SYNTHESIS AND UTILITY OF ELECTRONICALLY DIVERSE POLYCYCLIC AROMATICS

BY

JOHN DAYTON TOVAR

B. S., CHEMISTRY
UNIVERSITY OF CALIFORNIA, LOS ANGELES; 1997

SUBMITTED TO THE DEPARTMENT OF CHEMISTRY IN PARTIAL
FULFILLMENT OF THE REQUIREMENTS FOR THE DEGREE OF

DOCTOR OF PHILOSOPHY IN CHEMISTRY

AT THE

MASSACHUSETTS INSTITUTE OF TECHNOLOGY

JUNE 2002

SIGNATURE OF AUTHOR: _____
DEPARTMENT OF CHEMISTRY
MAY 2, 2002

CERTIFIED BY: _____
TIMOTHY M. SWAGER
PROFESSOR OF CHEMISTRY
THESIS SUPERVISOR

ACCEPTED BY: _____
ROBERT W. FIELD
CHAIRMAN, DEPARTMENTAL COMMITTEE ON GRADUATE STUDENTS

This doctoral thesis has been examined by a Committee of the Department of Chemistry as follows:

Professor Timothy F. Jamison: _____
Chairman

Professor Timothy M. Swager: _____
Thesis Advisor

Professor Rick L. Danheiser: _____

With humility and with pride,
I dedicate this thesis to my family.

Synthesis and Utility of Electronically Diverse Polycyclic Aromatics

by

JOHN DAYTON TOVAR

Submitted to the Department of Chemistry on May 2, 2002
in partial fulfillment of the requirements for the degree of
Doctor of Philosophy in Chemistry

ABSTRACT

This dissertation examines the synthesis of electronically diverse polycyclic aromatics within discrete molecular regimes and as incorporated into robust conjugated polymers. We have pursued two strategies for obtaining these large aromatics from rather elaborate yet readily available pendant aromatic precursors: electrophilic and oxidative cyclizations. Chapters One and Two describe research directed towards expansion of electrophilic cyclizations that utilize alkyne functionality to construct aromatized systems. Strongly-acidic conditions provide transient cationic intermediates that participate in annulations with adjacent arenes or amides to yield dibenzanthracenes or dioxanthracenes, respectively. In the latter case (Chapter Two), smaller model compounds confirmed this unique reactivity and helped to establish synthetic routes that yield isoquinolines in one synthetic step from aryl carbonyls appended with *ortho*-substituted alkynes. Chapters Three and Four describe efforts directed towards thiophene-based polycyclic aromatics. Tandem cyclization-polymerizations of pendant thiophenes provide robust electrochromic materials with readily tuneable optical bandgaps. Arenes placed adjacent to the highly-reactive oxidized thienyl moieties force this unique reactivity by biasing the system toward intramolecular cyclization. Chemical and electrochemical studies of related model systems further established the tandem reactivity. The generality of this controlled oxidative cyclization provided several readily-functionalized sulfur-based polycyclics. Using this chemistry, larger molecular and polymeric structures with tailored functionality may allow for a survey of electronic applications such as plastic organic field-effect transistors.

After employing the new routes to large polycyclic aromatics, these scaffolds helped to study the optimization of exciton migration and the mechanical tuneability of polymer chromicity. The thiophene-based platforms allowed for an assessment of the photophysical effects of chromophore aromatization within conjugated arylene-ethynylene polymers. As detailed in Chapter Four, the incorporation of planar and aromatized moieties greatly reduces the rate of fluorescence decay relative to closely-related yet non-aromatized structures. These easily-functionalized substrates also led to an examination of a new type of mechanochromism as introduced in Chapter Five. Conformational alterations within the polymer could lead to attenuated excimer-like behavior, and the synthetic schemes presented allow for the incorporation of a variety of discrete chromophores that may provide clean and sharp optical properties when compared to conformationally-disordered conjugated polymers.

Thesis Supervisor: Timothy M. Swager
Title: Professor of Chemistry

Preface

The Mahayanas tell the story of a sage who once stood on a riverbank looking across at the opposite shore. Although the far side was but dimly visible through the river mists, he could see that it was unspeakably beautiful. The hills were green and the trees were all in blossom. So he said to himself, "I want to go there."

There was a raft tied at the river's edge. He untied the raft and began to paddle toward the distant shore. The journey was long and hazardous for the currents in midstream were swift. The raging rapids tossed and turned the raft, and he had to work with all his strength to maintain his balance. From the center of the river, both shores were lost from view, and there were times when he was not sure which way he was drifting. But he continued paddling, and in due time, he reached the far shore.

He got out of the raft and said, "Ah, at last I am here. It was a perilous journey, but now I have reached nirvana." He looked about him. The hills were green and the trees were all in blossom. Then he turned around and looked back. He could not see the opposite shore from whence he came.

Nor was there any river to be seen.

And there was no raft.

J. L. Christian, *Philosophy* (6th ed), Harcourt Brace College Publishers: New York, 1994. p 624.

A note on style:
I have made every attempt to conform the main text of this dissertation to the standards of E-prime, an academic dialect of English that does not use the verb "to be." However, the experimental sections adopt the written conventions typically used in the literature. The acknowledgements section also does not adhere to this restriction.

Table of Contents

Chapter 1

An introduction to ladder polymers: Dibenz[*a,h*]anthracenes and related sytems *via* directed electrophilic cyclization

Adapted in part from:
Tovar, J. D.; Swager, T. M. *J. Organomet. Chem.* **2002**, *in press.*

Introduction

Substantial research efforts have focused on fully aromatic ladder polymers and related types of highly unsaturated organic materials as potential substrates for a variety of electronic applications such as light-emitting diodes, non-linear optics and thin film transistors. These structural motifs represent extended electronic structures of high stability, and they derive their unusual properties from the rigid aromatic frameworks that foster extensive π electron delocalization reminiscent of the two- and three-dimensional architecture found in graphite.[1] This field emerged from work conducted in the laboratories of Shirakawa, MacDiarmid and Heeger that led to the discovery of copper-like conductivity in iodine-doped poly(acetylene).[2] While this major finding earned these three the 2000 Nobel Prize in Chemistry, technological applications employing poly(acetylene) practically do not exist. Not only do the poly(acetylene)s exhibit relatively high reactivities, but poor solubilities have rendered these materials extremely difficult to process. As a result, many groups have endeavored to synthesize more robust materials that possess a poly(acetylene)-like conjugated backbone yet offer better solubility or stability. Two structural derivatives of poly(acetylene) broadly define these strategies: bridged repeat units and fused ladder systems (Figure 1).

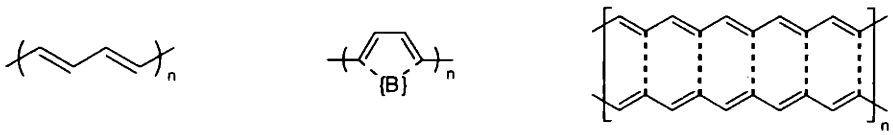

poly(acetylene) "bridged" "fused"

Figure 1: Broad variants of poly(acetylene)

Polymers with bridged units comprise the most studied and applied group of conducting polymers. Such polymers have non-degenerate ground state resonance structures referred to as the aromatic and the quinoidal forms. (Figure 2, top).[3] In the neutral state of the polymer, the aromatic form dominates, but upon oxidation, these materials adopt more of the quinoidal form in order to better delocalize the charge carriers (*i.e.* the polarons and "bipolarons").[4] While the poly(phenylene)s formally fall into this category, they typically exhibit low conductivity. This results from the torsional strain between solublizing groups on adjacent phenyl units that limits overall planarity and thus, effective conjugation length. Furthermore, extended quinoidal delocalization requires that several phenyl units must overcome their inherent aromatic resonance stabilizations. The poly(thiophene)s and poly(pyrrole)s ease these issues: the five-membered heterocycles minimize steric torsion in the backbone while the lesser degree of aromatic resonance energy facilitates quinoidal delocalization around the charge carrier. In fact, Roncali has found that thiophene monomers held into geometric planarity through annulation posess lower monomer and polymer oxidation potentials.[5] Although not formal "ladder polymers," these studies emphasize the importance molecular rigidity plays in determining the macroscopic properties of a bulk material. As such, Chapter 3 will go into further detail about these and other strategies to planarize "bridged" polyacetylene.

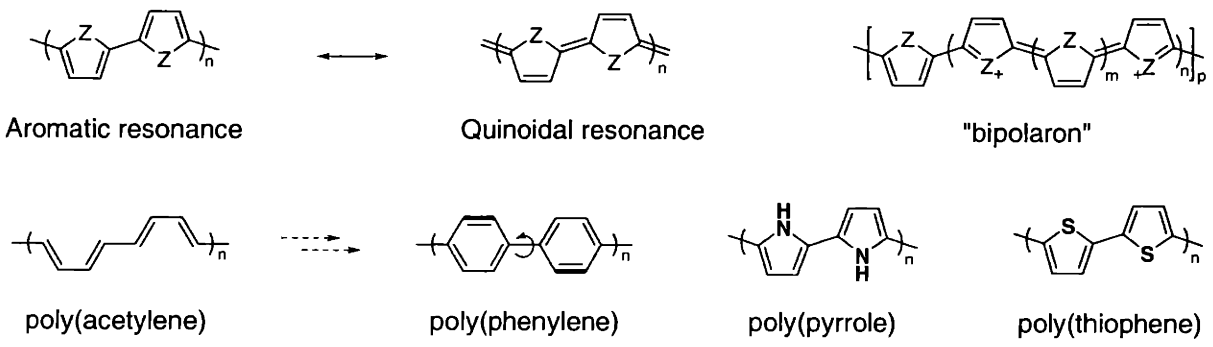

Figure 2: "Bridged" poly(acetylene)s

The second approach toward more robust derivatives of poly(acetylene) consists of a schematic fusion of two polymer chains. These rigid structures make up a sub-category of ladder polymers, materials where repeat units have more than one rigid, independent link between monomers such that a schematic rupture of one linking unit will not break the polymer into separate components. The poly(acene)s best epitomize this idea; in fact, Kivelson and Chapman postulated that these materials would have intrinsic conductivity.[6] However, their predictions from 1983 have remained largely untested as these systems suffer from severe reactivities after six fused repeat units (hexacene). To further frustrate this synthetic goal, strategies currently do not exist that allow for polymer-grade acene synthesis and for the incorporation of solubilizing groups. To circumvent these issues, several groups have directed more academically oriented research towards other ladder systems with a variety of linear and kinked molecular topologies that incorporate side chains for solubility. Defined ribbons with pendant functionality offer the possibility to alter electronic properties through substituent appendages off of the polymer backbone, and these substituents simultaneously offer solubilizing groups to facilitate structural characterization and processing. As with the poly(acene)s, these systems comprise discrete segments cut out of the graphite layer structure.

The variety of routes to ladder polymer systems illustrated in the following schemes indeed prove that pictures speak a thousand words. Nevertheless, a few prefacing remarks will follow. Schlüter first elaborated the synthesis of a fully aromatized ribbon *via* dehydrogenation of a polymeric Diels-Alder adduct.[7] The insolubility demonstrated by this polymer required the incorporation of hydrocarbon cyclophanes (through 'R') as opposed to the standard long alkyl chain solubilizing groups. Scherf and Müllen prepared the methylene-bridged poly(*p*-phenylene) in Scheme 2 (top) through a BF_3-mediated electrophilic cyclization of a poly(phenylene) with

appended hydroxymethyl arenes.[8] Here, the pendant arene on the bridging sp^3-carbon provides additional solubility by decreasing the extent of polymer chain interactions. This polymer displays strong blue emission in analogy to the related poly(phenylene) and poly(fluorene) materials, a testament to the intrinsic "phenylene" character maintained in the backbone despite the loss of rotational freedom. Scherf has carried out extensive electroluminescence and optical lasing studies to harness the intense blue emission observed from these materials.[9]

Scheme 1

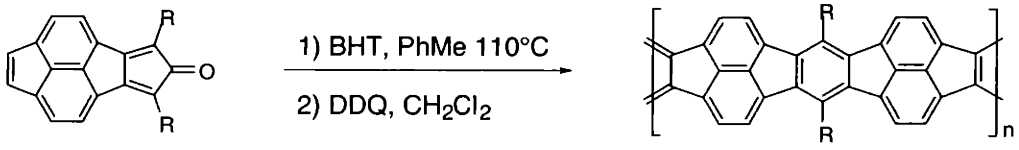

Schlüter, *et al.*

Scheme 2

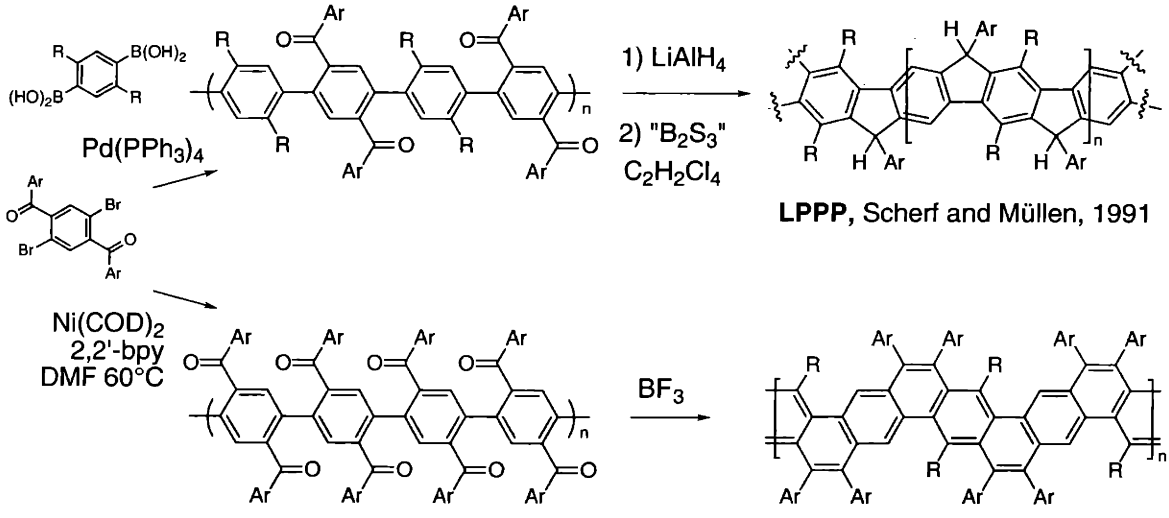

LPPP, Scherf and Müllen, 1991

Chmil and Scherf, 1993

Chmil and Scherf later disclosed a homopolymer from the same starting material to provide phenacene-type graphite ribbons *via* post-polymerization ketone condensation (Scheme 2, bottom).[10] The chromophore electronics significantly changed after cyclization due to the conjugative participation of the bridging olefin holding the poly(phenylene) backbone into planarity. This resulted in a red-shifted emission when compared to planarized yet not

completely aromatized LPPP system. In addition to these carbonoid systems, other investigations have examined heteraromatic ladder structures. Tour has studied fully aromatized systems that incorporate heteroatoms into the ladder backbone such as "donor-acceptor" thienyl- and pyridyl-based ribbon systems (Scheme 3, top).[11] These synthetic strategies parallel those used by Chmil and Scherf, where carbonyl-containing repeat units undergo acid-induced imine formation between repeat units to cyclize and aromatize the polymer. Unfortunately, many of Tour's systems suffer from severe insolubilities, often requiring dissolution in strong acids. Recently, Tsuda and Osuka reported the preparation of discrete porphyrin "tapes" on the order of 100 Å by DDQ/$Sc(OTf)_3$-mediated cyclizations (Scheme 3, bottom).[12] These tapes absorbed into the near IR, exemplifying their high degree of conjugation. Such robust organic materials with strong near IR activity may prove useful as third-order non-linear optical materials.

Scheme 3

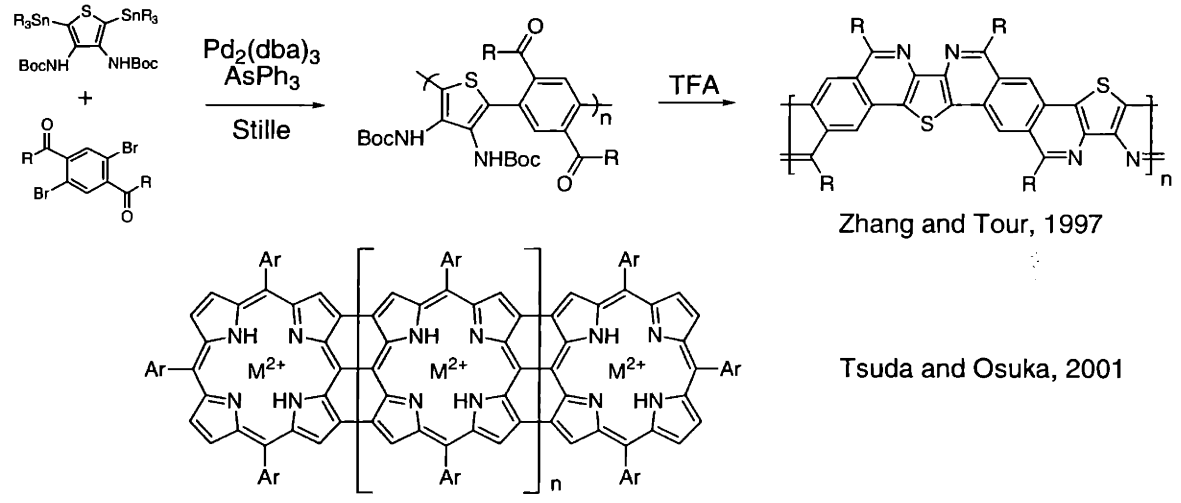

Up to this point, the discussion of ladder polymers has focused on linear ribbon structures. Introducing *meta* kinks into a polymer backbone opens possibilities for the study of helically oriented polymers.[13] Nature currently supplies one of the most important and most powerful helical polymers, DNA strands. Of course, smaller niche markets still exist that demand more rigid scaffolds. Specifically, rigid helical materials hold promise in "chiral separation technologies" where the inherently chiral pore of a helical strand may allow for selective adsorption and removal of an analyte. The periodic twisting of aromatic rungs could help to study several important questions concerning the relative importance of through-bond or through-space charge transport mechanisms. With a responsive helical material, environmental conditions may physically alter the helical pitch, thus affecting inter-rung distance and correlating with an observable change in optical or electronic properties (absorption, conductivity, *etc.*) However, no reliable methods exist for constructing fully aromatized, helical ladder materials. Katz has extensively studied helicene derivatives obtained through Diels-Alder chemistry, and he reported a conjugated but not fully aromatized helical ladder polymer by condensing a salicylaldehyde-based helicene with *o*-phenylenediamine and a nickel salt to form the Schiff-base helicene polymer (Scheme 4).[14] Beside this effort, no studies have successfully examined helical ribbon polymers.

Scheme 4

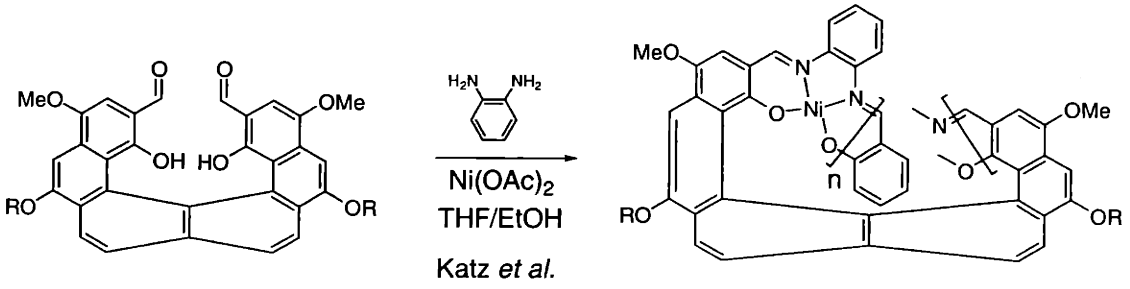

On the other hand, several groups have studied new strategies to form large helical segments as "bottom-up" models for the analogous helical ribbons. For example, the most commonly employed methods of thiahelicene synthesis consist of the representative routes depicted retrosynthetically in Figure 3. Rajca and co-workers have recently reported fused thiophene systems by constructing smaller oligomeric units through a "connect-annulate" approach.[15] The helicene formation then proceeds through a final lithiation and subsequent trapping with bis(phenylsulfonyl)sulfide. Being cross-conjugated, this system did not display extended aromatic delocalization ($\lambda_{max} < 300$ nm). As illustrated by the thiahelicenes of Tanaka *et al.*, Mallory-type photocyclization of thienyl-based 1,2-diarylethenes have afforded cyclized, aromatized helicenes.[16] However, photochemical routes do not readily allow for large quantities of cyclized materials, and the strong acid byproducts (HI) do not allow for diverse functional group incorporation. To overcome this, McMurry-type approaches have also succeeded in constructing helicenes from arene dimers with *o,o'*-dial functionality. To date, none of these strategies has led to the successful synthesis of fully aromatized helicene ladder polymers.

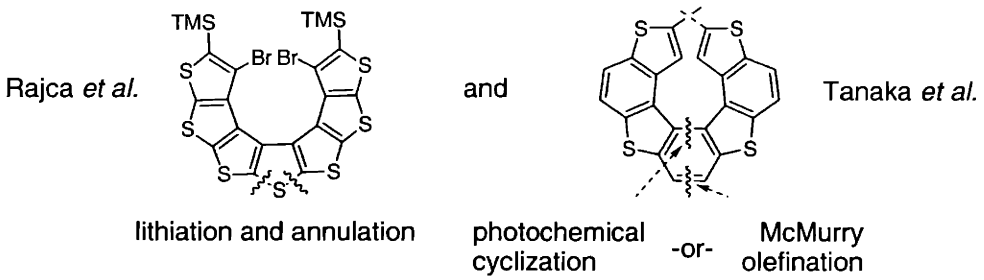

Figure 3: Synthetic routes to thiahelicenes

The nature of the oligo- or poly(arene) structural topology plays a significant role in the ultimate helical "zipping up" step, regardless of the synthetic approach applied. In many cases, properly substituted arenes will allow for only one molecular orientation that presents reactive functional groups in such a way that the photochemical or chemical annulation event can occur.

This idea follows from a typical stilbene photocyclization, where *cis* and *trans* stilbene both lead to the cyclized phenanthrene upon irradiation. Of course, the *trans* stilbene must first isomerize to *cis* prior to cyclization. Chain dynamics complicate this idea in polymer systems, where the relative hydrophobicity of the chain has dramatic impacts on the chain topology in spite of any latent reactive functionality. Moore elegantly has demonstrated the effects that non-solvents – solvents that do not appreciably dissolve a polymer of interest - have on the chain conformations of *meta*-phenylene ethynylene oligomers.[17] As a paragraph in an introduction cannot do proper justice to the beauty of these studies, Scheme 5 depicts a similarly simplified illustration of these effects. In chloroform, the oligomer chain adopts a zig-zag structure. By incorporating hydrophilic groups at the third *meta* site of the benzene repeat unit (R), this oligomer folds into a helical conformation upon addition of acetonitrile, a non-solvent. The favorable interactions of the hydrophilic side chain with acetonitrile relative to the hydrophobic inner core drive this folding. This concept will factor in largely to the work presented later in this chapter.

Scheme 5

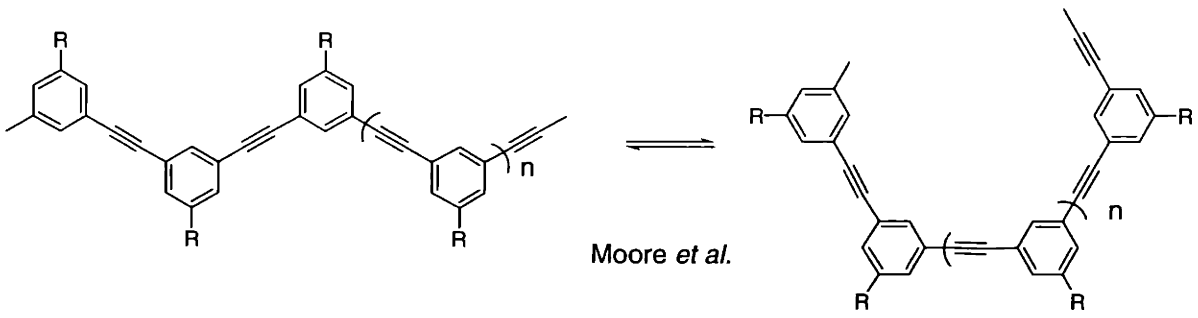

Besides aromatized ladder polymers, other semiconductor applications may benefit from the use of large molecular systems. The potential for utilizing highly conjugated yet *discrete* polycyclic aromatics as higher mobility FET materials has spurred the development of synthetic methods for new and otherwise challenging polycyclic scaffolds.[18] Most importantly, the covalent π-conjugated organic network mimics the extended σ-networks found in the crystal

lattices of inorganic semiconductors. Unlike ladder polymers, discrete molecular systems allow for sublimation and zone-refining purification, two techniques often employed to achieve materials of electronic-grade purity. Anthony has developed a strategy to access higher acenes and rylenes through sequential Bergman cyclizations (Scheme 6, top).[19] Here, the bromoethyne moieties help to drive the cycloaromatization, and they serve as handles to couple additional alkynes after cyclization for step-wise extension of the acene core. Müllen has elegantly applied oxidative cyclodehydrogenations to the synthesis of "superacene" graphite sheets (Scheme 6, bottom).[20a] A variety of dendritic oligo(phenylene) substrates readily undergo exhaustive cyclization in a similar fashion to the hexaphenylbenzene shown in Scheme 6. Such large molecular species have exhibited discotic-like liquid crystal character, and they possess sufficient inter-chromophore order to allow for modest charge transport (*ca.* 0.13 cm^2/Vs).[20b] Beside these rather specific cyclization chemistries, Mallory has extended the classic oxidative arene photocyclization to the synthesis of fused phenanthrenes.[21] Step-wise Wittig-Mallory sequences allow for the preparation of large fused ribbon oligomers.

Scheme 6

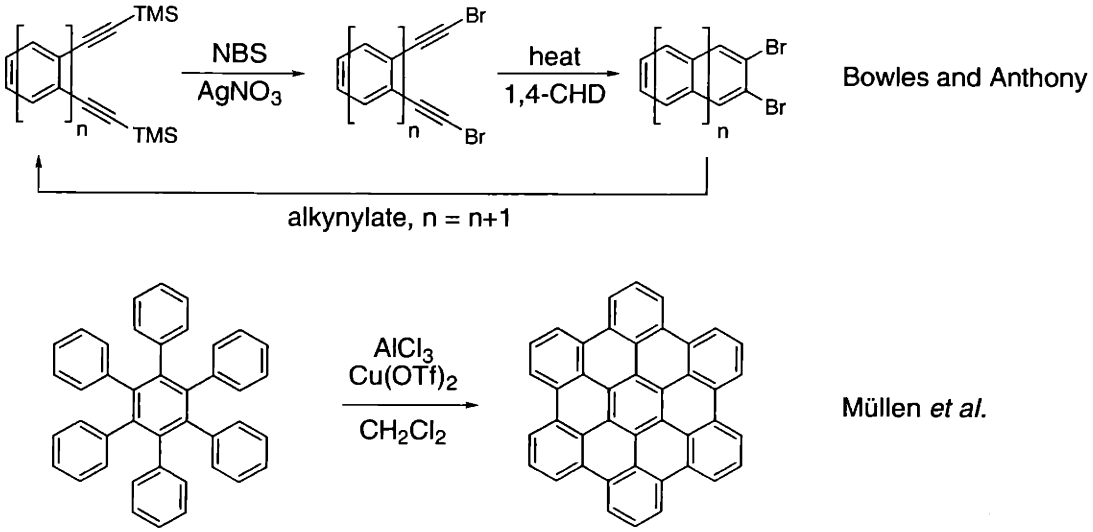

Bowles and Anthony

Müllen *et al.*

Earlier work led by Marc Goldfinger, a former Swager graduate student, examined a series of directed electrophilic cyclizations of alkyne-appended terphenyl and quinquephenyl systems into the corresponding aromatized polycyclics.[22] He found conditions to effect high yielding, often quantitative, cyclization to the benzo- and phenanthro-fused anthracenes by treating the alkynes with moderately strong electrophiles (Scheme 7, top).[22b,c] This reactivity relied upon lone-pair donation into the alkyne to facilitate electrophilic attack by the β-sp-carbon as indicated in Scheme 7. This chemistry also succeeded in cyclizing alkynylated poly(phenylene)s into aromatized ladder polymers (Scheme 7, bottom),[22a] structurally similar to the system reported by Chmil and Scherf.[10] In this chapter, we report an extension of this methodology where we now utilize stronger amine donors as cyclization-directing groups.

Scheme 7

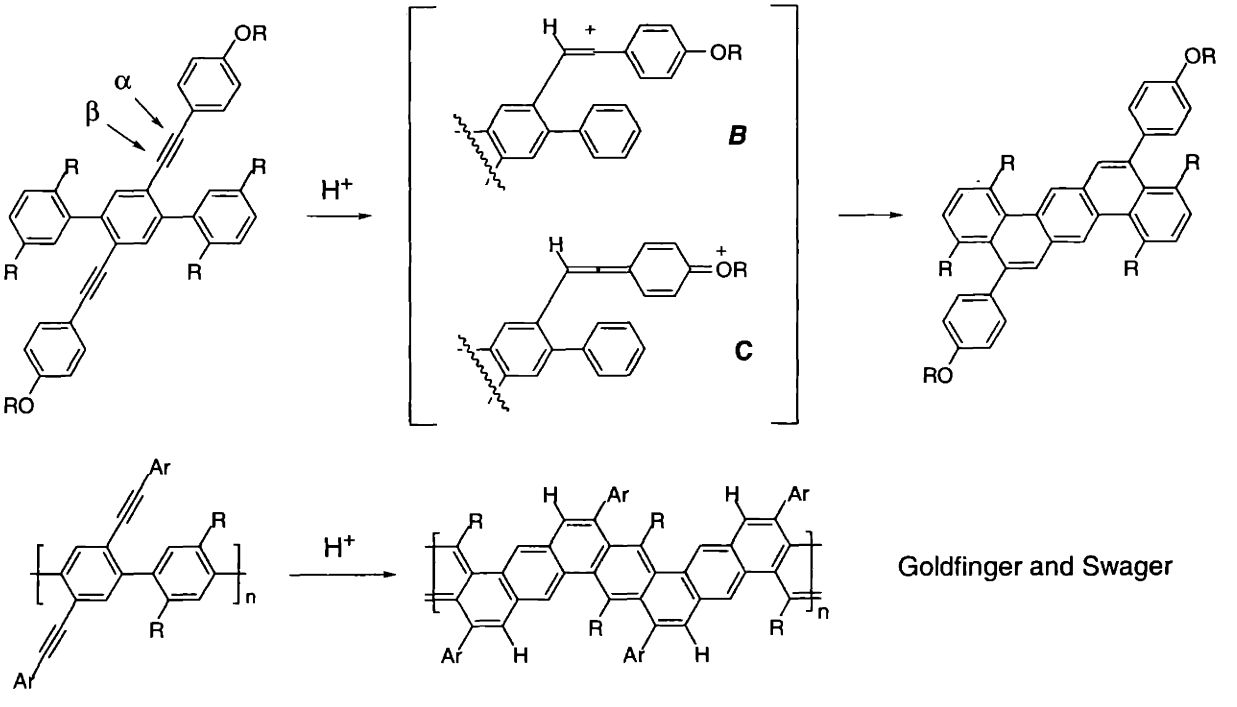

We sought to examine new donors with the goals of enhancing post-polymerization chemistry and eliminating undesired isomerization events (Scheme 8). In earlier studies, Goldfinger found that many thiophene-containing systems underwent arene migration to form

aromatized yet nonsymmetrical materials. While these isomerizations have minimal impact on the energetics of a polymer backbone, they could have serious implications for crystalline solid-state packing within molecular derivatives. One other limitation of the earlier methodology arose from the fact that ethynyl cyclization onto an unsubstituted thiophene moiety did not proceed at all. This effectively eliminates any potential for further synthetic manipulation after cyclization (*e.g.* bromination). Therefore, we initially sought to study cyclization efficiencies in the presence of stronger dibutylamine donors as an entry into more regiochemically well-defined annulations.

Scheme 8

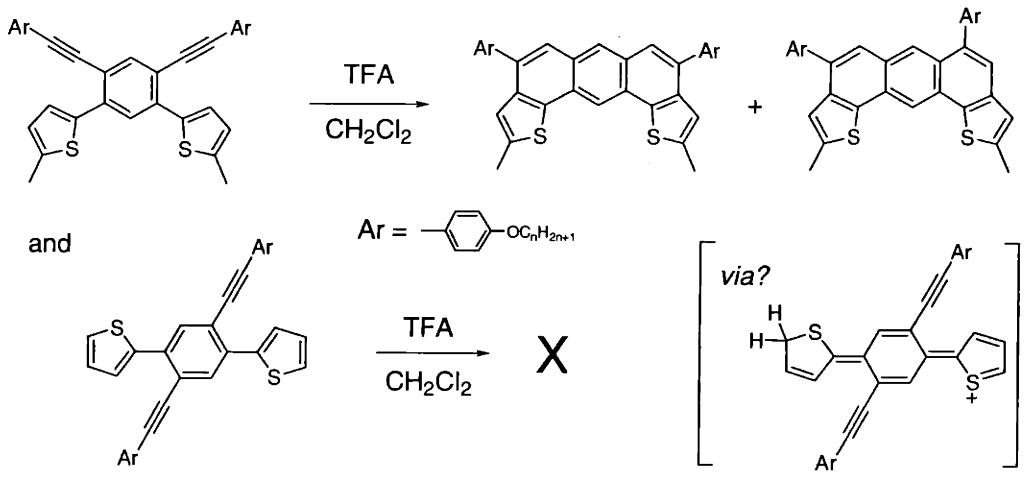

The Swager group's interest in chemosensory materials, coupled with the limitations of current methodologies, has led us to expand the scope of existing electrophilic cyclization strategies that efficiently effect the construction of soluble polycyclic aromatic structures within monomeric and polymeric regimes. With this goal in mind, this chapter will describe our studies directed towards systems falling under two major categories: *para*-substituted systems ultimately leading to ladder polymers (Scheme 9, top) and *meta*-substituted systems leading to rigid helical materials *via* chemical or electrochemical polymerization (Scheme 9, bottom). The small Stokes' shift observed for Goldfinger's *para* fused polymers hinted that these ribbons may

facilitate exciton migration thus serving as backbones for efficient chemosensory devices. The *meta* systems attracted us due to the potential of new chemosensory materials which exploit inherent backbone helicities. To explore both of these systems, two factors needed consideration: quantitative aryl-aryl coupling for high molecular weight materials and cyclization efficiency for defect-free materials. We examined Suzuki, Stille and Negishi couplings to address the former consideration and used these models to study the latter.

Scheme 9

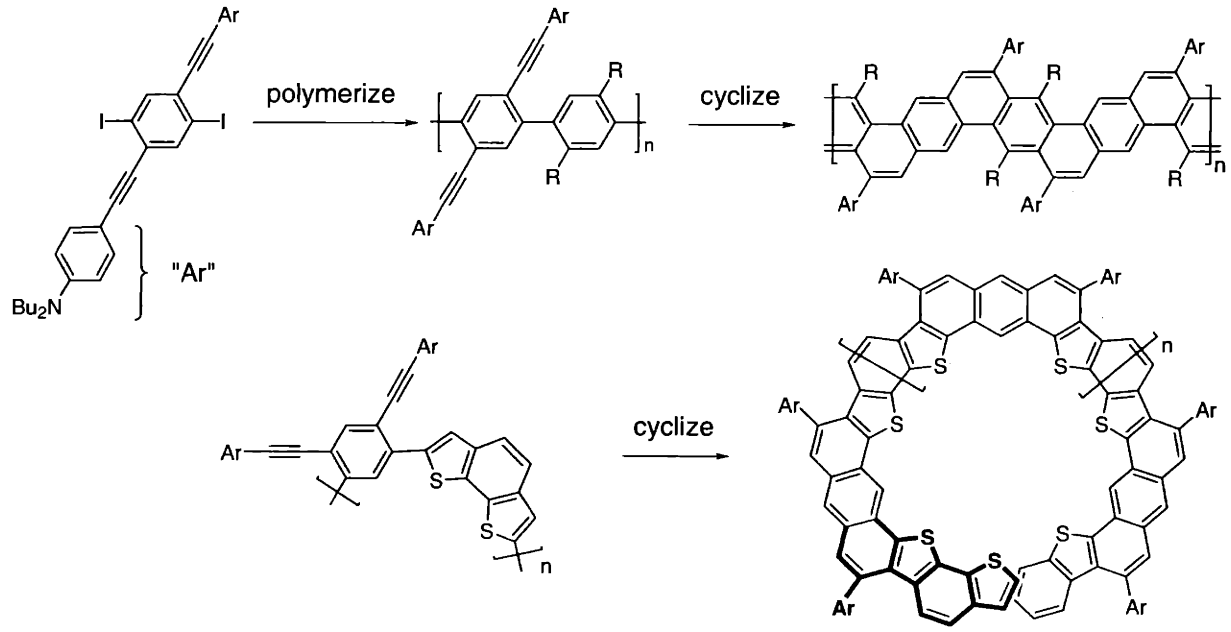

Results and Discussion

We developed two different synthetic routes to obtain the desired amine-donor terphenyl models **1** and **2**, both of which rely on Sonogashira and Suzuki protocols.[23,24] The first route paralleled that used by Goldfinger and incorporated the alkyne moieties onto the halide scaffold **3** thus allowing for the synthesis of polymerizable monomers (Scheme 10).[22b] Starting from **3**,[25] Sonogashira cross-coupling of TMS acetylene installed two alkynes chemoselectively at the iodo positions. Subsequent protiodesilylation and Sonogashira cross-coupling of *N,N*-dibutyliodo-aniline[26] provided the dibromide **4**. Despite the electron-rich nature of the iodoaniline, the

differential reactivity existing between bromo- and iodo-substituted arenes provided sufficient chemoselectivity to provide **4** in high yield. Unlike Goldfinger's approach to couple 4-dodecyloxyphenylacetylene with **3**, we had to rely on this stepwise route with TMS acetylene due to the oxidative instability of the analogous 4-aminophenylacetylene. For polymer studies, we prepared diiodide **5** *via* lithium/halogen exchange followed by an iodine quench. From **4**, Suzuki cross coupling of dimethyl- or dimethoxy phenylboronic acid provided the terphenyls **1** and **2**, respectively, in high but not quantitative yields. We surveyed a range of Suzuki conditions and found that conditions closely resembling those initially published by Suzuki provided optimal results. However, these methods will not adequately furnish high molecular weight materials during Suzuki-type polymerizations.

Scheme 10[a]

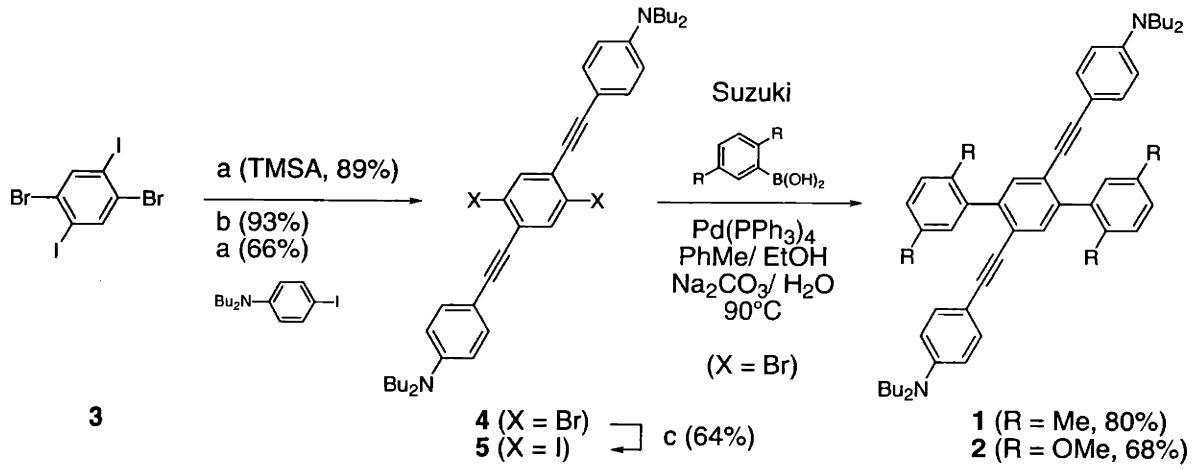

[a] Reagents and conditions: (a) *Sonogashira:* $(Ph_3P)_2PdCl_2$, CuI, PhMe, DIPA; (b) *deprotection:* K_2CO_3, THF, MeOH, rt; (c) *iodination*: i. *t*-BuLi, THF, -78°C; ii. I_2, THF.

The second route (Scheme 11) initially constructs the terphenyl moiety, allowing for the addition of a donor directing functionality at a later stage. This strategy avoided issues of oxidative sensitivity displayed by the aminated phenylacetylene that hampered large-scale purification on silica. Analogous to the preparation of **4**, chemoselective Sonogashira cross-coupling of TIPS acetylene provided the dibromide **6**. The robustness of the TIPS protecting groups allowed for clean Suzuki cross-coupling with dimethyl- or dimethoxy phenylboronic acid without apparent desilylation. Fluoride-promoted deprotection of the TIPS moieties then provided **7-8** in modest overall yields from **6**. From these terminal alkynes, Sonogashira cross-coupling with *N,N*-dibutyliodoaniline again provided **1-2** in high yields. Over both four-step procedures, the first route provided higher overall yields from the halide parent **3**: **1** (Scheme 10, 44%; Scheme 11, 30%), **2** (Scheme 10, 37%; Scheme 11, 25%).

Scheme 11[a]

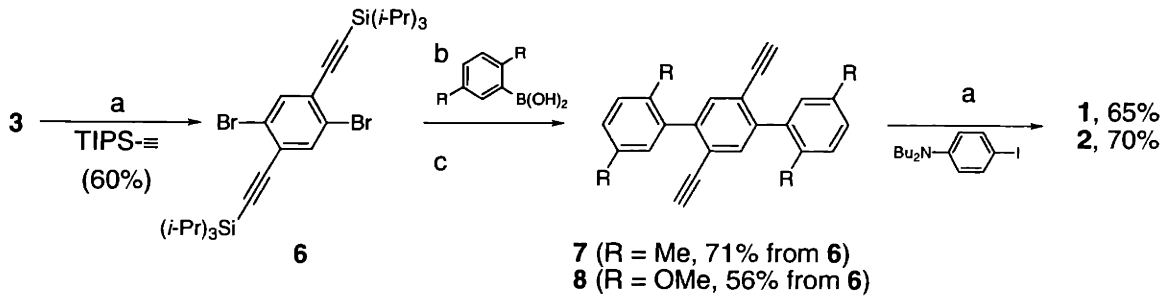

[a] Reagents and conditions: (a) *Sonogashira:* $(Ph_3P)_2PdCl_2$, CuI, PhMe, DIPA; (b) *Suzuki:* $Pd(PPh_3)_4$, PhMe, EtOH, Na_2CO_3, H_2O, 90°C; (c) *deprotection:* *n*-Bu_4NF, THF, H_2O, rt.

With these precursor models readily available, we could assess the competency of the stronger amine donors in the electrophilic cyclization. In line with Goldfinger's previous results, the starting terphenyls reacted immediately upon addition of trifluoroacetic acid (TFA); however, a basic workup only regenerated the starting materials. We postulated that the enhanced basicity of the amine-substituted terphenyls allowed for mere protonation of the amino moiety rather than an electrophilic attack and cyclization onto the acetylene. To support this claim, NMR experiments with **1** at room temperature indicated no formation of new aryl or olefinic protons after TFA addition. These measurements revealed that the alkynes persisted under such acidic conditions (^{13}C resonances at 92.1 and 91.6 ppm) while the *N*-butyl amine chains exhibited a downfield α-methylene resonance at 59.9 ppm compared to the value of 50.9 ppm for **1**. The absence of any new products resulting from rehybridization of the alkynes of **1** confirms that the reaction equilibria favored protonated donor *A* under the cyclization conditions at room temperature (depicted in Scheme 12).

Scheme 12

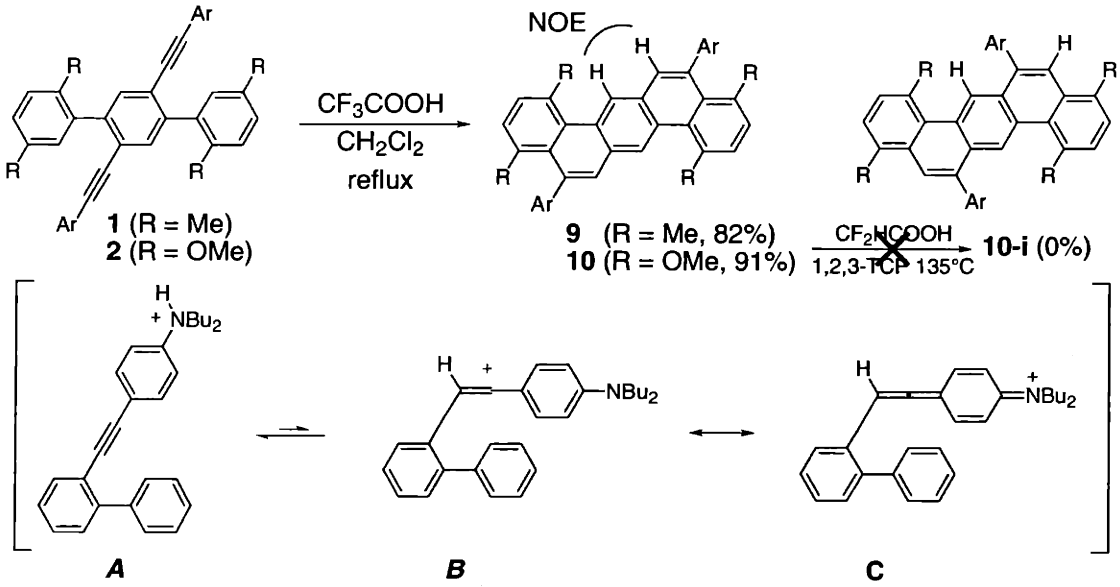

Subsequently, we found that the cyclization proceeded smoothly under refluxing conditions to provide the cyclized dibenz[*a,h*]anthracene systems **9-10** in excellent yields (Scheme 12). The enhanced degree of aromaticity in the cyclized materials resulted in downfield proton NMR shifts for the dibenz[*a,h*]anthracene ring protons. Furthermore, the extension of the π-conjugated pathway *via* rigidification provided red-shifted (*ca.* 28 nm between **2** and **10**) and weakly-allowed transitions often observed in similar polycyclic aromatic systems. As this chemistry required slightly elevated temperatures, we feared aryl isomerizations in accord with those observed in Goldfinger's studies; however, we have no evidence for the formation of isomerized products. Firstly, ^{1}H NMR shifts of the dibenz[*a,h*]anthracene ring systems within **9** and **10** matched those found in Goldfinger's alkoxy donor systems. ROESY analysis of **10** indicated the presence of a through-space interaction between the two dibenz[*a,h*]anthracenyl singlets: the proximal arene singlets of **10** should exhibit this interaction while the hypothetical isomer **10-i** should not (as noted in Scheme 12). Unlike Goldfinger's studies, we could not thermally isomerize **10** to the aryl-migrated product **10-i** despite harsher reaction conditions indicating that the apparently protonated aryl amines pendant to the newly-aromatized ring system inhibit thermally-promoted isomerizations.

Despite the modest yields obtained for Suzuki-type terphenyl construction, we performed initial studies towards poly(phenylene)-based cyclization precursors also bearing pendant alkynes. After screening several Suzuki polymerization conditions with both the dibromide **4** and the diiodide **5**, the best results only led to a polymer with M_n = 15,000 (Scheme 13, n = *ca.* 16). Nevertheless, our efforts to effect electrophilic cyclizations onto this polymer did not succeed. As we could not recover the starting polymer, we may attribute this lack of directed reactivity to decomposition or crosslinking of individual reactive sites during the refluxing post-polymerization modification attempts.

Scheme 13

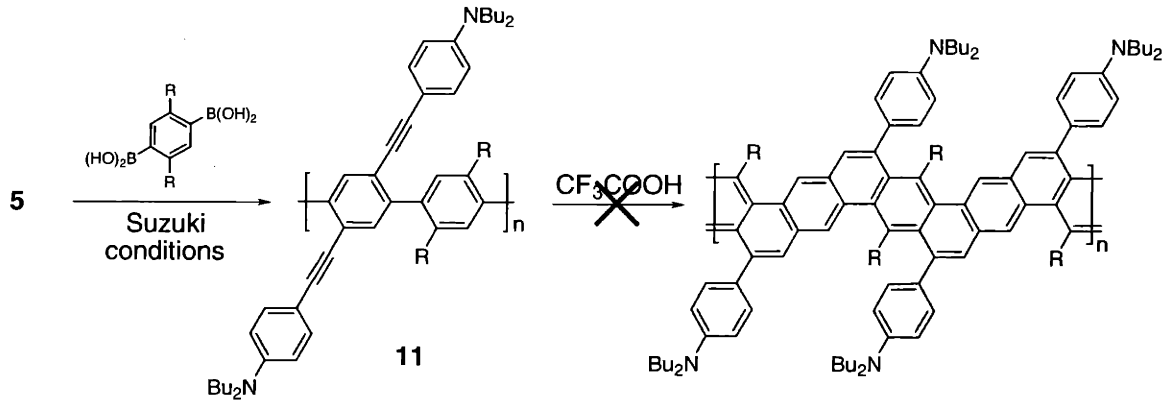

To test if the amine donor would allow for more efficient entry into other linear (*para*) systems such as thiophene-fused anthracenes, we prepared *para*-dithienyl derivative **12** through Stille cross-coupling between **4** and tributyltin thiophene (Scheme 14).[27] Initial cyclization attempts with TFA provided no reaction, even under refluxing conditions. When we employed the much stronger triflic acid as the electrophilic proton source, we obtained the cyclized anthradithiophene **13** in moderate yield. Similar to the case of **10**, ROESY analysis helped to confirm the structural connectivity of **13**. We envisioned that an unsubstituted thiophene-based monomer such as **13** would allow for electrodeposition of highly stable, electroactive polymer films; however, the readily oxidized aryl amines pendant to the aromatic scaffold complicated efforts to characterize the electrochemical behavior of **13**. As a result, anodic oxidation led to completely irreversible activity but no apparent polymer film deposition. Other thiophene-based polycyclic aromatics of comparable size to **13** have afforded highly stable, multiply charged species upon electrochemical oxidation, and polymers incorporating such units exhibit electrochromicity and robust environmental stability.[28] Chapters 3 and 4 will describe our work in these areas.

Scheme 14

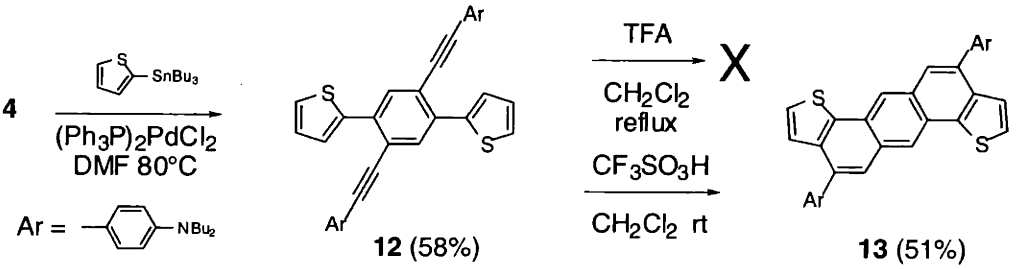

Switching to the *meta* systems, we chose benzodithiophene **14** for preliminary investigation.[29] In general, the helical shape of such a molecule coupled with the two synthetically addressable α-sites would allow for the study of model monomers as well as provide an entry toward polymers. Lithiating such monomers *in situ* would furnish a Negishi-

type reagent for monomer coupling or for polymerization.[30] Khushrav B. Crawford, a former Swager postdoctoral associate, worked out a synthetically simple approach to **14** depicted in Scheme 15 (top). The tetrabromide **15** underwent selective dehalogenation at the 2,5' bithiophene sites, and a second lithium-halogenation exchange followed by a DMF quench provided the dial **16**. McMurry coupling ultimately afforded the benzodithiophene **14** in 9-37% overall yield from tetrabromide **15**.[31] Unfortunately, the variable yields obtained for the second lithiation step and the high dilution required for the McMurry coupling hindered larger scale syntheses of **14** and thus, a thorough examination of the Negishi coupling. However, we should note that we used Aldrich Sure-Seal THF - not rigorously dried THF - for the lithiation step. While this has not posed problems for most of the chemistry in this chapter, perhaps drier solvents may improve the formylation yields.

Scheme 15[a]

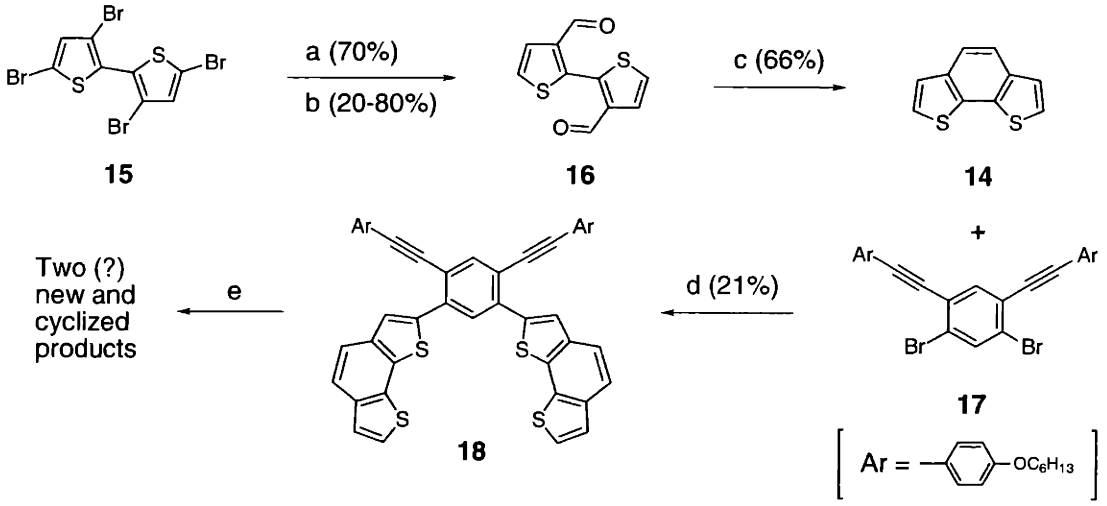

[a]Reagents and conditions: (a) i. *n*-BuLi, THF, -78°C; ii. AcOH; (b) i. *t*-BuLi, THF, -78°C; ii. DMF; (c) *McMurry:* $Zn/TiCl_4$, THF, reflux; (d) *Negishi:* i. *n*-BuLi, $ZnCl_2$, **14**, THF, -78°C; ii. $Pd(PPh_3)_4$, **17**, THF, rt; (e) CF_3COOH, CH_2Cl_2, reflux.

In light of the problematic protonations during cyclizations with *para* amine donor terphenyls (**1** and **2**), we used the *meta* alkoxy donor monomer **17** for initial *meta* pre-helical studies as synthesized by Goldfinger.[22b] Negishi protocols afforded 21% of the doubly

substituted benzodithiophene **18** (7 mg). Unfortunately, this poor yield prohibited an extensive examination of the electrophilic cyclization. Initial results indicated that one unsymmetrical (or at least two symmetrical products) had formed during the cyclization, although we could not isolate or characterize these products in pure form due to materials constraints. Again, distilled or otherwise dry THF may increase this cross-coupling step.

As a result, we sought to obtain other dithiophene monomers amenable to gram-scale preparation. We chose to synthesize extended dithiophene units *via* transition metal catalyzed electrophilic cyclizations of the readily-obtainable terminal acetylenes **19** and **20** shown in Scheme 16. Chemoselective Sonogashira coupling on the iodides of **21**[25] and **22**[22b] proceeded with 75 and 78% yields, respectively, and subsequent Stille coupling led to 58 and 83% yields, respectively. Deprotection of the acetylenes led to near quantatitative yields of **19** and **20**, but their rapid decomposition prevented rigorous purification.

Scheme 16[a]

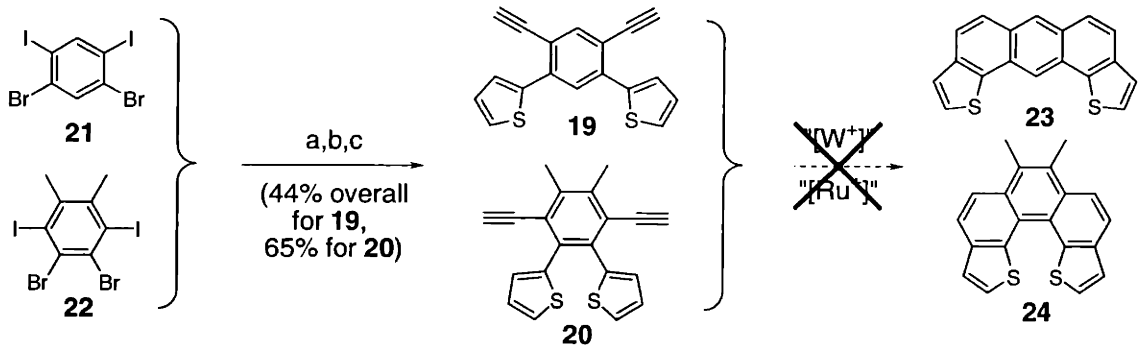

[a] Reagents and conditions: (a) *Sonogashira*: TMS-CCH, $(Ph_3P)_2PdCl_2$, CuI, PhMe, DIPA; (b) *Stille*: 2-(*n*-Bu_3Sn)thiophene, $(Ph_3P)_2PdCl_2$, DMF, PhMe, 80°C; (c) *deprotection*: K_2CO_3, THF, MeOH, rt.

The word "unfortunately" plays a key role in this chapter, and this holds true for the final cyclization step illustrated in Scheme 16. Cyclizations mediated by $W(CO)_5$(thf) only provided small percentages of mono-cyclized materials alongside recovered starting material.[32] Subjecting the crude reaction mixture to fresh cyclization conditions did not significantly drive the reactions

to further completion. We also prepared ruthenium complexes (η^6-C_6H_6)- and (η^6-*p*-cymene)-$RuCl_2(PPh_3)$ in accordance with reports for similar electrophilic alkynyl cyclizations.[33] Although this method eventually provided 21% of **23**, the reaction did not proceed to completion even after 7 to 14 days of reaction. Given this failure, we turned our attention to simpler systems not incorporating the alkyne moieties, and Chapters 3 and 4 detail this work.

Concluding Remarks

In closing, we have described extensions to acid-induced electrophilic cyclizations of pendant alkynes to provide electronically diverse families of polycyclic aromatics. By harnessing the versatility of the organometallic cross-coupling reaction, we may readily construct a variety of substrates to design and examine new reaction manifolds. The array of polyaromatics available on behalf of this generality stands to provide exciting new materials for current electronics and photonics applications. Concerning helical materials, the electrophilic cyclization failed in polar solvents such as acetonitrile. From Moore's studies, such polar, hydrophilic solvents will drive a pre-cyclized *meta* polymer into a helical conformation. As such, cyclization approaches will not readily allow for helical ladder materials unless they offer conditions compatible with both the helix formation and the cyclization chemistry. Chapter 4 will present another approach toward this goal.

Experimental Section

General: All air and water-sensitive synthetic manipulations were performed under an argon atmosphere using standard Schlenk techniques. Anhydrous diisopropylamine (DIPA), toluene (PhMe), methylene chloride and tetrahydrofuran (THF) were purchased from Aldrich and used without further purification. *n*-BuLi in hexane was titrated *versus* diphenylacetic acid before use. All other chemicals were of reagent grade and used as received. *N,N*-Dibutyl-4-iodoaniline[26] was prepared from NIS iodination of *N,N*-dibutylaniline; 2,5-dimethylphenyl boronic acid was prepared from bromo-*p*-xylene *via* lithiation and quenching with tri(isopropyl)borate; 2,5-dimethoxyphenyl boronic acid was prepared *via* lithiation of 1,4-dimethoxybenzene followed by quenching with tri(isopropyl)borate. Compounds **3** and **21** were prepared by the methods described by Hart from the corresponding dibromobenzenes (periodic acid, KI, H_2SO_4).[25] The diboronic acids used for **11** were prepared *via* lithiation of the respective 1,4-dialkoxy-2,5-diiodobenzene and quenching with trimethoxyborate.[22a] Compound **15** was prepared *via* exhaustive bromination of 2,2'-bithiophene. Compound **17** was prepared through Sonogashira coupling of 4-hexyloxyphenylacetylene with **21**.[22b] Compound **22** was prepared by sequential halogenation of *o*-xylene.[22b] The complex $(\eta^6\text{-}C_6H_6)RuCl_2PPh_3$ was prepared from $RuCl_3 \bullet x\ H_2O$ after step-wise treatment with cyclohexadiene and PPh_3.[33b]

Column chromatography was performed using Baker 40 μm silica gel. All organic extracts were dried over $MgSO_4$ and filtered prior to removal. NMR spectra were obtained on a Bruker AC-250, Varian Mercury-300 or Varian Inova-500 spectrometers, and all chemical shifts are referenced to $CHCl_3$ (7.26 ppm for ^1H, 77.23 ppm for ^{13}C) and TMS or $CHDCl_2$ (5.32 ppm). High resolution mass spectra were obtained at the MIT Department of Chemistry Instrumentation Facility (DCIF) on a Finnigan MAT 8200 using a peak matching protocol to determine the mass and error range of the molecular ion; FAB spectra were obtained using a 3-nitrobenzyl alcohol matrix. Molecular weight determination by gel permeation chromatography (GPC) was performed in THF versus polystyrene standards (PolySciences) on a HP 1100 HPLC system equipped with a Plgel 5 mm Mixed C column (300 x 7.5 mm). UV-Vis measurements were obtained on a Hewlett-Packard 8452A diode array spectrophotometer. Fluorescence measurements were recorded on a SPEX Fluorolog-τ2 fluorimeter (450 W Xe lamp). Elemental analyses were obtained at Desert Analytics (Tucson, AZ). Melting points are uncorrected.

2',5'-Bis[4-(*N,N*-dibutylamino)phenylethynyl]-2,2",5,5"-tetramethyl-1,1':4',1"-terphenyl (**1**)

From 4: A mixture of **4** (99.6 mg, 0.144 mmol), 2,5-dimethylphenyl boronic acid (108 mg, 0.721 mmol), KOH (113 mg, 2.01 mmol) and $Pd(PPh_3)_4$ (18 mg, 0.016 mmol) were placed under argon followed by the addition of PhMe (1.5 mL), EtOH (0.5 mL) and water (1.0 mL), A reflux condenser was attached under a purge of argon, and the reaction was stirred at reflux for 20 h at which point the solution was cooled to

room temperature and diluted with PhMe, ether and 2M KOH (aq). The organic layer was worked up as described below to provide a reddish oil. Chromatography on silica (3.5:1 hexane/CH_2Cl_2) yielded the desired product as a yellow solid (85.7 mg, 0.116 mmol, 80%).

From 7: *N,N*-Dibutyl-4-iodoaniline (336 mg, 1.01 mmol) was placed in a 10 mL Schlenk flask under argon and diluted with PhMe (3 mL). To another 10 mL Schlenk flask was added **7** (148 mg, 0.442 mmol) and PhMe (3 mL). A 25 mL Schlenk flask was charged with $(Ph_3P)_2PdCl_2$ (31 mg, 0.044 mmol) and CuI (28 mg, 0.145 mmol) and was placed under argon. The *N,N*-dibutyl-4-iodoaniline solution was then transferred into the catalyst mixture followed by a PhMe rinse (1 mL) and the dropwise addition of DIPA (0.6 mL). This solution was stirred for 10 min at which point the solution of **7** was cannulated in dropwise followed by a PhMe rinse (1 mL) and a THF rinse (1 mL). The reaction was stirred at room temperature for 20 h, diluted with ether and washed with NH_4Cl and NaCl. The organic phase was dried and removed *in vacuo*. Silica gel chromatography of the crude material (4:1 hexanes/CH_2Cl_2) yielded the product as an oily yellow solid (212 mg, 0.286 mmol, 70%). Recrystallization from CH_2Cl_2/EtOH again yielded the desired product as a yellow solid (151 mg, 71% recovery). mp 123-124.5°C. ^{1}H NMR (250 MHz, $CDCl_3$) δ: 7.44 (s, 2H), 7.19 (d, 2H, J = 7.6 Hz), 7.15 (s, 2H), 7.11 (d, 2H, J = 7.6 Hz), 6.98 (d, 4H, J = 8.7 Hz), 6.46 (d, 4H, J = 8.8 Hz), 3.22 (t, 8H, J = 7.3 Hz), 2.37 (s, 6H), 2.27 (s, 6H), 1.50 (quin, 8H, J = 6.2 Hz), 1.32 (sex, 8H, J = 7.6 Hz), 0.93 (t, 12H, J = 7.2 Hz). ^{13}C NMR (125 MHz, $CDCl_3$) δ: 148.0, 142.8, 140.4, 134.6, 133.7, 132.9, 132.2, 130.9, 129.7, 128.3, 122.8, 111.3, 109.1, 95.2, 87.3, 50.9, 29.6, 21.2, 20.5, 19.8, 14.2. FT-IR (KBr): ν/cm^{-1}: 2955, 2928, 2870, 2202, 1605, 1521, 1367, 1193, 1136, 811. HR-MS (EI): found m/z = 740.5070 ± 0.0015 (M^+); calc. for $C_{54}H_{64}N_2$: 740.5070.

2',5'-Bis[4-(*N,N*-dibutylamino)phenylethynyl]-2,2",5,5"-tetramethoxy-1,1':4',1"-terphenyl (**2**)

From 4: A mixture of **4** (339.5 mg, 0.4916 mmol), 2,5-dimethoxyphenylboronic acid (534 mg, 2.93 mmol), Na_2CO_3 (858 mg, 8.09 mmol) and $Pd(PPh_3)_4$ (79.8 mg, 0.0691 mmol) was placed under argon followed by the addition of PhMe (19 mL), EtOH (4 mL) and water (4 mL), The system was opened and purged for 10 minutes to allow for attachment of a reflux condenser, and the reaction was stirred at reflux for 19 h. The reaction was worked up as for compound **1** and subsequent chromatography on silica (1:1 hexane/CH_2Cl_2) yielded 306 mg of the desired product as a reddish white solid. Recrystallization from CH_2Cl_2/MeOH yielded a pure product as a fluffy pale yellow solid (269 mg, 0.334 mmol, 68%).

From 8: Following a similar procedure as described for the conversion of **7** into **1**, *N,N*-dibutyl-4-iodo-aniline (291 mg, 0.877 mmol) in THF (3 mL) was transferred to the catalyst mixture of $(Ph_3P)_2PdCl_2$ (26 mg, 0.038 mmol) and CuI (22 mg, 0.12 mmol). A solution of **8** (149 mg, 0.375 mmol) in THF (3 mL) was then added to the reaction. The reaction was stirred at room temperature for 2 d and worked up similar to **1**. Silica gel chromatography (1:1 hexanes/CH_2Cl_2) yielded the product as a pale yellow solid

(211 mg, 0.262 mmol, 70%). Recrystallization from CH_2Cl_2/MeOH provided the desired compound as faint beige needles (141 mg, 67% recovery). mp 168-169°C. ^{1}H NMR (300 MHz, $CDCl_3$) δ: 7.57 (s, 2H), 7.05 (d, 4H, *J* = 8.7 Hz), 7.02 (d, 2H, *J* = 2.4 Hz), 6.93 (m, 4H), 6.47 (d, 4H, *J* = 9.0 Hz), 3.81 (s, 6H), 3.78 (s, 6H), 3.23 (t, 8H, *J* = 7.8 Hz), 1.53 (quin, 8H, *J* = 8.1 Hz), 1.33 (sex, 8H, *J* = 7.5 Hz), 0.94 (t, 12H, *J* = 7.2 Hz). ^{13}C NMR (125 MHz, $CDCl_3$) δ: 153.3, 151.7, 147.9, 139.3, 133.2, 132.9, 130.6, 123.0, 116.8, 114.6, 112.5, 111.3, 109.4, 94.7, 87.6, 56.7, 56.1, 50.9, 29.6, 20.5, 14.2. FT-IR (KBr): ν/cm^{-1}: 2951, 2921, 2863, 2013, 1604, 1520, 1473, 1366, 1225, 1194, 1054, 812. UV-Vis ($CHCl_3$) λ/nm (log ε): 314 (4.46), 387 (4.74), 402 (4.73). Emission ($CHCl_3$) λ_{max}/nm: 437. HR-MS (EI): found *m/z* = 804.4866 ± 0.0016 (M^+); calc. for $C_{54}H_{64}N_2O_4$: 804.4866.

1,4-Bis(trimethylsilylethynyl)-2,5-dibromobenzene (*en route* to **4**): Under an argon atmosphere, THF (125 mL) was added to **3** (6.00 g, 12.3 mmol), $(Ph_3P)_2PdCl_2$ (860.3 mg, 1.226 mmol) and CuI (745 mg, 3.91 mmol). After the addition of DIPA (15 mL), the solution was stirred at room temperature for 15 min followed by the dropwise addition of TMS acetylene (3.65 mL, 25.8 mmol). After stirring for 17 h at room temperature, an ethereal solution of the reaction mixture was worked up as **1**. The crude material was chromatographed on silica gel (hexane) to yield the desired product (4.67 g, 10.9 mmol, 89%) as a pale yellow solid that was used without further purification. ^{1}H NMR (250 MHz, $CDCl_3$) δ: 7.67 (s, 2H), 0.27 (s, 18H). ^{13}C NMR (125 MHz, $CDCl_3$) δ: 136.6, 126.6, 123.9, 103.3, 101.6, -0.1.

2,5-Dibromo-1,4-diethynylbenzene (*en route* to **4**): A solution of 1,4-bis(trimethylsilylethynyl)-2,5-dibromobenzene (4.439 g, 10.36 mmol) and K_2CO_3 (5.73 g, 41.5 mmol) in THF (65 mL) and MeOH (65 mL) was stirred at room temperature for 7 h. The reaction was worked up as for **1** to yield a light brown solid (2.734 g, 9.628 mmol, 93%) that was of limited stability and was therefore used without further purification. ^{1}H NMR (250 MHz, $CDCl_3$) δ: 7.72 (s, 2H), 3.50 (s, 2H). HR-MS (EI): found *m/z* = 281.8680 ± 0.0056 (M^+); calc. for $C_{10}H_4Br_2$: 281.8680.

1,4-Bis[4-(*N,N*-dibutylamino)phenylethynyl]-2,5-dibromobenzene (**4**): A solution of *N,N*-dibutyl-4-iodo-aniline (7.14 g, 21.6 mmol), $(Ph_3P)_2PdCl_2$ (519 mg, 0.739 mmol) and CuI (541 mg, 2.84 mmol) in THF (75 mL) and DIPA (10 mL) was stirred under argon for 20 min. To this, a solution of 2,5-dibromo-1,4-diethynylbenzene (2.77 g, 9.76 mmol) in THF (25 mL) was transferred dropwise under argon, followed by a THF rinse (25 mL). The reaction was stirred at room temperature for 17 h at which point it was worked up as for **1**. The crude material was chromatographed on silica gel (4:1 hexane/CH_2Cl_2). Recrystallization from CH_2Cl_2/MeOH yielded an orange powder (4.47 g, 6.47 mmol, 66%). mp 143-144.5°C. ^{1}H NMR (250 MHz, $CDCl_3$) δ: 7.69 (s, 2H), 7.39 (d, 4H, *J* = 8.6 Hz), 6.58 (d, 4H, *J* = 8.7 Hz),

3.29 (t, 8H, J = 7.2 Hz), 1.57 (quin, 8H, J = 6.3 Hz), 1.35 (sex, 8H, J = 7.4 Hz), 0.96 (t, 12H, J = 7.2 Hz). ^{13}C NMR (125 MHz, $CDCl_3$) δ: 148.6, 135.4, 133.4, 126.4, 123.3, 111.4, 107.9, 98.7, 85.7, 50.9, 29.6, 20.5, 14.2. FT-IR (KBr): ν/cm^{-1}: 2955, 2929, 2870, 2208, 1604, 1520, 1373, 1287, 1191, 1144, 1055, 811, 423. HR-MS (EI): found m/z = 688.2028 ± 0.0014 (M^+); calc. for $C_{38}H_{46}Br_2N_2$: 688.2028.

1,4-Bis[4-(*N,N*-dibutylamino)phenylethynyl]-2,5-diiodobenzene (**5**): To a 1L three-neck flask and THF (150 mL) under argon at -78°C was added 1.7 M *t*-butyllithium in pentane (13.6 mL, 23.1 mmol), and the solution was stirred for 5 min. A solution of **4** (1.999 g, 2.894 mmol) in THF (50 mL) under argon was transferred dropwise to the *t*-BuLi solution followed by a THF rinse (50 mL), and the reaction was stirred at -78°C for 1h at which point a solution of iodine (9.38 g, 40.0 mmol) in THF (50 mL) under argon was added rapidly. The reaction was allowed to warm to room temperature and quenched with $Na_2S_2O_3$. After dilution with ether, the organic layer was washed with NaCl (x2), dried and removed *in vacuo* to provide a red-brown solid. Following chromatography on silica (4:1 hexane/CH_2Cl_2), the isolated solids were recrystallized from CH_2Cl_2/MeOH to yield an orange powdery solid (1.447 g, 1.845 mmol, 64%). mp 150.5-151.5°C. ^{1}H NMR (250 MHz, $CDCl_3$) δ: 7.89 (s, 2H), 7.41 (d, 4H, J = 8.8 Hz), 6.58 (d, 4H, J = 8.9 Hz), 3.29 (t, 8H, J = 7.4 Hz), 1.58 (quin, 8H, J = 8.3 Hz), 1.36 (sex, 8H, J = 7.6 Hz), 0.96 (t, 12H, J = 7.2 Hz). ^{13}C NMR (125 MHz, $CDCl_3$) δ: 148.6, 140.5, 133.2, 130.8, 111.3, 107.9, 99.6, 97.8, 89.0, 50.9, 29.5, 20.5, 14.2. FT-IR (KBr): ν/cm^{-1}: 2955, 2928, 2863, 2204, 1603, 1521, 1404, 1372, 1192, 1142, 811. HR-MS (EI): found m/z = 784.1751 ± 0.0015 (M^+); calc. for $C_{38}H_{46}I_2N_2$: 784.1751.

1,4-Bis(triisopropylsilylethynyl)-2,5-dibromobenzene (**6**): Under an argon atmosphere, THF (200 mL) was added to **3** (9.88 g, 20.3 mmol), $(Ph_3P)_2PdCl_2$ (1.01 g, 1.43 mmol) and CuI (0.596 g, 3.13 mmol). After the addition of DIPA (25 mL), the solution was stirred at room temperature for 15 min followed by the dropwise addition of triisopropylsilylacetylene (10.0 mL, 44.6 mmol). After stirring for 40 h at room temperature, the reaction was worked up as described for **1**. The crude material was pushed through a silica gel plug to provide 11 g of a white solid contaminated with the starting diiodide. Recrystallization from CH_2Cl_2/hexane provided 4.75 g of a purer product, and recrystallization of the mother liquor residue from isopropanol provided an additional 3.77 g. All collected solids were chromatographed on silica (hexanes) to yield 6.62 g of the desired product as a white solid in pure form next to 0.95 g of a mixture containing an additional 0.686 g of the desired product as determined by ^{1}H NMR integration against an internal standard. In addition, 534 mg of the starting material was recovered (1.09 mmol, 5.4%). Total desired product: 7.31 g (12.3 mmol, 64% based on recovered starting material). ^{1}H NMR (250 MHz, $CDCl_3$) δ: 7.67 (s, 2H), 1.14 (s, 42H). ^{13}C NMR (125 MHz, $CDCl_3$) δ: 136.7, 126.8, 124.0, 103.4, 100.0, 18.9, 11.5. FT-IR (KBr): ν/cm^{-1}: 2924, 2864, 2164, 1460, 1342, 1064, 883, 811, 674, 585.

2',5'-Bis(triisopropylsilylethynyl)-2,2",5,5"-tetramethyl-1,1':4',1"-terphenyl (en route to **7**): A 100 Schlenk flask was charged with **6** (1.004 g, 1.683 mmol), 2,5-dimethylphenyl boronic acid (1.11 g, 7.41 mmol), KOH (1.5 g, 27 mmol) and $Pd(PPh_3)_4$ (278 mg, 0.241 mmol) and placed under argon. PhMe (19 mL), EtOH (10 mL) and water (15 mL) were added, and the system was purged for 15 min to allow for the installation of a reflux condenser. The reaction was heated at reflux for 14 h and worked up similar to **1**. The crude material was chromatographed on silica gel (hexanes) to yield the desired product as a white solid (820 mg, 1.27 mmol, 75%). ^{1}H NMR (500 MHz, $CDCl_3$) δ: 7.39 (s, 2H), 7.10 (d, 2H, J = 8.0 Hz), 7.04 (m, 4h), 2,32 (s, 3H), 2.17 (s, 3H), 0.90 (s, 42H). ^{13}C NMR (125 MHz, $CDCl_3$) δ: 143.9, 140.0, 134.9, 133.3, 130.3, 129.9, 128.5, 123.1, 105.7, 95.4, 21.1, 19.8, 18.6, 11.4. FT-IR (KBr): ν/cm^{-1}: 2941, 2863, 2157, 1482, 1460, 1188, 995, 882, 808, 677, 594, 422. HR-MS (EI): found m/z = 646.4390 ± 0.0013 (M^+); calc. for $C_{44}H_{62}Si_2$: 646.4390.

2',5'-Diethynyl-2,2",5,5"-tetramethyl-1,1':4',1"-terphenyl (**7**): 2',5'-Bis(triisopropylsilylethynyl)-2,2", 5,5"-tetramethyl-1,1':4',1"-terphenyl (301 mg, 0.465 mmol) was placed in a 50 mL round bottom flask and dissolved in THF (25 mL) and water (2 mL). The system was briefly purged with a stream of argon at which point a 1M solution of TBAF in THF (5 mL, 5 mmol) was added dropwise. The reaction was stirred at room temperature for 45 hr and the reaction was diluted with ether and washed with NaCl (x3). The organic layer was dried and removed *in vacuo* to yield a white solid (148 mg, 0.442 mmol, 95%) that was used without further purification. ^{1}H NMR (500 MHz, $CDCl_3$) δ: 7.44 (s, 2H), 7.17 (d, 2H, J = 8.0 Hz), 7.12 (d, 2H, J = 7.5 Hz), 7.07 (s, 2H), 3.01 (s, 2H), 2.36 (s, 6H), 2.20 (s, 6H).

2',5'-Bis(triisopropylsilylethynyl)-2,2",5,5"-tetramethoxy-1,1':4',1"-terphenyl (en route to **8**): A 100 Schlenk flask was charged with **6** (1.005 g, 1.684 mmol), 2,5-dimethoxyphenyl boronic acid (1.35 g, 7.40 mmol), KOH (1.4 g, 25 mmol) and 278 mg $Pd(PPh_3)_4$ (278 mg, 0.241 mmol) and placed under argon. After following the procedure for the tetramethyl derivative above (*en route* to **7**), the reaction was worked up similar to **1**. The crude material was chromatographed on silica gel (2:1 hexanes/CH_2Cl_2) to yield the desired product as a white solid (750 mg, 1.06 mmol, 63%). ^{1}H NMR (500 MHz, $CDCl_3$) δ: 7.48 (s, 2H), 8.86 (m, 6H), 3.77 (s, 6H), 3.74 (s, 6H), 0.93 (s, 42H). ^{13}C NMR (125 MHz, $CDCl_3$) δ: 153.5, 151.3, 140.5, 134.1, 130.3, 123.4, 116.9, 114.2, 112.3, 106.1, 94.8, 56.5, 56.0, 18.7, 11.4. HR-MS (EI): found m/z = 710.4187 ± 0.0014 (M^+); calc. for $C_{44}H_{62}O_4Si_2$: 710.4187.

2',5'-Diethynyl-2,2",5,5"-tetramethoxy-1,1':4',1"-terphenyl (**8**): 2',5'-Bis(triisopropylsilylethynyl)-2,2", 5,5"-tetramethoxy-1,1':4',1"-terphenyl (299.5 mg, 0.4211 mmol) was subjected to similar conditions as

for **7**. The reaction was stirred at room temperature for 5 d, and an additional 5 mL of TBAF solution (5 mmol) was added. After a total of 6 d, workup as described for **7** provided a white solid (149 mg, 0.375 mmol, 89%) that was used without further purification. ^{1}H NMR (250 MHz, $CDCl_3$) δ: 7.57 (s, 2H), 6.92 (bm, 6H), 3.80 (s, 6H), 3.78 (s, 6H), 3.03 (s, 2H). ^{13}C NMR (125 MHz, $CDCl_3$) δ: 153.4, 151.3, 140.3, 135.0, 129.4, 122.5, 117.0, 114.6, 112.5, 82.9, 80.8, 56.5, 56.0.

5,12-Bis[4-(*N,N*-dibutylamino)phenylethynyl]-1,4,8,11-tetramethyldibenz[*a,h*]anthracene (**9**): To a solution of **1** (20 mg, 0.027 mmol) in CH_2Cl_2 (3 mL) under argon was added trifluoroacetic acid (80 μL, 1 mmol), and the reaction was refluxed for 2 d, cooled and quenched with $NaHCO_3$(aq). After dilution with CH_2Cl_2, the organic layer was washed with $NaHCO_3$ and brine, dried and removed *in vacuo*. The crude solid was chromatographed on silica (1:1 hexane/CH_2Cl_2) to yield the desired product as a yellow solid (16 mg, 0.022 mmol, 82%). mp 211-213°C. ^{1}H NMR (300 MHz, CD_2Cl_2) δ: 9.09 (s, 2H), 7.72 (s, 2H), 7.44 (d, 2H, J = 7.5 Hz), 7.26 (d, 2H, J = 7.5 Hz), 7.21 (d, 4H, J = 8.4 Hz), 6.72 (d, 4H, J = 8.7 Hz), 3.34 (t, 8H, J = 7.5 Hz), 3.20 (s, 6H), 2.11 (s, 6H), 1.64 (quin, 8H, J = 7.8 Hz), 1.40 (sex, 8H, J = 8.1 Hz), 0.99 (t, 12H, J = 7.2 Hz). ^{13}C NMR (125 MHz, $CDCl_3$) δ: 147.4, 139.1, 134.4, 133.3, 132.8, 132.6, 132.3, 130.9, 130.3, 130.1, 129.98, 129.88, 129.5, 127.1, 111.5, 51.1, 29.7, 26.9, 25.4, 20.7, 14.3. FT-IR (KBr): ν/cm^{-1}: 2954, 2930, 2868, 1609, 1517, 1457, 1365, 1180, 1105, 915, 817, 784. HR-MS (EI): found m/z = 740.5070 ± 0.0015 (M^+); calc. for $C_{54}H_{64}N_2$: 740.5070.

5,12-Bis[4-(N,N-dibutylamino)phenylethynyl]-1,4,8,11-tetramethoxydibenz[*a,h*]anthracene (**10**): To a solution of **2** (49 mg, 0.061 mmol) in CH_2Cl_2 (6 mL) under argon was added trifluoroacetic acid (60 μL, 0.8 mmol), and the reaction was refluxed for 20 h. After working up as for **9**, the residual crude solid was chromatographed on silica (3:2 CH_2Cl_2/hexane) to yield the desired product as a yellow solid (44 mg, 0.055 mmol, 91%). ^{1}H NMR (250 MHz, $CDCl_3$) δ: 10.10 (s, 2H), 7.84 (s, 2H), 7.30 (d, 4H, J = 8.5 Hz), 7.19 (d, 2H, J = 8.6 Hz), 7.07 (d, 2H, J = 8.8 Hz), 6.73 (d, 4H, J = 8.4 Hz), 4.14 (s, 6H), 3.47 (s, 6H), 3.34 (t, 8H, J = 7.2 Hz), 1.62 (quin, 8H, J = 6.3 Hz), 1.40 (sex, 8H, J = 7.5 Hz), 0.99 (t, 12H, J = 7.2 Hz). ^{13}C NMR (125 MHz, $CDCl_3$) δ: 154.3, 152.0, 146.7, 136.1, 133.7, 132.9, 131.3, 129.1, 128.1, 127.9, 125.1, 122.9, 111.7, 111.1, 109.7, 57.6, 56.5, 51.3, 29.8, 20.7, 14.3. FT-IR (KBr): ν/cm^{-1}: 2928, 2868, 1612, 1518, 1428, 1371, 1254, 1186, 1115, 1068, 1033, 922, 796, 731, 415. UV-Vis ($CHCl_3$) λ/nm (log ε): 251 (4.60), 281 (4.76), 319 (4.71), 405 (4.22), 431 (4.15). Emission ($CHCl_3$) λ_{max}/nm: 437, 468. HR-MS (EI): found m/z = 804.4866 ± 0.0016 (M^+); calc. for $C_{54}H_{64}N_2O_4$: 804.4866.

Polymer **11**: A 25 mL Schlenk tube was charged with **5** (78.6 mg, 0.100 mmol), 2,5-didecyloxybenzene-1,4-diboronic acid (49.1 mg, 0.103 mmol), and Na_2CO_3 (214 mg, 2.02 mmol) and placed under argon.

$Pd(PPh_3)_4$ (*ca.* 0.4 mg, $4x10^{-4}$ mmol) was transferred under an inert atmosphere, sealed in a glovebox and brought to the bench where tube was placed under argon. PhMe (1 mL), EtOH (1 mL) and water (1 mL) were added, and a cold-finger was attached under a 10 min argon purge. The system was heated at reflux for 3 days. After cooling to room temperature, the reaction was precipitated into MeOH, filtered and washed to provide the polymer as a fibrous brown solid. M_n = 14,700.

2,5-Bis[4-(*N,N*-dibutylamino)phenylethynyl]-1,4-di(2-thienyl)benzene (**12**): A 50 mL Schlenk flask was charged with **4** (1.000 g, 1.448 mmol) and $(Ph_3P)_2PdCl_2$ (50.1 mg, 0.0714 mmol) and placed under argon. DMF was added (15 mL) and heated to 80°C. Upon complete dissolution of the solids, 2-(tributylstannyl)thiophene was added dropwise (1.13 mL, 3.56 mmol), and the reaction stirred at 80°C for 68 h. Upon cooling, the mixture was pushed through a pad of celite. The organic eluent was diluted with ether, washed with NaCl (x3), dried and removed *in vacuo*. The crude material was pushed through a silica plug (hexane to 1:1 hexane/CH_2Cl_2) to provide a brown material subjected to further chromatography on silica (hexane to 2:1 hexane/CH_2Cl_2). Removal of the solvents provided the desired product as a bright yellow solid (753 mg, 1.08 mmol, 75%). mp 157.5-158.5°C. ^{1}H NMR (500 MHz, $CDCl_3$) δ: 7.82 (s, 2H), 7.74 (d, 2H, *J* = 2.5 Hz), 7.37 (d, 4H, *J* = 8.5 Hz), 7.14 (dd, 2H, *J* = 4.5, 4.5 Hz), 6.59 (d, 4H, *J* = 8.5 Hz), 3.29 (t, 8H, *J* = 7.0 Hz), 1.58 (m, 8H), 1.36 (sex, 8H, *J* = 8.0 Hz), 0.97 (t, 12H, *J* = 7.5 Hz). ^{13}C NMR (125 MHz, $CDCl_3$) δ: 148.3, 141.7, 133.8, 133.3, 133.0, 127.3, 127.0, 126.0, 120.8, 111.4, 108.8, 97.3, 87.5, 50.9, 29.6, 20.5, 14.2. FT-IR (KBr): ν/cm^{-1}: 2953, 2927, 2868, 2198, 1604, 1520, 1367, 1192, 1135, 810. UV-Vis ($CHCl_3$) λ/nm (log ε): 289 (4.54), 334 (4.68), 417 (4.73). HR-MS (EI): found *m/z* = 696.3572 ± 0.0014 (M^+); calc. for $C_{46}H_{52}N_2S_2$: 696.3572.

4,10-Bis[4-(*N,N*-dibutylamino)phenyl]anthra[1,2-*b*:5,6-*b'*]dithiophene (**13**): A 200 mL Schlenk flask was charged with **12** (205 mg, 0.294 mmol) and placed under argon. CH_2Cl_2 (100 mL) was added and stirred vigorously as TfOH was added dropwise (0.52 mL, 5.9 mmol). After 2 h, the reaction was quenched with $NaHCO_3$ and the organic phase was washed with $NaHCO_3$ (x2) and NaCl, dried and removed. The crude material was purified on silica gel (3:1 hexane/CH_2Cl_2) to provide the desired product as a deep burgundy-red solid (105 mg, 0.151 mmol, 51%). mp 208-209°C. ^{1}H NMR (500 MHz, $CDCl_3$) δ: 7.76 (s, 2H), 7.59 (d, 4H, *J* = 8.5 Hz), 7.48 (s, 2H), 7.46 (d, 2H, *J* = 5.0 Hz), 7.14 (d, 2H, *J* = 5.0 Hz), 6.70 (d, 4H, *J* = 9.0 Hz), 3.35 (t, 8H, *J* = 7.0 Hz), 1.64 (m, 8H), 1.40 (m, 8H), 0.99 (t, 12H, *J* = 7.5 Hz). ^{13}C NMR (125 MHz, $CDCl_3$) δ: 148.5, 145.6, 142.1, 141.9, 132.7, 131.8, 129.3, 127.0, 125.1, 123.5, 123.3, 111.2, 110.6, 51.0, 29.7, 20.6, 14.3. FT-IR (KBr): ν/cm^{-1}: 2954, 2858, 1594, 1520, 1367, 1186, 1140. UV-Vis ($CHCl_3$) λ/nm (log ε): 287 (4.46), 314 (4.53), 361 (4.55), 470 (4.74). HR-MS (EI): found *m/z* = 696.3561

± 0.0020 (M^+); calc. for $C_{46}H_{52}N_2S_2$: 696.3572. Anal: calc. for $C_{46}H_{52}N_2S_2$: C, 79.26; H, 7.52; N, 4.02. Found: C, 78.98; H, 7.74; N, 3.89.

Benzo[2,1-*b*:3,4-*b'*]dithiophene (**14**):[29] A 50 mL Schlenk flask was charged with **16** (251 mg, 1.13 mmol), placed under argon and dissolved in THF (25 mL). To a rigorously dried 250 mL 3-necked flask equipped with a reflux condenser was added zinc powder (946 mg, 14.5 mmol), and the system was placed under reduced pressure and heated (*via* Bunsen burner) to ensure removal of any residual water. The system was placed under argon, and THF (50 mL) was added. To the stirred slurry of zinc was added a solution of 1.0 M $TiCl_4$ in CH_2Cl_2 (7.2 mL, 7.2 mmol) DIRECTLY into the slurry and the reaction was stirred at reflux for 1.5 h. The solution of **16** was then added dropwise over a period of 4 h and stirred further at reflux for 1.5 h. After cooling to room temperature, the reaction mixture was pushed through a silica gel plug (1:1 hexane/CH_2Cl_2) followed by removal of the solvents to provide a greenish sludge. Chromatography on silica (hexanes) provided the desired product (142 mg, 0.744 mmol, 66%) in pure form as a clear oil which solidified at 0°C into a pasty white solid. ^{1}H NMR (250 MHz, $CDCl_3$) δ: 7.76 (s, 2H), 7.42 (d, 2H, J = 5.4 Hz), 7.38 (d, 2H, J = 5.4 Hz). ^{13}C NMR (125 MHz, $CDCl_3$) δ: 137.3, 133.8, 125.0, 124.4, 120.6. HR-MS (EI): found m/z = 189.9911 ± 0.0004 (M^+); calc. for $C_{10}H_6S_2$: 189.9911.

3,3'-Dibromo-2,2'-bithiophene (*en route* to **16**):[34] A dry 1L three-neck flask was charged with **15** (19.29 g, 40.03 mmol) and placed under argon followed by the addition of THF (500 mL). The solution was stirred at -78°C and 1.413 M *n*-BuLi in hexanes (58 mL, 82 mmol) was added dropwise *via* addition funnel. After addition, the reaction was stirred at -78°C for 3 min, quenched with 8 mL glacial AcOH and warmed to room temperature. The reaction mixture was diluted with ether and washed with $NaHCO_3$ (x2), NH_4Cl and NaCl. The organic layer was dried and removed *in vacuo* to provide a yellowish oil with suspended white solids. Chromatrography on silica (hexanes) followed by recrystallization from MeOH provided the desired product (9.065 g, 27.97 mmol, 70%) as a white crystalline solid. mp 92.5-95°C. ^{1}H NMR (250 MHz, $CDCl_3$) δ: 7.39 (d, 2H, J = 5.4 Hz), 7.07 (d, 2H, J = 5.4 Hz). ^{13}C NMR (125 MHz, $CDCl_3$) δ: 131.0, 129.1, 127.7, 112.9. FT-IR (KBr): ν/cm^{-1}: 3111, 1082, 1551, 1486, 1443, 1340, 1076, 858, 719, 705, 596. HR-MS (EI): found m/z = 321.8121 ± 0.0006 (M^+); calc. for $C_8H_4Br_2S_2$: 321.8121.

2,2'-Bithiophene-3,3'-dicarbaldehyde (**16**):[31b] THF (200 mL) was added under argon to a 500 mL Schlenk flask, and the system was cooled to -78°C. Additionally, a 100 mL flask was charged with 3,3'-dibromo-2,2'-bithiophene (1.000 g 3.085 mmol), placed under argon and filled with 100 mL THF. To the cooled 500 mL flask was added 1.7 M *t*-BuLi in pentane (15 mL, 26 mmol), and the solution was stirred for 5 min followed by the slow addition of the bithiophene solution. The reaction was stirred for 5 min,

quenched with DMF (2.5 mL) and stirred at -78°C for an additional 3 h. The reaction mixture was warmed to room temperature, diluted with $CHCl_3$ and worked up as **1** to provide a yellowish solid. Recrystallization from PhMe yielded the product (419 mg, 1.89 mmol, 61%) as a light brown solid. ^1H NMR (250 MHz, $CDCl_3$) δ: 9.86 (s, 2H), 7.65 (d, 2H, *J* = 5.4 Hz), 7.49 (d, 2H, *J* = 5.4 Hz). ^{13}C NMR (125 MHz, $CDCl_3$) δ: 184.4, 141.4, 140.7, 128.5, 127.5. FT-IR (KBr): ν/cm^{-1}: 3112, 3087, 2839, 2795, 2737, 1662, 1500, 1382, 1359, 1223, 825, 744, 725. HR-MS (EI): found *m/z* = 221.9809 ± 0.0004 (M^+); calc. for $C_{10}H_6O_2S_2$: 221.9809.

2,5-Bis(4-hexyloxyphenylethynyl)-1,4-di(benzo[2,1-*b*:3,4-*b'*]dithiophen-2-yl)benzene (**18**): A dry 10 mL Schlenk flask was charged with **17** (35 mg, 0.055 mmol) and $Pd(PPh_3)_4$ (5 mg, 0.004 mmol) and placed under Ar, and the solids were dissolved in THF (1 mL). A second dry 10 mL Schlenk flask was charged with **14** (31 mg, 0.16 mmol) and placed under Ar, and the material was dissolved in THF (1 mL). To the solution of **14**, a 1.54 M solution of *n*-BuLi in hexanes (0.25 mL, 0.38 mmol) was added dropwise at room temperature and stirred for 30 min followed by the dropwise addition of a 0.5 M solution of $ZnCl_2$ in THF (0.4 mL, 0.2 mmol). After stirring for 5 min, this reaction mixture was cannulated to the solution of **17** in THF followed by two THF rinses (0.5 mL). The entire reaction stirred for 40 h and then heated at reflux for 7 h. The reaction was quenched with MeOH and diluted with ether. The organics were washed twice with NH_4Cl, once with NaCl, dried and removed. Purification on silica gel (7:1 hexane/CH_2Cl_2) provided the desired product (7 mg, 0.008 mmol, 15%) alongside the mono addition product (16 mg, 0.021 mmol, 38%) and recovered **17** (11 mg, 0.017 mmol) and recovered **14** (17 mg, 0.089 mmol). Correcting for these recoveries, the desired product was obtained in 21% yield. ^1H NMR (300 MHz, $CDCl_3$) δ: 8.17 (s, 2H), 8.05 (d, 1H, *J* = 0.6 Hz), 7.95 (d, 1H, *J* = 0.6 Hz), 7.79 (d, 4H, *J* = 1.2 Hz), 7.50 (d, 4H, *J* = 8.7 Hz), 7.45 (d, 4H, *J* = 0.6 Hz), 6.89 (d, 4H, *J* = 9.0 Hz), 3.98 (t, 4H, *J* = 6.6 Hz), 1.80 (m, 4H), 1.65 (m, 4H), 1.36 (m, 8H), 0.89 (m, 6H). ^{13}C NMR (125 MHz, $CDCl_3$) δ: 159.8, 139.8, 138.7, 137.7, 134.9, 134.2, 133.33, 133.18, 131.1, 129.9, 129.0, 125.18, 125.14, 124.9, 120.97, 120.81, 115.09, 114.92, 96.2, 87.7, 68.3, 31.8, 29.4, 25.9, 22.8, 14.3.

1,5-Bis(trimethylsilylethynyl)-2,4-dibromobenzene (*en route* to **19**): A 250 Schlenk flask was charged with **21** (5.007 g, 10.27 mmol), $(Ph_3P)_2PdCl_2$ (575 mg, 0.820 mmol) and CuI (582 mg, 3.06 mmol) and placed under argon. THF (75 mL) and DIPA (25 mL) were transferred to the flask and stirred for 20 min at which point trimethylsilylacetylene was added dropwise (3.10 mL, 21.94 mmol) over a 3 h period *via* syringe. The reaction was stirred at room temperature for 20 h, and the reaction mixture was poured through a silica gel plug and eluted with CH_2Cl_2. Solvent removal *in vacuo* provided a brownish oil which was further purified by silica gel chromatography (hexane) to provide the desired product as a

yellow oil (3.303 g, 7.712 mmol, 75%). ^{1}H NMR (300 MHz, $CDCl_3$) δ: 7.80 (s, 1H), 7.59 (s, 1H), 0.26 (s, 18H). ^{13}C NMR (75 MHz, $CDCl_3$) δ: 137.6, 135.7, 125.8, 124.6, 101.6, 101.4, 0.0. FT-IR (neat): ν/cm^{-1}: 3082, 2965, 2892, 2164, 1449, 1333, 1172, 1056, 837 (vb), 764. HR-MS (EI): Found *m/z* = 425.9474 ± 0.0012 (M^+); calc. for $C_{16}H_{20}Br_2Si_2$: 425.9470.

2,4-Bis(trimethylsilylethynyl)-1,5-di(2-thienyl)-benzene (*en route* to **19**): A 25 mL Schlenk tube was charged with 1,5-bis(trimethylsilylethynyl)-2,4-dibromobenzene (1.00 g, 2.33 mmol) and $(Ph_3P)_2PdCl_2$ (65 mg, 0.093 mmol) and placed under argon. DMF (5 mL) was added to the tube and heated to 80°C. Upon complete dissolution of all solids, 2-(tributylstannyl)thiophene (1.95 mL, 5.83 mmol) was added dropwise. The reaction stirred for 52 h, cooled to room temperature, and an ethereal solution of the reaction mixture was washed with NH_4Cl (x5) and pushed through two silica gel plugs. The crude material was precipitated from MeOH, filtered and washed to provide the desired product as a white powder (591 mg, 1.36 mmol, 58%). mp 111-112°C. ^{1}H NMR (300 MHz, $CDCl_3$) δ: 7.75 (m, 4H), 7.38 (d, 2H, *J* = 4.8 Hz), 7.10 (t, 2H, *J* = 3.9 Hz), 0.25 (s, 18H). ^{13}C NMR (75 MHz, CD_2Cl_2) δ: 141.2, 140.4, 136.5, 129.2, 128.1, 127.8, 127.1, 119.3, 103.9, 101.4, -0.1. FT-IR (KBr): ν/cm^{-1}: 3096, 2957, 2892, 2152, 1485, 1249, 1136, 850 (vb), 704, 642. HR-MS (EI): Found *m/z* = 434.1024 ± 0.0012 (M^+); calc. for $C_{24}H_{26}S_2Si_2$: 434.1015.

2,4-Diethynyl-1,5-di(2-thienyl)benzene (**19**): A 25 mL round bottom flask was charged with 2,4-bis(trimethylsilylethynyl)-1,5-di(2-thienyl)benzene (204 mg, 0.468 mmol) and K_2CO_3 (516 mg, 3.73 mmol) and purged with argon. A degassed mixture of THF (2.5 mL), MeOH (2.5 mL) and H_2O (1.0 mL) were added to the flask and stirred for 4 h at room temperature. An ethereal solution of the crude reaction mixture was washed with NaCl (x3), dried and removed *in vacuo* to provide 138 mg of the desired product in impure form as a brownish solid which further darkened under argon and was used without further purification. ^{1}H NMR (300 MHz, $CDCl_3$) δ: 7.83 (s, 1H), 7.70 (m, 3H), 7.40 (d, 2H, *J* = 4.2 Hz), 7.13 (m, 2H), 3.33 (s, 2H). ^{13}C NMR (75 MHz, $CDCl_3$) δ: 140.8, 140.7, 136.9, 129.7, 127.86, 127.74, 126.8, 118.4, 83.1, 82.3. HR-MS (EI): Found *m/z* = 290.0228 ± 0.0008 (M^+); calc. for $C_{18}H_{10}S_2$: 290.0224.

3,6-Bis(trimethylsilylethynyl)-4,5-dibromo-*o*-xylene (*en route* to **20**): Subjecting **22** (5.290 g, 10.26 mmol), to similar Sonogashira conditions as described for **21** above (*en route* to **19**) in THF (40 mL), PhMe (40 mL) and DIPA (25 mL) followed by similar workup and silica gel chromatography (hexane) provided a yellow solid. Recrystallization from $CHCl_3$/MeOH provided the desired product as white needle-like solids (3.655 g, 8.008 mmol, 78%). mp 168.5-169°C. ^{1}H NMR (300 MHz, $CDCl_3$) δ: 2.42 (s, 6H), 0.29 (s, 18H). ^{13}C NMR (75 MHz, $CDCl_3$) δ: 139.6, 126.6, 125.8, 105.7, 103.1, 19.5, 0.1. FT-IR

(KBr): ν/cm^{-1}: 2955, 2158, 1376, 1250, 1081, 159, 759, 634. HR-MS (EI): Found *m/z* = 453.9794 ± 0.0013 (M^+); calc. for $C_{18}H_{24}Br_2Si_2$: 453.9783.

3,6-Bis(trimethylsilylethynyl)-4,5-di(2-thienyl)-*o*-xylene (*en route* to **20**): 3,6-Bis(trimethylsilylethynyl)-4,5-dibromo-*o*-xylene (1.001 g, 2.193 mmol) was subjected to similar Stille conditions as described above en route to **19**. The reaction stirred for 3d and was then cooled to room temperature and pushed through a silica gel plug to give an oily yellow solid. Recrystallization from $CHCl_3$/MeOH provided the desired product as a yellow crystalline solid (843 mg, 1.82 mmol, 83%). mp 160-161°C. ^{1}H NMR (300 MHz, $CDCl_3$) δ: 7.19 (m, 2H), 6.85 (m, 4H), 2.49 (s, 6H), 0.06 (s, 18H). ^{13}C NMR (75 MHz, $CDCl_3$) δ: 140.4, 139.2, 136.1, 128.8, 125.9, 125.9, 124.7, 104.5, 103.1, 19.0, -0.1. FT-IR (KBr): ν/cm^{-1}: 3096, 2957, 2896, 2149, 1391, 1248, 1220, 1083, 847, 704, 640. HR-MS (EI): Found *m/z* = 462.1319 ± 0.0013 (M^+); calc. for $C_{26}H_{30}S_2Si_2$: 462.1328.

3,6-Diethynyl-4,5-di(2-thienyl)-*o*-xylene (**20**): 3,6-Bis(trimethylsilylethynyl)-4,5-di(2-thienyl)-*o*-xylene (303 mg, 0.655 mmol) was subjected to similar deprotection conditions as described for **19** for 20 h at room temperature. Workup as described for **19** provided 206 mg of the desired product in impure form. A portion of this material was further purified on silica to the desired product as a white powder that slowly decomposed (in solution and as a solid) and was used without further purification. ^{1}H NMR (300 MHz, $CDCl_3$) δ: 7.23 (d, 2H, *J* = 3.9 Hz), 6.89 (m, 4H), 3.31 (s, 2H), 2.54 (s, 6H). ^{13}C NMR (75 MHz, $CDCl_3$) δ: 140.0, 136.1, 128.9, 126.2, 126.1, 124.0, 86.7, 81.6, 19.0. HR-MS (EI): Found *m/z* = 318.0531 ± 0.0009 (M^+); calc. for $C_{20}H_{14}S_2$: 318.0537.

Anthra[1,2-*b*:8,7-*b'*]dithiophene (**23**): A 10 mL Schlenk flask was charged with **19** (101 mg, 0.348 mmol), (η^6-C_6H_6)$RuCl_2PPh_3$ (26 mg, 0.051 mmol) and NH_4PF_6 (12 mg, 0.074 mmol) and dissolved in CH_2Cl_2 (5 mL). Under an Ar purge, a reflux condenser was equipped. The system was heated to reflux over a period of 6 days. Twice during the reaction, TLC monitoring indicated incomplete reaction, so additional catalyst was added (*ca.* 25 mg each time). The crude reaction was pushed through a plug of silica gel and then purified on silica (hexane) to provide the product as a yellow solid (21 mg, 0.073 mmol, 21%). ^{1}H NMR (500 MHz, $CDCl_3$) δ: 8.89 (s, 1H), 8.53 (s, 1H), 7.87 (d, 2H, *J* = 9.0 Hz), 7.81 (d, 2H, *J* = 9.0 Hz), 7.59 (d, 2H, *J* = 5.0 Hz), 7.50 (d, 2H, *J* = 5.0 Hz). ^{13}C NMR (125 MHz, $CDCl_3$) δ: 137.5, 137.0, 129.5, 128.9, 128.1, 125.88, 125.77, 125.51, 122.1, 117.0. HR-MS (EI): found *m/z* = 290.0228 ± 0.0008 (M^+); calc. for $C_{18}H_{10}S_2$: 290.0224.

References

(1) For reviews of this area, see: (a) Wuckel, L. *Mater. Sci. Forum* **1989**, *42*, 121-130; (b) Yu, L.; Chen, M.; Dalton, L. R. *Chem. Mater.* **1990**, *2*, 649-659; (c) Scherf. U.; Müllen, K. *Adv. Poly. Sci.* **1995**, *123*, 1-40; (d) Scherf. U. *J. Mater. Chem.* **1999**, *9*, 1853-1864.

(2) Chiang, C. K.; Fincher, C. R.; Park, Y. W.; Heeger, A. J.; Shirakawa, H.; Louis, E. J.; Gau, S. C.; MacDiarmid, A. G. *Phys. Rev. Lett.* **1977**, *39*, 1098-1101.

(3) Patil, A. O.; Heeger, A. J.; Wudl, F. *Chem. Rev.* **1988**, *88*, 183-200.

(4) Brédas, J. L. *J. Chem. Phys.* **1985**, *82,* 3808-3811.

(5) Roncali, J. *Chem. Rev.* **1997**, *97*, 173-205.

(6) Kivelson, S.; Chapman, O. L. *Phys. Rev. B* **1983**, *28*, 7236-7243.

(7) (a) Schlüter, A.-D. *Adv. Mater.* **1991**, *3*, 282-291; (b) Schlüter, A.-D.; Löffler, M.; Enkelmann, V. *Nature* **1994**, *368*, 831-834.

(8) Scherf, U.; Müllen, K. *Makromol. Chem., Rapid Commun.* **1991**, *12*, 489-497.

(9) (a) Grem, G.; Leising, G. *Synth. Met.* **1993**, *55-57*, 4105-4110; (b) Graupner, W.; Leising, G.; Lanzani, G.; Nisoli, M.; De Silvestri, S.; Scherf, U. *Phys. Rev. Lett.* **1996**, *76*, 847-850.

(10) Chmil, K.; Scherf. U. *Makromol. Chem., Rapid Commun.* **1993**, *14*, 217-222.

(11) Zhang, Q. T.; Tour, J. M. *J. Am. Chem. Soc.* **1997**, *119*, 9624-9631.

(12) Tsuda, A.; Osuka, A. *Science* **2001**, *293*, 79-82.

(13) For reviews on polymer helicity in general, see: (a) Laarhoven, W. H.; Prinsen, W. J. C. *Top. Curr. Chem.* **1984**, *125*, 63-131; (b) Meurer, K. P.; Vögtle, F. *Top. Curr. Chem.* **1985**, *127*, 1-76.

(14) Dai, Y.; Katz, T. J.; Nichols, D. A. *Angew. Chem. Int. Ed. Engl.* **1996**, *35*, 2109-2111.

(15) Rajca, A.; Wang, H.; Pink, M.; Rajca, S. *Angew. Chem. Int. Ed.* **2000**, *39*, 4481-4483.

(16) Tanaka, K.; Suzuki, H.; Osuga, H. *J. Org. Chem.* **1997**, *62*, 4465-4470.

(17) Nelson, J. C.; Saven, J. G.; Moore, J. S.; Wolynes, P. G. *Science* **1997**, *277*, 1793-1796.

(18) Katz, H. E.; Bao, Z.; Gilat, S. L. *Acc. Chem. Res.* **2001**, *34*, 359-369.

(19) Bowles, D. M.; Anthony, J. E. *Org. Lett.* **2000**, *2*, 85-87.

(20) (a) Dötz, F.; Brand, J. D.; Ito, S.; Gherghel, L.; Müllen, K. *J. Am. Chem. Soc.* **2000**, *122*, 7707-7717; (b) van de Craats. A. M.; Warman, J. M.; Müllen, K.; Geerts, Y.; Brand, J. D. *Adv. Mater.* **1998**, *10*, 36-38.

(21) Mallory, F. B.; Butler, K. E.; Bérubé, A.; Luzik, E. D.; Mallory, C. W.; Brondyke, E. J.; Hiremath, R.; Ngo, P.; Carroll, P. J. *Tetrahedron* **2001**, *57*, 3715-3724.

(22) (a) Goldfinger, M. B.; Swager, T. M. *J. Am. Chem. Soc.* **1994**, *116*, 7895-7896; (b) Goldfinger, M. B.; Crawford, K. B.; Swager, T. M. *J. Am. Chem. Soc.* **1997**, *119*, 4578-4593; (c) Goldfinger, M. B.; Crawford, K. B.; Swager, T. M. *J. Org. Chem.* **1998**, *63*, 1668-1675.

(23) Sonogashira, K.; Tohda, Y.; Hagihara, N. *Tetrahedron Lett.* **1975**, 4467-4470.

(24) Miyaura, N.; Yanagi, T.; Suzuki, A. *Synth. Commun.* **1981**, *11*, 513-519.

(25) Hart, H.; Harada, K.; Du, C.-J. F. *J. Org. Chem.* **1985**, *50*, 3104-3110.

(26) Hassner, A.; Birnbaum, D.; Loew, L. M. *J. Org. Chem.* **1984**, *49*, 2546-2551.

(27) Milstein, D.; Stille, J. K. *J. Am. Chem. Soc.* **1979**, *101*, 4992-4998.

(28) Tovar, J. D.; Swager, T. M. *Adv. Mater.* **2001**, *13*, 1775-1780.

(29) (a) Rao, D. S.; Tilak, B. D. *J. Sci. Ind. Res.* **1958**, *17B*, 260-266; (b) Gronowitz, S.; Dahlgren, T. *Chem. Scr.* **1977**, *12*, 57-67.

(30) Negishi, E.; King, A. O.; Okukado, N. *J. Org. Chem.* **1977**, *42*, 1821-1823.

(31) (a) McMurry, J. E.; Kees, K. L. *J. Org. Chem.* **1977**, *42*, 2655-2656; (b) Yoshida, S.; Fujii, M.; Aso, Y.; Otsubo, T.; Ogura, F. *J. Org. Chem.* **1994**, *59*, 3077-3081.

(32) Maeyama, K.; Iwasawa, N. *J. Org. Chem.* **1999**, *64*, 1344-1346.

(33) (a) Merlic, C. A.; Pauly, M. E. *J. Am. Chem. Soc.* **1996**, *118*, 11319-11320; (b) Bennett, M. A.; Smith, A. K. *J. Chem. Soc., Dalton Trans.* **1974**, 233-241.

(34) Gronowitz, S. *Acta Chem. Scand.* **1961**, *15*, 1393-1395.

Chapter 2

New routes to electron-deficient aromatics: Isobenzopyrylium salts and isoquinolines *via* electrophilic cyclization

Adapted in part from:
Tovar, J. D.; Swager, T. M. *J. Org. Chem.* **1999**, *64*, 6499-6504;
Tovar, J. D.; Swager, T. M. *J. Organomet. Chem.* **2002**, *in press.*

Introduction

Pyrylium salts have found uses in many areas of pharmaceutical and materials chemistry as versatile synthetic intermediates for complex heterocyclic skeletons and for their intriguing physical properties.[1] Their uses range from photosensitizers for photographic applications and fluorescent laser dyes to versatile synthons for numerous heterocyclic ring systems. Furthermore, the unusual charged oxygen component within the ring has provoked several theoretical and experimental studies aimed at examining the aromaticity of these systems. The pyrylium salts and the associated acid-base equilibria existing under physiological conditions provide an array of intensely colored dyes often found in nature (Scheme 1).[2] The anthocyanins and the flavilium salts undergo a cascade of ring openings and closings, where each new molecular state corresponds to a detectable photochromic change. Of course, Man too has attempted to synthetically emulate these colors. Aside from applications as food dyestuffs, photochromic multi-state switching schemes have taken advantage of these solution equilibria. Scheme 1 juxtaposes natural anthocyanins with classic syntheses of pyrylium and isobenzopyrylium salts. Stetter and Reischl demonstrated that *Z*-1,5-diphenyl-2-penten-4-ynone underwent cyclization to the pyrylium perchlorate upon exposure to perchloric acid.[4] Blount and Robinson synthesized and studied the related isobenzopyrylium salt.[5]

Scheme 1

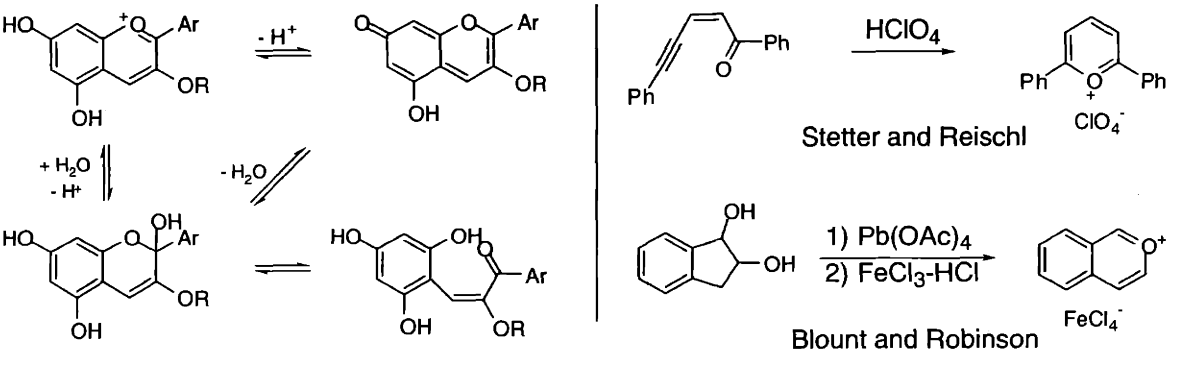

Baeyer first demonstrated the synthetic utility of these charged heterocycles by converting them to the corresponding aza-derivatives (*e.g.* pyrylium to pyridine) through treatment with ammonia gas.[6] Blount and Robinson showed that the isobenzopyrylium readily incorporated nitrogen within the ring in a similar fashion to provide isoquinoline.[5] In addition, several textbook strategies exist for more traditional construction of the isoquinoline ring system.[7] Scheme 2 depicts representative examples of these route (bottom). These reactions typically proceed by way of an electrophilic attack of the adjacent arene onto an electron-deficient moiety appended to the ring, such as the imine generated *in situ* during a Pictet-Spengler cyclization. Other syntheses utilize Bischler-Napieralski cyclization to construct the isoquinoid ring system, but the use of this procedure for constructing 3-arylisoquinoline ring systems (where R = phenyl, *etc.*) gives rise to competitive stilbenic side products after formal nitrile elimination as depicted in Scheme 2.[8]

Scheme 2

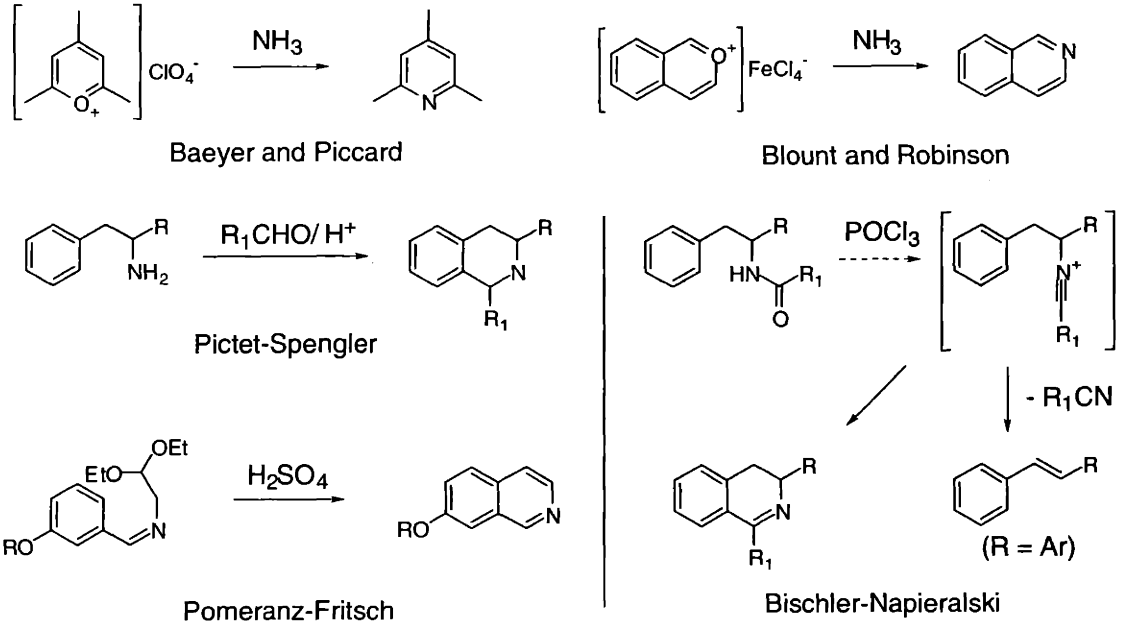

Although a rather specific sub-category of the isoquinoline family, the 3-aryl systems have attracted synthetic interest to circumvent this undesired elimination. Scheme 3 depicts

several representative routes to a common target, 3-phenyl isoquinoline. For example, Olofson anionically opened benzocyclobuten-2-ol to an *o*-tolualdehyde anion that then attacked and cyclized with benzonitrile.[9] Schiess employed a related benzocyclobutene ring opening of the analogous acyloxy system under flash vacuum pyrolysis.[10] Exposure of the resulting ring-opened formyl benzyl ketone to ammonium hydroxide furnished the isoquinoline. Scheme 3 also depicts two routes from related ortho-substituted arenes. Following Pd-catalyzed Sonogashira alkyne coupling onto an iodoimine, Larock used the catalytic CuI present in the reaction mixture to subsequently mediate an intramolecular cyclization of the iminoalkyne.[11] Using this strategy, they reported an improved total synthesis of the small isoquinoline natural product decumbenine B.[11b] Sakamoto *et al.* reported a similar alkyne cyclization where a *o*-alkynylated carboxaldehyde cyclized into the isoquinoline after exposure to ammonia gas, presumably by way of an aldimine intermediate.[12]

Scheme 3

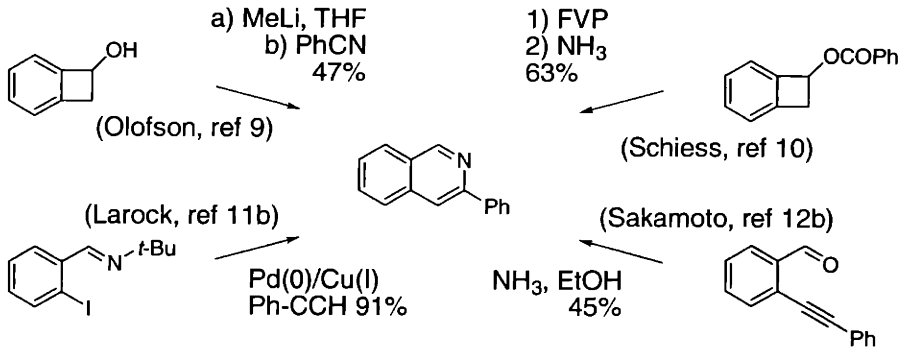

With a variety of established methods available for constructing aza-aromatics, materials scientists have used these electron-deficient materials for electronic applications involving electron transport (Scheme 4). Initial work synthesized and studied these materials as rigid-rod poly(imide) analogues with even more robust thermal properties. In fact, Arnold and Van Deusen's synthesis of the BBL ladder polymer closely paralleled that used in the preparation of conventional poly(imide)s (Scheme 4, top).[13] Other studies have investigated the electrical conductivity and the n-type (electron) semiconducting properties of nitrogen heterocycle-based polymers. Their higher electron affinities allow for efficient electron injection in organic polymer light-emitting diodes thus motivating the design of new and more robust n-type polymers. Stille has studied poly(quinoline)s derived from self-condensation polymerizations of benzophenones in Freidlander-type quinoline ring constructions.[14] These polymers displayed modest levels of conductivity after treatment with sodium metal. Hay has studied the synthesis of the related poly(isoquinoline)s by condensing aromatic poly(ketone)s with benzylamine, and these materials had high thermal and mechanical strength.[15] Other groups have synthesized electron-deficient monomers for chemical co-polymerization, such as Masuda's highly soluble phenazines or Wudl's benzo[*c*]thiophene incorporating a fused dicarboxylic imide (Scheme 4, bottom).[16,17] Recent work in Jenekhe's group has also targeted the poly(quinoline) systems due to their high electron affinity and n-type transport characteristics. They have demonstrated tuneable emission from a variety of structurally distinct quinoline-based co-polymers while maintaining high electron affinities.[18] Another possibility for such materials lies in the field of organic transistors. The very few reports of n-type behavior in organic materials reflect the rapid environmental decomposition of the organic substrate after electron injection.[19] In fact, Jenekhe very recently demonstrated the first polymer n-type material with the BBL ladder polymer under

ambient conditions.[18b] While most organic aromatics can allow for high *hole* mobilities, organic transistor schemes will require materials capable of supporting high *electron* mobilities as well. This n-type polymer stands to further develop more readily accessable ambipolar organic-based circuits.

Scheme 4

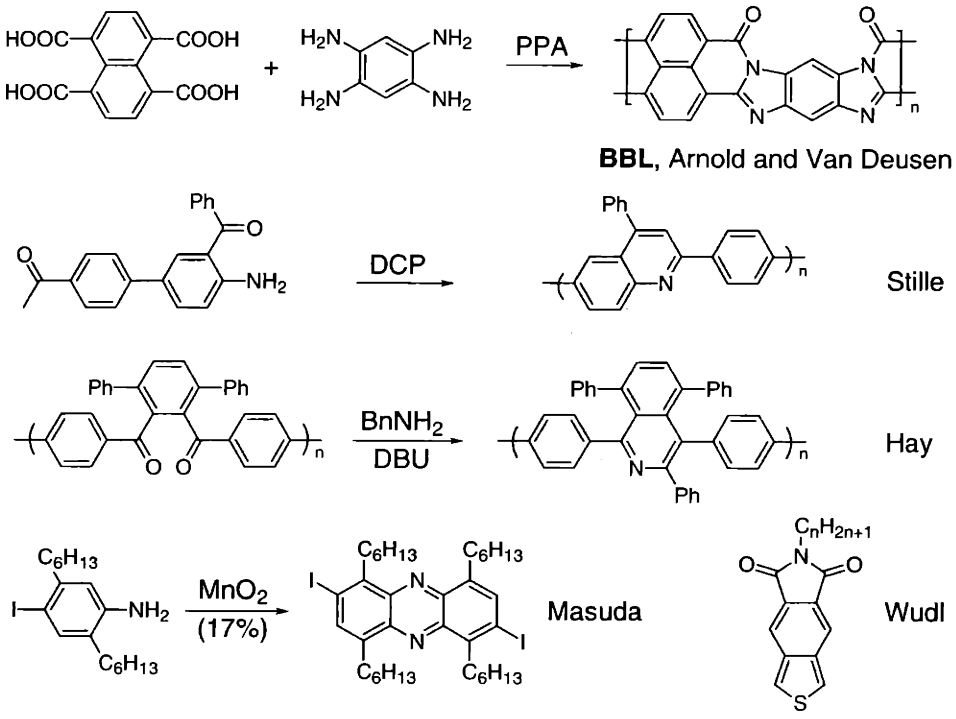

In conjunction with earlier work in our laboratories led by Marc Goldfinger, Chapter 1 explored acid-catalyzed electrophilic cyclizations of aryl acetylenes to provide conjugated and fully aromatized materials.[20] Our group has utilized Sonogashira polymerizations to obtain very high molecular weight arylene-ethynylene polymers for molecular wire applications.[21,22] However, post-polymerization strategies that use the alkyne moieties rationally in further chemistries remain sparse, if not non-existent.[23] Our continued interest in highly unsaturated ladder polymers and related materials has led us to consider the use of a carbonyl group in lieu of a proximal arene moiety as a way of harnessing these arylene-ethynylene polymers for further chemistry. Accordingly, electrophilic attack by the β-carbon of alkyne **1** results in carbocation formation at the α–carbon, thereby leading to ring closure of intermediate **A** *via* lone pair attack (Scheme 5). In Chapter 1, a proximal arene attacked this vinyl cation moiety in the key cyclization event. In this chapter, we present the scope of a novel acid-induced cyclization of *ortho*-alkynylated aromatic carbonyl functionalities (**1**) into the isobenzopyrylium salts depicted by **2**. In addition, this chapter describes efficient preparations of the corresponding 3-arylisoquinolines **3** that can serve as key intermediates in the synthesis of many isoquinoline alkaloids but have proven difficult to access through current methodology.[24]

Scheme 5

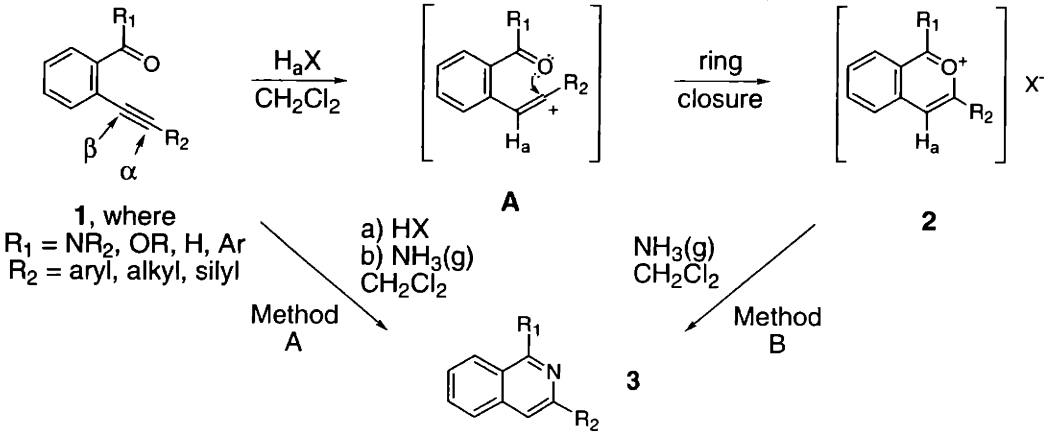

Results and Discussion

Several former group members of the Swager group have studied amide-containing poly(*p*-phenylene ethynylene)s (PPEs) such as **4**, and we saw them as suitable candidates for post-polymerization modification involving a pyrylium intermediate.[22a,25] To assess this, we used the iodo monomer **5** to prepare the model benzamide **6** by way of Sonogashira cross-coupling (Scheme 6). Subjection of **6** to the TFA cyclization conditions presented in Chapter 1 failed to provide any isolable, cyclized materials. The use of a stronger acid (HBF_4) allowed the deep burgundy-colored cyclized salt **7** to precipitate upon addition of ethyl ether to the reaction solution. This salt exhibits lower energy charge-transfer optical transitions upon cyclization (λ_{max} = 539 nm in $CHCl_3$). Although model **6** successfully cyclized, extensions to post-polymerization cyclizations of polymer **4** failed. Adding acid to extremely dilute solutions of **4** led to the immediate formation of black intractable materials. To help identify better polymer systems amenable to exhaustive ethynyl cyclizations, we examined smaller model systems to elucidate the scope of this reaction and to uncover any possibilities for further synthetic manipulation.

Scheme 6

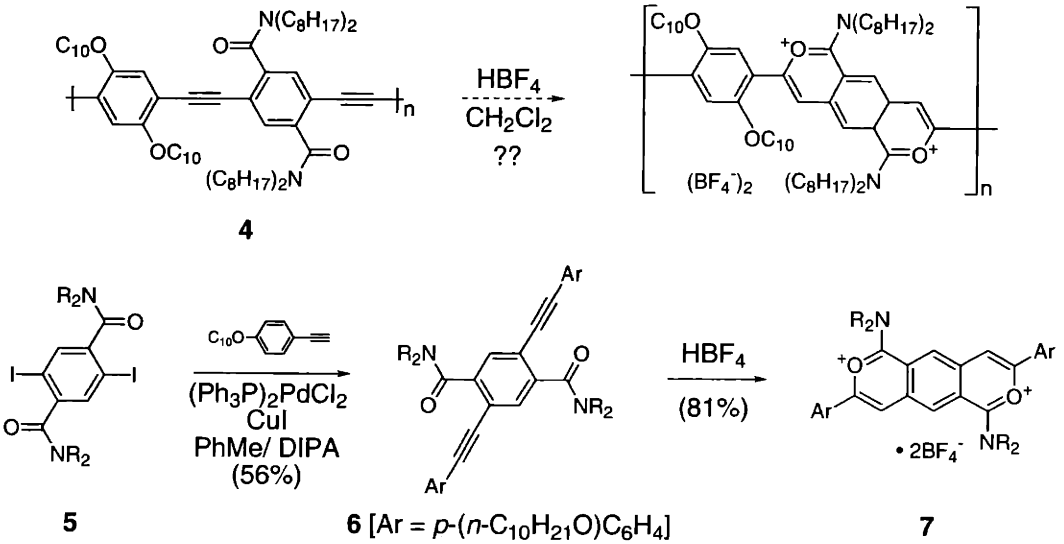

4 **5** **6** [Ar = *p*-(*n*-$C_{10}H_{21}O$)C_6H_4] **7**

We chose to study simple, unsubstituted arenes with carbonyl and alkyne functionalities positioned *ortho* to each other as represented generally by **1** (Scheme 5). This structural motif would mimic that of the polymer **4** and the model **6**. In these studies, we targeted aryl amides, esters, aldehydes and ketones to serve as representative carbonyl examples. We synthesized the amide and ester carbonyl equivalents from *o*-iodobenzoic acid: amides *via* amination of the acid chloride and esters by esterification with ethanol. Utilization of a synthetically facile modified Sonogashira-Hagihara protocol provided a variety of *o*-ynone cyclization precursors from these iodides as presented in Table 1. For aldehydes, we used *o*-iodobenzyl alcohol for the Sonogashira coupling prior to PCC oxidation of the coupling product.

With these precursors, we investigated the scope of the proposed cyclization. In initial studies, trifluoroacetic acid induced a partial degree of apparent cyclization, but the reaction proceeded slowly and the resulting products eluded isolation. In general, stronger acids such as HBF_4 and TfOH provide instant and essentially quantitative cyclizations. These reactions require high dilution (0.005 M) and exclusion of water in order to suppress intermolecular chemistry and hydrolysis, respectively. Significantly higher concentrations led to the formation of intractable materials. Concerning the alkyne moieties, our findings show that the cyclization requires alkynes with phenyl substitution in order to obtain the desired reactivity: the use of alkyl acetylenes (R_2 = *n*-Bu in Scheme 5) led to at least two different and unisolable products while silyl and free acetylenes (R_2 = TMS, H) led to the formation of undesired and apparently non-cyclized olefinic products as determined by *in situ* ^{1}H NMR.[26] However, the *o*-ynone cyclization does not require a strong *para* electron-donating group on the aryl acetylene to stabilize the positive charge density of the α-carbon of intermediate ***A*** in Scheme 5 as evidenced by the *o*-ynones with pendant phenyl and tolyl groups.

In accordance with literature precedents,[5] we used anhydrous ammonia to transform the isobenzopyrylium salts **2** into the corresponding isoquinolines **3**. Investigations toward efficient methodologies led to the conclusion that exposure of a triflate salt generated *in situ* (method A) and a two-pot isolation-exposure protocol (method B) provided comparable yields, as summarized in Table 1. Thus, method A serves as an attractive one-pot synthetic strategy for constructing isoquinoline ring systems. Table 1 complies the results of our synthetic studies related to these model systems as described in greater detail in the remainder of this chapter.

Table 1: Synthesis of acetylenes **1**, pyrylium salts **2** and isoquinolines **3**.

Entry	R_1	R_2 [b]	Acetylene Yield/% [a]	X	Pyrylium Yield/% [d]	Method	Isoquinoline Yield/% [g]
a	NMe_2	TMS	81	TfO	0 [e]	N/A	N/A
b		H	85		0 [e]	N/A	N/A
c		Ph	87 [c]		63	A	22 (32)
d		*p*-tol	67 [c]		64	B	30 (45)
e		*p*-OC_{10}	66		50	A	0 (52)
f	OEt	TMS	89	BF_4	N/A	N/A	N/A
g		Ph	84		66 [c] (83) [f]	B	23 (11) [h]
h		*p*-tol	90		88 [c] (95) [f]	A	21 (66)
i		*p*-OC_{10}	55		0 (67) [f]	N/A	N/A
j	H	TMS	84	TfO	0 [e]	N/A	N/A
k		Ph	36		>95 [e]	A	74
l		*p*-tol	79		>95 [e]	A	67
m		*p*-OC_{10}	72		>90 [e]	A	65
n	Ph	Ph	65	TfO	74	B	38
o		*p*-tol	54		84	A	67
p		*n*-C_4H_9	87		0	N/A	N/A

[a] **1a, c-e** prepared from *N,N*-dimethyl-2-iodobenzamide *via* Sonogashira coupling with R_2-CCH [$(Ph_3P)_2PdCl_2$, CuI, THF, DIPA]; **1b** prepared by deprotection of **1a** (K_2CO_3/MeOH/THF); **2f-i** prepared from ethyl-2-iodobenzoate *via* similar Sonogashira conditions as for **1a, c-e**; overall yield of **1j-m** prepared in two steps from Sonogashira coupling with *o*-iodobenzyl alcohol as for **1a, c-e** followed by PCC oxidation (CH_2Cl_2); **1n-p** prepared *via* Sonogashira conditions as for **1a, c-e**; [b] *p*-tol = 4-Me-C_6H_4-; *p*-OC_{10} = 4-(*n*-$C_{10}H_{21}O$)-C_6H_4-; [c] determined by ^1H NMR integration; [d] isolated and analytically pure unless otherwise noted; [e] *in situ* ^1H NMR determination of the transient intermediate; [f] isolated yield of **9** after hydrolysis; [g] values in parentheses refer to **8**; [h] accompanied by **9g** (30% by GC-MS).

Distinct spectroscopic changes accompanied all isobenzopyrylium formations. Immediately upon acid addition, an intense red to yellow UV fluorescence developed that persisted in the precipitate. Representative fluorescence data for the isolated salts displayed Stokes' shifts of greater than 100 nm suggesting excited state planarization of the pendant aryl moiety relative to the newly formed aromatic core. All isolated salts lacked the alkynyl C-C stretch in the infrared spectra (2200 cm^{-1}) while they exhibited an intense stretching band characteristic of their respective counteranion (1260 cm^{-1} for TfO^-, 1060 cm^{-1} for BF_4^-). High resolution MS provided evidence for the intact cation (EI or FAB) as well as the counteranion (negative ion FAB), and all isolated salts gave satisfactory elemental analyses. In the ^{13}C NMR, the two 85-100 ppm ethynyl carbon resonances disappeared and a new resonance corresponding

to the former carbonyl carbon (C_1 of **2**) appeared at 170-180 ppm. A new aromatic singlet (H_a of **2**) appeared in the ^1H spectra upon cyclization but did not appear during TfOD-induced cyclizations.

For the benzamide systems (Scheme 7), the triflate salts **2c**, **d** and **e** that formed upon cyclization precipitated readily from diethyl ether and maintained stability under ambient conditions. Dissolving the salt in acetonitrile followed by re-precipitation from diethyl ether provided analytically pure samples in high yields. For decyloxy-substituted **2e**, reaction times greater than 30 minutes led to the observation of a new and apparently de-alkylated species as observed by *in situ* ^1H NMR experiments. These salts displayed strong solution and solid-state emission characteristics: **2c** displayed a low-energy solution absorbance at 370 nm and fluoresced at 474 nm. Although we could easily isolate and purify these salts, we encountered problematic reactivity during subsequent aminations. We observed that these compounds underwent competitive transformation into the corresponding free amino isoquinolines **8c-e** in both the one-pot and two-pot methods.

Scheme 7

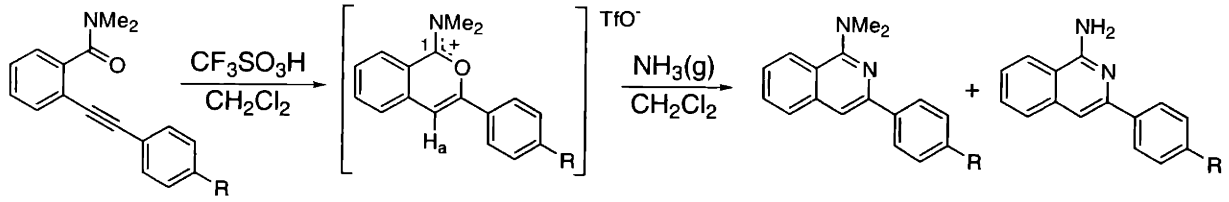

1c (R = H)
d (R = Me)
e (R = $OC_{10}H_{21}$)

2c (63%)
d (64%)
e (50%)

3c-d **8c-e**

From **1c**: 22% **3c**, 32% **8c**
From **2d**: 30% **3d**, 45% **8d**
From **1e**: 52% **8e**

In concurrence with the results for other α-amino pyrylium salts,[27] NMR data indicated that these aminated salts displayed a significant degree of exocyclic charge localization onto the nitrogen substituent. The *N*-methyl protons appeared as two distinct singlets in the ^1H spectrum between 3.7-3.9 ppm, and two distinct *N*-methyl carbon resonances appeared around 43-46 ppm

in the ^{13}C spectrum. The persistence of imine character in these salts displayed itself in the small upfield shift of the carbonyl carbon observed in the ^{13}C spectrum upon cyclization (C_1 of **2**). When compared to the other pyrylium salts discussed below, the new proton singlet observed at 7.5-7.6 ppm upon cyclization (H_a of **2**) indicated decreased aromatic character, lending credence to the argument that exocyclic charge localization reduces aromaticity. To further verify this claim, the crystal structure determined for **2d** supports a structure with significant exocyclic double bond character as evidenced by the short C_1-N bond of 1.314 Å (typical arylamine value 1.39 Å, Figure 1). This exocyclic resonance served to reduce the full pyrylium character of **2c-e** and thus inhibited the reactivities typically associated with pyrylium compounds. We should expect that such localized electronic structures would not react in a manner typical of pyrylium or isobenzopyrylium salts, as indeed evidenced by competitive over-amination to afford **8**.

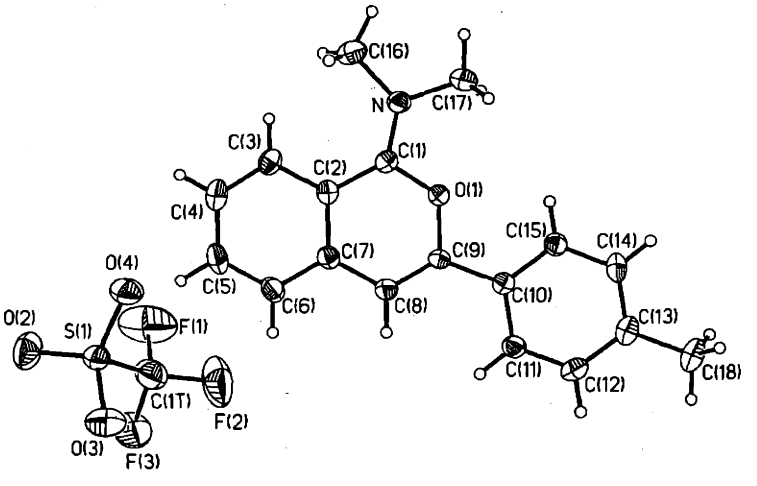

Bond Lengths/ Å	
C(1) – N	1.313
C(1) – O(1)	1.337
C(1) – C(2)	1.449
O(1) – C(9)	1.390
C(8) – C(9)	1.323
C(7) – C(8)	1.434
Bond Angles/ deg	
C(2)-C(1)-O(1)	119.5
C(1)-O(1)-C(9)	123.7
O(1)-C(8)-C(7)	119.0
C(7)-C(8)-C(9)	121.2

Figure 1: X-ray crystal structure and selected structural data for **1d**.

By incorporating a weaker oxygen donor into the carbonyl (an ester; Scheme 8), the ethoxy pyrylium systems formed upon cyclization should exhibit stronger aromaticity. Indeed, H_a resonated as a singlet at 8.1 ppm in these systems. Unfortunately, the isolation of these salts proved problematic. The tetrafluoroborate salts **2g-h** precipitated out of solution but slowly

hydrolyzed at ambient conditions to provide the corresponding isocoumarin compounds **9g-h** within hours. This instability precluded isolation and characterization in pure form, but full characterization of the hydrolysis products **9g** and **9h** agreed with data found in the literature for the pure isocoumarins.[28] Attempts to precipitate **2i** only resulted in immediate hydrolysis to **9i**. Unlike other functionalities studied, the ethyl esters **1g-i** required the use of HBF_4 to induce cyclization: treatment of **1i** with TfOH led to a significant amount of isocoumarin formation upon isolation. However, **1g** cyclized cleanly in the presence of TfOD as observed by ^1H NMR. Unfortunately, the ester model systems that could cyclize also underwent competitive transformation to the free amino-substituted isoquinolines under both amination methods. In the one-pot method (A), we obtained the over-aminated isoquinoline **8h** in a predominant 66% yield from **1h**, while the isolation-amination method (B) applied to salt **2g** provided a reaction mixture contaminated with the isocoumarin hydrolysis product **9g** formed upon initial isolation of the salt beside both **3g** and **8g**. As with the benzamide systems, this result stands in agreement with the idea that charge donation into the electron-deficient pyrylium ring reduces the overall pyrylium character of these substrates.

Scheme 8

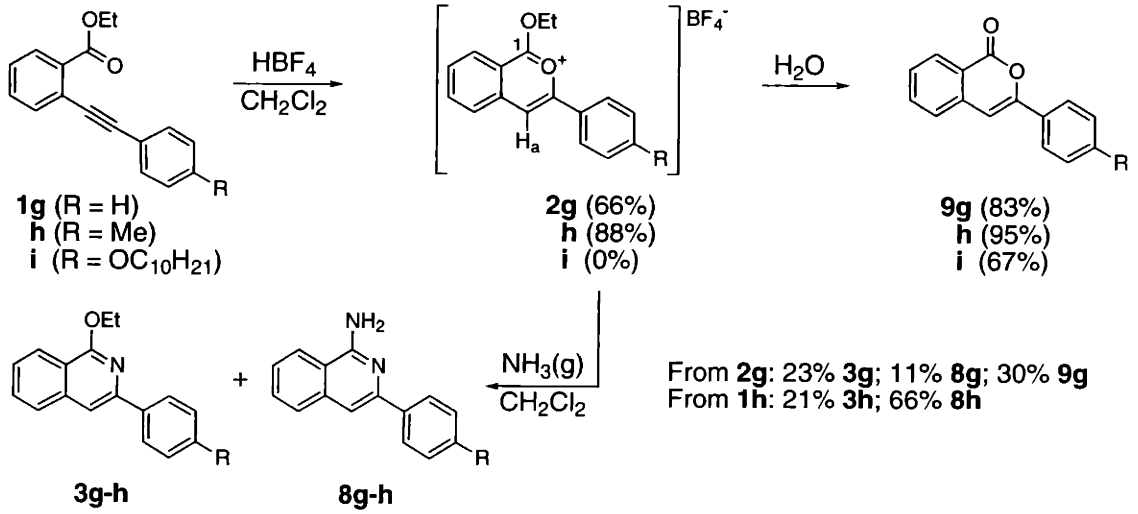

With the absence of strong nitrogen or oxygen donors in the aldehyde substrates (Scheme 9), aromaticity should dominate for the resulting *protio* pyrylium systems. We could not precipitate or otherwise isolate the triflate salts **2k-m** from the reaction mixture, so we relied on *in situ* ^{1}H NMR to characterize these transient intermediates using both TfOH and TfOD prior to further synthetic manipulations. Alkynes **1k** and **1l** cyclized quantitatively while a second undetermined side-product competitively formed during the cyclization of **1m**, a possible result of acid induced aryl ether cleavage. These systems displayed lower-field ^{1}H singlet resonances for H_a at 8.6 ppm. The lack of heteroatomic appendages allowed for less charge donation into the pyrylium ring, thus enhancing the degree of aromaticity within the system and shifting the H_a resonance to even lower field. As we may now consider these salts more delocalized and "authentic" pyrylium compounds, they readily aminated under both the one-pot and two-pot methods in very high yields. We observed no evidence for competitive over-amination or hydrolysis under these conditions.

Scheme 9

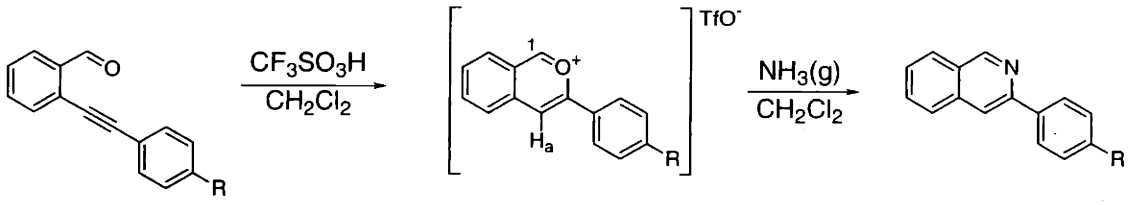

1k (R = H)
l (R = Me)
m (R = $OC_{10}H_{21}$)

2k (>95% NMR)
l (>95% NMR)
m (>90% NMR)

3k (74% from **1k**)
l (67% from **1l**)
m (65% from **1m**)

Due to the charge localization found in the amino compounds and the problematic isolations of the 1-*protio* and ethoxy salts, we studied the more traditional pyrylium systems **2n-o** (Scheme 10). As with the benzamide models, the benzophenone derivatives allowed for analytical purification *via* two precipitations from diethyl ether. Upon cyclization, the observed downfield proton singlet for H_a at 8.8 ppm indicates the greater expected degree of aromaticity within these systems. Relative to the benzophenone carbonyl ^{13}C NMR resonance, C_1 of **2n-o** shifted upfield by 20 ppm: carbon NMR data for **2n** (but where BF_4^- replaces TfO^-) correlated well with literature values.[29] The 1-phenyl pyrylium salts absorbed at 440-450 nm and fluoresced weakly at 538 nm, again displaying a significant Stokes' shift upon emission. As with the aldehyde model systems, the one-pot cyclization-amination protocol provided high yields of the 1,3-diaryl isoquinoline with no apparent hydrolysis or over-amination.

Scheme 10

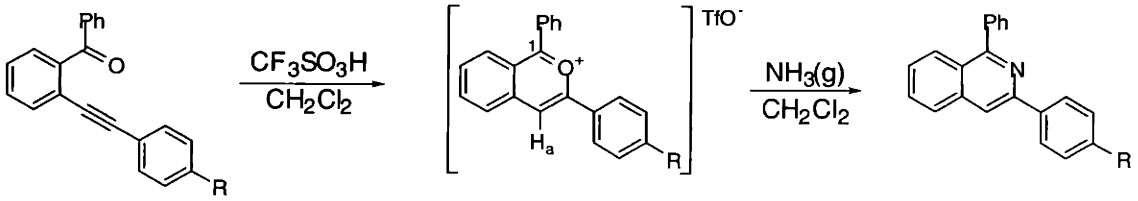

1n (R = H)
o (R = Me)

2n (74%)
o (84%)

3n (38% from **1n**)
o (67% from **1o**)

With this general survey of functional group compatibilities completed, we could then return to study post-polymerization functionalization. Recall from Scheme 6 that we initially targeted the cyclization of the amide-containing PPE **4**. The results from model systems **1c-e** indicated that the benzamide systems provided multiple products and poor yields of the desired isoquinolines. This may help to explain the poor results we obtained in initial attempts to effect post-polymerization cyclization of **4**. We then turned to the model studies to identify a better polymer system that may prove more amenable to this cyclization. We pursued the aldehyde systems as they provided essentially quantitative cyclizations (as judged by ^1H NMR) and clean

aminations. We sought to investigate the model terephthaldehyde **10** for initial cyclization studies in addition to the aldehyde-based PPE **11** (Scheme 11). Starting from the halide scaffold **12**, Sonogashira coupling installed the phenylacetylene moieties, and lithium-halogen exchange followed by a DMF quench of the dianion provided **10**. Similarly, TIPS-acetylene coupling under Sonogashira conditions provided **13**. We obtained the dial monomer **14** by subjecting **13** to similar formylation conditions used to obtain **10** followed by TBAF desilylation. Unfortunately, we ran into problems during the investigations of both of these compounds: **10** failed to provide isolable materials after the one-pot cyclization-amination conditions, and the monomer **14** failed to polymerize under Sonogashira conditions. Future work will need to study other types of more soluble derivatives such as alkyl or aryl diketones as carbonyl equivalents.

Scheme 11[a]

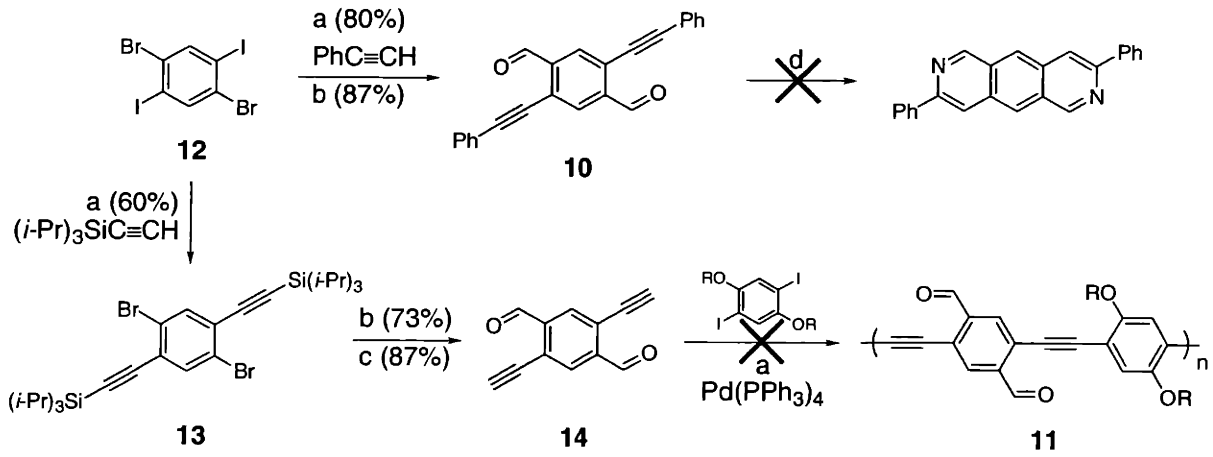

[a] Reagents and conditions: (a) *Sonogashira:* $(Ph_3P)_2PdCl_2$, CuI, PhMe, DIPA; (b) i. *t*-BuLi, THF -78°C; ii. DMF; (c) *n*-Bu_4NF, THF, MeOH, H_2O; (d) i. TfOH, CH_2Cl_2; ii. NH_3.

Concluding Remarks

In closing, we have shown that the acid-induced intramolecular electrophilic cyclizations of alkynes with carbonyl oxygens provide new and efficient routes to pyrylium salts and their isoquinoline analogues. We anticipate that this methodology should prove useful for the development of more convergent syntheses of aryl isoquinolines. Future work shall focus on expanding this methodology to other aza-aromatic systems and to polymeric systems in order to open new avenues of post-polymerization chemistry. These modifications will help to provide novel n-dopable monomers and polymeric systems capable of providing high electron mobilities.

Experimental Section

General: All synthetic manipulations were performed under an argon atmosphere using standard Schlenk techniques unless otherwise noted. Anhydrous diisopropylamine (DIPA), methylene chloride and tetrahydrofuran (THF) were purchased from Aldrich and used without further purification. All other chemicals were of reagent grade and used as received. *N,N*-Dimethyl-2-iodobenzamide (precursor to **1a-e**)[30] was prepared by refluxing 2-iodobenzoic acid in $SOCl_2$ followed by addition of dimethylamine in THF; ethyl-2-iodobenzoate (precursor to **1f-i**)[31] was prepared by refluxing 2-iodobenzoic acid and 12 M HCl in ethanol; 2-iodobenzophenone (precursor to **1n-p**)[32] was prepared *via* the diazonium salt of 2-aminobenzophenone (HCl-$NaNO_2$) by treatment with aqueous KI; 4-Decyloxyphenylacetylene[33] was prepared by a Williamson ether synthesis on 4-iodophenol (1-bromodecane, K_2CO_3, KI, acetone) followed by Sonogashira coupling of trimethylsilylacetylene [$(Ph_3P)_2PdCl_2$, CuI, DIPA/PhMe] and subsequent deprotection (KOH, MeOH/H_2O). Compounds **4** and **5** were prepared by the published routes.[25] Compound **12** was prepared through iodination of 1,4-dibromo benzene (H_5IO_6, KI, H_2SO_4).[34] 1,4-bis(phenylethynyl)-2,5-dibromobenzene was prepared from **12** by Sonogashira coupling of **12** and phenylacetylene.[20b] Compound **13** was prepared as described in Chapter 1.

Column chromatography was performed using Baker 40 μm silica gel. All organic extracts were dried over $MgSO_4$ and filtered prior to removal. NMR spectra were obtained on a Bruker AC-250, Varian Mercury-300 or Varian Inova-500 spectrometers, and all chemical shifts are referenced to $CHCl_3$ (7.26 ppm for ^1H, 77.23 ppm for ^{13}C) and TMS or CD_2HCN (1.94 ppm for ^1H, 1.39 ppm for ^{13}C). High resolution mass spectra were obtained at the MIT Department of Chemistry Instrumentation Facility (DCIF) on a Finnigan MAT 8200 using a peak matching protocol to determine the mass and error range

of the molecular ion; FAB spectra were obtained using a 3-nitrobenzyl alcohol matrix. UV-Vis measurements were obtained on a Hewlett-Packard 8452A diode array spectrophotometer. Fluorescence measurements were recorded on a SPEX Fluorolog-τ2 fluorimeter with a 450 W xenon lamp. Elemental analyses were obtained at Desert Analytics (Tucson, AZ). Melting points are uncorrected.

Ethynyl benzamides (1a, c–e): Representative procedure for *N,N*-dimethyl-2-(trimethylsilylethynyl) benzamide (**1a**)**:** A dry Schlenk flask was charged with 1 eq of *N,N*-dimethyl-2-iodobenzamide (4.00 g, 14.5 mmol), 0.04 eq $(Ph_3P)_2PdCl_2$ (407 mg, 0.579 mmol), and 0.1 eq CuI (275 mg, 1.44 mmol) and placed under an argon atmosphere. THF (120 mL) and DIPA (40 mL) were transferred into the flask, and the reaction was stirred at room temperature for 20 min at which point 1.1 eq of degassed trimethylsilylacetylene (2.25 mL, 15.9 mmol) was added over a 3 hr period *via* syringe. The reaction was stirred for a total of 20 h and filtered through a pad of celite. The filtered solvents were removed *in vacuo* and the residual oil was purified on silica (1:1 hexane/ethyl acetate) to provide **1a** (2.886 g, 11.76 mmol, 81%) as a brownish-red oil which solidified upon standing and was used without further purification. mp 52.0–54.0°C. ^{1}H NMR (500 MHz, $CDCl_3$) δ: 7.46 (m, 1H), 7.36 (m, 1H), 7.31 (m, 2H), 3.12 (s, 3H), 2.90 (s, 3H), 0.23 (s, 9H). ^{13}C NMR (125 MHz, $CDCl_3$) δ: 170.1, 140.3, 132.2, 129.1, 128.7, 126.6, 120.1, 102.2, 97.8, 38.3, 34.8, 0.0. FT-IR (neat) ν/cm^{-1}: 3057, 2958, 2159, 1645, 1504, 1394, 1250, 1109, 1073, 865, 759, 647. HR-MS (EI): found *m/z* = 245.1238 ± 0.0007 (M^+); calc. for $C_{14}H_{19}NOSi$: 245.1236.

N,N-Dimethyl-2-ethynylbenzamide (**1b**)**:** A 50 mL round bottom flask was charged with **1a** (301 mg, 1.23 mmol) and K_2CO_3 (693 mg, 5.02 mmol) and the flask was placed under argon. A degassed mixture of MeOH (7 mL), THF (7 mL) and water (3 mL) was added to the flask, and the reaction stirred at room temperature for 45 min at which point TLC indicated complete consumption of starting material. The reaction was diluted with ether, and the organic phase was washed with NaCl (x3), dried and removed *in vacuo* to yield a crude yellowish solid. The solids were pushed through a silica gel plug (1:1 ethyl acetate/CH_2Cl_2) to provide **1b** as a yellow-white solid (181 mg, 1.05 mmol, 85%) that was used without further purification. mp 93-95°C. ^{1}H NMR (500 MHz, $CDCl_3$) δ: 7.53 (d, 1H, *J* = 7.5 Hz), 7.40 (td, 1H, *J* = 7.5, 1.0 Hz), 7.34 (td, 1H, *J* = 7.0, 1.5 Hz), 7.31 (d, 1H, *J* = 7.5 Hz), 3.17 (s, 1H), 3.14 (s, 3H), 2.89 (s, 3H). ^{13}C NMR (125 MHz, $CDCl_3$) δ: 169.9, 140.3, 132.8, 129.3, 128.7, 126.4, 119.1, 80.8, 80.6, 38.4, 34.8. FT-IR (KBr) ν/cm^{-1}: 3228, 3067, 3009, 2930, 2105, 1619, 1507, 1410, 1397, 1278, 1262, 1073, 782, 713. HR-MS (EI): found *m/z* = 173.0838 ± 0.0005 (M^+); calc. for $C_{11}H_{11}NO$: 173.0841.

N,N-Dimethyl-2-(phenylethynyl)benzamide (**1c**)**:**[35] Prepared as **1a** from *N,N*-dimethyl-2-iodobenzamide (561 mg, 2.04 mmol) and phenylacetylene (0.24 mL, 2.2 mmol), column chromatography (1:1 ethyl

acetate/hexanes) provided 3 major fractions: 85 mg of **1c** as a brown oil in pure form besides 375 mg of a 12:1 mixture of **1** and starting benzamide and 29 mg of a 1:1 mixture, as determined by ^{1}H NMR integration. From integration ratios, a total of 1.77 mmol was obtained (87%). Based on NMR estimates of recovered **1** (47 mg, 0.188 mmol), the overall corrected yield was 96%. ^{1}H NMR (300 MHz, $CDCl_3$) δ: 7.54 (m, 1H), 7.45 (m, 2H), 7.35 (m, 6H), 3.18 (s, 3H), 2.95 (s, 3H). ^{13}C NMR (125 MHz, $CDCl_3$) δ: 170.3, 139.8, 132.0, 131.7, 128.9, 128.9, 128.7, 128.5, 126.7, 123.0, 120.3, 92.7, 86.8, 38.5, 35.0. FT-IR (neat) ν/cm^{-1}: 3059, 2927, 2207, 1634, 1492, 1395, 1273, 1070, 758, 460. HR-MS (EI): found *m/z* = 249.1150 ± 0.0007 (M^+); calc. for $C_{17}H_{15}NO$: 249.1154.

N,N-Dimethyl-2-(4-methylphenylethynyl)benzamide **(1d):** Prepared as **1a** from *N,N*-dimethyl-2-iodobenzamide (200 mg, 0.727 mmol) and 4-ethynyltoluene (0.10 mL, 0.79 mmol), column chromatography (CH_2Cl_2 followed by 2:1 ethyl acetate/hexane) provided 130 mg of **1d** as an extremely viscous dark brown oil; NMR data indicated that a residual amount of starting iodide was present (2.7%). From NMR integration ratios, 0.481 mmol of **1d** was obtained (67%). ^{1}H NMR (500 MHz, $CDCl_3$) δ: 7.53 (m, 1H), 7.36 (m, 5H), 7.15 (d, 2H, *J* = 8.0 Hz), 3.17 (s, 3H), 2.94 (s, 3H), 2.37 (s, 3H). ^{13}C NMR (125 MHz, $CDCl_3$) δ: 170.2, 139.6, 138.8, 131.7, 131.5, 129.2, 128.7, 128.5, 126.5, 120.3, 119.8, 92.8, 86.0, 38.4, 34.8, 21.5. FT-IR (neat) ν/cm^{-1}: 3027, 2923, 2207, 1646, 1510, 1395, 1273, 1211, 1106, 1070, 817, 758, 460. HR-MS (EI): found *m/z* = 263.1313 ± 0.0007 (M^+); calc. for $C_{18}H_{17}NO$: 263.1310.

2-(4-Decyloxyphenylethynyl)-*N,N*-dimethylbenzamide **(1e):** Prepared as **1a** from *N,N*-dimethyl-2-iodobenzamide (218 mg, 0.792 mmol) and 4-decyloxyphenylacetylene (216 mg, 0.838 mmol) taken up in THF (2 mL), column chromatography (1:1 ethyl acetate/hexanes) provided **1e** as a viscous brown oil (213 mg, 0.524 mmol, 66%). ^{1}H NMR (300 MHz, $CDCl_3$) δ: 7.51 (m, 1H), 7.36 (m, 5H), 6.85 (d, 2H, *J* = 9.0 Hz), 3.96 (t, 2H, *J* = 6.6 Hz), 3.17 (s, 3H), 2.94 (s, 3H), 1.77 (quin, 2H, *J* = 6.9 Hz), 1.45 (m, 2H), 1.28 (m, 12H), 0.88 (t, 3H, *J* = 6.6 Hz). ^{13}C NMR (300 MHz, $CDCl_3$) δ: 170.3, 159.5, 139.5, 133.1, 131.7, 128.8, 128.4, 126.6, 120.7, 114.7, 114.6, 92.9, 85.4, 68.2, 38.4, 34.9, 32.0, 29.6, 29.5, 29.4, 29.2, 26.1, 22.8, 14.2. FT-IR (neat) ν/cm^{-1}: 3057, 2925, 2854, 2212, 1645, 1605, 1511, 1394, 1285, 1248, 1175, 1070, 832, 756. HR-MS (EI): found *m/z* = 405.2664 ± 0.0012 (M^+); calc. for $C_{27}H_{35}NO_2$: 405.2668.

Ethynyl esters (1f–i): Representative procedure for ethyl-2-(trimethylsilylethynyl)benzoate **(1f):**[35] One eq of ethyl-2-iodobenzoate (4.717 g, 17.09 mmol) was placed under argon in a dry 25 mL Schlenk flask and dissolved in THF (20 mL). A dry 500 mL Schlenk flask was charged with 0.16 eq CuI (528 mg, 2.77 mmol) and 0.04 eq $(Ph_3P)_2PdCl_2$ (538 mg, 0.766 mmol) and placed under argon. The benzoate solution was transferred into the catalyst flask at which point additional THF (100 mL) and DIPA (40 mL) were

added, and the solution was stirred at room temperature for 20 min. 1.1 eq of degassed trimethylsilylacetylene (2.7 mL, 19 mmol) was added over a 3 h period *via* syringe and further stirred for a total of 20 h. The reaction was filtered through a pad of silica, and the solvents were removed *in vacuo* to provide a black oil. Column chromatography on silica (3:2 hexane/CH_2Cl_2) provided a light reddish brown oil with residual solid impurities that were removed by filtration of an ethereal solution of the product. Ether removal *in vacuo* yielded **1f** as a brown oil (3.73 g, 15.1 mmol, 89%). ^{1}H NMR (300 MHz, $CDCl_3$) δ: 7.89 (dd, 1H, J = 7.5, 0.9 Hz), 7.58 (dd, 1H, J = 7.5, 0.9 Hz), 7.43 (td, 1H, J = 7.5, 1.5 Hz), 7.36 (td, 1H, J = 7.8, 1.5 Hz), 4.40 (q, 2H, J = 7.2 Hz), 1.42 (t, 3H, J = 7.2 Hz), 0.26 (s, 9H). ^{13}C NMR (125 MHz, $CDCl_3$) δ: 166.7, 134.9, 132.9, 131.5, 130.3, 128.3, 123.2, 103.5, 99.7, 61.4, 14.5, 0.1. FT-IR (neat) ν/cm^{-1}: 2067, 2960, 2159, 1731, 1715, 1594, 1294, 1250, 1131, 1078, 844, 759, 453. HR-MS (EI): found m/z = 246.1073 ± 0.0007 (M^+); calc. for $C_{14}H_{18}O_2Si$: 246.1076.

Ethyl-2-(phenylethynyl)benzoate (**1g**):[35] Prepared as **1f** from ethyl-2-iodobenzoate (2.00 g, 7.24 mmol) and phenylacetylene (0.85 mL, 7.7 mmol), column chromatography (1:1 hexane/CH_2Cl_2) provided **1g** as a reddish brown oil (1.516 g, 6.056 mmol, 84%). ^{1}H NMR (500 MHz, $CDCl_3$) δ: 7.95 (dd, 1H, J = 8.0, 1.0 Hz), 7.61 (dd, 1H, J = 7.5, 0.5 Hz), 7.57 (dd, 2H, J = 8.0, 2.0 Hz), 7.41 (td, 1H, J = 7.5, 1.0 Hz), 7.31 (m, 3H), 4.39 (q, 2H, J = 7.0 Hz), 1.36 (t. 3H, J = 7.0 Hz). ^{13}C NMR (125 MHz, $CDCl_3$) δ: 166.2, 134.0, 132.1, 131.64, 131.55, 130.4, 128.48, 128.36, 127.9, 123.54, 123.34, 94.2, 88.4, 61.2, 14.4. FT-IR (neat) ν/cm^{-1}: 3062, 2982, 2221, 1727, 1716, 1599, 1494, 1443, 1366, 1290, 1249, 1129, 1076, 755, 691, 438. HR-MS (EI): found m/z = 250.0995 ± 0.0007 (M^+); calc. for $C_{17}H_{14}O_2$: 250.0994.

Ethyl-2-(4-methylphenylethynyl)benzoate (**1h**): Prepared as **1f** from ethyl-2-iodobenzoate (2.01 g, 7.28 mmol) and 4-ethynyltoluene (1.0 mL, 7.9 mmol), column chromatography (1:1 hexane/CH_2Cl_2) provided **1h** as a brown oil (1.726 g, 6.529 mmol, 90%). ^{1}H NMR (500 MHz, $CDCl_3$) δ: 7.96 (dd, 1H, J = 7.5, 1.0 Hz), 7.63 (dd, 1H, J = 7.5, 1.0 Hz), 7.46 (m, 3H), 7.35 (td, 1H, J = 7.5, 1.0 Hz), 7.16 (dd, 2H, J = 8.0, 0.5 Hz), 4.42 (q, 2H, J = 7.5 Hz), 2.36 (s, 3H), 1.40 (t, 3H, J = 7.0 Hz). ^{13}C NMR (125 MHz, $CDCl_3$) δ: 166.6, 138.8, 134.1, 132.3, 131.72, 131.67, 130.5, 129.3, 127.9, 123.9, 120.4, 94.6, 87.8, 61.4, 21.7, 14.5. FT-IR (neat) ν/cm^{-1}: 2981, 2217, 1728, 1511, 1290, 1248, 1130, 1075, 817, 757, 460. HR-MS (EI): found m/z = 264.1152 ± 0.0007 (M^+); calc. for $C_{18}H_{16}O_2$: 264.1150.

2-(4-Decyloxyphenylethynyl)ethylbenzoate (**1i**): Prepared as **1f** from ethyl-2-iodobenzoate (0.46 g, 1.7 mmol) and 4-decyloxyphenylacetylene (451 mg, 1.74 mmol) taken up in THF (3 mL), column chromatography (3:2 hexane/CH_2Cl_2) provided **1i** as a yellow solid (372 mg, 0.915 mmol, 55%). mp 40.5-41.5°C. ^{1}H NMR (500 MHz, $CDCl_3$) δ: 7.96 (d, 1H, J = 8.0 Hz), 7.62 (d, 1H, J = 7.5 Hz), 7.48 (m,

3H), 7.36 (t, 1H, J = 7.5 Hz), 6.87 (d, 2H, J = 8.5 Hz), 4.42 (q, 2H, J = 7.0 Hz), 3.97 (t, 2H, J = 6.0 Hz), 1.79 (m, 2H), 1.41 (m, 4H), 1.28 (bm, 10H), 0.89 (t, 3H, J = 6.0 Hz). ^{13}C NMR (125 MHz, $CDCl_3$) δ: 166.7, 159.6, 134.0, 133.3, 132.1, 131.7, 130.6, 127.7, 124.2, 115.4, 114.7, 94.7, 87.2, 68.3, 61.3, 32.1, 29.78, 29.76, 29.60, 29.53, 29.39, 26.2, 22.9, 14.6, 14.3. FT-IR (KBr) ν/cm^{-1}: 2923, 2851, 2215, 1705, 1510, 1286, 1247, 1129, 1040, 832, 758. HR-MS (EI): found m/z = 406.2501 ± 0.0012 (M^+); calc. for $C_{27}H_{34}O_3$: 406.2508.

Ethynyl benzyl alcohols (Precursors to **1j-m**): representative procedure for 2-(trimethylsilylethynyl) benzyl alcohol (precursor to **1j**): A dry Schlenk flask was charged with 1 eq of 2-iodobenzyl alcohol (4.002 g, 17.10 mmol), 0.04 eq $(Ph_3P)_2PdCl_2$ (538 mg, 0.766 mmol) and 0.16 eq CuI (535 mg, 2.81 mmol) and placed under an argon atmosphere. To this flask was added THF (120 mL) and diisopropylamine (40 mL) *via* cannula, and the reaction was stirred at room temperature for 20 min at which point 1.12 eq of degassed trimethylsilylacetylene (2.7 mL, 19 mmol) was added over a 3 hr period *via* syringe. The reaction was stirred for a total of 20 h and filtered through a pad of silica. The filtered solvents were then removed *in vacuo*, and the residual oil was then purified further on silica (4:1 hexanes/ethyl acetate). Solvent removal provided the desired ethynyl alcohol (3.037 g, 14.86 mmol, 87%) as a brown oil used without further purification. ^{1}H NMR (500 MHz, $CDCl_3$) δ: 7.47 (dd, 1H, J = 7.5, 1.0 Hz), 7.41 (d, 1H, J = 8.0 Hz), 7.34 (td, 1H, J = 7.5, 1.0 Hz), 7.24 (td, 1H, J = 7.0, 1.0 Hz), 4.82 (d, 2H, J = 6.5 Hz), 2.21 (t, 1H, J = 7.0 Hz), 0.27 (s, 9H). ^{13}C NMR (125 MHz, $CDCl_3$) δ: 143.3, 132.6, 129.1, 127.49, 127.29, 121.3, 102.8, 99.8, 64.2, 0.1. FT-IR (neat) ν/cm^{-1}: 3346, 3067, 2959, 2898, 2155, 1480, 1450, 1250, 1042, 866, 842, 759, 645, 430. HR-MS (EI): found m/z = 204.0973 ± 0.0006 (M^+); calc. for $C_{12}H_{16}OSi$: 204.0970.

2-(Phenylethynyl)benzyl alcohol (precursor to **1k**):[36] Prepared as above from 2-iodobenzyl alcohol (4.709 g, 20.12 mmol) and phenylacetylene (2.40 mL, 21.9 mmol), column chromatography (CH_2Cl_2) provided **1k** in clean form as a pale yellow solid (1.87 g, 8.98 mmol, 45%). ^{1}H NMR (250 MHz, $CDCl_3$) δ: 7.53 (m, 4H), 7.38 (m, 5H), 4.92 (d, 2H, J = 6.5 Hz), 2.10 (t, 1H, J = 5.6 Hz).

2-(4-Methylphenylethynyl)benzyl alcohol (precursor to **1l**): Prepared as above from 2-iodobenzyl alcohol (4.708 g, 20.12 mmol) and 4-ethynyltoluene (2.40 mL, 21.9 mmol), column chromatography (CH_2Cl_2) provided the product as a chaulky white-orange powder (3.456 g, 15.55 mmol, 91%) used without further purification. ^{1}H NMR (500 MHz, $CDCl_3$) δ: 7.53 (dd, 1H, J = 7.5, 1.0 Hz), 7.47 (d, 1H, J = 7.5 Hz), 7.43 (d, 2H, J = 8.0 Hz), 7.35 (td, 1H, J = 7.5, 1.5 Hz), 7.28 (td, 1H, J = 7.0, 1.5 Hz), 7.17 (dd, 2H, J = 8.5, 0.5 Hz), 4.91 (d, 2H, J = 6.5 Hz), 2.38 (s, 3H), 2.13 (t, 1H, J = 6.5 Hz). ^{13}C NMR (125 MHz, $CDCl_3$) δ:

142.6, 138.9, 132.2, 131.6, 129.4, 128.7, 127.61, 127.38, 121.6, 120.0, 94.6, 86.3, 64.2, 21.7. FT-IR (KBr) ν/cm^{-1}: 3339, 3249, 3057, 2926, 2212, 1510, 1450, 1032, 818, 760, 521. HR-MS (EI): found *m/z* = 222.1040 ± 0.0007 (M^+); calc. for $C_{16}H_{14}O$: 222.1045.

2-(4-Decyloxyphenylethynyl)benzyl alcohol (precursor to **1m**): Prepared as above from 2-iodobenzyl alcohol (471 mg, 2.01 mmol) and 4-decyloxyphenylacetylene (545 mg, 2.11 mmol) taken up in THF (3 mL), column chromatography (CH_2Cl_2) provided the product as a beige-white solid (631 mg, 1.73 mmol, 86%) used without further purification. mp 76.5-78.5°C. ^{1}H NMR (500 MHz, $CDCl_3$) δ: 7.52 (dd, 1H, *J* = 7.5, 1.5 Hz), 7.46 (m, 3H), 7.34 (td, 1H, *J* = 7.0, 1.0 Hz), 7.28 (td, 1H, *J* = 7.5, 1.0 Hz), 6.88 (m, 2H), 4.91 (d, 2H, *J* = 6.5 Hz), 3.98 (t, 2H, *J* = 7.0 Hz), 2.11 (t, 1H, *J* = 6.5 Hz), 1.79 (quin, 2H, *J* = 7.0 Hz), 1.46 (m, 2H), 1.29 (m, 12H), 0.89 (t, 3H, *J* = 7.0 Hz). FT-IR (KBr) ν/cm^{-1}: 3357, 2921, 2852, 1605, 1510, 1474, 1247, 1046, 834, 759. HR-MS (EI): found *m/z* = 364.2407 ± 0.0011 (M^+); calc. for $C_{25}H_{32}O_2$: 364.2402.

Ethynyl aldehydes (1j–m): representative procedure for 2-(trimethylsilylethynyl)benzaldehyde (**1j**): To a dry Schlenk flask was added 2 eq PCC (6.14 g, 28.5 mmol) with equal weights of dry molecular sieves and celite, and the solids were placed under argon. CH_2Cl_2 (240 mL) was transferred into the flask, and the mixture was stirred vigorously. Following dissolution of the PCC, a solution of 2-(trimethylsilyl-ethynyl)benzyl alcohol (2.90 g, 14.2 mmol) in CH_2Cl_2 (40 mL) was added dropwise *via* syringe and stirred at room temperature for 7 h. The reaction solvents were pushed through a silica gel plug and removed *in vacuo* to provide **1j** as a brown oil (2.75 g, 13.6 mmol, 96%) which solidified into a brown solid upon freezing and was used without further purification. mp 50.5-51.5°C (lit.[37] 51-53°C). ^{1}H NMR (300 MHz, $CDCl_3$) δ: 10.56 (s, 1H), 7.91 (dd, 1H, *J* = 7.2, 0.6 Hz), 7.58 (m, 1H), 7.54 (td, 1H, *J* = 7.5, 1.5 Hz), 7.44 (td, 1H, *J* = 6.9, 0.9 Hz), 0.27 (s, 9H). ^{13}C NMR (75 MHz, $CDCl_3$) δ: 192.0, 136.3, 133.86, 133.67, 129.0, 127.04, 126.96, 102.6, 100.2, -0.0. FT-IR (KBr) ν/cm^{-1}: 2955, 2853, 2766, 2151, 1697, 1593, 1248, 1090, 867, 846, 765, 653. HR-MS (EI): found *m/z* = 202.0811 ± 0.0006 (M^+); calc. for $C_{12}H_{14}OSi$: 202.0814.

2-(Phenylethynyl)benzaldehyde (**1k**):[38] Prepared as **1j** from 2-(phenylethynyl)benzyl alcohol (1.87 g, 8.98 mmol), **1k** was obtained as a yellow oil (1.492 g, 7.234 mmol, 81%). ^{1}H NMR (500 MHz, $CDCl_3$) δ: 10.66 (s, 1H), 7.95 (d, 1H, *J* = 7.5 Hz), 7.64 (d, 1H, *J* = 7.0 Hz), 7.57 (m, 3H), 7.44 (t, 1H, *J* = 7.0 Hz), 7.39 (m, 3H). ^{13}C NMR (125 MHz, $CDCl_3$) δ: 191.8, 135.9, 133.9, 133.3, 131.8, 129.2, 128.74, 128.66, 127.4, 127.0, 122.4, 96.5, 85.1. FT-IR (neat) ν/cm^{-1}: 3061, 3033, 2839, 2746, 2215, 1697, 1592, 1492,

1266, 1193, 1070, 757, 690, 430. HR-MS (EI): found m/z = 206.0733 ± 0.0006 (M^+); calc. for $C_{15}H_{10}O$: 206.0732.

2-(4-Methylphenylethynyl)benzaldehyde (**1l**): Prepared as **1j** from 2-(4-methylphenylethynyl)benzyl alcohol (3.006 g, 13.52 mmol), **1l** was obtained as a maize yellow solid (2.58 g, 11.7 mmol, 87%). mp 42.5-44.5°C (lit.[39] 38°C). ^{1}H NMR (300 MHz, $CDCl_3$) δ: 10.65 (s, 1H), 7.95 (dd, 1H, J = 7.5, 1.0 Hz), 7.64 (dd, 1H, J = 7.5, 0.5 Hz), 7.59 (td, 1H, J = 7.0, 1.5 Hz), 7.46 (m, 3H), 7.20 (d, 2H, J = 8.0 Hz), 2.39 (s, 3H). ^{13}C NMR (125 MHz, $CDCl_3$) δ: 192.0, 139.6, 135.9, 133.9, 133.3, 131.8, 129.5 [2 peaks], 128.6, 127.3, 119.4, 96.8, 84.5, 21.8. FT-IR (KBr) ν/cm^{-1}: 3028, 2912, 2839, 2751, 2212, 1693, 1592, 1508, 1472, 1388, 1263, 1192, 813, 764, 638, 518. HR-MS (EI): found m/z = 220.0887 ± 0.0007 (M^+); calc. for $C_{16}H_{12}O$: 220.0888.

2-(4-Decyloxyphenylethynyl)benzaldehyde (**1m**): Prepared as **1j** from 2-(4-decyloxyphenylethynyl)-benzyl alcohol (365 mg, 1.00 mmol), **1m** was obtained as a faint orange solid (305 mg, 0.841 mmol, 84%). mp 41.5-42.0°C. ^{1}H NMR (500 MHz, $CDCl_3$) δ: 10.65 (s, 1H), 7.94 (d, 1H, J = 8.0 Hz), 7.62 (d, 1H, J = 8.0 Hz), 7.57 (t, 1H, J = 7.5 Hz), 7.49 (d, 2H, J = 8.5 Hz), 7.43 (t, 1H, J = 7.5 Hz), 6.90 (d, 2H, J = 8.0 Hz), 3.99 (t, 2H, J = 6.5 Hz), 1.80 (m, 2H), 1.46 (m, 2H), 1.28 (bm, 12H), 0.89 (t, 3H, J = 6.5 Hz). ^{13}C NMR (75 MHz, $CDCl_3$) δ: 192.1, 160.0, 135.8, 133.9, 133.4, 133.2, 128.4, 127.6, 127.35, 114.9, 114.2, 97.0, 83.9, 68.3, 32.1, 29.77, 29.75, 29.58, 29.52, 29.35, 26.2, 22.9, 14.3. FT-IR (KBr) ν/cm^{-1}: 2922, 2853, 2212, 1693, 1605, 1591, 1509, 1253, 1013, 830, 771. HR-MS (EI): found m/z = 362.2240 ± 0.0011 (M^+); calc. for $C_{25}H_{30}O_2$: 362.2246.

Ethynyl benzophenones (1n–p): Representative procedure for 2-(phenylethynyl)benzophenone (**1n**):[40] A dry 10 mL Schlenk flask was charged with 1 eq of 2-iodobenzophenone (1.000 g, 3.244 mmol), placed under argon and dissolved in 8 mL THF. A dry 100 mL Schlenk flask was charged with 0.1 eq CuI (61 mg, 0.32 mmol) and 0.04 eq $(Ph_3P)_2PdCl_2$ (91 mg, 0.13 mmol) and placed under argon. The benzophenone solution was transferred into the catalyst flask at which point additional THF (2 x 8 mL) and DIPA (8 mL) were successively used to transfer any residual benzophenone, and the solution was stirred at room temperature for 40 min. Degassed phenylacetylene (0.40 mL, 3.6 mmol, 1.1 eq) was added over a 2 h period *via* syringe and further stirred for a total of 24 h. The reaction was filtered through a pad of silica, and the solvents were removed *in vacuo* to provide a brown oil. Column chromatography on silica (2:1 hexanes/CH_2Cl_2) provided **1n** as an orange oil (593 mg, 2.10 mmol, 65%) that solidified upon standing to a orange-brown powdery solid and was used without further purification. mp 45.0-47.0°C. ^{1}H NMR (500 MHz, $CDCl_3$) δ: 7.89 (d, 2H, J = 7.0 Hz), 7.53 (m, 7H), 7.22 (m, 3H),

7.04 (d, 2H, J = 7.0 Hz). ^{13}C NMR (125 MHz, $CDCl_3$) δ: 197.3, 141.7, 137.6, 133.4, 132.8, 131.6, 130.52, 130.46, 128.9, 128.6 (2C), 128.40, 128.28, 122.8, 122.1, 95.4, 87.7. FT-IR (KBr) ν/cm^{-1}: 3062, 2216, 1659, 1596, 1578, 1492, 1450, 1320, 1291, 1244, 1151, 928, 752, 692, 634. UV-Vis (CH_3CN) λ_{max}/nm (log ε): 195 (4.76), 256 (4.41), 282 (s, 4.30). HR-MS (EI): found m/z = 282.1039 ± 0.0008 (M^+); calc. for $C_{21}H_{14}O$: 282.1045.

2-(4-Methylphenylethynyl)benzophenone (**1o**): Prepared as **1n** from 2-iodobenzophenone (1.002 g, 3.252 mmol) and 4-ethynyltoluene (0.45 mL, 3.6 mmol), column chromatography (2:1 hexanes/CH_2Cl_2) provided **1o** as a reddish brown solid (523 mg, 1.76 mmol, 54%) which was used without further purification. mp 67.5-69.5°C. ^{1}H NMR (500 MHz, $CDCl_3$) δ: 7.88 (d, 2H, J = 7.0 Hz), 7.51 (m, 7H), 7.01 (d, 2H, J = 8.0 Hz), 6.92 (d, 2H, J = 8.0 Hz), 2.30 (s, 3H). ^{13}C NMR (125 MHz, $CDCl_3$) δ: 197.4, 141.6, 138.8, 137.6, 133.3, 132.6, 131.5, 130.50, 130.43, 129.0, 128.86, 128.56, 128.2, 122.2, 119.7, 95.7, 87.1, 21.7. FT-IR (KBr) ν/cm^{-1}: 3062, 3018, 2916, 2202, 1662, 1594, 1509, 1449, 1318, 1288, 1245, 1152, 935, 922, 813, 767, 707, 635. UV-Vis (CH_3CN) λ_{max}/nm (log ε): 194 (4.75), 256 (4.41), 286 (4.33), 293 (4.31). HR-MS (EI): found m/z = 296.1197 ± 0.0009 (M^+); calc. for $C_{22}H_{16}O$: 296.1201.

2-(Butylethynyl)benzophenone (**1p**): Prepared as **1n** from 2-iodobenzophenone (1.001 g, 3.249 mmol) and 1-hexyne (0.42 mL, 3.7 mmol), column chromatography (2:1 hexane/CH_2Cl_2) provided **1p** as a reddish-brown oil (741 mg, 2.82 mmol, 87%). ^{1}H NMR (500 MHz, $CDCl_3$) δ: 7.82 (d, 2H, J = 7.5 Hz), 7.56 (t, 1H, J = 7.5 Hz), 7.44 (m, 5H), 7.37 (m, 1H), 2.10 (t, 2H, J = 6.5 Hz), 1.17 (m, 4H), 0.77 (t, 2H, J = 7.0 Hz). ^{13}C NMR (125 MHz, $CDCl_3$) δ: 197.6, 141.9, 137.4, 133.1, 132.7, 130.28, 130.12, 128.39, 128.20, 127.5, 122.6, 96.7, 78.7, 30.4, 21.9, 19.1, 13.7. FT-IR (neat) ν/cm^{-1}: 3067, 2957, 2931, 2863, 2222, 1668, 1596, 1449, 1316, 1289, 1158, 928, 756, 704. HR-MS (EI): found m/z = 262.1354 ± 0.0008 (M^+); calc. for $C_{19}H_{18}O$: 262.1358.

Isobenzopyrylium salts (2): Representative procedure.

One eq. of an alkyne precursor **1** was added to a dry Schlenk flask and placed under argon. A 0.005 M solution of the alkyne in CH_2Cl_2 was prepared and stirred vigorously as 20 eq. of the acid (neat trifluoromethanesulfonic acid unless otherwise noted) was added dropwise. The reaction stirred at room temperature for 0.5–1.5 h at which point the salts were precipitated with diethyl ether or used for amination studies as described individually below. For NMR studies, chloroform-d (and CF_3SO_3D when specified) was used in lieu of CH_2Cl_2.

1-(*N,N*-Dimethylamino)-3-phenylisobenzopyrylium trifluoromethane sulfonate (**2c**): Starting from **1c** (101 mg, 0.406 mmol), the reaction stirred for 1h at which point solvent volume was reduced *in vacuo* by approx. 50%. **2c** was precipitated twice from diethyl ether followed by filtration to provide a greenish-yellow fluffy solid (102 mg, 0.254 mmol, 63%). mp 204.5–206.0°C. ^{1}H NMR (500 MHz, CD_3CN) δ: 8.44 (d, 1H, *J* = 8.5 Hz), 8.03 (t, 1H, *J* = 8.0 Hz), 7.96 (m, 2H), 7.88 (d, 1H, *J* = 8.0 Hz), 7.77 (t, 1H, *J* = 8.5 Hz), 7.63 (s, 1H), 7.61 (m, 3H), 3.87 (s, 3H), 3.69 (s, 3H). ^{13}C NMR (125 MHz, CD_3CN) δ: 165.3, 152.5, 139.2, 138.4, 132.3, 131.3, 130.8, 130.5, 130.4, 129.0, 126.5, 122.2 (q, 319 Hz), 116.3, 106.6, 46.0, 43.6. FT-IR (KBr): ν/cm^{-1}: 1661, 1610, 1484, 1420, 1266 (vs). UV-Vis (CH_3CN) λ_{max}/nm (log ε): 271 (4.38), 303 (s, 4.20), 370 (3.94). Emission (CH_3CN) λ_{max}/nm: 474. HR-MS (EI): found *m/z* = 250.1226 ± 0.0007 (M^+); calc. for $C_{17}H_{16}NO^+$: 250.1232. HR-MS [FAB (-)]: found *m/z* = 148.9522 ± 0.0005 (M^-); calc. for $CF_3SO_3^-$: 148.9520. Anal.: calc. for $C_{18}H_{16}F_3NO_4S$: C, 54.13; H, 4.04; N, 3.51. Found: C, 53.90; H, 3.91; N, 3.75.

1-(*N,N*-dimethylamino)-3-(4-methylphenyl)isobenzopyrylium trifluoromethane sulfonate (**2d**): Starting from **1d** (103 mg, 0.390 mmol), the reaction stirred for 1h at which point solvent volume was reduced *in vacuo* by approx. 50%. **2d** was precipitated twice from diethyl ether followed by filtration to provide a greenish-yellow fluffy solid (104 mg, 0.251 mmol, 64%). mp 208-209°C. ^{1}H NMR (500 MHz, CD_3CN) δ: 8.43 (d, 1H, *J* = 8.5 Hz), 8.01 (t, 1H, *J* = 7.5 Hz), 7.85 (m, 2H), 7.75 (t, 1H, *J* = 8.0 Hz), 7.57 (s, 1H), 7.41 (d, 2H, *J* = 7.5 Hz), 3.86 (s, 3H), 3.67 (s, 3H), 2.43 (s, 3H). ^{13}C NMR (125 MHz, CD_3CN) δ: 165.2, 152.7, 143.1, 139.3, 138.26, 131.3, 131.0, 130.1, 128.8, 128.0, 126.4, 122.2 (q, *J* = 328 Hz), 116.1, 105.7, 46.0, 43.6, 21.6. FT-IR (KBr): ν/cm^{-1}: 1658, 1607, 1479, 1420, 1262 (s). UV-Vis (CH_3CN) λ_{max}/nm (log ε): 306 (s, 4.28), 376 (3.95). Emission (CH_3CN) λ_{max}/nm: 487. HR-MS (EI): found *m/z* = 264.1385 ± 0.0009 (M^+); calc. for $C_{18}H_{18}NO^+$: 264.1388. HR-MS [FAB (-)]: found *m/z* = 148.9519 ± 0.0005 (M^-); calc. for $CF_3SO_3^-$: 148.9520. Anal.: calc. for $C_{19}H_{18}F_3NO_4S$: C, 55.20; H, 4.39; N, 3.39. Found: C, 54.95; H, 4.20; N, 3.35.

3-(4-Decyloxyphenyl)-1-(*N,N*-dimethylamino)isobenzopyrylium trifluoromethane sulfonate (**2e**): Starting from **1e** (82 mg, 0.20 mmol), **2e** was precipitated twice from diethyl ether followed by filtration to provide a yellow fluffy solid (55.7 mg, 0.100 mmol, 50%). mp 136.5-138°C. ^{1}H NMR (500 MHz, CD_3CN) δ: 8.41 (d, 1H, *J* = 8.5 Hz), 7.99 (t, 1H, *J* = 8.0 Hz), 7.87 (d, 2H, *J* = 9.0 Hz), 7.82 (d, 1H, *J* = 7.0 Hz), 7.72 (td, 1H, *J* = 7.5, 1.0 Hz), 7.48 (s, 1H), 7.09 (d, 2H, *J* = 9.0 Hz), 4.07 (t, 2H, *J* = 6.5 Hz), 3.85 (s, 3H), 3.66 (s, 3H), 1.78 (quin, 2H, *J* = 6.5 Hz), 1.46 (quin, 2H, *J* = 6.5 Hz), 1.30 (m, 12H), 0.89 (t, 3H, *J* = 7.0 Hz). ^{13}C NMR (125 MHz, CD_3CN) δ: 165.3, 162.7, 152.9, 139.7, 138.3, 131.2, 129.8, 128.6, 128.3, 122.9, 122.2 (q, *J* = 319 Hz), 116.3, 115.8, 104.8, 69.4, 46.0, 43.5, 32.7, 30.4, 30.3, 30.1, 29.8, 26.7, 23.5,

14.5. FT-IR (KBr): ν/cm^{-1}: 1656, 1604, 1516, 1481, 1260 (s). UV-Vis (CH_3CN) λ_{max}/nm (log ε): 239 (4.16), 273 (4.32), 313 (4.39), 387 (4.03). Emission (CH_3CN) λ_{max}/nm: 527. HR-MS (EI): found *m/z* = 406.2736 ± 0.0012 (M^+); calc. for $C_{27}H_{36}NO_2^+$: 406.2746. HR-MS [FAB (-)]: found *m/z* = 148.9522 ± 0.0005 (M^-); calc. for $CF_3SO_3^-$: 148.9520. Anal.: calc. for $C_{28}H_{36}F_3NO_5S$: C, 60.52; H, 6.53; N, 2.52. Found: C, 60.18; H, 6.54; N, 2.58.

1-Ethoxy-3-phenylisobenzopyrylium tetrafluoroborate (**2g**): Starting from **1g** (103 mg, 0.412 mmol) and a 54% solution of HBF_4 in diethyl ether (2.5 mL, 18 mmol), **2g** was precipitated with diethyl ether alongside hydrolysis product **9g** to provide 136 mg of a pale yellow fluffy solid. The instability of this compound prevented isolation in pure form, so peaks attributed to **2g** were assigned by comparison with a pure sample of isocoumarin **9g**. Literature values for 3-phenylisocoumarin were consistent with those obtained for hydrolysis product **9g**. Using ^1H NMR integration ratios, 0.272 mmol of **2g** was obtained (66%). ^1H NMR (500 MHz, CD_3CN) δ: 8.54 (d, 1H, *J* = 8.5 Hz), 8.29 (td, 1H, *J* = 8.5, 1.0 Hz), 8.17 (s, 1H), 8.09 (d, 1H, *J* = 8.0 Hz), 8.04 (m, 2H), 7.96 (td, 1H, *J* = 7.0, 1.0 Hz), 7.67 (m, 3H), 5.27 (q, 2H, *J* = 7.0 Hz), 1.74 (t, 3H, *J* = 7.0 Hz).

1-Ethoxy-3-(4-methylphenyl)isobenzopyrylium tetrafluoroborate (**2h**): Starting from **1h** (108 mg, 0.409 mmol) and a 54% solution of HBF_4 in diethyl ether (1.15 mL, 8.35 mmol), **2h** was precipitated with diethyl ether alongside hydrolysis product **9h** to provide 138 mg of a pale yellow fluffy solid. The instability of this compound prevented isolation in pure form, so peaks attributed to **2h** were assigned by comparison with a pure sample of isocoumarin **9h**. Literature values for 3-(4-methylphenyl)isocoumarin were consistent with those obtained for hydrolysis product **9h**. Using ^1H NMR integration ratios, 0.360 mmol of **2h** was obtained (88%). ^1H NMR (500 MHz, CD_3CN) δ: 8.51 (d, 1H, *J* = 8.0 Hz), 8.27 (td, 1H, *J* = 8.0, 1.0 Hz), 8.10 (s, 1H), 8.06 (d, 1H, *J* = 8.5 Hz), 7.93 (m, 3H), 7.47 (d, 2H, *J* = 8.0 Hz), 5.25 (q, 2H, *J* = 7.0 Hz), 2.46 (s, 3H), 1.73 (t, 3H, *J* = 7.0 Hz).

3-Phenylisobenzopyrylium trifluoromethane sulfonate (**2k**): Generated *in situ* from **1k** (3.2 mg, 0.016 mmol) in 2 mL of $CDCl_3$ to provide a greenish-yellow fluorescent intermediate which could not be isolated but was observed by ^1H NMR approx 1 hr into the reaction. Further structural proof was obtained after exposure to ammonia: characterization data for **3k** was consistent with literature values. ^1H NMR (500 MHz, $CDCl_3$) δ: 10.18 (s, 1H), 8.67 (s, 1H), 8.57 (d, 1H, *J* = 8.5 Hz), 8.54 (t, 1H, *J* = 8.5 Hz), 8.29 (d, 1H, *J* = 8.5 Hz), 8.16 (m, 3H), 7.78 (t, 1H, *J* = 7.0 Hz), 7.71 (t, 2H, *J* = 7.5 Hz).

4-*Deuterio*-3-phenylisobenzopyrylium trifluoromethane sulfonate: Generated as **2k** using TfOD. ^{1}H NMR (500 MHz, $CDCl_3$) δ: 10.19 (s, 1H), 8.58 (d, 1H, *J* = 8.5 Hz), 8.54 (td, 1H, *J* = 8.0, 1.0 Hz), 8.29 (d, 1H, *J* = 8.5 Hz), 8.16 (m, 3H), 7.78 (t, 1H, *J* = 7.5 Hz), 7.71 (t, 2H, *J* = 8.0 Hz).

3-(4-Methylphenyl)isobenzopyrylium trifluoromethane sulfonate (**2l**): Generated *in situ* from **1l** (3.4 mg, 0.015 mmol) in $CDCl_3$ (2 mL) to provide an intensely yellow fluorescent intermediate which could not be isolated but was observed by ^{1}H NMR approx. 1 hr into the reaction. Further structural proof was obtained after exposure to ammonia: characterization data for **3l** was consistent with literature values. ^{1}H NMR (500 MHz, $CDCl_3$) δ: 10.11 (s, 1H), 8.60 (s, 1H), 8.52 (d, 1H, *J* = 8.5 Hz), 8.49 (td, 1H, *J* = 8.5, 1.0 Hz), 8.24 (d, 1H, *J* = 8.5 Hz), 8.11 (t, 1H, *J* = 7.0 Hz), 8.04 (d, 2H, *J* = 8.5 Hz), 7.51 (d, 2H, *J* = 8.0 Hz), 2.53 (s, 3H).
4-*Deuterio*-3-(4-methylphenyl)isobenzopyrylium trifluoromethane sulfonate: Generated as **2l** using TfOD. ^{1}H NMR (500 MHz, $CDCl_3$) δ: 10.12 (s, 1H), 8.52 (d, 1H, *J* = 8.0 Hz), 8.49 (t, 1H, *J* = 7.0 Hz), 8.24 (d, 1H, *J* = 8.5 Hz), 8.12 (t, 1H, *J* = 8.0 Hz), 8.04 (d, 2H, *J* = 8.5 Hz), 7.51 (d, 2H, *J* = 7.5 Hz), 2.53 (s, 3H).

3-(4-Decyloxyphenyl)isobenzopyrylium trifluoromethane sulfonate (**2m**): Generated *in situ* from **1m** (5.3 mg, 0.015 mmol) in $CDCl_3$ (2 mL) of to provide an intense burgandy intermediate which could not be isolated but was observed by ^{1}H NMR after 10 min (NMR data listed below), 60 min (3:1 mixture of products) and 4 d into the reaction (one product, no evidence for alkoxy protons). Further structural proof was obtained after exposure to ammonia: characterization data for **3m** was consistent with the proposed isoquinoline structure. ^{1}H NMR (500 MHz, $CDCl_3$) δ: 10.02 (s, 1H), 8.51 (s, 1H), 8.43 (m, 2H), 8.18 (d, 1H, *J* = 7.5 Hz), 8.11 (d, 2H, *J* = 9.0 Hz), 8.05 (t, 1H, *J* = 8.5 Hz), 7.19 (d, 2H, *J* = 9.0 Hz), 4.18 (t, 2H, *J* = 6.5 Hz), 1.86 (quin, 2H, *J* = 7.5 Hz), 1.48 (quin, 2H, *J* = 7.5 Hz), 1.29 (bm, 12H), 0.88 (t, 3H, *J* = 7.0 Hz).

1,3-Diphenylisobenzopyrylium trifluoromethane sulfonate (**2n**): Starting from **1n** (101 mg, 0.358 mmol) and following addition of diethyl ether, the solution was stored overnight at 0°C. The resulting solids were filtered and washed with ether to give **2n** as an orange powder (114 mg, 0.264 mmol, 74%). mp 189.5-190.0°C. ^{1}H NMR (500 MHz, CD_3CN) δ: 8.80 (s, 1H), 8.68 (d, 1H, *J* = 8.5 Hz), 8.46 (t, 1H, *J* = 7.0 Hz), 8.34 (d, 1H, *J* = 8.0 Hz), 8.23 (m, 4H), 8.09 (t, 1H, *J* = 7.5 Hz), 7.99 (t, 1H, *J* = 7.5 Hz), 7.87 (t, 2H, *J* = 8.5 Hz), 7.73 (m, 3H). ^{13}C NMR (125 MHz, CD_3CN) δ: 182.2, 161.8, 145.1, 144.1, 136.6, 134.2, 134.1, 134.0, 133.7, 131.0 (2 Cs), 130.5, 130.3, 129.4, 127.9, 124.3, 122.2 (q, *J* = 319 Hz), 116.5. FT-IR (KBr): ν/cm^{-1}: 1621, 1541, 1499, 1417, 1272 (vs). UV-Vis (CH_3CN) λ_{max}/nm (log ε): 228 (4.22), 267

(4.44), 303 (s, 4.36), 441 (3.99). HR-MS (EI): found m/z = 283.1126 ± 0.0008 (M^+); calc. for $C_{21}H_{15}O^+$: 283.1123. HR-MS [FAB (-)]: found m/z = 148.9522 ± 0.0005 (M^-); calc. for $CF_3SO_3^-$: 148.9520. Anal.: calc. for $C_{22}H_{15}F_3O_4S$: C, 61.11; H, 3.50. Found: C, 60.98; H, 3.45.

1,3-Diphenylisobenzopyrylium tetrafluoroborate:[29] Starting from **1n** (101 mg, 0.358 mmol), this salt was precipitated with diethyl ether followed by filtration to provide an orange solid used to compare with literature ^{13}C data (87.9 mg, 0.238 mmol, 66%). mp 241-242.5°C (dec). ^1H NMR (500 MHz, CD_3CN) δ: 8.80 (s, 1H), 8.68 (d, 1H, J = 8.5 Hz), 8.46 (t, 1H, J = 7.0 Hz), 8.34 (d, 1H, J = 8.5 Hz), 8.23 (m, 4H), 8.09 (t, 1H, J = 7.0 Hz), 7.99 (t, 1H, J = 7.5 Hz), 7.87 (t, 2H, J = 8.0 Hz), 7.73 (m, 3H). ^{13}C NMR (125 MHz, CD_3CN) δ: 182.2, 161.8, 145.1, 144.1, 136.6, 134.2, 134.1, 134.0, 133.7, 131.0 (2C), 130.5, 130.3, 129.4, 127.9, 124.3, 116.5. FT-IR (KBr): ν/cm^{-1}: 1619, 1540, 1502, 1417, 1056 (vs). UV-Vis (CH_3CN) λ_{max}/nm (log ε): 302 (4.36), 440 (4.01). Emission (CH_3CN) λ_{max}/nm: 538 (very weak). HR-MS (EI): found m/z = 283.1117 ± 0.0008 (M^+); calc. for $C_{21}H_{15}O^+$: 283.1123. HR-MS [FAB (-)]: found m/z = 87.0028 ± 0.0003 (M^-); calc. for BF_4^-: 87.0029.

3-(4-Methylphenyl)-1-phenylisobenzopyrylium trifluoromethane sulfonate (**2o**): Starting from **1o** (100 mg, 0.338 mmol) and following addition of diethyl ether, the solution was stored at 0°C overnight. The precipitated solids were filtered off and washed with ether to provide **2o** as an orange solid (126 mg, 0.283 mmol, 84%). mp 220.5-221.5°C (sub). ^1H NMR (500 MHz, CD_3CN) δ: 8.76 (s, 1H), 8.66 (d, 1H, J = 9.0 Hz), 8.45 (t, 1H, J = 7.5 Hz), 8.32 (d, 1H, J = 8.5 Hz), 8.23 (d, 2H, J = 7.0 Hz), 8.14 (d, 2H, J = 8.0 Hz), 8.08 (t, 1H, J = 7.5 Hz), 8.00 (t, 1H, J = 7.5 Hz), 7.88 (t, 2H, J = 8.0 Hz), 7.55 (d, 2H, J = 8.0 Hz), 2.51 (s, 3H). ^{13}C NMR (125 MHz, CD_3CN) δ: 181.6, 162.1, 145.6, 145.3, 143.9, 136.4, 133.8, 133.8, 133.6, 131.7, 131.0, 130.5, 129.3, 127.9, 127.5, 124.1, 122.2 (q, J = 318 Hz), 115.9, 21.8. FT-IR (KBr): ν/cm^{-1}: 1621, 1540, 1499, 1418, 1265 (vs). UV-Vis (CH_3CN) λ_{max}/nm (log ε): 233 (4.23), 271 (4.41), 304 (4.35), 329 (s), 452 (3.98). HR-MS (FAB): found m/z = 297.1276 ± 0.0009 (M^+); calc. for $C_{22}H_{17}O$: 297.1279. HR-MS [FAB (-)]: found m/z = 148.9523 ± 0.0005 (M^-); calc. for $CF_3SO_3^-$: 148.9520. Anal.: calc. for $C_{23}H_{17}F_3O_4S$: C, 61.88; H, 3.84. Found: C, 61.93; H, 3.73.

Isoquinolines (3): representative procedures.

Method A: Starting from alkyne precursors **1**, the pyrylium salts **2** were prepared as described above at which point anhydrous ammonia was bubbled through the reaction mixture for 30-45 min, placed under a positive pressure of ammonia and stirred for a total of 20 h. The reaction mixture was washed with $NaHCO_3$ (aq) and NaCl (aq). The organic layer was separated, dried and removed *in vacuo* to provide a crude material which was purified on silica gel to yield the isoquinolines listed below.

Method B: the isolated salt **2** was placed under argon in a dry Schlenk flask and brought to a concentration of 0.005 M in CH_2Cl_2. The suspension was stirred vigorously to effect some dissolution, and anhydrous ammonia was bubbled through the flask for 30-45 min. The system was placed under a positive ammonia pressure and stirred for a total of 20 hr. Washing the organic phase as described for method A followed by column chromatography provided the desired isoquinolines.

For further purification, the isoquinolines were taken up in ether and precipitated as the hydrochloride salts upon addition of 12 M HCl. Rinsing the solids twice with ether and a basic workup (2M KOH, $NaHCO_3$ and NaCl) again provided the isoquinolines which were pure by ^1H and GC-MS (96%+). Reported yields are for products obtained after chromatography.

1-(*N,N*-Dimethylamino)-3-phenylisoquinoline (**3c**): Using **1c** (106 mg, 0.425 mmol) in method A followed by column chromatography (3:1 hexane/ethyl acetate) provided **3c** as a yellow oil (24 mg, 0.095 mmol, 22%). ^1H NMR (500 MHz, $CDCl_3$) δ: 8.19 (d, 2H, *J* = 7.5 Hz), 8.14 (d, 1H, *J* = 8.5 Hz), 7.79 (d, 1H, *J* = 8.5 Hz), 7.65 (s, 1H), 7.58 (td, 1H, *J* = 8.0, 1.0 Hz), 7.47 (m, 3H), 7.38 (t, 1H, *J* = 7.5 Hz), 3.20 (s, 6H). ^{13}C NMR (75 MHz, $CDCl_3$) δ: 161.4, 148.1, 140.0, 139.4, 129.6, 128.7, 128.3, 127.7, 126.8, 126.2, 125.4, 120.5, 110.3, 43.3. FT-IR (KBr) ν/cm^{-1}: 1618, 1561, 1501, 1385, 1344. HR-MS (EI): found *m/z* = 248.1309 ± 0.0007 (M^+); calc. for $C_{17}H_{16}N_2$: 248.1313.
Further elution with 2:1 hexane/ ethyl acetate provided 1-amino-3-phenylisoquinoline (**8c**) as a pale yellow solid (34 mg, 0.135 mmol, 32%). Characterization data below.

1-(*N,N*-Dimethylamino)-3-(4-methylphenyl)isoquinoline (**3d**): Using **2d** (49.5 mg, 0.120 mmol) in method B followed by column chromatography (2:1 hexane/CH_2Cl_2) provided **3d** as a yellow oil (9.4 mg, 0.036 mmol, 30%). ^1H NMR (500 MHz, $CDCl_3$) δ: 8.12 (d, 1H, *J* = 8.0 Hz), 8.08 (d, 2H, *J* = 8.0 Hz), 7.76 (d, 1H, *J* = 8.0 Hz), 7.61 (s, 1H), 7.56 (td, 1H, *J* = 7.0, 1.0 Hz), 7.43 (td, 1H, *J* = 7.0, 1.0 Hz), 7.28 (d, 2H, *J* = 8.0 Hz), 3.19 (s, 6H), 2.41 (s, 3H). ^{13}C NMR (125 MHz, $CDCl_3$) δ: 161.4, 148.3, 139.6, 138.2, 137.3, 129.6, 129.5, 127.6, 126.7, 126.3, 125.3, 120.4, 109.9, 43.2, 21.5. FT-IR (KBr): ν/cm^{-1}: 1616, 1561, 1515, 1497, 1385. HR-MS (EI): found *m/z* = 262.1464 ± 0.0008 (M^+); calc. for $C_{18}H_{18}N_2$: 262.1470.
Further elution with 3:1 hexane/ ethyl acetate afforded 1-amino-3-(4-methylphenyl)isoquinoline (**8d**) as a pale yellow oil which solidified upon standing (13 mg, 0.054 mmol, 45%). Characterization data below.

1-Ethoxy-3-phenylisoquinoline (**3g**):[41] The salt **2g** was prepared from **1g** (106 mg, 0.424 mmol) by as described above. The precipitate was filtered, washed with ether and immediately placed under argon.

Using method B followed by column chromatography (3:1 hexane/CH_2Cl_2) provided **3g** as a white oily solid (24.5 mg, 0.0298 mmol, 23%). ^{1}H NMR (500 MHz, $CDCl_3$) δ: 8.27 (d, 1H, *J* = 8.0 Hz), 8.16 (d, 2H, *J* = 7.5 Hz), 7.78 (d, 1H, *J* = 8.0 Hz), 7.68 (s, 1H), 7.64 (t, 1H, *J* = 7.0 Hz), 7.49 (m, 3H), 7.39 (t, 1H, *J* = 7.5 Hz), 4.72 (q, 2H, *J* = 7.0 Hz), 1.56 (t, 3H, *J* = 7.0 Hz). ^{13}C NMR (75 MHz, $CDCl_3$) δ: 160.2, 147.9, 139.7, 138.9, 130.6, 128.7, 128.4, 126.8, 126.7 (2C), 126.4, 124.4, 119.1, 110.3, 62.2, 15.0. FT-IR (KBr) ν/cm^{-1}: 1626, 1574, 1500, 1378. HR-MS (EI): found *m/z* = 249.1157 ± 0.0007 (M^+); calc. for $C_{17}H_{15}NO$: 249.1154.

Gradually increasing the elution solvent polarity led to the isolation of 44 mg of a solid containing primarily the isocoumarin **9g** (65% by GC-MS, 30% estimated overall yield). Further elution provided **8g** (11 mg, 0.047 mmol, 11%) as a yellowish solid.

1-Ethoxy-3-(4-methylphenyl)isoquinoline (**3h**): Using **1 h** (102 mg, 0.384 mmol) in method A with ethereal HBF_4 in lieu of TfOH followed by chromatography (2:1 hexane/CH_2Cl_2) provided **3h** as a oily white solid (21 mg, 0.079 mmol, 21%). Further elution with 4:1 hexane/ ethyl acetate also provided free-amine **8h** (59 mg, 0.25 mmol, 66%). ^{1}H NMR (500 MHz, $CDCl_3$) δ: 8.25 (d, 1H, *J* = 8.0 Hz), 8.05 (d, 2H, *J* = 8.0 Hz), 7.76 (d, 1H, *J* = 8.0 Hz), 7.63 (m, 2H), 7.48 (t, 1H, *J* = 8.0 Hz), 7.28 (d, 2H, *J* = 8.0 Hz), 4.71 (q, 2H, *J* = 7.0 Hz), 2.42 (s, 3H), 1.55 (t, 3H, *J* = 6.5 Hz). ^{13}C NMR (125 MHz, $CDCl_3$) δ: 160.2, 148.1, 139.1, 138.4, 137.0, 130.6, 129.5, 126.7 (2C), 126.2, 124.4, 119.1, 109.8, 62.1, 21.5, 14.9. FT-IR (KBr): ν/cm^{-1}: 1626, 1576, 1411, 1377. HR-MS (EI): found *m/z* = 263.1304 ± 0.0007 (M^+); calc. for $C_{18}H_{17}NO$: 263.1310.

3-Phenylisoquinoline (**3k**): Using **1k** (106 mg, 0.515 mmol) in method A followed by column chromatography (7.5:1 hexane/ethyl acetate) provided **3k** as yellow flakes (78 mg, 0.38 mmol, 74%). mp 101-101.5°C (lit.[28] 102.5-103.5°C). ^{1}H NMR (500 MHz, $CDCl_3$) δ: 9.35 (s, 1H), 8.13 (d, 2H, *J* = 7.5 Hz), 8.08 (s, 1H), 8.00 (d, 1H, *J* = 8.0 Hz), 7.88 (d, 1H, *J* = 8.5 Hz), 7.71 (t, 1H, *J* = 7.0 Hz), 7.59 (t, 1H, *J* = 7.5 Hz), 7.52 (t, 2H, *J* = 8.0 Hz), 7.42 (t, 1H, *J* = 7.5 Hz). ^{13}C NMR (125 MHz, $CDCl_3$) δ: 152.6, 151.5, 139.8, 136.8, 130.7, 128.99, 128.71, 127.95, 127.76, 127.26, 127.20, 127.11, 116.7. FT-IR (KBr): ν/cm^{-1}: 3027, 2957, 2925, 2855, 1728, 1624, 1589, 1492, 1453, 1280, 1130, 1072, 962, 942, 884, 786, 762, 688. HR-MS (EI): found *m/z* = 205.0890 ± 0.0006 (M^+); calc. for $C_{15}H_{11}N$: 205.0891.

3-(4-Methylphenyl)isoquinoline (**3l**): Using **1l** (101 mg, 0.458 mmol) in method A followed by purification on silica gel (5:1 hexane/ethyl acetate) provided **3l** as a light brown solid (67.2 mg, 0.306 mmol, 67%). mp 74-75°C (lit.[28] 76-76.5°C). ^{1}H NMR (500 MHz, $CDCl_3$) δ: 9.33 (s, 1H), 8.05 (s, 1H), 8.03 (d, 2H, *J* = 8.5 Hz), 7.99 (d, 1H, *J* = 8.5 Hz), 8.87 (d, 1H, *J* = 8.0 Hz), 7.69 (td, 1H, *J* = 7.0, 1.0 Hz),

7.57 (t, 1H, 8.0 Hz), 7.32 (d, 2H, J = 8.0 Hz), 2.43 (s, 3H). ^{13}C NMR (125 MHz, $CDCl_3$) δ: 152.5, 151.5, 138.6, 136.99, 136.88, 130.6, 129.7 (3C), 127.84, 127.75, 127.0, 116.2, 21.48. FT-IR (KBr): ν/cm^{-1}: 3028, 2912, 2853, 1624, 1585, 1515, 1446, 1279, 1177, 1017, 944, 883, 822, 748, 716, 680. HR-MS (EI): found m/z = 219.1046 ± 0.0007 (M^+); calc. for $C_{16}H_{13}N$: 219.1048.

3-(4-Decyloxyphenyl)isoquinoline (**3m**): Using **1m** (49.9 mg, 0.138 mmol) in method A followed by column chromatography (9:1 hexane/ethyl acetate) provided **3m** as a light brown solid (32.2 mg, 0.0891 mmol, 65%). Further purification as described above gave **3m** as a white solid (16 mg, 0.043 mmol, 31%). mp 78.5-79°C. ^{1}H NMR (500 MHz, $CDCl_3$) δ: 9.30 (s, 1H), 8.07, d, 2H, J = 8.5 Hz), 7.99 (s, 1H), 7.97 (d, 1H, J = 8.5 Hz), 7.84 (d, 1H, J = 8.0 Hz), 7.67 (t, 1H, J = 7.0 Hz), 7.55 (t, 1H, J = 7.5 Hz), 7.03 (d, 2H, J = 8.5 Hz), 4.03 (t, 2H, J = 7.0 Hz), 1.82 (quin, 2H, J = 6.5 Hz), 1.48 (quin, 2H, J = 6.5 Hz), 1.28 (bm, 12H), 0.89 (t, 3H, J = 6.5 Hz). ^{13}C NMR (125 MHz, $CDCl_3$) δ: 160.0, 152.5, 151.4, 137.0, 132.2, 130.6, 128.4, 127.8, 127.6, 127.0, 126.8, 115.5, 115.0, 68.3, 32.1, 29.82, 29.79, 29.66, 29.56, 29.52, 26.3, 22.9, 14.4. FT-IR (KBr): ν/cm^{-1}: 1625, 1605, 1512, 1446, 1251. HR-MS (EI): found m/z = 361.2402 ± 0.0010 (M^+); calc. for $C_{25}H_{31}NO$: 361.2406.

1,3-Diphenylisoquinoline (**3n**): Using **2n** (80.2mg, 0.186 mmol) in method B followed by column chromatography (1:1 hexane/CH_2Cl_2) provided **3n** as an oily opaque solid (19.8 mg, 0.0704 mmol, 38%). mp 73-74.5°C (lit.[42] 71-73°C). ^{1}H NMR (500 MHz, $CDCl_3$) δ: 8.22 (d, 2H, J = 7.5 Hz), 8.13 (d, 1H, J = 8.5 Hz), 8.08 (s, 1H), 7.94 (d, 1H, J = 8.5 Hz), 7.82 (d, 2H, J = 6.5 Hz), 7.68 (t, 1H, J = 7.5 Hz), 7.53 (m, 6H), 7.40 (t, 1H, J = 7.5 Hz). ^{13}C NMR (125 MHz, $CDCl_3$) δ: 160.5, 150.3, 140.0, 139.8, 138.0, 130.4, 130.2, 128.89, 128.78, 128.65, 128.46, 127.72, 127.63, 127.3, 127.1, 126.0, 115.9. FT-IR (KBr): ν/cm^{-1}: 3048, 2960, 2931, 2844, 1619, 1560, 1497, 1386, 1336, 1138, 978, 876, 775, 766, 691. HR-MS (EI): found m/z = 281.1199 ± 0.0008 (M^+); calc. for $C_{21}H_{15}N$: 281.1205.

3-(4-Methylphenyl)-1-phenylisoquinoline (**3o**): Using **1o** (99.8 mg, 0.337 mmol) in method A followed by column chromatography (2:2 hexane/CH_2Cl_2) provided **3o** as a pale orange solid (66.8 mg, 0.226 mmol, 67%). mp 116-117°C. ^{1}H NMR (500 MHz, $CDCl_3$) δ: 8.12 (d, 3H, J = 8.0 Hz), 8.04 (s, 1H), 7.92 (d, 1H, J = 8.5 Hz), 7.81 (d, 2H, J = 7.5 Hz), 7.67 (t, 1H, J = 7.0 Hz), 7.52 (m, 4H), 7.30 (d, 2H, J = 7.5 Hz), 2.42 (s, 3H). ^{13}C NMR (125 MHz, $CDCl_3$) δ: 160.4, 150.4, 140.1, 138.5, 138.0, 137.0, 130.4, 130.1, 129.6, 128.7, 128.5, 127.71, 127.57, 127.1, 126.9, 125.8, 115.4, 21.5. FT-IR (KBr): ν/cm^{-1}: 1621, 1562, 1516, 1445, 1386. HR-MS (EI): found m/z = 295.1356 ± 0.0009 (M^+); calc. for $C_{22}H_{17}N$: 295.1361.

2,5-Bis(4-decyloxyphenylethynyl)-1,4-di(*N,N*-dioctylcarbamoyl)benzene (**6**): A 10 mL Schlenk flask was charged with **5** (400.4 mg, 0.4625 mmol), $(Ph_3P)_2PdCl_2$ (18 mg, 0.026 mmol) and CuI (11 mg, 0.056 mmol) and placed under argon. THF (2 mL) and DIPA (1 mL) were added, and the solution was stirred at room temperature during the addition of a solution of 4-decyloxyphenylacetylene (254 mg. 0.983 mmol) in THF (0.5 mL). After addition, very thick precipitates formed, and toluene was added to facilitate stirring (1 mL). After 3 h at room temperature, the reaction was diluted with ether and washed with NaCl (x3). The organics were dried and removed to provide a crude brown solid. Subsequent purification on silica gel (9:1 hexane/EtOAc) yielded a yellowish solid (310 mg, 0.28 mmol, 60%). ^{1}H NMR (250 MHz, $CDCl_3$): 7.42 (s, 2H), 7.38 (d, 4H, J = 8.7 Hz), 6.83 (d, 4H, J = 8.8 Hz), 3.95 (t, 4H, J = 6.5 Hz), 3.75 (bm, 2H), 3.16 (bm, 6H), 1.0-1.9 (bm, 80H), 0.85 (m, 18H). ^{13}C NMR (75 MHz, $CDCl_3$): 168.9, 159.8, 139.8, 133.4, 130.2, 120.5, 114.67, 114.63, 95.2, 85.2, 68.3, 48.8, 44.9, 32.1, 31.9, 29.77, 29.71, 29.60, 29.53, 29.44, 29.39, 29.32, 28.8, 27.9, 27.4, 26.9, 26.2, 22.88, 22.83, 14.34, 14.28. FT-IR (KBr): ν/cm^{-1}: 2923, 2853, 2212, 1636, 1603, 1512, 1249, 1173, 837. HR-MS (FAB): found m/z = 1125.9304 $(M+H)^+$; calc. for $C_{76}H_{120}N_2O_4$+H: 1125.9326.

3,7-Bis(4-decyloxyphenylethynyl)-1,5-bis(*N,N*-dioctylcarbamoyl)-2,6-dioxanthracene bis (tetrafluoro borate) (**7**): A 100 mL Schlenk flask was charged with **6** (80.3 mg, 0.0713 mmol) and placed under argon. After the addition of CH_2Cl_2 (15 mL), the solution was stirred vigorously as HBF_4 (0.50 mL of a 40% solution in diethyl ether, 3.6 mmol) was added dropwise. The reaction stirred for 1h at which point diethyl ether was added. The intensely colored material that precipitated was collected by filtration and washed with ether to provide a fluffy burgundy solid product (74.7 mg, 0.0574 mmol, 81%). ^{1}H NMR (300 MHz, CD_3CN): 8.32 (s, 2H), 7.84 (d, 4H, J = 8.7 Hz), 7.51 (s, 2H), 7.13 (d, 4H, J = 9.0 Hz), 4.10 (m, 12H), 1.80 (m, 4H), 1.7-1.2 (bm, 76H), 0.89 (m, 18H). UV-Vis ($CHCl_3$) λ/nm (log ε): 302 (4.40), 389 (4.74), 539 (3.79).

1-Amino-3-phenylisoquinoline (**8c** and **8g**):[43] mp 95.5-96.5°C (lit. 97.5-99°C). ^{1}H NMR (500 MHz, $CDCl_3$) δ: 8.06 (d, 2H, J = 7.0 Hz), 7.81 (d, 1H, J = 8.0 Hz), 7.78 (d, 1H, J = 8.5 Hz), 7.63 (t, 1H, J = 7.0 Hz), 7.51 (s, 1H), 7.47 (m, 3H), 7.37 (t, 1H, J = 7.5 Hz), 5.19 (bs, 2H). ^{13}C NMR (75 MHz, $CDCl_3$) δ: 156.0, 149.7, 140.0, 138.3, 130.4, 128.7, 128.3, 127.7, 127.0, 126.0, 122.7, 117.1, 109.0. FT-IR (KBr) ν/cm^{-1}: 3459, 3359, 3057, 1617, 1564, 1498, 1425, 1343, 1206, 1075, 1032, 770, 690. HR-MS (EI): found m/z = 220.1002 ± 0.0020 (M^+); calc. for $C_{15}H_{12}N_2$: 220.1000.

1-Amino-3-(4-methylphenyl)isoquinoline (**8d** and **8h**): mp 105.5-106.5°C. ^{1}H NMR (500 MHz, $CDCl_3$) δ: 7.96 (d, 2H, J = 8.5 Hz), 7.71 (m, 2H), 7.56 (t, 1H, J = 7.5 Hz), 7.44 (s, 1H), 7.38 (t, 1H, J = 7.0 Hz),

7.26 (d, 2H, J = 8.0 Hz), 5.29 (bs, 2H), 2.39 (s, 3H). ^{13}C NMR (125 MHz, $CDCl_3$) δ: 156.1, 149.8, 138.4, 138.2, 137.3, 130.3, 129.5, 127.6, 126.9, 125.8, 122.8, 117.0, 108.5, 21.5. FT-IR (KBr) ν/cm^{-1}: 3487, 3453, 3290, 1620, 1561, 1495, 1432. HR-MS (EI): found m/z = 234.1155 ± 0.0007 (M^+); calc. for $C_{16}H_{14}N_2$: 234.1157.

1-Amino-3-(4-decyloxyphenyl)isoquinoline (**8e**): Using **1e** (49 mg, 0.12 mmol) in method A followed by column chromatography (4:1 hexane/ethyl acetate) provided **8e** as a clear oil (25.4 mg, 0.0675 mmol, 52%). Purification as described above provided **8e** as a white solid (13.4 mg, 0.0356 mmol, 27%). mp 66-67.5°C. ^{1}H NMR (500 MHz, $CDCl_3$) δ: 7.99 (d, 2H, J = 8.5 Hz), 7.79 (d, 1H, J = 8.0 Hz), 7.73 (d, 1H, J = 8.0 Hz), 7.60 (t, 1H, J = 7.5 Hz), 7.43 (t, 1H, J = 7.5 Hz), 7.41 (s, 1H), 6.98 (d, 2H, J = 8.5 Hz), 5.26 (s, 2H), 4.01 (t, 2H, J = 6.5 Hz), 1.81 (quin, 2H, J = 7.5 Hz), 1.47 (quin, 2H, J = 7.5 Hz), 1.28 (bm, 12H), 0.89 (t, 3H, J = 6.5 Hz). ^{13}C NMR (125 MHz, $CDCl_3$) δ: 159.7, 156.0, 149.4, 138.6, 132.3, 130.5, 128.2, 127.6, 125.8, 122.8, 116.8, 114.8, 108.0, 68.3, 32.1, 29.81, 29.79, 29.66, 29.56, 29.51, 26.3, 22.9, 14.36. FT-IR (KBr) ν/cm^{-1}: 3466, 3393, 3347, 1605, 1563, 1513, 1420. HR-MS (EI): found m/z = 376.2518 ± 0.0011 (M^+); calc. for $C_{25}H_{32}N_2O$: 376.2515.

3-Phenylisocoumarin (**9g**): A 200 mL Schlenk flask was charged with **1g** (109 mg, 0.435 mmol) and placed under argon. CH_2Cl_2 (90 mL) was transferred to the flask followed by the dropwise addition of a 54% solution of HBF_4 in diethyl ether (1.1 mL, 8.0 mmol). After stirring for 1 h at room temperature, diethyl ether was added, and the precipitated solids were removed by filtration. The solids were placed into an Erlenmeyer flask with ether (100 mL) and NaCl (aq, 100 mL) and stirred for 30 min. Upon complete hydrolysis, the ether layer was washed NaCl (x3), dried and removed *in vacuo* to provide **9g** as a white solid (79.9 mg, 0.360 mmol, 83%). mp 85-86°C (lit.[28a] 86-86.5°C). ^{1}H NMR (500 MHz, CD_3CN) δ: 8.22 (d, 1H, J = 8.0 Hz), 7.90 (d, 2H, J = 7.0 Hz), 7.80 (td, 1H, J = 8.0, 1.5 Hz), 7.63 (d, 1H, J = 8.0 Hz), 7.52 (m, 4H), 7.21 (s, 1H). ^{13}C NMR (125 MHz, $CDCl_3$) δ: 162.5, 153.8, 137.7, 135.1, 132.1, 130.2, 129.8, 129.0, 128.3, 126.2, 125.4, 120.7, 102.0. FT-IR (KBr) ν/cm^{-1}: 3106, 3033, 2917, 1720, 1639, 1483, 1447, 1239, 1071, 1028, 761, 685. HR-MS (EI): found m/z = 222.0679 ± 0.0007 (M^+); calc. for $C_{15}H_{10}O_2$: 222.0681.

3-(4-Methylphenyl)isocoumarin (**9h**): A 500 mL Schlenk flask was charged with **1h** (103 mg, 0.388 mmol) and placed under argon. CH_2Cl_2 (100 mL) was transferred to the flask followed by the dropwise addition of TfOH (0.52 mL, 5.9 mmol). After stirring for 3 h at room temperature, NaCl (aq) was added and the reaction was stirred overnight. The organic layer was washed NaCl (x3), dried and removed in vacuo to provide a crude material further purified on silica gel (2:1 CH_2Cl_2/hexanes) to yield **9h** as a

white powder (86.9 mg, 0.368 mmol, 95%). mp 113-114.5°C (lit.[28b] 116°C). ^{1}H NMR (500 MHz, $CDCl_3$) δ: 8.31 (d, 1H, *J* = 8.5 Hz), 7.79 (d, 2H, *J* = 8.5 Hz), 7.72 (td, 1H, *J* = 6.5, 1.5 Hz), 7.49 (m, 2H), 7.28 (d, 2H, *J* = 8.0 Hz), 6.92 (s, 1H), 2.41 (s, 3H). ^{13}C NMR (125 MHz, $CDCl_3$) δ: 162.7, 154.1, 140.5, 137.9, 135.0, 129.87, 129.77, 129.41, 128.1, 126.1, 125.4, 120.6, 101.3, 21.6. FT-IR (KBr): ν/cm^{-1}: 3077, 3033, 2917, 1733, 1630, 1607, 1511, 1482, 1299, 1236, 1067, 1008, 817, 753, 689, 527. HR-MS (EI): found *m/z* = 236.0835 ± 0.0007; calc. for $C_{16}H_{12}O_2$: 236.0837.

3-(4-Decyloxyphenyl)isocoumarin (**9i**): A 200 mL Schlenk flask was charged with **1i** (21 mg, 0.051 mmol) and placed under argon. CH_2Cl_2 (30 mL) was transferred to the flask followed by the dropwise addition of a 54% soltuion of HBF_4 in diethyl ether (0.35 mL, 2.5 mmol). After stirring for 1 h at room temperature, diethyl ether was added at which point the solution's fluorescence changed from yellow to purple-blue. The solids were filtered off but apparently hydrolyzed immediately to **9i**. Purification on silica gel (3:2 CH_2Cl_2/ hexane) provided **9i** as a yellowish-white solid (13 mg, 0.034 mmol, 67%). mp 67.5-69°C. ^{1}H NMR (500 MHz, $CDCl_3$) δ: 8.29 (d, 1H, *J* = 8.5 Hz), 7.82 (d, 2H, *J* = 8.5 Hz), 7.70 (td, 1H, *J* = 7.5, 1.0 Hz), 7.46 (m, 2H), 6.96 (d, 2H, *J* = 8.5 Hz), 6.84 (s, 1H), 4.01 (t, 2H, *J* = 6.5 Hz), 1.81 (quin, 2H, *J* = 7.0 Hz), 1.47 (quin, 2H, *J* = 7.5 Hz), 1.28 (bm, 12H), 0.88 (t, 3H, *J* = 6.5 Hz). ^{13}C NMR (125 MHz, $CDCl_3$) δ: 162.5, 160.9, 154.0, 138.2, 135.0, 129.9, 127.8, 127.0, 125.9, 124.5, 120.5, 114.9, 100.3, 68.4, 32.1, 29.79, 29.77, 29.60, 29.54, 29.39, 26.23, 22.9, 14.4. FT-IR (KBr) ν/cm^{-1}: 2921, 2852, 1723, 1633, 1515, 1260, 1236, 1180, 1066, 1017, 828. HR-MS (EI): found *m/z* = 378.2204 ± 0.0011 (M^+); calc. for $C_{25}H_{30}O_3$: 378.2195.

2,5-Di(phenylethynyl)terephthaldehyde (**10**): A dry 25 mL Schlenk flask was placed under argon and filled with THF (10 mL). After cooling to -78°C a solution of 1.7 M *t*-butyllithium in pentane (3.25 mL, 5.53 mmol) was added, and the solution was stirred for 5 min. A solution of 1,4-di(phenylethynyl)-2,5-dibromobenzene (229 mg, 0.686 mmol) in dry THF (5 mL) under argon was transferred dropwise to the *t*-BuLi solution, and the reaction was stirred at -78°C for 1h at which point dry DMF (1 mL) was added rapidly. The reaction was allowed to warm to room temperature and quenched with NH_4Cl. After dilution with ether, the organic layer was washed with NH_4Cl and NaCl, dried and removed *in vacuo* to provide a fibrous bright yellow solid. Chromatography on silica (2:1 hexane/CH_2Cl_2) provided the product as a yellow powder (200.2 mg, 0.5987 mmol, 87%). mp 181-182°C (lit.[44] 179-181°C). ^{1}H NMR (300 MHz, $CDCl_3$) δ: 10.66 (s, 2H), 8.19 (s, 2H), 7.58 (m, 4H), 7.42 (m, 6H). ^{13}C NMR (125 MHz, $CDCl_3$) δ: 190.6, 138.4, 132.6, 132.1, 129.8, 128.8, 126.3, 121.9, 99.2, 84.2. FT-IR (KBr): ν/cm^{-1}: 2917, 2849, 2742, 2197, 1692, 1497, 1410, 1393, 1268, 1127, 764, 695. HR-MS (EI): found *m/z* = 334.0987 ± 0.0010 (M^+); calc. for $C_{24}H_{14}O_2$: 334.0994.

2,5-Bis(triisopropylsilylethynyl)terephthaldehyde (*en route* to **14**): A dry 100 mL Schlenk flask was placed under argon and filled with THF (10 mL). After cooling to -78°C a solution of 1.7 M *t*-butyllithium in pentane (4.0 mL, 6.8 mmol) was added, and the solution was stirred for 5 min. A solution of 1,4-bis(triisopropylsilylethynyl)-2,5-dibromobenzene (500 mg, 0.8 mmol) in dry THF (5 mL) under argon was transferred dropwise to the *t*-BuLi solution, and the reaction was stirred at -78°C for 1h at which point dry DMF (2 mL) was added rapidly. The reaction was allowed to warm to room temperature and quenched with NH_4Cl. After dilution with ether, the organic layer was washed with NH_4Cl (x3), NaCl, dried and removed *in vacuo* to provide black solids. Chromatography on silica (hexane to 4:1 hexane/CH_2Cl_2) provided the product as a very fainy yellow solid (302 mg, 0.611 mmol, 73%). mp 125.5-127°C. ^{1}H NMR (500 MHz, $CDCl_3$) δ: 10.60 (s, 2H), 8.08 (s, 2H), 1.14 (s, 42H). ^{13}C NMR (125 MHz, $CDCl_3$) δ: 190.7, 138.8, 132.8, 126.5, 103.0, 100.8, 18.9, 11.4. FT-IR (KBr): ν/cm^{-1}: 2944, 2865, 2154, 1695, 1471, 1388, 1144, 882, 736. HR-MS (EI): found *m/z* = 451.2494 ± 0.0013 [(M-C_3H_7)$^+$]; calc. for $C_{27}H_{39}O_2Si_2$: 451.2489

2,5-Di(ethynyl)terephthaldehyde (**14**): 2,5-Bis(triisopropylsilylethynyl)terephthaldehyde (200.2 mg, 0.4046 mmol) was placed in a 100 mL Schlenk flask and placed under argon. THF (18 mL), MeOH (2 mL) and water (2 mL) were added, and the solution was stirred as a 1M solution of TBAF in THF (2 mL, 2 mmol) was added dropwise. The reaction was stirred at room temperature for 20 hr and the reaction was diluted with ether and washed with NaCl (x3). The organic layer was dried and removed *in vacuo* to yield a pale brown solid. This crude material was purified on silica gel (1:1 hexane/CH_2Cl_2) to provide the product as an off-white powder solid (64.0 mg, 0.351 mmol, 87%). ^{1}H NMR (500 MHz, $CDCl_3$) δ: 10.54 (s, 2H), 8.15 (s, 2H), 3.62 (s, 2H). FT-IR (KBr): ν/cm^{-1}: 3264, 3028, 2883, 2105, 1686, 1470, 1408, 1387, 1280, 1150, 910, 862, 694, 676. HR-MS (EI): found *m/z* = 182.0364 (M^+); calc. for $C_{12}H_6O_2$: 182.0368.

References

(1) For some leading reviews, see: (a) Dimroth, K.; Wolf, K. H. In *Newer Methods of Preparative Organic Chemistry*. Foerst, W., Ed. Academic Press: New York, 1964. Vol. 3, pps 357-423; (b) Balaban, A. T.; Schroth, W.; Fischer, G. In *Advances in Heterocyclic Chemistry*. Katritzky, A. R.; Boulton, A. J.; Eds. Academic Press: New York, 1969. Vol. 10, pps 241-326; (c) Balaban, A. T.; Dinculescu, A.; Dorofeenko, G. N.; Fischer, G. W.; Koblik, A. V.; Mezheritskii, V. V.; Schroth, W. *Pyrylium Salts: Syntheses, Reactions, and Physical Properties*. Academic Press: New York, 1982.

(2) *Anthocyanins as Food Colors*; Markakis, P., ed. Academic Press: New York, 1982.

(3) (a) Brouillard, R.; Dubois, J.-E. *J. Am. Chem. Soc.* **1977**, *99*, 1359-1364; (b) Pina, F.; Maestri, M.; Balzani, V. *Chem. Commun.* **1999**, 107-114.

(4) Stetter, H.; Reischl, A. *Chem. Ber.* **1960**, *93*, 1253-1256.

(5) Blount, B. K.; Robinson, R. *J. Chem. Soc.* **1933**, 555-557.

(6) Baeyer, A.; Piccard, J. *Ann. Chem.* **1911**, *384*, 208-224.

(7) (a) Gilchrist, T. L. *Heterocyclic Chemistry*, 3rd. ed. Addison Wesley Longman: Harlow (Essex, England), 1997; (b) Kametani, T.; Fukumoto, K. In *Isoquinolines*. Grethe, G., Ed. John Wiley & Sons: New York, 1981. Part I, pps 139-274.

(8) (a) Fodor, G.; Nagubandi, S. *Tetrahedron* **1980**, *36*, 1279-1300; (b) Larsen, R. D.; Reamer, R. A.; Corley, E. G.; Davis, P.; Grabowski, E. J. J.; Reider, P. J.; Shinkai, I. *J. Org. Chem.* **1991**, *56*, 6034-6038 and references therein.

(9) Fitzgerald, J. J.; Michael, F. E.; Olofson, R. A. *Tetrahedron Lett.* **1994**, *35*, 9191-9194.

(10) Schiess, P.; Huys-Francotte, M.; Vogel, C. *Tetrahedron Lett.* **1985**, *26*, 3959-3962.

(11) (a) Roesch, K. R.; Larock, R. C. *J. Org. Chem.* **1998**, *63*, 5306-5307; (b) Roesch, K. R.; Larock, R. C. *Org. Lett.* **1999**, *1*, 553-556.

(12) (a) Numata, A.; Kondo, Y.; Sakamoto, T. *Synthesis* **1999**, 306-311; (b) Sakamoto, T.; Numata, A.; Kondo, Y. *Chem. Pharm. Bull.* **2000**, *48*, 669-672.

(13) Arnold, F. E.; Van Deusen, R. L. *Macromolecules* **1969**, *2*, 497-502.

(14) (a) Tunney, S. E.; Suenaga, J.; Stille, J. K. *Macromolecules* **1983**, *16*, 1398-1399; (b) Tunney, S. E.; Suenaga, J.; Stille, J. K. *Macromolecules* **1987**, *20*, 258-264.

(15) Singh, R.; Hay, A. S. *Makromol. Chem., Macromol. Symp.* **1992**, *54/55*, 357-363.

(16) Izumi, A.; Nomura, R.; Masuda, T. *Macromolecules* **2000**, *33*, 8918-8920.

(17) Meng, H.; Wudl, F. *Macromolecules* **2001**, *34*, 1810-1816.

(18) (a) Zhang, X.; Shetty, A. S.; Jenekhe, S. A. *Macromolecules* **1999**, *32*, 7422-7429; (b) Babel, A.; Jenekhe, S. A. *Adv. Mater.* **2002**, *14*, 371-374.

(19) Bao, Z. *Adv. Mater.* **2000**, *12*, 227-230.

(20) (a) Goldfinger, M. B.; Swager, T. M. *J. Am. Chem. Soc.* **1994**, *116*, 7895-7896; (b) Goldfinger, M. B.; Crawford, K. B.; Swager, T. M. *J. Am. Chem. Soc.* **1997**, *119*, 4578-4593; (c) Goldfinger, M. B.; Crawford, K. B.; Swager, T. M. *J. Org. Chem.* **1998**, *63*, 1668-1675.

(21) Sonogashira, K.; Tohda, Y.; Hagihara, N. *Tetrahedron Lett.* **1975**, 4467-4470.

(22) (a) Zhou, Q.; Swager, T. M. *J. Am. Chem. Soc.* **1995**, *117,* 7017-7018; (b) Yang, J.-S.; Swager, T. M. *J. Am. Chem. Soc.* **1998**, *120*, 5321-5322.

(23) For another recent approach, see: Yamaguchi, S.; Swager, T. M. *J. Am. Chem. Soc.* **2001**, *123*, 12087-12088.

(24) See also: (a) Bradsher, C. K.; Wallis, T. G. *Tetrahedron Lett.* **1972**, 3149-3150; (b) Garcia, A.; Lete, E.; Villa, M. J.; Dominguez, E.; Badia, M. D. *Tetrahedron* **1988**, *44*, 6681-6686.

(25) (a) Zhou, Q.; Swager, T. M. *J. Am. Chem. Soc.* **1995**, *117*, 12593-12602; (b) Levitsky, I. A.; Kim, J.; Swager, T. M. *J. Am. Chem. Soc.* **1999**, *121*, 1466-1472; (c) Kim, J.; McHugh, S. K.; Swager, T. M. *Macromolecules* **1999**, *32*, 1500-1507.

(26) A distinct ^{1}H NMR resonance initially appeared at 5.70 ppm (dd, 2H, J = 13.5, 5.0 Hz) and with further exposure to TfOH shifted to 5.83 ppm (dd, J = 19.5, 4.5 Hz) for both **3a** and **b**, indicative of olefinic protons and residual F^--promoted TMS cleavage.

(27) (a) Kleinpeter, E.; Spitzner, R.; Schroth, W. *Magn. Reson. Chem.* **1987**, *25*, 688-695; (b) Kleinpeter, E.; Spitzner, R.; Schroth, W; Pihlaja, K.; Mattinen, J. *Magn. Reson. Chem.* **1988**, *26*, 707-713.

(28) (a) Bradsher, C. K.; Wallis, T. G. *J. Org. Chem.* **1978**, *43*, 3817-3820; (b) Ruhemann, A. *Chem. Ber.* **1891**, *24*, 3964-3976.

(29) Saba, A.; Sib, F. S.; Aycard, J.-P. *Spectroscopy Lett.* **1993**, *26*, 491-496.

(30) Fong, C. W.; Lincoln, S. F.; Williams, E. H. *Aust. J. Chem.* **1978**, *31*, 2623-2628.

(31) Högler, R.; Kahovec, L. *Monatsh. Chem.* **1946**, *76*, 27-31.

(32) Bacon, R. G. R.; Lindsay, W. S. *J. Chem. Soc.* **1958**, 1382-1389.

(33) Seto, K.; Shimojitosho, H.; Imazaki, H.; Matsubara, H.; Takahashi, S. *Bull. Chem. Soc. Jpn.* **1990**, *63*, 1020-1025.

(34) Hart, H.; Harada, K.; Du, C.-J. F. *J. Org. Chem.* **1985**, *50*, 3104-3110.

(35) Sakamoto, T.; An-naka, M.; Kondo, Y.; Yamanaka, H. *Chem. Pharm. Bull.* **1986**, *34*, 2754-2759.

(36) Padwa, A.; Krumpe, K. E.; Weingarten, M. D. *J. Org. Chem.* **1995**, *60*, 5595-5603.

(37) Austin, W. B.; Bilow, N.; Kelleghan, W. J.; Lau, K. S. Y. *J. Org. Chem.* **1981**, *46*, 2280-2286.

(38) Fairfax, D. J.; Austin, D. J.; Xu, S. L.; Padwa, A. *J. Chem. Soc., Perkin. Trans. 1* **1992**, 2837-2844.

(39) Schmittel, M.; Keller, M.; Kiau, S.; Strittmatter, M. *Chem., Eur. J.* **1997**, *3*, 807-816.

(40) Wang, K. K.; Zhang, H.-R.; Petersen, J. L. *J. Org. Chem.* **1999**, *64*, 1650-1656.

(41) Kirby, G. W.; Tan, S. L.; Uff, B. C. *J. Chem. Soc., Perkin Trans. 1* **1979**, 266-269.

(42) Ford, A.; Sinn, E.; Woodward, S. *J. Chem. Soc., Perkin Trans. 1* **1997**, 927-934.

(43) Casey, M.; Moody, C. J.; Rees, C. W. *J. Chem. Soc., Perkin Trans. 1* **1984**, 1933-1941.

(44) Evers, R. C.; Moore, G. J.; Abraham, T. *J. Polym. Sci. A, Polym. Chem.* **1988**, *26*, 3213-3228.

Chapter 3

Elucidation of a tandem cyclization-polymerization sequence: Poly(naphthodithiophene)s

Adapted in part from:
Tovar, J. D.; Swager, T. M. *Adv. Mater.* **2001**, *13*, 1775-1780;
Tovar, J. D.; Rose, A.; Swager, T. M. *J. Am. Chem. Soc.*, accepted.

Introduction

Following the first synthesis of conductive poly(thiophene) by Garnier,[1] extensive efforts have targeted new thiophene architectures that allow for enhanced materials properties, easier processing, and higher stability.[2] Processing requirements for characterization and application dictated a need for soluble polymers, and substituents at the β-sites of the thiophene ring met this need.[3,4] Alkylated or arylated monomers readily polymerize upon treatment with chemical oxidants such as $FeCl_3$ to provide soluble, processable polymers.[5] Similarly, electrochemical oxidation allowed for the deposition of electrode-immobilized polymers. Both of these routes involve initial oxidation of the thiophene monomer to an extremely reactive radical cation that couples to additional radical cations or undergoes electrophilic attack by a neutral thiophene monomer. This type of coupling proceeds primarily through the α-sites of the ring (Scheme 1). While investigations of a variety of poly(thiophene)s traditionally employ these synthetic routes, they often result in defects from regiochemical irregularities. Such defects arise from the high reactivity of the thienyl radical cations allowing for uncontrolled chemical couplings during polymerization (Scheme 1, bottom).

Scheme 1

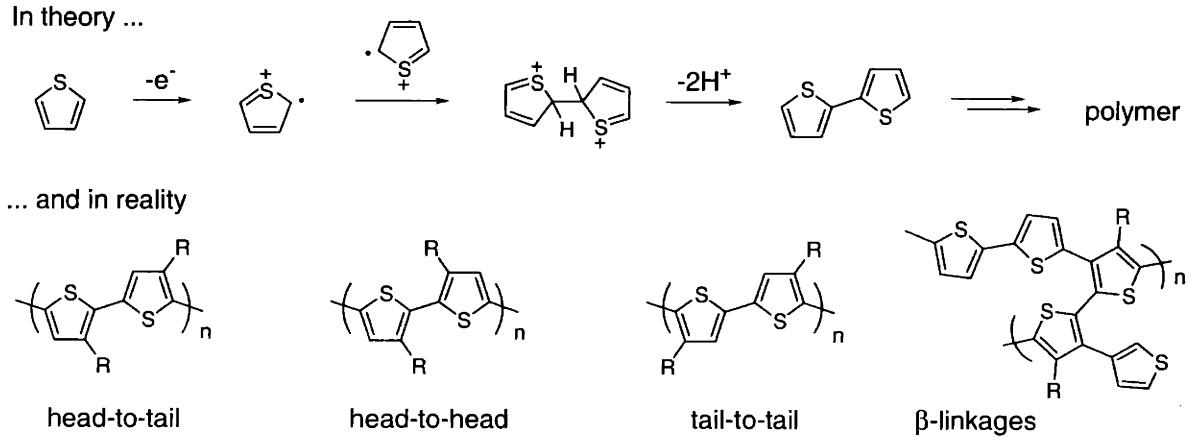

"Head-to-head" linkages will introduce steric strain between repeat units thus forcing the thiophene backbone to twist locally out of co-planarity. In the presence of a strong electronic bias (*e.g.* 3-phenylthiophene), the chemically oxidized monomer can polymerize with high degrees of regioregularity (*ca.* 90%).[5] On the other hand, electrochemical oxidative strategies often provide defect linkages through the β-ring positions of the monomer that also reduce the effective conjugation length. Other studies examined chemical homopolymerization of dibromothiophenes to minimize the presence of β-defects.[6] While successful in this regard, these chemical cross-coupling approaches exerted little control over the head-to-tail connectivities.[7]

The torsional rotation between repeat units has significant impacts on the physical properties of poly(thiophene)s. Seemingly a matter of conventional wisdom, early studies from the Swager group physically demonstrated the connection between planarity and effective conjugation length (Scheme 2). Marsella and Swager synthesized bithiophene monomers strapped with a bridging crown ether linkage chosen to specifically bind Na^+.[8] After polymerization, this material had dramatic blue-shifts in the UV when exposed to Na^+ in solution. From the molecular design, a binding event within the crown moiety enforced a structural twist in the repeat unit of the polymer backbone. The crown-strapped polymer system only displayed these effects in the presence of Na^+, other cations had minor effects on the observed absorbance. Therefore, the crown-ether strapped polymer served as a sodium sensor where molecular cation binding events elicited a bulk response. Roncali has studied several thienyl systems where the π-conjugated system has been geometrically fused into planarity as a means of ensuring maximal π orbital overlap.[9] Scheme 2 (right) illustrates two of these monomers that differ only by the incorporation of bridging etheno moieties.[10] The planarized chromophore provided a lower monomer oxidation potential, and the resulting polymer

displayed smaller optical and electrical band gaps. Therefore, geometric topologies within a repeat unit and steric torsion between repeat units dictate several bulk polymer properties.

Scheme 2

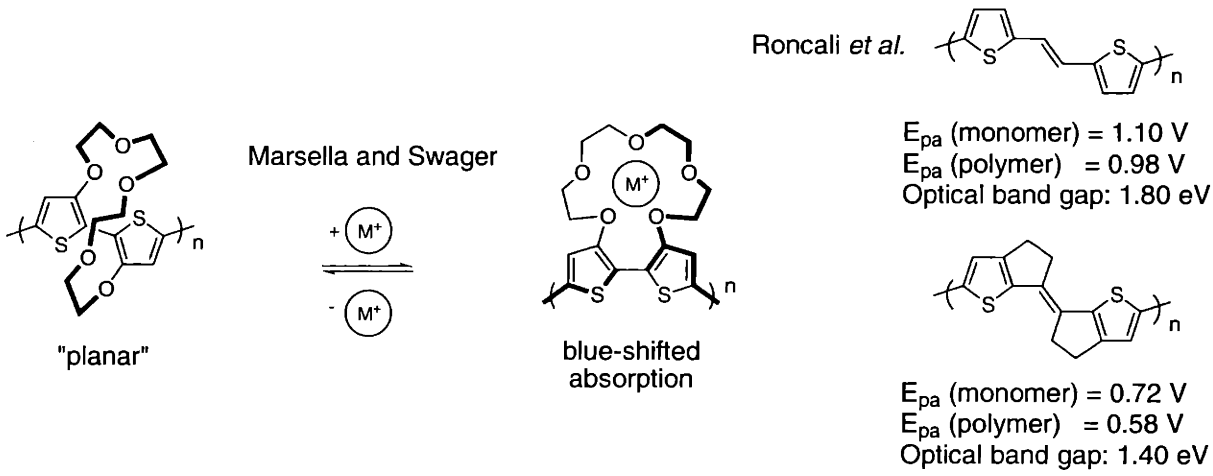

While elegant, the systems studied by Swager and Roncali require rather elaborate syntheses. Important synthetic efforts to enhance polymer conductivities from standard, readily available thienyl halides used selectively metallated substrates for transition metal mediated cross-coupling polymerizations (Scheme 3). In 1992, McCullough developed a powerful Kumada-type polymerization strategy where the unsubstituted α-sites of 2-bromothiophenes underwent selective deprotonation to form Grignard reagents.[11] Subsequent nickel-mediated polymerization through the bromo-functionalized site furnished regioregular poly(thiophene)s with *ca.* 91% head-to-tail couplings. Shortly thereafter, Rieke independently reported even higher degrees of regioregular poly(thiophene)s from dibromothiophene monomers.[12] Highly active Rieke zinc selectively metallated the 5-bromo site, and this bromozincio thienyl bromide then polymerized under palladium catalysis to provide greater than 98% head-to-tail ratios. The controlled regioregularity resulted in decreased optical bandgaps and conductivities on the order of 60-fold higher than those measured for the regiorandom counterparts.

Scheme 3

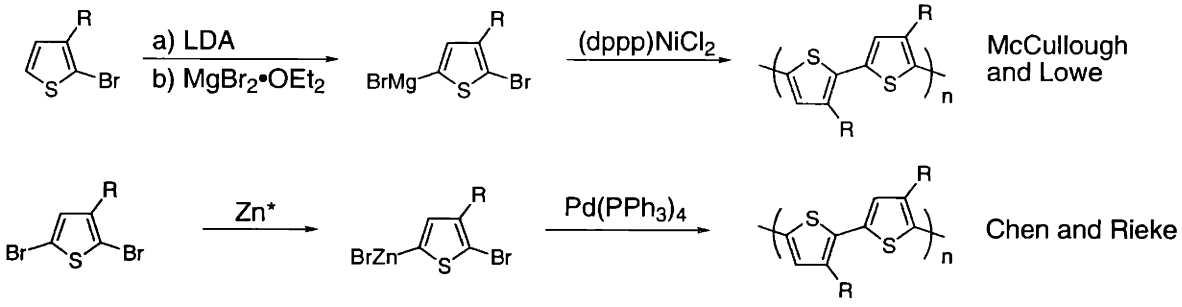

Several conducting polymer studies employ cyclic voltammetry (CV) to grow and study electroactive polymers. Figure 1 depicts a generic electrochemical cell (top left), and the bottom plots depict random *i*-V curves from CV. Cyclic voltammetry involves the application of a linearly-changing potential over time through an electrochemical cell between a working electrode and a counter electrode, relative to a known redox couple (Figure 1, top right). As the bulk of the next two chapters deals with electrochemical oxidation, this brief discussion will focus on anodic processes.[13] CV essentially monitors the potential required to allow for current flow through the cell. Therefore, any increases in anodic current indicate the removal of more electrons from the system and thus, the oxidation of species near the working electrode. If the oxidized material does not react or decompose, it will undergo reduction by the flow of electrons from the working electrode during the reverse scan. This results in the offset humps depicted in the leftmost CV of Fig 1, where E_{pa} defines the peak oxidation potential, and E_{pc} defines the cathodic peak potential. For an electrochemically reversible process, the average of E_{pa} and E_{pc} defines the half-wave potential ($E_{1/2}$). However, if an electrochemically-oxidized monomer possesses sufficient reactivity, it may undergo chemical coupling on the time scale of the CV scan. In this case, no strong reduction occurs during the reverse sweep (middle CV of Figure 1), and subsequent cycling often results in greater amounts of current passing through the working electrode with each scan (leftmost CV). This larger current flow at a given potential indicates an enlargement of the electrode's effective surface area. In practice, this enlarged surface area consists of electrically conductive polymeric material. Passivation of the electrode surface due to the deposition of decomposed or electrochemically inactive material would result in decreased current flowing with successive sweeps. Typically, as a polymer deposits on the working electrode, waves at less-positive potential grow in during cyclic sweeping indicating the

oxidation (or electrochemical doping) of the polymer immobilized on the electrode surface along with monomer oxidations occurring at more-positive potentials in solution. Rinsing the deposited films and performing CV in fresh, monomer-free electrolytic solvent allows for measurement of the polymer's electrical properties.

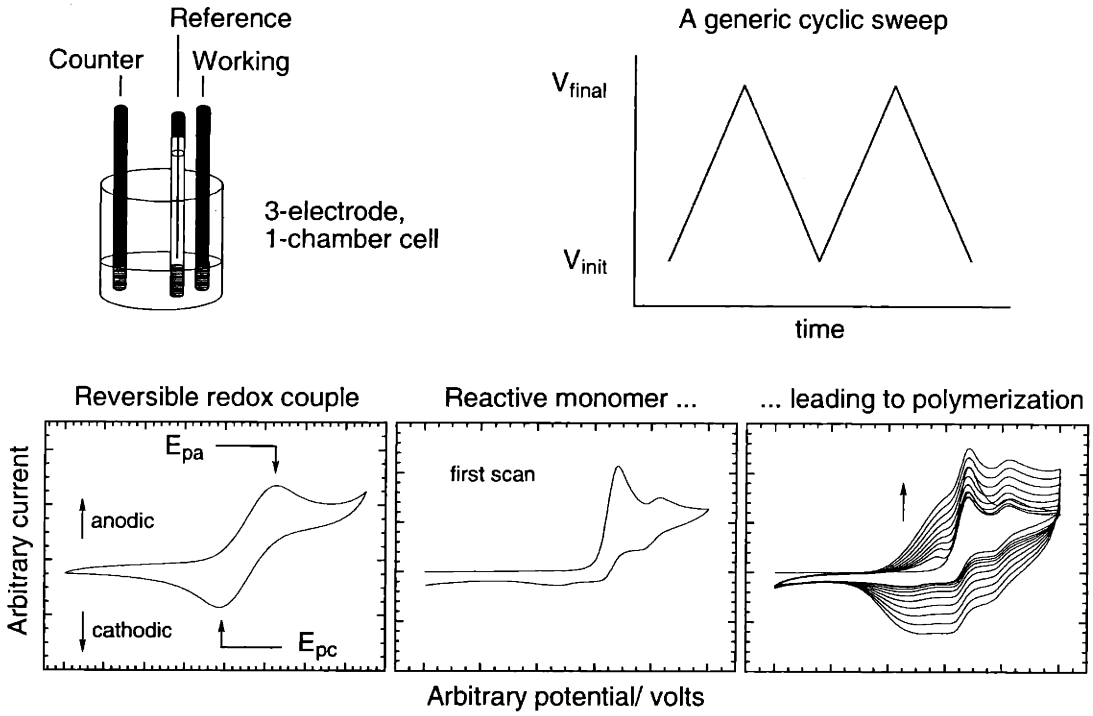

Figure 1: Cyclic voltammetry in a half-page. Standard electrochemical cell geometry (top, left); CV potential profile as a function of time (top, right); examples of reversible (bottom left) and irreversible electrochemical oxidation (bottom middle and right).

The high stability of both neutral and charged poly(thiophene)-based materials has allowed for the development of applications taking advantage of optical absorption changes during electrochemical doping.[14] Such electrochromic polymers can serve as flexible, transparent coatings with externally tuneable colors.[15] This phenomenon stems from the energetic parallels between standard inorganic and organic semiconductors. In the neutral state, poly(thiophene) adopts the insulating aromatic form with a bandgap of *ca.* 2.20 eV (560 nm). With electrochemical doping, the holes (or cationic charges) introduced into the backbone induce structural changes within the polymer to compensate for the removal of charge. These structural

changes result in the formation of quinoidal-type geometries and ultimately lead to molecular HOMO destabilization.[16] Such quinoidal structures have bandgaps well below 2 eV, providing optical absorption into the near IR. The polymer adopts a quinoidal structure upon oxidation to better delocalize and stabilize the charge carriers throughout the backbone rather than localizing these charges on individual aromatic repeat units. Despite the lower energy for the aromatic form in the pristine polymer, the quinoidal resonance structures help to accommodate the charge of the doped polymer more favorably. These electronic alterations create mid-gap states within the bandgap that give rise to near IR absorptivity (Scheme 2). In semiconductor parlance, mid-gap states arise from the dopant "impurities" rather than the structural changes, *i.e.* electrolytic counteranions that swell into the polymer to compensate the removal of electrons during oxidation. The *a priori* inclusion of predetermined concentrations of small impurity ions dopes inorganic semiconductors by filling the interstitial sites of the material's crystal lattice. Once grown, these crystals have a set dopant level and thus, a fixed Fermi level. Organic polymers offer the ability to tune the dopant (and thus, the polymer band gap) selectively and reversibly *in situ* simply by changing the potential applied to the polymer film. The electrochromic effect arises from this reversible alteration of optical absorptivities through controlling the influence of mid-gap states at energies lower than the pristine bandgap.

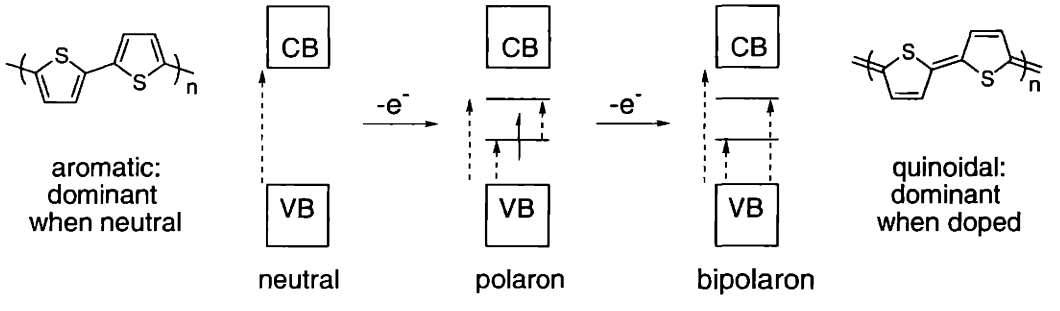

Figure 2: Poly(thiophene) *ground-state* resonance forms and optical changes resulting from polymer oxidation. For a more realistic illustration of an oxidized backbone, see Chapter 1, Figure 2.

In search of highly stable electrochromic materials, several groups have become interested in the incorporation of polycyclic aromatic residues into a conjugated polymer backbone. Bard has used polycylic precursors to prepare electrochromic ladder-type materials as shown in Equation 1. These carbonoid ladder systems imparted a large degree of stability into the resulting electrochromic material,[17] and we envisioned that the inclusion of thiophene-based polycyclic aromatics would offer additional enhancement of stability relative to poly(thiophene)-based electrochromics. Many synthetic routes to large aromatic molecules amenable to the synthesis of electrochromic ladder polymers employ oxidative cyclizations from pendant arene precursors. The highly reactive nature of oxidized thiophene moieties has not allowed for the development of similarly well-defined, thiophene-centered oxidative cyclizations as these materials often polymerize rather than undergo discrete monomer cyclizations upon oxidation.[18]

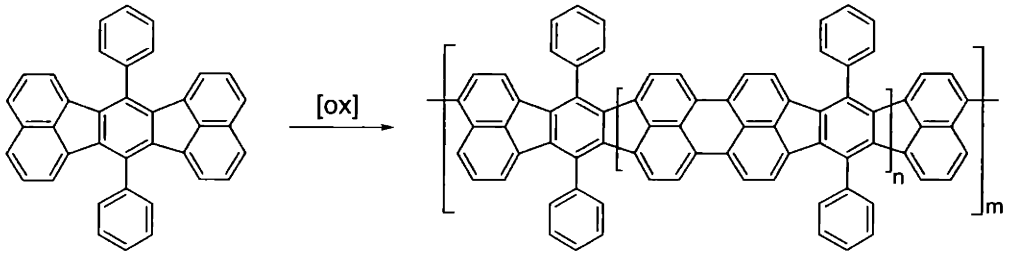

(1)

To effectively synthesize such materials, we describe herein a tandem cyclization-polymerization scheme to produce aromatized monomers *in situ* prior to oxidative polymerization. Within this context, Scheme 4 depicts such a sequence where a generic pendant thienyl monomer undergoes an oxidative cyclization to provide an aromatized material containing a bithiophene repeat unit planarized by a bridging benzeno segment. A related TTF system studed by Kalaji and Murphy also bore pendant 3-thienyl moieties; however, the oxidized TTF dication apparently prohibited chemical cyclization and polymer growth.[19] The *a priori* regularity afforded by the symmetry of these fused monomers eliminates any regiochemical head-to-tail coupling issues during polymerization,[10,11] allowing for a greater degree of coplanarity between repeat units and hence, enhanced conductivity. The topological similarity of these fused monomers to triphenylene offers an opportunity to utilize this discotic organizational element in the design of new liquid crystalline[20] or electronic materials.[21] The introduction of fused thiophene moieties simplifies synthetic manipulation relative to triphenylene cores thereby enabling greater flexibility to fine-tune a desired molecular property. In this regard, we discuss spectroelectrochemical data that demonstrates the significant electronic differences available through facile structural variations within the precursor monomers.

Scheme 4

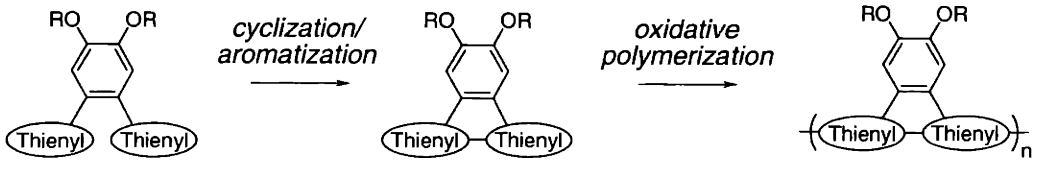

pendant monomer ***fused aromatic*** ***poly(naphtho dithiophene)***

Results and Discussion

From common intermediates, we could obtain two distinct isomeric systems with linkages at α- or β-sites of the thienyl ring (Scheme 5). Although a seemingly trivial structural alteration, this geometric connectivity will prove to have dramatic consequences for the energetics of the resulting polymer. To obtain the β-isomer, we utilized Suzuki couplings with dialkoxy dibromobenzenes and 3-thiophene boronic acid to provide the β-thienyl redoxophores **1** in high yield.[22] This quite general Suzuki procedure routinely provided isolated, recrystallized, multigram quantities in yields over 90%. For the corresponding α-isomer, Stille coupling with 2-tributylstannyl thiophene provided **α-1** in high yield.[23] As a comparison, we prepared the mono β-thienyl (**mono**β) as an electrochemically polymerizable control system lacking additional *ortho*-positioned substituents.

Scheme 5

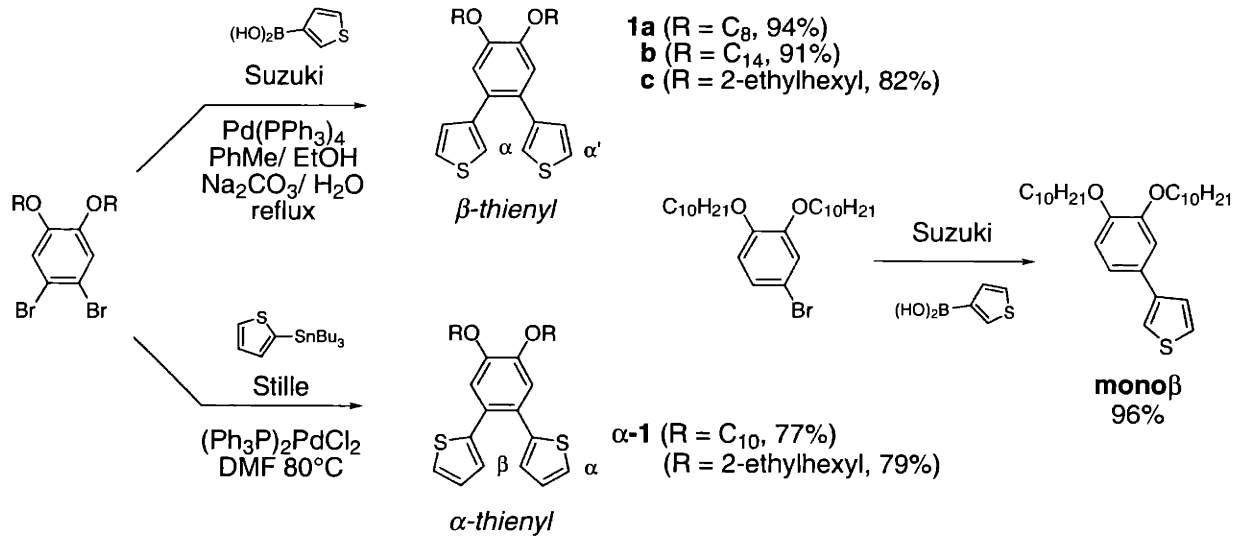

Electrochemical polymerization: Cyclic voltammetry (CV) of **1a** (Figure 3, top) and α-**1** (Figure 3, middle) revealed two distinct and irreversible monomer oxidation peaks as the only anodic signals present in the first oxidative scan (with E_{pa}s of 0.83 and 0.91 V for **1a**; 0.87 and *ca.* 1.07 V for α-**1**). Subsequent voltammetric sweeps revealed the growth of low potential polymer-based redox activity that increased with additional scanning. Deposition required successive cycling to the most positive monomer oxidation potential as no polymer film growth occurred at applied potentials below *ca.* 0.90 V. For comparison, **mono**β demonstrates a typical thiophene electropolymerization, where sweeping through a single monomer oxidation potential (with an E_{pa} of 0.86 V) led to polymer growth (Figure 3, bottom). Note that this potential corresponded to those observed for the first oxidation of **1a** and α-**1**. Furthermore, the polymer redox activity for **mono**β grew in at much higher potentials when compared to the corresponding double-thienyl system **1a**.

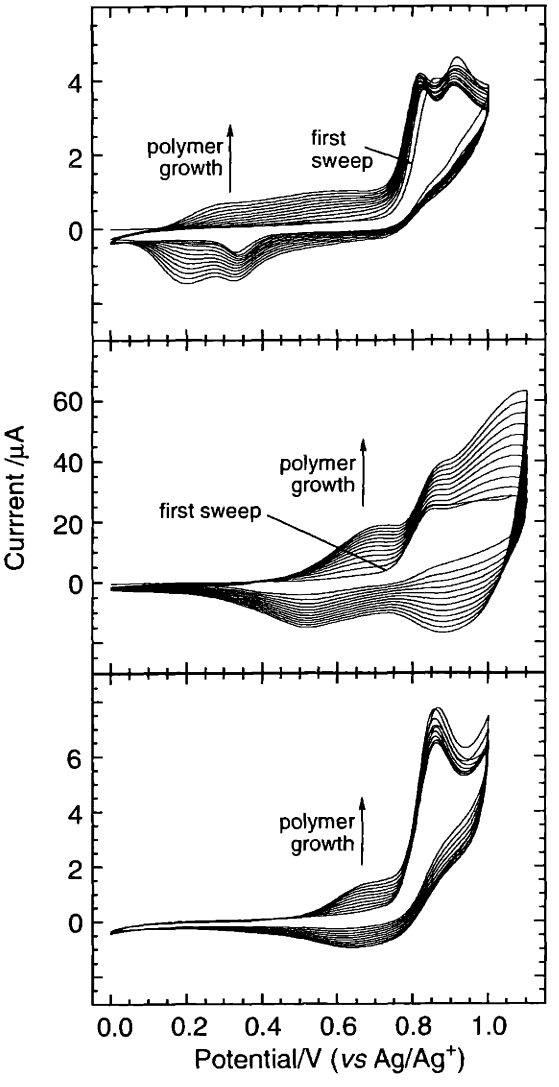

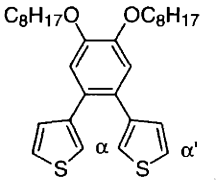

1a

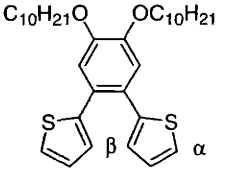

α-1

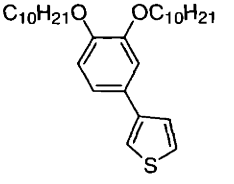

monoβ

Figure 3: Monomer cyclic voltammetry: **1a** (top, 0.27 mM), **α-1** (middle, 1.7 mM) and **monoβ** (bottom, 2.4 mM) at a 2 mm^2 Pt button electrode in 0.1 M *n*-Bu_4PF_6 (CH_3CN) cycled at 100 mV/s. $E_{1/2}(Fc/Fc^+)$: +0.086 V.

From these data, we propose the two major mechanistic steps illustrated in Scheme 6 for isomers **1a** and α-**1**. After electrochemical oxidation of a pendant thienyl moiety of **1a**, an intramolecular α-α cyclization and deprotonation provides the aromatized naphthodithiophene **2a**.[24] Further oxidation of **2a** at higher potential ultimately leads to polymer growth through the remaining α' sites. In an analogous fashion, oxidation of α-**1** leads to the isomeric aromatized monomer by way of a β-β cyclization followed by higher potential polymerization through the vacant α-sites to provide poly(α-**2**). Typical monomers undergo uncontrolled polymerization after oxidation as opposed to an apparently controlled chemical cyclization due to the adjacent *ortho*-substituted thienyl ring. We could also use this controlled approach to provide high-yielding syntheses of the corresponding molecular systems (*e.g.* **2**). We performed a series of chemical and electrochemical studies in order to ascertain the nature of this unique oxidative reactivity as described in the remainder of this chapter.

Scheme 6

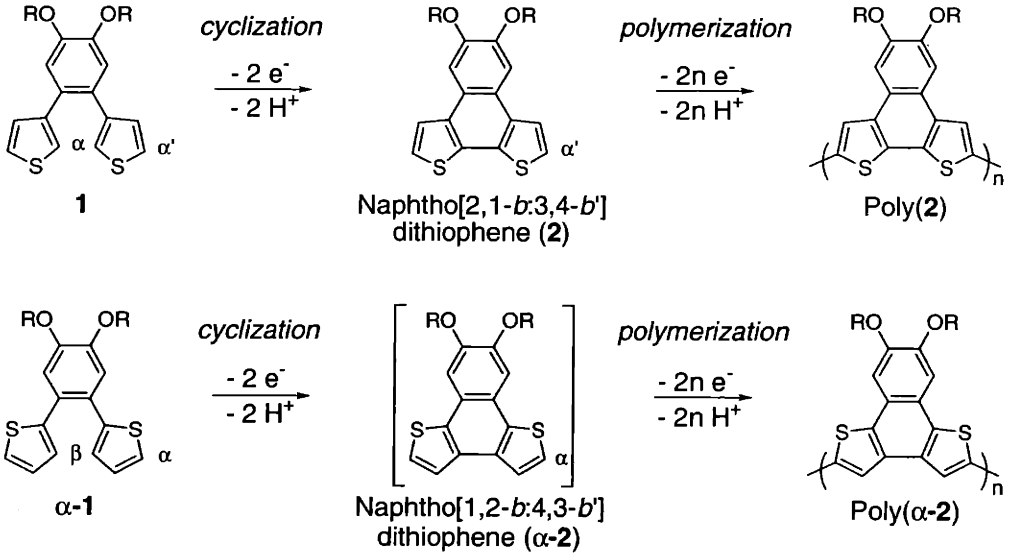

To support our mechanism and shed light on the tandem cyclization-polymerization sequence of Scheme 6, we prepared **2a** in high yield through the use of $FeCl_3$ as an oxidant. While $FeCl_3$ has served as a suitable chemical oxidant during *poly*(thiophene) synthesis,[5] we could minimize undesired polymerization during the cyclization of **1a** to **2a** through use of short reaction times with near-stoichiometric amounts of oxidant. As the two different α-sites of **1** should exhibit the highest degrees of chemical and electrochemical reactivity (labeled α and α'), we used **2a** to address the first mechanistic step (the α-α coupling). Compound **2a** eliminates the need for a distinct chemical cyclization event prior to polymerization and thus, the "tandem cyclization" element. We subjected a saturated solution of sparingly soluble **2a** to the same electropolymerization conditions as monomer **1a** and obtained the growth profile in Figure 4B. Note that the first sweep displayed only *one* monomer oxidation peak with an E_{pa} of 0.88 V, a value that corresponded to the E_{pa} of the second monomer oxidation displayed by **1** (placed again in Figure 4A). Subsequent sweeps revealed lower potential polymer-based redox activity similar to that observed in the CV of **1a**. The close resemblance of the polymer films obtained from **1a** and from **2a** (Figure 4C and D, respectively) supports the fact that the deposited materials have the same structural connectivity. However, polymer CVs provide little detailed structural information and essentially no mechanistic data. Poor film solubilities and trace amounts of electrochemically deposited material prevent rigorous structural determinations often employed (and often taken for granted) to characterize small molecules.

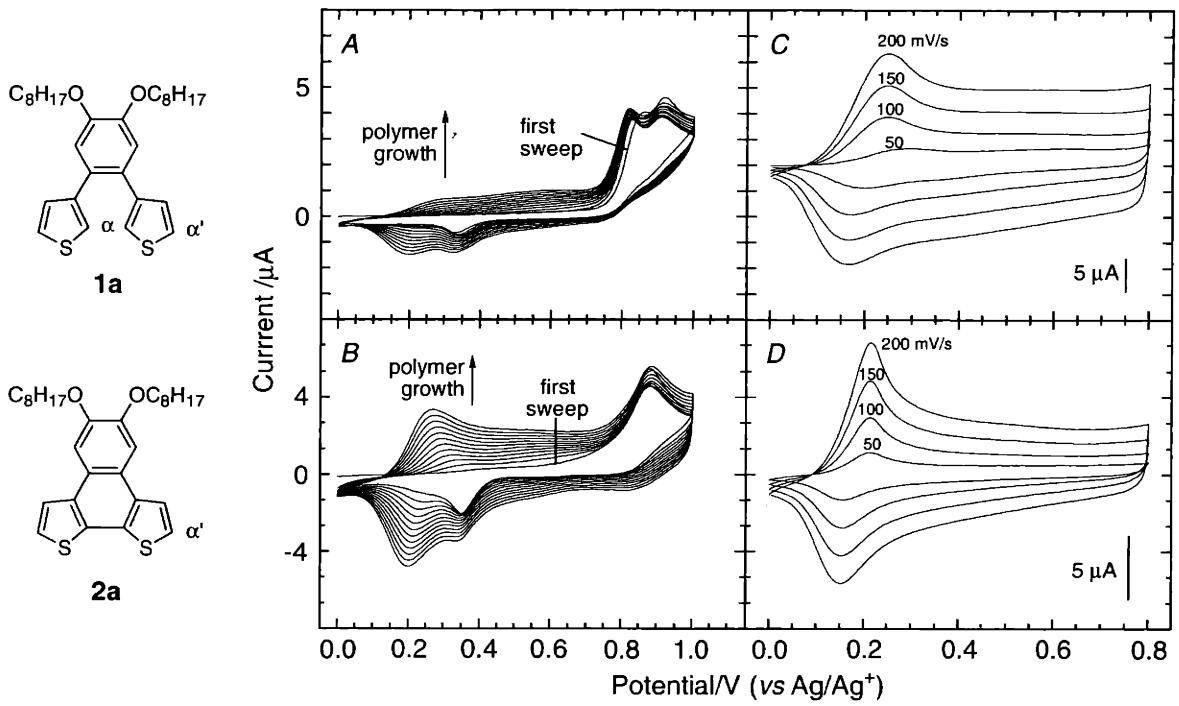

Figure 4: Monomer (A, B) and polymer (C, D) cyclic voltammetry: **1a** (A; 0.27 mM), **2a** (B; sat. *ca.* 0.3 mM), leading to poly(**2**) (C and D) at a 2 mm^2 Pt button electrode in 0.1 M *n*-Bu_4PF_6 (CH_3CN). Monomer CVs cycled at 100 mV/s; polymer CVs obtained at 50-200 mV/s. $E_{1/2}(Fc/Fc^+)$: +0.086 V.

Our efforts to further clarify this connectivity centered on examinations of model, non-polymerizable systems and of chemically synthesized polymers. The remainder of this chapter will examine both of these topics in turn.

Investigation of molecular models: In order to accomplish the first aim, we needed models that would allow for electrochemically-mediated cyclization events without undergoing oxidative polymerization. We envisioned the generic structural motifs presented in Scheme 7 to serve in this regard. Model A has pendant 3-thienyl groups where blocking groups at the 5-position α-sites prevent polymerization. For the substitutional isomer, we chose model B, where the pendant 2-thienyl rings also have blocking groups on the polymerizable α-sites. If these polymers indeed propagate through the α-sites now blocked in these models, CV should detect the redox activities of any new electroactive species formed at the electrode rather than irreversible follow-up chemical polymerization. Furthermore, these models would shed light on the propensities (if any) toward coupling defects through vacant aryl or β-sites on the aromatized models. Specifically, we synthesized several model systems with judiciously placed blocking groups - with both pendant and cyclized topologies - designed to mimic in part the overall structural connectivity of the isomeric poly(naphthodithiophene) families.

Scheme 7

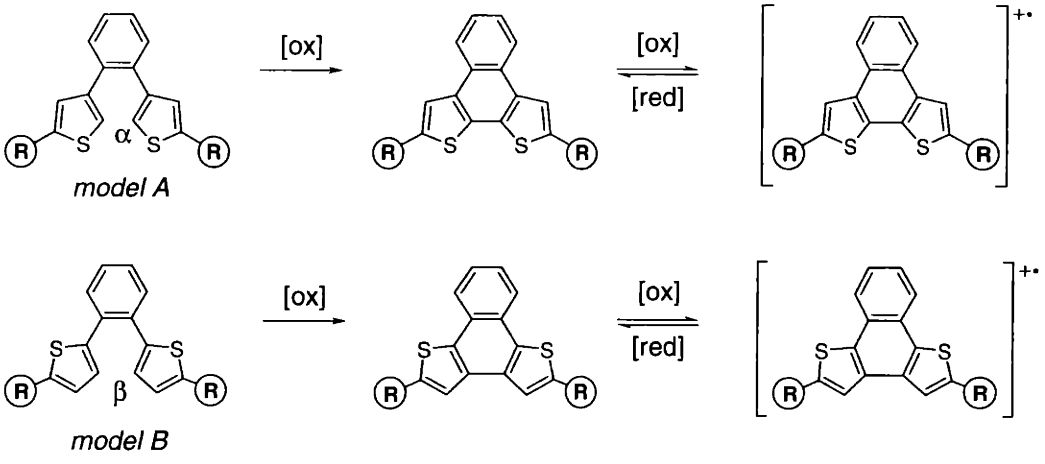

Using standard thiophene halogenation chemistry and Suzuki cross-coupling techniques, we obtained the α'-blocked, non-polymerizable **3** (representing model A). As outlined in Scheme 8, bromination occurred regioselectively at the α-positions of **1b**, and subsequent iodination occurred at the remaining α'-positions to provide **4**.[25] Although the high reactivity of both thienyl halides provided low chemoselectivity for the Suzuki cross-coupling, we obtained modest yields of the desired iodo-coupled product corresponding to aryl installation at the α'-site. Finally, debromination *via* lithium-halogen exchange provided α-unsubstituted **3**. To assess the specificity of the oxidative cyclization under chemical conditions, we subjected **3** to $FeCl_3$ oxidation to obtain **5** in high yield. Unlike the situation for pendant **1**, we could employ several molar excesses of oxidant in order to drive the cyclizations to completion without apparent oligomerization or polymerization.

Scheme 8[a]

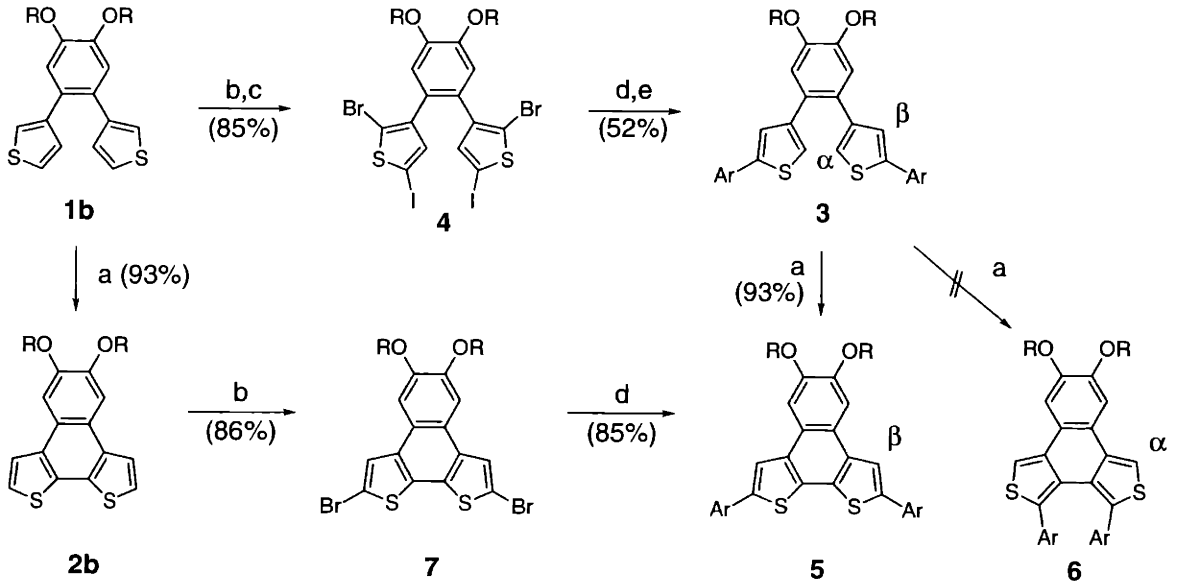

[a] R = *n*-$C_{14}H_{29}$, Ar = 2,5-$Me_2C_6H_3$-; Reagents and conditions: (a) $FeCl_3$, CH_2Cl_2; (b) Br_2, CH_2Cl_2; (c) $PhI(OCOCF_3)_2$, I_2, CCl_4 (no light); (d) *Suzuki*: $ArB(OH)_2$, $Pd(PPh_3)_4$, Na_2CO_3, PhMe/EtOH/H_2O; (e) i. *n*-BuLi, THF, -78°C; ii. AcOH, -78°C-rt.

Remarkably, this reaction provided only one product, indicating that the α-α sites of **3** had participated in the cyclization. The two naphthodithiophene singlets observed in the ^1H

NMR reflected a high degree of symmetry within the cyclized product. We observed no evidence for the formation of the second hypothetical β-β coupled isomer **6**; however, the insolubility of the product prevented an adequate ROESY analysis to assess the overall connectivity. To verify the assignment of **5**, we conducted a parallel synthesis from **1b**. Chemical cyclization of **1b** (to **2b**) followed by selective bromination at the α'-sites provided **7**. Subsequent Suzuki coupling yielded an identical product to that obtained through oxidative cyclization of **3**. This further supports our hypothesis that in the presence of both vacant α and β positions, the more reactive α-sites of **3** indeed participate in the cyclization to afford **5** selectively and in high yield.

Cyclic voltammetric (CV) analysis of **3** and **5** revealed corroborating oxidation activity. Both **3** and **5** shared reversible redox characteristics when swept at 100 mV/s: **3** exhibited two redox waves with half-wave potentials ($E_{1/2}$) of 0.86 and 1.31 V (Figure 5, top) while **5** displayed two redox waves with $E_{1/2}$s of 0.88 and 1.28 V (Figure 5, bottom). The lower potential anodic wave observed for **3**, with an E_{pa} of 0.93 V, appeared much stronger and broader than that for **5**, indicating a possible superposition of an irreversible oxidation and a reversible redox couple. Indeed, slower scans (25 mV/s) through the first half-wave potential of both compounds helped to better resolve this difference (insets in Figure 5). These data clearly show two distinct oxidations occurring within the first broad redox wave of **3** (top inset): one irreversible oxidation with an E_{pa} of 0.85 V and one reversible couple with an $E_{1/2}$ of 0.85 V (E_{pa} = 0.89 V, peak-peak separation ΔE_p = 88 mV). In comparison, **5** only exhibits the redox wave with an $E_{1/2}$ of 0.85 V (bottom inset; E_{pa} = 0.90 V, ΔE_p = 98 mV).[26]

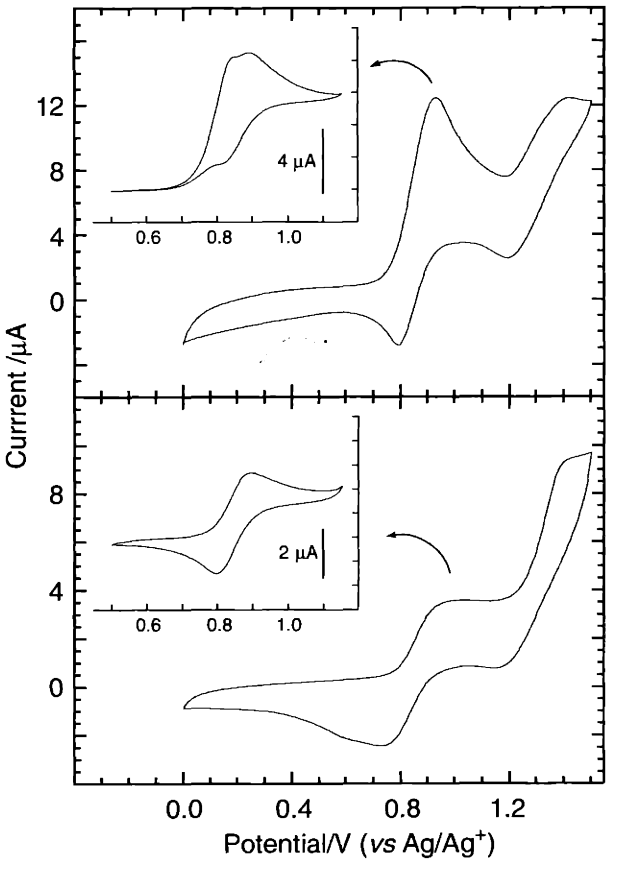

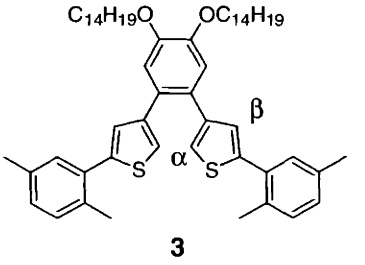

3

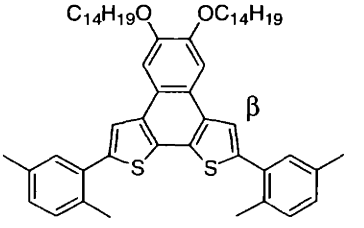

5

Figure 5: CVs of **3** (top, 1.2 mM) and **5** (bottom, 1.0mM) at a 2 mm^2 Pt button electrode in 0.1 M *n*-Bu_4PF_6 (CH_2Cl_2) scanned at 100 mV/s; inset scans taken at 25 mV/s. $E_{1/2}(Fc/Fc^+)$: +220 mV.

In line with the independent chemical syntheses of **5**, the initial oxidation of **3** leads to an intramolecular α-α cyclization. Subsequent deprotonation and rearomatization leads to **5**, and this product undergoes reversible redox chemistry at a higher potential essentially identical to that displayed by the chemically synthesized **5**. With the α'-sites blocked, we observed no evidence for irreversible chemical follow-up reactions upon oxidation (*e.g.* dimerization or polymerization). In the absence of aryl groups blocking the reactive α'-positions of **5**, radical cations derived from such an electrode-aromatized product (*e.g.* $\mathbf{2}^{\bullet+}$) then engage in follow-up chemical couplings and subsequent growth of poly(**2**) as opposed to the reversible redox chemistry observed for the blocked model.

As the cyclization-polymerization reactivity depicted in Scheme 4 also applied to the substitutional α-linked thiophene isomers, we sought to explore the electrochemical activity of non-polymerizable α-thienyl derivatives such as **8** (model B), readily obtained through Stille cross-coupling (Scheme 9). Unlike **3**, methyl-blocked **8** only has one vacant site available for oxidative cyclization that would lead to an aromatized system. Accordingly, chemical oxidation of **8** furnished the naphthodithiophene **9** in modest yield. Both **8** and **9** provided distinct electrochemical signatures that also shed light into the general mechanism of Scheme 6.

Scheme 9[a]

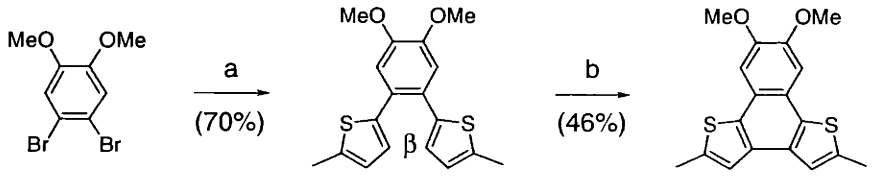

8 **9**

[a] Reagents and conditions: (a) *Stille*: 5-methyl-2-tributylstannylthiophene, $(Ph_3P)_2PdCl_2$, DMF, 80°C; (b) $FeCl_3$, CH_2Cl_2, rt.

Figure 6 displays these signatures at different scan rates. The CV of **8** displayed two strong oxidation peaks at 100 mV/s scan rates (Figure 6, top; solid line): one irreversible wave with an E_{pa} of 0.74 V attributed oxidation of the pendant thienyl ring of **8** followed by a β-β chemical cyclization and deprotonation process, and one well-defined and reversible redox wave with an $E_{1/2}$ of 0.82 V (E_{pa} = 0.87 V, ΔE_p = 110 mV) attributed to electrochemical formation of a stable radical cation species. Subjecting **9** to the same conditions provided the reversible redox process only with an $E_{1/2}$ of 0.82 V (dashed line; E_{pa} = 0.89 V, ΔE_p = 130 mV). Furthermore, repetitive fast CV scans of **8** at 750 mV/s resulted in a decrease in intensity for the initial oxidative peak (E_{pa} = 0.79 V) followed by a *pseudo* steady-state buildup of an electrochemically active product in the vicinity of the electrode (Figure 6, bottom). The *quasi*-reversible redox couple with an $E_{1/2}$ of 0.82 V (E_{pa} = 0.89 V, ΔE_p = 130 mV) resembled that obtained

independently through fast scan sweeps of **9** (Figure 6, bottom; dashed line). As with **3** and **5**, we observed no evidence for dimerization or polymer growth with cyclic sweeping through oxidizing potentials. In total, the data for **3** and **5** and for **8**-**9** support a coupled and electrochemically-mediated cyclization/polymerization process, where the oxidized form of a monomer initially cyclized *in situ* (such as **2**) participates in intermolecular couplings leading to polymer growth through the remaining unsubstituted sites α to the sulfur atoms.

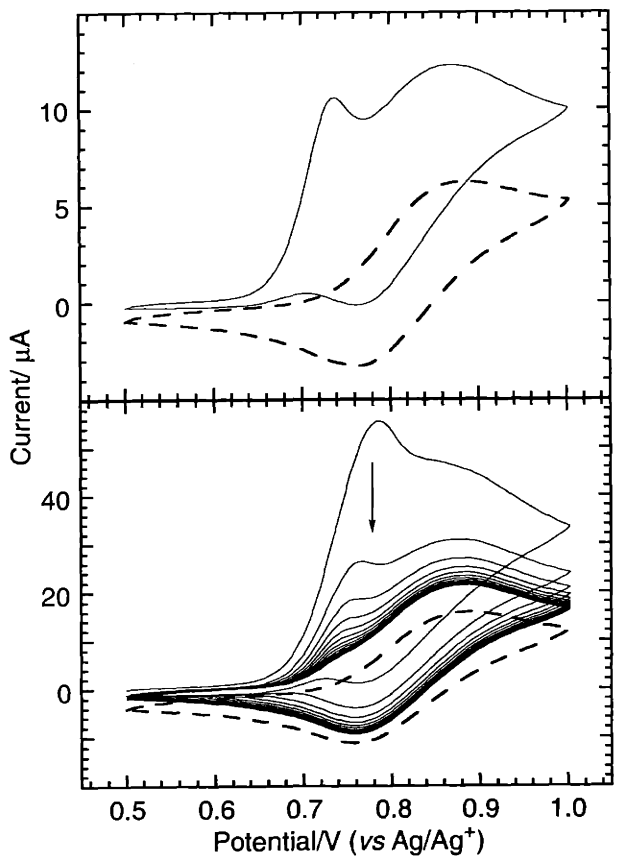

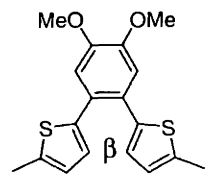

8

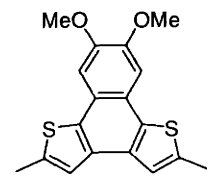

9

Figure 6: Cyclic voltammetry of **8** (—, 1.1 mM) and **9** (-----, 1.2 mM) at a 2 mm^2 Pt button electrode in 0.1 M *n*-Bu_4PF_6 (CH_3CN) scanned at 100 mV/s (top) and at 750 mV/s (bottom); $E_{1/2}(Fc/Fc^+)$: +84 mV.

In collaboration with the group of Professor Allen J. Bard group at UT Austin, we utilized the technique of Scanning Electrochemical Microscopy (SECM) to electrochemically observe the highly reactive oxidized intermediates generated at the working electrode before they could undergo subsequent chemical cyclization and reversible redox events.[27] In this technique, one observes changes in current profiles between an oxidizing tip electrode (*ca.* 10 μm diameter) and a reducing substrate collection electrode (*ca.* 250 μm diameter) as the tip approaches the substrate (Figure 7). As the distance to the substrate electrode decreases, the oxidized intermediates at the tip quantitatively undergo reduction at the substrate. At longer distances, the intermediates have lifetimes shorter than the diffusion times required to reach the substrate, and they react in solution to form neutral, substrate-inactive materials. This powerful technique can observe these highly reactive intermediates and measure any associated chemical rate constants (dimerization, *etc.*). Indeed, we could observe reactive intermediates when we applied SECM to **8**: at small distances, the substrate collects two intermediate species, while longer distances provide no collection of reactive intermediates. In comparison, **9** essentially provides quantitative collection of all oxidized species at the substrate regardless of the tip-substrate distance. This indicates that the radical cations of **9** do not undergo dimerization or polymerization through the unsubstituted sites on the naphthodithiophene core; namely, coupling predominantly occurs through the α-sites.

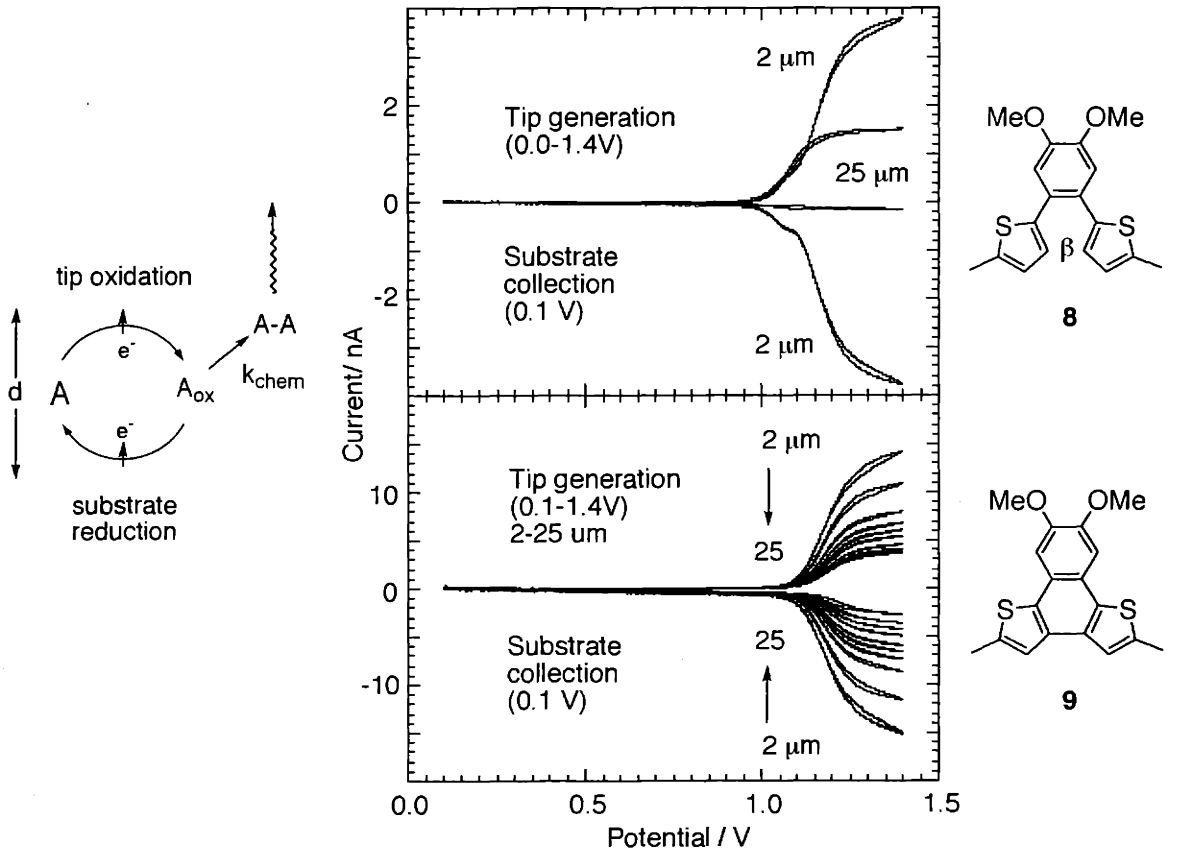

Figure 7: Schematic SECM and measurements of **8** and **9** (2 mM in CH_3CN) at a tip diameter of 10 μm and a collection substrate diameter of 250 μm.

While the SECM measurements revealed the presence of at least one reactive intermediate, we could not definitively back out a rate constant for the cyclization. Most SECM studies involve reactions with simple electrochemical descriptions such as an electrochemical reduction and subsequent dimerization (an EC mechanism).[27b] The earlier discussion for **8** grouped the thienyl oxidation (E) together with the cyclization step (C) and the deprotonation step (C). On the time scale of SECM, the individual rate constants of each of these processes become important. As such, several different, charged intermediates will indiscriminantly undergo reduction at the substrate. In addition, the deprotonation steps result in a local pH increase at the electrodes to further complicate analysis. When determining kinetic rate equations, the observed effects of different reactant concentrations can provide mechanistic

insight. This intramolecular process will not show a dependence on concentration, thus removing one of the variables SECM utilizes to assess rate constants. Despite these drawbacks, we could use SECM to prove the stability of the blocked and cyclized models (such as **9**), although not a particularly glamorous application of this technique.

Investigation of polymer connectivity and electronics: Our second aim focused on analysis of the structural connectivity of the polymers derived through tandem cyclization-polymerizations. While the models presented earlier provided strong monomer-based evidence for the cyclization-polymerization reactivities, electrochemically synthesized poly(thiophene)s often have poor regiochemical integrity. During uncontrolled polymerization of reactive thiophene radical cations, defects arising from head-to-tail scrambling and from β linkages significantly affect bulk properties of the resulting polymers. To evaluate the selectivity of our chemistry, we performed bulk electrolyses on the 2-ethylhexyl derivatives **1c** and **2c** (Scheme 10). Chronocoulometry indicated that the conversion of **1c** to **2c** consumed 2.1 e^-/mol at 0.85 V to provide a 75% isolated yield of **2c**. Holding solutions of **1c** at 0.90-1.20 V provided a fully characterized, *doubly cyclized* dimer **10** (n=0 in Scheme 10) alongside higher oligomers and polymers. Likewise, subjecting **2c** to a 0.90 V potential yielded trace yet spectroscopically useful amounts of trimeric and tetrameric materials (**10** where n=1 and 2 of Scheme 10) again along with higher insoluble materials that prohibited GPC analysis. UV-vis analysis of the GPC eluents reflected the oligomeric nature of the THF-soluble materials as evidenced by the similarly-structured yet increasingly lower energy λ_{max} absorptions corresponding to dimeric (404 nm), trimeric (448 nm) and tetrameric (468 nm) oligo(**2**)s. The eluted GPC fractions of THF-soluble oligomers derived either from bulk electrolysis or chemical oxidation of pendant monomer **1c** displayed comparable UV-vis absorptions to materials derived from **2c**, thus

serving to further establish the tandem cyclization-polymerization reactivity. If incomplete cyclizations occurred within these oligomeric materials, we would expect to see significant optical differences on account of the greater rotational degrees of freedom (*i.e.* lower effective conjugation length) available to a hypothetical oligomer such as **11**. For example, aryl-appended thienyl monomer **3** displays the lowest energy absorption at 271 nm (in CH_2Cl_2, log ε = 4.51) while the lowest-energy transition for cyclized **5** falls at 354 nm (log ε = 4.43).

Scheme 10

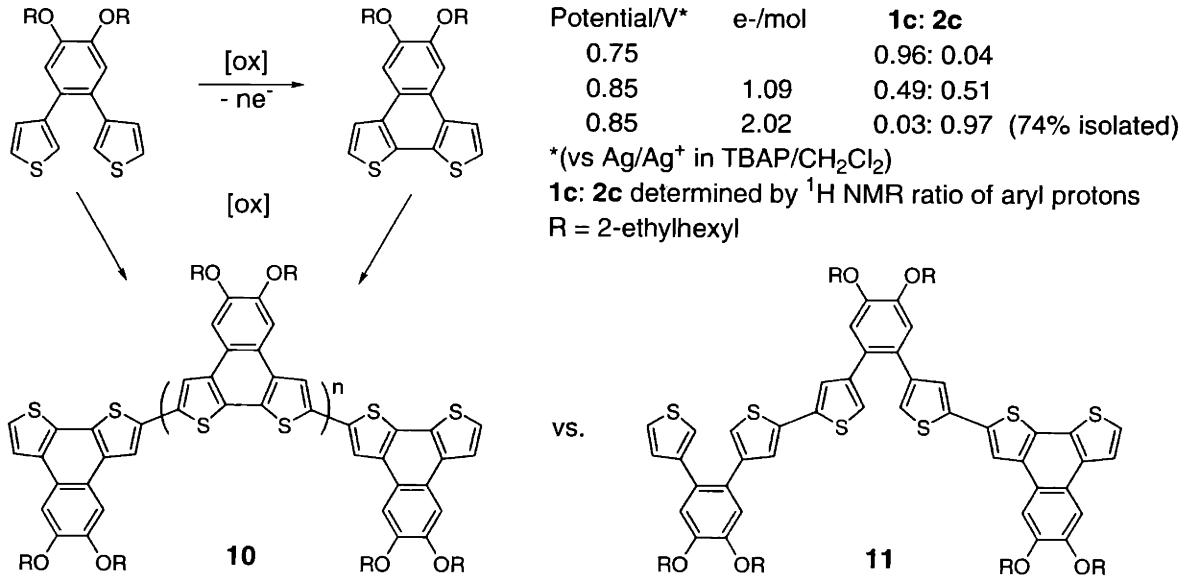

Potential/V*	e-/mol	**1c**: **2c**
0.75		0.96: 0.04
0.85	1.09	0.49: 0.51
0.85	2.02	0.03: 0.97 (74% isolated)

*(vs Ag/Ag^+ in $TBAP/CH_2Cl_2$)
1c: **2c** determined by ^1H NMR ratio of aryl protons
R = 2-ethylhexyl

In parallel, we prepared the soluble iodide **12** as a means of obtaining poly(**2**) through relatively more mild Pd-catalyzed cross-coupling conditions (Scheme 11, top). This would provide poly(**2**) with well-defined α-α linkages between repeat units. Lithiation of **2c** ultimately led to the diiodide **12** in high yield. To further verify the structural connectivity of electrochemically prepared poly(**2**), we used Kelly's *in situ* stannylation/ cross-coupling strategy to obtain regiochemically well-defined poly(**2**) from **12**.[28] As with bulk electrochemical polymerization, we obtained insoluble materials that precipitated during the course of the reaction, apparently a result of aggregation between the naphthodithiophene repeat units.

However, sufficient amounts of the polymer dissolved in hot *o*-dichlorobenzene to allow for the preparation of dark red drop-cast films suitable for four-point probe conductivity determination. Taken in ambient atmosphere, these measurements revealed a conductivity of 1.3 S/cm with saturative doping by iodine vapor. In line with the material derived from oxidative polymerization, UV-vis analysis of the GPC eluents for THF soluble, cross-coupled oligo(**2**) showed a similar λ_{max} progression to lower energies for the dimer (412 nm), trimer (452 nm) and tetramer (476 nm) as depicted in Figure 8 below. When taken together with the electrochemical observations and the UV data observed for the GPC eluents of materials derived through chemical oxidation, we can offer strong evidence to conclude that **1** undergoes a tandem cyclization-polymerization sequence to provide a poly(naphthodithiophene) isomer, poly(**2**).

Scheme 11[a]

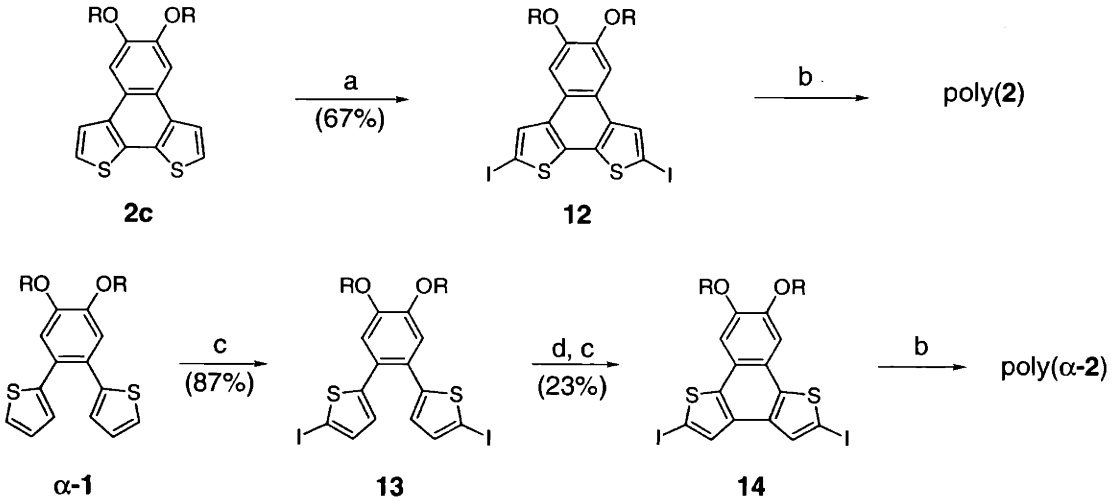

[a] R = 2-ethylhexyl. Reagents and conditions: (a) i. *n*-BuLi, TMEDA, THF, -78°C; ii. I_2; (b) $Me_3SnSnMe_3$, $Pd(PPh_3)_4$, DMF, PhMe, 80°C; (c) i. $Hg(OAc)_2$, CH_2Cl_2, rt; ii. I_2; (d) $FeCl_3$, CH_2Cl_2, rt.

We also synthesized the isomeric poly(α-**2**) by chemical means despite a much more problematic route (Scheme 11, bottom). We could not isolate the cyclized monomer α-**2** (where R = 2-ethylhexyl in Scheme 6) after exposure of α-**1** to $FeCl_3$, perhaps reflecting a higher degree of reactivity of this cyclized monomer upon oxidation. On the other hand, oxidation of α-

iodinated **13** resulted in complete cyclization as judged by NMR, but significant amounts of apparently monodehalogenated yet cyclized material also formed under these conditions. Re-iodination of the crude mixture did not proceed to completion; however, we could isolate useful amounts of the diiodide **14**. Again, Kelly's stannylation/cross-coupling route led to poly(α-**2**). The problems associated for all of these steps prevented thorough comparisons between cross-coupled and oxidatively-derived poly(α-**2**) as discussed above for poly(**2**). However, THF-soluble oligomers of chemically cross-coupled poly(α-**2**) of undetermined number of repeat units all displayed similar absorption profiles with λ_{max} values around 380 nm, again reflecting the localized electronic structure of poly (α-**2**). For comparison, cyclized model **9** displays a lowest-energy absorption at 367 nm (in CH_2Cl_2, log ε = 3.93). This 13 nm difference between monomer and oligomer reflects the weak conjugation through oligomers of poly(α-**2**). Figure 8 juxtaposes these absorbances (right) with those obtained for the corresponding oligo(**2**)s (left).

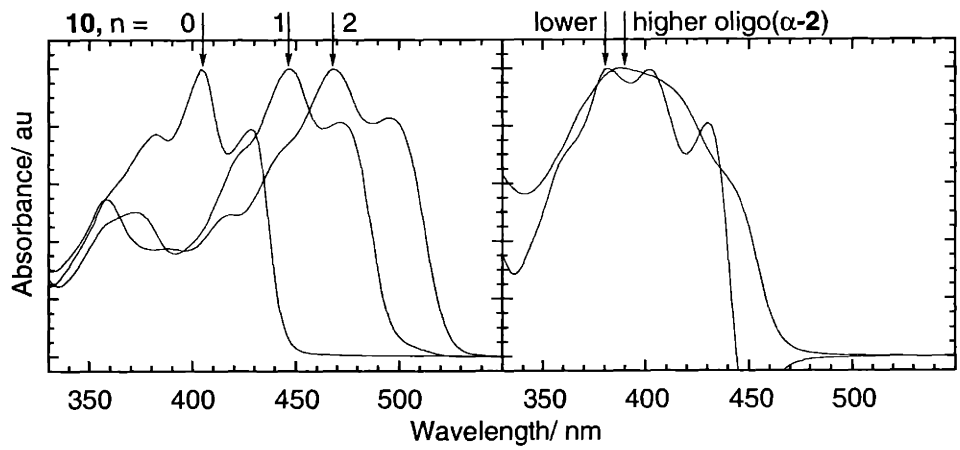

Figure 8: Normalized UV-vis absorptions (from GPC eluents) for a series of oligo(**2**)s (left) and oligo(α-**2**)s (right) in THF.

The CVs for poly(**2**) obtained anodically exhibit reversible electroactivity over a broad range of potentials consistent with a highly delocalized system (Figure 9, top). In contrast, poly(α-**2**) requires higher potentials for electroactivity and displays less reversible behavior (Figure 9, bottom). The problems encountered during the attempted chemical synthesis of poly(α-**2**) did not allow for suitably high molecular weight material in order to make a direct bulk conductivity comparison with poly(**2**). Attempts to obtain *in situ* conductivites also did not succeed due to poor adhesion of uniform polymer films on interdigitated microelectrodes, so we cannot offer any quantitative comparisons between poly(**2**) and poly(α-**2**). However, the more diffuse electroactivity and the higher oxidation potential observed for poly(α-**2**) would indicate that this material has a more localized electronic structure and exhibits a lesser degree of conductivity.

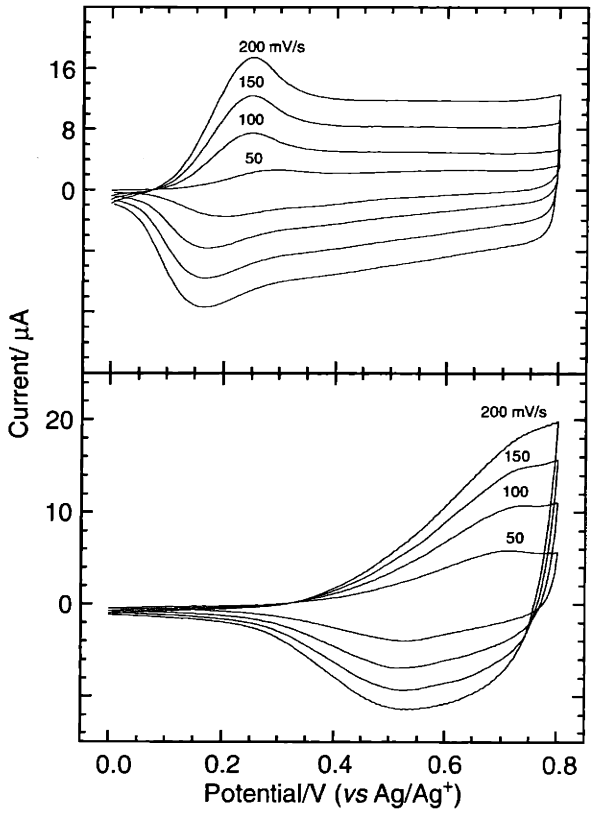

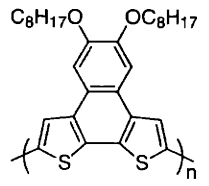

Poly(**2**)

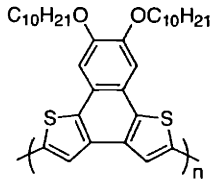

Poly(α-**2**)

Figure 9: Polymer cyclic voltammetry: poly(**2**) (top) and poly(α-**2**) (bottom) at a 2 mm^2 Pt button electrode in 0.1 M *n*-Bu_4PF_6 (CH_3CN) obtained at 50-200 mV/s. $E_{1/2}(Fc/Fc^+)$: +0.086 V.

These differing degrees of backbone delocalization available to poly(**2**) and isomeric poly(α-**2**) manifest themselves upon inspection of the spectroelectrochemistry presented in Figure 10. Electrodeposition on transparent In-SnO_2 glass electrodes of red poly(**2**) films and yellow poly(α-**2**) films (from **1a** and α-**1**, respectively) provided films that transformed to dark blue as the anodic potential cycled through values sufficiently high to oxidize the polymer. On account of this transparency, we could monitor the electrochromicity of the deposited materials as the oxidation potential increased. Attesting to the extraordinary stability imparted by the naphthodithiophene moieties, the electroactivity and electrochromicity of these films persisted after over 10,000 scans under ambient atmospheric conditions. Poly(**2**) displayed a low energy absorption centered at 620 nm along with a near-IR absorbance that increased with further oxidation (Figure 10, top). For poly(α-**2**), a low energy band centered at 550 nm appeared with increased oxidation along with a broad near-IR band that drifted to higher energy with further doping (Figure 10, bottom). The well-defined higher energy transition coupled with this NIR drift implies that poly(α-**2**) has a more localized electronic structure than that of poly(**2**). After considering the quinoidal polymer resonance structures illustrated in Figure 10, poly(α-**2**) should possess a low degree of electronic delocalization due to the necessary disruption of aromaticity within the fused benzo fragment of the repeat unit. Indeed, the higher oxidation potential and UV-vis absorbances of poly(α-**2**) reflect the energetic cost of delocalizing charge within the oxidized material. From this argument, it follows that poly(**2**) oxidizes at lower potential due to the extended thiophene-centered quinoidal delocalization available without requiring significant aromatic perturbation in the benzo fragment. The relative energies of such quinoidal resonance contributions play important roles in determining the band gaps of conjugated polymers.[29]

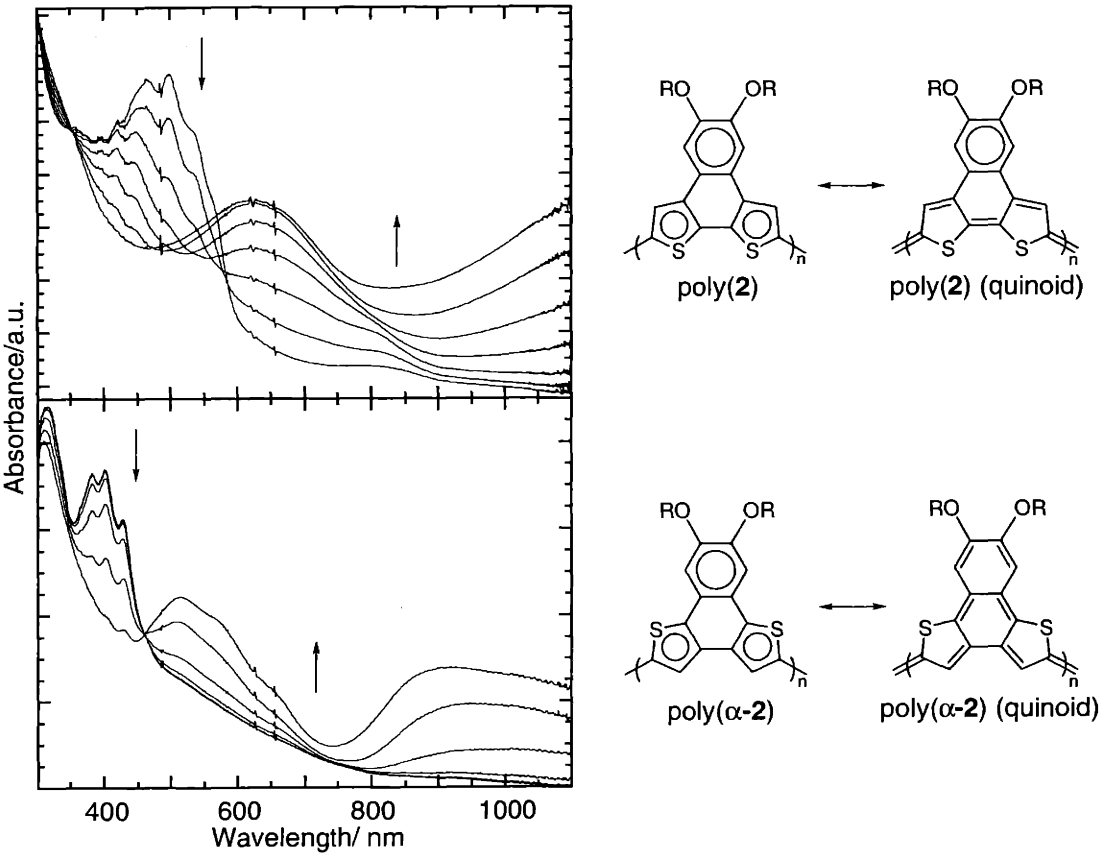

Figure 10: Changes in UV-vis absorption upon increased oxidation for poly(**2**) (top) and poly(α-**2**) (bottom) grown on ITO-coated electrodes and held at *ca.* 120 mV steps between 0.15-0.90 V. Other conditions as in Figure 3. The exaggerated resonance structures to the right depict possible ground-state *and* oxidized resonance contributions: they do not imply that the entire charged polymer exists in the as-drawn quinoidal bonding scheme.

Concluding Remarks

In summary, we have designed and synthesized a series of pendant aromatic monomers that display excellent chemical and electrochemical behavior. The pendant thienyls **1** and **α-1** undergo a tandem cyclization/polymerization process to yield a new class of robust electrochromic materials. To further study this process, we developed efficient chemical and electrochemical syntheses of the naphtho[2,1-*b*:3,4-*b*']dithiophene core **2**, a monomer poised for further investigation. In analogy to the iodination/cross-coupling route to poly(**2**), preliminary work has shown that Suzuki, Stille and Sonogashira[15] protocols can also provide easy access to a variety of extended *monomeric* systems. Through judicious choices of pendant functionality, we can tune the liquid crystallinity and electroactivity of these systems. The following chapter describes our efforts to utilize this chemistry for the syntheses of larger monomers for subsequent incorporation into novel organic materials.

Experimental Section

General: Air and water sensitive reactions employed standard Schlenk techniques under argon atmosphere. Methylene chloride, THF and TMEDA were passed through activated alumina columns prior to use and TMEDA was then distilled from KOH; *n*-BuLi in hexane was titrated *versus* diphenylacetic acid before use. All other chemicals were of reagent grade and used as received. 1,2-dialkoxy-4,5-dihalobenzenes were obtained via Williamson etherification of catechol followed by bromination with molecular bromine[30,31] or iodination with $Hg(OAc)_2$ and I_2.[32] 1,2-Didecyloxybenzene was monobrominated with NBS for preparation of **monoβ**. 4,5-Dibromoveratrole was obtained through bromination of veratrole with molecular bromine. 2,5-Dimethylphenyl boronic acid was prepared *via* lithiation and subsequent quenching with tri(isopropyl)borate. 5-Methyl-2-(tributylstannyl)thiophene was obtained *via* lithiation of 2-methylthiophene and quenching with tributylstannyl chloride.

Column chromatography was performed using Baker 40 μm silica gel. All organic extracts were dried over $MgSO_4$ and filtered prior to removal under reduced presure. NMR spectra were obtained on Varian Unity or Mercury 300, Bruker Avance 400 or Varian Inova 500 spectrometers, and all chemical shifts are referenced to residual $CHCl_3$ (7.26 ppm for ^1H, 77.23 ppm for ^{13}C) or $CHDCl_2$ (5.32 ppm for ^1H,

54.00 ppm for ^{13}C); aromatic carbon multiplicities were determined by DEPT analysis. High resolution mass spectra were obtained at the MIT Department of Chemistry Instrumentation Facility (DCIF) on a Bruker Daltronics APEX II 3 Tesla FT-ICR-MS. Molecular weight determination by gel permeation chromatography (GPC) was performed in THF versus polystyrene standards (PolySciences) on a HP 1100 HPLC system equipped with a Plgel 5 mm Mixed C column (300 x 7.5 mm). UV-Vis measurements were obtained on a Hewlett-Packard 8452A diode array spectrophotometer. Elemental analyses were obtained at Desert Analytics (Tucson, AZ). Melting points are uncorrected. Conductivity measurements were determined by the four-point probe method; film thicknesses were determined on surface profiler.

All electrochemical measurements were made with an Autolab PGSTAT 20 potentiostat (Eco Chemie). Cyclic voltammetry was performed in oven-dried, argon-purged one chamber three electrode cells *versus* a *quasi*-internal Ag wire reference electrode (BioAnalytical Systems) submersed in 0.01 M $AgNO_3$/0.1 M *n*-Bu_4NPF_6 (TBAP) in anhydrous MeCN. All studies employed TBAP electrolyte in MeCN or CH_2Cl_2 as noted. **Spectroelectrochemistry** was performed under ambient laboratory conditions on polymer films electrodeposited onto ITO coated glass electrodes. The films were placed in a quartz cuvette in the path of the light source along with counter and reference electrodes as used above. The film was allowed to equilibrate for 30 sec at a given oxidation potential prior to measuring the absorption spectrum. **Bulk electrolyses** were conducted *vs.* Ag/Ag^+ at a *ca* 4 cm^2 Pt gauze electrode in a 2 chambered cell separated by a glass frit to allow for isolation of the Pt gauze (ca. 6 cm^2) counterelectrode.

4.5-Dioctyloxy-1,2-di(3-thienyl)benzene (**1a**): A three-necked 1 L flask was charged with 4,5-dibromo-1,2-dioctyloxybenzene[30] (8.74 g, 17.8 mmol), 3-thiophene boronic acid (5.00 g, 39.1 mmol), Na_2CO_3 (15.01 g, 141.6 mmol) and equipped with a condenser. PhMe (285 mL), EtOH (70 mL) and H_2O (70 mL) were added to the flask and the solution was vigorously stirred during a 1 hr purge with argon. Under a gentle argon stream, $Pd(PPh_3)_4$ (605 mg, 0.524 mmol) was added to the solution, and the system was heated at reflux for 18h, cooled to room temperature and diluted with ether. After removing the aqueous layer, the organics were washed with 2M KOH (x2), and NaCl (aq), and the organic phase was dried ($MgSO_4$) and removed *in vacuo*. Chromatography of the crude material on silica gel (3:1 hexane/CH_2Cl_2) provided the product as a chaulky white solid (8.330 g, 16.70 mmol, 94%). mp 74-75°C. ^1H NMR (300 MHz, $CDCl_3$) δ: 7.17 (dd, 2H, J = 3.0, 4.8 Hz), 7.01 (dd, 2H, J = 1.2, 3.0 Hz), 6.96 (s, 2H), 6.78 (dd, 2H, J = 1.1, 5.0 Hz), 4.05 (t, 4H, J = 6.6 Hz), 1.85 (quin, 4H, J = 6.9 Hz), 1.49 (m, 4H), 1.30 (bm, 16H), 0.90 (t, 6H, J = 6.3 Hz). ^{13}C NMR (100 MHz, $CDCl_3$) δ: 148.5, 142.2, 129.3, 128.1, 124.7, 122.5, 115.9, 69.6, 32.0, 29.57, 29.50 (2 C), 26.2, 22.9, 14.3. FT-IR (KBr): ν/cm^{-1}: 3096, 2954, 2921, 2852, 1602, 1536,

1505, 1467, 1386, 1259, 1163, 1060, 781, 676. UV-vis ($CHCl_3$) λ/nm (log ε): 241 (4.29), 279 (3.94). HR-MS (EI): found *m/z* = 498.2617 ± 0.0015 (M^+); calc. for $C_{30}H_{42}O_2S_2$: 498.2626.

4,5-Bis(tetradecyloxy)-1,2-di(3-thienyl)benzene (**1b**): 1,2-Bis(tetradecyloxy)-4,5-dibromobenzene[30] (11.69 g, 17.70 mmol) was treated to the same conditions as for **1b**. The reaction was worked up as described for **1a**, and the crude material was initially pushed through a plug of silica gel (CH_2Cl_2). Recrystallization from $CHCl_3$/MeOH provided the product as opaque white plates (10.73 g, 16.08 mmol, 91%). mp 88.5°C. ^{1}H NMR (300 MHz, $CDCl_3$) δ: 7.17 (dd, 2H, *J* = 3.2, 5.0 Hz), 7.01 (dd, 2H, *J* = 1.1, 2.9), 6.96 (s, 2H), 6.77 (dd, 2H, *J* = 1.4, 5.0 Hz), 4.05 (t, 4H, *J* = 6.6 Hz), 1.85 (quin, 4H, *J* = 6.6 Hz), 1.49 (m, 4H), 1.27 (bm, 40H), 0.89 (t, 6H, *J* = 6.6 Hz). ^{13}C NMR (75 MHz, $CDCl_3$) δ: 148.4, 142.1, 129.2, 128.1, 124.6, 122.4, 115.8, 69.7, 32.2, 30.01, 29.97, 29.95, 29.72, 29.67, 29.60, 26.3, 23.0, 14.5. FT-IR (KBr): ν/cm^{-1}: 3096, 2917, 2849, 1602, 1506, 1467, 1259, 1163, 1055, 845, 783. HR-MS (EI): found *m/z* = 666.4526 ± 0.0019 (M^+); calc. for $C_{42}H_{66}O_2S_2$: 666.4505. Anal: Calcd for $C_{42}H_{66}O_2S_2$: C, 75.62; H, 9.97. Found: C, 75.78; H, 10.24.

4,5-Di(2-ethylhexyloxy)-1,2-di(3-thienyl)benzene (**1c**): Following the procedure for **1a** except for the use of 4,5-dibromo-1,2-di(2-ethylhexyloxy)benzene[31] (4.93 g, 10.0 mmol) and a reaction time of 45h, chromatography of the crude material on silica gel (hexane to 3:1 hexane/CH_2Cl_2) provided the product as a viscous, opaque white oil (4.068 g, 8.156 mmol, 82%). ^{1}H NMR (400 MHz, $CDCl_3$) δ: 7.17 (dd, 2H, *J* = 3.0, 4.9 Hz), 7.02 (m, 2H, apparent dd), 6.95 (s, 2H), 6.79 (dd, 2H, *J* = 0.8, 5.0 Hz), 3.92 (m, 4H), 1.79 (m, 2H), 1.31-1.54 (bm, 16H), 0.93 (m, 12H). ^{13}C NMR (100 MHz, $CDCl_3$) δ: 149.0, 142.4, 129.3, 128.0, 124.7, 122.4, 115.6, 72.0, 39.8, 30.8, 29.3, 24.2, 23.3, 14.3, 11.4. FT-IR (neat): ν/cm^{-1}: 3101, 2958, 2927, 2871, 1614, 1542, 1500, 1465, 1256, 1161, 1032, 846, 780. UV-vis (CH_2Cl_2) λ/nm (log ε): 231 (4.49), 278 (4.11). HR-MS (EI): found *m/z* = 498.2615 ± 0.0014 (M^+); calc. for $C_{30}H_{42}O_2S_2$: 498.2626.

4,5-Didecyloxy-1,2-di(3-thienyl)benzene (**α-1**): A 25 mL Schlenk tube was charged with 1,2-didecyloxy-4,5-diiodobenzene[32] (0.999 g, 1.55 mmol) and $(Ph_3P)_2PdCl_2$ (51 mg, 0.073 mmol) and placed under argon. Degassed PhMe (1 mL) and DMF (3 mL) were added and the system was heated to 80°C. 2-(Tributylstannyl)thiophene (1.3 mL, 3.9 mmol) was added dropwise, and the reaction was stirred at 80°C for 6h. After cooling, the mixture was pushed through a silica gel plug (1:1 hexane/CH_2Cl_2) and the solvents were removed. The crude material was dissolved in ether and washed with NH_4Cl, 1M HCl, NaF (x2), and NH_4Cl (x2). The organic phase was dried ($MgSO_4$) and removed *in vacuo* to provide a yellow solid. Recrystallization from $CHCl_3$/MeOH provided the product as a chaulky white solid (733 mg, 1.32 mmol, 85%). mp 68.5-69°C. ^{1}H NMR (500 MHz, $CDCl_3$) δ: 7.22 (d, 2H, *J* = 6.0 Hz), 6.99 (s,

2H), 6.93 (m, 2H), 6.83 (d, 2H, J = 3.0 Hz), 4.04 (t, 4H, J = 6.5 Hz), 1.84 (quin, 4H, J = 7.0 Hz), 1.47 (quin, 4H, J = 7.0 Hz), 1.28 (m, 28H), 0.88 (t, 6H, J = 7.0 Hz). ^{13}C NMR (125 MHz, $CDCl_3$) δ: 148.8, 143.1, 128.0, 126.9, 126.5, 125.6, 116.3, 69.6, 32.1, 29.85, 29.80, 29.62, 29.57, 29.43, 26.2, 22.9, 14.4. FT-IR (KBr): ν/cm^{-1}: 2955, 2919, 2850, 1600, 1504, 1467, 1260, 1233, 1160, 1074, 857, 692. UV-vis ($CHCl_3$) λ/nm (log ε): 241 (4.27), 296 (4.24). HR-MS (EI): found m/z = 554.3243 ± 0.0016 (M^+); calc. for $C_{34}H_{50}O_2S_2$: 554.3252.

4,5-Di(2-ethylhexyloxy)-1,2-di(2-thienyl)benzene (α-**1**, except R = 2-ethylhexyl): A solution of 4,5-dibromo-1,2-di(2-ethylhexyloxy)benzene[31] (6.86 g, 13.9 mmol) in DMF (100 mL) was purged with a flow of argon in a 100 mL Schlenk flask followed by the addition of $(Ph_3P)_2PdCl_2$ (441 mg, 0.628 mmol). The system was heated to 80°C, and 2-(tributylstannyl)thiophene (12.60 g, 32.08 mmol) was added dropwise. After 21h at 80°C, the reaction was cooled and diluted with ether. After vigorous stirring with 1M NaF, the aqueous layer was removed and washed with ether. The combined organics were stirred again with 1M NaF followed by washes with NH_4Cl (x3). The organics were dried and removed to provide a brown oil. This crude material was purified on silica (hexane to 6:1 hexane/CH_2Cl_2) to provide a bright yellow oil used without further purification (5.459 g, 10.94 mmol, 79%). ^{1}H NMR (400 MHz, $CDCl_3$) δ: 7.20 (dd, 2H, J = 1.1, 5.1 Hz), 6.99 (s, 2H), 6.92 (dd, 2H, J = 3.5, 5.1 Hz), 6.84 (dd, 2H, J = 1.2, 3.5 Hz), 3.91 (m, 4H), 1.79 (m, 2H), 1.3-1.6 (bm, 16H), 0.92 (m, 12H). ^{13}C NMR (100 MHz, $CDCl_3$) δ: 149.1, 143.2, 126.96, 126.84, 126.3, 125.6, 115.9, 71.8, 39.7, 30.8, 29.3, 24.1, 23.3, 14.3, 11.4. FT-IR (neat): ν/cm^{-1}: 3104, 3070, 2964, 2927, 2871, 1599, 1537, 1501, 1465, 1433, 1380, 1256, 1231, 1159, 1029, 828, 693. HR-MS (EI): found m/z = 498.2612 (M^+); calc. for $C_{30}H_{42}O_2S_2$: 498.2621.

3-(3,4-Didecyloxyphenyl)thiophene (**mono**β): Following the procedure for **1a** except substituting 1,2-didecyloxy-4-bromobenzene (1.870 g, 3.983 mmol), the crude material was chromatographed on silica gel (4:1 hexane/CH_2Cl_2) provided the product as a white solid (1.811 g, 3.831 mmol, 96%). mp 66.5-67°C. ^{1}H NMR (400 MHz, $CDCl_3$) δ: 7.33 (m, 3H), 7.11 (m, 2H), 6.89 (d, 1H, J = 8.8 Hz), 4.03 (m, 4H, apparent 2 t), 1.82 (m, 4H), 1.48 (m, 4H), 1.27 (bm, 16H), 0.88 (t, 6H, 6.56 Hz). ^{13}C NMR (100 MHz, $CDCl_3$) δ: 149.5, 148.8, 142.5, 129.3, 126.6, 126.2, 119.3 (2C), 114.2, 112.8, 69.7, 69.5, 32.1, 29.9, 29.8, 29.7, 29.6, 29.5, 26.3, 22.9, 14.3. FT-IR (KBr): ν/cm^{-1}: 2958, 2918, 2850, 1601, 1585, 1509, 1475, 1258, 1213, 1144, 1028, 773. HR-MS (EI): found m/z = 472.3363 (M^+); calc. for $C_{30}H_{48}O_2S$: 472.3370.

8,9-Dioctyloxynaphtho[2,1-*b*:3,4-*b*']dithiophene (**2a**): A solution of **1a** (330 mg, 0.66 mmol) in CH_2Cl_2 (15 mL) was stirred vigorously under argon as a suspension of $FeCl_3$ (450 mg, 2.77 mmol) in CH_2Cl_2 (7 mL) was added dropwise. The solution was stirred under an argon purge for 30 min at which point

anhydrous MeOH was added and stirred for 30 min. The solvents were removed, and the residue was taken up in CH_2Cl_2 and stirred vigorously with NH_4OH (aq). The aqueous layer was washed twice with CH_2Cl_2, and the combined organics were washed with NH_4OH and NH_4Cl, dried and removed. Purification on silica (hexane to 4:1 hexane/CH_2Cl_2) provided the product as very faint yellow solid (216 mg, 0.435 mmol, 66%). mp 118.5-121°C. ^{1}H NMR (400 MHz, $CDCl_3$) δ: 7.87 (d, 2H, *J* = 5.4 Hz), 7.69 (s, 2H), 7.46 (d, 2H, *J* = 5.3), 4.20 (m, 4H), 1.95 (m, 2H), 1.56 (m, 4H), 1.32 (bm, 16H), 0.91 (t, 6H, *J* = 6.5 Hz), 0.94 (t, 6H, *J* = 7.1 Hz). ^{13}C NMR (100 MHz, $CDCl_3$) δ: 149.0, 134.1, 130.6, 123.6, 122.90, 122.74, 106.9, 69.4, 32.1, 29.7, 29.53, 29.49, 26.3, 22.9, 14.4. FT-IR (KBr): ν/cm^{-1}: 2953, 2925, 2851, 1618, 1517, 1467, 1391, 1252, 1181, 1108, 1069, 840, 728. UV-vis ($CHCl_3$) λ/nm (log ε): 262 (4.58), 311 (3.80), 321 (3.84), 333 (3.75), 350 (3.75). HR-MS (ESI): found *m/z* = 519.2384 [(M+Na)$^+$]; calc. for $C_{30}H_{40}O_2S_2$+Na: 519.2362.

8,9-Bis(tetradecyloxy)naphtho[2,1-*b*:3,4-*b*']dithiophene (**2b**): A solution of **1b** (668 mg, 1.00 mmol) in CH_2Cl_2 (100 mL) was stirred vigorously under argon as a solution of $FeCl_3$ (343 mg, 2.11 mmol) in $MeNO_2$ (10 mL) was added dropwise over 5 min. Anhydrous MeOH was added at 30 min and stirred for 1 hr. The resulting precipitates were filtered and washed with MeOH to provide 527 mg of product as a faint green-yellow solid. The remaining organics were diluted with CH_2Cl_2 and stirred with NH_4OH (aq). The organic layer was washed with aqueous NH_4OH and NH_4Cl, dried and removed. This residue was dissolved in CH_2Cl_2 and diluted with hexanes (300% v/v) and pushed through a plug of silica gel (3:1 hexane/CH_2Cl_2). The organics were removed and the material was dissolved in CH_2Cl_2, precipitated into MeOH and filtered. The filtrate provided an additional 95 mg of product. Overall, 622 mg was obtained (0.935 mmol, 93%). mp 115-115.5°C. ^{1}H NMR (300 MHz, $CDCl_3$) δ: 7.88 (d, 2H, *J* = 5.4 Hz), 7.70 (s, 2H), 7.47 (d, 2H, *J* = 5.7 Hz), 4.21 (t, 4H, *J* = 6.3 Hz), 1.96 (m, 4H), 1.56 (m, 4H), 1.28 (bm, 40H), 0.90 (t, 6H, *J* = 6.6 Hz). FT-IR (KBr): ν/cm^{-1}: 3092, 2918, 2849, 1619, 1515, 1469, 1390, 1252, 1183, 1107, 840, 727, 639. HR-MS (EI): found *m/z* = 664.4360 (M$^+$); calc. for $C_{42}H_{64}O_2S_2$: 664.4342. Anal: Calcd for $C_{42}H_{64}O_2S_2$: C, 75.85; H, 9.70. Found: C, 76.16; H, 9.91.

8,9-Di(2-ethylhexyloxy)naphtho[2,1-*b*:3,4-*b*']dithiophene (**2c**): Subjecting **1c** (504 mg, 1.01 mmol) to the same procedure as described for **2b** above, the crude mixture was pushed through a plug of silica. The eluent was concentrated and added dropwise to MeOH. After filtering off the precipitated yellow solids, the filtrate was evaporated, and the crude product purified on silica gel (hexane to to 8:1 hexane/CH_2Cl_2) to provide the product as a faint yellow oil (272 mg, 0.548 mmol, 54%) alongside the previously precipitated, doubly cyclized dimer **10** (n=0; 94 mg, 0.095 mmol, 19%) and higher oligomers. ^{1}H NMR (400 MHz, $CDCl_3$) δ: 7.89 (d, 2H, *J* = 5.4 Hz), 7.69 (s, 2H), 7.47 (d, 2H, *J* = 5.3), 4.09 (m, 4H), 1.89 (m,

2H), 1.37-1.62 (m, 16H), 1.01 (t, 6H, J = 7.5 Hz), 0.94 (t, 6H, J = 7.1 Hz). ^{13}C NMR (125 MHz, $CDCl_3$) δ: 149.3, 134.1, 130.4, 123.5, 122.76, 122.74, 106.4, 71.6, 39.8, 30.9, 29.4, 24.25, 24.23, 23.3, 14.4, 11.5. FT-IR (neat): ν/cm^{-1}: 3101, 3072, 2957, 2927, 2871, 1619, 1515, 1448, 1380, 1252, 1190, 1107, 1017, 839, 720, 641. UV-vis (CH_2Cl_2) λ/nm (log ε): 228 (4.43), 263 (4.81), 310 (4.00), 321 (4.04), 334 (3.93), 350 (3.96). HR-MS (EI): found m/z = 496.2458 ± 0.0014 (M^+); calc. for $C_{30}H_{40}O_2S_2$: 496.2470.

1,2-Bis[2-bromo-5-(2,5-dimethylphenyl)-3-thienyl]-4,5-bis(tetradecyloxy)benzene (en route to **3**): A 100 mL three-necked flask equipped with a condenser was charged with **4** (1.301 g, 1.208 mmol), 2,5-dimethylphenyl boronic acid (380 mg, 2.5 mmol), and the solids were dissolved in PhMe (35 mL) and EtOH (5 mL). With vigorous stirring, a solution of Na_2CO_3 (999 mg, 9.43 mmol) in water (5 mL) was added, and the biphasic system was purged with a strong flow of argon for 45 min. Under a gentle argon stream, $Pd(PPh_3)_4$ (41 mg, 0.036 mmol) was added to the solution, and the system was heated at reflux for 8 h, cooled to 70°C and stirred for an additional 18 h. After cooling to room temperature, the reaction was diluted with ether. After removing the aqueous layer, the organics were washed with NH_4Cl (aq) and pushed through a plug of silica. Removal of the eluents provided a crude orange oil. Two purifications on silica gel (hexane, then gradually to 6:1 hexane/CH_2Cl_2) provided the product as a viscous faint yellow oil (664 mg, 0.643 mmol, 53%). ^{1}H NMR (400 MHz, $CDCl_3$) δ: 7.07 (m, 8H), 6.57 (s, 2H), 4.08 (t, 4H, J = 6.6 Hz), 2.28 (s, 6H), 2.18 (s, 6H), 1.85 (m, 4H), 1.49 (m, 4H), 1.26 (bm, 44H), 0.88 (t, 6H, J = 6.6 Hz). ^{13}C NMR (100 MHz, $CDCl_3$) δ: 148.5, 142.7, 141.4, 135.6, 133.1, 132.9, 131.0, 130.7, 129.3, 129.0, 127.2, 115.6, 109.5, 69.3, 32.2, 29.9, 29.68, 29.62, 29.4, 26.3, 22.9, 21.0, 20.7, 14.4.

1,2-Bis[5-(2,5-dimethylphenyl)-3-thienyl]-4,5-bis(tetradecyloxy)benzene (**3**): A solution of 1,2-bis[2-bromo-5-(2,5-dimethylphenyl)-3-thienyl]-4,5-bis(tetradecyloxy)benzene (659 mg, 0.638 mmol) in THF (50 mL) was cooled to -78°C, and *n*-BuLi was added (2.4 mL, 3.8 mmol). The reaction stirred for 5 min, and AcOH (1 mL) was added to quench any lithiated species. After warming to room temperature, the solution was washed with 2M KOH (x2) and NH_4Cl, dried and removed to provide a clear yellow oil. After purification on silica, the product was obtained as a clear oil (552 mg, 0.631 mmol, 99%). ^{1}H NMR (400 MHz, $CDCl_3$) δ: 7.16 (m, 2H, apparent d, J = 1.0 Hz), 7.11 (d, 2H, J = 1.4 Hz), 7.09 (d, 2H, J = 7.8 Hz), 7.02 (m, 4H, apparent s and dd, J = 1.3, 7.5 Hz), 6.81 (d, 2H, J = 1.4 Hz), 4.07 (t, 4H, J = 6.6 Hz), 2.30 (s, 6H), 2.23 (s, 6H), 1.86 (m, 4H), 1.49 (m, 4H), 1.26 (bm, 44H), 0.88 (t, 6H, J = 6.6 Hz). ^{13}C NMR (100 MHz, $CDCl_3$) δ: 148.6, 142.7, 142.5, 135.5, 134.0, 132.9, 131.0 (CH), 130.9 (CH), 128.8 (CH), 128.58 (CH), 128.37, 122.0 (CH), 115.7 (CH), 69.6, 32.15, 29.94, 29.89, 29.88, 29.65, 29.60, 29.52, 26.3, 22.9, 21.0, 20.9, 14.4. FT-IR (KBr): ν/cm^{-1}: 2920, 2851, 1602, 1539, 1514, 1497, 1467, 1378, 1360,

1256, 1212, 1153, 1036, 846, 807. UV-Vis (CH_2Cl_2) λ/nm (log ε): 233 (4.66), 243 (4.68), 271 (4.51). HR-MS (EI): found *m/z* = 874.5774 (M^+); calc. for $C_{58}H_{82}O_2S_2$: 874.5751.

1,2-Bis(2-bromo-3-thienyl)-4,5-bis(tetradecyloxy)benzene (en route to **4**): A solution of **1b** (2.003 g, 3.003 mmol) in CH_2Cl_2 (150 mL) was stirred at room temperature while bromine (0.32 mL, 6.2 mmol) was added dropwise. Precipitates formed at 20 min, but the reaction was stirred for an additional 3.5 h, at which point 2M KOH was added. Washing with 2M KOH and NaCl and drying the organics provided a crude oily solid that was purified on silica gel (hexane) to yield an off-white yellowish solid (2.373 g, 2.876 mmol, 96%). mp 44.5-46°C. ^{1}H NMR (300 MHz, $CDCl_3$) δ: 7.07 (d, 2H, *J* = 5.4 Hz), 6.96 (s, 2H), 6.52 (d, 2H, *J* = 5.7 Hz), 4.06 (t, 4H, *J* = 6.6 Hz), 1.86 (m, 4H), 1.49 (m, 4H), 1.27 (bm, 40H), 0.89 (t, 6H, *J* = 6.3 Hz). ^{13}C NMR (100 MHz, $CDCl_3$) δ: 148.5, 141.1, 130.0, 127.0, 125.0, 115.6, 110.6, 69.3, 32.2, 29.7-29.9 (unresolved Cs), 29.6, 29.4, 26.3, 22.9, 14.4. FT-IR (KBr): ν/cm^{-1}: 2918, 2850, 1603, 1545, 1504, 1467, 1262, 1232, 1190, 1073, 989. HR-MS (EI): found *m/z* = 822.2710 (M^+); calc. for $C_{42}H_{64}Br_2O_2S_2$: 822.2709.

1,2-Bis(2-bromo-5-iodo-3-thienyl)-4,5-bis(tetradecyloxy)benzene (**4**): To a solution of 1,2-bis(2-bromo-3-thienyl)-4,5-bis(tetradecyloxy)benzene (1.600g, 1.940 mmol) in CCl_4 (32 mL) was added I_2 (503 mg, 1.98 mmol) and $PhI(OCOCF_3)_2$ (888 mg portionwise, 2.07 mmol). The reaction was stirred while excluding light for 37 h, at which point NMR monitoring showed essentially complete conversion to the apparent product. The reaction was quenched with 2M KOH, and the organics were diluted with $CHCl_3$ and washed with 2M KOH (x2). The combined aqueous layers were washed with CH_2Cl_2, and the combined organics were washed with NH_4Cl (aq), dried and removed to provide a crude oily solid. The crude material was pushed through a plug of silica (4:1 hexane/CH_2Cl_2) to provide the product as a yellow-orange solid (1.859 g, 1.727 mmol, 89%). mp 79-80.5°C. ^{1}H NMR (400 MHz, $CDCl_3$) δ: 6.87 (s, 2H), 6.74 (s, 2H), 4.03 (t, 4H, *J* = 6.6 Hz), 1.85 (m, 4H), 1.47 (m, 4H), 1.26 (bm, 44H), 0.88 (t, 6H, *J* = 6.5 Hz). ^{13}C NMR (100 MHz, $CDCl_3$) δ: 148.8, 142.8, 139.3, 125.7, 115.2, 113.7, 71.2, 69.4, 32.1, 29.93, 29.89, 29.85, 29.64, 29.60, 29.36, 26.23, 22.9, 14.4. FT-IR (KBr): ν/cm^{-1}: 2916, 2848, 1499, 1468, 1429, 1388, 1339, 1258, 1213, 1075, 827.

2,5-Bis(2,5-dimethylphenyl)-8,9-bis(tetradecyloxy)naphtho[2,1-*b*:3,4-*b*']dithiophene (**5**)

Route A – $FeCl_3$ cyclization: A solution of **3** (344 mg, 0.393 mmol) in CH_2Cl_2 (35 mL) was stirred vigorously under argon as a suspension of $FeCl_3$ (255 mg, 1.57 mmol) in CH_2Cl_2 (5 mL) under argon was added dropwise over 2 min. The solution was stirred under an argon purge for 15 min at which point MeOH (approx. 20 mL) was added and stirred. NH_4OH was added to the reaction, and the aqueous layer

was removed and washed twice with CH_2Cl_2. The combined organics were washed with NH_4OH and NH_4Cl, dried and removed. The residue was dissolved in CH_2Cl_2 and precipitated into MeOH. The solids were filtered and rinsed with MeOH to provide the product as a pale yellow chaulky solid (319 mg, 0.365 mmol, 93%).

Route B - Suzuki coupling: A 50 mL two-necked flask equipped with a condenser was charged with **7** (118 mg, 0.143 mmol) and 2,5-dimethylphenyl boronic acid (45 mg, 0.30 mmol), and the solids were dissolved in PhMe (5 mL) and EtOH (1 mL). During vigorous stirring, a solution of Na_2CO_3 (118 mg, 1.11 mmol) in water (1 mL) was added, and the biphasic system was purged with a strong flow of argon for 30 min. Under a gentle argon stream, $Pd(PPh_3)_4$ (5 mg, 0.005 mmol) was added to the solution, and the system was heated at reflux for 15 h. After cooling to room temperature, the reaction was diluted with ether, washed twice with NH_4Cl (aq), dried and removed. Purification on a silica plug (3:1 hexane/CH_2Cl_2) and removal of the eluents provided a product that was dissolved in CH_2Cl_2 and precipitated from MeOH. Filtering and rinsing the solids with MeOH provided the product as a yellow chalky solid (106 mg, 0.121 mmol, 85%). mp 67-68.5°C. ^{1}H NMR (400 MHz, $CDCl_3$) δ: 7.78 (s, 2H), 7.68 (s, 2H), 7.40 (d, 2H, J = 1.0 Hz), 7.21 (d, 2H, J = 7.8 Hz), 7.12 (dd, 2H, J = 1.4, 7.8 Hz), 4.20 (t, 4H, J = 6.6 Hz), 2.52 (s, 6H), 2.39 (s, 6H), 1.92 (m, 4H), 1.53 (m, 4H), 1.26 (bm, 44H), 0.88 (t, 6H, J = 6.7 Hz). FT-IR (KBr): ν/cm^{-1}: 2918, 2849, 2360, 2342, 1618, 1520, 1465, 1256, 1187, 1098, 669. UV-Vis (CH_2Cl_2) λ/nm (log ε): 233 (4.59), 269 (4.75), 354 (4.43). HR-MS (EI): found m/z = 872.5588 (M^+); calc. for $C_{58}H_{80}O_2S_2$: 872.5594.

2,5-Dibromo-8,9-bis(tetradecyloxy)naphtho[2,1-*b*:3,4-*b'*]dithiophene (**7**): A solution of **2 b** (116 mg, 0.174 mmol) in CH_2Cl_2 (17 mL) was stirred at room temperature while Br_2 (18.3 μL, 0.357 mmol) was added dropwise. Thick precipitates formed after 15 min. The reaction stirred for 1.5 h, at which MeOH was added to the mixture. The solids were filtered and rinsed with MeOH to provide a yellow solid that was used without further purification (123 mg, 0.149 mmol, 86%). ^{1}H NMR (400 MHz, $CDCl_3$) δ: 7.82 (s, 2H), 7.50 (s, 2H), 4.17 (t, 4H, J = 6.6 Hz), 1.93 (m, 4H), 1.53 (m, 4H), 1.26 (bm, 44H), 0.87 (t, 6H, 6.7 Hz). HR-MS (EI): found m/z = 820.2575 (M^+); calc. for $C_{42}H_{62}Br_2O_2S_2$: 820.2552.

4,5-Bis(5-methyl-2-thienyl)veratrole (**8**): A 25 mL Schlenk flask was charged with 4,5-dibromoveratrole (889 mg, 3.00 mmol) and $(Ph_3P)_2PdCl_2$ (105 mg, 0.150 mmol) and placed under argon. Degassed DMF (7 mL) was added and the system was heated to 80°C. 5-Methyl-2-(tributylstannyl)thiophene (3.48 g, 8.99 mmol) was added dropwise, and the reaction was stirred at 80°C for 16h. After cooling, the mixture was diluted with ether and stirred with NaF (aq). The aqueous layer was washed with ether, and the combined organics were washed with NaCl, dried and removed. The crude material was pushed through

a silica gel plug followed by careful column chromatography on silica (hexane to 1:1 hexane/CH_2Cl_2) to provide the product as a white solid. Recrystallization from $CHCl_3$/MeOH provided the product as a clear needle-like solid (696 mg, 2.11 mmol, 70%). mp 88-91°C. ^{1}H NMR (300 MHz, $CDCl_3$) δ: 6.94 (s, 2H), 6.67 (d, 2H, *J* = 3.3 Hz), 6.61 (m, 2H), 3.92 (s, 6H), 2.46 (s, 6H). ^{13}C NMR (75 MHz, $CDCl_3$) δ: 148.1, 140.5, 139.9, 126.58, 126.44, 125.1, 113.8, 56.1, 15.5. FT-IR (KBr): ν/cm^{-1}: 3057, 2999, 2955, 2911, 2839, 1600, 1515, 1439, 1352, 1231, 1142, 1017, 871, 800. UV-Vis (CH_2Cl_2) λ/nm (log ε): 233 (4.29), 268 (4.26), 304 (4.17). HR-MS (EI): found *m/z* = 330.0753 ± 0.0010 (M^+); calc. for $C_{18}H_{18}O_2S_2$: 330.0748. Anal: Calcd for $C_{18}H_{18}O_2S_2$: C, 65.42; H, 5.49. Found: C, 65.11; H, 5.47.

8,9-Dimethoxy-2,5-dimethylnaphtho[1,2-*b*:4,3-*b*']dithiophene (**9**): A solution of **8** (165 mg, 0.498 mmol) in CH_2Cl_2 (35 mL) was stirred vigorously under argon as a suspension of $FeCl_3$ (488 mg, 3.01 mmol) in CH_2Cl_2 (15 mL) under argon was added dropwise over 5 min. The solution was stirred under an argon purge for 45 min at which point MeOH was added and stirred. Water and NH_4OH were added to the solution and stirred. The aqueous layer was removed and washed with CH_2Cl_2 (x2). The combined organics were washed with 1M HCl, dried and removed to provide a crude purple material. Chromatography on silica (1:1 CH_2Cl_2/hexane) provided the product as a yellowish powder (75 mg, 0.23 mmol, 46%). mp 202-204°C. ^{1}H NMR (400 MHz, CD_2Cl_2) δ: 7.32 (d, 2H, *J* = 1.2 Hz), 7.29 (s, 2H), 4.00 (s, 6H), 2.68 (d, 6H, *J* = 1.2 Hz). ^{13}C NMR (100 MHz, $CDCl_3$) δ: 149.0, 138.9, 133.4, 132.3, 121.32, 121.25, 104.3, 56.2, 16.4. FT-IR (KBr): ν/cm^{-1}: 2995, 2911, 2848, 1621, 1513, 1478, 1435, 1284, 1238, 1165, 1118, 1022, 833. UV-Vis (CH_2Cl_2) λ/nm (log ε): 231 (4.57), 278 (4.91), 288 (5.12), 310 (4.49), 332 (3.67), 349 (3.85), 367 (3.93). HR-MS (EI): found *m/z* = 328.0586 (M^+); calc. for $C_{18}H_{16}O_2S_2$: 328.0586.

Oligo(**2**) characterization (**10**):

Dimer (n = 0): ^{1}H NMR (400 MHz, $CDCl_3$) δ: 8.06 (s, 2H), 7.89 (d, 2H, *J* = 5.4 Hz), 7.663 (s, 2H), 7.658 (s, 2H), 7.50 (d, 2H, *J* = 5.3 Hz), 4.14 (m, 4H), 4.09 (m, 4H), 1.90 (m, 4H), 1.3-1.7 (bm, 32H), 1.04 (m, 6H), 0.96 (m, 6H), 0.88 (m, 12H). ^{13}C NMR (100 MHz, $CDCl_3$) δ: 149.47, 149.43, 135.0, 134.57, 134.51, 129.73, 129.66, 123.8 (CH), 122.87, 122.83 (CH), 122.4, 119.6 (CH), 106.3 (CH), 106.0 (CH), 71.63, 71.58, 39.90, 39.77, 30.9, 29.51, 29.44, 24.2, 23.38, 23.35, 14.42, 14.37, 11.60, 11.54. HR-MS (FAB): found *m/z* = 990.4812 ± 0.0030 (M^+); calc. for $C_{60}H_{78}O_4S_4$: 990.4783.

Trimer (n = 1): ^{1}H NMR (400 MHz, $CDCl_3$) δ: 7.99 (s, 2H), 7.96 (s, 2H), 7.83 (d, 2H, *J* = 5.4 Hz), 7.61 (s, 2H), 7.59 (s, 4H), 7.46 (d, 2H, *J* = 5.3 Hz), 4.12 (bm, 8H), 4.06 (bm, 4H), 1.92 (m, 6H), 1.2-1.8 (bm, 48H), 0.95-1.05 (m, 36H). MS (MALDI): found *m/z* = 1484.5768 [$(M+H)^+$]; calc. For $C_{90}H_{116}O_6S_6$+H: 1485.7181.

8,9-Di(2-ethylhexyloxy)-2,5-diiodonaphtho[2,1-*b*:3,4-*b*']dithiophene (**12**): A dry 100 mL Schlenk flask containing a solution of TMEDA (0.80 mL, 5.3 mmol) in 40 mL THF was cooled to -78°C followed by the addition of 2.30 mL *n*-BuLi in hexanes (1.577 M, 3.63 mmol). The solution was stirred for 5 min, at which point a solution of **2c** (595 mg, 1.20 mmol) in 5 mL THF was added dropwise. After being held for 30 min at -78°C, a solution of I_2 (2.18 g, 8.59 mmol) in 5 mL THF was added. After addition, the reaction was stirred from -78°C to 25°C over 5 h. 2M KOH was added to quench the reaction and stirred overnight. The aqueous phase was washed with ether, and the combined organics were washed further with NH_4Cl (aq) and water. After drying ($MgSO_4$) and removing the solvent *in vacuo*, the pale yellow solid was dissolved in minimal CH_2Cl_2 and precipitated into MeOH. The collected solids were then recrystallized from $CHCl_3$/MeOH to provide the product as a fluffy pale yellow solid (603 mg, 0.8055 mmol, 67%). mp 154.5-155°C. ^{1}H NMR (400 MHz, $CDCl_3$) δ: 7.89 (s, 2H), 7.41 (s, 2H), 4.05 (m, 4H), 1.90 (m, 2H), 1.40-1.60 (bm, 16H), 1.01 (t, 6H, J = 7.4 Hz), 0.95 (t, 6H, J = 6.7 Hz). ^{13}C NMR (100 MHz, $CDCl_3$) δ: 149.7, 135.0, 133.9, 132.5, 121.2, 105.7, 74.0, 71.6, 39.8, 30.9, 29.4, 24.3, 23.3, 14.4, 11.5. FT-IR (KBr): ν/cm^{-1}: 2957, 2925, 2857, 1617, 1519, 1447, 1380, 1259, 1189, 1084, 822. UV-vis ($CHCl_3$) λ/nm (log ε): 267 (4.61), 335 (4.14), 350 (4.12). HR-MS (EI): found m/z = 748.0372 (M^+); calc. for $C_{30}H_{38}I_2O_2S_2$: 748.0397.

Poly(**2**), *representative procedure* from **1c** via oxidative cyclization-polymerization: A solution of **1c** (240 mg, 0.48 mmol) in CH_2Cl_2 (100 mL) was stirred vigorously under argon as a suspension of $FeCl_3$ (600 mg, 3.7 mmol) in CH_2Cl_2 (8 mL) under argon was added dropwise over 10 min. The solution was stirred under an argon purge for 3.5 hr at which point methanol was added. After stirring for approx 1 hr, the solvents were removed under reduced pressure, and the crude solids were redissolved in CH_2Cl_2. The organic phase was washed with NH_4OH (x2) and NaCl (aq), dried ($MgSO_4$) and removed *in vacuo* to provide the material as a dark burgandy red solid (208 mg).

Representative procedure from **12** via Pd catalyzed polymerization: A 25 mL screw cap tube was charged with $Pd(PPh_3)_4$ (5 mg, 4 μmol) and **12** (74 mg, 98 μmol) and purged gently with argon. To a tared vial containing degassed toluene (1.5 mL) and DMF (0.5 mL) was added $Me_3SnSnMe_3$ (43 mg, 130 μmol), and this solution was added to the screw cap tube. [CAUTION: $Me_3SnSnMe_3$ is highly toxic and readily absorbed through the skin!] After brief argon purging and sealing of the tube, the system was heated to 90°C for 4 days at which point the reaction mixture was added dropwise to methanol. The precipitates were filtered to provide poly(**2**) as a burgundy red solid.

1,2-Bis(5-iodo-2-thienyl)-4,5-di(2-ethylhexyloxy)benzene (**13**): A solution of α-1 (except R = 2-ethylhexyl, 473 mg, 0.948 mmol) in CH_2Cl_2 (15 mL) was stirred at room temperature as $Hg(OAc)_2$ was added portionwise (606 mg, 1.90 mmol). The reaction was stirred with exclusion of light for 45 min followed by the addition of solid iodine (500 mg, 2 mmol). After stirring for 5 more hours, the reaction was quenched with water, diluted with CH_2Cl_2 and stirred with 2M KOH. The aqueous layer was removed and washed with CH_2Cl_2, and the combined organics were washed with 2M KOH and NH_4Cl, dried and removed. Purification on silica (hexane to 6:1 hexane/CH_2Cl_2) provided the product as a yellow oil used without further purification (617 mg, 0.822 mmol, 87%). ^{1}H NMR (400 MHz, $CDCl_3$) δ: 7.10 (d, 2H, *J* = 3.7 Hz), 6.90 (s, 2H), 6.54 (d, 2H, *J* = 3.7 Hz), 3.90 (m, 4H), 1.79 (m, 2H), 1.3-1.6 (bm, 16H), 0.93 (m, 12H). ^{13}C NMR (100 MHz, $CDCl_3$) δ: 149.4, 148.8, 137.1, 128.6, 125.2, 115.5, 73.2, 71.7, 39.6, 30.7, 29.3, 24.1, 23.3, 14.3, 11.4. FT-IR (neat): ν/cm^{-1}: 2957, 2926, 2870, 1597, 1538, 1500, 1464, 1253, 1221, 1156, 1028, 795. HR-MS (EI): found *m/z* = 750.0545 (M^+); calc. for $C_{30}H_{40}I_2O_2S_2$: 750.0554.

8,9-Di(2-ethylhexyloxy)-2,5-diiodonaphtho[1,2-*b*:4,3-*b'*]dithiophene (**14**): A solution of **13** (308 mg, 0.410 mmol) in CH_2Cl_2 (35 mL) was stirred vigorously under argon as a suspension of $FeCl_3$ (140 mg, 0.86 mmol) in CH_2Cl_2 (5 mL) under argon was added dropwise over 5 min. The solution was stirred under an argon purge for 45 min at which point MeOH was added. After stirring for approx 1 hr, the solvents were removed under reduced pressure and the crude solids were redissolved in CH_2Cl_2. The organic phase was stirred with NH_4OH and removed. The aqueous layer was washed twice with CH_2Cl_2. The combined organics were washed with NH_4OH and NH_4Cl (x2), dried ($MgSO_4$) and removed *in vacuo* to provide the crude product. This material was chromatographed on silica, and subjected to further iodination similar to **13** using $Hg(OAc)_2$ (70.1 mg, 0.220 mmol) and iodine (67 mg, 0.26 mmol) in CH_2Cl_2 (7 mL). Workup as described for **13** and chromatography on silica gel (hexane to 10:1 hexane/CH_2Cl_2) provided the product as a white solid that was dissolved in CH_2Cl_2 and precipitated into MeOH. This material was filtered and rinsed with MeOH to provide the product as a white fibrous solid (72 mg, 0.096 mmol, 23%). mp 105.5-106°C. ^{1}H NMR (400 MHz, $CDCl_3$) δ: 7.78 (s, 2H), 7.20 (s, 2H), 4.02 (m, 4H), 1.86 (m, 2H), 1.3-1.7 (bm, 16H), 0.94 (m, 12H). ^{13}C NMR (125 MHz, $CDCl_3$) δ: 150.1, 139.7, 132.8, 131.5, 120.5, 105.2, 74.2, 71.6, 39.6, 30.9, 29.4, 24.2, 23.3, 14.4, 11.5. FT-IR (KBr): ν/cm^{-1}: 2957, 2926, 2857, 1618, 1518, 1465, 1277, 1232, 1190, 1032, 812. HR-MS (EI): found *m/z* = 748.0417 (M^+); calc. for $C_{30}H_{38}I_2O_2S_2$: 748.0397.

References

(1) Tourillon, G.; Garnier, F. *J. Electroanal. Chem.* **1982**, *135*, 173-178.

(2) *Handbook of Conducting Polymers*, 2nd ed (Eds: T. A. Skotheim, R. L. Elsenbaumer, J. R. Reynolds). Marcel Dekker, New York **1998**.

(3) (a) Elsenbaumer, R. L.; Jen, K. Y.; Oboodi, R. *Synth. Met.* **1985**, *15*, 169-174; (b) Sato, M.; Tanaka, S.; Kaeriyama, K. *J. Chem. Soc., Chem. Commun.* **1986**, 873-874.

(4) Sato, M.; Tanaka, S.; Kaeriyama, K. *J. Chem. Soc., Chem. Commun.* **1987**, 1725-1726.

(5) Andersson, M. R.; Selse, D.; Berggren, M.; Järvinen, H.; Hjertberg, T.; Inganäs, O.; Wennerström, O.; Österhelm, J.-E. *Macromolecules* **1994**, *27*, 6503-6506.

(6) Yamamoto, T.; Sanechika, K.; Yamamoto, A. *J. Polym. Sci., Polym. Lett. Ed.* **1980**, *18*, 9-12.

(7) McCullough, R. D. *Adv. Mater.* **1998**, *10*, 93-116.

(8) Marsella, M. J.; Swager, T. M. *J. Am. Chem. Soc.* **1993**, *115*, 12214-12215.

(9) Roncali, J. *Chem. Rev.* **1997**, *97*, 173-205.

(10) Roncali, J.; Thobie-Gautier, C.; Elandaloussi, E. H.; Frere, P. *J. Chem. Soc., Chem. Commun.* **1994**, 2249-2250.

(11) McCullough, R. D.; Lowe, R. D. *J. Chem. Soc., Chem. Commun.* **1992**, 70-72.

(12) Chen, T.-A.; Rieke, R. D. *J. Am. Chem. Soc.* **1992**, *114*, 11087-11088.

(13) Bard, A. J.; Faulkner, L. R. *Electrochemical Methods*. 2nd ed. Wiley: New York, 2001.

(14) Patil, A. O.; Heeger, A. J.; Wudl, F. *Chem. Rev.* **1988**, *88*, 183-200.

(15) Monk, P. M. S.; Mortimer, R. J.; Rosseinsky, D. R. *Electrochromism*. VCH: New York, 1995.

(16) (a) Brédas, J. L.; Thémans, B.; Fripiat, J. G.; André, J. M. *Phys. Rev. B* **1984**, *29*, 6761-6773; (b) Lee, Y.-S.; Kertesz, M. *Chem. Mater.* **1990**, *2*, 526-530.

(17) Debad, J. D.; Bard, A. J. *J. Am. Chem. Soc.* **1998**, *120*, 2476-2477.

(18) See for example: Naudin, E.; El Mehdi, N.; Soucy, C.; Breau, L.; Bélanger, D. *Chem. Mater.* **2001**, *13*, 634-642.

(19) Charlton, A.; Kalaji, M.; Murphy, P. M.; Salmaso, S.; Underhill, A. E.; Williams, G.; Hursthouse, M. B.; Malik, K. M. A. *Synth. Met.* **1998**, *95*, 75-78.

(20) Billard, J.; Dubois, J. C.; Tinh, N. H.; Zann, A. *Nouv. J. Chim.* **1978**, *2*, 535-540.

(21) For example, related fused-thiophenes have achieved high organic field-effect mobilities (0.15 cm^2/Vs): (a) Laquindanum, J. G.; Katz, H. E.; Lovinger, A. J. *J. Am. Chem. Soc.* **1998**, *120*, 664-672; (b) Sirringhaus, H.; Friend, R. H.; Wang, C.; Leuninger, J.; Müllen, K. *J. Mater. Chem.* **1999**, *9*, 2095-2101.

(22) Miyaura, N.; Yanagi, T.; Suzuki, A. *Synth. Commun.* **1981**, *11*, 513-519.

(23) Milstein, D.; Stille, J. K. *J. Am. Chem. Soc.* **1979**, *101*, 4992-4998.

(24) For a discussion of radical-radical couplings and radical cation electrophilic substitution pertinent to thiophene polymerizations, see: Wei, Y.; Chan, C.-C.; Tian, J.; Jang, G.-W.; Hsueh, K. F. *Chem. Mater.* **1991**, *3*, 888-897.

(25) D'Auria, M.; Mauriello, G. *Tetrahedron Lett.* **1995**, *36*, 4883-4884.

(26) Although a formally reversible one-electron redox couple requires a peak to peak separation of 59 mV, we observed similar broadening behavior under identical conditions for the known, reversible one-electron ferrocene/ferrocenium couple. For another recent observation of such non-nernstian behavior in aprotic solvents, see: Lai, R. Y.; Fabrizio, E. F.; Lu, L.; Jenekhe, S. A.; Bard, A. J. *J. Am. Chem. Soc.* **2001**, *123*, 9112-9118.

(27) (a) Bard, A. J.; Fan, F.-R. F.; Mirkin, M. V. In *Electroanalytical Chemistry.* Bard, A. J., ed. Marcel Dekker, Inc.: New York, 1994. Vol. 18, pps 243-373; (b) for a representative demonstration of SECM applied to mechanistic studies, see: Zhou, F.; Bard, A. J. *J. Am. Chem. Soc.* **1994**, *116*, 393-394.

(28) Kelly, T. R.; Li, Q.; Bhushan, V. *Tetrahedron Lett.* **1990**, *31*, 161-164.

(29) Brédas, J. L. *J. Chem. Phys.* **1985**, *82*, 3808-3811.

(30) Sauer, T.; Wegner, G. *Mol. Cryst. Liq. Cryst.* **1988**, *162B*, 97-118.

(31) Ford, W. T.; Sumner, L.; Zhu, W.; Chang, Y. H.; Um, P. J.; Choi, K. H.; Heiney, P. A.; Maliszewskyj, N. C. *New J. Chem.* **1994**, *18*, 495-505.

(32) Zhou, Q.; Carroll, P. J.; Swager, T. M. *J. Org. Chem.* **1994**, *59*, 1294-1301.

Chapter 4

Functionalizable polycyclic aromatics *via* oxidative cyclization: From dibenzanthradithiophenes to fluorescent polymers

Adapted in part from:
Tovar, J. D.; Rose, A.; Swager, T. M., *J. Am. Chem. Soc.* accepted.

Introduction

In 1978, Billard *et al.* observed the first discotic liquid crystal phase within triphenylene.[1] Their *disquotique* description reflected the apparent disk-like ordering of the triphenylene cores into organized columns. Since then, several studies have investigated this new phase. These studies have found that high degrees of molecular planarity and aromaticity, two key design parameters, often lead to discotic properties in a bulk material by taking advantage of favorable π-π interactions between neighboring molecules.[2] The order imposed within a discotic phase results in unusual properties such photoconduction through an organized array of stacked molecules. In fact, the related hexakis(hexylthio) triphenylene exhibited hole mobilities of *ca.* 0.1 cm^2/Vs.[3] Efforts in the Swager group have pursued novel aromatic topologies leading to new discotic liquid crystals. Work led by Hsiu-Fu Hsu and Alexander Paraskos used classical $FeCl_3$ arene oxidations to construct the discotic diphenanthrothiophenes in high yields (Scheme 1). Due to the complete aryl substitution on the thiophene ring, chemical oxidation did not lead to undesired polymerization. This work served as one inspiration for the molecular oxidative cyclizations presented in Chapter 3.

Scheme 1

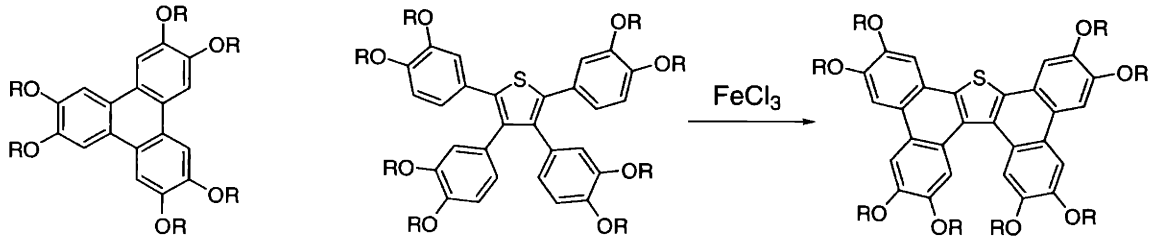

The incorporation of sulfur has also met with success in the design of new organic semiconductors that exhibit conductivity upon application of an electric bias to a device. Chart 1 shows one such candidate, Lucent's anthradithiophene,[4] compared to the analogous carbonoid system, pentacene. Pentacene comprises the "gold standard" of organic semiconductors, exhibiting a variety of unique properties upon charge injection.[5] The anthradithiophene has lower hole mobilities relative to pentacene, reflecting the relative ease of charge transport through these two materials. Although this difference could correspond to an intrinsic structural difference between pentacene and anthradithiophene, it could also relate to the maturity of processing techniques that exist for pentacene (crystal purification and growth, specifically). One reason for incorporating atomic sulfur stemmed from the field of molecular conductors. The charge-transfer salt TTF•TCNQ stands as one of the first organic metals.[6] Furthermore, several derivatives of the highly chalcogenated BEDT-TTF core have demonstrated high-temperature 2-D superconductivity.[7] Both systems apparently take advantage of the greater radial extension within the sulfur components that ultimately leads to more polarizable crystals. Therefore, large aromatic cores containing sulfur offer great promise towards the development of organic electronics.

Chart 1

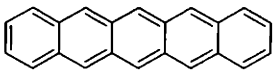

pentacene
μ_h = 3 cm^2/Vs

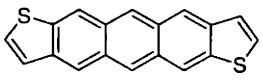

anthradithiophene
μ_h = 0.09 cm^2/Vs

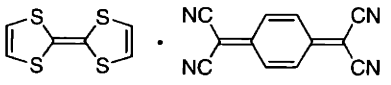

TTF•TCNQ

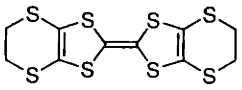

BEDT-TTF

Any extensions to new electronic applications will require reliable synthetic routes. Thiophene-based systems do not enjoy the fruits of the established synthetic literature that exist for the carbon-based analogues. Many of the traditional strategies to synthesize polycyclic aromatics such as those presented in Chapter 1 do not carry over to thienyl-based polycyclics, attesting to the high reactivity and sensitivity of the thienyl core. Two of the most common arene-based routes involve oxidative or photochemical cyclization. As discussed in Chapter 3, the first route often fails for thiophene-based systems. For example, Naudin *et al.* examined a variety of aryl-appended systems (thiophenes and terthiophenes) and only observed polymerization under oxidative conditions.[8] These authors did not present any evidence for discrete monomer cyclizations, neither on an analytical nor on a preparative scale. The second common approach, the Mallory photocyclization, often fails for 3-thienyl systems as demonstrated by the series of 1,2-dithienylethene isomers depicted in Scheme 2.[9] While the 2-substituted isomers cyclize in high yield, the 3-thienyl systems often lead to reactive ring-opened thiyl radicals that decompose *via* polymerization. Note in Scheme 2 that as the "ratio" of 3-thienyl units increases, the cyclization yield drops measurably. Photoexcitation of aryl-substituted thienyl cores can lead to aryl-scrambled isomerizations as opposed to cyclization.[10]

Scheme 2

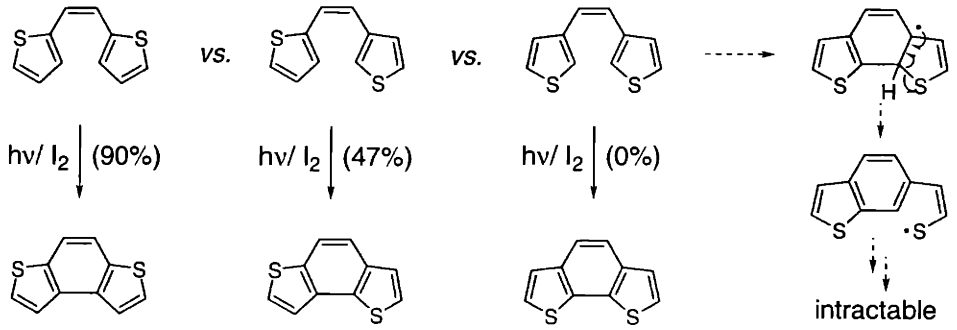

Scheme 3 depicts other routes that have led to successful syntheses of large thiophene-based polycyclics. For example, Ladquindanum *et al.* have used chemistry reminiscent of that used for pentacene to synthesize the anthradithiophenes,[4] while Sirringhaus *et al.* have employed electrophilic ring closures of sulfones under strongly acidic conditions.[11] Both of these routes provided isomeric mixtures of the cyclized products. Ryashentseva *et al.* reported even harsher conditions to prepare benzodithiophenes through brutal treatment of diethylbenzene and H_2S with catalytic Cr_2O_3 at 600°C to afford 19% of an isomeric benzodithiophene mixture.[12] Several of these examples have vacant sites on the sites α to the sulfur atoms, potentially amenable to further synthetic manipulation. Rational alterations of the molecular properties will require efficient and specific synthetic handles for further functionalization. Smaller thiophene-based aromatics such as benzo[*b*]- and naphtho[2,1-*b*]thiophenes undergo selective lithiation, halogenation and acylation at the α-positions reminiscent of thiophene itself.[13] The aromatic character of a larger polycyclic molecule may possibly dilute the separate contribution of a thienyl moiety that allows for such remarkable selectivities, where the electronics of the whole aromatic system dictate the preferred sites of electrophilic attack. However, the synthetic chemistries of larger thiophene-based aromatics essentially have remained unexplored.

Scheme 3

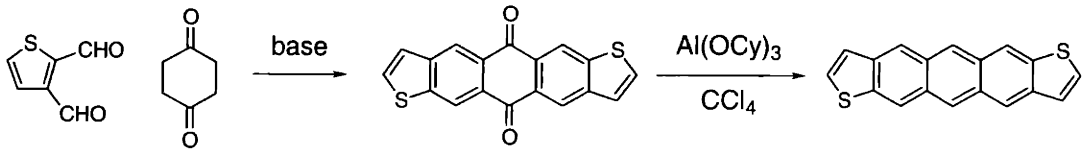

Laquindanum *et al.* (53% overall)

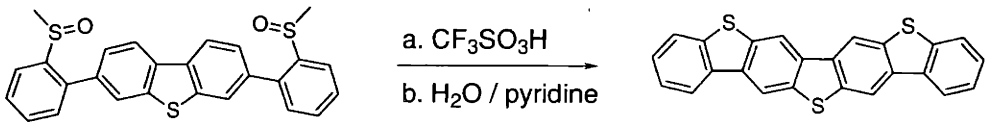

Sirringhaus *et al.* (88%)

With methods in hand for synthesis and functionalization, we may incorporate these scaffolds into conjugated polymers. Several ongoing projects in the Swager group examine the general phenomenon of energy migration within conjugated polymers. To optimize exciton migration and thereby enhance a sensory response, the electronic structure of the polymer needs to facilitate extensive delocalization, and the excited state must persist for as long as possible. This would allow the exciton to travel the longest distance, thus being able to sample a maximal amount of sensory receptors or potential trap sites.[14] In the view of our group, highly conjugated graphite ribbons (as presented in Chapter 1) would serve as one of the best systems to study this concept. Here, the extended π conjugation would foster electronic delocalization while the anticipated weakly-allowed transitions (as observed for other large polycyclic aromatics) would provide a longer excited-state lifetime. Although our group has synthesized and studied such systems,[15] the large π surfaces have a propensity for self-quenching resulting from favorable inter-polymer interactions. This aggregation dramatically lowers the solubility of the polymers.

Our group has also examined this issue from the bottom-up by synthesizing arylene-ethynylene polymers (AEs) with functionalized aromatic co-monomers of varied molecular sizes.[16] This approach provides for better control over solubility and polymer-polymer interactions through effective use of solubilizing side chains or sterically bulky co-monomers. Aimee Rose and Claus Lugmair have studied several triphenylene-based AEs such as the series shown in Chart 2.[17] In all systems studied, the triphenylene AEs exhibited longer fluorescence lifetimes and led to greater degrees of exciton migration when compared to the phenylene-based AEs (PPEs). Both of these observations affirm the effects that rigidified, aromatic comonomers impart to the polymer. Shigehiro Yamaguchi later developed unique cyclization chemistry that afforded functionalizable dibenzo[*g,p*]chrysenes (Chart 3).[18] When co-polymerized with dialkynes, these polymers exhibited fluorescence lifetimes up to 2.5 ns, perhaps representing the highest reported value for an AE polymer. As a testament to the idea that optimizing exciton migration will improve a sensory response, these polymers displayed some of the best performances to date for the detection of the electron-deficient explosive, trinitrotoluene (TNT). The greater degrees of electronic delocalization within the monomer repeat units coupled with the excited-state lifetime enhancements gave rise to this improved sensory behavior.

Chart 2

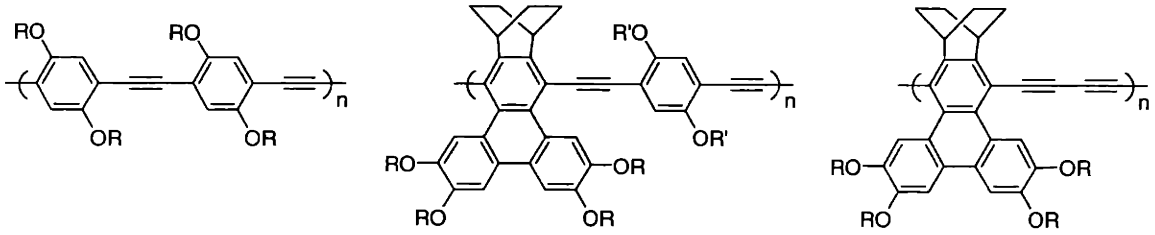

τ = 0.52 ns
ϕ = 0.45

τ = 0.71 ns
ϕ = 0.27

τ = 1.27 ns
ϕ = 0.14

These studies provided empirical demonstrations of excited-state lifetime extension in that the dominant conjugation pathways through a *p*-phenylene, a dibenzochrysene and a triphenylene core have different geometric and electronic properties. One could ask if these effects arose from the incorporation of the large aromatic monomer or if the electronics of differentially-substituted monomers inherently provide longer fluorescence lifetime regardless of the degree of aromatization or rigidity. Another fundamental issue lies with the effects that molecular rigidity and symmetry have on a photophysical property. In theory, synthetic analogues that maintain the conjugation pathway of a triphenylene or of a dibenzochrysene without the extended planarity or aromaticity would help to answer these questions. To some extent, comparisons between triphenylene AEs and phenylene-based PPEs have helped to resolve this. A comparison between the dibenzochrysene AE shown in Chart 3 and the hypothetical phenylene-vinylene AE would also prove instructive, synthesis permitting.

Chart 3

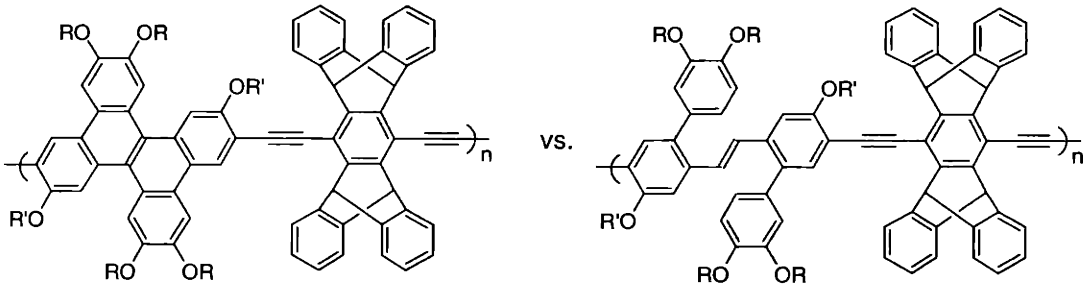

τ = 2.5 ns τ = ??

Studies on a molecular level have not yielded definitive structural principles for guiding polymer design and synthesis in this regard. In general, rigidification of a chromophore will result in weaker oscillator strengths of the lower-energy (0,0) absorption, decreased quantum yields, and smaller differences between the (0,0) absorption and emission λ_{max} (the Stokes' shift). In addition, polycyclic aromatics tend to have longer lifetimes relative to oligo-arenes of comparable size but not covalently held into rigid conjugation. Chart 4 illustrates the lack of

predictive ability even when investigating biphenyl and terphenyl "geometric planarity" (*i.e.* the bridge itself does not electronically interact to a significant extent with the π system of the chromophore). In the biphenyl case, geometric planarization decreases the fluorescence lifetime, while in the terphenyl system, molecular rigidity enhances the lifetime.[19] Despite this apparent contradiction, aromatized phenanthrene and dibenz[*a,h*]anthracene ("electronic planarity" where the bridge offers greater electronic delocalization through the π system) exhibit remarkably longer fluorescence lifetimes as often observed for large polycyclic aromatics. We sought to study the manifestations of these effects within conjugated polymer systems.

Chart 4[a]

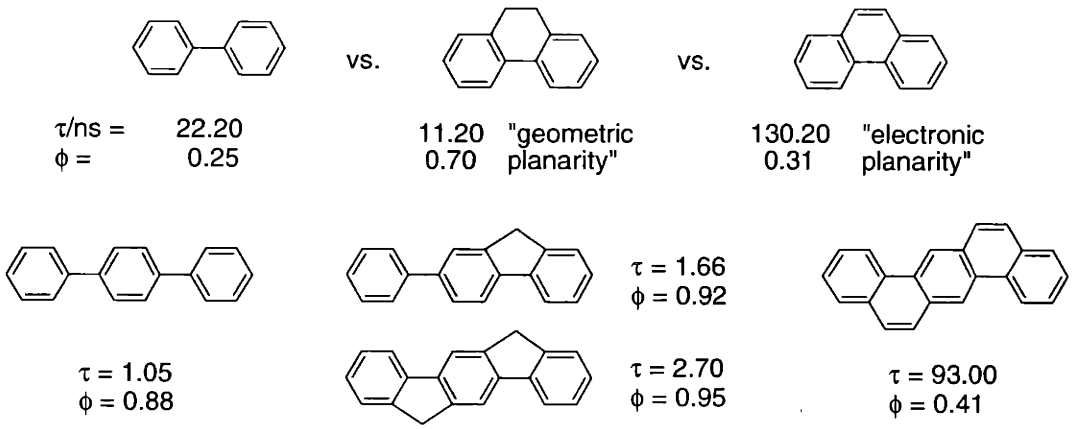

[a] Data taken from Nijegorodov and Downey (ref. 19).

This chapter will apply the strategies outlined in Chapter 3 toward the synthesis of a variety of extended thiophene-based molecular aromatics from pendant thienyl precursors. By placing thienyl moieties in close proximity to adjacent arenes, we can direct the oxidized intermediates into controlled cyclization pathways, effectively suppressing polymer formation. As with the naphthodithiophenes, the unsubstituted positions α to the sulfur within these large aromatic cores allowed for efficient halogenation and further functionalization. To demonstrate this ease, we prepared a series of arylene-ethynylene polymers with varying degrees of chromophore aromatization and used them to probe the effects of synthetically imposed rigidity

on polymer photophysical behavior. We found that the symmetries and effective conjugation pathways within the monomers play a key role in determining photophysical properties.

Results and Discussion

Chapter 3 presented examples of efficient thienyl-thienyl carbon-carbon bond formation where a reactive intermediate underwent intramolecular coupling in a relatively controlled fashion prior to oxidative polymerization. We sought to employ such oxidative cyclizations in constructing larger thiophene-based systems. In earlier studies toward this end, we could obtain the anthratetrathiophene **1** in 17% unoptimized yield. Although quite poor by many standards, such a complex sulfur-containing structure involved only two linear steps from tetrabromobenzene (Scheme 4): Stille coupling provided tetrathienyl **2** and subsequent cyclization yielded **1**.[20] This simple route comprises a quick yet rational approach to such a target when compared to other common routes used to obtain thiophene-based systems. We initially presumed that this reactivity would require alkyl chains on the α-sites in order to prevent polymerization. Unfortunately, this also prevents straightforward functionalization of the molecular core.

Scheme 4

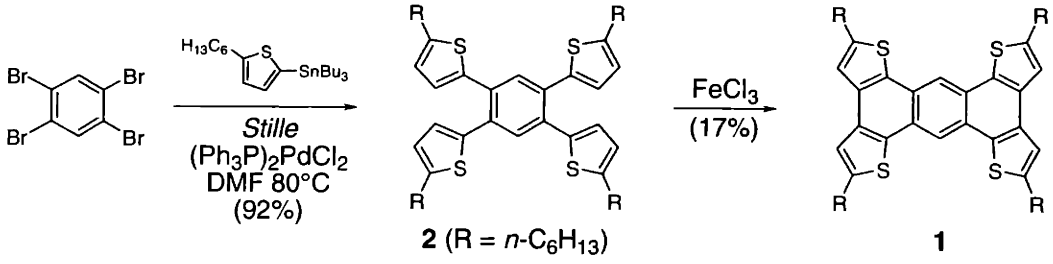

To solve this problem, we examined cyclizations of systems that incorporated free, unsubstituted thiophenes. From the versatile *meta*-oriented halide scaffold **3**,[21] chemoselective cross-coupling under palladium catalysis provided the differentially-substituted pendant monomer **4** *via* sequential Stille and Suzuki cross-couplings (Scheme 5).[22] For the smaller systems discussed in Chapter 3, very slight excesses of oxidant effectively suppressed competitive polymerization after cyclization. Surprisingly, after application of similar oxidative conditions to **4** ($FeCl_3/CH_2Cl_2$), we obtained a mixture of monocyclized product alongside the desired extended aromatic **5**. We could drive this reaction to completion with several molar excesses of oxidant (*ca.* 10-15 equiv.) to afford **5** in respectable yield; however, the significant excesses of iron oxidant apparently led to some decomposition.

Scheme 5[a]

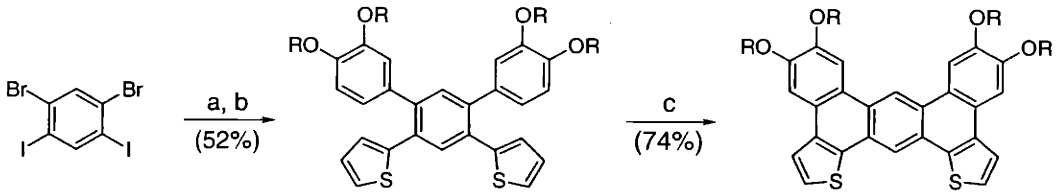

3 **4** **5**

[a] R = 2-ethylhexyl; Reagents and conditions: (a) *Stille*: 2-tributylstannyl thiophene, $(Ph_3P)_2PdCl_2$, DMF, 80°C; (b) *Suzuki*: 3,4-di(2-ethylhexyloxy)phenylpinacolatoborane, $Pd(PPh_3)_4$, Na_2CO_3, PhMe, EtOH, H_2O, 90°C; (c) $FeCl_3$, CH_2Cl_2, rt.

We then wanted to examine the electronic effects exerted by the individual thiophene units within these large systems as pertinent to the halogenation of **5**. For example, thiophene undergoes lithiation and electrophilic bromination at either the 2- or both the 2- and 5-positions, depending on the reaction stoichiometries and conditions used. We worried about the potential for poor regioselectivity during functionalization of these larger cores where the overall aromaticity may dilute the individual thiophene electronic contributions. Fortunately, these systems provided regioselective halogenation at the α-sites of **5** only (Scheme 6). Molecular bromine allowed for regiospecific dibromination to provide **6** in excess of 90% yields. Likewise,

the dianion of **5** generated from *n*-BuLi deprotonation provided the diiodide **7** after an iodine quench. In both of these cases, ROESY spectroscopy helped to determine connectivity: **6** and **7** both displayed two through-space interactions of protons associated with the aromatic cores as illustrated in Scheme 6, consistent with selective α-halogenations.

Scheme 6

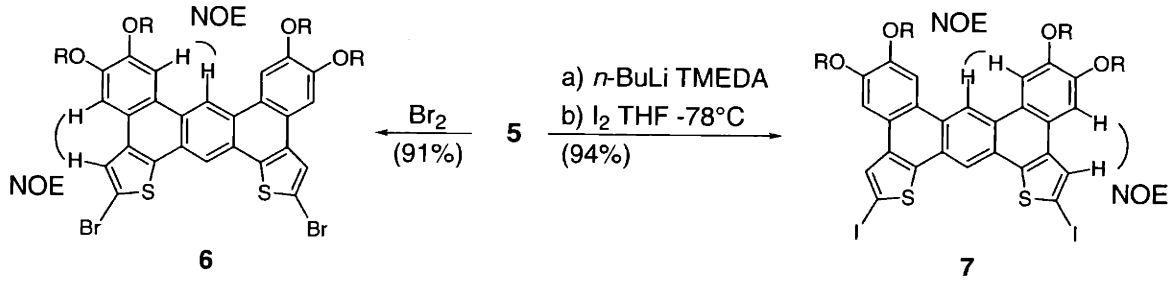

6 **7**

Analogous to the studies detailed in Chapter 3, repetitive fast scan cyclic voltammetry (CV) at 750 mV/s with **4** indicated one initial peak oxidation (E_{pa}) at 1.32 V, and successive scans eventually reached a *pseudo* steady-state voltammogram exhibiting two reversible waves with half-wave potentials ($E_{1/2}$) at 0.84 V (E_{pa} = 0.95 V, peak-to-peak separation (ΔE_p) = 220 mV) and 1.11 V (E_{pa} = 1.23 V, ΔE_p ca. 200 mV; Figure 1). For comparison, the CV of **5** under identical conditions exhibited two reversible processes with $E_{1/2}$s at 0.83 V (E_{pa} = 0.96 V, ΔE_p = 240 mV) and 1.11 V (E_{pa} = 1.23 V, $\Delta E_{p\text{-}p}$ = 230 mV; Figure 1, dashed line). This indicates the buildup of a new electroactive species at the working electrode resulting from an oxidatively-induced aryl-thienyl bond formation. When compared to naphthodithiophene systems and their non-cyclized parent compounds (Chapter 3), the more positive initial E_{pa} for **4** reflects the lesser degree of electronic induction afforded by the pendant alkoxy groups. This results from the additional phenylene spacer placed between the dialkoxy arene and the thienyl moiety. After cyclization, **5** then exhibits two reversible oxidations at less positive potentials than in **4** due to the extended delocalization offered to the charged species by a completely aromatized system.

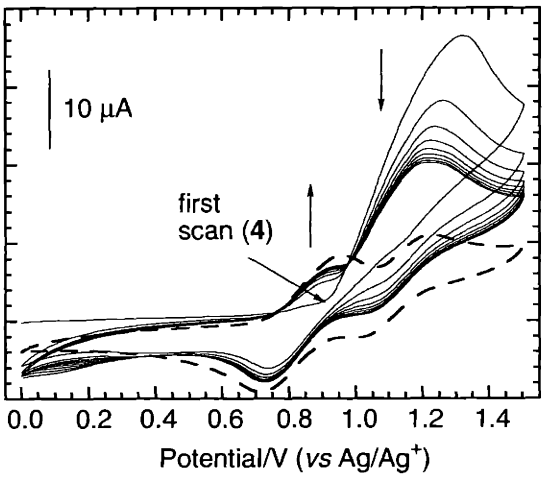

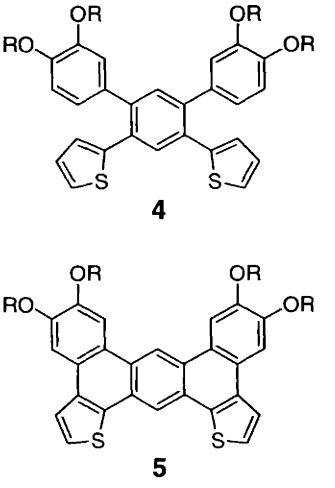

Figure 1: CVs of **4** (—, 1.0 mM) and **5** (-----, 1.1 mM) at a 2 mm^2 Pt button electrode in 0.1 M *n*-Bu_4PF_6 (CH_2Cl_2) scanned at 750 mV/s; $E_{1/2}(Fc/Fc^+)$: +230 mV.

We employed scanning electrochemical microscopy (SECM) in an effort to detect reactive intermediates formed upon oxidation. As discussed for the naphthodithiophene cyclizations in Chapter 3, the series of distinct chemical and electrochemical steps that actually form the cyclized and aromatized **5** would provide several charged intermediates thus complicating SECM analysis. However, we could use SECM to verify that the aromatized core **5** can support radical cations and dications in solution without apparent dimerization or attack by solvent (Figure 2). This stable scaffold may find use in electrochemically generated chemiluminescence (ECL) schemes upon covalent attachment of a moiety capable of supporting radical anions. Here, ECL can generate radical cations and anions simultaneosly on the same scaffold, thus leading to charge annihilation and the emission of light.

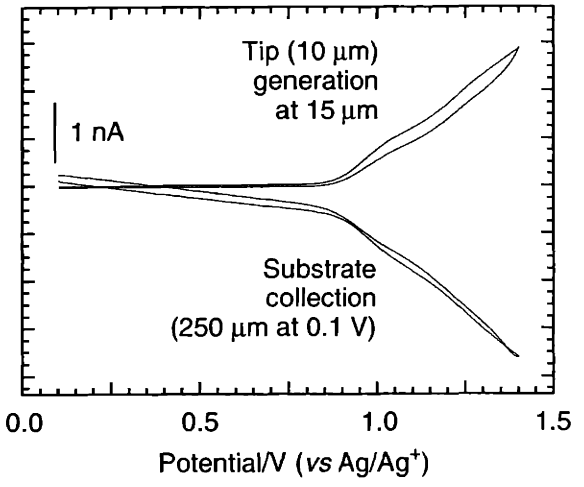

Figure 2: SECM measurement of **5** (2 mM in CH_2Cl_2) at a tip diameter of 10 μm and a collection substrate diameter of 250 μm.

The monomer synthetic scheme allowing entry into the *para* systems paralleled that used for constructing the *meta* system **4** (Scheme 7). Sequential Stille and Suzuki cross-couplings onto the isomeric *para* scaffold **8**[21] afforded the thienyl-substituted terphenyl **9** (X = H), and halogenation proceeded in high yield to provide the dibromide **10** or diiodide **11**. The oxidative conversion of **9** directly into the aromatized system failed due to unavoidable polymer formation,[23] in stark contrast to the relatively clean cyclization of *meta* system **4** into **5**. Therefore, we hoped to prevent this by employing the halogens to block the reactive and polymerizable α-sites. The carbon-iodine bond lability of **11** apparently led to significant dehalogenation and dimerization during chemical cyclization; however, bromide **10** cleanly cyclized under the $FeCl_3$ oxidation conditions to afford **12**. Despite the sparingly soluble nature of **12**, exhaustive purification of the crude product (and concomitant material losses) provided modest isolated yields.

Scheme 7[a]

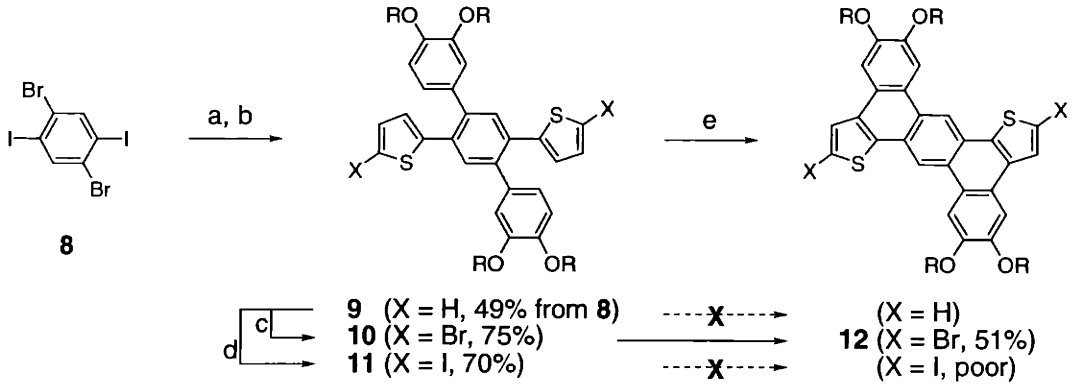

[a] R = 2-ethylhexyl; Reagents and conditions: (a) *Stille*: 2-tributylstannyl thiophene, $(Ph_3P)_2PdCl_2$, DMF, 80°C; (b) *Suzuki*: 3,4-di(2-ethylhexyloxy)phenylpinacolatoborane, $Pd(PPh_3)_4$, Na_2CO_3, PhMe, EtOH, H_2O, 90°C; (c) NBS, DMF, CH_2Cl_2, rt; (d) i. $Hg(OAc)_2$; ii. I_2, CH_2Cl_2, rt; (e) $FeCl_3$, CH_2Cl_2, rt.

To demonstrate generality, we examined if extended benzannulation on the thiophene moiety would affect the cyclization efficiency. Chapter 1 introduced an interest in helical ribbon polymers, and we wanted to lay out initial groundwork for entry to such structures *via* oxidative cyclization. We prepared model compound **13** through similar cross-coupling strategies used for **4**, where the benzo[*b*]thiophen-2-yl groups of **13** replace the thienyl groups of **4** (Scheme 8).[24] Similar oxidative conditions provided the doubly-cyclized **14** in moderate yield. Despite the aromaticity within the benzo[*b*]thiophene units, the Clar structures depicted in Scheme 8 indicate the persistence of olefinic character when compared to **5**. As with the conversion to **5**, extensive decomposition occurred during $FeCl_3$-promoted cyclization of **13**, and the reaction mixture proved difficult to purify. The use of this chemistry on larger heteroaromatics indicates that such oxidative cyclizations extend beyond simple thiophene derivatives. We then sought to functionalize **14** by using the sulfur atoms to direct lithiation or mercuration of the core, although these strategies did not succeed in ultimate halogenation. Owing to the favorable cofacial interactions possible between such large planar π systems, fused compounds **5** and **14** exhibited concentration dependent ^{1}H NMR shifts as expected for a strongly aggregating system. We anticipate that this propensity will allow for extended intermolecular organization, making more crystalline derivatives of **5** and **14** (where R = OMe for example) suitable for FET applications.

Scheme 8[a]

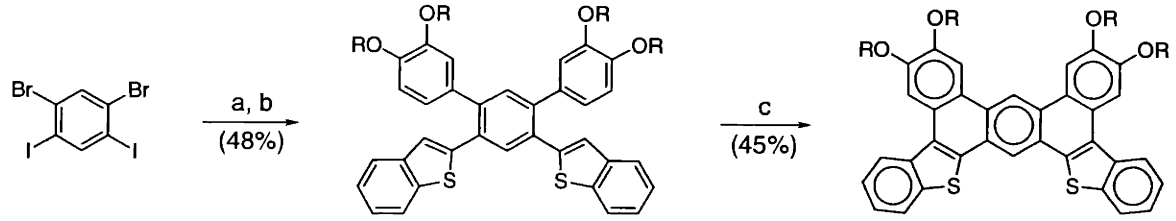

3 **13** **14**

[a] R = 2-ethylhexyl; Reagents and conditions: (a) *Stille*: 2-tributylstannybenzo[*b*]thiophene, $(Ph_3P)_2PdCl_2$, DMF, 80°C; (b) *Suzuki*: 3,4-di(2-ethylhexyloxyphenylpinacolatoborane, $Pd(PPh_3)_4$, Na_2CO_3, PhMe, EtOH, H_2O, 90°C; (c) $FeCl_3$, CH_2Cl_2, rt.

Repetitive fast-scan CV cycling appeared to indicate an efficient conversion of **13** to **14** although undesired electrode passivation at higher potentials complicated CV analysis. The CVs of very dilute samples of **13** (Figure 3, top) provided only capacitive current until sweeping through the initial E_{pa} at 1.11 V. Subsequent scans revealed a less-positive potential redox couple with an $E_{1/2}$ at 0.78 V (E_{pa} = 0.84 V, ΔE_p = 120 mV) and a concurrent decrease in anodic current of the higher potential oxidation step, analogous to **4** (Figure 1). In comparison, we observed a similar redox couple for very dilute solutions of **14** with an $E_{1/2}$ at 0.75 V (E_{pa} = 0.83 V, ΔE_p = 150 mV; Figure 3, bottom); again, sweeping in solutions on the order of 1 mM at more positive potentials also led to passivation. Future efforts will need to incorporate more soluble units to avoid passivation and more stable redoxophores to foster greater electrochemical reversibility.

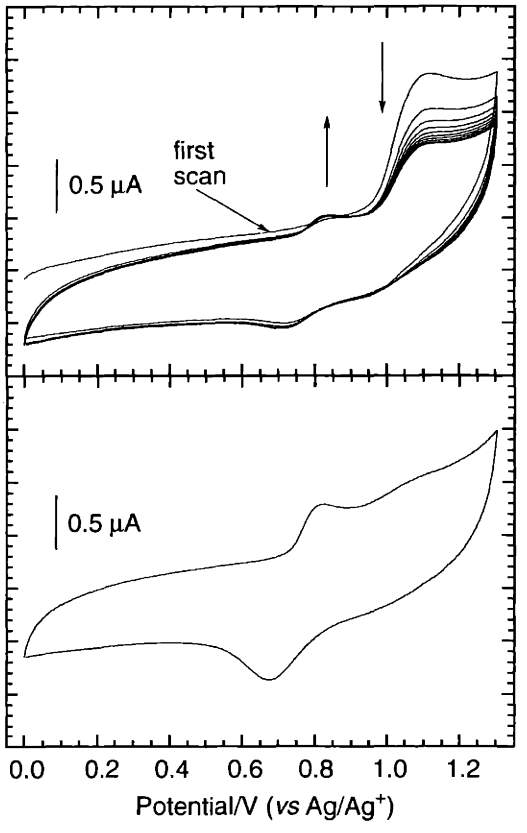

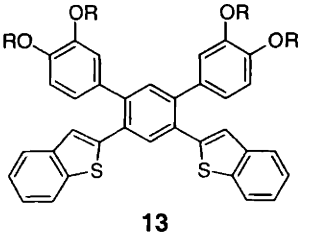

13

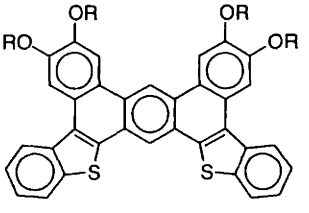

14

Figure 3: CVs of **13** (repetitive scans, top, *ca.* 0.09 mM) and **14** (bottom, *ca.* 0.22 mM) taken at 500 mV/s, conditions as in Figure 1; $E_{1/2}(Fc/Fc^+)$: +231 mV.

These studies may open the door to helical polymer-functionalized electrodes. Chapter 1 referred to Moore's studies of conformational dynamics within *meta*-phenylene ethynylene oligomers where polar non-solvents (acetonitrile) enforced a helical twist of the oligomer.[25] However, the chemistry presented in Chapter 1 initially used to construct the linear ladder polymers could not proceed in the presence of polar solvents such as acetonitrile. Therefore, a *meta*-oriented polymeric material could not undergo the zig-zag-to-helix conformational change under those electrophilic cyclization conditions. With this oxidative chemistry, a *meta*-substituted polymer resembling model monomer **13** may helicize in electrochemistry-friendly acetonitrile as directed by the incorporation of polar crown ether moieties on the periphery of the polymer (Scheme 9). After helix formation, electrochemical oxidation may "zip up" the polymer backbone by effecting a cascade of oxidative cyclizations. The *meta* substitution will minimize the degree of communication between oxidized sites thus helping to allow for the formation of multiple charges on one polymer backbone during the cyclization event.

Scheme 9

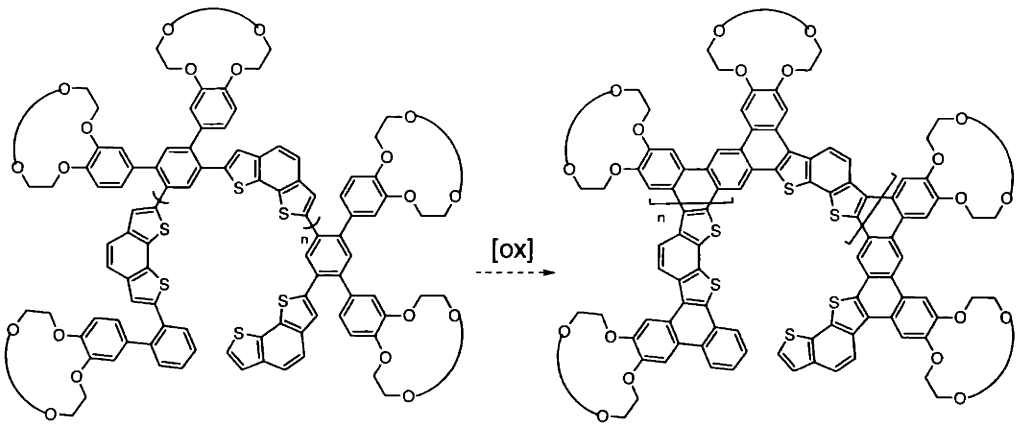

Incorporation into conjugated polymers. In line with our group's earlier studies,[17,18] we anticipated that the extended planarity and rigidity of co-monomers derived from **5** and **12** would also offer a long-lived excited-state. As the parent non-cyclized materials themselves readily halogenated (*e.g.* **9** to **10** or **11**), we now have access to systems where the co-monomer structures and electronics have more similarities. This could allow us to carefully probe the effects that result upon chromophore rigidification. A systematic study of such large aromatic chromophores would assess the relative photophysical contributions of molecular symmetry and planarity within conjugated polymer systems and would help to outline parameters required for more efficient sensory materials. Even within molecular systems, planarized chromophores do not show predictable trends in photophysical properties.[19] We sought to study these trends within polymeric systems of varied symmetries and structural constraints.

We synthesized four distinct arylene-ethynylene polymers through Sonogashira co-polymerization with a halogenated monomer and diethynylpentiptycene (**15**) as illustrated in Scheme 10.[26,27] Two polymers fall into the *meta* category: the *meta* "pendant" polymer (**16**) and the *meta* "planar" (**17**). The other two polymers have *para* substitution, thus having a higher degree of through-bond conjugation: the *para* "pendant" (**18**) and the *para* "planar" (**19**). In both families, the pendant polymers should have larger degrees of torsional flexibility that would restrict the effective conjugation lengths in the ground state while the aromatic core present in the planar polymers will offer more structural rigidity. We chose to keep all polymers as identical as possible in order to observe the effects that rigidity plays in determining excited-state properties. Note that for **16**, we first iodinated **4** in high yield through treatment with $Hg(OAc)_2$ and iodine. Given the insolubility of both pentiptycene **15** and the halogenated co-monomers, we could only obtain materials with lower-than-desired molecular weights.

Scheme 10

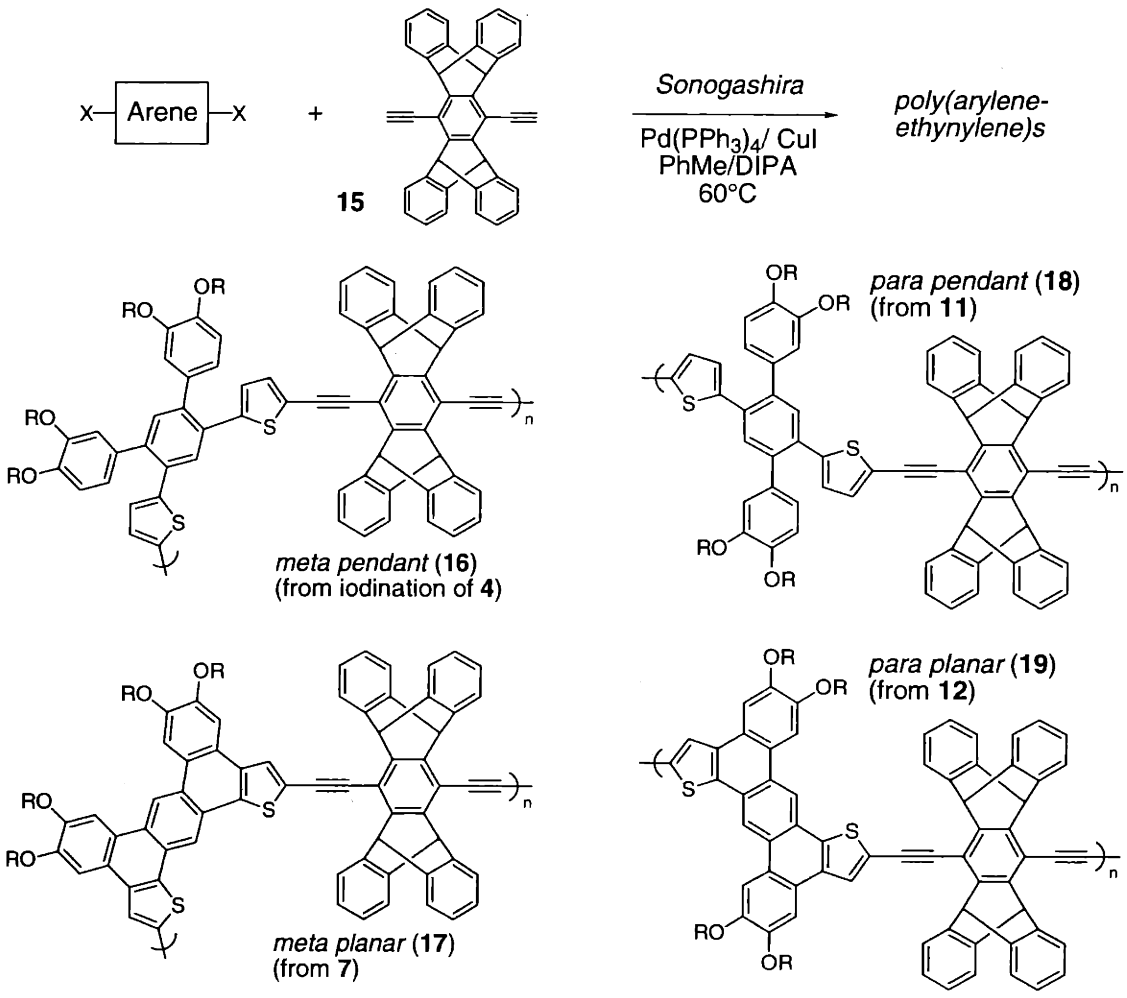
X—Arene—X
+
15
Sonogashira
Pd(PPh3)4/ CuI
PhMe/DIPA
60°C
poly(arylene-ethynylene)s
meta pendant (16)
(from iodination of 4)
para pendant (18)
(from 11)
meta planar (17)
(from 7)
para planar (19)
(from 12)

Simple inspection of the absorption and emission spectra for both the *meta* family (**16** and **17**) and the *para* family (**18** and **19**) reveal the electronic effects of chromophore planarization (Figures 4 and 5). When compared to the conformationally flexible **16** and **18**, the more rigid, aromatized units present in **17** and **19** offer more defined vibronic structure and significant reduction in energy between the (0,0) absorption and the emission λ_{max}. The relative oscillator strengths for the low-energy absorbances of *meta* polymer **17** have lower intensities when compared to the analogous low-energy absorptions for *para* **19**. While significantly altering the absorption profiles, monomer aromatization within a family only results in a slightly red-shifted emission maximum (*meta*: 14 nm; *para*: 10 nm). Despite the differences in ground state geometries within both families of polymers, these close resemblances in emission λ_{max} indicate similar excited-state conjugation lengths between the flexible and the rigidified polymers. This supports the fact that the pendant arenes of non-cyclized **16** and **18** adopt a more planar conformation after initial excitation in order to allow for greater excited-state delocalization. The slightly blue-shifted emissions observed in the pendant systems (**16** and **18**) indicate a minor persistence of localized poly(phenylene) character in their excited states. This would suggest that charge localization still exists on the phenylene (or thienylene) segments in spite of any excited-state planarization effects.

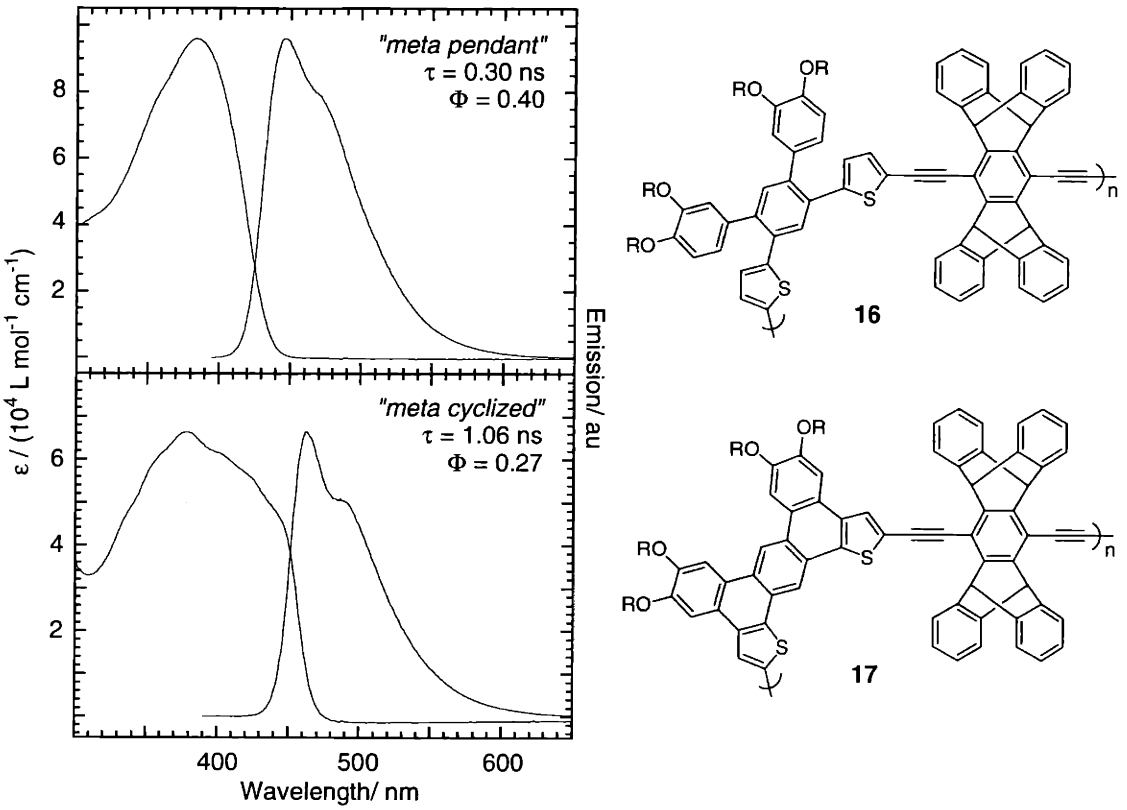

Figure 4: Absorption and emission spectra for **16** (top) and **17** (bottom) acquired at room temperature in CH_2Cl_2.

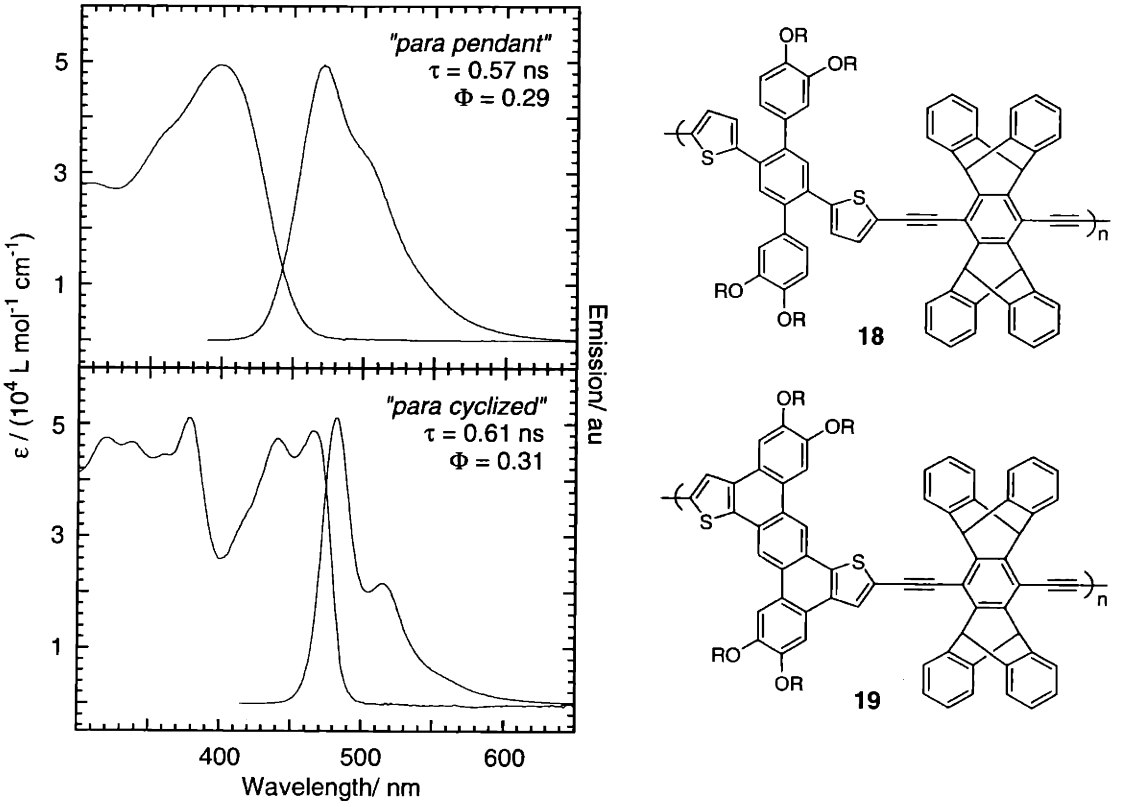

Figure 5: Absorption and emission spectra for **18** (top) and **19** (bottom) acquired at room temperature in CH_2Cl_2.

With both isomeric sets of polymers displaying absorption and emission characteristics expected after incorporating a more rigid aromatic chromophore, we measured the fluorescence lifetimes and quantum yields of these polymers. Pendant *meta* polymer **16** had a solution lifetime of 0.30 ns (Φ = 0.40) whereas aromatized **17** displayed a lifetime of 1.06 ns (Φ = 0.27), a 3.5-fold larger value. A correlation of the lifetimes with the quantum yield measurements indicated a decreased rate of radiative decay for the aromatized **17**. In contrast, *para* polymers **18** and **19** exhibited *identical* solution lifetimes (0.57 and 0.61 ns, respectively) and quantum yields (Φ = 0.29 and 0.31, respectively), suggesting that the inclusion of the aromatized system effects no significant change in the radiative rate. This result surprised us at first.

To further investigate this interplay between chromophore aromaticity and symmetry, we synthesized alkynylated *meta* models **20** and **21** and the related *para* derivatives **22** and **23** as shown in Chart 5. Unlike the polymers, these systems possess shorter, well-defined conjugation lengths thus allowing for a clear assessment of planarization effects within molecular systems without significant contributions from variations in effective conjugation lengths. While we initially anticipated the use of oxidative cyclizations to obtain the alkynyl-appended polycyclic aromatics (*e.g.* **20** to **21**), extensive decomposition during the reaction led to unidentifiable materials, apparently a result of alkyne degradation.[22] Cyclic voltammetric studies of **20** and **22** show a lack of new electroactive products formed near the electrode surface as well as complete anodic irreversibility over a range of potential scan rates (0.1–10 V/s). However, despite the problematic purification of the *para* bromide **12**, Sonogashira cross-coupling of the respective dihalides with alkyne **24**[28] provided all four alkynylated models in high yields.

Chart 5[a]

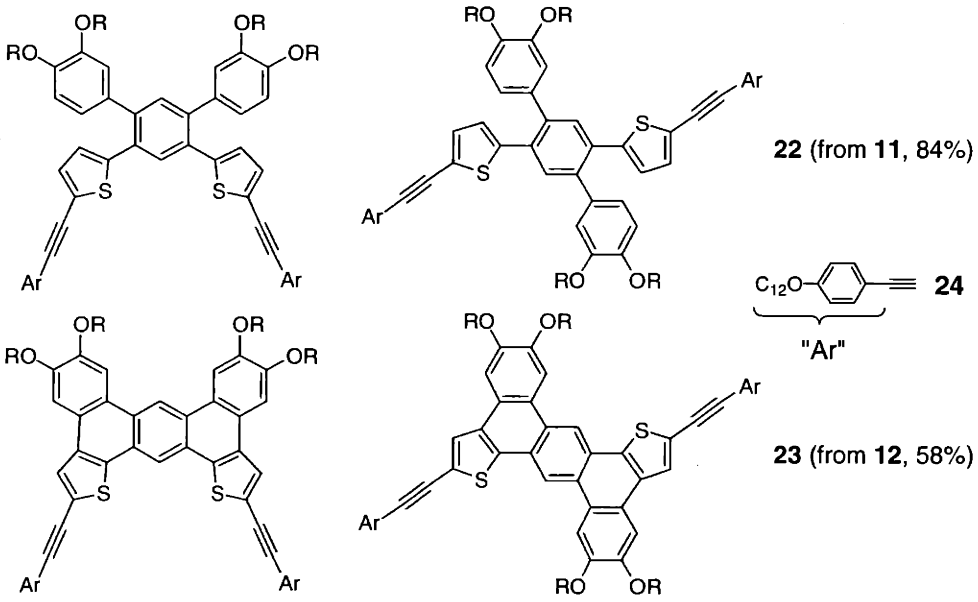

[a] Obtained from Sonogashira coupling between a given dihalide and **24**.

In agreement with the optical trends observed for the polymer systems, the aromatized systems **21** and **23** displayed sharper vibronic structure and decreased Stokes' shifts when compared to the pendant analogues **20** and **22** (Figures 6 and 7). Again in line with the polymer electronic properties, the low oscillator strength of the (0,0) absorption observed for **21** (436 nm, log ε = 3.63) when compared to that in **23** (also at 436 nm, log ε = 4.69) indicates a much more weakly allowed process. We then measured the fluorescence lifetimes and quantum yields for these molecular systems of shorter and more defined conjugation lengths. Consistent with the polymeric systems, we found a near nine-fold increase in lifetime in the cyclized *meta* system **21** (**20**: 0.58 ns; **21**: 5.00 ns) while the quantum yields for the two remained equal (Φ = 0.17). The cyclized *para* system **23** displayed a much less pronounced extension upon planarization (**22**: 0.80 ns; **23**: 1.12 ns) while the quantum yield decreased slightly (**22**: 0.54; **23**: 0.41). For both systems, the decreases in radiative rates upon planarization within an isomeric family give rise to the lifetime extensions.

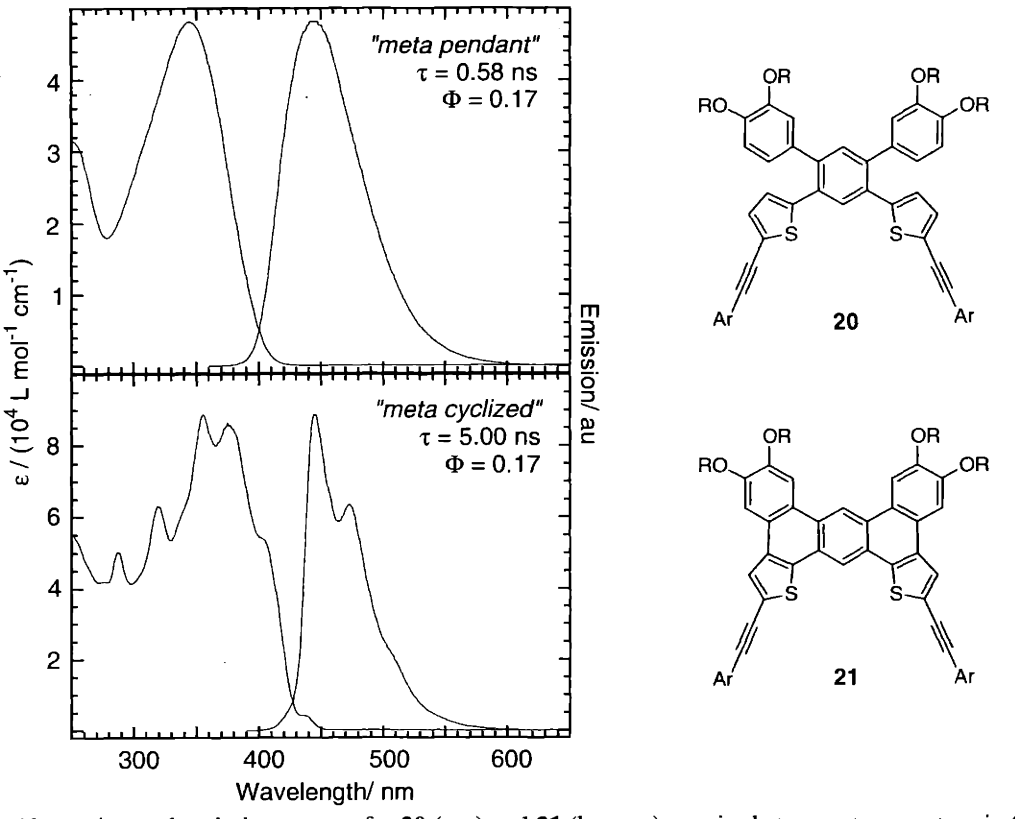

Figure 6: Absorption and emission spectra for **20** (top) and **21** (bottom) acquired at room temperature in CH_2Cl_2.

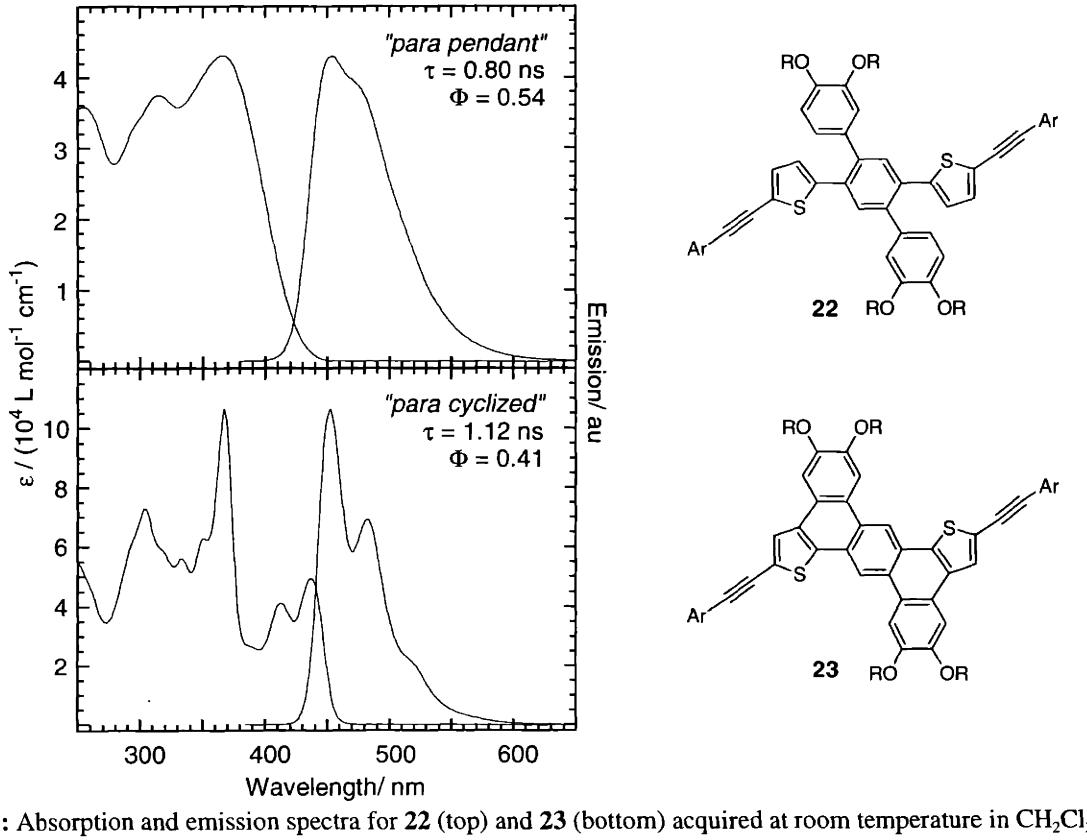

Figure 7: Absorption and emission spectra for **22** (top) and **23** (bottom) acquired at room temperature in CH_2Cl_2.

To further study the effect within carbonoid polymers more comparable to traditional PPEs, we prepared the "non-cyclized triphenylene" derivative to serve as an additional comparison to Rose's triphenylene-based polymers.[17] Suzuki coupling of the *ortho*-dibromide shown in Scheme 11 (synthesis described in Chapter 1) followed by silyl deprotection led to the dialkyne **25**. Sonogashira polymerization provided the *o*-terphenyl-based PPE **26**. This polymer apparently had a rather high molecular weight due to the tough free-standing nature of the isolated polymer despite the low measured GPC values. This material displayed a strong aggregate absorption; however, the aggregated and less-aggregated polymers had identical lifetimes. In comparison to Rose's triphenylene polymer **27**, the less-planar **26** exhibited a higher quantum yield and a lower fluorescence lifetime. This system removes elements of high conductivity potentially present in thiophene-based systems such as **18** and **19**. The data obtained for **26** corresponded quite well to data for standard PPEs studied in our group (*e.g.* τ = 0.52 ns; ϕ = 0.45).[17]

Scheme 11[a]

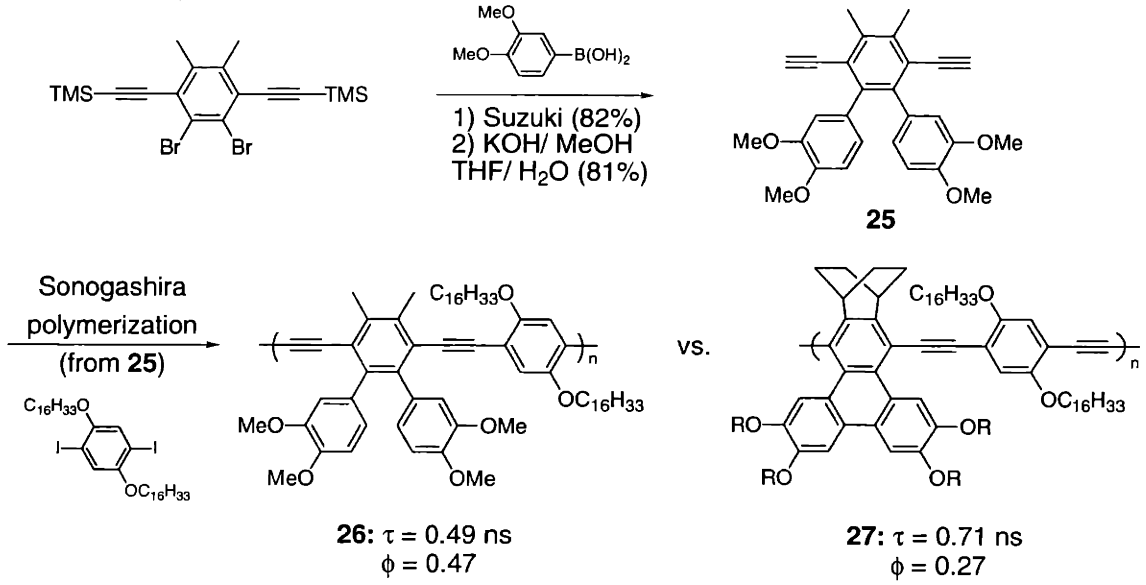

[a] Data for **27** taken from ref. 17.

These results stand in agreement with similar lifetime enhancements resulting from symmetry-forbidden transitions in conjugated polymers containing triphenylene cores.[17] In line with our earlier findings related to the electrochromicity and conductivity of the poly(naphthodithiophene)s,[29] the set of *para* model systems (**22** and **23**) and the related *para* polymers (**18** and **19**) appear to maintain much longer excited-state conjugation pathways localized through the thienyl-aryl-thienyl segments despite any structural rigidification. As such, the differences in radiative rates within the planarized *para* polymers are not as severe as in the less delocalized *meta* systems. Ridigification provides a consistent explanation for the observed changes in optical properties upon chromophore aromatization, but the lack of significant excited-state lifetime enhancement within the planarized *para* **19** indicates that simple rigidification of a given chromophore does not necessarily couple to an increase in lifetime. We should emphasize that both the *meta* and *para* systems compare the effects of electronic planarity since the bridging arene should help to further delocalize the chromophore as opposed to the more electronically passive geometric planarity. In the *para* systems, the strong conjugation through the central thienylene-phenylene core does not allow (or require) the exciton to significantly interact with the bridging unit *via* delocalization. Within systems that had stronger resemblances to the PPE systems (**26** and **27**), we find that triphenylene-based **27** indeed exhibits a higher lifetime. This indicates that the excited state may delocalize throughout the large triphenylene core thus enhancing the lifetimes and extending exciton migration. Future studies will assess the physical properties of these molecular ensembles as well as continue to investigate the effects of repeat unit aromatization on enhancing excited-state lifetimes in systems of other symmetries.

Concluding Remarks

We have shown that oxidative couplings of pendant thienyl moieties allow for construction of discrete molecular structures as a complement to well-established arene-based molecular cyclizations and to thiophene-based polymerization strategies. The ease of synthesis for the pendant aromatic precursors has allowed us to expand upon the cyclization-polymerization strategy we described in Chapter 3 by providing a powerful route to electroactive and emissive aromatic structures. We have demonstrated that both the α- and the β-sites of pendant monomers may undergo cyclization under oxidative conditions and have applied this to the synthesis of a variety of large thiophene-based polycyclics from readily-synthesized pendant polyaromatic precursors. By incorporating the thiophene moieties, we included a synthetic handle through which even more elaborate scaffolds become available. We then used this chemistry as a platform to demonstrate the effects of chromophore aromatization on photophysical properties of conjugated polymers. From these studies, we have established further structural groundwork to aid in the design of new sensory materials. This chemistry stands poised to provide polarizable materials for liquid crystal and field-effect transistor applications, two areas of interest to the organic electronics community.

Experimental Section

General: All air and water sensitive synthetic manipulations were performed under an argon atmosphere using standard Schlenk techniques. Diisopropylamine (DIPA) was distilled from KOH; methylene chloride (CH_2Cl_2), toluene (PhMe), and tetrahydrofuran (THF) were passed through activated alumina columns prior to storage in dry airfree vessels. Methanol (MeOH) and nitromethane ($MeNO_2$) were dried over sieves and stored under argon. TMEDA was passed through activated alumina and then distilled from KOH; *n*-BuLi in hexane was titrated *versus* diphenylacetic acid before use. All other solvents and chemicals were of reagent grade and used as received. 5-Hexyl-2-tributylstannylthiophene was obtained by lithiating 2-hexylthiophene and quenching the anion with Bu_3SnCl. 1,3-Dibromo-4,5-diiodobenzene **3** was obtained by iodination of 1,3-dibromobenzene (H_5IO_6, KI, H_2SO_4).[21] Likewise, 1,4-dibromo-2,5-diiodobenzene **8** was obtained from 1,4-dibromobenzene.[15] 3,4-Di(2-ethylhexyloxy)phenyl-1-pinacolatoborane was obtained from Williamson etherification of catechol with 2-ethylhexylbromide, mono-bromination with NBS in DMF and subsequent Miyaura coupling with bis(pinacolato)diboron.[22] Tri-*n*-butylstannyl-2-benzo[*b*]thiophene was prepared by lithiation of benzo[*b*]thiophene and trapping with *n*-Bu_3SnCl.[24] Diethynyl pentiptycene **15** was prepared as previously desribed.[27] Alkyne **24** was prepared by a Williamson ether synthesis on 4-iodophenol (1-bromodecane, K_2CO_3, KI, acetone) followed by a Sonogashira coupling of trimethylsilylacetylene [$(Ph_3P)_2PdCl_2$, CuI, DIPA/PhMe] and subsequent deprotection (KOH, MeOH/H_2O).[15] 3,6-Bis(trimethylsilylethynyl)-4,5-dibromo-*o*-xylene, used for **25**, was prepared as described in Chapter 1.

Column chromatography was performed using Baker 40 μm silica gel. All organic extracts were dried over $MgSO_4$ and filtered prior to removal under reduced presure. NMR spectra were obtained on Varian Unity or Mercury 300, Bruker Avance 400 or Varian Inova 500 spectrometers, and all chemical shifts are referenced to residual $CHCl_3$ (7.26 ppm for ^1H, 77.23 ppm for ^{13}C) or $CHDCl_2$ (5.32 ppm for ^1H, 54.00 ppm for ^{13}C); aromatic carbon multiplicities were determined by DEPT analysis. High resolution mass spectra were obtained at the MIT Department of Chemistry Instrumentation Facility (DCIF) on a Bruker Daltronics APEX II 3 Tesla FT-ICR-MS. Molecular weight determination by Gel permeation chromatography (GPC) was performed in THF versus polystyrene standards (PolySciences) on a HP 1100 HPLC system equipped with a Plgel 5 mm Mixed C column (300 x 7.5 mm). UV-Vis measurements were obtained on a Hewlett-Packard 8452A diode array spectrophotometer. Fluorescence measurements were recorded on a SPEX Fluorolog-τ2 fluorimeter with a 450 W xenon lamp. Quantum yield measurements are relative to quinine sulfate in 0.1 N H_2SO_4 ($\phi = 0.55$); lifetime data were obtained by phase-modulation techniques. Elemental analyses were obtained at Desert Analytics (Tucson, AZ). Melting points are uncorrected. All electrochemical measurements were made with an Autolab PGSTAT

20 potentiostat (Eco Chemie). Cyclic voltammetry was performed at Pt electrodes in oven-dried, argon-purged, one chamber/three electrode cells versus a quasi-internal Ag wire reference electrode (BioAnalytical Systems) submersed in 0.01 M $AgNO_3$/ 0.1 M *n*-Bu_4NPF_6 in anhydrous acetonitrile (MeCN). All experiments were conducted in freshly prepared solutions of 0.1 M *n*-Bu_4NPF_6 in anhydrous MeCN or CH_2Cl_2 stored over activated 4Å sieves.

3,4-Di(2-ethylhexyloxy)phenylpinacolatoborane: A solution of 1,2-di(2-ethylhexyloxy)-4-bromobenzene (12.401 g, 29.995 mmol), bis(pinacolato)diborane (8.924 g, 35.14 mmol) and KOAc (10.304 g, 104.98 mmol) in DMSO (200 mL) was purged with argon for 1 hr in a dry 500 mL round-bottom flask followed by the addition of (dppf)$PdCl_2$ (714 mg, 0.874 mmol). The reaction was held under argon at 80°C for 22h. After cooling, the reaction was diluted with ether and carefully washed with NaCl (x3). [CAUTION: the reaction mixture reacts vigorously with water, so the water must be added slowly!] The first aqueous extraction was washed with ether, and the separated organic layer was further washed with NaCl (x2). The combined organics were dried and removed to provide a dark brown oil. The crude material was pushed through a plug of silica (hexane to 1:1 hexane/ CH_2Cl_2) to yield the product as a faint green oil that was used without further purification (12.329 g, 26.773 mmol, 89%). ^{1}H NMR (300 MHz, CD_2Cl_2) δ: 7.30 (dd, 1H, *J* = 1.5, 7.8 Hz), 7.22 (d, 1H, *J* = 1.2 Hz), 6.87 (d, 1H, *J* = 8.1 Hz), 3.87 (m, 4H), 1.73 (m, 2H), 1.2-1.6 (bm, 28H), 0.90 (m, 12H). ^{13}C NMR (100 MHz, $CDCl_3$) δ: 152.5, 149.0, 128.7, 119.0, 112.6, 83.7, 71.56, 71.33, 39.86, 39.64, 30.81, 30.75, 29.35, 29.28, 25.03, 24.14, 24.07, 23.28, 23.27, 14.31, 14.29, 11.41, 11.34. FT-IR (neat): ν/cm^{-1}: 2928, 2873, 1599, 1518, 1465, 1418, 1353, 1257, 1137, 1031, 857, 685. HR-MS (EI): found *m/z* = 460.3734 (M^+); calc. for $C_{28}H_{49}O_4B$: 460.3718.

2,5,8,11-Tetrahexylanthra[1,2-*b*:4,3-*b'*:5,6-*b''*:8,7-*b'''*]tetrathiophene (**1**): A solution of **2** (75.1 mg, 0.101 mmol) in CH_2Cl_2 (30 mL) was brought to 0°C under argon and stirred vigorously as a solution of $FeCl_3$ (70 mg, 0.4 mmol) in CH_2Cl_2 (20 mL) under argon at 0°C was added dropwise over 10 min. Upon addition, the solution was kept in the 0°C water bath and was allowed to slowly warm to room temperature. Stirring for approx 17 h under argon followed by the addition of MeOH (approx. 50 mL) provided a brown-green solution. Removal of the solvents *in vacuo* provided a crude reddish-brown material that was adsorbed onto silica and purified on silica gel (hexane) to yield the product as a yellow solid (13 mg, 0.018 mmol, 17%). ^{1}H NMR (500 MHz, $CDCl_3$) δ: 8.58 (s, 2H), 7.30 (s, 4H), 3.01 (t, 8H, *J* = 7.0 Hz), 1.85 (quin, 8H, *J* = 8.0 Hz), 1.45 (m, 24H), 0.93 (t, 12H, *J* = 7.0 Hz). ^{13}C NMR (125 MHz, $CDCl_3$) δ: 146.4, 133.51, 133.40, 125.3, 120.3, 118.2, 31.90, 31.82, 31.80, 31.08, 29.1, 22.8, 14.4. FT-IR (KBr): ν/cm^{-1}: 2950, 2922, 2849, 1520, 1463, 1401, 1278, 848, 819. HR-MS (EI): found *m/z* = 738.3437 ± 0.0022 (M^+); calc. for $C_{46}H_{58}S_4$: 738.3421.

1,2,4,5-Tetra(5'-hexyl-2'-thienyl)benzene (**2**): A 25 mL Schlenk flask was charged with 1,2,4,5-tetrabromobenzene (275 mg, 0.677 mmol) and $(Ph_3P)_2PdCl_2$ (40 mg, 0.057 mmol) and placed under argon. DMF (3 mL) was added and the reaction was heated to 80°C until all solids dissolved. 5-Hexyl-2-(tributylstannyl)thiophene (1.837 g, 4.017 mmol) was added dropwise and stirred further for 24h. After cooling, the reaction mixture was diluted with ether and 1M NaF and stirred for 30 min. The mixture was diluted further with ether and washed with NaF, NH_4Cl (x3) and NaCl. The organic layer was dried and removed *in vacuo* to provide a brown oil which was chromatographed on silica gel (hexanes) to provide a clear viscous oil with suspended white solids. This material was taken up in MeOH and the resulting white precipitate was filtered and dried to provide 198 mg of the product as a fluffy white solid. The supernatant was concentrated and treated again with MeOH to provide an additional 263 mg of a pale yellow solid that was pure by ^{1}H NMR. Total yield: 461 mg (0.620 mmol), 92%. mp 62.5-64°C. ^{1}H NMR (500 MHz, $CDCl_3$) δ: 7.57 (s, 2H), 6.75 (d, 4H, J = 4.0 Hz), 6.63 (d, 4H, J = 3.5 Hz), 2.76 (t, 8H, J = 8.0 Hz), 1.64 (quin, 8H, J = 7.0 Hz), 1.33 (m, 24H), 0.89 (t, 12H, J = 6.5 Hz). ^{13}C NMR (125 MHz, $CDCl_3$) δ: 147.1, 139.5, 133.2 (x2), 127.0, 124.2, 31.85, 31.80, 30.3, 29.0, 22.8, 14.3. FT-IR (KBr): ν/cm^{-1}: 3072, 2955, 2925, 2850, 1505, 1466, 1377, 1338, 1231, 911, 799. HR-MS (EI): found m/z = 742.3724 ± 0.0021 (M^+); calc. for $C_{46}H_{62}S_4$: 742.3734. Anal: Calcd for $C_{46}H_{62}S_4$: C, 74.44; H, 8.64. Found: C, 74.55; H, 8.86.

4,6-Dibromo-1,3-di(2-thienyl)benzene (en route to **4**): A 100 mL Schlenk flask was charged with **3** (4.881 g, 10.01 mmol) and $(Ph_3P)_2PdCl_2$ (249 mg, 0.355 mmol) and placed under argon. DMF (25 mL) was added, and the reaction was heated to 80°C. 2-(Tributylstannyl)thiophene (7.0 mL, 21 mmol) was added dropwise and stirred further for 42 h. After cooling, the reaction mixture was worked up as described for **2** to provide a yellow oil that solidified upon freezing. Recrystallization from MeOH provided 2.024 g of a faint yellow product, and the material in the mother liquor was chromatographed on silica gel (hexane) and recrystallized to provide an additional 606 mg of product as fluffy white needles. Both cuts were clean by ^{1}H NMR to give a total yield of 2.630 g (6.572 mmol, 66%). mp 73-74°C. ^{1}H NMR (300 MHz, $CDCl_3$) δ: 8.00 (s, 1H), 7.59 (s, 1H), 7.42 (dd, 2H, J = 5.1, 0.9 Hz), 7.33 (dd, 2H, J = 3.6, 1.2 Hz), 7.12 (dd, 2H, J = 3.6, 5.1 Hz). ^{13}C NMR (125 MHz, $CDCl_3$) δ: 140.3, 137.9, 134.9, 134.3, 128.4, 127.4, 126.9, 122.3. FT-IR (KBr): ν/cm^{-1}: 3101, 3072, 1527, 1463, 1294, 1055, 885, 684. HR-MS (EI): found m/z = 397.8427 ± 0.0012 (M^+); calc. for $C_{14}H_8Br_2S_2$: 397.8434. Anal: Calcd for $C_{14}H_8Br_2S_2$: C, 42.02; H, 2.02. Found: C, 42.06; H, 1.97.

4',6'-Di(2-thienyl)-3,3'',4,4''-tetra(2-ethylhexyloxy)-1,1':3',1''-terphenyl (**4**): A three-necked 25 mL flask was charged with 4,6-dibromo-1,3-di(2-thienyl)benzene (108 mg, 0.269 mmol), 3,4-di(2-ethylhexyloxy)phenylpinacolatoborane (267 mg, 0.580 mmol), Na_2CO_3 (220 mg, 2.1 mmol) and

equipped with a condenser. Toluene (7 mL), EtOH (2 mL) and H_2O (2 mL) were added to the flask and the solution was purged with an argon flow with vigorous stirring for 30 min. Under a gentle argon stream, $Pd(PPh_3)_4$ (11 mg, 0.0095 mmol) was added to the solution and the system was heated at reflux for 21 h, cooled to room temperature. After removing the aqueous layer, the organics were filtered through silica gel (2:1 hexane/CH_2Cl_2). Purification of the crude material on silica gel (hexane to 3:1 hexane/CH_2Cl_2) provided the product as a white solid (209 mg, 0.230 mmol, 86%). mp 83.5-86.0°C. ^{1}H NMR (400 MHz, $CDCl_3$) δ: 7.72 (s, 1H), 7.47 (s, 1H), 7.22 (dd, 2H, *J* = 1.14, 5.08 Hz), 6.92 (dd, 2H, *J* = 3.6, 5.1 Hz), 6.85 (m, 4H; apparent d, 2H, *J* = 1.7 Hz and s, 2H), 6.82 (dd, 2H, *J* = 1.2, 3.6 Hz), 6.78 (d, 2H, *J* = 1.6 Hz), 3.88 (m, 4H), 3.66 (m, 4H), 1.77 (m, 2H), 1.7 (m, 2H), 1.3-1.6 (bm, 32H), 0.93 (m, 24H). ^{13}C NMR (100 MHz, $CDCl_3$) δ: 149.1, 148.96, 142.9, 140.4, 133.3, 133.0 (CH), 132.9 (CH), 132.2, 127.2 (CH x2), 125.8 (CH), 121.9 (CH), 115.4 (CH), 113.3 (CH), 71.79, 71.59, 39.8, 39.5, 30.8, 30.7, 29.37, 29.26, 24.13, 24.06, 23.3, 14.3, 11.45, 11.34. FT-IR (KBr): ν/cm^{-1}: 2958, 2926, 2859, 1602, 1580, 1513, 1467, 1255, 1137, 1027, 697. HR-MS (EI): found *m/z* = 906.5691 (M^+); calc. for $C_{58}H_{82}O_4S_2$: 906.5649.

5,6,10,11-Tetra(2-ethylhexyloxy)dibenz[3',4';5',6']anthra[1,2-*b*:8,7-*b*']dithiophene (**5**): A solution of **4** (1.000 g, 1.102 mmol) in CH_2Cl_2 (110 mL) was stirred vigorously under argon as a solution of $FeCl_3$ (2.85 g, 17.8 mmol) in $MeNO_2$ (15 mL) was added dropwise over 5 min. Anhydrous MeOH was added at 25 min and stirred for 1 hr. The reaction was diluted with CH_2Cl_2 and stirred with NH_4OH (aq). The aqueous layer was removed and washed with CH_2Cl_2 (x2). The combined organic layers were washed with aqueous NH_4OH and water. The solvent was removed, and the crude material was pushed through a plug of silica gel (4:1 hexane/ CH_2Cl_2) to provide the product as a waxy yellow solid (739 mg, 0.818 mmol, 74%). mp 126.5-127.5°C. ^{1}H NMR (400 MHz, $CDCl_3$) δ: 9.32 (s, 1H), 8.50 (s, 1H), 8.17 (s, 2H), 7.77 (d, 2H, *J* = 5.4 Hz), 7.54 (s, 2H), 7.51 (d, 2H, *J* = 5.3 Hz), 4.23 (m, 4H), 4.08 (m, 4H), 1.93 (m, 4H), 1.3-1.75 (bm, 32 H), 1.11 (t, 6H, *J* = 7.4 Hz), 1.05 (t, 6H, *J* = 7.4 Hz), 0.98 (m, 12H, apparent 2 t). ^{13}C NMR (100 MHz, $CDCl_3$) δ: 150.3, 149.0, 135.0, 134.7, 126.8, 126.1, 124.8 (CH), 124.0, 123.5, 123.2 (CH), 118.2 (CH), 116.9 (CH), 107.6 (CH), 107.1 (CH), 72.2, 71.6, 40.0, 39.8, 30.94, 30.90, 29.48, 29.44, 24.2, 23.37, 23.36, 14.41, 14.39, 11.63, 11.51. FT-IR (KBr): ν/cm^{-1}: 2957, 2927, 1618, 1610, 1525, 1509, 1458, 1421, 1251, 1179, 1040, 839. UV-Vis (CH_2Cl_2) λ/nm (log ε): 322 (4.92), 337 (5.14), 370 (4.25), 389 (3.91), 412 (3.51). HR-MS (EI): found *m/z* = 902.5333 (M^+); calc. for $C_{58}H_{78}O_4S_2$: 902.5336.

2,14-Dibromo-5,6,10,11-tetra(2-ethylhexyloxy)dibenz[3',4';5',6']anthra[1,2-*b*:8,7-*b*']dithiophene (**6**): A solution of **5** (568 mg, 0.629 mmol) in CH_2Cl_2 (25 mL) was stirred at room temperature as bromine (66 μL, 1.3 mmol) was added dropwise. The reaction was stirred for 4 h with a gentle argon purge and

quenched with 2M KOH. The organic layer was washed with NH_4Cl, dried and removed. The crude material was chromatographed on silica gel (hexane to 7:1 hexane/CH_2Cl_2) to provide the product as a waxy yellow gum This material was dissolved in CH_2Cl_2 and precipitated into MeOH. The precipitates were filtered, rinsed with MeOH and pumped dry to provide the product as gummy yellow solids (604 mg, 0.569 mmol, 91%). ^{1}H NMR (400 MHz, $CDCl_3$) δ: 8.63 (s, 1H), 7.73 (s, 2H), 7.33 (s, 2H), 7.05 (s, 1H), 7.02 (s, 2H), 4.18 (m, 4H), 3.98 (m, 4H), 2.00 (m, 2H), 1.95 (m, 2H), 1.4-1.8 (bm, 32H), 0.99-1.15 (m, 24H). ^{13}C NMR (100 MHz, $CDCl_3$) δ: 149.8, 149.0, 135.0, 134.5, 125.93, 125.79 (CH), 124.01, 122.9, 122.3, 116.3 (CH), 115.7 (CH), 112.2, 106.42 (CH), 106.25 (CH), 71.85, 71.65, 39.89, 39.71, 30.88, 30.83, 29.54, 29.49, 24.16, 23.44, 23.40, 14.48, 14.45, 11.75, 11.53. HR-MS (EI): found *m/z* = 1058.3537 (M^+); calc. for $C_{58}H_{76}Br_2O_4S_2$: 1058.3546.

2,14-Diiodo-5,6,10,11-tetra(2-ethylhexyloxy)dibenz[3',4';5',6']anthra[1,2-*b*:8,7-*b'*]dithiophene (**7**): A solution of dry THF (25 mL), *n*-BuLi (0.74 mL, 1.2 mmol) and TMEDA (0.18 mL, 1.2 mmol) were stirred in a 100 mL Schlenk flask under argon at –78°C for 10 min. A solution of **5** (350.4 mg, 0.3879 mmol) in THF (5 mL) was cooled to –78°C and added dropwise to the *n*-BuLi solution followed by a 5 mL THF rinse. The reaction was stirred for 30 min at –78°C at which point a solution of iodine (395 mg, 1.56 mmol) in THF (5 mL) was added dropwise. The reaction was allowed to warm to room temperature and was then quenched with 2M KOH. After the disappearance of the iodine color, the aqueous layer was removed and washed with ether; the combined organics were washed with NH_4Cl (x2), dried and removed. The crude material was pushed through a silica plug (4:1 hexane/ CH_2Cl_2) followed by purification by silica gel chromatography (hexane to 7:1 hexane/CH_2Cl_2) to provide the product as a yellow solid gum (421 mg, 0.364 mmol, 94%). ^{1}H NMR (400 MHz, $CDCl_3$) δ: 8.81 (s, 1H), 7.84 (s, 2H), 7.63 (s, 2H), 7.35 (s, 1H), 7.17 (s, 2H), 4.20 (m, 4H), 4.03 (m, 4H), 2.00 (m, 4H), 1.5-1.8 (bm, 32H), 0.97-1.15 (m, 24H). ^{13}C NMR (125 MHz, $CDCl_3$) δ: 150.1, 149.1, 139.3, 135.9, 132.9, 126.2, 124.3, 123.0, 122.3, 117.4, 115.9, 106.6, 74.2, 72.1, 71.7, 39.93, 39.75, 30.90, 30.86, 29.56, 29.51, 24.20, 23.44, 23.42, 14.49, 14.47, 11.80, 11.56. FT-IR (KBr): ν/cm^{-1}: 2957, 2926, 2870, 2857, 1619, 1525, 1457, 1419, 1381, 1261, 1227, 1175, 1076, 1041, 836. HR-MS (EI): found *m/z* = 1154.3258 (M^+); calc. for $C_{58}H_{76}I_2O_4S_2$: 1154.3269.

2,5-Dibromo-1,4-di(2-thienyl)benzene (en route to **9**): A 100 mL Schlenk flask was charged with **8** (9.764 g, 20.02 mmol) and $(Ph_3P)_2PdCl_2$ (352 mg, 0.501 mmol) and placed under argon. DMF (50 mL) was added and the reaction was heated to 80°C. 2-(Tributylstannyl)thiophene (14 mL, 42 mmol) was added dropwise and stirred further for 40 h. After cooling, the reaction mixture was worked up as for **2** to provide a yellow oil that solidified in the freezer. Recrystallization from CH_2Cl_2/MeOH provided needle-like solids that were subsequently adsorbed onto silica. Chromatography on silica gel (hexane) provided

the product as a white solid (4.640 g, 11.60 mmol, 58%). mp 131.5-133°C. ^{1}H NMR (400 MHz, $CDCl_3$) δ: 7.80 (s, 2H), 7.44 (dd, 2H, *J* = 1.2, 5.1 Hz), 7.36 (dd, 2H, *J* = 1.2, 3.6 Hz), 7.13 (dd, 2H, *J* = 3.6, 5.1 Hz). ^{13}C NMR (100 MHz, $CDCl_3$) δ: 139.9, 136.2, 135.9, 128.6, 127.4, 127.1, 121.4. FT-IR (KBr): ν/cm^{-1}: 3092, 1532, 1467, 1420, 1247, 1202, 1072, 957, 832, 689. HR-MS (FAB): found *m/z* = 397.8426 ± 0.0012 (M^+); calc. for $C_{14}H_8Br_2S_2$: 397.8434. Anal: Calcd for $C_{14}H_8Br_2S_2$: C, 42.02; H, 2.02. Found: C, 42.35; H, 1.92.

2',5'-Di(2-thienyl)-3,3",4,4"-tetra(2-ethylhexyloxy)-1,1':4',1"-terphenyl (**9**): A 500 mL three-necked flask equipped with a condenser was charged with 2,5-dibromo-1,4-di(2-thienyl)benzene (1.599 g, 3.996 mmol) and 3,4-di(2-ethylhexyloxy)phenyl pinacolatoborane (3.914 g, 8.499 mmol) and dissolved in PhMe (100 mL) and EtOH (20 mL). During vigorous stirring, a solution of Na_2CO_3 (3.323 g, 31.35 mmol) in water (20 mL) was added, and the biphasic system was purged with a strong flow of argon for 60 min. Under a gentle argon stream, $Pd(PPh_3)_4$ (120 mg, 0.10 mmol) was added to the solution and the system was heated at reflux for 56 h. After cooling to room temperature, the reaction was diluted with PhMe, washed twice with NH_4Cl (aq), dried and removed. Two purifications on silica (hexane to 8:1 hexane/CH_2Cl_2) provided the product as an opaque oil that slowly solidified into a white waxy solid (298 mg, 0.398 mmol, 58%). mp 48.5-50.0°C. ^{1}H NMR (400 MHz, $CDCl_3$) δ: 7.58 (s, 2H), 7.20 (dd, 2H, *J* = 1.1, 5.1 Hz), 6.89 (dd, 2H, *J* = 3.6, 5.1 Hz), 6.86 (m, 4H), 6.80 (dd, 2H, *J* = 1.1, 3.6 Hz), 6.77 (d, 2H, *J* = 1.2 Hz), 3.88 (m, 4H), 3.66 (m, 4H), 1.77 (m, 2H), 1.6 (m, 2H), 1.4 (bm, 32H), 0.9 (m, 24H). ^{13}C NMR (100 MHz, $CDCl_3$) δ: 149.2, 149.0, 143.0, 139.8, 133.4, 132.84 (CH), 132.73, 127.21 (CH), 127.18 (CH), 125.8 (CH), 121.9 (CH), 115.6 (CH), 113.5 (CH), 71.87, 71.67, 39.85, 39.58, 30.85, 30.76, 29.39, 29.28, 24.15, 24.08, 23.3, 14.3, 11.45, 11.34. FT-IR (KBr): ν/cm^{-1}: 2958, 2926, 2871, 1603, 1581, 1517, 1466, 1437, 1378, 1241, 1193, 1138, 1031, 697. HR-MS (EI): found *m/z* = 906.5873 (M^+); calc. for $C_{58}H_{82}O_4S_2$: 906.5649.

2',5'-Di(5-bromo-2-thienyl)-3,3",4,4"-tetra(2-ethylhexyloxy)-1,1':4',1"-terphenyl (**10**): A solution of **9** (837 mg, 0.923 mmol) in CH_2Cl_2 (5 mL) and DMF (10 mL) was stirred in the absence of light as NBS (337 mg, 1.87 mmol) was added portionwise. The reaction was stirred at room temperature for 19 h at which point NMR indicated a complete reaction. At 25 h, the reaction was quenched with 2M KOH and diluted with CH_2Cl_2. The aqueous layer was washed twice with CH_2Cl_2 and the combined organics were washed with 2M KOH and NH_4Cl (x3). The organic layer was dried and removed to provide an orange-brown oil. The crude material was chromatographed on silica gel (hexane to 6:1 hexane/CH_2Cl_2) to provide the product as a viscous oil contaminated with a trace impurity (742 mmol, *ca.* 0.697 mmol, 75%). This material was used without further purification or characterization. ^{1}H NMR (300 MHz,

$CDCl_3$) δ: 7.50 (s, 2H), 6.85 (m, 6H), 6.75 (s, 2H), 6.55 (d, 2H), 3.90 (m, 4H), 3.70 (m, 4H), 1.75 (m, 2H), 1.70 (m, 2H), 1.2-1.6 (bm, 32H), 0.90 (m, 24H).

2',5'-Di(5-iodo-2-thienyl)-3,3",4,4"-tetra(2-ethylhexyloxy)-1,1':4',1"-terphenyl (**11**): A solution of **9** (837 mg, 0.923 mmol) in CH_2Cl_2 (20 mL) was stirred at room temperature as $Hg(OAc)_2$ was added portionwise (603 mg, 1.89 mmol). The reaction was stirred with exclusion of light for 1 hr followed by the addition of solid iodine (496 mg, 1.95 mmol). After stirring for 5 more hours, the reaction was quenched with water, diluted with CH_2Cl_2 and stirred with 2M KOH. The aqueous layer was removed and washed with CH_2Cl_2, and the combined organics were filtered and washed with 2M KOH and NH_4Cl, dried and removed. The crude material was precipitated into vigorously stirred MeOH. After initial oil formation, continued stirring provided a waxy solid. Filtration and rinsing provided 850 mg of a pale yellow solid. Chromatography on silica gel (hexane to 7:1 hexane/CH_2Cl_2) provided a solid that was precipitated again into MeOH. Filtration and rinsing the solids provided the product as a white powder (748 mg, 0.645 mmol, 70%). mp 66-67°C. ^{1}H NMR (400 MHz, $CDCl_3$) δ: 7.51 (s, 2H), 7.04 (d, 2H, J = 3.7 Hz), 6.87 (m, 4H), 6.77 (d, 2H, J = 1.4 Hz), 6.49 (d, 2H, J = 3.8 Hz), 3.91 (m, 4H), 3.71 (m, 4H), 1.8 (m, 2H), 1.7 (m, 2H), 1.40 (m, 32H), 0.94 (m, 24H). ^{13}C NMR (100 MHz, $CDCl_3$) δ: 149.24, 149.21, 148.9, 139.7, 137.2, 132.6, 132.2, 128.8, 121.9, 115.4, 113.5, 73.8, 71.80, 71.75, 39.76, 39.52, 30.81, 30.76, 29.36, 29.26, 24.12, 24.07, 23.32, 23.30, 14.36, 11.45, 11.37. FT-IR (KBr): ν/cm^{-1}: 2958, 2927, 2859, 1602, 1578, 1516, 1465, 1250, 1235, 1196, 1137, 1026, 797, 669.

2,10-Dibromo-5,6,13,14-tetra(decyloxy)dibenz[3',4';7',8']anthra[1,2-*b*:5,6-*b'*]dithiophene (**12**): A solution of **10** (742 mg, 0.697 mmol) in CH_2Cl_2 (25 mL) was stirred vigorously under argon as a suspension of $FeCl_3$ (677 mg, 4.17 mmol) in $MeNO_2$ (3 mL) under argon was added dropwise over 2 min. The solution was stirred under an argon purge for 10 min at which point MeOH (approx. 25 mL) was added and stirred. The precipitates that formed were collected by filtration and washed with MeOH. The crude solids were dissolved in boiling $CHCl_3$ and hot hexane was added to this solution such that the approximate solvent ratio was 7:1 hexane/$CHCl_3$. This solution was then applied to a silica column packed with warm solvent and eluted with 4:1 hexane/CH_2Cl_2 to provide the product as a fluffy yellow solid (378 mg, 0.356 mmol, 51%). mp 168-170°C. ^{1}H NMR (300 MHz, $CDCl_3$) δ: 8.80 (s, 2H), 8.05 (s, 2H), 7.82 (s, 2H), 7.47 (s, 2H), 4.20 (m, 4H), 4.08 (m, 4H), 1.91 (m, 4H), 1.4 (bm, 32H), 1.0 (m, 12H). FT-IR (KBr): ν/cm^{-1}: 2957, 2928, 2871, 1614, 1523, 1460, 1428, 1264, 1244, 1188, 1049, 837. HR-MS (MALDI): found m/z = 1058.3549 (M^+); calc. for $C_{58}H_{76}Br_2O_4S_2$: 1058.3546.

1,3-Di(benzo[*b*]thiophen-2-yl)-4,6-dibromobenzene (en route to **13**): A 100 mL Schlenk flask was charged with **3** (4.884 g, 10.01 mmol) and $(Ph_3P)_2PdCl_2$ (246 mg, 0.351 mmol) and placed under argon.

DMF (25 mL) was added and the reaction was heated to 80°C. 2-(Tributylstannyl)benzo[*b*]thiophene (10.873 g, 25.167 mmol) was added dropwise and stirred for 46 h. Upon cooling, the resulting precipitates were filtered off and recrystallized from $CHCl_3$/MeOH to provide the product as a fibrous, chalky white solid (3.120 g, 6.237 mmol, 62%). mp 186°C. ^{1}H NMR (400 MHz, $CDCl_3$) δ: 8.08 (s, 1H), 7.84 (m, 4H), 7.74 (s, 1H), 7.56 (s, 2H), 7.39 (m, 4H). ^{13}C NMR (100 MHz, $CDCl_3$) δ: 140.4, 140.3, 139.8, 138.1 (CH), 135.0, 134.8 (CH), 125.2 (CH), 125.1 (CH), 124.8 (CH), 124.2 (CH), 123.1, 122.3 (CH). FT-IR (KBr): ν/cm^{-1}: 3061, 2928, 2849, 1653, 1522, 1459, 1430, 1180, 1055, 823, 718. HR-MS (EI): found *m/z* = 497.8723 (M^+); calc. for $C_{22}H_{12}Br_2S_2$: 497.8742.

4',6'-Di(benzo[*b*]thiophen-2-yl)-3,3'',4,4''-tetra(2-ethylhexyloxy)-1,1':3',1''-terphenyl (**13**): A three-necked 500 mL flask was charged with 1,3-di(benzo[*b*]thiophen-2-yl)-4,6-dibromobenzene (2.004 g, 4.006 mmol), 3,4-di(2-ethylhexyloxy)phenyl pinacolatoborane (4.403 g, 9.561 mmol), followed by the addition of PhMe (100 mL), EtOH (20 mL) and an aqueous solution of Na_2CO_3 (333 mg, 3.14 mmol dissolved in 20 mL water). After attaching a reflux condenser, the solution was purged with an argon flow for 1h with vigorous stirring. Under a gentle argon stream, $Pd(PPh_3)_4$ (120 mg, 0.10 mmol) was added to the solution, and the system was heated at reflux for 39 h, cooled to room temperature, diluted with ether and stirred with 2M KOH. The aqueous layer was removed and washed with ether; the combined organics were washed with 2M KOH (aq) and NH_4Cl, dried and removed. The crude material was chromatographed on silica gel (hexane to 4:1 hexane/ CH_2Cl_2) to provide the product as a waxy white solid (3.091 g, 3.068 mmol, 77%). mp 98-100°C. ^{1}H NMR (100 MHz, CD_2Cl_2) δ: 7.89 (s, 1H), 7.76 (d, 2H, *J* = 7.6 Hz), 7.69 (d, 2H, *J* = 7.7 Hz), 7.56 (s, 1H), 7.30 (m, 4H), 7.16 (s, 2H), 6.90 (m, 6H), 3.87 (m, 4H), 3.58 (m, 4H), 1.74 (m, 2H), 1.2-1.7 (bm, 34H), 0.92 (m, 18H), 0.79 (t, 6H, *J* = 7.4 Hz). ^{13}C NMR (100 MHz, CD_2Cl_2) δ: 149.70, 149.58, 143.7, 141.7, 141.0, 140.6, 133.9 (CH), 133.4 (CH), 133.1, 132.5, 124.84 (CH), 124.70 (CH), 124.2 (CH), 124.0 (CH), 122.52 (CH), 122.38 (CH), 116.0 (CH), 113.6 (CH), 72.10, 71.98, 40.2, 39.9, 31.15, 30.98, 29.7, 29.5, 24.5, 24.3, 23.66, 23.64, 14.46, 14.44, 11.56, 11.31. FT-IR (KBr): ν/cm^{-1}: 2960, 2927, 2858, 1600, 1579, 1510, 1467, 1245, 1133, 1026, 857, 743. HR-MS (EI): found *m/z* = 1006.5970 (M^+); calc. for $C_{66}H_{86}O_4S_2$: 1006.5962.

Compound **14**: A solution of **13** (32 mg, 0.032 mmol) in CH_2Cl_2 (4 mL) was stirred vigorously under argon as a solution of $FeCl_3$ (88 mg, 0.54 mmol) in CH_2Cl_2 (1 mL) under argon was added dropwise over 5 min. Anhydrous MeOH was added at 45 min and stirred for 30 min. To remove iron impurities, the reaction was diluted with CH_2Cl_2 and stirred with NH_4OH (5 mL). The aqueous layer was washed with CH_2Cl_2 (x2); the combined organics were washed with aqueous NH_4OH and NH_4Cl, dried and removed to provide a crude material. Purification on silica gel (hexane to 5:1 hexane/ CH_2Cl_2) provided the product as a yellow film (14.5 mg, 0.0145 mmol, 45%). ^{1}H NMR (400 MHz, CD_2Cl_2) δ: 9.21 (s, 1H),

8.45 (d, 2H, J = 8.0 Hz), 8.28 (s, 1H), 8.11 (s, 2H), 8.05 (s, 2H), 7.96 (dd, 2H, J = 1.0, 7.6 Hz), 7.49 (m, 4H), 4.18 (m, 4H), 4.09 (m, 4H), 1.95 (m, 4H), 1.5-1.8 (m, 32H), 0.99-1.15 (m, 24H). ^{13}C NMR (100 MHz, CD_2Cl_2) δ: 150.5, 148.9, 139.9, 137.9, 136.2, 128.10, 128.04, 125.7, 125.34 (CH), 125.25 (CH), 125.19, 124.40, 123.59 (CH), 120.3 (CH), 116.5 (CH), 107.51 (CH), 107.41 (CH), 72.07, 71.94, 40.34, 40.18, 31.27, 31.24, 29.85, 24.59, 24.54, 23.79, 23.77, 14.58, 14.55, 11.82, 11.72. FT-IR (KBr): ν/cm^{-1}: 2957, 2926, 2871, 2857, 1610, 1530, 1456, 1378, 1256, 1208, 1378, 1256, 1042, 720. HR-MS (ESI): found m/z = 1003.5725 [(M+H)$^+$]; calc. for $C_{66}H_{82}O_4S_2$+H: 1003.5727.

4',6'-Di(5-iodo-2-thienyl)-3,3'',4,4''-tetra(2-ethylhexyloxy)-1,1':3',1"-terphenyl (en route to **16** and **20**): A solution of **4** (453 mg, 0.499 mmol) in CH_2Cl_2 (10 mL) was stirred at room temperature as $Hg(OAc)_2$ was added portionwise (326 mg, 1.02 mmol). The reaction was stirred with exclusion of light for 1 hr followed by the addition of solid I_2 (268 mg, 1.06 mmol). After stirring for 5 more hours, the reaction was quenched with water, diluted with CH_2Cl_2 and stirred with 2M KOH. The aqueous layer was removed and washed with CH_2Cl_2, and the combined organics were filtered and washed with 2M KOH and NH_4Cl, dried and removed. The crude material was precipitated into vigorously stirred MeOH and the solids were collected by filtration and rinsing to provide the product as a waxy white solid (510 mg, 0.44 mmol, 88%). mp 84.5-85.5°C. ^{1}H NMR (400 MHz, $CDCl_3$) δ: 7.57 (s, 1H), 7.44 (s, 1H), 7.05 (d, 2H, J = 3.8 Hz), 6.85 (s, 4H), 6.76 (s, 2H), 6.48 (d, 2H, J = 3.7 Hz), 3.90 (m, 4H), 3.69 (m, 4H), 1.78 (m, 2H), 1.7 (m, 2H), 1.40 (bm, 32H), 0.93 (m, 24H). ^{13}C NMR (100 MHz, $CDCl_3$) δ: 149.28, 149.25, 148.9, 140.7, 137.2 (CH), 133.2 (CH), 132.7, 132.3 (CH), 131.4, 128.8 (CH), 121.9 (CH), 115.4 (CH), 113.5 (CH), 73.6, 71.86, 71.81, 39.8, 39.6, 30.83, 30.79, 29.38, 29.28, 24.15, 24.11, 23.32, 23.30, 14.4, 11.45, 11.38. FT-IR (KBr): ν/cm^{-1}: 29587, 2926, 2858, 1601, 1511, 1466, 1254, 1136, 1024.

Polymer **16**: A 25 mL Schlenk tube was charged with 4',6'-di(5-iodo-2-thienyl)-3,3'',4,4''-tetra(2-ethylhexyloxy)-1,1':3',1"-terphenyl (116 mg, 0.100 mmol), **15** (48 mg, 0.10 mmol) and CuI (4 mg, 0.02 mmol), and the flask was placed under argon. In an inert atmosphere, $Pd(PPh_3)_4$ was added (5 mg, 0.004 mmol), and the flask was again placed under argon at the bench. Under an argon purge, 3 mL of a 3:2 PhMe/DIPA mixture was added. The system was heated at 85°C for 62 h at which point the Pd catalyst precipitated out. The reaction mixture was precipitated into MeOH, redissolved in CH_2Cl_2 and washed with NH_4OH and H_2O. Drying and removal of the solvent provided a yellow film. This material was dissolved into CH_2Cl_2 and reprecipitated from MeOH. The polymer was filtered and washed thoroughly with boiling MeOH and boiling acetone to provide a yellow powder (114 mg, 82% mass yield). M_n = 21,000.

Polymer **17**: Following a similar procedure for **16**, a mixture of **7** (116 mg, 0.101 mmol), **15** (48.6 mg, 0.102 mmol), CuI (1 mg, 0.006 mmol) and $Pd(PPh_3)_4$ (5 mg, 0.004 mmol) in PhMe (4 mL) and DIPA (1.5 mL) was stirred at 85°C for 6.5 d. Work up and precipitation as described for **16** provided the polymer as a light brown waxy solid (93 mg, 67% mass yield). M_n = 16,500.

Polymer **18**: Following a similar procedure for **16**, **11** (116 mg, 0.100 mmol), **15** (48 mg, 0.10 mmol), CuI (1 mg, 0.004 mmol) and $Pd(PPh_3)_4$ (6 mg, 0.005 mmol) in 3.5 mL of a 3:1 mixture of toluene and DIPA was stirred at 80°C for 48 h at which point the Pd catalyst precipitated out. Work up and precipitation as described for **16** provided the polymer as a dark yellow solid that had a high degree of static charge, making accurate weight determination impossible. M_n = 15,000.

Polymer **19**: Following a similar procedure for **16**, **12** (105.7 mg, 0.0996 mmol) and **15** (47.8 mg, 0.0999 mmol), CuI (2 mg, 0.02 mmol) and $Pd(PPh_3)_4$ (5 mg, 0.004 mmol) in toluene (2.5 mL) and DIPA (0.8 mL) was stirred at 60°C for 4 d. Work up and precipitation as described for **16** provided the polymer as a fluffy yellow solid (118 mg, 86% mass yield). M_n = 20,000.

4',6'-Bis(5-[4-dodecyloxyphenylethynyl]-2-thienyl)-3,3'',4,4''-tetra(2-ethylhexyloxy)-1,1':3',1''-terphenyl (**20**): A 25 mL Schlenk tube was charged with 4',6'-di(5-iodo-2-thienyl)-3,3'',4,4''-tetra(2-ethylhexyloxy)-1,1':3',1''-terphenyl (205 mg, 0.177 mmol), $(Ph_3P)_2PdCl_2$ (4.1 mg, 0.0058 mmol) and CuI (2.5 mg, 0.013 mmol) and placed under argon. THF (5 mL) and DIPA (1 mL) were added, and the reaction was heated to 50°C for 20 min. A solution of **24** in THF (1.21 mL of a 88.3 mg/mL solution in THF, 0.374 mmol) was added dropwise, and the reaction was stirred under argon for 16 h. Upon cooling, the reaction was diluted with ether, washed with NH_4Cl and DI water, and removed. Chromatography on silica gel (hexane to 3:1 hexane/CH_2Cl_2) provided the product as a waxy yellow solid (228 mg, 0.154 mmol, 87%). ^{1}H NMR (400 MHz, $CDCl_3$) δ: 7.71 (s, 1H), 7.47 (s, 1H), 7.43 (d, 4H, *J* = 8.8 Hz), 7.05 (d, 2H, *J* = 3.8 Hz), 6.86 (m, 10H), 6.71 (d, 2H, *J* = 3.7 Hz), 3.98 (t, 4H, *J* = 6.6 Hz), 3.91 (m, 4H), 3.73 (m, 4H), 1.80 (m, 6H), 1.7 (m, 2H), 1.40 (bm, 68H), 0.93 (m, 30H). ^{13}C NMR (100 MHz, $CDCl_3$) δ: 159.5, 149.30, 149.23, 144.0, 140.6, 133.3 (CH), 133.1 (CH), 132.9, 132.4 (CH), 131.76 (CH), 131.74, 127.3 (CH), 124.2, 122.0 (CH), 115.4 (CH), 115.0, 114.7 (CH), 113.5 (CH), 94.1, 81.6, 71.8, 68.3, 39.8, 39.6, 32.1, 31.8, 30.85, 30.76, 29.88, 29.86, 29.81, 29.79, 29.60, 29.57, 29.40, 29.38, 29.25, 26.2, 24.16, 24.08, 23.3, 22.91, 22.87, 14.34, 14.32, 11.45, 11.32. FT-IR (KBr): ν/cm^{-1}: 2957, 2925, 2854, 2221, 1604, 1506, 1467, 1247, 1172, 1135, 1026, 830, 813. UV-Vis (CH_2Cl_2) λ/nm (log ε): 260 (4.49), 344 (4.68). HR-MS (MALDI): found *m/z* = 1474.9913 (M^+); calc. for for $C_{98}H_{138}O_6S_2$: 1474.9929.

2,14-Bis(4-dodecyloxyphenylethynyl)-5,6,10,11-tetra(2-ethylhexyloxy)dibenz[3',4';5',6']anthra[1,2-*b*:8,7-*b*']dithiophene (**21**): A 25 mL Schlenk tube was charged with **7** (130 mg, 0.11 mmol), $(Ph_3P)_2PdCl_2$

(2.5 mg, 0.0036 mmol) and CuI (1.3 mg, 0.0068 mmol) and placed under argon. THF (4 mL) and DIPA (1 mL) were added, and the reaction was heated to 50°C for 20 min. A solution of **24** in THF (0.51 mL of a 134 mg/mL solution, 0.24 mmol) was added dropwise, and the reaction was stirred under argon for 16 h. Upon cooling, the reaction mixture was worked up as described for **20** and chromatographed on silica gel (hexane to 4:1 hexane/CH_2Cl_2) to provide the product as a waxy yellow solid. (124 mg, 0.0842 mmol, 75%). mp 94.5-96°C. ^{1}H NMR (400 MHz, $CDCl_3$) δ: 8.87 (s, 1H), 7.92 (s, 1H), 7.87 (s, 2H), 7.77 (s, 2H), 7.56 (d, 4H, *J* = 8.6 Hz), 7.34 (s, 2H), 6.94 (d, 4H, *J* = 8.2 Hz), 4.18 (m, 4H), 4.03 (m, 8H), 1.97 (m, 4H), 1.83 (m, 4H), 1.68 (m, 8H), 1.4 (bm, 60H), 0.99 (m, 30H). ^{13}C NMR (100 MHz, $CDCl_3$) δ: 159.7, 150.1, 149.1, 135.1, 134.6, 133.2 (CH), 127.4 (CH), 127.0, 125.0, 123.30, 123.12, 122.2, 116.6 (CH), 116.2, (CH), 115.1, 114.8 (CH), 106.85 (CH), 106.68 (CH), 94.9, 82.6, 72.1, 71.7, 68.3, 39.88, 39.71, 32.2, 30.82, 30.78, 29.91, 29.88, 29.85, 29.83, 29.65, 29.59, 29.46, 26.28, 24.11, 23.43, 23.38, 23.93, 14.42, 14.35, 11.67, 11.46. FT-IR (KBr): ν/cm^{-1}: 2955, 2924, 2853, 2201, 1606, 1519, 1456, 1254, 1171, 1038, 828. UV-Vis (CH_2Cl_2) λ/nm (log ε): 240 (4.76), 287 (4.70), 319 (4.80), 355 (4.95), 375 (4.94), 401 (sh, 4.73), 436 (sh, 3.63). HR-MS (MALDI): found *m/z* = 1470.9638 (M^+); for $C_{98}H_{134}O_6S_2$: 1470.9616.

2',5'-Bis(5-[4-dodecyloxyphenylethynyl]-2-thienyl)-3,3",4,4"-tetra(2-ethylhexyloxy)-1,1':4',1"-terphenyl (**22**): A 50 mL Schlenk tube was charged with **11** (351 mg, 0.302 mmol), $(Ph_3P)_2PdCl_2$ (6.7 mg, 0.0095 mmol) and CuI (3.7 mg, 0.019 mmol) and placed under argon. THF (6 mL) and DIPA (1 mL) were added, and the reaction was heated to 50°C for 20 min. A solution of **24** in THF (2.07 mL of a 88.3 mg/mL solution, 0.638 mmol) was added dropwise, and the reaction was stirred under argon for 16 h. Upon cooling, the reaction was worked up as described for **20**. Two chromatographies on silica gel (hexane to 5:1 hexane/CH_2Cl_2) provided the product as a yellow solid (373 mg, 0.253 mmol, 84%). mp 87.5-88.0°C. ^{1}H NMR (400 MHz, $CDCl_3$) δ: 7.56 (s, 2H), 7.39 (d, 4H, *J* = 8.7 Hz), 7.01 (d, 2H, *J* = 3.7 Hz), 6.84 (m, 10H), 6.67 (d, 2H, *J* = 3.8 Hz), 3.96 (t, 4H, *J* = 6.6 Hz), 3.90 (m, 4H), 3.72 (m, 4H), 1.78 (m, 6H), 1.70 (m, 2H), 1.40 (bm, 68H), 0.92 (m, 30H). ^{13}C NMR (100 MHz, $CDCl_3$) δ: 159.5, 149.34, 149.26, 144.0, 139.8, 133.03 (CH), 132.90, 132.75 (CH), 132.4, 131.8 (CH), 127.3 (CH), 124.2, 122.0 (CH), 115.5 (CH), 115.0, 114.7 (CH), 113.6 (CH), 94.1, 81.6, 71.86, 71.83, 68.3, 39.83, 39.59, 32.1, 31.8, 30.85, 30.76, 29.87, 29.85, 29.80, 29.78, 29.59, 29.56, 29.39, 29.26, 26.22, 24.16, 24.08, 23.3, 22.90, 22.87, 14.3, 11.45, 11.33. FT-IR (KBr): ν/cm^{-1}: 2958, 2925, 2855, 2203, 1605, 1509, 1458, 1288, 1249, 1175, 1016, 829. UV-Vis (CH_2Cl_2) λ/nm (log ε): 255 (4.55), 315 (4.57), 367 (4.64). HR-MS (MALDI): found *m/z* = 1474.9943 (M^+); calc. for $C_{98}H_{138}O_6S_2$: 1474.9929.

2,10-Bis(4-dodecyloxyphenylethynyl)-5,6,13,14-tetra(2-ethylhexyloxy)dibenz[3',4';7',8']anthra[1,2-*b*:5,6-*b'*]dithiophene (**23**): A 25 mL Schlenk tube was charged with **12** (106 mg, 0.100 mmol),

$(Ph_3P)_2PdCl_2$ (2.0 mg, 0.0028 mmol) and CuI (1.2 mg, 0.0063 mmol) and placed under argon. PhMe (4 mL) and DIPA (1 mL) were added, and the reaction was heated to 75°C for 20 min; however, some material did not dissolve. A solution of **24** in THF (0.36 mL of a 167 mg/mL solution, 0.21 mmol) was added dropwise, and the reaction was stirred under argon for 22 h. Upon cooling, the reaction was worked up as described for **20**. Chromatography on silica gel (hexane to 5:1 hexane/CH_2Cl_2) provided the product as a waxy yellow solid-oil (85 mg, 0.058 mmol, 58%). mp 153-154°C. ^{1}H NMR (400 MHz, $CDCl_3$) δ: 8.75 (s, 2H), 7.96 (s, 2H), 7.92 (s, 2H), 7.54 (d, 4H, *J* = 8.8 Hz), 7.46 (s, 2H), 6.91 (d, 4H, *J* = 8.8 Hz), 4.20 (m, 4H), 4.04 (m, 4H), 3.99 (t, 4H, *J* = 6.5 Hz), 1.9 (m, 4H), 1.8 (m, 4H), 1.4 (bm, 68H), 1.0 (m, 30H). ^{13}C NMR (100 MHz, $CDCl_3$) δ: 159.7, 150.2, 149.1, 135.8, 134.6, 133.2 (CH), 127.7 (CH), 127.1, 125.5, 122.95, 122.78, 122.1, 117.4 (CH), 114.99, 114.82 (CH), 106.54 (CH), 106.41 (CH), 95.0, 82.6, 71.72, 71.60, 68.3, 39.72, 39.65, 32.2, 30.98, 30.79, 29.93, 29.90, 29.87, 29.84, 29.67, 29.61, 29.56, 29.46, 29.41, 26.3, 24.26, 24.15, 23.47, 23.43, 22.9, 14.48, 14.42, 14.38, 11.71, 11.48. FT-IR (KBr): ν/cm^{-1}: 2955, 2922, 2852, 2208, 1605, 1515, 1459, 1431, 1244, 1187, 1172, 1041, 829. UV-Vis (CH_2Cl_2) λ/nm (log ε): 248 (4.74), 304 (4.86), 333 (4.75), 351 (4.80), 367 (5.03), 412 (4.61), 436 (4.69). HR-MS (MALDI): found *m/z* = 1471.9694 ([M+H]$^+$); calc. for $C_{98}H_{134}O_6S_2$+H: 1471.9695.

4,5-Bis(dimethoxyphenyl)-3,6-bis(trimethylsilylethynyl)-*o*-xylene (en route to **25**): A two-necked 50 mL flask was charged with 3,6-bis(trimethylsilylethynyl)-4,5-dibromo-*o*-xylene (229 mg, 0.503 mmol), 3,4-dimethoxyphenylboronic acid (192 mg, 1.05 mmol) and dissolved in PhMe (9 mL) and EtOH (2 mL). A solution of Na_2CO_3 (424 mg, 4.00 mmol) in water (2 mL) was added, a condenser was equipped, and the solution was purged with argon for 30 min. Under a gentle argon stream, $Pd(PPh_3)_4$ (12 mg, 0.010 mmol) was added to the solution and the system was heated at reflux for 48 h and cooled to room temperature. The solvents were removed and the crude material was dissolved in CH_2Cl_2, washed with NH_4Cl. The organic phase was dried and removed to provide light brown solids. Purification on silica gel (CH_2Cl_2) provided the product as a yellow solid (268 mg, 0.469 mmol, 82%). ^{1}H NMR (300 MHz, $CDCl_3$) δ: 6.65 (s, 4H), 6.57 (s, 2H), 3.81 (s, 6H), 3.65 (s, 6H), 2.50 (s, 6H), 0.03 (s, 18H). ^{13}C NMR (100 MHz, $CDCl_3$) δ: 147.73, 147.51, 141.8, 138.1, 132.8, 123.5, 123.2 (CH), 114.3 (CH), 110.1 (CH), 104.1, 103.6, 55.91, 55.75, 18.7, -0.1. HR-MS (EI): found *m/z* = 570.2604 (M$^+$); calc. for $C_{34}H_{42}O_4Si_2$: 570.2616.

4,5-Bis(dimethoxyphenyl)-3,6-diethynyl-*o*-xylene (**25**): A 25 mL flask was charged with 4,5-bis(dimethoxy phenyl)-3,6-bis(trimethylsilylethynyl)-*o*-xylene (147 mg, 0.256 mmol) and placed under argon. A degassed solution of THF (8 mL) and MeOH (2 mL) was added, and the solution was stirred under an argon purge as a solution of KOH (1 pellet, 138 mg, 2.46 mmol) in water (1 mL) was added dropwise. During the course of the reaction, an oily white material deposited on the flask. After 21h, the reaction was diluted with CH_2Cl_2 and washed with NH_4Cl. The aqueous layer was washed once with

CH_2Cl_2, and the combined organics were washed with NH_4Cl and DI water. The organic phase was dried and removed to provide the product as white solids. This material was purified on silica gel (1:1 hexane/CH_2Cl_2 to 100% CH_2Cl_2) to provide 90 mg of the produce as a white solid film (89.5 mg, 0.210 mmol, 81%). ^{1}H NMR (400 MHz, $CDCl_3$) δ: 6.65 (3 broad peaks, 6H), 3.82 (s, 6H), 3.64 (s, 6H), 3.23 (s, 2H), 2.54 (s, 6H). ^{13}C NMR (400 MHz, $CDCl_3$) δ: 147.82, 147.66, 141.9, 138.9, 132.4, 123.2, 122.8, 114.3, 110.0, 86.1, 82.4, 55.85, 55.78, 18.8.

Polymer **26**: A 25 mL Schlenk tube was charged with **25** (36 mg, 0.083 mmol), 1,4-bis(hexadecyloxy)-2,5-diiodobenzene (68 mg, 0.084 mmol) and CuI (1 mg, 0.005 mmol) and placed under argon. In an inert atmosphere, $Pd(PPh_3)_4$ (3 mg, 0.003 mmol) was added, and the tube was capped removed from the inert atmosphere and placed under argon on a Schlenk line. Under a gentle purge of argon, the solids were dissolved in PhMe (1.5 mL) and DIPA (0.5 mL) and heated to 60°C for 2 days at which point a solid gel formed. The gel was dissolved in $CHCl_3$ and washed with NH_4Cl. The organic layer was removed and the crude polymer was redissolved in minimal $CHCl_3$ and precipitated into MeOH. The polymer was filtered and rinsed with MeOH and boiling MeOH to provide the polymer as an orange free-standing film (74 mg, 90% mass yield). ^{1}H NMR (400 MHz, $CDCl_3$) δ: 6.75-6.71 (2s, 6H), 6.19 (s, 2H), 3.82 (s, 16H), 3.64 (s, 6H), 2.64 (s, 6H), 1.77 (bs, 4H), 1.49 (bs, 4H), 1.25 (bs, 48H), 0.87 (m, 6H).

References

(1) Billard, J.; Dubois, J. C.; Tinh, N. H.; Zann, A. *Nouv. J. Chim.* **1978**, *2*, 535-540.

(2) *Handbook of Liquid Crystals;* Demus, D.; Goodby, J.; Gray, G. W.; Spiess, H.-W.; Vill, V., Eds.; Wiley-VCH, New York: 1998. Vol. 2B.

(3) Adam, D.; Schuhmacher, P.; Simmerer, J.; Häussling, L.; Siemensmeyer, K.; Etzbach, K. H.; Ringsdorf, H.; Haarer, D. *Nature* **1994**, *371*, 141-143.

(4) Laquindanum, J. G.; Katz, H. E.; Lovinger, A. J. *J. Am. Chem. Soc.* **1998**, *120*, 664-672.

(5) See for example: (a) Dimitrakopoulos, C. D.; Malenfant, P. R. L. *Adv. Mater.* **2002**, *14*, 99-117; (b) Schön, J. H.; Berg. S.; Kloc, C.; Batlogg, B. *Science* **2000**, *287*, 1022-1023.

(6) Coleman, L. B.; Cohen, M. J.; Sandman, D. J.; Yamagishi, F. G.; Garito, A. F.; Heeger, A. J. *Solid State Commun.* **1973**, *12*, 1125-1132.

(7) Parkin, S. S. P.; Engler, E. M.; Schumaker, R. R.; Lagier, R.; Lee, V. Y.; Scott, J. C.; Greene, R. L. *Phys. Rev. Lett.* **1983**, *50*, 270-273.

(8) Naudin, E.; El Mehdi, N.; Soucy, C.; Breau, L.; Bélanger, D. *Chem. Mater.* **2001**, *13*, 634-642.

(9) (a) Mallory, F. B.; Mallory, C. W. *Org. React.* **1984**, *30*, 1-456; for specific examples of 3-thienyl decomposition and photoisomerizations, see: (b) Kellogg, R. M.; Groen, M. B.; Wynberg, H. *J. Org. Chem.* **1967**, *32*, 3093-3100.

(10) Wynberg, H.; van Driel, H.; Kellogg, R. M.; Buter, J. *J. Am. Chem. Soc.* **1967**, *89*, 3487-3494.

(11) Sirringhaus, H.; Friend, R. H.; Wang, C.; Leuninger, J.; Müllen, K. *J. Mater. Chem.* **1999**, *9*, 2095-2101.

(12) Ryashentseva, M. A.; Belanova, E. P.; Minachev, Kh. M.; Polosin, V. M.; Bogdanov, V. S.; Petukhov, V. A.; Maksimov, B. I. *Bull. Acad. Sci. USSR* **1988**, *37*, 2579-2581.

(13) (a) Shirley, D. A.; Cameron, M. D. *J. Am. Chem. Soc.* **1950**, *72*, 2788-2789; (b) Clarke, K.; Rawson, G.; Scrowston, R. M. *J. Chem. Soc. C.* **1969**, 537-540.

(14) Swager, T. M. *Acc. Chem. Res.* **1998**, *31*, 201-207.

(15) Goldfinger, M. B.; Swager, T. M. *J. Am. Chem. Soc.* **1994**, *116*, 7895-7896.

(16) Bunz, U. H. F. *Chem. Rev.* **2000**, *100*, 1605-1644.

(17) Rose, A.; Lugmair, C. G.; Swager, T. M. *J. Am. Chem. Soc.* **2001**, *123*, 11298-11299.

(18) Yamaguchi, S.; Swager, T. M. *J. Am. Chem. Soc.* **2001**, *123*, 12087-12088.

(19) Nijegorodov, N. I.; Downey, W. S. *J. Phys. Chem.* **1994**, *98*, 5639-5643.

(20) Milstein, D.; Stille, J. K. *J. Am. Chem. Soc.* **1979**, *101*, 4992-4998.

(21) Hart, H.; Harada, K.; Du, C.-J. F. *J. Org. Chem.* **1985**, *50*, 3104-3110.

(22) Miyaura, N.; Yanagi, T.; Suzuki, A. *Synth. Commun.* **1981**, *11*, 513-519.

(23) For $FeCl_3$ polymerizations of the base 1,4-di(2-thienyl)benzene moiety, see: Reynolds, J. R.; Ruiz, J. P.; Child, A. D.; Nayak, K.; Marynick, D. S. *Macromolecules*, **1991**, *24*, 678-687.

(24) Liebeskind, L. S.; Wang, J. *J. Org. Chem.* **1993**, *58*, 3550-3556.

(25) Nelson, J. C.; Saven, J. G.; Moore, J. S.; Wolynes, P. G. *Science*, **1997**, *277*, 1793-1796.

(26) Sonogashira, K.; Tohda, Y.; Hagihara, N. *Tetrahedron Lett.* **1975**, 4467-4470.

(27) Yang, J.-S.; Swager, T. M. *J. Am. Chem. Soc.* **1997**, *120*, 11864-11873.

(28) Goldfinger, M. B.; Crawford, K. B.; Swager, T. M. *J. Am. Chem. Soc.* **1997**, *119*, 4578-4593.

(29) Tovar, J. D.; Swager, T. M. *Adv. Mater.* **2001**, *13*, 1775-1780.

Chapter 5

Towards new mechanochromic responses: Unusual optical properties of "polymeric oligomers"

Introduction

During the course of our studies towards the development of new routes to large polycyclic aromatic systems, we became interested in novel chromic applications that may utilize some of the structural features contained within the thiophene-based systems of Chapters 3 and 4. From the synthesis of models to explain tandem cyclization-polymerization sequences (Chapter 3), we realized that the pendant thienyl moieties halogenated selectively and in high yields. As portrayed in Scheme 1, we envisioned a variety of systems that could employ this facile functionalization to provide formally conjugated polymers with well-defined chromophores in the repeat unit. The choice of bridging arenes with *ortho* or *meta* conjugation pathways coupled with the chromophore's expected lack of co-planarity with the bridging unit will minimize inter-chromophore electronic communication yet allow for spatial interaction. As such, these systems should maintain the optical characteristics of the isolated chromophore while providing mechanical properties found in polymeric systems. They should also exhibit remarkable optical changes as a function of chromophore conformation. This idea may translate to mechanochromic transduction events where physical stresses applied to polymer films would induce differences in optical characteristics. It also may find use in solid-state polymer architectures that utilize polymer aggregation phenomena to enhance electronic coupling.

Scheme 1

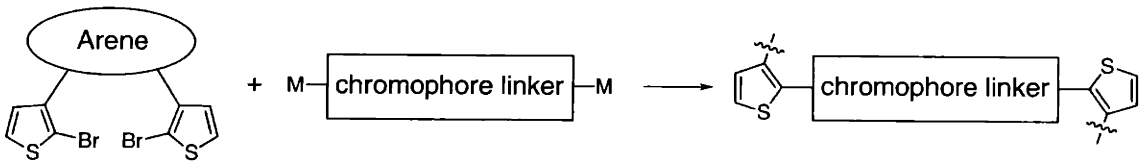

Crystalline poly(diacetylene) (PDA) has exhibited this mechanochromic effect; however, such studies resulted in new, irreversibly-formed crystalline domains attributed to changes in the

electronic configuration within the polymer.[1] Patel *et al.* established solution-based conformational transitions in urethane-substituted PDAs.[2] They found that the addition of non-solvents – solvents that provide sparing polymer solubility - to solvated polymer solutions fostered greater intrapolymer hydrogen bonding among the pendant urethane moieties as illustrated in Scheme 2. This hydrogen bonding served to planarize the diacetylene backbone and resulted in dramatic optical changes related to the overall effective conjugation length of the material. This precedent set the stage for Rubner's mechanochromic investigations of segmented PDA-poly(urethane)s where physical stretching led to blue-shifted optical absorbances arising from greater disorder within the hard PDA segments of the bulk material.[3] Upon releasing the applied stress, the system returned to its initial absorptivity. These reversible optical effects indicate that environmental strain on the bulk material can enforce microscopic structural reorganization in a controllable fashion. Very recent work by Carpick *et al.* has led to nanometer-scale observation of irreversible mechanochromism after AFM tips physically stressed self-assembled PDA trilayers.[4] While Rubner argued that changes in domain packing led to the macroscopic chromicity, this recent study concluded that disruption of the trilayer ultimately forced the PDA to reorganize into a higher-energy backbone conformation. Neither study assessed the nature of the polymer backbone conformational dymanics during the application of the physical stresses.

Scheme 2

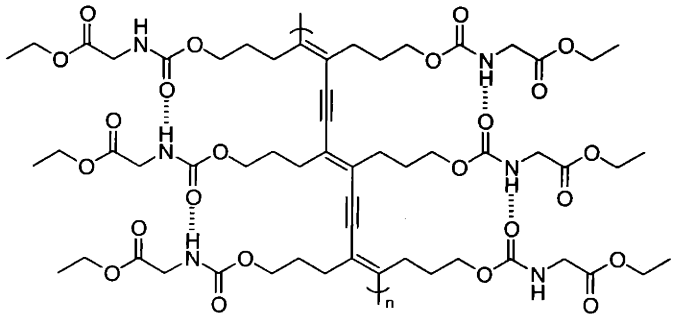

in $CHCl_3$: λ_{max} = 475 nm

with non-solvent:
λ_{max} = 560 nm

One of the biggest technical problems within the conducting polymer field lies with the relatively high polydispersities obtained after synthesis when compared to standard commodity plastics. These molecular weight and conjugation length distributions serve to broaden the observed optical properties due to the fact that several similar polymeric chromophores with slightly different optical profiles can actively absorb and emit light. The PDAs, generated from photochemically-induced topochemical polymerization, also suffer from large polydispersities. Other efforts have explored the incorporation of non-conjugative spacers to allow for several independent and discrete chromophores within one mechanically-robust polymer. Much of this work has stemmed from the LED field in search of better and purer blue emitters. Karasz and co-workers synthesized oligo-*p*-phenylene-vinylene (PPV) copolymers where the discrete PPV moiety offered sharper optical properties while the aliphatic moiety of the polymer main chain provided mechanical stability.[5] Yoshino *et al.* have investigated the incorporation of silicon atoms into conjugated polymers where the silicon atom served to interrupt polymer conjugation.[6] Both of these approaches succeeded in providing blue electroluminescent materials, but the extreme conformational disorder expected for Karasz's systems or the relative rigidity of silyl-based conducting polymers would not readily allow for rational control of the chromophore order and any resulting optical properties.

In other applications, strong ordering in the solid-state leads to decreased fluorescence or electroluminescence efficiencies. This results from the tendency of rigid-rod conjugated polymers to preferentially and strongly self-associate. On a molecular scale, this aggregation arises from favorable π-π interactions that offer lower-energy, non-radiative pathways through which an exciton may decay. Therefore, several groups have looked at ways to minimize such self-quenching through the use of steric bulk to prevent aggregation. Moore demonstrated

efficient blue LED emission from emissive anthracene moieties encapsulated by large dendrimeric structures.[7] Our group has reported enhancements of solid-state fluorescence properties made possible through the use of rigid 3D pentiptycene scaffolds within PPE backbones that served to minimize aggregation.[8] Aida has extended these ideas to highly emissive, apparently non-aggregating PPEs displaying quantum yields of essentially 100% by covalently linking dendrimeric side-groups onto monomer units prior to polymerization.[9] As most materials scientists do not have the expertise or the facilities to synthetically eliminate polymer aggregation, new processing techniques have also received attention. Schwartz has shown that the optical properties of spin-coated PPV polymer films exhibit strong dependence on the processing history, *i.e.* the extent of aggregation pre-existing within the solution used to cast the material.[10] On the other hand, very recent work out of our laboratories has attacked this problem from a different angle by *harnessing* these aggregation events to provide enhanced solid-state emission properties.[11] Steffen Zahn in our group has demonstrated that oblique ordering of polymer chains within chiral aggregates can provide high quantum yields, an important finding for optimizing fluorescent responses and other types of electronic coupling in the solid-state.[11b]

In the systems proposed in Scheme 1, the issue of conformational disorder within a polymer backbone will not play as pivotal of a role given that the small chromophore linker should more effectively allow for complete planarization relative to the disorder found in conjugated polymer backbones. Several studies led by Jinsang Kim in our group have examined the subtleties of repeat-unit conformational changes through physical alterations of these conformations in Langmuir monolayers.[12] Although connected by an aromatic spacer, the linkers of Scheme 3 should exhibit localized optical properties since the electronics and the

sterics of the bridging arene will minimize efficient through-bridge conjugation. The inclusion of defined chromophores into a polymer backbone offers an opportunity to separate the effects of repeat-unit torsional conformation from macromolecular conformations that spatially affect this discrete chromophore. This would allow for the electronics of the chromophore linker to dominate the polymer's optical properties as opposed to those for an array of electronically distinct absorbing and emitting moieties within several different polymer chains of polydisperse lengths. As these polymer have covalent linkages to a rigid spacer, we may consider the opportunities for new conformationally-responsive mechanochromic materials.

Unlike the poly(diacetylene)s, the polymers presented in this chapter will derive their optical differences from attenuation of excimer-like photophysical behavior resulting from spatial reorientation of the chromophore linker moieties during stretching or swelling.[13] We would expect macroscopic stresses upon the bulk polymer film to result in molecular alterations of the inter-chromophore distance. As illustrated in Scheme 3, a bulk stress that leads to a decrease in the inter-chromophore distance could facilitate the formation of an intramolecular excimer. The photophysics of this excimer would lead to dramatic optical effects if these molecular effects translated into a bulk observable. Likewise, swelling events such as redox-mediated electrolyte influx could lead to an increase in the inter-chromophore distance and a subsequent decrease in the excimer-like photophysical contributions. Swelling or other types of film strain could also foster new absorptions due to altered stabilization of charge between the chromophore linkers (for instance *via* π-dimers). Although Scheme 3 depicts a specific chromophore linker, molecular design should allow for a quite general survey of optically and electrochemically responsive linkers.

Scheme 3

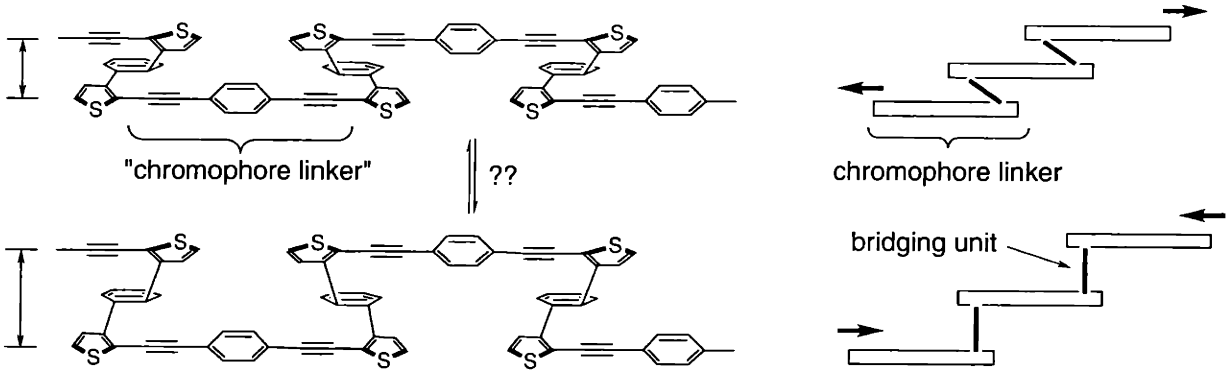

The structural motif of Scheme 3 attracted us due to the potential for chirality within the *o*-dithienyl benzene moiety upon polymerization. While Zahn's studies employed chiral side-chains to enforce chiral aggregates, this approach will incorporate chirality (although essentially racemic mixtures) into the main chain of the polymer. Chiral co-monomers possibly may help to bias the main chain during polymerization to favor one particular orientation. A recent study by Lere-Porte *et al.* synthesized the chiral polymer depicted in Chart 1 based upon a functionalized (1*R*,2*R*)-diaminocyclohexane.[14] Unlike the polymer illustrated in Scheme 3, the flexibility of their bridging spacer group did not allow for defined interactions between the rigid chromophores. While the chromophore itself absorbed at 325 ($CHCl_3$, log ε = 4.32) and 377 nm (log ε = 4.43), the polymer absorbed at 329 and 385 nm with emission bands at 497 and 519(sh) nm. The intense fluorescence reported for the chiral polymer indicates that the individual chromophores do not significantly interact with each other. Other than these data, they reported no other optical properties as their primary interest centered on asymmetric catalysis.

Chart 1

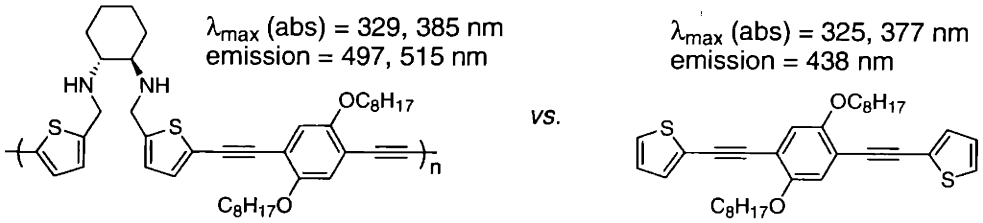

This chapter will emphasize the "utility" aspect of this thesis as it will not introduce any significantly new synthetic approaches, primarily bromination and palladium-mediated cross-couplings as described in previous chapters. This does not reflect the lack of synthetic work required: the monomers employed for co-polymerizations typically require several synthetic steps. Rather, this chapter will showcase the synthetic versatility of the simple *ortho*-linked dithienyl molecules as related to the construction of larger polymerizable monomers. We will

then turn to one of the functionalizable *meta* scaffolds presented in Chapter 4 to further examine the potentials of mechanochromic responses as dictated generally by Schemes 1 and 3 where the larger arene bridge will further isolate the individual chromophore linkers. This chapter will detail synthetic routes to the mechanochromic candidate materials and examine the optical properties of these new materials in solution as a function of non-solvent addition in order to initially assess any optical alterations possible within a bulk solid-state material.

Results and Discussion

We became interested in these polymer motifs after recognizing the ease through which **1** underwent bromination (Scheme 4). The presence of the arene at the 3-position of the thiophene ring provided for initial bromination of **1** selectively at the "*ortho* α" sites leading to **2**. Further bromination similarly afforded the tetra-α brominated **3**. Both **2** and **3** readily participated in Stille cross-couplings[15] with thienyl derivatives to provide the bis(bithiophene) **4** along with the bis(ter- and quinquethienyl) **5** and **6**, respectively, in high yield.

Scheme 4

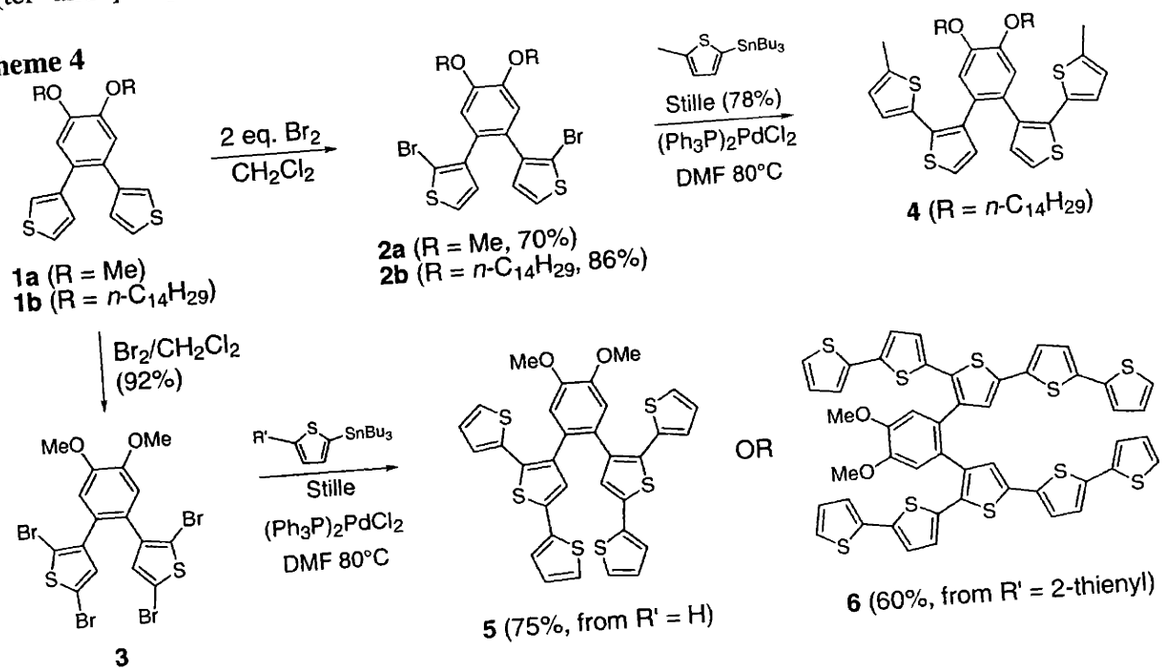

Such thienyl-based systems could allow for counteranion and solvent swelling upon electrochemical doping. Polymer actuators rely on this swelling mechanism to provide bulk spatial movement resulting from a collective response of doped conducting polymers as solvent and counteranions diffuse into an oxidized film to compensate charge.[16] Terthiophene **5** exhibited good solubilities in common solvents, while the quinquethiophene **6** had sparing solubility in essentially all common solvents. Solution studies revealed that monomer **5** absorbs broadly at 353 nm (in CH_2Cl_2, log $\varepsilon = 4.53$) and emits weakly and broadly at 468 nm ($\phi = 0.02$). For comparison, terthiophene itself absorbs at 354 nm and emits at *427 nm,* hinting that the red-shifted emission observed for **5** may stem from the pre-disposed orientation of the bridged chromophores toward excimer formation enforced by the bridging benzene unit.[17a] Indeed, the ^{1}H NMR shifts observed for **5** displayed significant shielding effects apparently arising from cofacial arrangement of the terthiophene moieties relative to reported values for 3'-phenylterthiophene.[17b]

Monomers such as **5** and **6** present four reactive electrochemical sites available for oxidative polymerization thus leading to poorly defined and highly crosslinked films. For example, Figure 1 presents the CV of a polymer derived electrochemically from monomer **5**. Judging by the broad electroactivity and the fast electrochemical kinetics, these materials appear to maintain the high conductivities of pure thiophene-based polymers. We also polymerized these monomers on transparent electrodes as a means of assessing the optical properties of the deposited polymer as a function of doping. In the neutral state, the film absorbs broadly at 445 nm. We could only observe one very broad low-energy absorbance during anodic doping centered at 760 nm at high doping levels. This optical behavior closely mimics that found in poly(terthiophene)s. However, the electrochemistry of **5** and terthiophene have significant differences that reflect the influence of closely-spaced redoxophores: **5** oxidizes at a much lower potential than does terthiophene under similar conditions,[17c] and poly(**5**) displays a highly reversible redox couple while poly(terthiophene) has a higher oxidation potential (*ca.* 400 mV) and a very pronounced hysteresis in the CV.[17d]

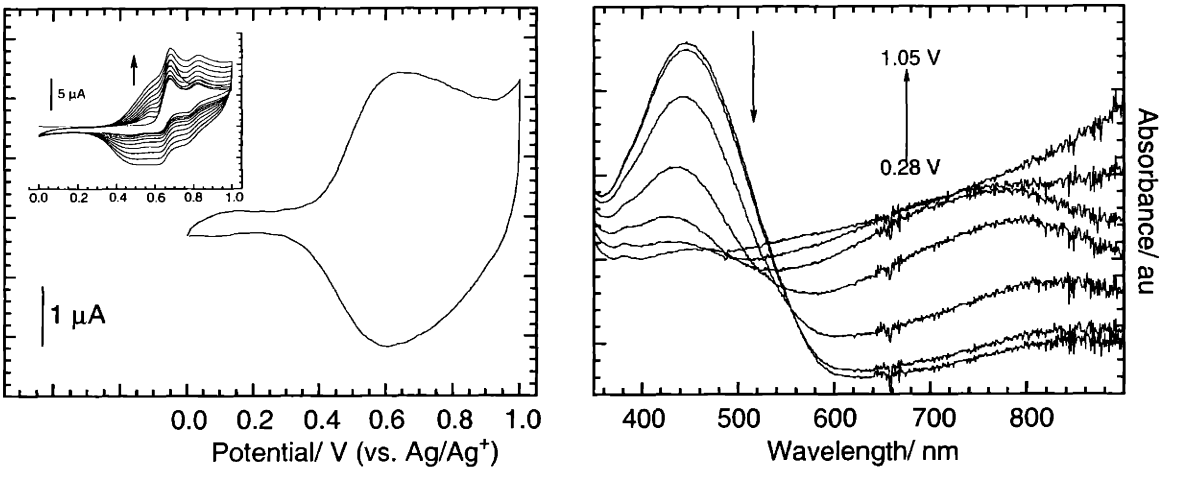

Figure 1: Poly(**5**) cyclic voltammetry at a 2 mm^2 Pt button (left) and spectroelectrochemistry (right) on ITO in 0.1 M *n*-Bu_4PF_6 (CH_3CN). UV-Vis measurements made at *ca.* 150 mV intervals. Inset graph depicts CVs of monomer **5** [1.0 mM] during polymer growth in the same electrolyte solution. $E_{1/2}(Fc/Fc^+)$: +0.096 V.

Although cross-linked materials should prove to have high strength, they also may complicate the subtle optical effects we wish to examine. As a second approach, we could employ a similar strategy used to construct **4** from **2b** for Sonogashira-type polymerizations of **2a** (Scheme 5).[18] Using diethynyl monomers **7**[19] and **8**,[8] we independently polymerized **2a** with two structurally distinct comonomers that should preserve the alkyne-arene-alkyne chromophrore. Polymer **9** incorporates the dialkoxy benzene co-monomer **7** while polymer **10** incorporates the bulky pentiptycene **8**. In principle, **9** should allow for physical interactions between the chromophore linkers, while the steric bulk imposed by the pentiptycene moiety should minimize or remove such an interaction completely within **10**. Unlike most arylene-ethynylene polymers (AEs) synthesized in our laboratories, the polymerization reaction mixtures for **9** and **10** exhibited very weak fluorescence under irradiation with UV light. This would indicate that neighboring chromophore linkers already share strong interactions thus forming weakly-emissive intra-polymer excimers after excitation. However, upon precipitation into the non-solvent methanol, **10** displayed an intense yellow emission typically associated with AEs. Polymer **9** had a dark burgundy color and displayed no intense solid-state fluorescence.

Scheme 5

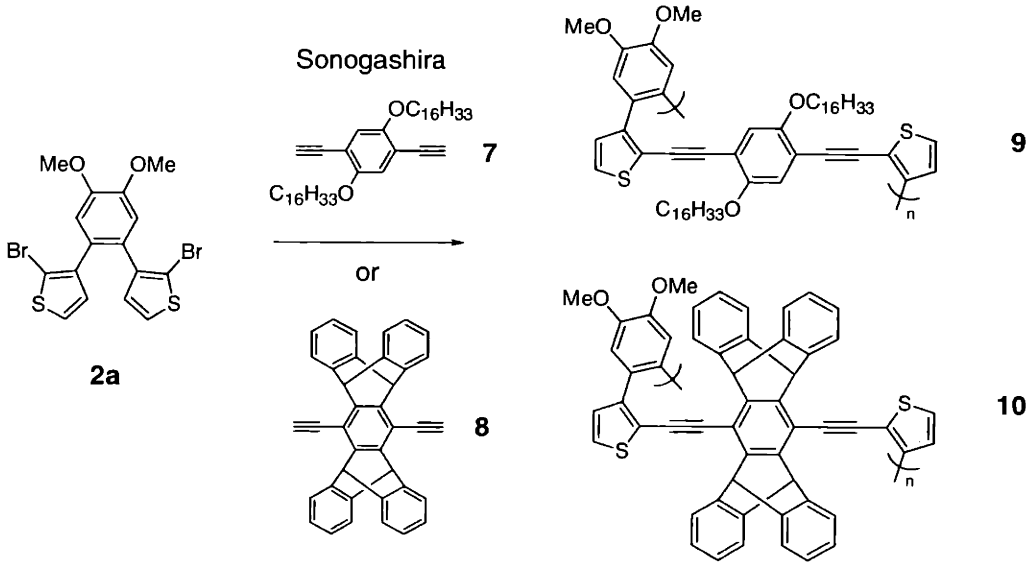

We performed solution studies to assess the optical properties of these materials during aggregation by measuring solution absorption and emission as a function of non-solvent composition. For typical PPEs, the addition of non-solvent leads to lower-energy aggregate absorptions coupled with new aggregate emission peaks and decreased fluorescence efficiencies.[20] We observed no new absorption or emission features with non-solvent addition to CH_2Cl_2 solutions of **9** (Figure 2). As shown in Figure 2 (right), the addition of methanol leads to quenching of the already weak fluorescence of **9**. Here, the absorption λ_{max} decreased slightly yet remained fixed at *ca.* 400 nm while all emission features decreased steadily. Compare this to the lowest energy absorbance for the chromophore pictured in Chart 1 (377 nm): the corresponding polymer in Chart 1 fluoresced at 497 nm.[14] In Figure 2, three-emission peaks appear in good solvent while a persistent emission band remained at 550 nm upon addition of non-solvent.

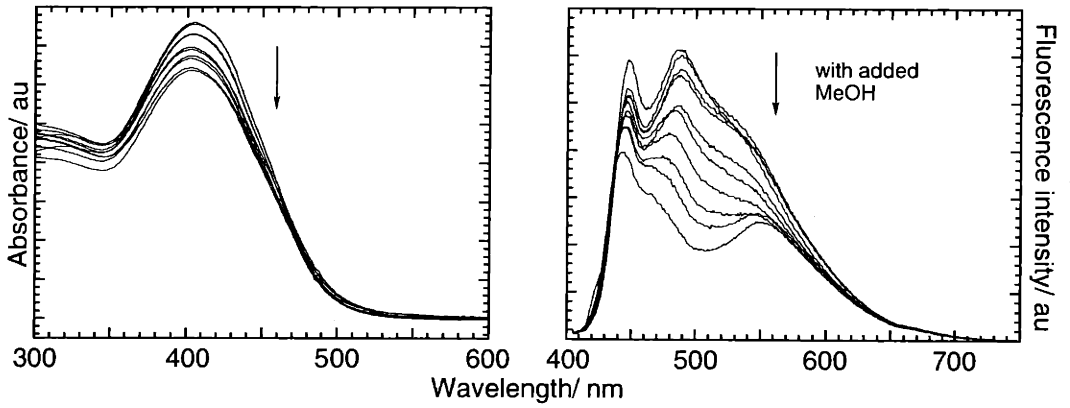

Figure 2: UV-Vis and emission spectra for **9** in CH_2Cl_2 with varying mole fractions of methanol and constant polymer concentration.

The pentiptycene polymer **10** displayed much different fluorescence behavior (Figure 3). The initial observation of enhanced fluorescence upon precipitation encouraged us to examine and quantify this effect in solution. Analogous to **9**, increasing amounts of methanol did not provide any new aggregation bands, and we observed a minimal decrease in the polymer's 360 nm absorbance at high methanol percentages (Figure 3, left). However, the fluorescence response did not resemble that observed for **9** despite the electronically similar chromophore linkers (Figure 3, right). While initial emission spectra in CH_2Cl_2 displayed a three-peak signature, higher methanol mole fractions led to an *increased* fluorescence (*ca.* 10%) due to the growth of the lowest energy 510 nm emission during aggregation. The emission spectra in Figures 2 and 3 plot absolute intensities as obtained from the fluorimeter response, although these general trends mirror those using corrected values that account for the refractive indices of the respective solvent compositions and the polymer absorption in a given mixture. However, to say that aggregated **10** comprises a "fluorescent aggregate" would mislead the reader: the initially well-solvated polymer displays a quantum yield of only 2% due to the pre-existing close association between chromophore linkers. Upon aggregation, the quantum yield "increases" to 2.2%.

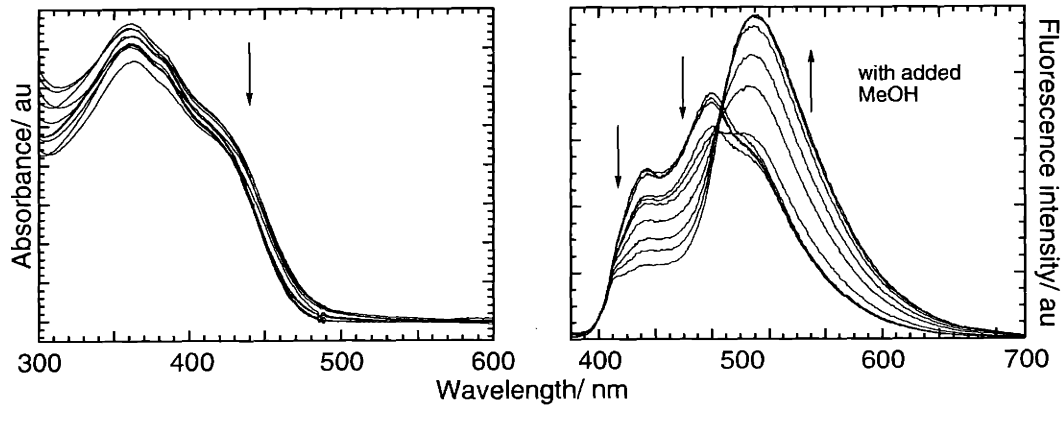

Figure 3: UV-Vis and emission spectra for **10** in CH_2Cl_2 with varying mole fractions of methanol and constant polymer concentration.

Although this data alone does not offer structural insight as to the nature of the aggregate state(s), we considered that the monomer has adapted a random yet chiral conformation during the polymerization. The low quantum yields indicate that the polymers **9** and **10** have efficient non-radiative pathways by way of excimer formations. Chart 2 depicts different monomer and polymer conformations possible within a repeat unit based upon **2**. Structures A and B have an enantiomeric relationship while structure C lacks chirality. The steric bulk of the chromophore linker would minimize the extent through which the linkers can interact electronically in achiral structure C while significant π-π interactions may still occur within A and B regardless of the steric demands imposed by the dialkyne monomer. Therefore, we should expect polymers based upon the motif of C to maintain high degrees of fluorescence while the interacting chromophores in A and B would lead to excimer formations and poor quantum yields. Indeed, the racemic nature of these chromophores resulted in the absence of significant circularly-polarized absorptions as measured by circular dichroism.

Chart 2

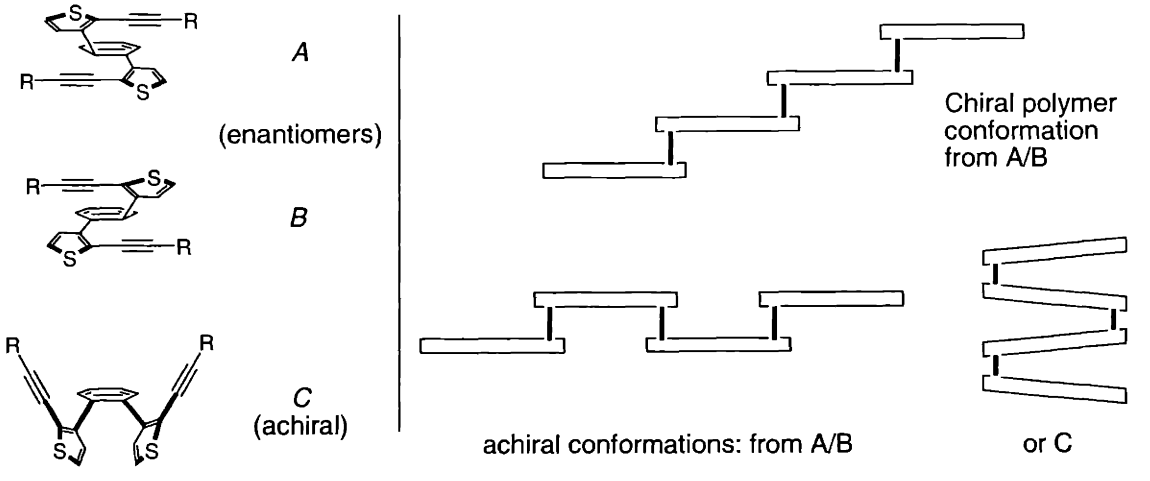

As an additional observation of this optical behavior within a more well-defined system, we prepared the strapped model **11** through $Hg(OAc)_2$-mediated iodination and subsequent Sonogashira cross-coupling with alkyne **12**. Although the structure as illustrated in Scheme 6 lacks chirality, we have not established the presence of the respective enantiomeric structures (or lack thereof). Consistent with the optical properties for the polymers, **11** absorbed at 359 nm ($\log \varepsilon = 4.65$) and fluoresced broadly yet weakly in solution at 470 nm. **11** displayed a solution quantum yield of 4%, again indicating a possible pre-existing disposition to forming an excited-state excimer.

Scheme 6[a]

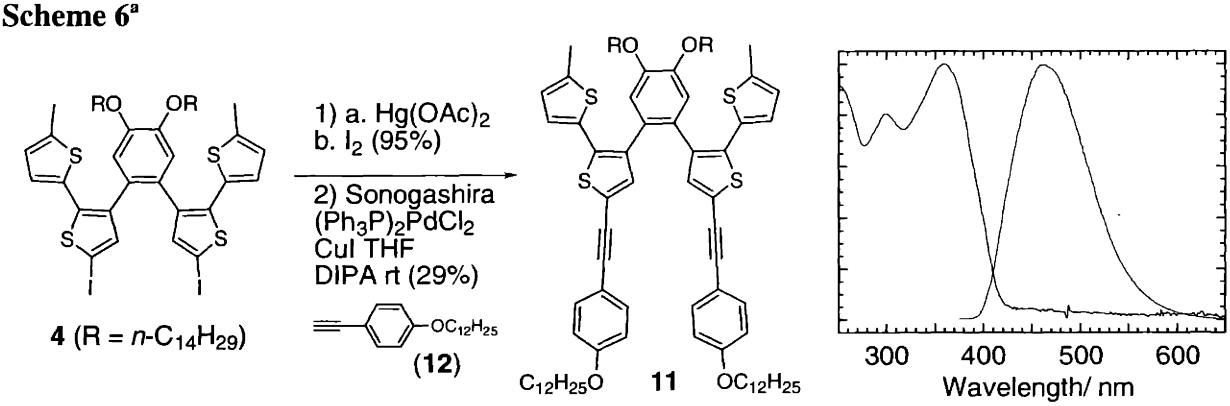

[a] The spectra depict UV-Vis and emission spectra for **11** obtained in CH_2Cl_2 at room temperature.

From our preliminary studies, polymers derived from the scaffold **2a** initially will exhibit low-energy optical properties due to the strongly-interacting chromophore linkers forming excited-state excimers in the as-synthesized polymer. We also wanted to examine the opposite scenario, where the polymers would initially lack significant intra-polymer chromophore interactions. For these studies, we employed the large *meta* scaffold **13** as introduced in Chapter 4. This dibromide readily coupled with 3-thiophene boronic acid in 94% yield, and subsequent *ortho*-α bromination of the pendant thiophenes provided **14** in 50% unoptimized yield (Scheme 7, top). This yield reflects the difficulties encountered during the removal of apparent side

reactions from the bromination. The use of solid NBS as a brominating agent (as opposed to liquid bromine) should circumvent this problem in the future by offering an experimentally more reliable stoichiometry measurement. Nevertheless, we could obtain **14** in greater than 95% purity as determined by NMR.

Scheme 7

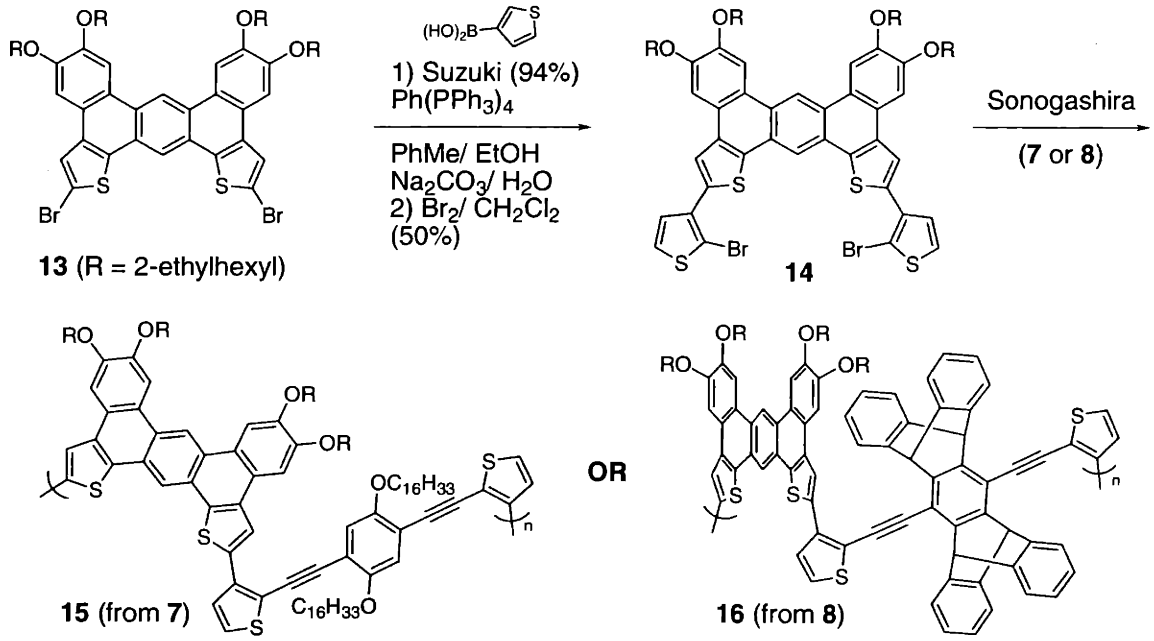

We employed the diethynyl monomers **7** and **8** to prepare polymers with the same chromophore linkers as contained in **9** and **10**. In these present systems, the co-monomer **14** imposes a greater distance between adjacent chromophores, thus allowing for fewer intra-polymer interactions between neighboring repeat units (Scheme 7, bottom). Indeed, the polymerization reaction mixtures during the preparation of polymers **15** and **16** remained strongly emissive under UV irradiation. Upon precipitation from methanol, both polymers exhibited strong solid-state fluorescence: **16** appeared intensely yellow to the eye while **15** had a more orange appearance. These polymers behaved in a manner more related to standard PPEs: new, low-energy absorptions appeared upon increased addition of non-solvent and fluorescence responses fell dramatically during aggregation. Figure 4 illustrates the photophysical responses

of **15**. Polymer **16** displayed similar trends although this material had a very low molecular weight (*ca.* trimer) thus precluding a legitimate comparison with **15** or the *ortho*-linked **9** and **10**. As with the *ortho*-systems, **15** did not display any significant CD signals, either in the fully-solvated state or after the addition of non-solvent.

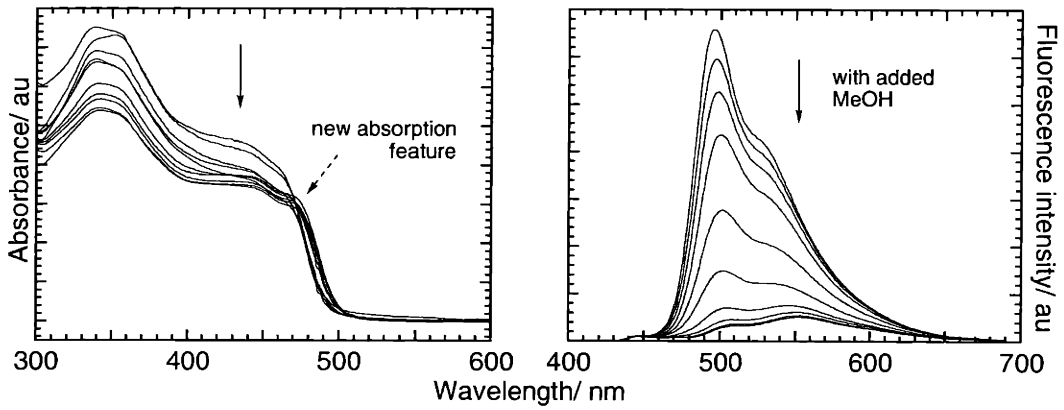

Figure 4: UV-Vis and emission spectra for **15** in CH_2Cl_2 with varying mole fractions of methanol and constant polymer concentration.

As mentioned earlier, we wanted to examine if a chiral co-monomer would relay chirality to the *ortho*-linked monomer (**2**) during polymerization. If this repeat unit did adopt a non-racemic backbone connectivity, we may have another opportunity to observe chiral aggregates where the chirality of both monomers plays a role in the electronic coupling within the aggregated system. We could also use a chiral monomer to provide chiral aggregates from polymers derived from the *meta* scaffold **14**. From the (*S*,*S*)-dialkyne **17**,[11b] we synthesized polymers **18** and **19** with structures very similar to the previously discussed **9** and **15** (Scheme 8). Polymers **18** and **19** displayed absorption characteristics identical to **9** and **15**. While the emission of the *meta* polymer **19** resembled those observed for **15**, *ortho* polymer **18** had a much lower high-energy fluorescence intensity (*ca.* 450 nm) when compared to **9** (Figure 5). This may result from an increase in inter-polymer interactions mediated by monomer chirality that minimizes the fluorescence of the "free" polymer relative to that of a new aggregate state.

However, these interactions lacked chirality: "chiral polymers" **18** and **19** did not display significant CD activity. This indicates that the chiral co-monomer (**17**) cannot enforce or bias chirality in the conformations of **2a** or **14** during polymerization. The lack of strong CD absorptivity does not rule out pre-existing chirality within the halogenated co-monomers themselves, and future work should examine new ways to impart chirality to related systems.

Scheme 8

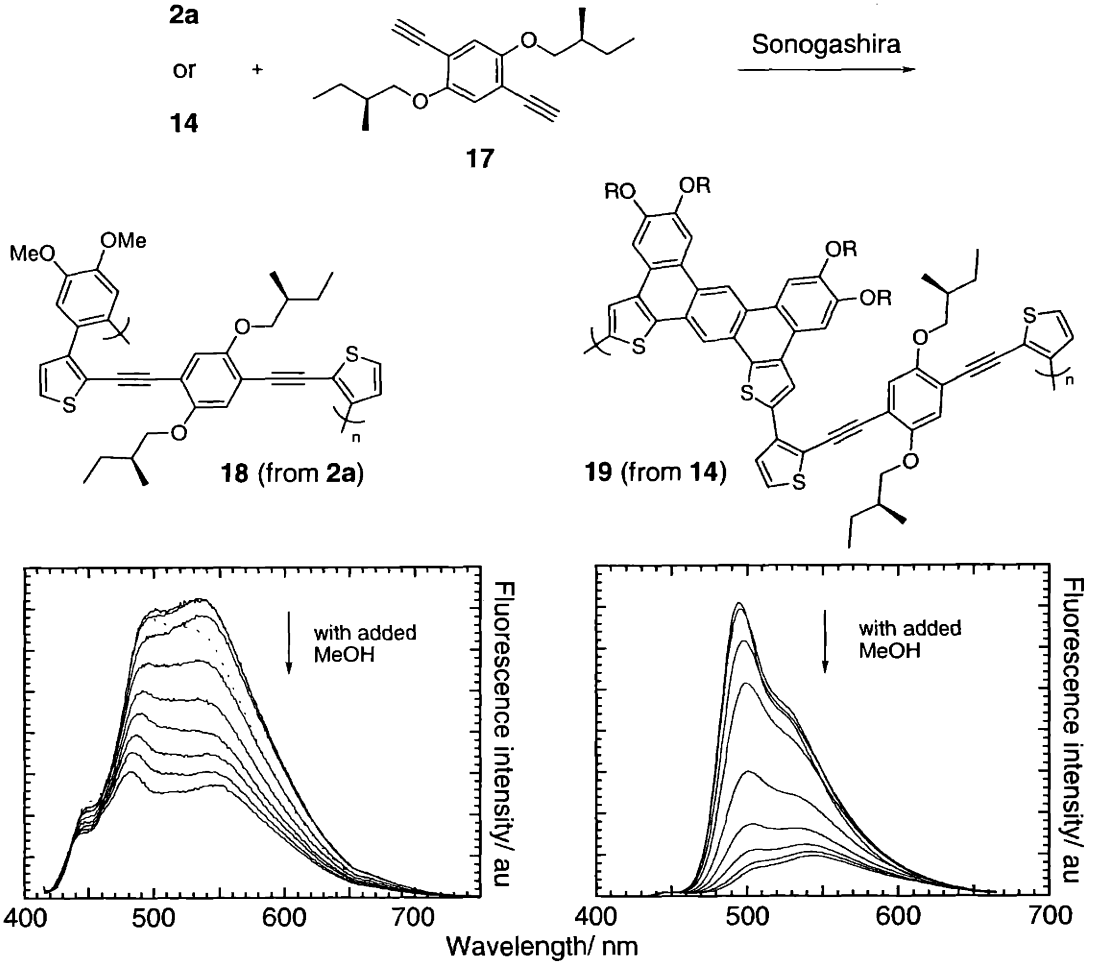

Figure 5: Emission spectra for **18** (left) and **19** (right) in CH_2Cl_2 with varying mole fractions of methanol and constant polymer concentration. The dotted spectrum in the left spectra depicts the emission of **18** in 100% CH_2Cl_2.

Concluding Remarks

This chapter has presented synthetic procedures for a variety of polymers that possess differing degrees of intra-polymer intereaction. From optical studies in solution, we can conclude that the close and pre-existing spacing between the chromophore linkers of **9** and **10** does not change upon aggregation in methanol. Remarkably, we observed an enhancement in fluorescence intensity for the pentiptycene-based **10** during methanol addition. On the other hand, polymers derived from the *meta* scaffold **14** did not allow for sufficient interaction between the linkers upon solution-based aggregation, and we observed standard aggregation behavior with increased methanol content. To optimize this effect in the solid-state, bridging units of intermediate size between that of **2a** and **14** may provide a more dramatic solution-based optical response. Furthermore, the inclusion of *two* well-defined chiral co-monomers may help to create new chiral polymer aggregates in line with Zahn's work in our group. Concerning mechanochromicity, these materials stand ready for examination in bulk polymer films as optically-responsive dopants. While we could not minimize the excimer-like behavior of **9** and **10** in solution, bulk films may allow for a realization of the opposite effect. As such, future studies will need to examine strategies to align such polymers in bulk polymer films in order to achieve optimal mechanochromic responses. We could also utilize *monomeric* materials of similar structural connectivity in this capacity as well (*e.g.* variants of **11**). The generality of Scheme 1 shows that a variety of electronically and sterically tuneable chromophore linkers may help to alter and enhance the desired optical characteristics of these unique polymers.

Experimental Section

General: All air and water sensitive synthetic manipulations were performed under an argon atmosphere using standard Schlenk techniques. Diisopropylamine (DIPA) was distilled from KOH; toluene (PhMe), and tetrahydrofuran (THF) were passed through activated alumina columns prior to storage in dry airfree vessels. All other solvents and chemicals were of reagent grade and used as received. 4,5-dibromoveratrole was prepared through bromination of veratrole with Br_2 in CH_2Cl_2. Compound **1b** was prepared as described in Chapter 3. 5-Methyl-2-(tributylstannyl)thiophene was obtained *via* lithiation of 2-methylthiophene and quenching with tributylstannyl chloride; likewise, 5-tributylstannyl-2,2'-bithiophene was prepared from 2,2'-bithiophene. Compounds **7**,[19] **8**,[8] **12**,[21] and **17**[11b] were prepared as described previously. Compound **13** was prepared as described in Chapter 4.

Column chromatography was performed using Baker 40 μm silica gel. All organic extracts were dried over $MgSO_4$ and filtered prior to removal under reduced presure. NMR spectra were obtained on Varian Unity or Mercury 300, Bruker Avance 400 or Varian Inova 500 spectrometers, and all chemical shifts are referenced to residual $CHCl_3$ (7.26 ppm for ^1H, 77.23 ppm for ^{13}C) or $CHDCl_2$ (5.32 ppm for ^1H, 54.00 ppm for ^{13}C); aromatic carbon multiplicities were determined by DEPT analysis. High-resolution mass spectra were obtained at the MIT Department of Chemistry Instrumentation Facility (DCIF) on a Bruker Daltronics APEX II 3 Tesla FT-ICR-MS. Molecular weight determination by Gel permeation chromatography (GPC) was performed in THF versus polystyrene standards (PolySciences) on a HP 1100 HPLC system equipped with a Plgel 5 mm Mixed C column (300 x 7.5 mm). UV-Vis measurements were obtained on a Hewlett-Packard 8452A diode array spectrophotometer. Fluorescence measurements were recorded on a SPEX Fluorolog-τ2 fluorimeter with a 450 W xenon lamp. Elemental analyses were obtained at Desert Analytics (Tucson, AZ). Melting points are uncorrected. All electrochemical measurements were made with an Autolab PGSTAT 20 potentiostat (Eco Chemie). Cyclic voltammetry was performed at Pt electrodes in oven-dried, argon-purged, one chamber/three electrode cells versus a quasi-internal Ag wire reference electrode (BioAnalytical Systems) submersed in 0.01 M $AgNO_3$/ 0.1 M *n*-Bu_4NPF_6 in anhydrous acetonitrile (MeCN). All experiments were conducted in freshly prepared solutions of 0.1 M *n*-Bu_4NPF_6 in anhydrous MeCN or CH_2Cl_2 stored over activated 4Å sieves.

4,5-Di(3-thienyl)veratrole (**1a**): A 250 mL Schlenk flask was charged with 4,5-dibromoveratrole (1.539 g, 5.200 mmol), 3-thiophene boronic acid (1.998 g, 15.61 mmol), Na_2CO_3 (4.42 g, 41.7 mmol) and $Pd(PPh_3)_4$ (193 mg, 0.167 mmol, transferred under an inert nitrogen atmosphere). After equipping a reflux condenser, the system was placed under argon and filled with PhMe (100 mL), EtOH (20 mL) and water (20 mL). The reaction was refluxed for 24 h, cooled and diluted with ether. The reaction was washed with 2M KOH (aq), NH_4Cl and NaCl, and the organic phase was dried and removed *in vacuo*.

Chromatography on silica gel (gradual change from hexane to 1:1 hexane/CH_2Cl_2) provided the product as a white solid (1.521 g, 5.029 mmol, 97%). mp 165-166.5°C. ^{1}H NMR (500 MHz, $CDCl_3$) δ: 7.18 (dd, 2H, J = 3.0, 5.0 Hz), 7.3 (dd, 2H, J = 1.0, 3.0 Hz), 6.95 (s, 2H), 6.70 (dd, 2H, J = 1.0, 5.0 Hz), 3.94 (s, 6H). ^{13}C NMR (125 MHz, $CDCl_3$) δ: 148.3, 142.1, 129.2, 128.1, 124.8, 122.6, 113.3, 56.2. FT-IR (KBr): ν/cm^{-1}: 3116, 3090, 2999, 2941, 2839, 1603, 1538, 1500, 1464, 1340, 1263, 1230, 1154, 1033, 846, 781. HR-MS (EI): found *m/z* = 302.0426 ± 0.0009 (M^+); calc. for $C_{16}H_{14}O_2S_2$: 302.0435. Anal: Calcd for $C_{16}H_{14}O_2S_2$: C, 63.55; H, 4.67. Found: C, 63.16; H, 4.54.

4,5-Di(2-bromo-3-thienyl)veratrole (**2a**): A solution of **1a** (1.752 g, 5.795 mmol) in CH_2Cl_2 (150 mL) was stirred at room temperature while Br_2 (0.60 mL, 12 mmol) was added dropwise. The reaction was purged with a gentle stream of argon for 1 hr and was stirred for an additional 3 h, at which point 2M KOH was added. The organic layer was worked up as for **1a**. The crude solids were dissolved in 1:1 hexane/CH_2Cl_2 and pushed through a silica plug with the same eluent. The material obtained was recrystallized from MeOH to provide the product as white needle-like solids (1.874 g, 4.072 mmol, 70%). mp 147-148°C. ^{1}H NMR (300 MHz, $CDCl_3$) δ: 7.09 (d, 2H, J = 5.7 Hz), 6.98 (s, 2H), 6.55 (d, 2H, J = 5.4 Hz), 3.95 (s, 6H). ^{13}C NMR (100 MHz, $CDCl_3$) δ: 148.5, 141.0, 130.0, 127.2, 125.2, 113.6, 110.7, 56.2. FT-IR (KBr): ν/cm^{-1}: 3113, 2995, 2946, 2930, 2900, 2033, 1603, 1547, 1504, 1461, 1410, 1354, 1333, 1262, 1249, 1207, 1171, 1048, 988, 864, 825.

4,5-Di(2-bromo-3-thienyl)-1,2-bis(tetradecyloxy)benzene (**2b**): A solution of **1b** (2.003 g, 3.003 mmol) in CH_2Cl_2 (150 mL) was stirred at room temperature while Br_2 (0.32 mL, 6.2 mmol) was added dropwise. Precipitates formed at 20 min, but the reaction was stirred for an additional 3.5 h, at which point 2M KOH was added. The reaction was worked up as for **1a** to provide a crude oily solid that was purified on silica gel (hexane) to yield an off-white yellowish solid (2.373 g, 2.876 mmol, 96%). mp 44.5-46°C. ^{1}H NMR (300 MHz, $CDCl_3$) δ: 7.07 (d, 2H, J = 5.4 Hz), 6.96 (s, 2H), 6.52 (d, 2H, J = 5.7 Hz), 4.06 (t, 4H, J = 6.6 Hz), 1.86 (m, 4H), 1.49 (m, 4H), 1.27 (bm, 40H), 0.89 (t, 6H, J = 6.3 Hz). ^{13}C NMR (100 MHz, $CDCl_3$) δ: 148.5, 141.1, 130.0, 127.0, 125.0, 115.6, 110.6, 69.3, 32.2, 29.7-29.9 (unresolved Cs), 29.6, 29.4, 26.3, 22.9, 14.4. FT-IR (KBr): ν/cm^{-1}: 2918, 2850, 1603, 1545, 1504, 1467, 1262, 1232, 1190, 1073, 989. HR-MS (EI): found *m/z* = 822.2710 (M^+); calc. for $C_{42}H_{64}Br_2O_2S_2$: 822.2709.

4,5-Bis(2,5-dibromo-3-thienyl)veratrole (**3**): A solution of **1a** (909 mg, 3.00 mmol) in CH_2Cl_2 (75 mL) was stirred at room temperature while a solution of Br_2 (0.63 mL, 12 mmol) in CH_2Cl_2 (5 mL) was added dropwise. The reaction was stirred with an argon purge for 1 h and further for 12 h. 2M KOH was added to quench the reaction, and the organic layer was worked up as for **1a** to provide a brownish-white solid.

This material was pushed through a silica gel plug (1:1 hexane/CH_2Cl_2) to provide a white powder used without further purification (1.709 g, 2.765 mmol, 92%). mp 180-181°C. ^{1}H NMR (400 MHz, $CDCl_3$) δ: 6.89 (s, 2H), 6.60 (s, 2H), 3.93 (s, 2H). ^{13}C NMR (100 MHz, $CDCl_3$) δ: 148.8, 141.4, 132.2, 126.2, 113.3, 110.7, 110.2, 56.2. FT-IR (KBt): ν/cm^{-1}: 3064, 2995, 2934, 2835, 1604, 1506, 1464, 1352, 1255, 1220, 1164, 1064, 993. HR-MS (EI): found *m/z* = 613.6854 (M^+); calc. for $C_{16}H_{10}Br_4O_2S_2$: 618.6850.

4,5-Bis(5'-methyl-2,2'-bithiophen-3-yl)-1,2-bis(tetradecyloxy)benzene (**4**): A 25 mL Schlenk flask was charged with **2b** (825 mg, 1.00 mmol) and $(Ph_3P)_2PdCl_2$ (40 mg, 0.06 mmol) and placed under argon. DMF (5 mL) was added and the reaction was heated to 80°C. 5-methyl-2-tributylstannylthiophene (865 mg, 2.23 mmol) was added dropwise and stirred for 39 h. Upon cooling, the reaction was diluted with ether and stirred and washed with 1M NaF (x2), NH_4Cl (x3) and dried. Removal of the solvent provided a yellow oil with suspended solids. Chromatography on silica (hexane to 7:1 hexane/CH_2Cl_2) provided the desired product contaminated with ca. 5% of cyclized naphthodithiophene (by NMR). The impure product was twice dissolved in hexane, filtered and stripped of solvent to provide the pure product as a yellow waxy solid (673 mg, 0.783 mmol, 78%). mp 55.5-57.0°C. ^{1}H NMR (400 MHz, $CDCl_3$) δ: 6.91 (m, 4H; apparent d, 2H, *J* = 5.4 Hz; and s, 2H), 6.69 (d, 2H, *J* = 3.5 Hz), 6.56 (d, 2H, *J* = 5.2 Hz), 6.53 (dd, 2H, *J* = 1.1, 3.5 Hz), 3.97 (t, 4H, *J* = 6.8 Hz), 2.40 (d, 6H, *J* = 0.6 Hz) 1.82 (m, 4H), 1.5 (m, 4H), 1.31 (bm, 40H), 0.93 (t, 6H, *J* = 6.6 Hz). ^{13}C NMR (100 MHz, $CDCl_3$) δ: 148.4, 139.8, 137.3, 134.2, 132.9, 131.0 (CH), 128.4, 125.6 (CH), 125.2 (CH), 122.1 (CH), 116.2 (CH), 69.1, 32.1, 29.91, 29.87, 29.83, 29.63, 29.57, 29.3, 26.2, 22.9, 15.4, 14.3. FT-IR (KBr): ν/cm^{-1}: 2917, 2849, 1601, 1533, 1502, 1467, 1377, 1242, 1187, 1053, 793, 677. HR-MS (EI): found *m/z* = 858.4578 (M^+); calc. for $C_{52}H_{74}O_2S_4$: 858.4566.

4,5-Bis(2,2':5',2"-terthiophen-3'-yl)veratrole (**5**): A 25 mL Schlenk tube was charged with **3** (617 mg, 0.999 mmol) and $(Ph_3P)_2PdCl_2$ (56 mg, 0.080 mmol) and placed under argon. DMF (5 mL) was added and the reaction was heated to 80°C. 2-Tributylstannylthiophene (1.72 g, 4.38 mmol) was added dropwise and stirred for 23 h. Upon cooling, the reaction was diluted with ether, filtered and worked up as described for **4** to provide a brown solid. The crude material was pushed through a plug of silica (2:1 CH_2Cl_2/hexane) to provide the product as a yellow solid. Recrystallization from $CHCl_3$/MeOH provided the product as yellow needles (473 mg, 0.750 mmol, 75%). mp 192-194°C. ^{1}H NMR (400 MHz, $CDCl_3$) δ: 7.17 (dd, 2H, J = 1.1, 5.1 Hz), 7.06 (dd, 2H, J = 1.1, 5.1 Hz), 7.03 (dd, 2H, J = 1.1, 3.6 Hz), 6.98 (dd, 2H, J = 3.6, 5.1 Hz), 6.88 (s, 2H), 6.79 (dd, 2H, J = 3.6, 5.1 Hz), 6.68 (dd, 2H, J = 1.1, 3.6 Hz), 6.41 (s, 2H), 3.91 (s, 6H). ^{13}C NMR (100 MHz, $CDCl_3$) δ: 148.8, 138.0, 137.3, 135.9, 134.6, 131.2, 128.1, 127.9 (CH), 127.3 (2Cs, CH), 125.76 (CH), 125.64 (CH), 124.42 (CH), 123.7 (CH), 113.7 (CH), 56.2. FT-IR

(KBr): ν/cm^{-1}: 3097, 2955, 2932, 2837, 1601, 1517, 1495, 1463, 1382, 1255, 1211, 1062, 829, 700, 686. UV-Vis (CH_2Cl_2) λ/nm (log ε): 353 (4.53). HR-MS (EI): found *m/z* = 629.9951 (M^+); calc. for $C_{32}H_{22}O_2S_6$: 629.9939.

4,5-Bis(2,2':5',2'':5''-2''':5''',2''''-quinquethiophen-3''-yl)veratrole (**6**): A 25 mL Schlenk tube was charged with **3** (618 mg, 0.999 mmol) and $(Ph_3P)_2PdCl_2$ (56 mg, 0.080 mmol) and placed under argon. DMF (5 mL) was added, and the reaction was heated to 80°C. 5-Tributylstannyl-2,2'-bithiophene (1.99 g, 4.37 mmol) was added dropwise and stirred for 23 h during which point thick precipitates formed. Upon cooling, the reaction was diluted with MeOH, filtered and rinsed to provide the product as a dark orange solid (572 mg, 0.596 mmol, 60%). The severe insolubility of this material prevented further purification. mp 250°C+. ^{1}H NMR (400 MHz, $CDCl_3$) δ: 7.21 (dd, 2H, J = 1.2, 5.0 Hz), 7.08 (dd, 2H, J = 1.1, 5.0 Hz), 7.03 (dd, 2H, J = 1.1, 3.6 Hz), 7.00 (m, 2H), 6.93 (m, 6H), 6.87 (m, 4H), 6.81 (d, 2H, J = 3.8 Hz), 6.48 (d, 2H, J = 3.8 Hz), 6.46 (s, 2H), 3.98 (s, 6H). FT-IR (KBr): ν/cm^{-1}: 3065, 2928, 1601, 1517, 1495, 1461, 1254, 1205, 1062, 835, 795, 693. UV-Vis (CH_2Cl_2) λ/nm (log ε): 406 (4.76). HR-MS (ESI): found *m/z* = 957.9481 (M^+); calc. for $C_{48}H_{30}O_2S_{10}$: 957.9447.

Polymer **9**: A 25 mL Schlenk tube was charged with dibromide **2a** (92.0 mg, 0.200 mmol), dialkyne **7** (121 mg, 0.200 mmol) and CuI (2 mg, 0.01 mmol), and the flask was placed under argon. In an inert atmosphere, $Pd(PPh_3)_4$ was added (10 mg, 0.009 mmol), and the flask was again placed under argon at the bench. Under an argon purge, PhMe (5 mL) and DIPA (1 mL) were added. The system was heated at 60°C for 60 h and cooled to room tmeperature. The reaction mixture was precipitated into MeOH, filtered, dissolved in CH_2Cl_2 and reprecipitated into MeOH. The polymer was then thoroughly washed with MeOH and boiling MeOH to provide a brick-red powder (105 mg, 60% mass yield). M_n: 24,000.

Polymer **10**: Following a similar procedure for **9**, a mixture of **2a** (46 mg, 0.10 mmol), **8** (48 mg, 0.10 mmol), CuI (1 mg, 0.006 mmol) and $Pd(PPh_3)_4$ (4 mg, 0.003 mmol) in PhMe (1,75 mL) and DIPA (0.5 mL) was stirred at 60°C for 4 d. The reaction was diluted with CH_2Cl_2 and washed with NH_4OH. The organic layer was removed and precipitated in to MeOH. Filtration and rinsing with MeOH provided the polymer as a yellow solid that could not be accurately weighed.. M_n: 4,000.

4,5-Bis(5-iodo-5'-methyl-2,2'-bithiophen-3-yl)-1,2-bis(tetradecyloxy)benzene (en route to **11**): A solution of **4** (643 mg, 0.748 mmol) in CH_2Cl_2 (25 mL) was stirred at room temperature as $Hg(OAc)_2$ was added portionwise (483 mg, 1.52 mmol). The reaction was stirred with exclusion of light for 1 hr followed by the addition of solid iodine (403 mg, 1.59 mmol). After stirring for 5 more hours, the

reaction was quenched with 2M KOH and diluted with CH_2Cl_2. The aqueous layer was removed and washed with CH_2Cl_2 (x2), and the combined organics were filtered, washed with 2M KOH and NH_4Cl, dried and removed. The crude material was purified on silica gel (hexane to 4:1 hexane/CH_2Cl_2) to provide the product as a waxy yellow solid (791 mg, 0.712 mmol, 95%). mp 69-71°C. ^{1}H NMR (400 MHz, $CDCl_3$) δ: 6.76 (s, 2H), 6.50 (dd, 2H, *J* = 1.0, 3.5 Hz), 6.38 (s, 2H), 6.34 (d, 2H, *J* = 3.5 Hz), 3.99 (t, 4H, *J* = 6.7 Hz), 2.41 (s, 6H), 1.84 (m, 4H), 1.47 (m, 4H), 1.27 (bm, 40H), 0.89 (t, 6H, *J* = 6.6 Hz). ^{13}C NMR (100 MHz, $CDCl_3$) δ: 148.7, 140.6, 140.4 (CH), 138.37, 138.26, 132.6, 127.1, 125.90 (CH), 125.69 (CH), 115.6 (CH), 70.1, 69.3, 32.2, 31.81, 29.94, 29.90, 29.69, 29.60, 29.46, 26.3, 22.92, 22.88, 15.6, 14.4. FT-IR (KBr): ν/cm^{-1}: 2919, 2849, 1506, 1468, 1364, 1256, 1238, 1211, 1167, 1057, 834, 800.

4,5-Bis(5-[4-dodecyloxyphenylethynyl]-5'-methyl-2,2'-bithiophen-3-yl)-1,2-bis(tetradecyloxy)benzene (**11**): A Schlenk flask was charged with 4,5-bis(5-iodo-5'-methyl-2,2'-bithiophen-3-yl)-1,2-bis (tetradecyloxy)benzene (203 mg, 0.183 mmol), $(Ph_3P)_2PdCl_2$ (5 mg, 0.007 mmol), CuI (3 mg, 0.02 mmol) and placed under argon. THF (4 mL) and DIPA (1 mL) were added, and the mixture was heated at 50°C for 20 minutes. A solution of alkyne **12** (111 mg, 0.387 mmol) in THF (1 mL) was added dropwise, and the reaction was stirred at 50°C for 3.5 days. Upon cooling, the reaction was diluted with ether and NH_4Cl, and the organic phase was removed. The crude residue was chromatographed on silica gel (hexane to 5:1 hexane/CH_2Cl_2) to provide the product as a waxy yellow solid (76 mg, 0.53 mmol, 29%). mp 59.5-60.5°C. ^{1}H NMR (400 MHz, $CDCl_3$) δ: 7.39 (d, 4H, J = 8.7 Hz), 6.84 (m, 6H), 6.52 (m, 6H), 3.98 (m, 8H), 2.39 (s, 6H), 1.80 (m, 8H), 1.45 (m, 8H), 1.27 (bm, 72H), 0.89 (m, 12H). ^{13}C NMR (100 MHz, $CDCl_3$) δ: 159.5, 148.7, 140.7, 136.9, 135.2 (CH), 133.9, 133.4, 133.0 (CH), 127.9, 126.0 (CH), 125.5 (CH), 120.4, 116.1 (CH), 115.1, 114.7 (CH), 93.7, 81.7, 69.3, 68.3, 32.15, 32.14, 29.94, 29.90, 29.87, 29.81, 29.78, 29.69, 29.60, 29.57, 29.45, 29.40, 26.26, 26.23, 22.9, 15.5, 14.3. FT-IR (KBr): ν/cm^{-1}: 2918, 2850, 1603, 1516, 1468, 1245, 1171, 1058, 828, 669. UV-Vis (CH_2Cl_2) λ/nm (log ε): 359 (4.65). HR-MS (MALDI): found *m/z* = 1426.8549 (M^+); calc. for $C_{92}H_{130}O_4S_4$: 1426.8846.

2,14-Di(3-thienyl)-5,6,10,11-tetra(2-ethylhexyloxy)dibenz[3',4';5',6']anthra[1,2-*b*:8,7-*b*']dithiophene (en route to **14**): A three-necked 25 mL flask was charged with **13** (570 mg, 0.54 mmol), 3-thiophene boronic acid (148 mg, 1.16 mmol) and dissolved in PhMe (12 mL) and EtOH (2.5 mL). A solution of Na_2CO_3 (455 mg, 4.29 mmol) in water (2.5 mL) was added, a condenser was equipped, and the solution was purged with argon for 30 min. Under a gentle argon stream, $Pd(PPh_3)_4$ (19 mg, 0.016 mmol) was added to the solution, and the system was heated at reflux for 23 h and cooled to room temperature. The reaction was diluted with ether and washed with NH_4Cl. The organic phase was concentrated and precipitated into MeOH to provide the product as yellow flakes (541 mg, 0.507 mmol, 94%). mp 147-

149°C. ^{1}H NMR (400 MHz, $CDCl_3$) δ: 9.34 (s, 1H), 8.30 (s, 1H), 8.16 (s, 2H), 7.77 (s, 2H), 7.60 (dd, 2H, J = 1.3, 2.9 Hz), 7.53 (dd, 1.3, 5.0 Hz), 7.51 (s, 2H), 7.45 (dd, 2H, J = 2.9, 5.0 Hz), 4.17 (m, 4H), 4.11 (m, 4H), 1.93 (m, 4H), 1.4-1.63 (bm, 32H), 1.05 (m, 12H), 0.96 (m, 12H). ^{13}C NMR (100 MHz, $CDCl_3$) δ: 150.1, 148.9, 137.6, 136.2, 135.4, 133.3, 126.58, 126.42 (CH), 126.34 (CH), 125.6, 123.59, 123.56, 120.2 (CH), 118.6 (CH), 117.4 (CH), 116.5 (CH), 107.3 (CH), 106.8 (CH), 72.1, 71.6, 39.88, 39.78, 30.85, 30.79, 29.47, 24.16, 24.05, 23.42, 23.39, 14.44, 11.60, 11.53. FT-IR (KBr): ν/cm^{-1}: 2954, 2925, 2853, 1520, 1506, 1455, 1262, 1229, 1075, 842, 768. HR-MS (MALDI): found *m/z* = 1066.5111 (M^+); calc. for $C_{66}H_{82}O_4S_4$: 1066.5090.

2,14-Di(2-bromo-3-thienyl)-5,6,10,11-tetra(2-ethylhexyloxy)dibenz[3',4';5',6']anthra[1,2-*b*:8,7-*b*'] dithiophene (**14**): A solution of 2,14-di(3-thienyl)-5,6,10,11-tetra(2-ethylhexyloxy)dibenz[3',4';5',6'] anthra[1,2-*b*:8,7-*b*']dithiophene (449 mg, 0.421 mmol) in CH_2Cl_2 (20 mL) was stirred at room temperature while a solution of Br_2 (44 μL, 0.86 mmol) in CH_2Cl_2 (2 mL) was added dropwise. The reaction was stirred with an argon purge for 2 h and further for 2 h. 2M KOH was added to quench the reaction, and the organic layer was removed and added dropwise to MeOH. The gummy solids that precipitated were filtered and washed to provide a dark yellow solid. This material was chromatographed on silica gel (4:1 to 2:1 hexane/CH_2Cl_2) to provide the product in two major fractions. The first was contaminated with an unidentified product, and the second fraction had clean product. This second fraction was dissolved in CH_2Cl_2 and precipitated into MeOH. Stirring overnight led to finer precipitates that were filtered off, rinsed with MeOH and dried under vacuum at 60°C to provide the product as a waxy yellow solid (260 mg, 0.21 mmol, 50%). mp 127-128.5°C. ^{1}H NMR (400 MHz, CD_2Cl_2) δ: 9.31 (s, 1H), 8.27 (s, 1H), 8.14 (s, 2H), 8.03 (s, 2H), 7.50 (s, 2H), 7.40 (d, 2H, J = 5.7 Hz), 7.35 (d, 2H, J = 5.7 Hz), 4.18 (m, 4H), 4.08 (m, 4H), 1.90 (m, 4H), 1.4-1.6 (bm, 32H), 1.06 (m, 12H), 0.97 (m, 12H). ^{13}C NMR (100 MHz, CD_2Cl_2) δ: 150.6, 149.5, 135.69, 135.12, 134.74, 134.40, 128.8 (CH), 127.2, 126.8 (CH), 125.7, 123.7, 121.9 (CH), 117.9 (CH), 117.0 (CH), 108.5, 107.35 (CH), 107.10 (CH), 72.35, 71.91, 40.32, 40.15, 31.31, 31.15, 29.8, 24.52, 24.43, 23.79, 23.77, 14.60, 14.58, 11.79, 11.72. FT-IR (KBr): ν/cm^{-1}: 2953, 2928, 2871, 1618, 1522, 1509, 1458, 1262, 1230, 1177, 1032, 839, 715, 605. MS (MALDI-TOF): found *m/z* = 1222.26 (M^+); calc. for $C_{66}H_{80}Br_2O_4S_4$: 1222.33.

Polymer **15**: Following a similar procedure for **9**, a mixture of dibromide **14** (88.5 mg, 0.0722 mmol), dialkyne **7** (43.8 mg, 0.0722 mmol), CuI (1 mg, 0.005 mmol) and $Pd(PPh_3)_4$ (4 mg, 0.004 mmol) in PhMe (2 mL) and DIPA (0.5 mL) was stirred at 60°C for 60 h. Work up and precipitation as described for **9** provided the polymer as an orange-yellow solid (100 mg, 83% mass yield). M_n: 18,000.

Polymer **16**: Following a similar procedure for **9**, a mixture of dibromide **14** (80.7 mg, 0.0659 mmol), dialkyne **8** (31.6 mg, 0.0660 mmol), CuI (1 mg, 0.006 mmol) and $Pd(PPh_3)_4$ (4 mg, 0.004 mmol) in PhMe (2 mL) and DIPA (0.5 mL) was stirred at 60°C for 60 h. Work up and precipitation as described for **9** provided the polymer as a bright yellow solid (80 mg, 79% mass yield). M_n: 5,000.

Polymer **18**: Following a similar procedure for **9**, a mixture of dibromide **2a** (92.2 mg, 0.200 mmol), dialkyne **17** (60.0 mg, 0.201 mmol), CuI (2 mg, 0.01 mmol) and $Pd(PPh_3)_4$ (11 mg, 0.0095 mmol) in PhMe (5 mL) and DIPA (1 mL) was stirred at 60°C for 48 h. Work up and precipitation as described for **9** provided the polymer as a brownish solid (84 mg, 63% mass yield). M_n: 10,000.

Polymer **19**: Following a similar procedure for **9**, a mixture of dibromide **14** (42.6 mg, 0.0348 mmol), dialkyne **17** (10.4 mg, 0.0352 mmol), CuI (0.6 mg, 0.003 mmol) and $Pd(PPh_3)_4$ (2 mg, 0.002 mmol) in PhMe (1 mL) and DIPA (0.5 mL) was stirred at 60°C for 60 h. Work up and precipitation as described for **9** provided the polymer as a yellow solid (24 mg, 51% mass yield). M_n: 10,400.

References

(1) Müller, H.; Eckhardt, C. J. *Mol. Cryst. Liq. Cryst.* **1978**, *45*, 313-318.

(2) (a) Patel, G. N.; Chance, R. R.; Witt, J. D. *J. Phys. Chem.* **1979**, *70*, 4387-4392; (b) Chance, R. R. *Macromolecules* **1980**, *13*, 396-398.

(3) (a) Rubner, M. F. *Macromolecules* **1986**, *19*, 2129-2138; (b) Nallicheri, R. A.; Rubner, M. F. *Macromolecules* **1991**, *24*, 517-525.

(4) Carpick, R. W.; Sasaki, D. Y.; Burns, A. R. *Langmuir* **2000**, *16*, 1270-1278.

(5) Yang, Z.; Sokolik, I.; Karasz, F. E. *Macromolecules* **1993**, *26*, 1188-1190.

(6) (a) Yoshino, K.; Fujii, A.; Nakayama, H.; Lee, S.; Naka, A.; Ishikawa, M. *J. Appl. Phys.* **1999**, *85*, 414-418; (b) Yoshida, Y.; Nishihara, Y.; Ootake, R.; Fujii, A.; Ozaki, M.; Yoshino, K.; Kim, H. K.; Baek, N. S.; Choi, S. K. *J. Appl. Phys.* **2001**, *90*, 6061-6065.

(7) (a) Wang, P. W.; Liu, Y.-J.; Devadoss, C.; Bharathi, P.; Moore, J. S. *Adv. Mater.* **1996**, *8*, 237-241; (b) Pillow, J. N. G.; Halim, M.; Lupton, J. M.; Burn, P. L.; Samuel, I. D. W. *Macromolecules* **1999**, *32*, 5985-5993.

(8) Yang, J.-S.; Swager, T. M. *J. Am. Chem. Soc.* **1997**, *120*, 11864-11873.

(9) Sato, T.; Jiang, D.-L.; Aida, T. *J. Am. Chem. Soc.* **1999**, *121*, 10658-10659.

(10) (a) Nguyen, T.-Q.; Doan, V.; Schwartz, B. J. *J. Chem. Phys.* **1999**, *110*, 4068-4078; (b) Nguyen, T.-Q.; Martini, I. B.; Liu, J.; Schwartz, B. J. *J. Phys. Chem. B* **2000**, *104*, 237-255.

(11) (a) Deans, R.; Kim, J.; Machacek, M. R.; Swager, T. M. *J. Am. Chem. Soc.* **2000**, *122*, 8565-8566; (b) Zahn, S.; Swager, T. M., *Science*, submitted for publication.

(12) Kim, J.; Swager, T. M. *Nature* **2001**, *411*, 1030-1034.

(13) (a) Jenekhe, S. A.; Osaheni, J. A. *Science* **1994**, *265*, 765-768; (b) Turro, N. J. *Modern Molecular Photochemistry*. University Science Books: Sausalito (CA), 1991.

(14) Lere-Porte, J.-P.; Moreau, J. J. E.; Serein-Spirau, F.; Wakim, S. *Tetrahedron Lett.* **2001**, *42*, 3073-3076.

(15) Milstein, D.; Stille, J. K. *J. Am. Chem. Soc.* **1979**, *101*, 4992-4998.

(16) Otero, T. F. In *Polymer Sensors and Actuators*, Osada, Y.; DeRossi, D. E., Eds. Springer: New York, 2000. pps 295-323.

(17) (a) Becker, R. S.; Seixas de Melo, J.; Maçanita, A. L.; Elisei, F. *Pure Appl. Chem.* **1995**, *67*, 9-16; (b) Kankare, J.; Lukkari, J.; Pasenen, P.; Sillanpää, R.; Laine, H.; Harmaa, K. *Macromolecules* **1994**, *27*, 4327-4334; (c) Roncali, J.; Gorgues, A.; Jubault, M. *Chem. Mater.* **1993**, *5*, 1456-1464; (d) Eales, R. M.; Hillman, R. M. *J. Mater. Sci.* **1990**, *25*, 3806-3813.

(18) Sonogashira, K.; Tohda, Y.; Hagihara, N. *Tetrahedron Lett.* **1975**, 4467-4470.

(19) Swager, T. M.; Gil, C. J.; Wrighton, M. S. *J. Phys. Chem.* **1995**, *99*, 4886-4893.

(20) Bunz, U. H. F. *Chem. Rev.* **2000**, *100*, 1605-1644.

(21) Goldfinger, M. B.; Swager, T. M. *J. Am. Chem. Soc.* **1994**, *116*, 7895-7896.

Chapter 6:

What lies ahead?
An introduction of sorts

"If we do not begin by giving a glance at the whole, if we pass at once to the consideration of the parts, we may perhaps see very well, but we do not know what we are looking at"
- Henri Bergson

Preface

Prior to writing this thesis, I envisioned including a broad discussion of "organic electronics" as an introductory chapter. Small molecules, polymers, single molecules, liquid crystals, monolayers ... transistors, light-emitting diodes, logic gates, sensors ... the lists (and the page lengths) go on. Realizing that this would present a quite formidable task, I started to focus in on more specific areas bearing a stronger relation to the work presented in this thesis. Given that my work has primarily focused on synthetic methods for large aromatic scaffolds, I then contemplated a general introduction to the prior art in the fields of polycyclic aromatics and ladder polymers. However, the four main synthetic chapters had sufficient differences that one comprehensive introduction would not provide a proper entry to each of the individual chapters. To get around this, I then chose to break up this large introduction into smaller synthetically-oriented segments in order to better integrate individual concepts with the systems best suited to exemplify them. For example, Chapter 1 discussed ladder polymers in the context of our work dealing with graphite ribbons and Chapter 3 linked issues of thiophene-based materials with our studies of tandem cyclization-polymerization. Each chapter has made allusions to potential electronics applications without going into incredibly detailed explanations. This chapter will serve to make up for this exclusion as applicable to one specific area, organic semiconductors. While this broad label formally encompasses any applications involving conducting polymers, I will focus the discussion to the phemonemon of organic semiconductivity within the context of organic field-effect transistors (OFETs).

All five chapters of this thesis deal with molecular and polymeric systems that may comprise ideal candidates for OFETs while not all systems may exhibit photoconductivity or emit light upon charge injection. Therefore, a discussion of OFETs, why particular organics

make good OFET candidates, what materials already find use in OFET architectures, and what applications these devices may offer would help in the design of new materials or the continued investigation of old materials. This chapter will draw parallels to inorganic semiconductors and briefly discuss basic device geometries and the empirical physics behind them. It will also survey some of the prototypical and well-studied OFET materials and discuss recent studies that have pushed the envelope of OFET design and application. Finally, tangible real-world uses for organic electronic materials will close the chapter. I by no means intend to deliver an all-inclusive discussion, and several reviews included as reference may better answer more specific questions that relate to materials design, synthesis, device performance and applications.[1,2] So with that said ...

Introduction to FETs and device geometries

Silicon-based semiconductor technology currently dictates all integrated circuitry performance or conversely, the rendering of old computers obsolete. New technological breakthroughs drive down circuit feature sizes and allow for greater processing speeds on smaller chips. The heavy price tag that accompanies these new chips reflects the exacting technical infrastructure required to grow pure inorganic materials and pattern active channels at smaller and smaller scales. As these feature sizes and the spacing between them shrink, electronic cross-talk has a larger influence by providing routes to device shorts through physical contact between two elements or through tunneling effects. For the high-performance semiconductor field, this physical limitation on feature size will challenge researchers in academia and industry for the next decade or so. At this point, I should cleverly make the case

for organic semiconductors and how they will change the world for high-performance silicon technology, but I cannot. So why use organic circuitry?

In essence, one may schematize a FET as a capacitor with a tuneable dielectric layer (*i.e.* the active semiconductor). As the dielectric layer in a standard capacitor will dictate how much charge the device will hold, this layer within a FET determines when and how fast charge may move. Scheme 1 depicts two common device geometries: the top-contact and the bottom-contact structures. These geometries find the most use in organic studies. High-performance applications utilize much more elaborate structures. The choice of device geometries typically reflects processing concerns of the organic material.

Scheme 1: Common OFET device geometries

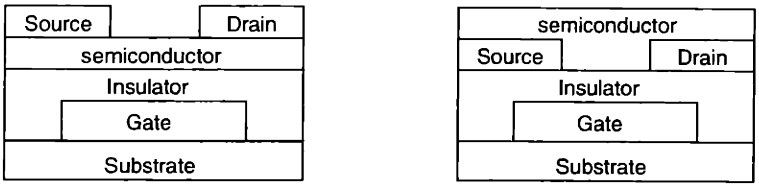

In both geometries, an insulating layer separates the bottom gate electrode from the active organic semiconductor and the source and drain electrodes. In the "off" state, with no voltage applied to the gate, the semiconductor does just that. Essentially no current flows between the source and drain electrodes. From the analogy above, this resembles a capacitor storing charge. Upon application of stronger voltages to the gate, electronic polarization within the semiconductor will introduce charge carriers (the ubiquitous "holes" or electrons). Keeping with the capacitor analogy, this represents an alteration of the dielectric constant of the material separating the capacitor plates. At sufficiently high charge carrier densities, the device enters the "on" state, and current flows between the source and drain, representing the firing of the capacitor. By removing the gate voltage, the device returns to the "off" state. Two key figures

of merit describe this activity: mobility and on-off ratio. The mobility refers to the speed of the charge carrier under an applied electric field and the on-off ratio measures the relative magnitudes of the intrinsic current flowing with no gate bias (off) and with field-effect gating (on). These general device structures serve as test-beds for organic semiconductivity in addition to legitimate device applications.

Inorganic vs. organic

Main group materials such as silicon and the III-Vs (GaN, InP and GaAs) exemplify commonly used inorganic semiconductors. Under the proper growth conditions, these materials provide essentially perfect crystal lattices covalently linked through large and diffuse sigma bonding. From the crystal structures of these materials, one can derive the expected electronic band diagrams that describe the conduction and valence bands of the materials. Within all semiconductors, purity dramatically affects performance. Impurities added in controlled amounts during the growth of inorganics also have strong influences on the resulting electronic properties. The addition of donor or acceptor impurities (dopants) into the crystal lattice tunes the electronics by shifting the electron density of the material. For example, p-doped materials have electron acceptor dopants that remove charge from the valence band to create positive charge carriers (holes). Once grown, these materials have fixed and permanent dopant levels. The larger and more diffuse sigma bonds for the heavier main group elements allow for extensive delocalization of the charge carriers. These carriers (referred to as Wannier excitons) have radii of *ca.* 100 Å, and this extensive delocalization explains the high carrier mobilities found in highly doped, single crystal silicon.

Chemists and physicists recognized the links between inorganic σ-delocalization and organic π-conjugation and pursued studies of charge transport phenomena within small acenes

such as anthracene in the 1970s.[3] These pursuits remained buried in academia until the discovery of conductivity in conjugated polymers. At this point, it became clear that π-delocalized systems can foster efficient charge transport. As discussed in Chapter 3, conducting polymers undergo reversible, controllable doping during electrochemical redox processes hinting that these materials would make ideal organic semiconductors. While true to some extent, the severe local disorder within conjugated polymers reduces the observed semiconducting behavior relative to a hypothetical "perfect" polymer. On the other hand, single organic crystals of molecular species offer such order. Here, much like inorganic crystals, one may use the crystal structure of the organic to derive a band diagram. Although quite a simplified picture, Scheme 2 illustrates the electronic convergence of a molecular HOMO-LUMO picture with a polymer valence-conduction picture. As we progress from this single molecule HOMO-LUMO picture to a crystal, the inter-molecular π-π interactions between adjacent aromatics provide extended delocalization.

Scheme 2: HOMO-LUMO/conduction-valence convergence

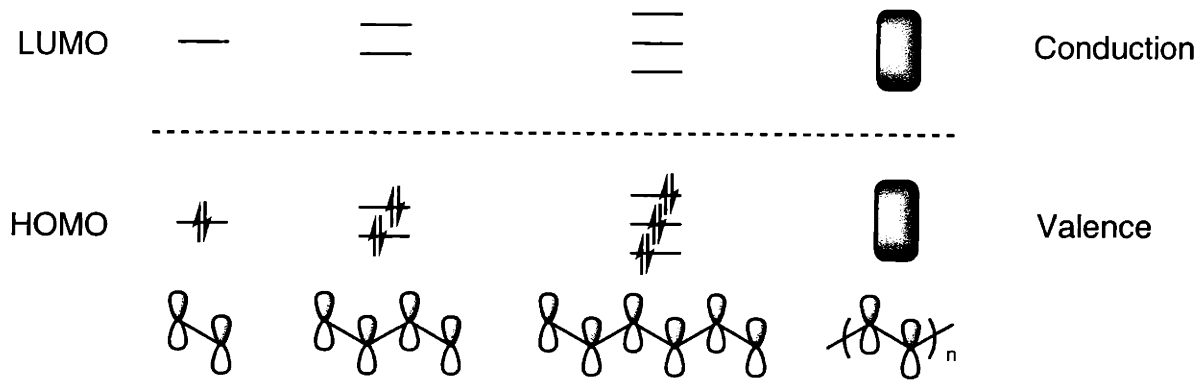

However, the exciton radii within these materials (referred to as Frenkel excitons) fall around 10 Å, essentially localizing charge on a single molecule within the crystal. Organic molecules undergo structural alterations during charge injection (*e.g.* aromatic to quinoidal structures for conducting polymers, Chapter 3). Physicists refer to such resonance structures as

electron-phonon couplings, basically saying that these structural reorganizations introduce defect sites into the lattice as if the crystal had cracked due to stress. As a result of these localized charges, organic charge-conduction typically relies on intermolecular "hopping" as opposed to the true band transport found in inorganics. All of these ideas translate into inherently smaller charge mobilities when compared to their inorganic counterparts.

Most of the organic semiconductor literature acknowledge these facts and clearly point out that this technology will not rival that of single-crystal silicon. So why pursue such materials? From a processing standpoint, organics allow for low temperature vacuum deposition (chemical vapor deposition, CVD) or for solution-based depostion such as spin casting from solution. These routes provide thin semiconducting layers in under a day as opposed to the several weeks required to grow and process an inorganic single crystal. However, spin-coating or CVD techniques typically provide polycrystalline materials having several grain boundaries that serve as trap sites for mobile charges. Low-temperature solution processability factors into two novel and practical aspects of organic semiconductors: ink-jet printing and device preparation on flexible substrates.[4] Circuitry design with computer-aided drafting could result in final circuit construction from the laser printer. Likewise, flexible polymer supports can support low-temperature deposition of active semiconducting layers and electrodes. The end of the chapter will elaborate upon this idea.

With respect to crystal morphology, one molecular compound may exist as numerous polymorphs with different unit cell properties. The formation of these polymorphs strongly depends on the processing methods used to deposit the material: solvents of crystallization, rate of CVD growth, substrate temperatures, *etc.* For example, pentacene adopts a herring-bone motif in the solution-grown crystal. However, pentacene has several polymorphs that provide

different carrier mobility characteristics. In addition, one polycrystalline film may have several different morphologies, thus complicating mobility measurements inherent to particular lattice constants. Figure 1 depicts the influence that crystal order has on the observed hole mobilities for CVD-grown pentacene thin films. Clearly, the more ordered film provides higher mobilities by minimizing grain boundaries and allowing for better π-π interactions throughout the channel. Keeping this idea in mind, the discussion that follows will not cite mobility data as this parameter varies widely depending on the materials processing or device geometries employed.

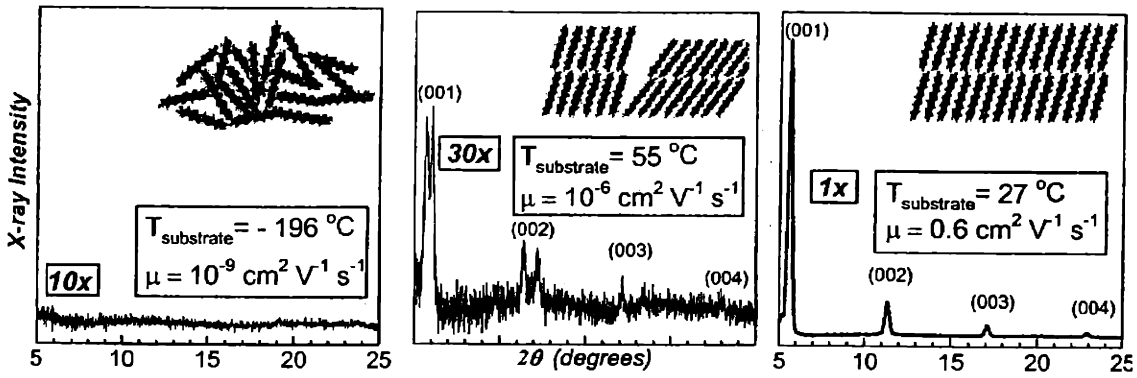

Figure 1: Effects of pentacene thin-film order on observed mobilities. Adapted from ref. 1b.

Organic semiconductor materials

For inorganics, one refers to p-type or n-type materials, a reference to the nature of the dopant and the type of majority charge carrier. P-type materials incorporate electron-accepting dopants that create holes in the valence band, thus allowing for hole mobility. N-type materials use electron donors to populate the conduction band for electron transport. While inorganics use lattice matching to ensure electronic continuity throughout a device, organic materials use "HOMO-LUMO matching," *i.e.* comparable LUMO (n-type) or HOMO energies (p-type) relative to a given electrode's work function. Therefore, the relative electron or hole affinities of the materials play an important role when constructing an OFET. In practice, electrochemical measurements may relate the organic's molecular orbital energies relative to vacuum for comparison and matching with metal work functions. By far, the vast majority of organic semiconductor research has focused on p-type materials since the parasitic impurities remaining in organics (although not intentionally as for inorganics) tend to trap electrons much more efficiently than they trap holes. Therefore, with the exception of the first materials discussed below, all references to "mobility" will imply hole mobility unless otherwise stated.

Before a structural survey, I must address one semantic point: "small molecules." This classification essentially consists of any non-polymeric material with a known chemical connectivity. For example, hexameric structures would fall under the "small molecule" umbrella regardless of the molecular weight. This label deals more with the fact that small molecules allow for sublimation under high vacuum while polymers typically require solution-processing.

n-type: Despite the relatively high level of electron-trapping impurities within organics when compared to the inorganic counterparts, a few materials have demonstrated suitable n-type characteristics. As the p-type materials now perform at the level of amorphous silicon, organic-

based p-n junctions and other types of complementary circuits will require suitable materials with improved n-type behavior. Although the materials set at present has few components, they do have some structural features in common. Chart 1 depicts some established n-type small molecules. These materials rely on high electron affinities imparted by the electron-deficient perfluorinated phthalocyanine (F-CuPc)[5] or perfluorinated alkyl chains of sexithiophene (F-α-6T).[6] PTCDI also has a large aromatic core but with strongly withdrawing imide moieties. Devices incorporating all of these materials tend to decompose quite rapidly under ambient atmosphere due to undesired chemical reactivity between the charged organic semiconductor and residual water. However, the hydrophobic alkyl "grease" appended to these cores may play a role in protecting from water permeation into the active organic layer.

Chart 1: n-type materials

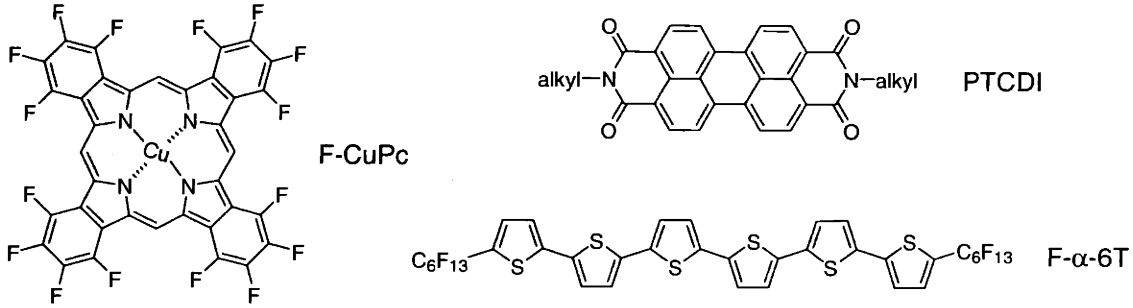

p-type: As several studies have revealed the hole mobilities within a variety of organics, we may break down p-type materials into subcategories comprised of fused-ring systems, well-defined oligomers and polymers. In general, the fused ring systems and the oligomers allow for rigorous purification yet tend to have poor solution solubilities. These materials readily sublime, making them amenable to vapor deposition techniques. Extensive synthetic work can tailor these molecules to include solubilizing alkyl groups as a means of rendering the insoluble material processable from solution. After solution processing, the thin organic layer has more intermolecular order relative to spin-cast polymers. Although not as ordered in a bulk film,

polymers have the advantages of durability, solubility, and mechanical strength. Regioregular polymers have minimized this disorder to a large extent; however, no one has yet reported a polymer single crystal.

Fused arenes: Chart 2 depicts some common fused arenes used for FETs. Pentacene and tetracene have by far received the most study in recent years. They readily sublime and form large single crystals during zone-refining. However, these reactive arenes must undergo rigorous purification and subsequent processing in oxygen-free environments. Other work has looked at more stable materials with similar structural motifs such as pyrene and the anthradithiophenes.[7] As the fused arenes generally have poor solubilities for solution processing, synthetic chemistry has tailored these cores to incorporate steric bulk or alkyl chains onto the polycyclic aromatic core. In fact, Anthony's studies of differentially alkynylated pentacenes demonstrated a great deal of crystal packing control from molecular design.[8]

Chart 2: p-type fused arenes

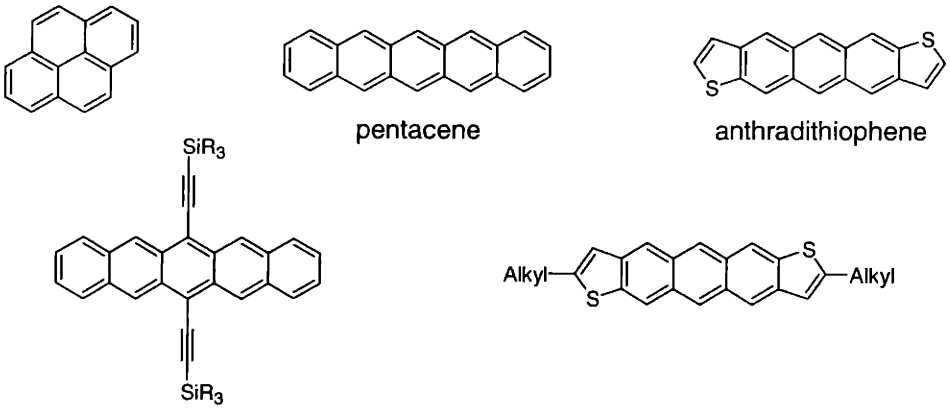

Oligomers: As poly(thiophene) allowed for the first demonstration of FET-behavior from an organic material,[9] other research has looked into more well-defined *oligo*(thiophene)s. The thiophene hexamer α-6T and the tetramer α-4T have also proven their FET worth (Chart 3). These offer a near convergence with the electronic properties of the analogous polymer and allow for more rigorous purification relative to polymeric samples. Katz and co-workers at Lucent have also combined the fused-ring scaffolds based on the benzodithiophenes (BDTs) into defined oligomeric structures.[1c] This strategy allows for a variety of molecular alterations *via* cross coupling onto common intermediates: electronic tuning from aromatic cross-couplings or solubilization through the incorporation of alkyl chains. As definitive OFET structure-function relationships do not yet exist, the ability to fine-tune a given molecular core will help to discover better materials.

Chart 3: p-type well-defined oligomers

α-6T 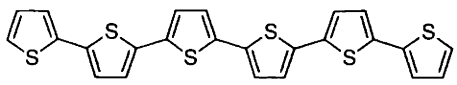 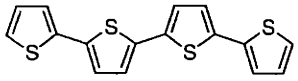 α-4T

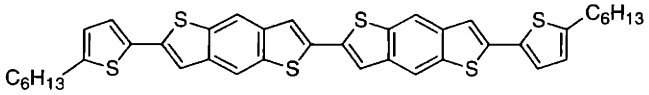 BDT oligomer

Polymers: One drawback to the small molecule FET materials consists of the issues of grain boundaries in crystalline domains. Spin-coating or CVD often results in several crystalline domains where each grain boundary limits the overall mobility of the device. Polymers have helped to overcome this issue. Even though polymers also may form crystalline domains, high molecular weight materials do not readily crack upon annealing. The poly(thiophene)s have provided the best mobilities to date for FET applications. With the advent of synthetic methods for regioregular poly(thiophene)s,[10] mobilities have increased markedly apparently due to the higher degree of interpolymer order relayed through ordered and more well-defined backbones.

As they exhibit high conductivities in their oxidized states, these materials may also serve as flexible anodes to drive all-organic circuitry. Towards this end, a complementary and stable n-type polymer FET constructed with the BBL ladder polymer recently provided respectable *electron* mobilities.[11]

Chart 4: Polymer semiconductors

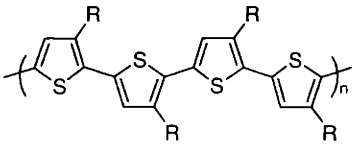

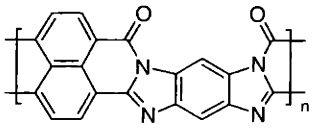

BBL

Applications and recent investigations

Industrial organic electronics groups continue to pioneer this emerging field. They have done tremendous work not only in the development of useful applications for OFETs, but they have also made important scientific contributions to the field. I will close this chapter by highlighting a few of these topics.

Ambipolar transport: Schön and colleagues at Bell Labs succeeded in getting ultra-pure pentacene to display both p *and* n-type field-effect gating.[12] In all examples before, organics only had p-type or n-type activity. Therefore, to construct a complementary circuit for performing logic or other computational functions, one would need to deposit separate organic layers as previously described by the Lucent group for α-6T/F-CuPc heterostructures.[13] As grain boundaries and interfacial contacts often supply the largest potential for trapping, such heterostructures would have limited efficiencies. This finding for pentacene may help to further develop such organic circuitry.

Lasing and light-emitting FETs: Schön, Batlogg, Dodabalapur and their crystal wizard, Kloc, reported optical emissions from FETs built with tetracene[14] and from α-6T[15] in 2000. By utilizing techniques for obtaining ambipolar transport characteristics now available to highly-

purified materials, they could introduce holes and electrons at two different device interfaces. As pictured in Scheme 4, they assembled two FETs onto one tetracene crystal. A typical light-emitting diode (LED, left diagram) uses separate hole and electron transporting layers to facilitate charge injection and recombination within the third emissive layer. By injecting holes and electrons at the two respective gates of the tetracene FET device (right diagram), they then played the two gates off of each other to effect an overall potential drop across the crystal. This electrical gradient resulted in holes and electrons migrating to the opposite poles, and upon annihilation they emitted highly-narrowed emission and eventually displayed electrically-pumped lasing. In addition, they observed similar non-lasing light emission from α-6T. This claim of electrically-pumped lasing comprises a significant advance for laser materials as they currently require optical input to obtain coherent optical output. This finding remains quite controversial.

Scheme 4: A comparison of LED and "lasing FET" geometries

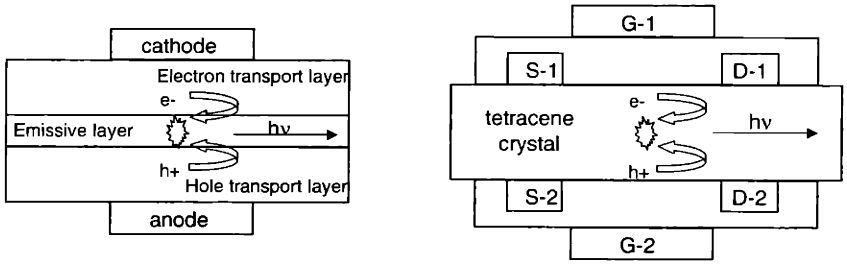

LED geometry Light-emitting FET (lasing?)

All-plastic circuitry: Rigorously prepared single crystal specimens made the previous two examples possible. Using these processing techniques to prepare large devices on an industrial level would not succeed, if not prove entirely impossible. The largest organic crystals commonly obtained through gradient sublimation size in on the order of a couple square millimeters. In 1998, Phillips Research disclosed a flexible, all-polymer integrated circuit that incorporated conductive poly(aniline) (PANI), semiconductive poly(thienylene-vinylene) (PTV) and

insulating poly(vinylphenol), all supported on a poly(imide) substrate.[16] They employed photolithography to pattern the conductive PANI interconnects used to modulate the semiconductive PTV layer. Although these devices performed quite poorly compared to standard circuitry, it stands as a strong proof-of-principle affirming the feasibility of flexible all-organic components. This work has led to the fabrication of flexible active-matrix displays several inches in size. For example, Lucent and E-Ink announced in November 2000 a joint development of "electronic paper" based on E-Ink's electrophoretic display technology and Lucent's flexible organic transistors.

The future? The solution-based processing conditions employed for organic materials may prove amenable to constructing very large-area devices. Some applications envisioned through this idea seek to develop products as diverse as roll-up computer displays and full-wall organic-based soft lighting. The relatively low fabrication costs involved for organic device preparation would pave the way for inexpensive, disposable devices that do not require significant (if any) inorganic semiconductor processing. Most importantly, solution processing may allow for reel-to-reel manufacturing as a means of integrating all facets of device preparation into one assembly line. The "smart card" illustrated in Scheme 5 represents one of the holy grails of the organic electronics field potentially available with such processing techniques. All references to Big Brother aside, such a card may allow for the storage and access of all personal information on a cheap, lightweight and durable card. Scheme 5 illustrates such a card, where active elements of memory, power, and communication co-exist within a small credit-card-type package. Here, the organic integrated circuit can perform computational operations and drive the other elements, the organic-based memory chip would provide permanent, non-volatile memory, and the photovoltaic solar cell would provide energy to power

the system. Organic light-emitting diodes and photodetectors would then provide external communication in order to interface with card readers or other computers.

Scheme 5: Flexible, all-organic "smart card"

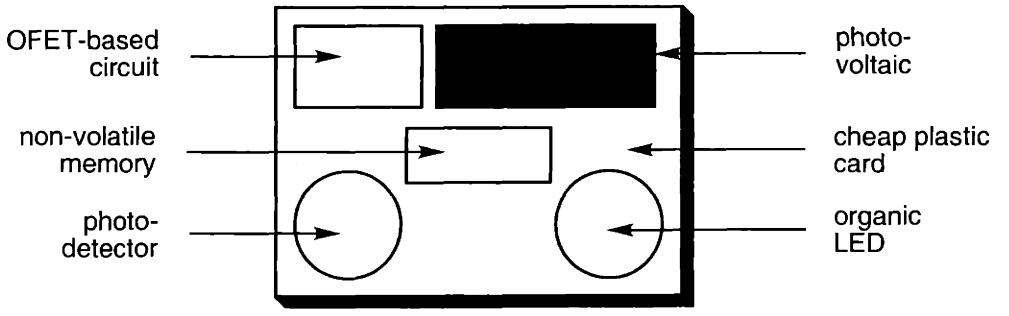

Concluding Remarks

I hope that this chapter may serve as a readable starting point for continued synthetic investigations directed towards harnessing organic semiconductivity. Until recent years, little cross-talk existed between the device physicists and the synthetic chemists: this largely explains the predominant use of pentacene at the industrial level. As chemists have now entered the arena, the field of organic electronics as a feasible goal stands to further benefit from the molecular insights available. Just as two diplomats find a common language to work out problems, organic chemists interested in organic electronics need to have an understanding of how the molecular properties of their materials will relate to bulk performance in a device and a working knowledge of device preparation. Likewise, engineers and materials scientists must realize and understand the extensive efforts sometimes required to make "trivial" structural changes. This cross-validation of specialties will eliminate the prevalent conceptions of "just give the EEs some materials" or "just have the chemists make it" that often permeate this field. And for every synthetic chemist discussing semiconductors in a thesis, hopefully there exists an engineer discussing organic chemistry ...

References

(1) (a) Horowitz, G.; *Adv. Mater.* **1998**, *10*, 365-377; (b) Dimitrakopoulos, C. D.; Mascaro, D. J. *IBM J. Res. Dev.* **2001**, *45*, 11-27; (c) Katz, H. E.; Bao, Z.; Gilat, S. L. *Acc. Chem. Res.* **2001**, *34*, 359-369; (d) Cornil, J.; Beljonne, D.; Calbert, J.-P.; Brédas, J.-L. *Adv. Mater.* **2001**, *13*, 1053-1067; (e) Dimitrakopoulos, C. D.; Malenfant, P. R. L. *Adv. Mater.* **2002**, *14*, 99-117.

(2) (a) Pierret, R. F. *Semiconductor Fundamentals*. Addison-Wesley: Reading (MA), 1983; (b) Omar, M. A. *Elementary Solid State Physics*. Addison-Wesley: Reading (MA), 1993; (c) Pope, M.; Swenberg, C. E. *Electronic Processes in Organic Crystals and Polymers* (2nd ed). Oxford University Press: New York, 1999.

(3) Karl, N. *Festkörperprobleme* **1974**, *XIV*, 261-290.

(4) (a) Bao, Z.; Rogers, J. A.; Katz, H. E. *Chem. Mater.* **1999**, *9*, 1895-1904; (b) Bao, Z. *Adv. Mater.* **2000**, *12*, 227-230.

(5) Bao, Z.; Lovinger, A. J.; Brown, J. *J. Am. Chem. Soc.* **1998**, *120*, 207-208.

(6) Facchetti, A.; Deng, Y.; Wang, A.; Koide, Y.; Sirringhaus, H.; Marks, T. J.; Friend, R. H. *Angew. Chem. Int. Ed.* **2000**, *39*, 4547-4551.

(7) Laquindanum, J. G.; Katz, H. E.; Lovinger, A. J. *J. Am. Chem. Soc.* **1998**, *120*, 664-672.

(8) Anthony, J. E.; Brooks, J. S.; Eaton, D. L.; Parkin, S. R. *J. Am. Chem. Soc.* **2001**, *123*, 9482-9483.

(9) Tsumura, A.; Koezuka, H.; Ando, T. *Appl. Phys. Lett.* **1986**, *18*, 1210-1212.

(10) (a) McCullough, R. D.; Lowe, R. D. *J. Chem. Soc., Chem. Commun.* **1992**, 70-72; (b) Chen, T.-A.; Rieke, R. D. *J. Am. Chem. Soc.* **1992**, *114*, 11087-11088.

(11) Babel, A.; Jenekhe, S. A. *Adv. Mater.* **2002**, *14*, 371-374.

(12) Schön, J. H.; Berg. S.; Kloc, C.; Batlogg, B. *Science* **2000**, *287*, 1022-1023.

(13) Crone, B.; Dodabalapur, A.; Lin, Y.-Y.; Filas, R. W.; Bao, Z.; LaDuca, A.; Sarpeshkar, R.; Katz, H. E.; Li, W. *Nature* **2000**, *403*, 521-523.

(14) Schön, J. H.; Kloc, C.; Dodabalapur, A.; Batlogg, B. *Science* **2000**, *289*, 599-601.

(15) Schön, J. H.; Dodabalapur, A.; Kloc, C.; Batlogg, B. *Science* **2000**, *290*, 963-965.

(16) Drury, C. J.; Mutsaers, C. M. J.; Hart, C. M.; Matters, M.; de Leeuw, D. M. *Appl. Phys. Lett.* **1998**, *73*, 108-110.

CURRICULUM VITAE

JOHN DAYTON TOVAR

ACADEMIC INTERESTS

Materials-oriented synthetic organic chemistry, electrochemistry, conjugated and conducting polymers, supramolecular chemistry, organic electronics.

EDUCATION

1997 - 2002 — *Massachusetts Institute of Technology* — *Cambridge, MA*
Ph.D., Chemistry
Dissertation Adviser: Professor Timothy M. Swager; "Synthesis and Utility of Electronically Diverse Polycyclic Aromatics"

1993 - 1997 — *University of California, Los Angeles* — *Los Angeles, CA*
B.S., Chemistry (March 1997; GPA 3.52/4.00)

1989 - 1994 — *Mount San Antonio College* — *Walnut, CA*
No Degree Objective (GPA 4.00/4.00)

AWARDS AND HONORS

Wyeth-Ayerst Scholar, MIT (2001)
Departmental Outstanding Teaching Award, MIT (1998)
Hypercube Scholar, UCLA (1997)
Departmental High Honors, UCLA (1997)
Golden Key National Honor Society, UCLA (1995)

PROFESSIONAL EXPERIENCE

1998 - 2002 — *Graduate Research Assistant* — *MIT Department of Chemistry*
- Developed new synthetic routes into electron-poor oxygen- and nitrogen-containing aromatic ring systems *via* electrophile-induced cyclizations.
- Elucidated new oxidation chemistry to explain novel thiophene cyclization-polymerization sequences and to obtain functionalizable polycyclic aromatics.
- Applied a variety of electrochemical methods for the synthesis and study of conductive electrochromic polymers with unique backbone energetics.
- With newly developed chemistry, demonstrated enhancements of conjugated polymer photophysics that follow from chromophore aromatization.

1997 - 1998 — *Teaching Assistant* — *MIT Department of Chemistry*
Undergraduate General Chemistry Laboratory
- Instructed and supervised introductory laboratory techniques.

1996 – 1997 — *Undergraduate Research* — *UCLA (Chemistry)*
Adviser: Professor Yves F. Rubin

• Synthesized highly unsaturated carbon macrocycles and networks.
• Utilized Diels-Alder chemistry to construct multiply alkynylated arenes as new conjugated organic scaffolds.

1995 - 1997 *Assistant Chemical Safety Officer* *UCLA Environment, Health and Safety*
UCLA Department of Chemistry and Biochemistry
• Handled general safety questions and concerns.
• Assessed and responded to departmental emergencies.

1995 - 1996 *Undergraduate Research* *UCLA (Civil and Environmental Engineering)*
Adviser: Professor Julius Glater
• Utilized reverse osmosis filtration to purify seleniferous synthetic waters.
• Worked on a preliminary protocol for selenium analysis in synthetic water using hydride-generation atomic absorption spectroscopy.

TECHNICAL PROFICIENCIES

Synthetic organic chemistry; small molecule purification and characterization
Polymer synthesis, purification and characterization
Molecular modeling and calculation (Spartan)
Inert atmosphere and Schlenk techniques
Trace metal analysis (HGAAS)
Structural characterization (1D and 2D NMR, surface profilometry)
Electrochemical characterization (voltammetry, spectroelectrochemistry)
Optical characterization (absorption, fluorescence)

PROFESSIONAL ACTIVITIES AND AFFILIATIONS

Member, Materials Research Society (2001-)
Chemistry Graduate Student Committee, MIT (2000-2002)
Chemical Hygiene and Safety Committee, MIT Chemistry (1999-2002)
Member, American Association for the Advancement of Science (1998-)
President, Student Affiliates of the American Chemical Society, UCLA (1997)
Member, American Chemical Society (1996-)
Advisory Board, UCLA Golden Key (1996)
UCLA Circle K (Kiwanis International, 1995)
California Scholarship Federation: Vice President (1992), 100% Life Member

SCIENTIFIC PRESENTATIONS

[4] J. D. Tovar and T. M. Swager, "Extended thiophene-based polycyclic aromatics: Oxidative cyclizations and core elaborations," presented to the Organic Division of the American Chemical Society (ORGN 134) at the 222nd National Meeting, Chicago, IL (26-30 Aug 2001).

[3] J. D. Tovar, T. M. Swager, "Chemical and electrochemical investigations of poly(naphtho-dithiophene)s: A new class of electroactive materials," presented to the Organic Division of the American Chemical Society (ORGN 48) at the 220th National Meeting, Washington, DC (20-24 Aug 2000).

[2] J. D. Tovar and T. M. Swager, "Naphthodithiophenes: A new class of electroactive materials," presented at the Gordon Conference on Organic Structures and Properties, New London, CT (17-22 June 2000).

[1] J. D. Tovar and T. M. Swager, "Pyrylium Salts *via* Electrophilic Cyclization: Applications for Novel 3-Arylisoquinoline Syntheses," presented to the Organic Division of the American Chemical Society (ORGN 473) at the 218th National Meeting, New Orleans, LA (22-26 Aug 1999).

PUBLICATIONS

[5] J. D. Tovar, A. Rose and T. M. Swager, "Functionalizable Polycyclic Aromatics Through Oxidative Cyclization of Pendant Thiophenes," in the Journal of the American Chemical Society (accepted).

[4] J. D. Tovar and T. M. Swager, "Exploiting the Versatility of Organometallic Cross-Coupling Reactions for Entry into Extended Aromatic Systems," invited by the Journal of Organometallic Chemistry, 2002 (in press).

[3] J. D. Tovar and T. M. Swager, "Poly(naphthodithiophene)s: Robust, Conductive Electrochromics *via* Tandem Cyclization-Polymerizations," in Advanced Materials, 2001 (13) 1775-1780.

[2] J. D. Tovar and T. M. Swager, "Pyrylium Salts *via* Electrophilic Cyclization: Applications for Novel 3-Arylisoquinoline Syntheses," in the Journal of Organic Chemistry, 1999 (64) 6499-6504.

[1] J. D. Tovar, N. Jux, T. Jarrosson, S. I. Khan and Y. F. Rubin, "Synthesis and X-Ray Characterization of an Octaalkynyldibenzooctadehydro[12]annulene," in the Journal of Organic Chemistry, 1997 (62) 3432-3433.

Acknowledgements

"In these Rude Collections, which are onely the Gleanings of my private diversions in broken hours, it may appear, that many Minds and Hands are in many places industriously employed ... in the pursuit of those Excellent Ends ..." (Oldenburg, H. *Royal Soc. London, Philos. Trans.* **1665**, 1-2). With that, I save the best part for last: thanking these many minds and hands.

First and foremost, I must give a great deal of thanks to Professor Timothy Swager. His passion for pushing the envelope has brushed off on all who have been associated with his group. When I was but a "starry eyed" young first-year, he did not fetter my own outside academic interests, allowing me to get more exposure to the very problems our group's chemistry helps to study. He truly takes an active role in the intellectual development of his group – most of us can be found in seminars spanning electrical engineering, biotechnology and the notorious PPST, in addition to the extensive organic chemistry program, and this attendance is encouraged rather than done in a "behind-the-back" manner. The scientific independence he has given the group – at least those who take it - must also be commended. You have been and will continue to be an important influence in my career.

I must also thank my undergraduate chemistry research advisor, Professor Yves Rubin. I had been locked up to a reverse osmosis pump in civil engineering, analyzing selenium and arsenic with HGAAS as necessary until I took a physical organic course from Yves. All of the pioneers in the membrane field were organic and polymer chemists by training, so I figured it wouldn't be a bad choice for study. From that point on, I was hooked. Perhaps a life of modeling membrane fouling would have been in store for me, but Yves let me join his research group where I had the chance to work on an exciting project with a supportive group of people – Dr. Norbert Jux, Dr. Tim Parker, Dr. Wenyuan Qian, Lance Kvetko, and Dr. Iris Lamparth were labmates that helped me make the decision to pursue graduate studies in organic chemistry.

Upon arrival into the Swager group, Khushrav Crawford helped get me up to speed with this weird contraption known as a Schlenk line, and Claus Lugmair gave me some solid air-sensitive techniques, and I am indebted to them for this help. I can only imagine the discussions in the computer room as my first exploits on the line were told to the senior group members at the time ...

Many in the group often joke or laugh when people provide long acknowledgements, but I feel this is better that those who provide none. However, I will be uncharacteristically brief here. A couple lines in this acknowledgement cannot express my gratitude to individual members of the group, but I will make an effort to highlight a few.

I must thank the general entity known as "the Swager group" – too many people and too many contributions to list ... whether it's Karen Warren making the MIT bureaucracy a bit easier to deal with, Jordan Wosnick coming to the rescue on the computers, or Karen Villazor's assistance with the CD. I am indebted to the group for their day-to-day assistance.

A great deal of thanks needs to go to the CpS seminar series, an informal "discussion group" we started several years ago. Such seminars typically ended with the chosen location closing up for the night and usually required one of the men in the group to play some type of fiancé capacity. Anyone who was anyone within the group attended these meetings, but a special thanks goes out to the regular participants: Aimee Rose, Alex Paraskos, Paul Byrne, Dr. Mark MacLachlan, Dr. Hindy Bronstein, Dr. Yutaka Nishiyama, and – for at least a couple hours into the seminars – Bruce Yu. The jokes, the political arguments, or the science discussions all helped to provide and maintain sanity throughout the years.

I also need to acknowledge my long-term baymate, Dr. Tyler McQuade. Tyler and I saw the collegial sides of each other that most never have (and probably should not see). After long conversations or arguments during chromatography and such, we often found that we stood on the same ground. Always quick with a question or two, he helped to keep me on my toes.

And my past-bay neighbors Karen and Phoebe Kwan need a shout out. They were the first class where I could play the "grandfatherly" senior student role. They provided sunshine and cheer and joy to what used to be an otherwise gloomy environment. I think many older group members were unsure how to deal with the sudden influx of such strong personalities over the past few years.

I am grateful to the patience demonstrated by Dr. Richard Kingsborough and Dr. Anthony Pullen as I started the more electrochemical portions of this thesis. The best way to learn electrochemistry is through trial and error, and they were there to help interpret the initial errors. Hsiao-hua "Bruce," my classmate and fellow electrochemical warrior, also provided an arena to discuss and argue new results.

Aimee Rose, another classmate and the group's "fluorescence god," generously performed the lifetime measurements in Chapter 4 and provided very helpful discussions. I don't know what I would have done if she weren't on such the same wavelength as I am on a variety of scientific and personal issues. Many a late night we've had during post-CpS sessions, and I'll miss those. She marked the entrance of strong assertive women in the group, and I think she's helped to make the lab environment much more enjoyable. Words can't express my thanks, even if she done f---ed up the CpS.

I am indebted to Alex, Karen (K-Ro), Aimee (A-Ro), and Jordan (J-Wo) for proofreading chapters of this thesis. Keep it real and forget about it. And how could I end without a final "heeey," "Really?," or "oooo" to people like Kenichi Kuroda, Dr. Zhengguo Zhu and Dr. Arkadi Vigalok?

Under a MURI grant that funded part of this research, a couple of collaborations developed. I thank Professor Allen J. Bard at UT Austin for allowing me to come to his labs to learn this technique. Dr. Zhifeng Deng provided invaluable experimental help and many late nights trying to align the tip and substrate. Dean DeLongchamp from the Hammond group in Chemical Engineering has also provided a source of cross-talk between disciplines, unfortunately, our multilayering ideas never came to fruition.

I also need to thank Professor Vladimir Bulovic and his group. By sharing common lab and office space, we've learned the basics of device physics from them, and they have gotten some chemistry basics from us. I've probably learned just as much about how to reduce difficult chemical concepts to the lowest common denominator as I have about the forefront of organic optoelectronics.

I also thank the staff in the DCIF, particularly Dr. Jeff Simpson for assistance with 2D pulse sequences. Li Li has also done her best to obtain molecular ion peaks from rather difficult compounds I threw her way. All together they continue to do a great job with the facility. Dr. Bill Davis collected the X-Ray data for the crystal presented in Chapter 2.

Of course, much sanity has been found outside of the lab sphere ... to all, bottoms up until we meet again. The Thanksgiving crew will be welcome to our new place in Chicago for the next few Novembers – I expect Bruce, the Chang's (Michelle and Chris) and Luis Melean to be there, as they've been solid attendees. At the bare minimum, I'll expect Bruce's fried rice. Thanks to the Indian food bunch – Jason Diffendal, Michele Harris and Luis – good reasons to escape for lunch and top the day off with a nap. Luis and Dilia, I owe you big time, not only for the Thursday night hospitality but for opening your homes in Venezuela over several trips. Luis also served as an important catalyst.

There is one more person who I ordinarily would have lumped into the last paragraph had it not been for the aforementioned catalytic activity: Melissa Da. Even though I may not always acknowledge it in the most serious way, I am touched and deeply grateful for all you have done to help keep me on track over these past few months ... above and beyond the already high background signal. I think her joy of cooking came in handy as she carefully proofread this thesis, even the experimentals! I only hope that I can return the favor to the extent you have done for me. Just as long as we can keep the policy rolling, the next couple years will fly by ... even with the early morning wake-up calls. Moving to a new city will be exciting, and it will only make us closer and more strong. I have no doubts that your worth will shine through to any school library out there - it definitely has for me.

Finally, I would like to thank my family. My mom, Dianne, my dad, John, and my sisters Sarah and Jessica, have been there through thick and thin, constantly offering to proofread papers if I so needed. I have yet to take them up on this. The sacrifices my parents made to ensure that we had the best opportunities available have definitely paid off for all of us. I could not have made it without knowing that my family was standing behind me. It is for their love and support that I dedicate this thesis to them.

Appendices

Appendix 1:

^{1}H and ^{13}C NMR spectra for Chapter 1

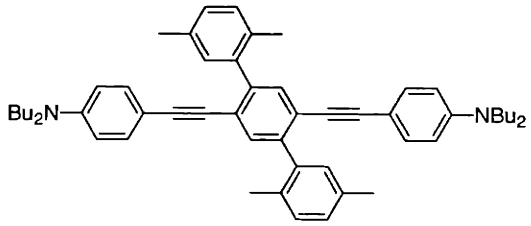

1

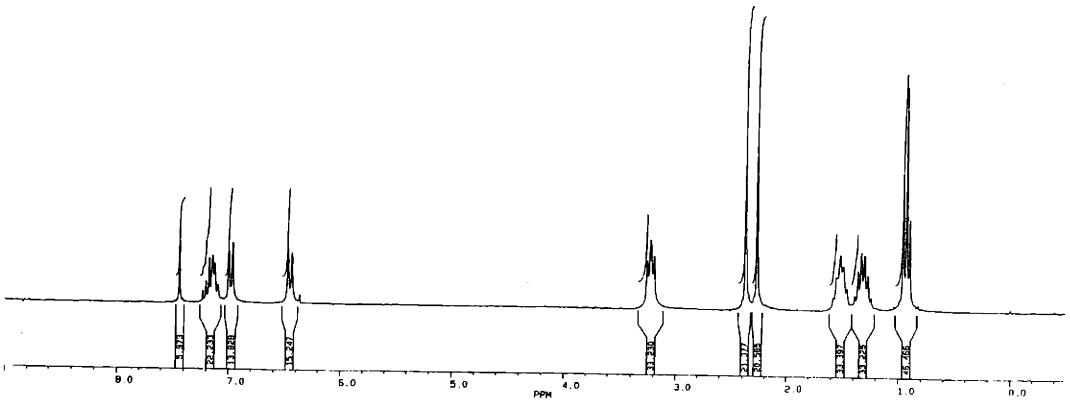

^{1}H NMR of **1** (250 MHz, $CDCl_3$)

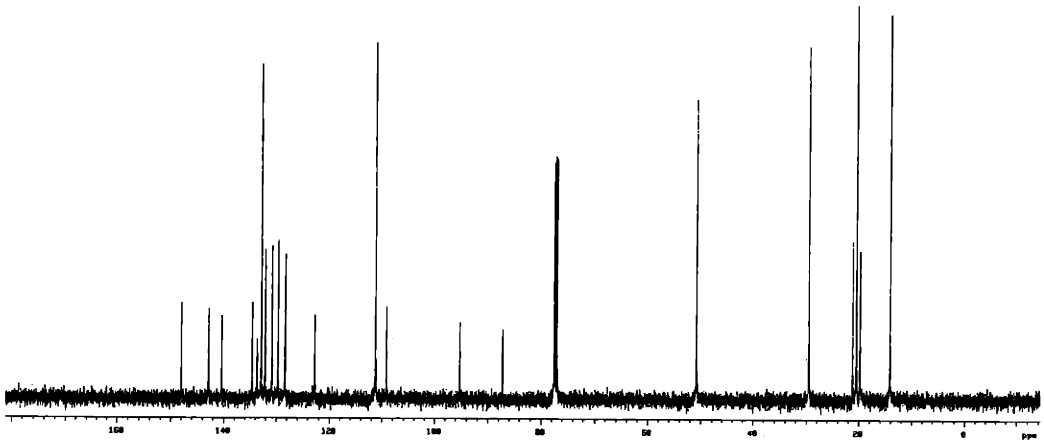

^{13}C NMR of **1** (125 MHz, $CDCl_3$)

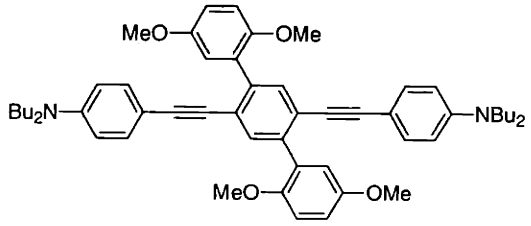

2

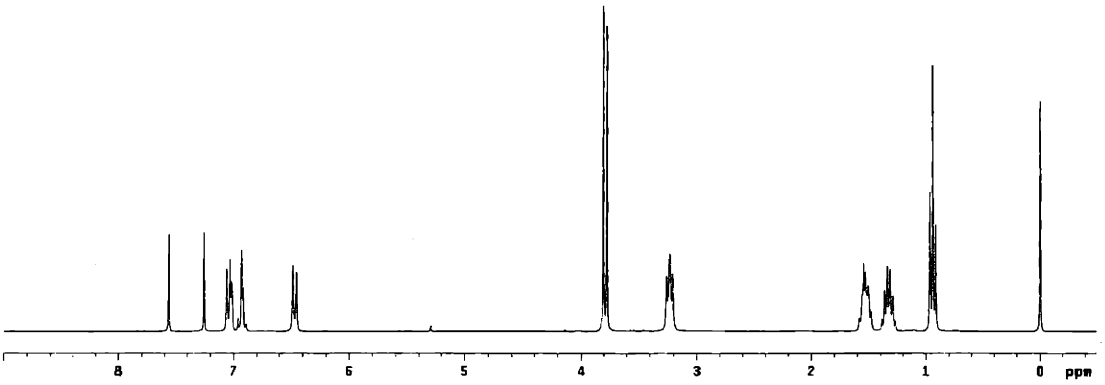

^{1}H NMR of **2** (300 MHz, $CDCl_3$)

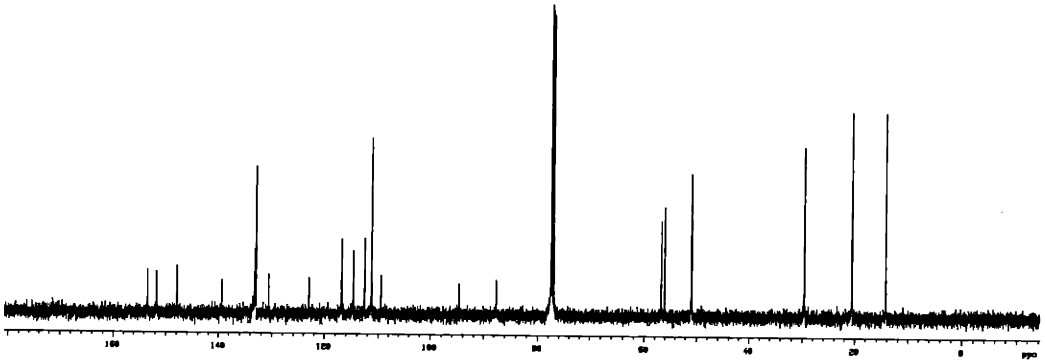

^{13}C NMR of **2** (125 MHz, $CDCl_3$)

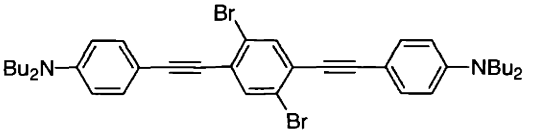

4

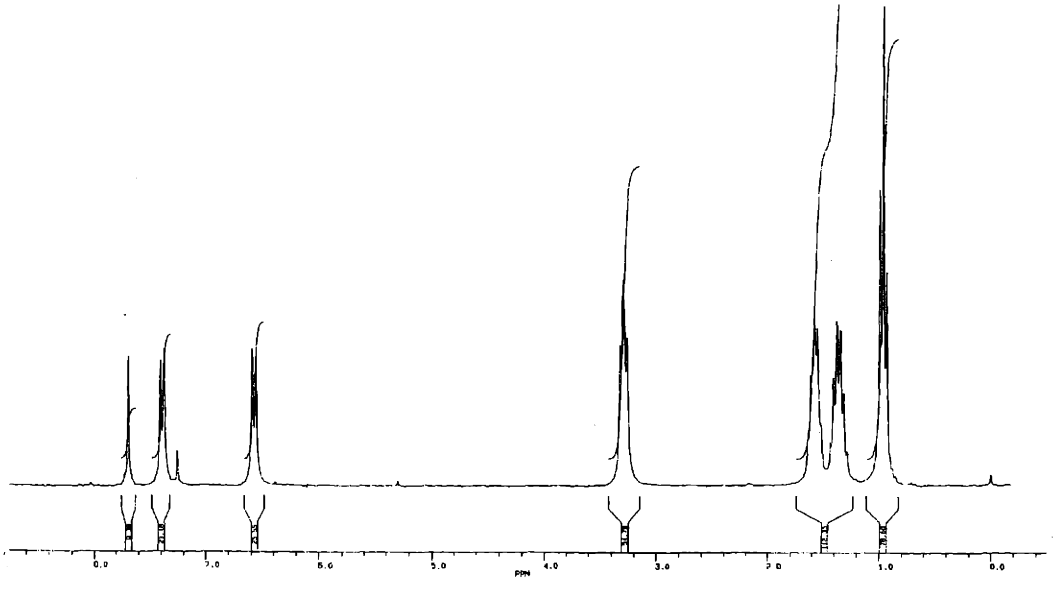

^{1}H NMR of **4** (250 MHz, $CDCl_3$)

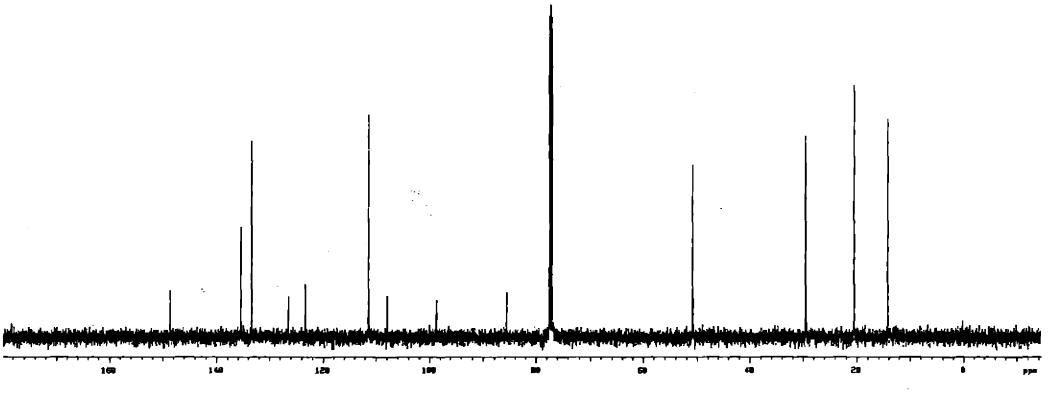

^{13}C NMR of **4** (125 MHz, $CDCl_3$)

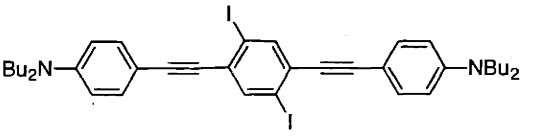

5

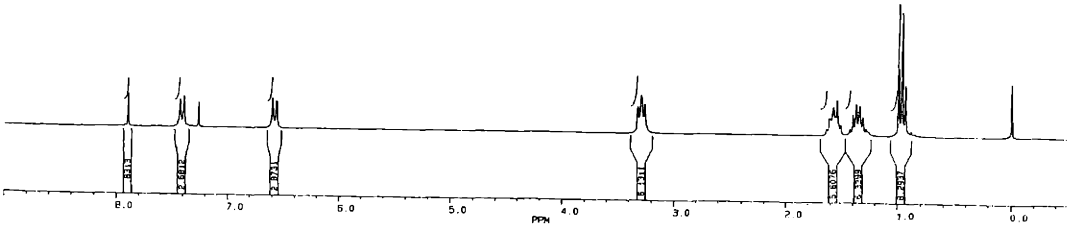

^{1}H NMR of **5** (250 MHz, $CDCl_3$)

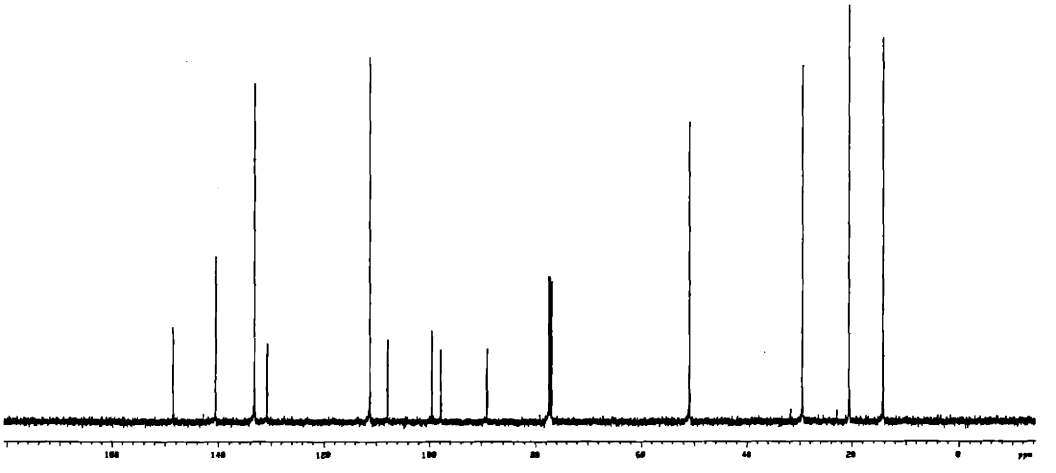

^{13}C NMR of **5** (125 MHz, $CDCl_3$)

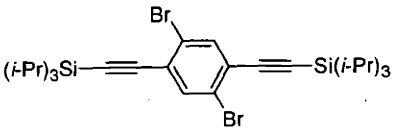

6

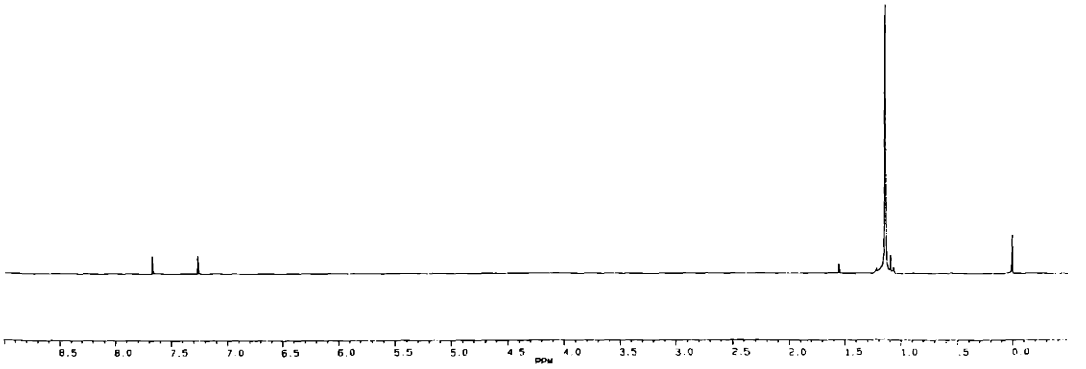

^{1}H NMR of **6** (250 MHz, $CDCl_3$)

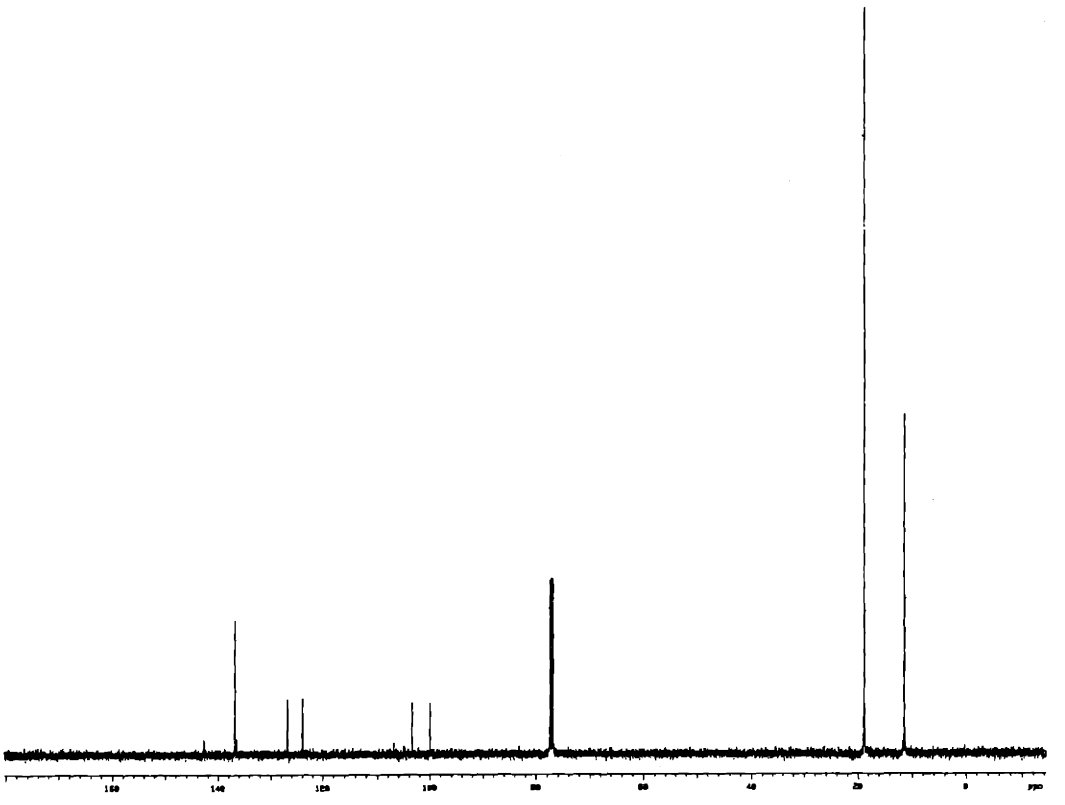

^{13}C NMR of **6** (125 MHz, $CDCl_3$)

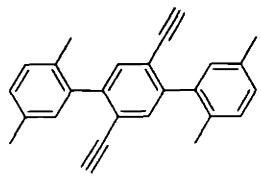

7

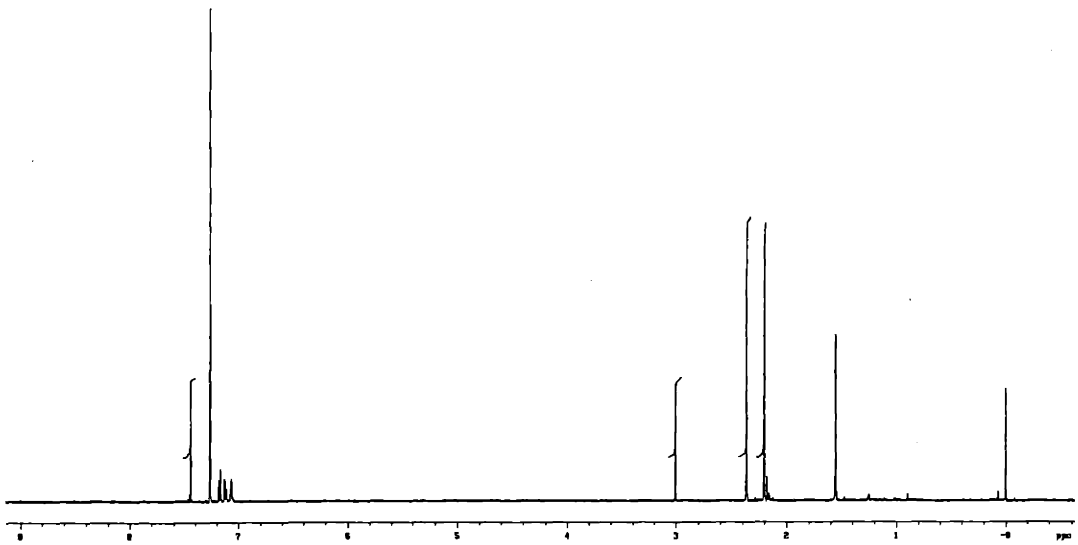

^{1}H NMR of **7** (300 MHz, $CDCl_3$)

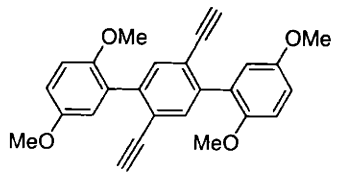

8

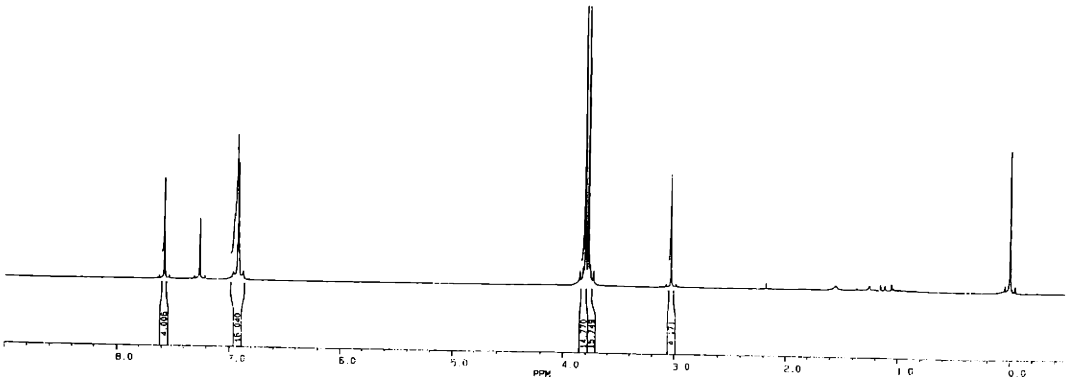

^{1}H NMR of **8** (250 MHz, $CDCl_3$)

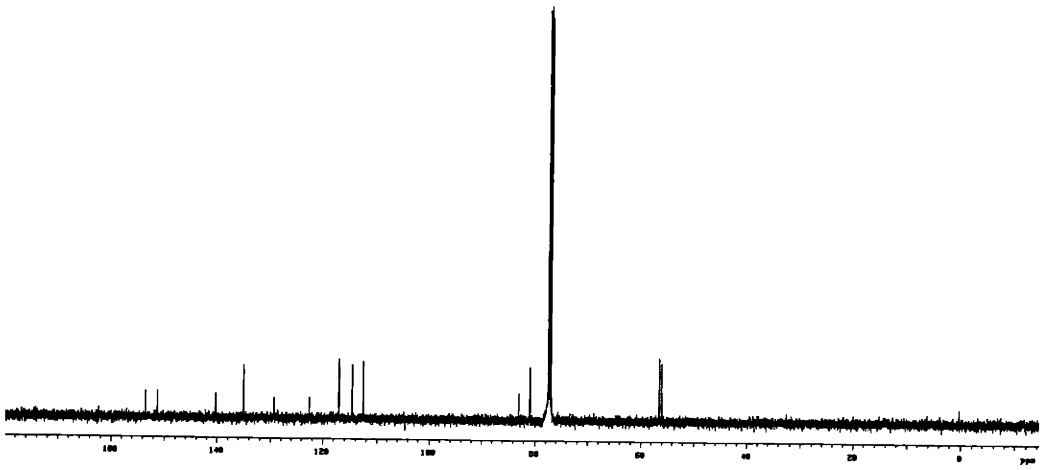

^{13}C NMR of **8** (125 MHz, $CDCl_3$)

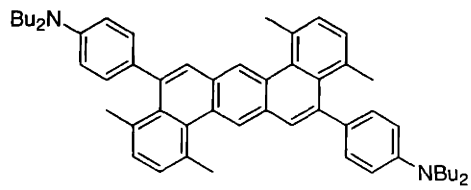

9

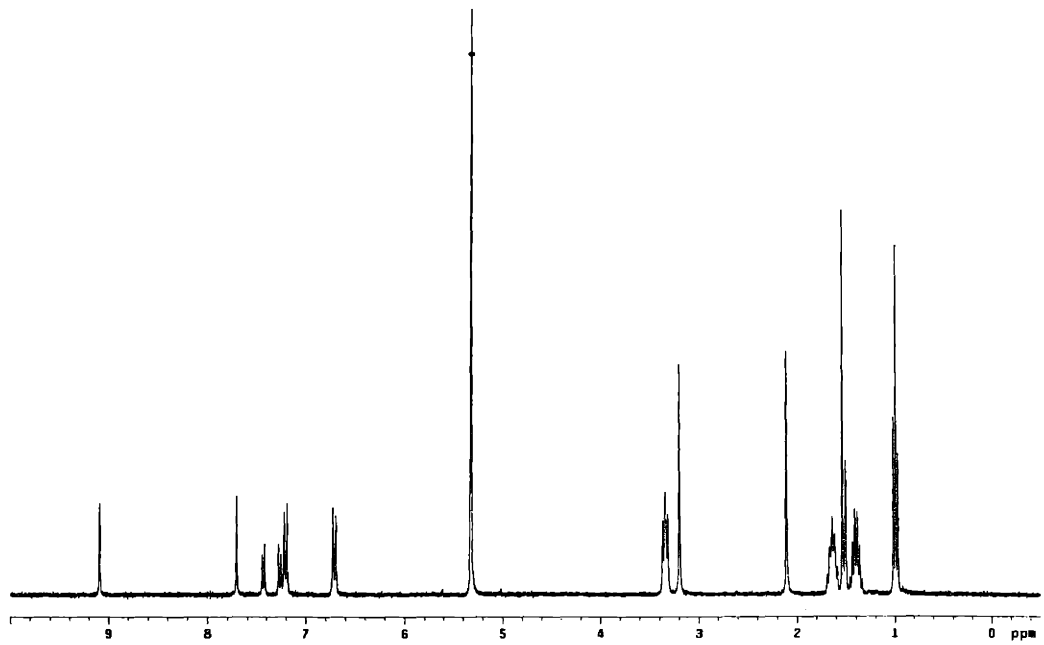

^{1}H NMR of **9** (300 MHz, CD_2Cl_2)

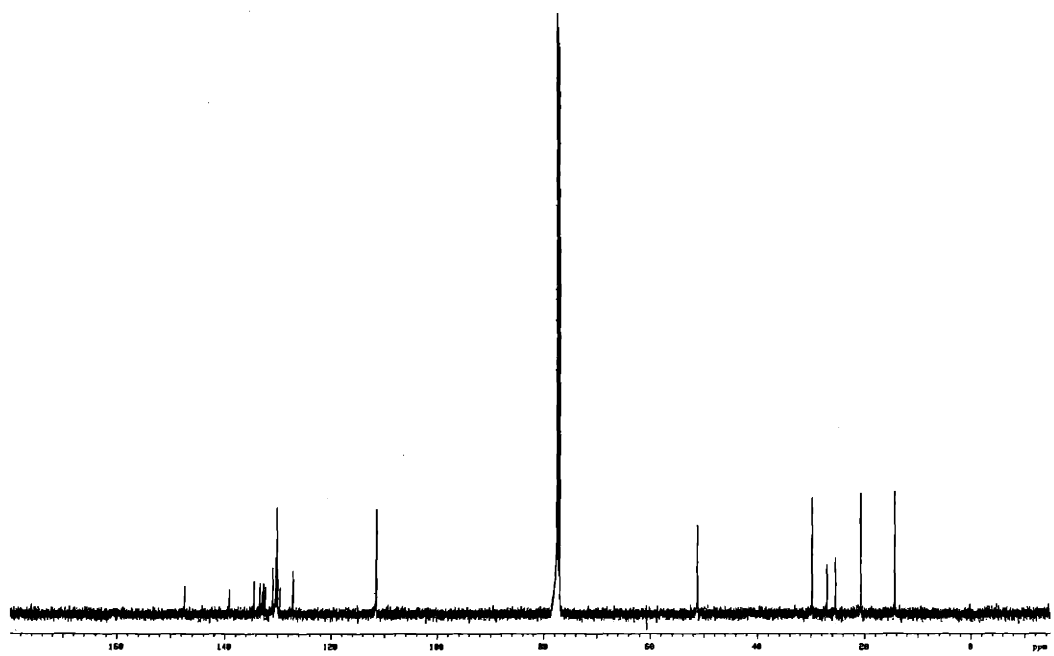

^{13}C NMR of **9** (125 MHz, $CDCl_3$)

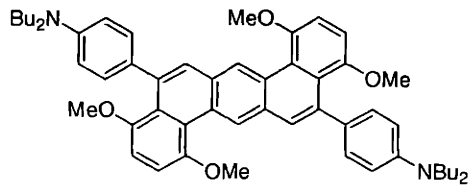

10

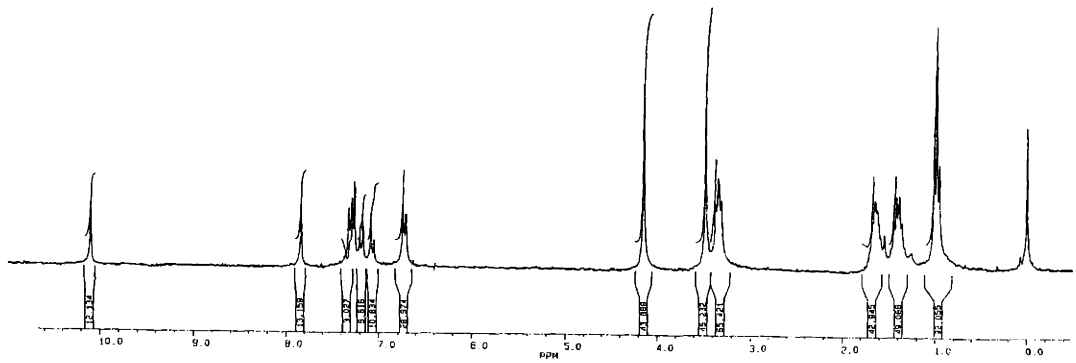

^{1}H NMR of **10** (250 MHz, $CDCl_3$)

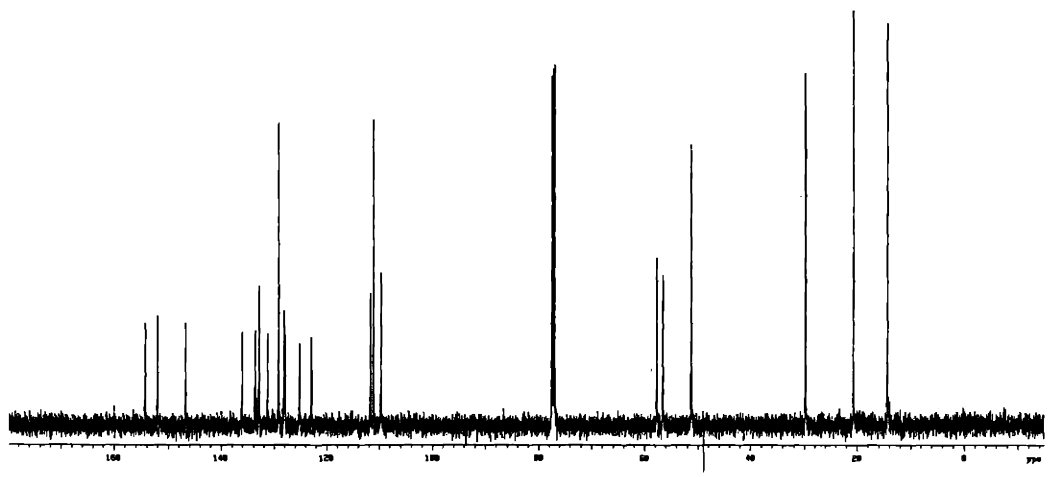

^{13}C NMR of **10** (125 MHz, $CDCl_3$)

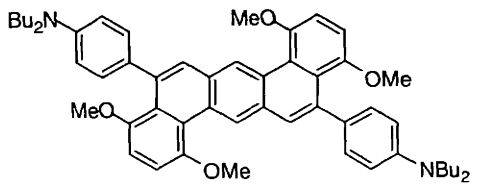

10

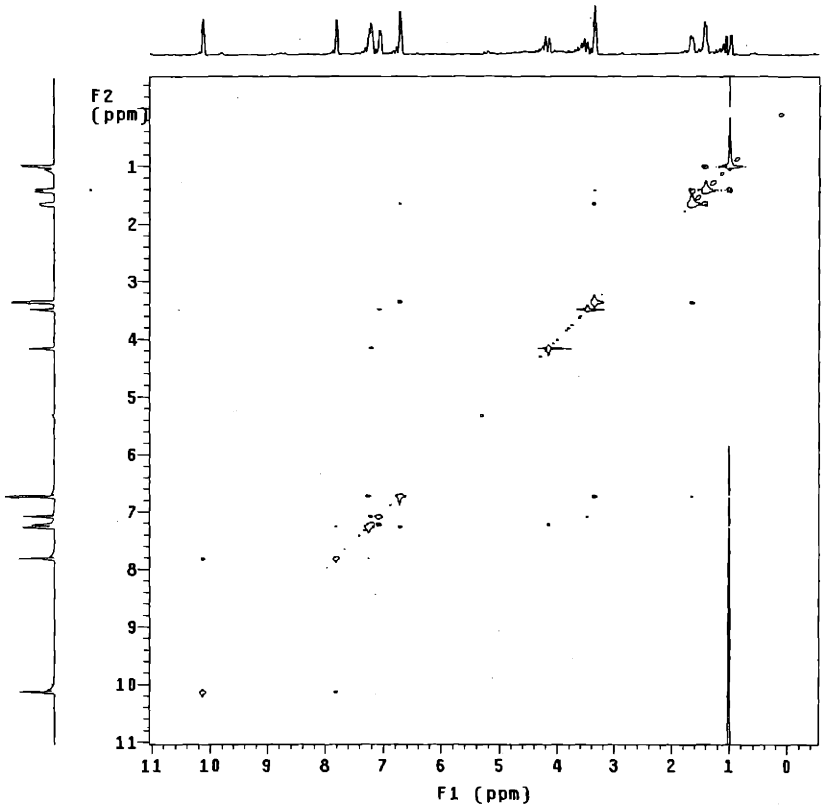

ROESY of **10** (500 MHz, CD_2Cl_2)

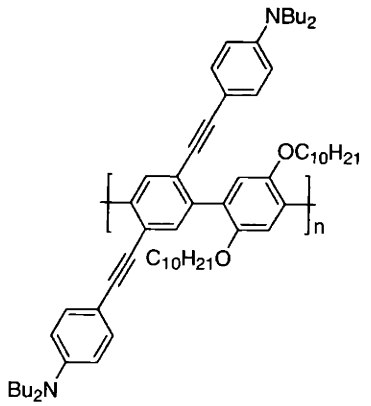

11

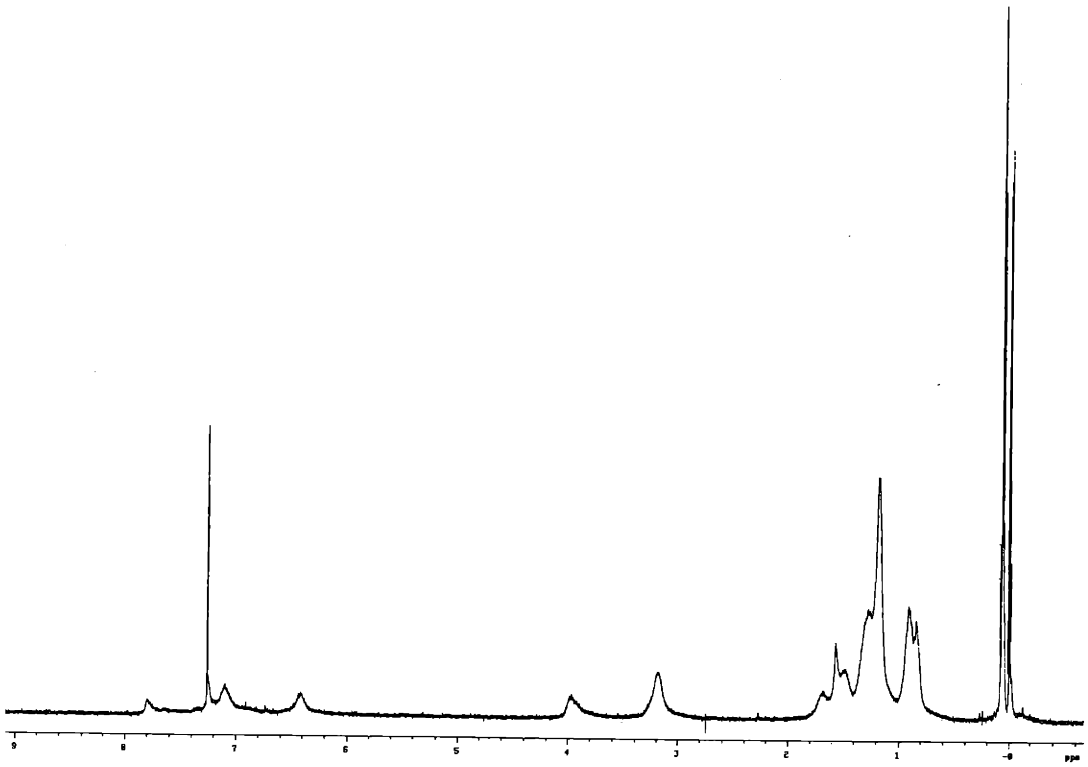

^{1}H NMR of **11** (300 MHz, $CDCl_3$)

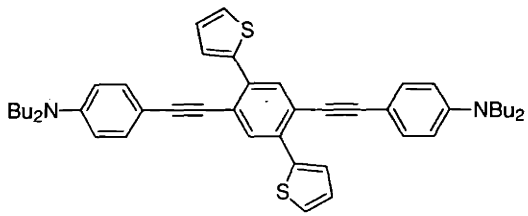

12

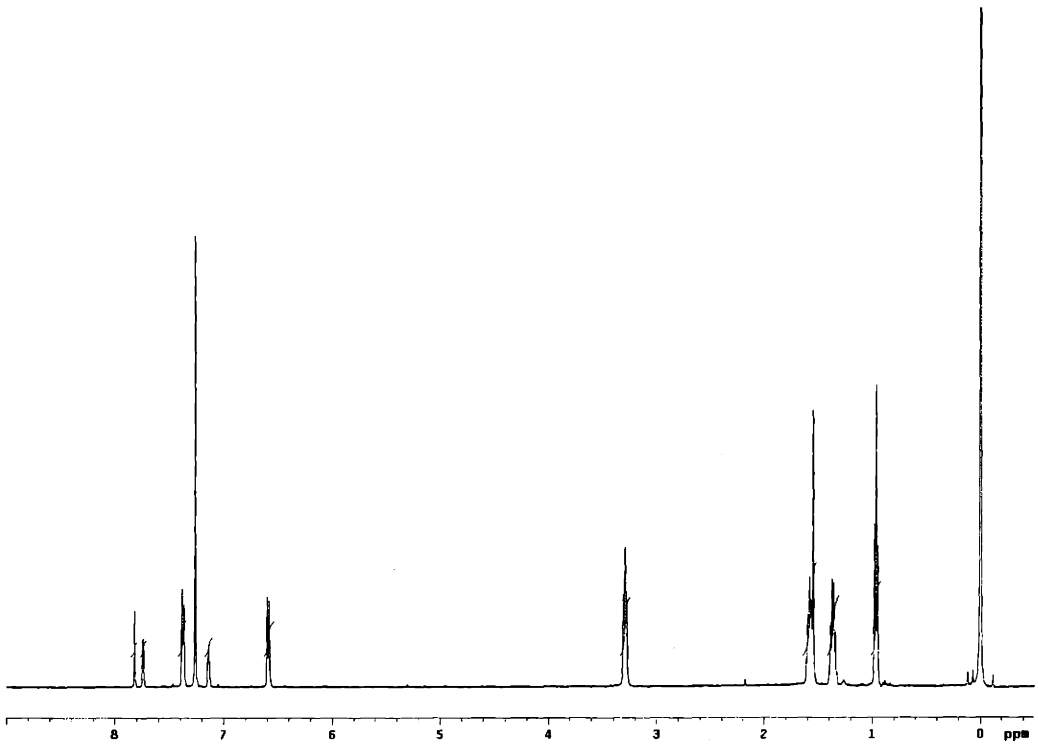

^{1}H NMR of **12** (500 MHz, $CDCl_3$)

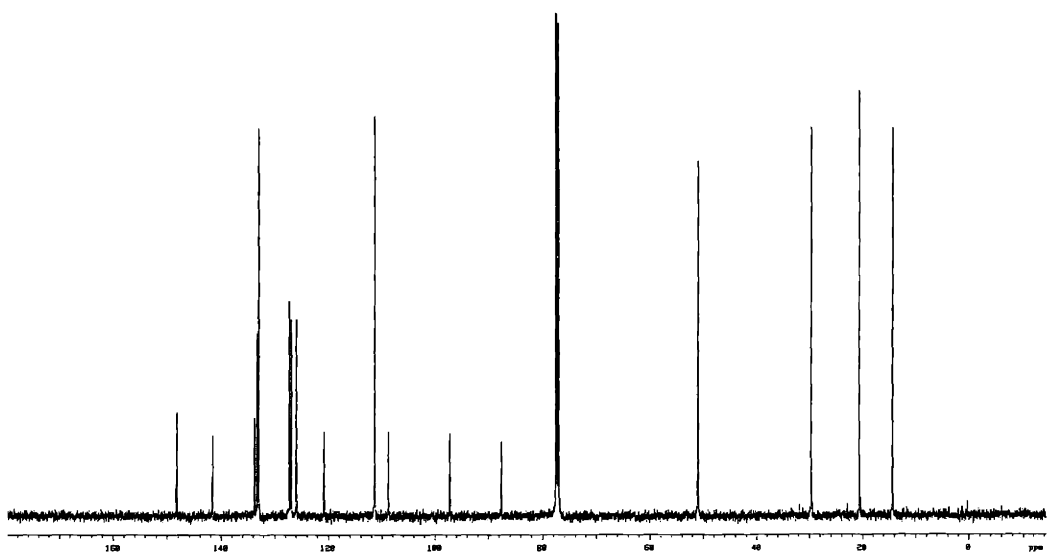

^{13}C NMR of **12** (125 MHz, $CDCl_3$)

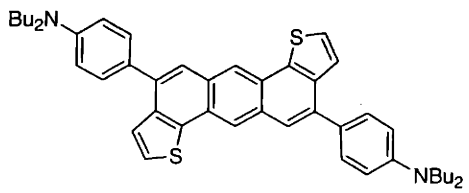

13

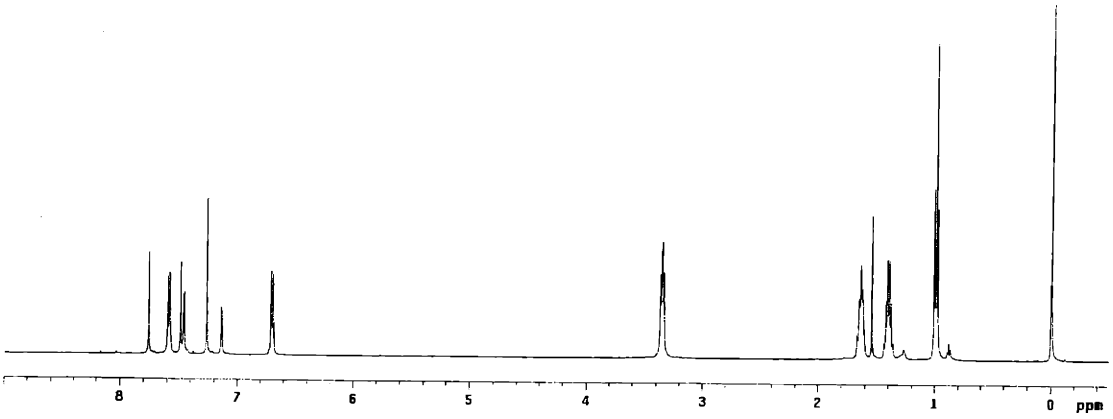

^{1}H NMR of **13** (500 MHz, $CDCl_3$)

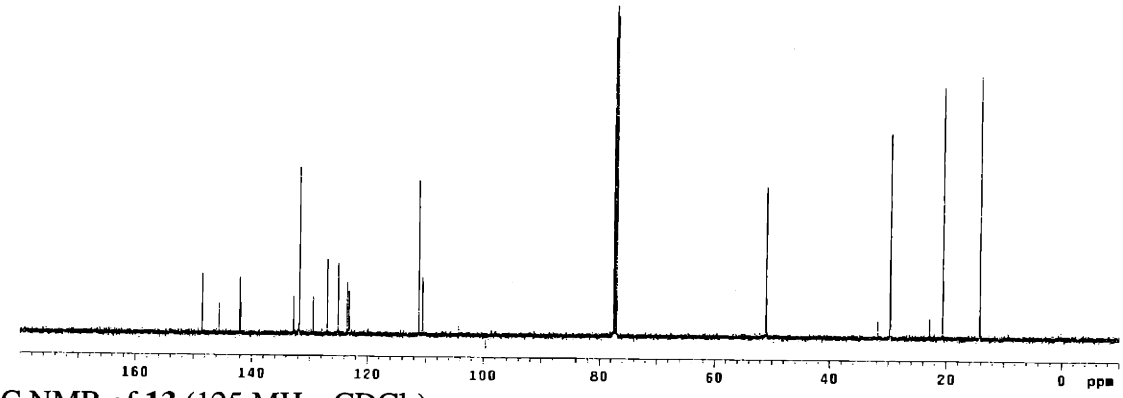

^{13}C NMR of **13** (125 MHz, $CDCl_3$)

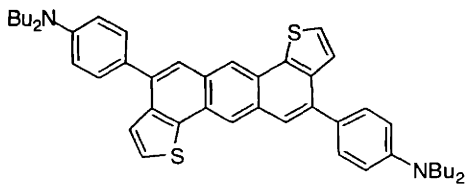

13

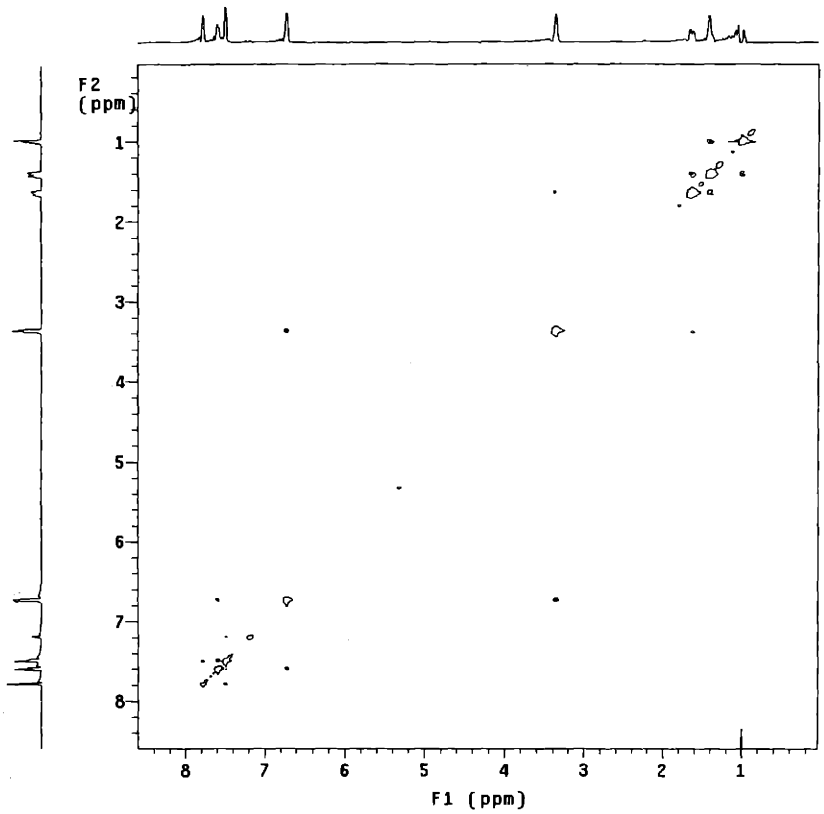

ROESY of **13** (500 MHz, CD_2Cl_2)

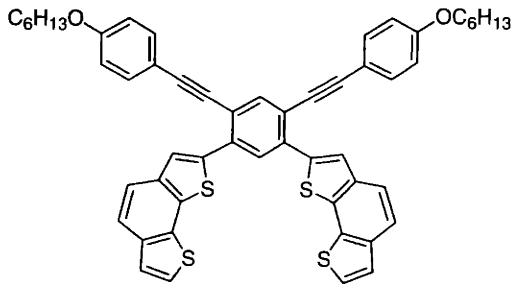

18

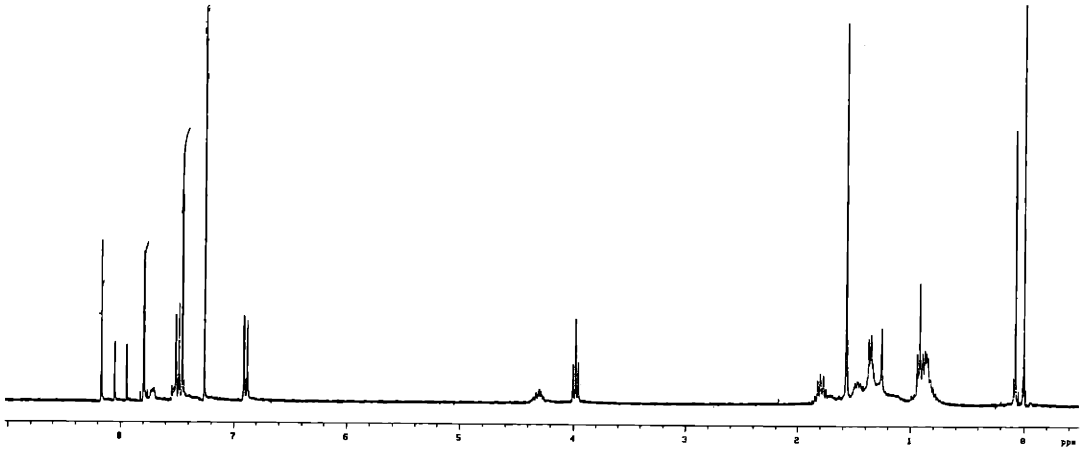

^{1}H NMR of **18** (300 MHz, $CDCl_3$)

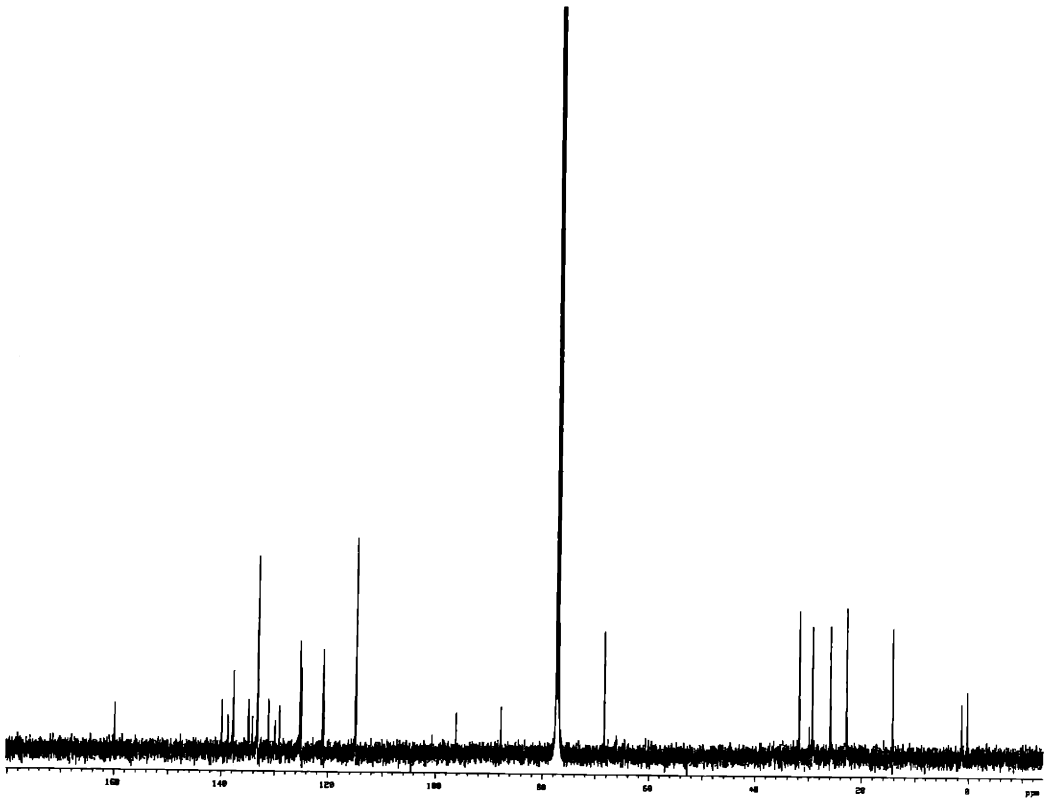

^{13}C NMR of **18** (125 MHz, $CDCl_3$)

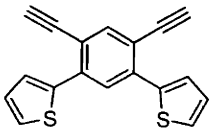

19

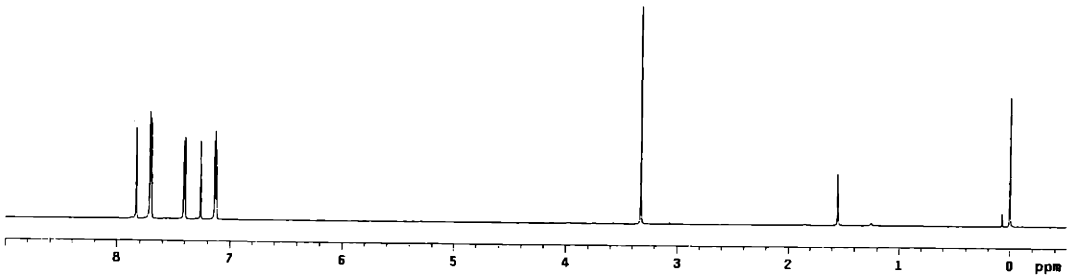

^{1}H NMR of **19** (500 MHz, $CDCl_3$)

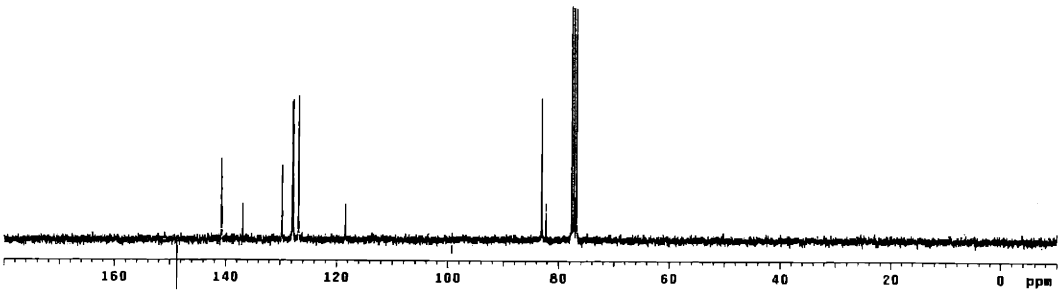

^{13}C NMR of **19** (75 MHz, $CDCl_3$)

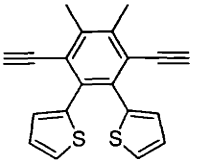

20

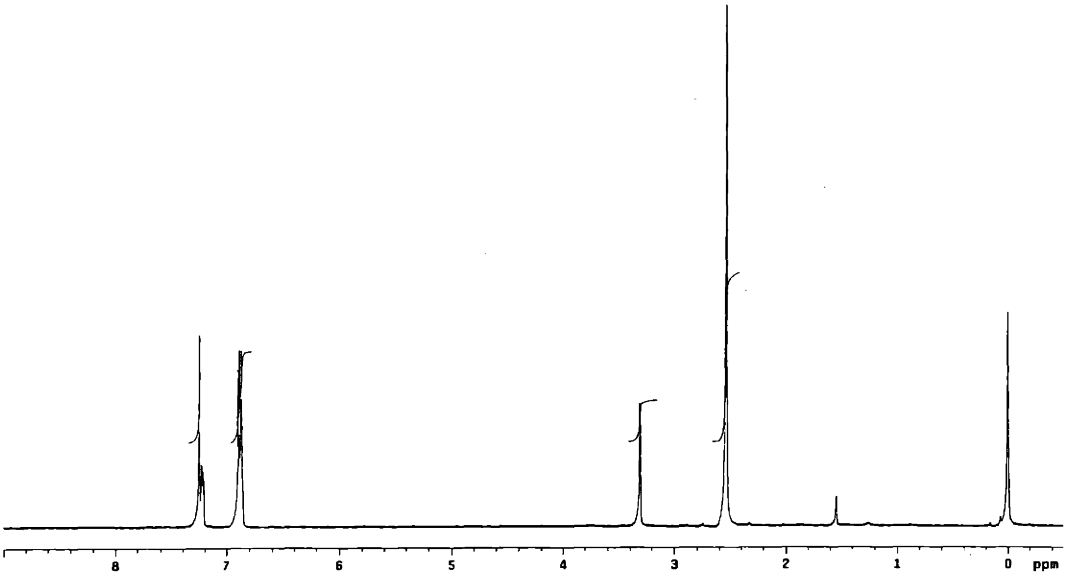

^{1}H NMR of **20** (300 MHz, $CDCl_3$)

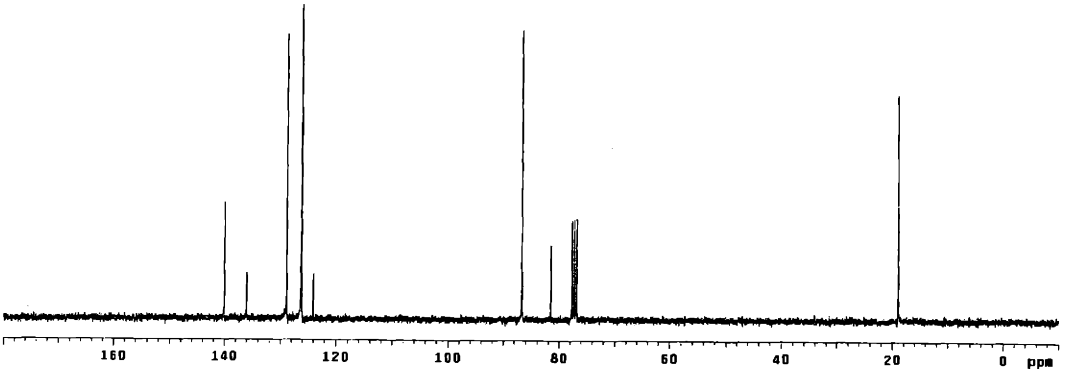

^{13}C NMR of **20** (75 MHz, $CDCl_3$)

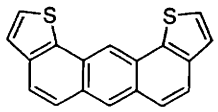

23

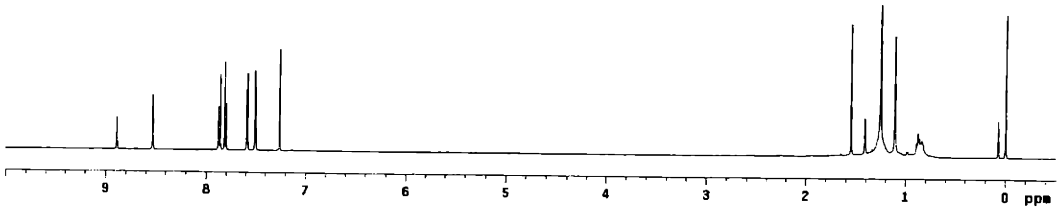

^{1}H NMR of **23** (500 MHz, $CDCl_3$)

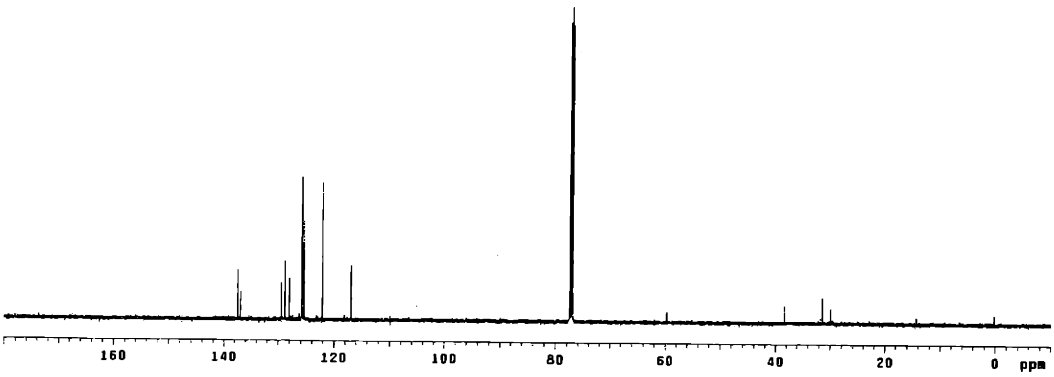

^{13}C NMR of **23** (125 MHz, $CDCl_3$)

Appendix 2:

^{1}H and ^{13}C NMR spectra for Chapter 2

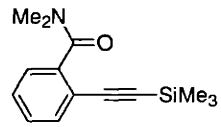

1a

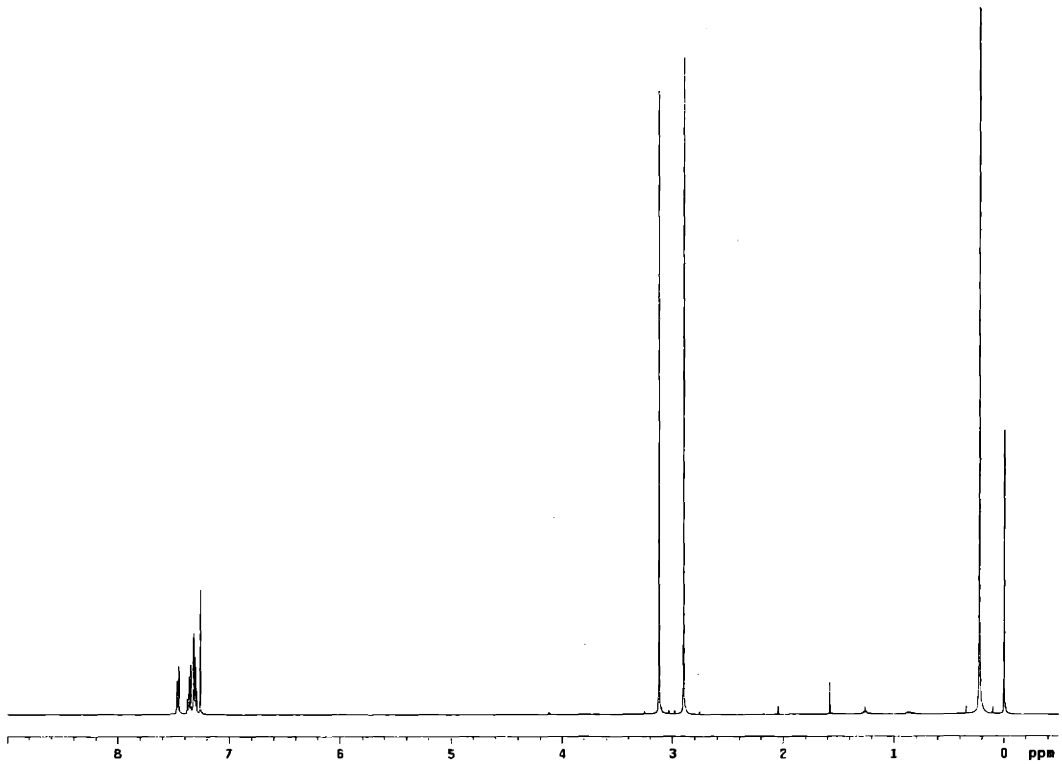

^{1}H NMR of **1a** (500 MHz, $CDCl_3$)

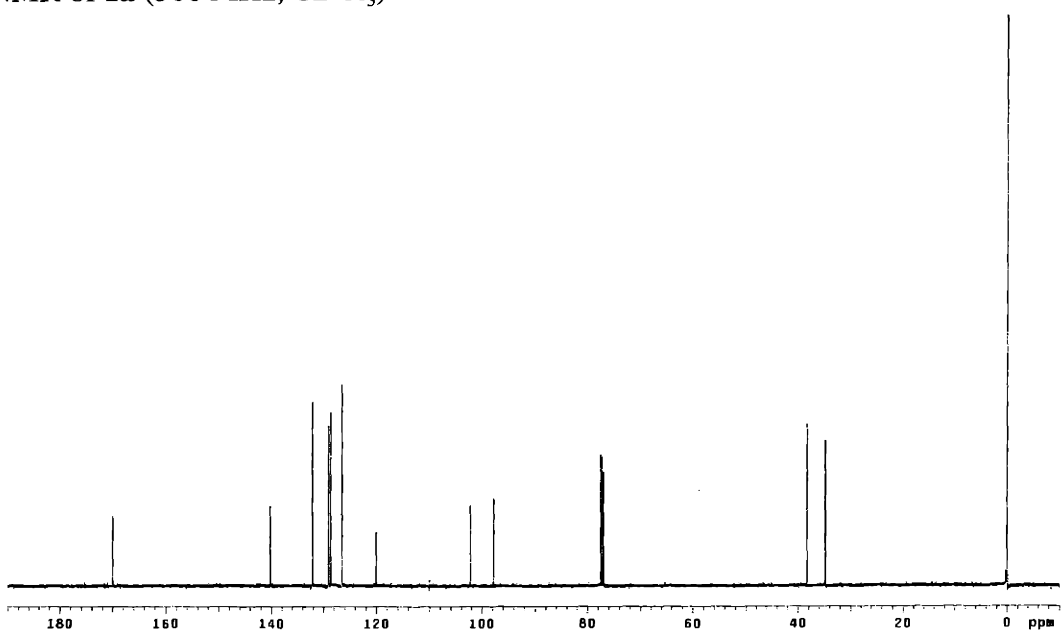

^{13}C NMR of **1a** (125 MHz, $CDCl_3$)

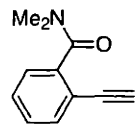

1b

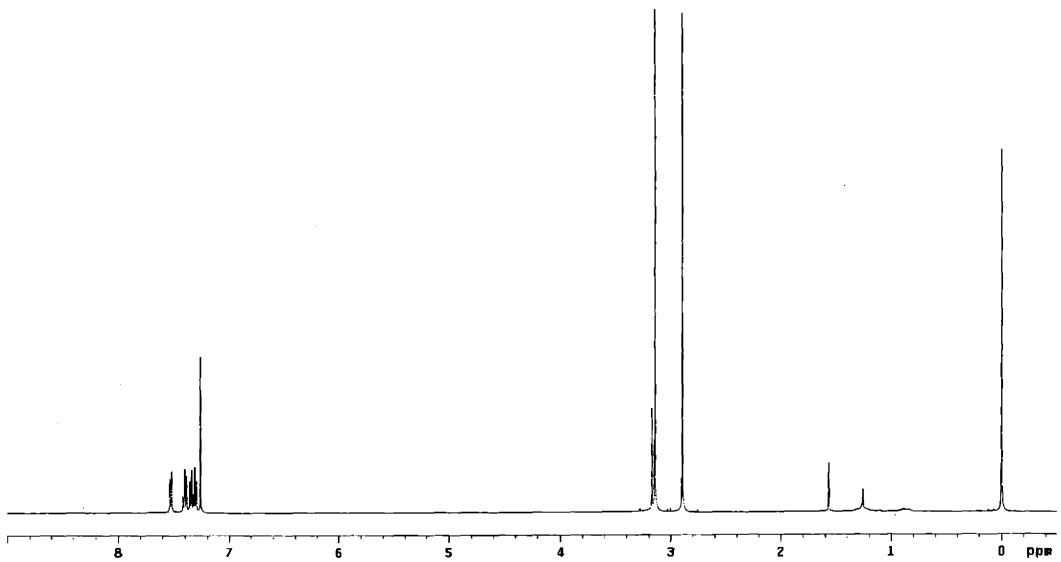

^{1}H NMR of **1b** (500 MHz, $CDCl_3$)

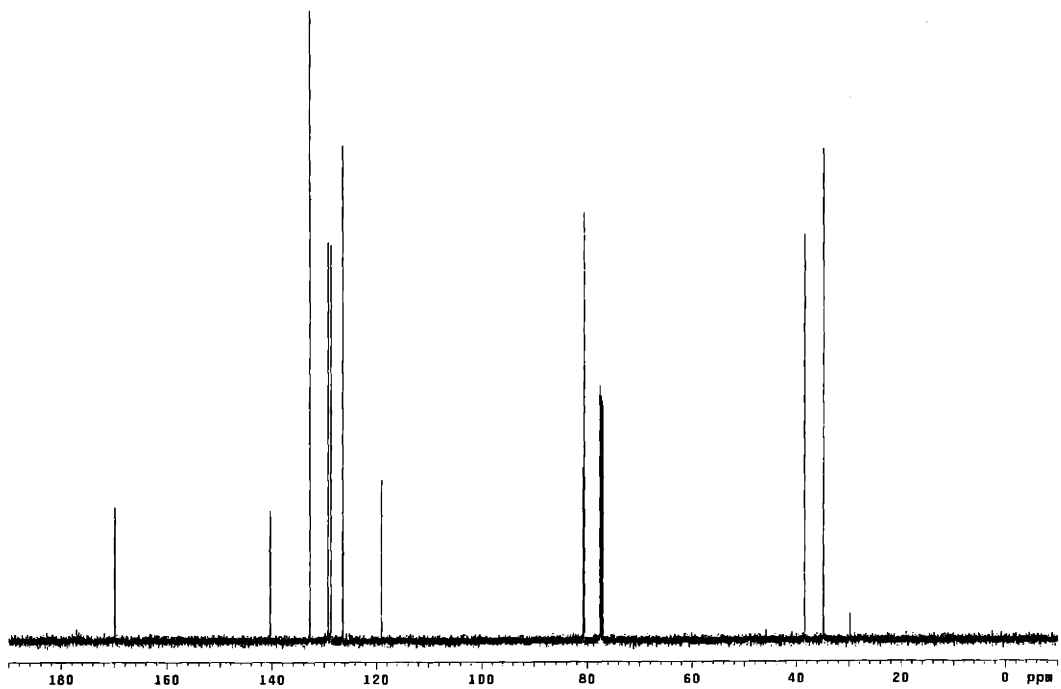

^{13}C NMR of **1b** (125 MHz, $CDCl_3$)

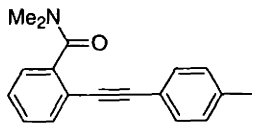

1d

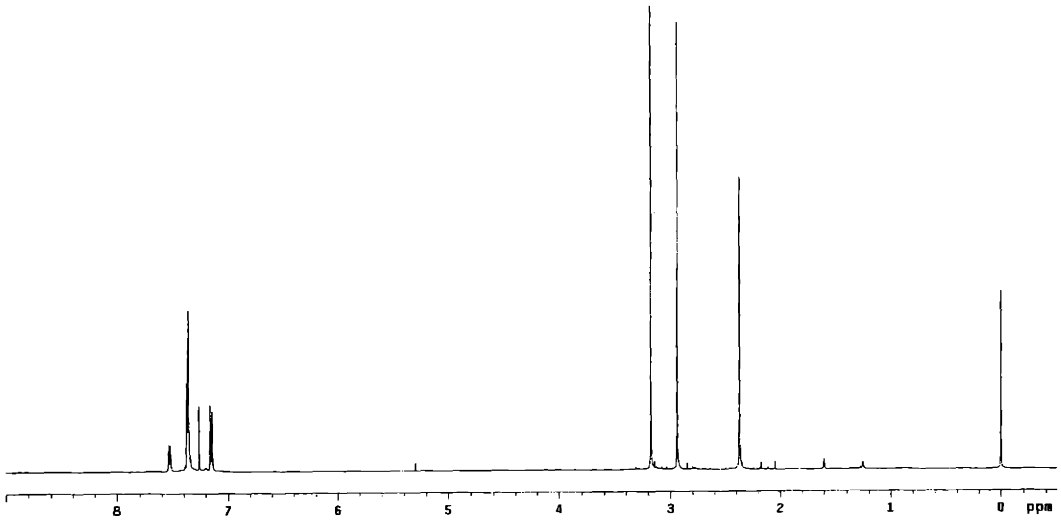

^{1}H NMR of **1d** (500 MHz, $CDCl_3$)

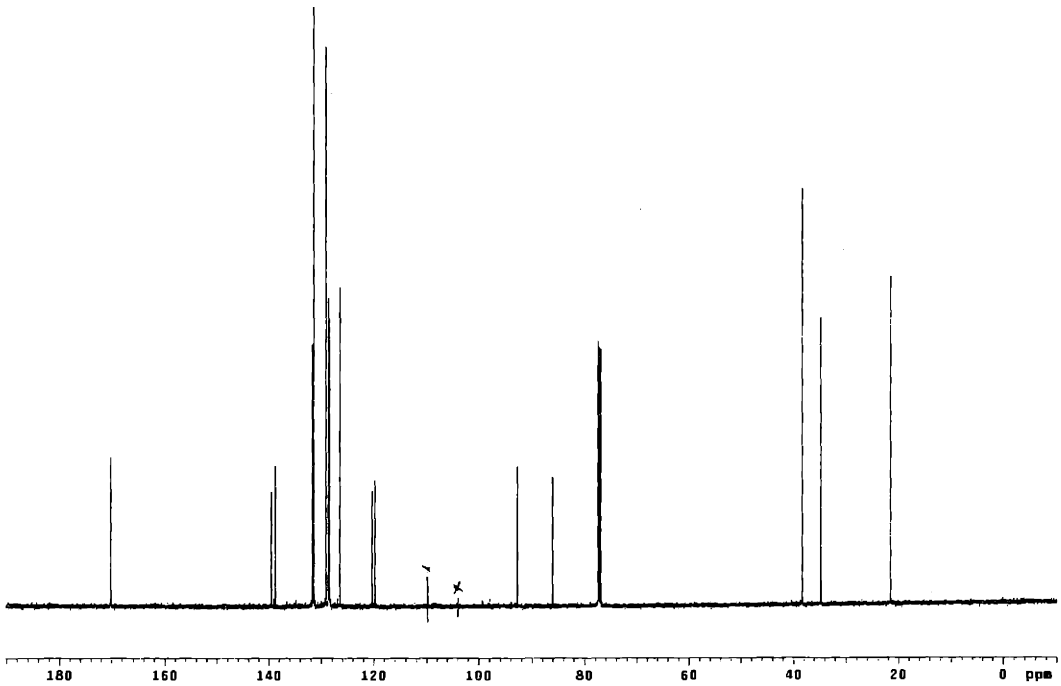

^{13}C NMR of **1d** (125 MHz, $CDCl_3$)

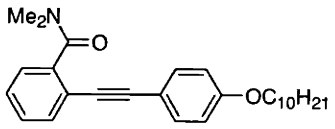

1e

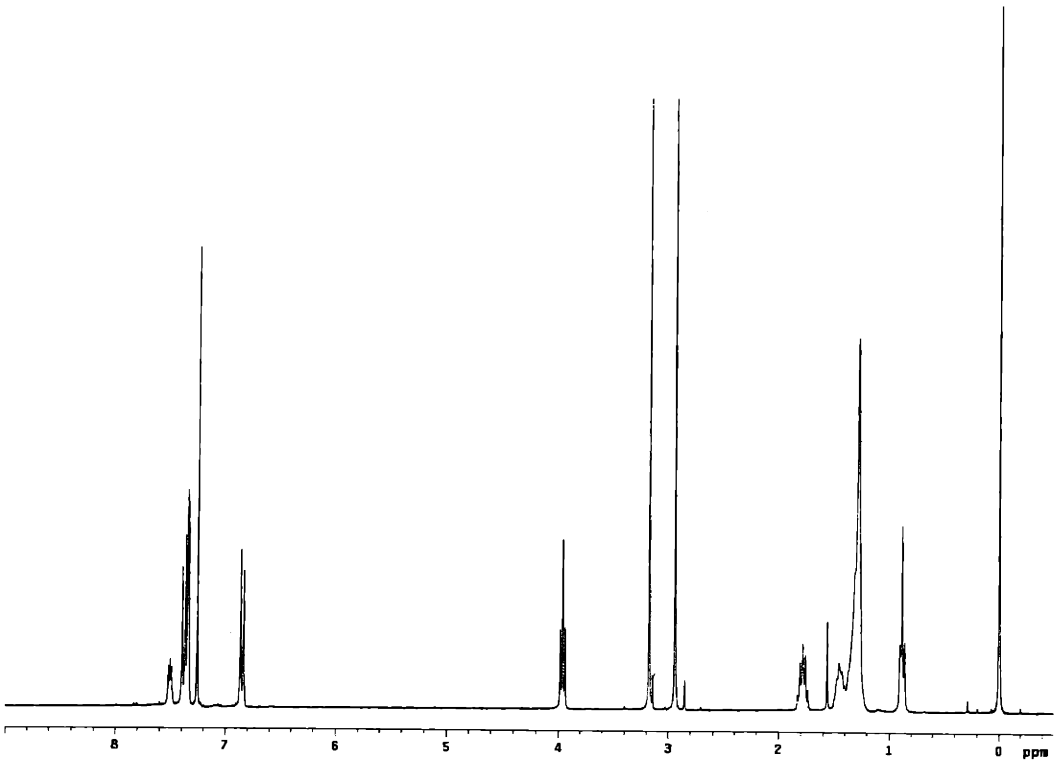

^{1}H NMR of **1e** (300 MHz, $CDCl_3$)

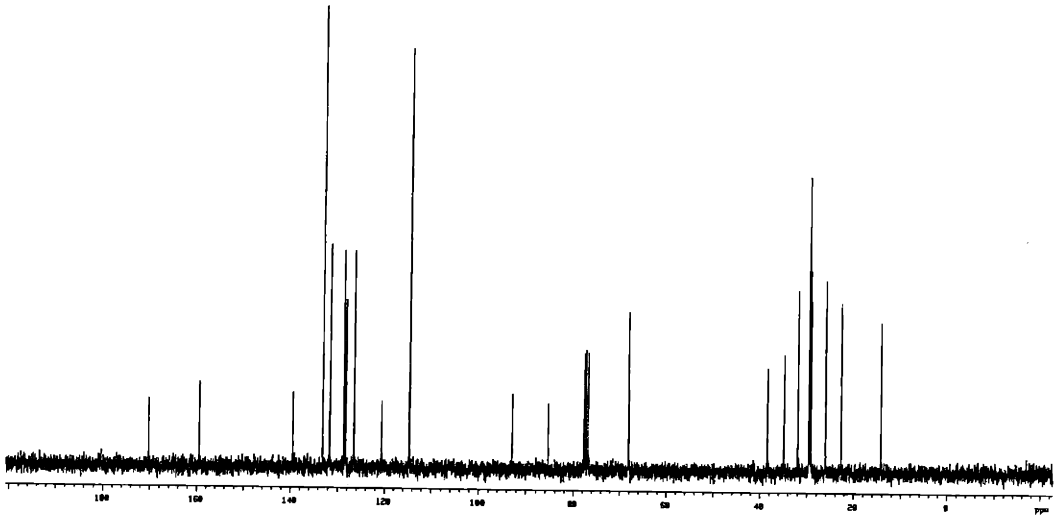

^{13}C NMR of **1e** (75 MHz, $CDCl_3$)

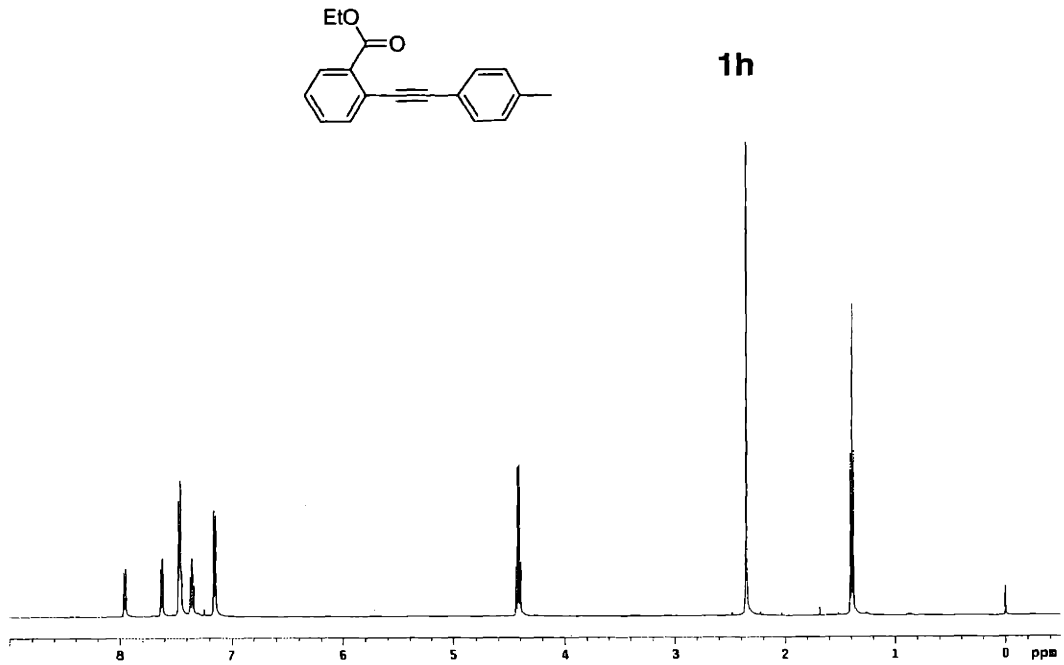

^{1}H NMR of **1h** (500 MHz, $CDCl_3$)

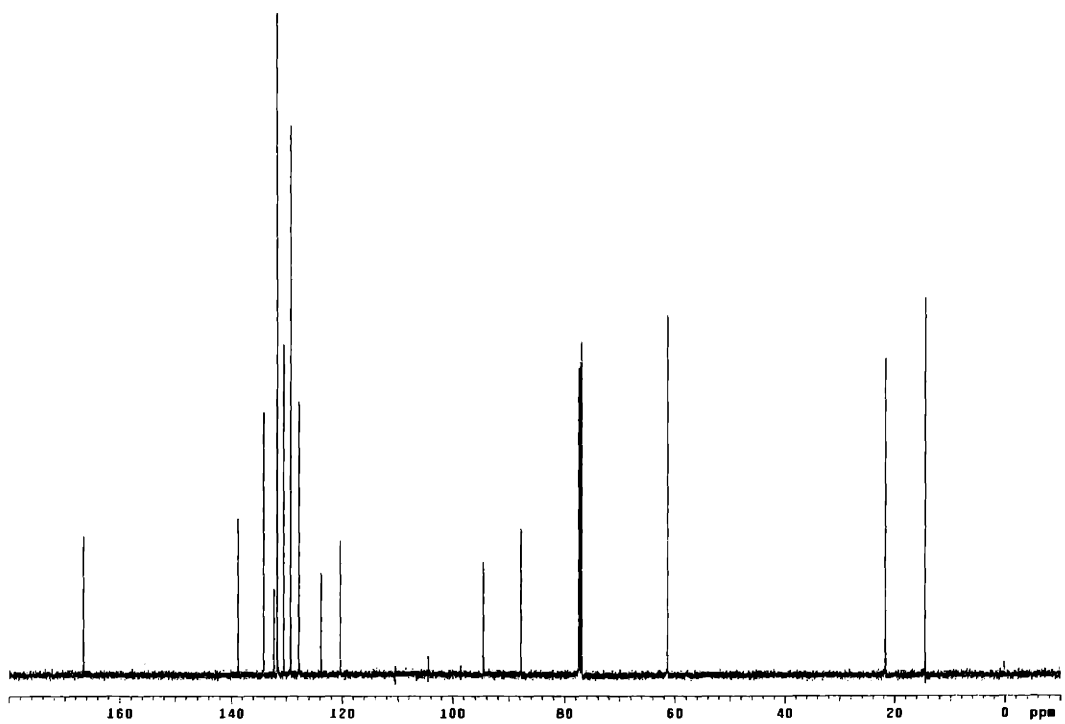

^{13}C NMR of **1h** (125 MHz, $CDCl_3$)

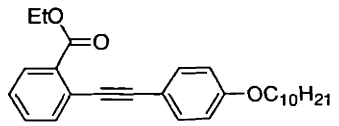

1i

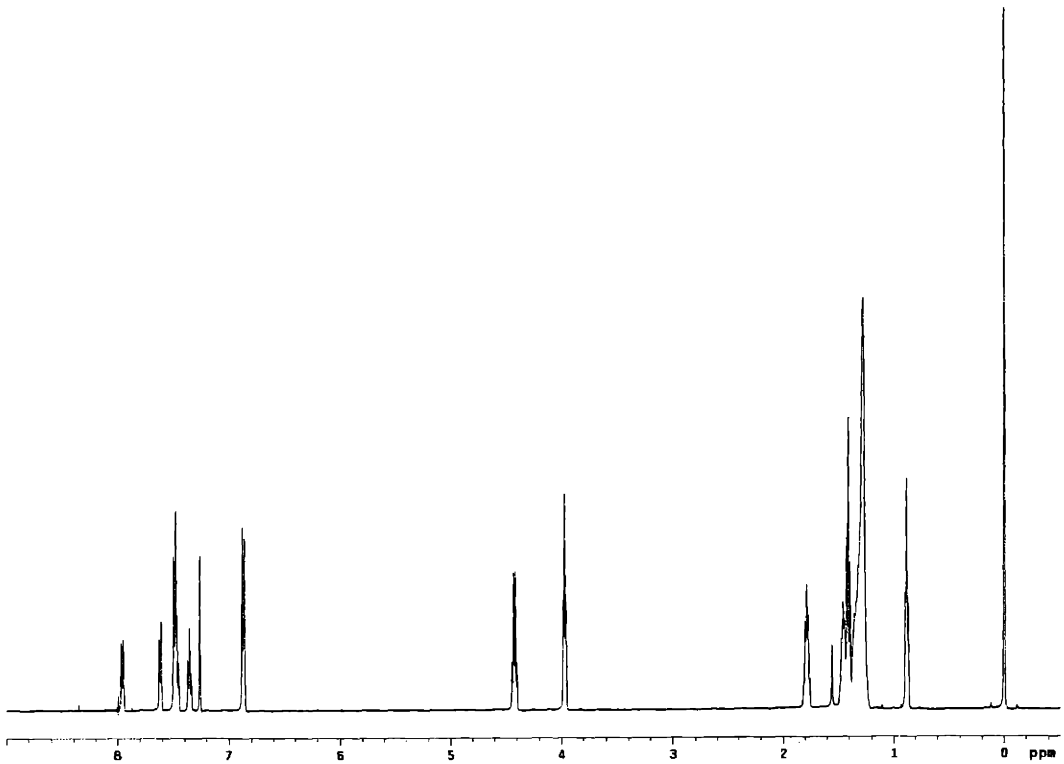

^{1}H NMR of **1i** (500 MHz, $CDCl_3$)

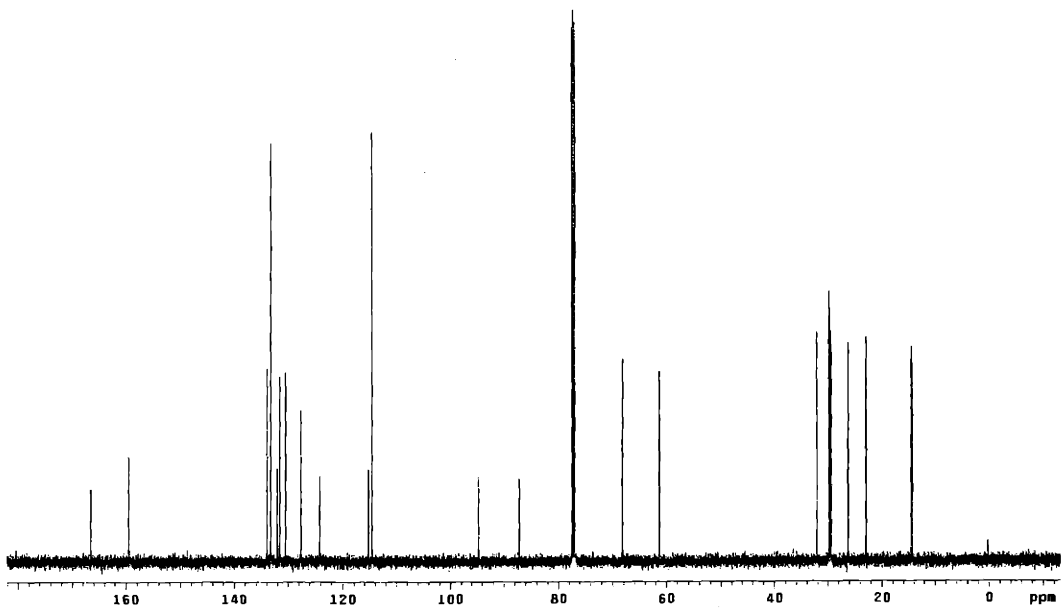

^{13}C NMR of **1i** (125 MHz, $CDCl_3$)

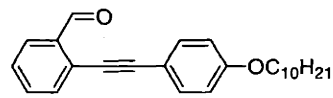

1m

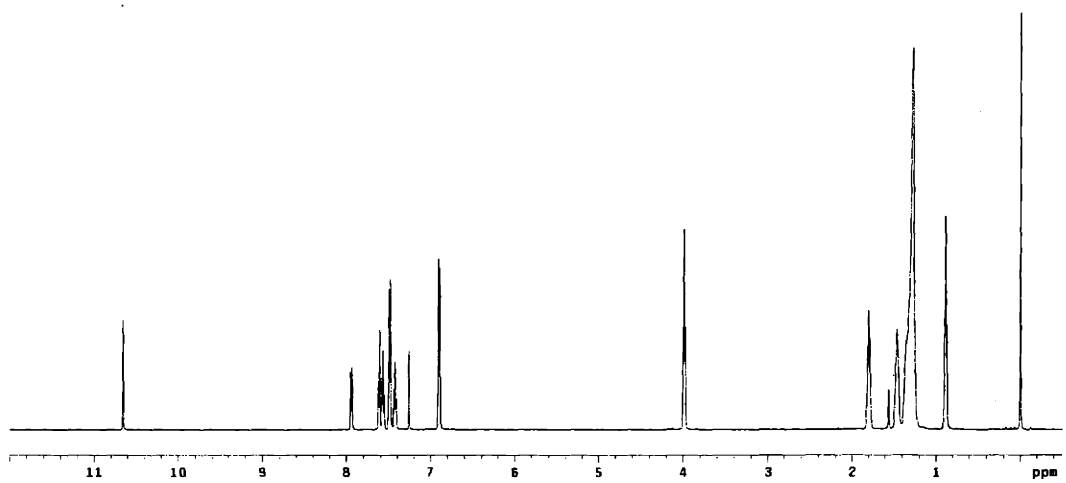

^{1}H NMR of **1m** (500 MHz, $CDCl_3$)

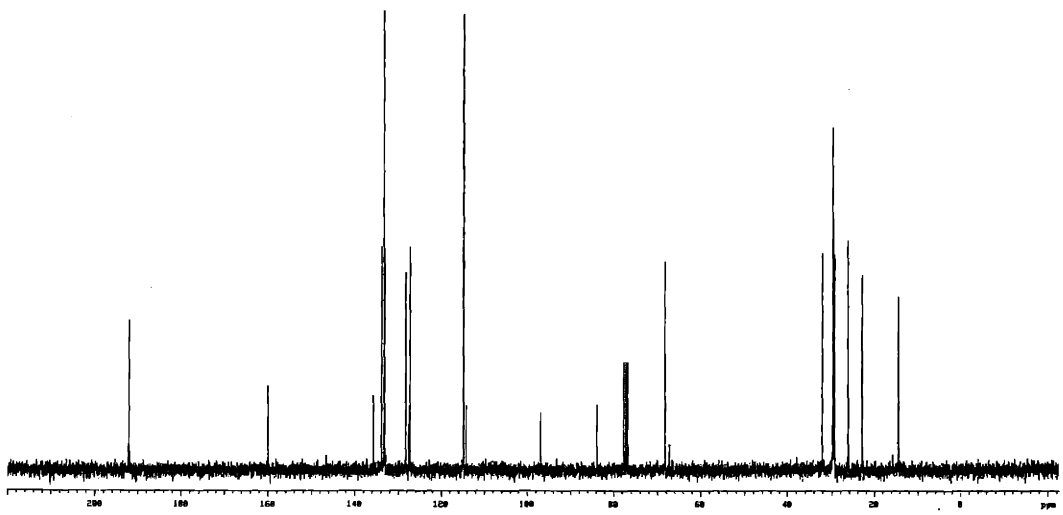

^{13}C NMR of **1m** (75 MHz, $CDCl_3$)

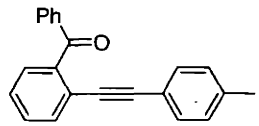

1o

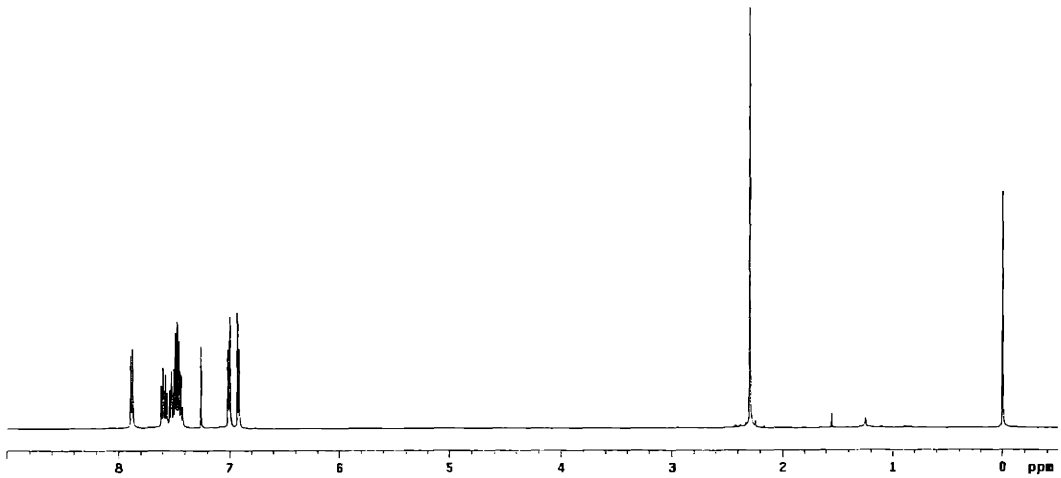

^{1}H NMR of **1o** (500 MHz, $CDCl_3$)

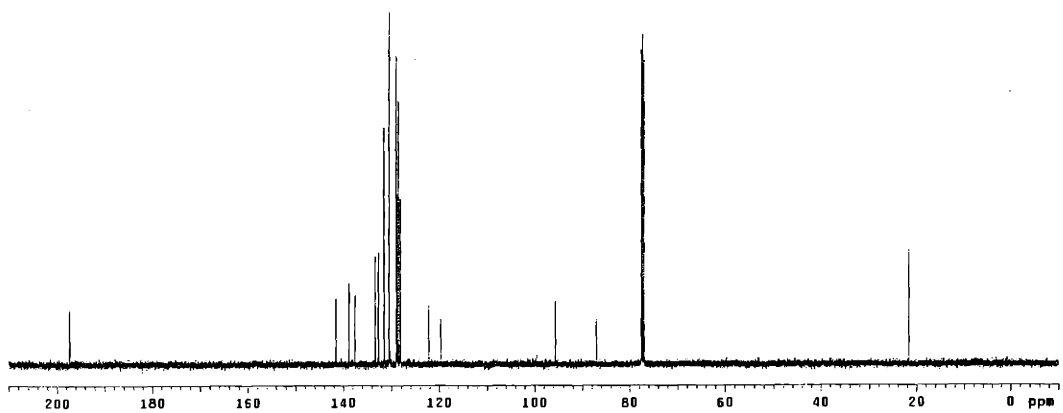

^{13}C NMR of **1o** (125 MHz, $CDCl_3$)

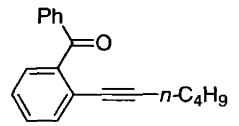

1p

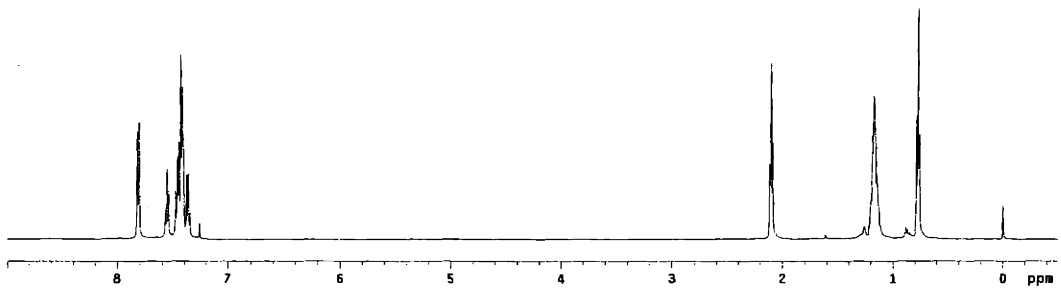

^{1}H NMR of **1p** (500 MHz, $CDCl_3$)

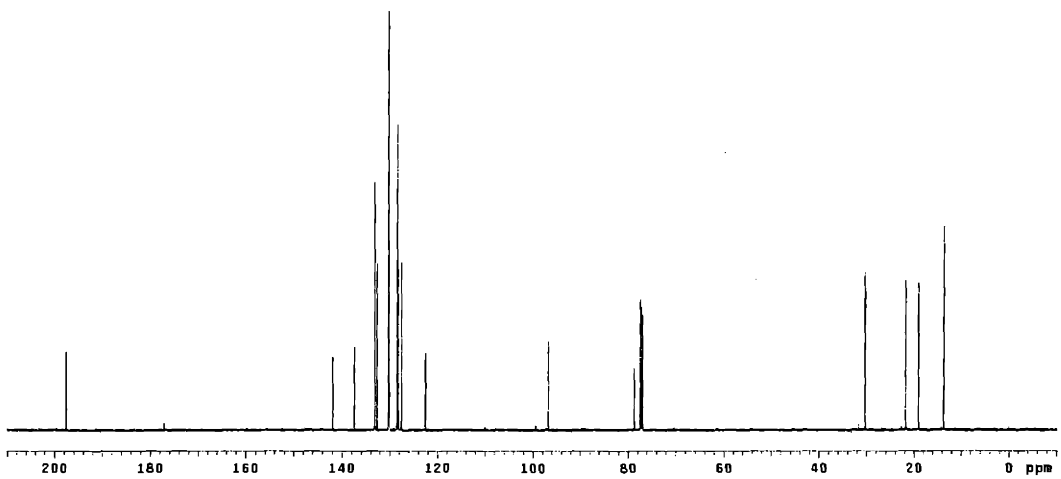

^{13}C NMR of **1p** (125 MHz, $CDCl_3$)

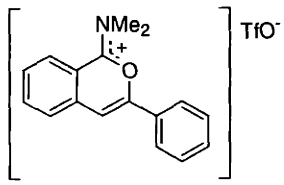

2c

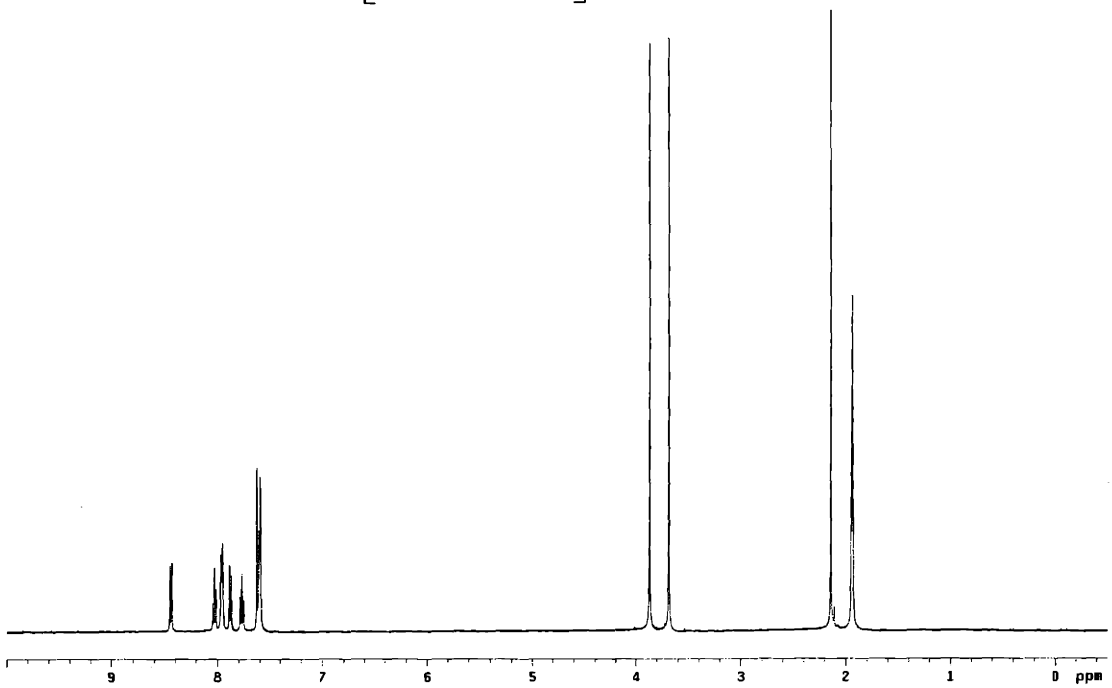

^{1}H NMR of **2c** (500 MHz, CD_3CN)

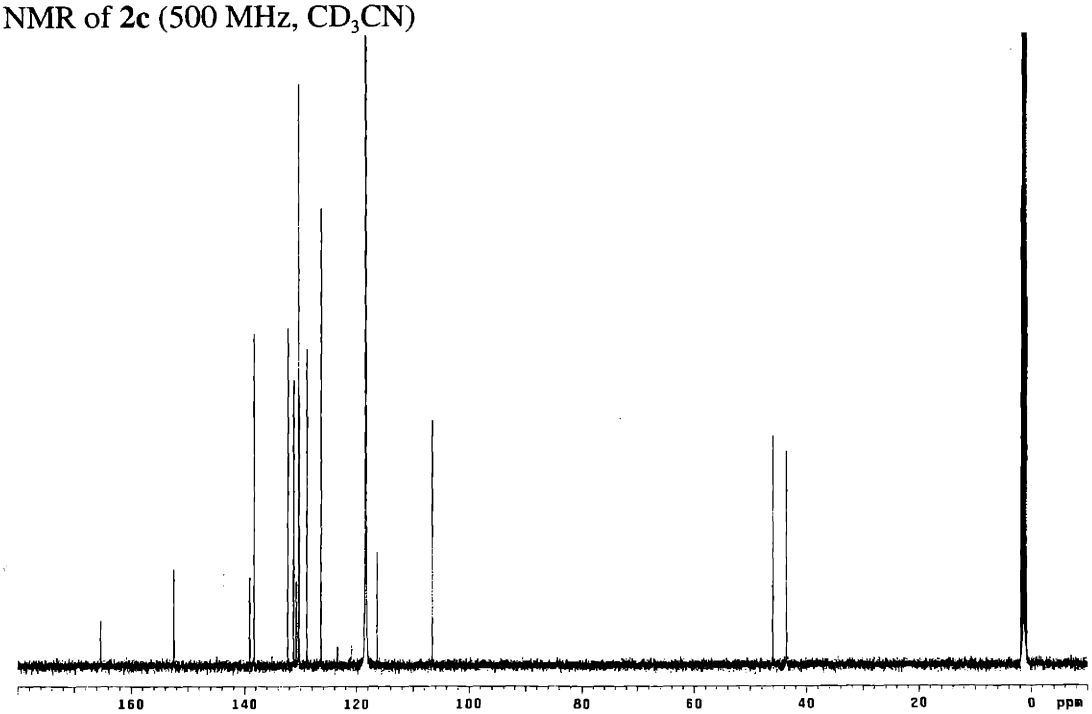

^{13}C NMR of **2c** (125 MHz, CD_3CN)

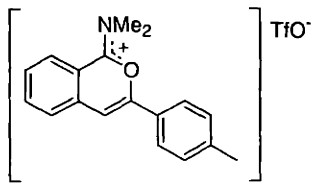

2d

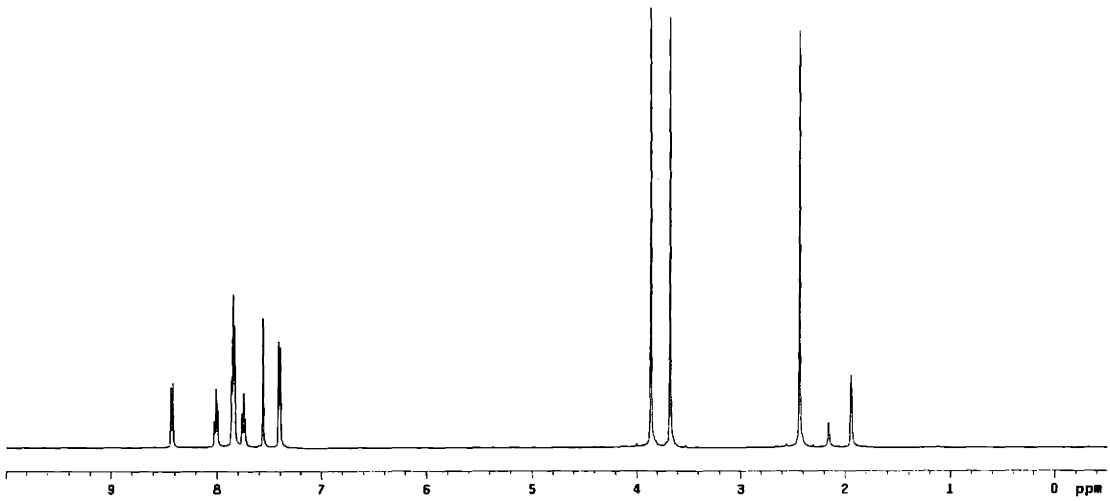

^{1}H NMR of **2d** (500 MHz, CD_3CN)

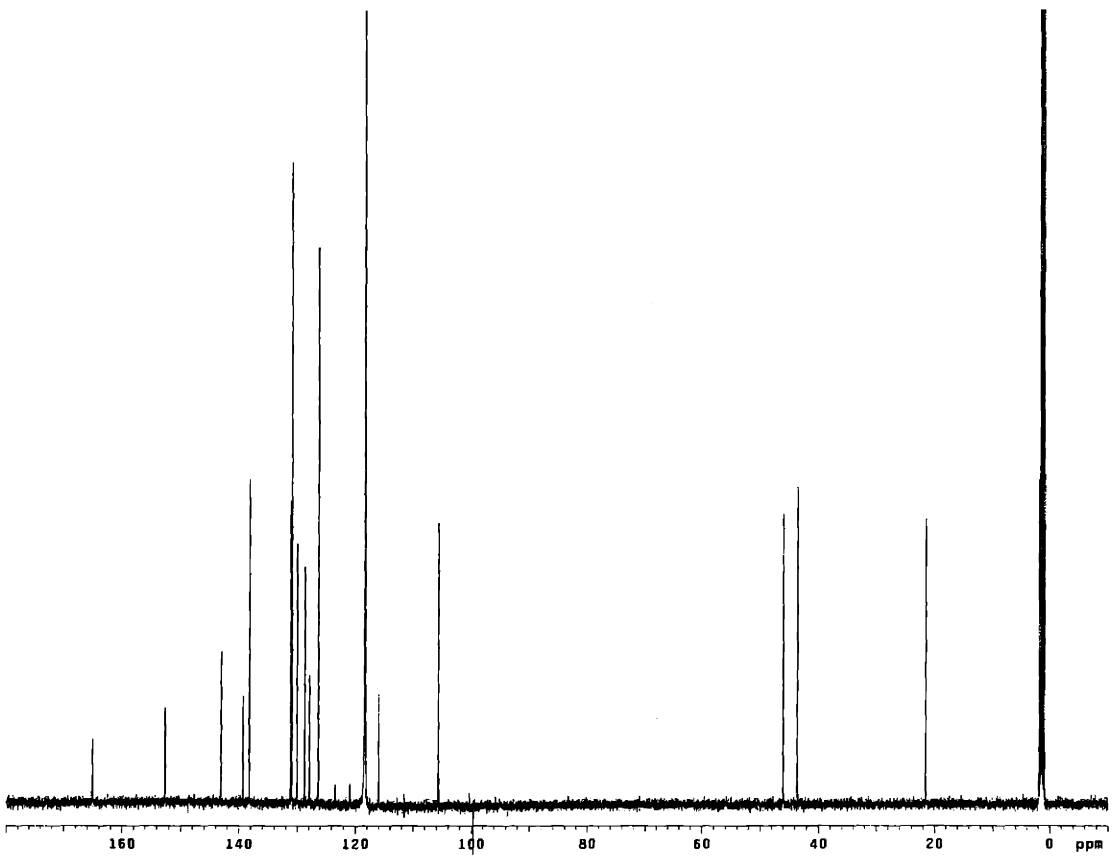

^{13}C NMR of **2d** (125 MHz, CD_3CN)

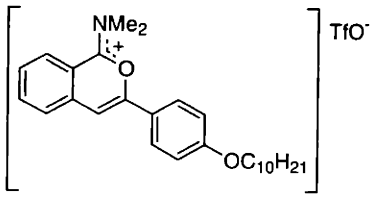

2e

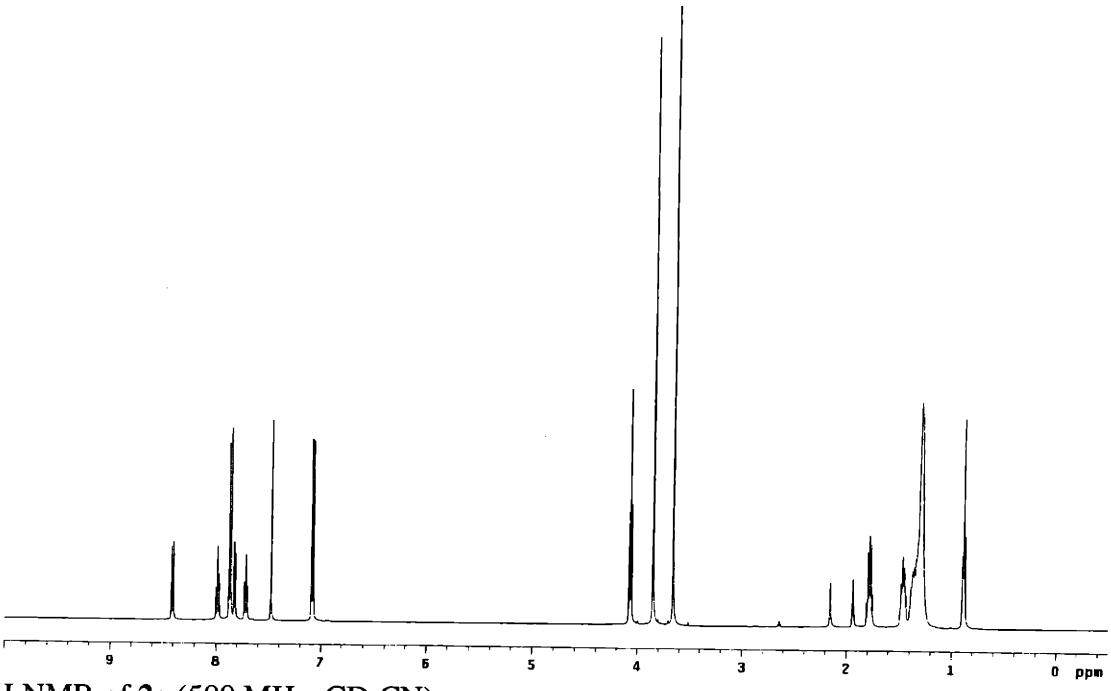

^{1}H NMR of **2e** (500 MHz, CD_3CN)

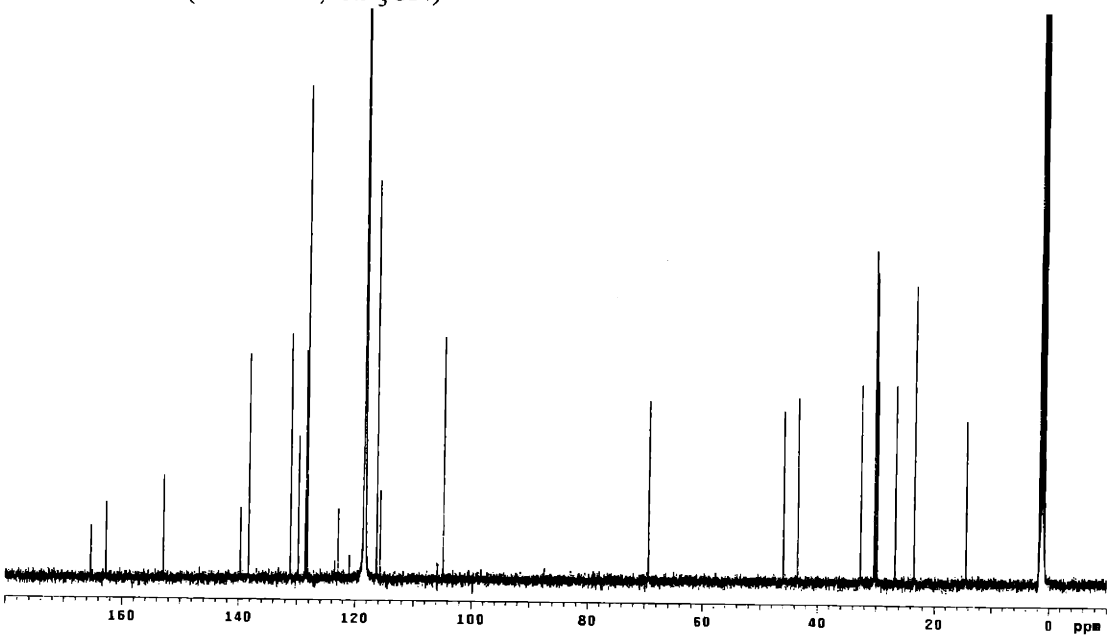

^{13}C NMR of **2e** (125 MHz, CD_3CN)

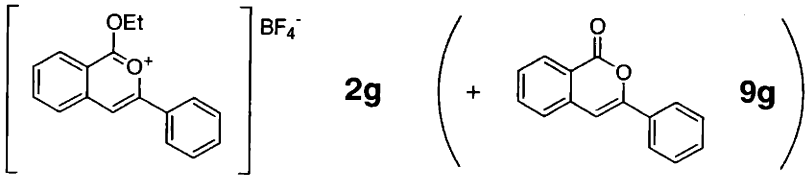

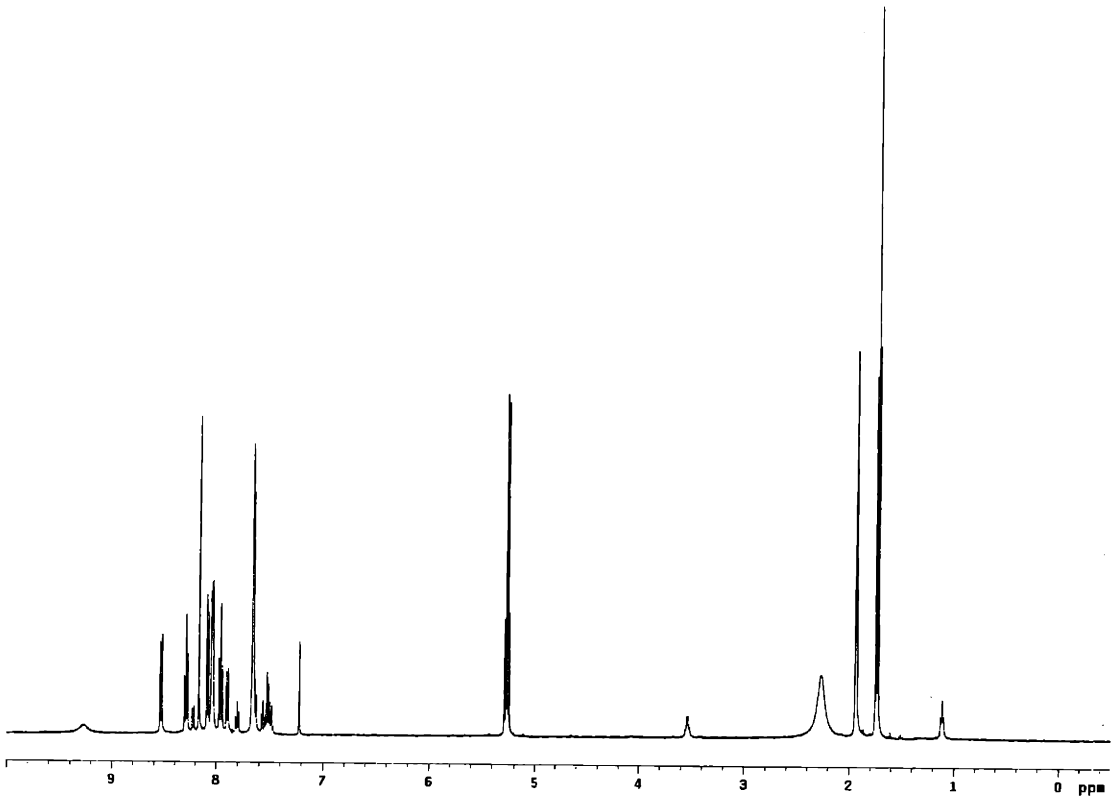

^{1}H NMR of isolated **2g** contaminated with **9g** (500 MHz, CD_3CN)

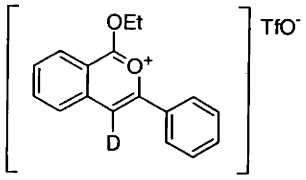

2g-*d*

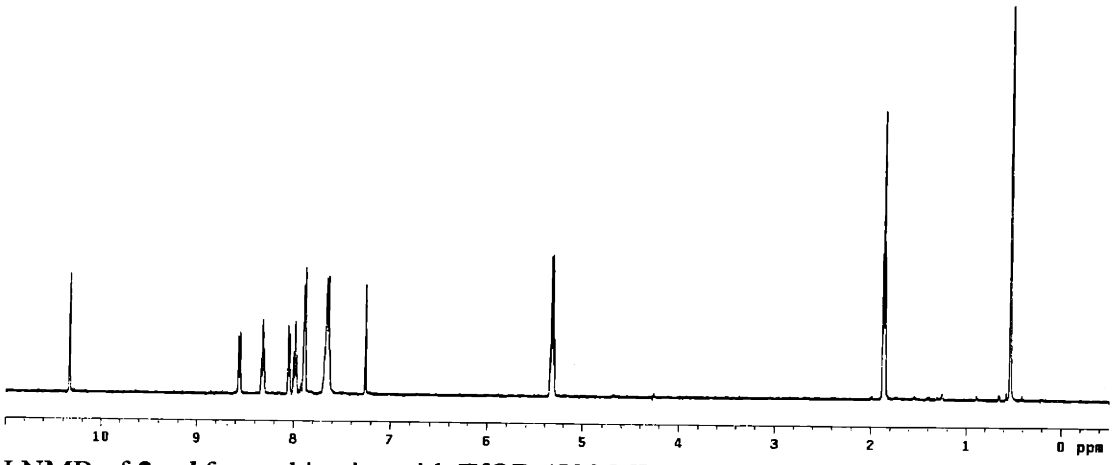

^{1}H NMR of **2g-*d*** formed in situ with TfOD (500 MHz, $CDCl_3$)

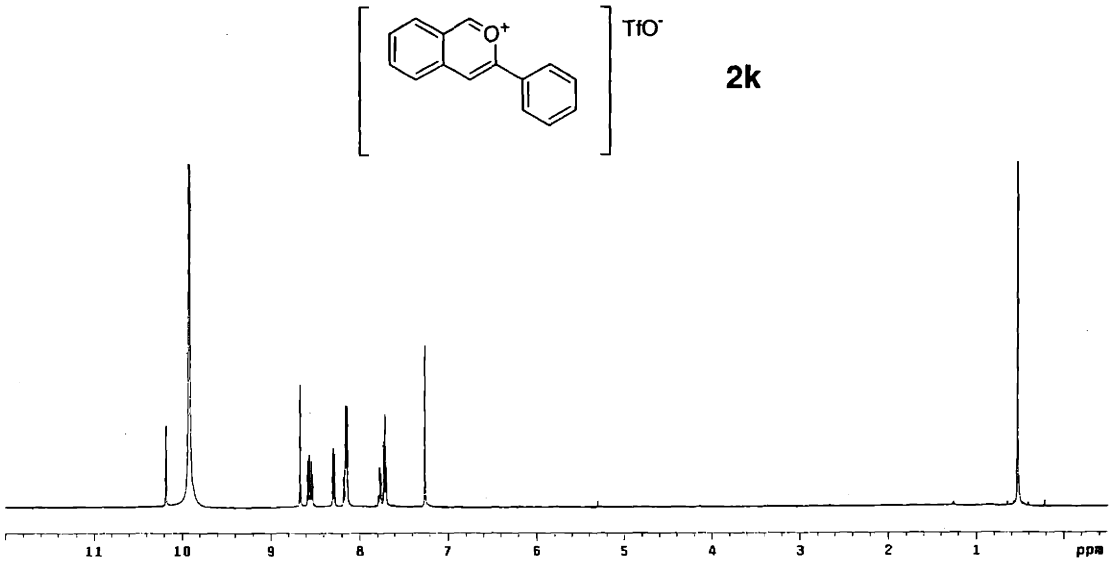

^{1}H NMR of **2k** generated in situ (500 MHz, $CDCl_3$)

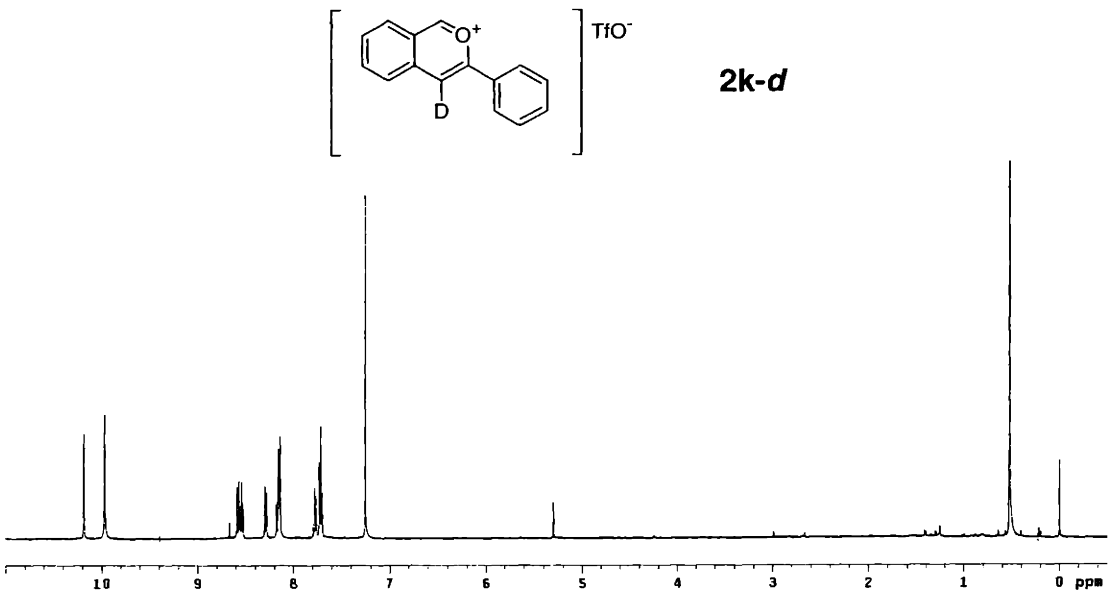

^{1}H NMR of **2k-*d*** generated in situ (500 MHz, $CDCl_3$)

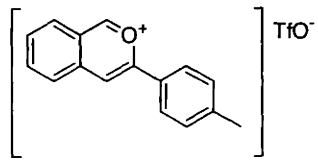

2l

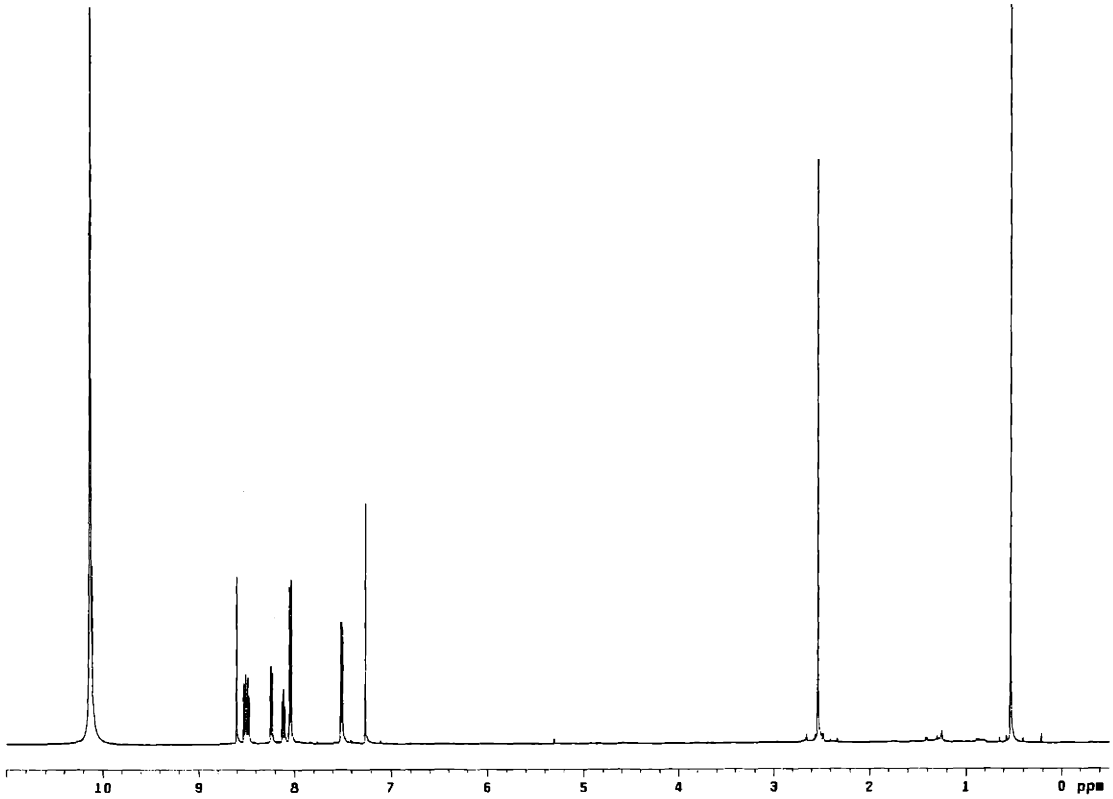

^{1}H NMR of **2l** generated in situ (500 MHz, $CDCl_3$)

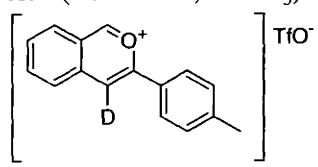

2l-*d*

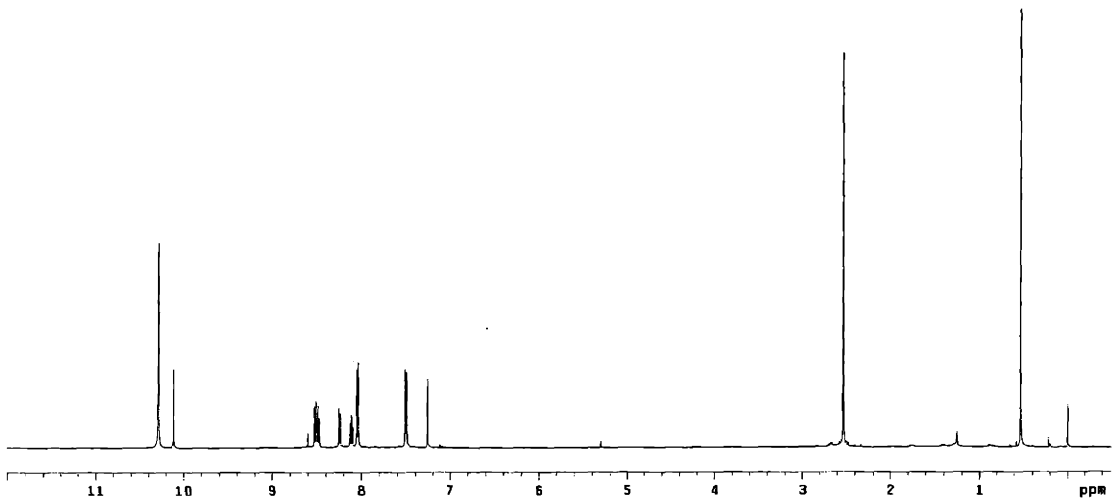

^{1}H NMR of **2l-*d*** generated in situ (500 MHz,, $CDCl_3$)

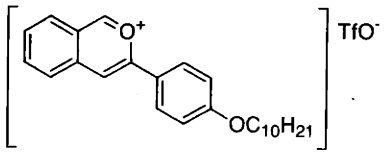

2m

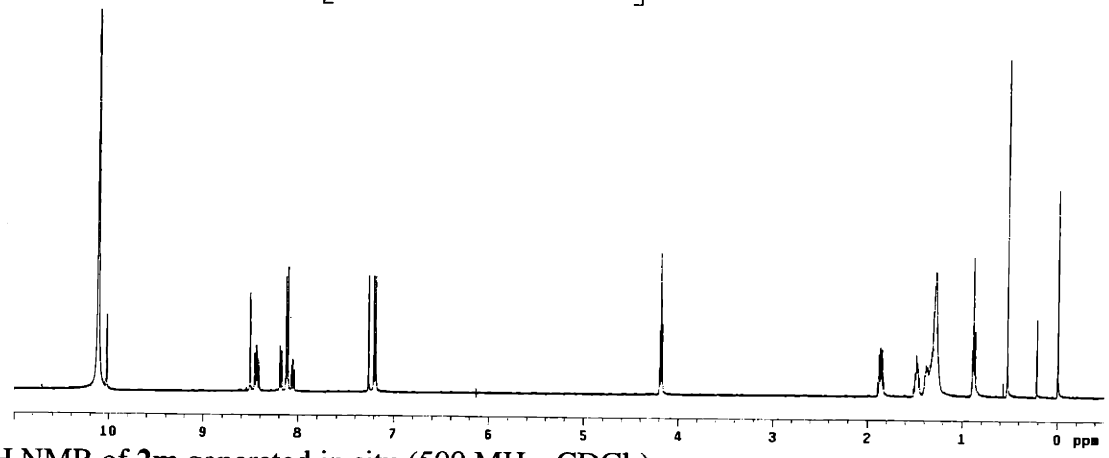

^{1}H NMR of **2m** generated in situ (500 MHz, $CDCl_3$)

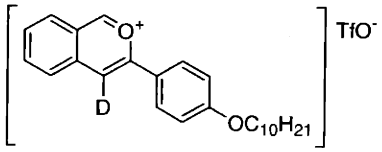

2m-*d*

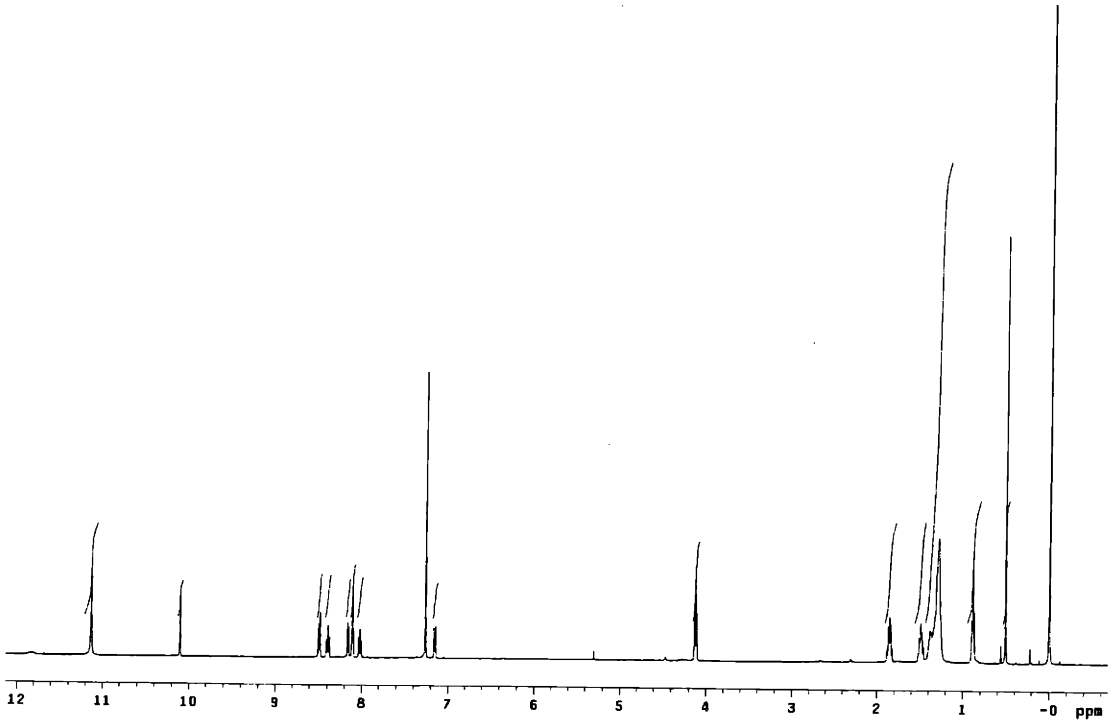

^{1}H NMR of **2m-*d*** generated in situ (500 MHz, $CDCl_3$)

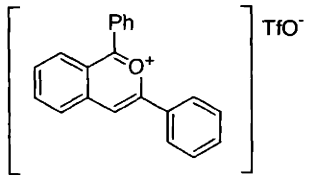

2n

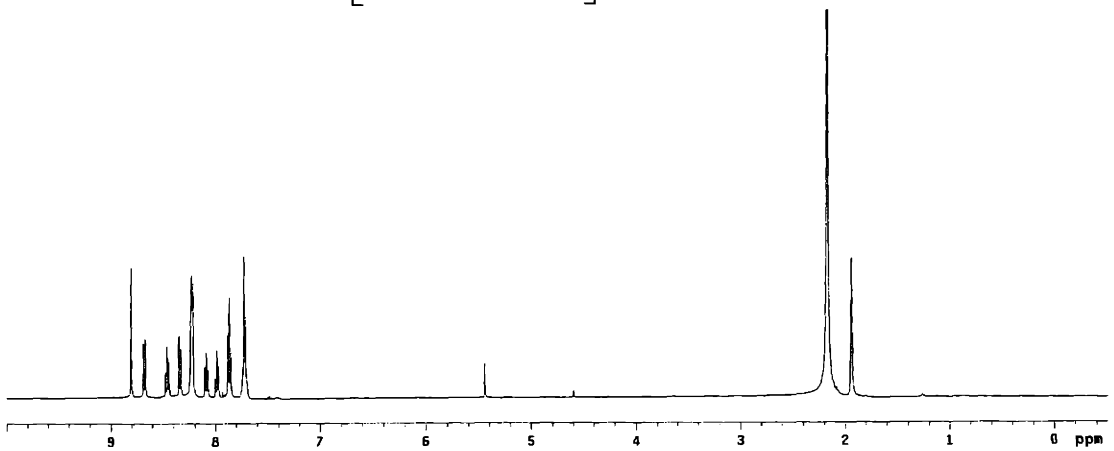

^{1}H NMR of **2n** (500 MHz, CD_3CN)

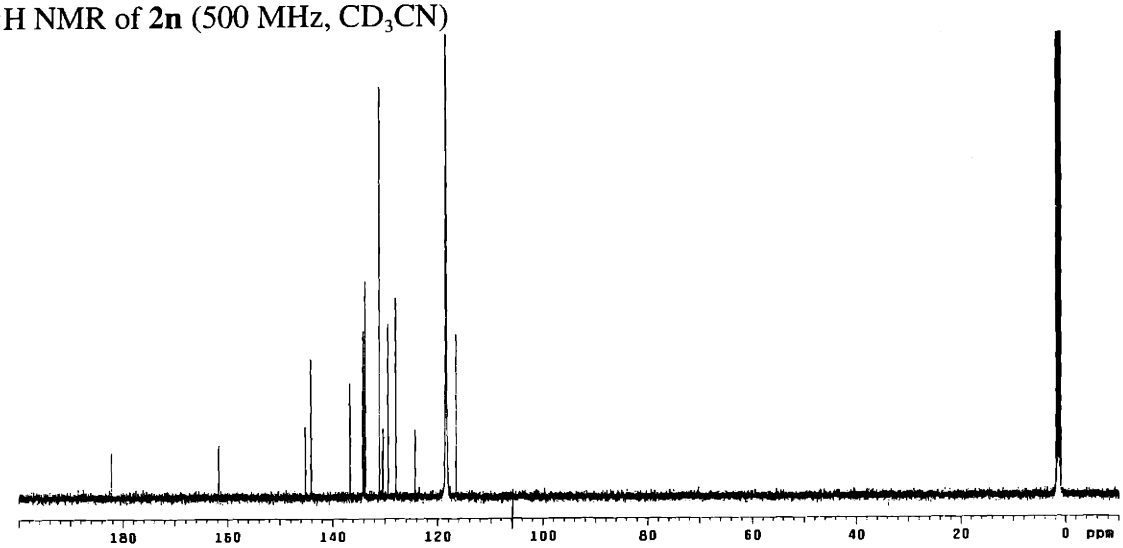

^{13}C NMR of **2n** (125 MHz, CD_3CN)

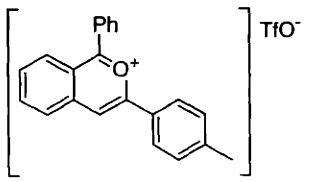

2o

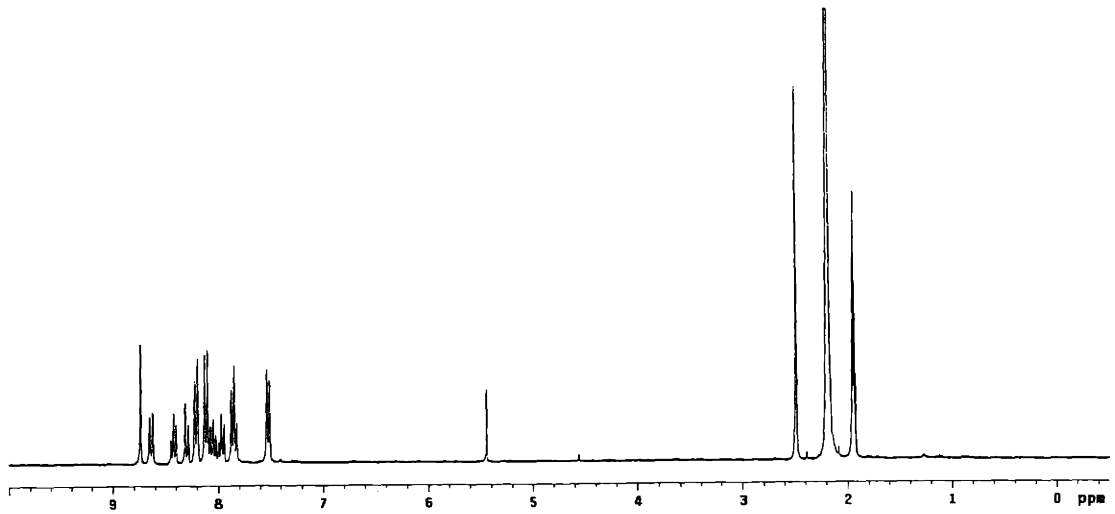

^{1}H NMR of **2o** (300 MHz, CD_3CN)

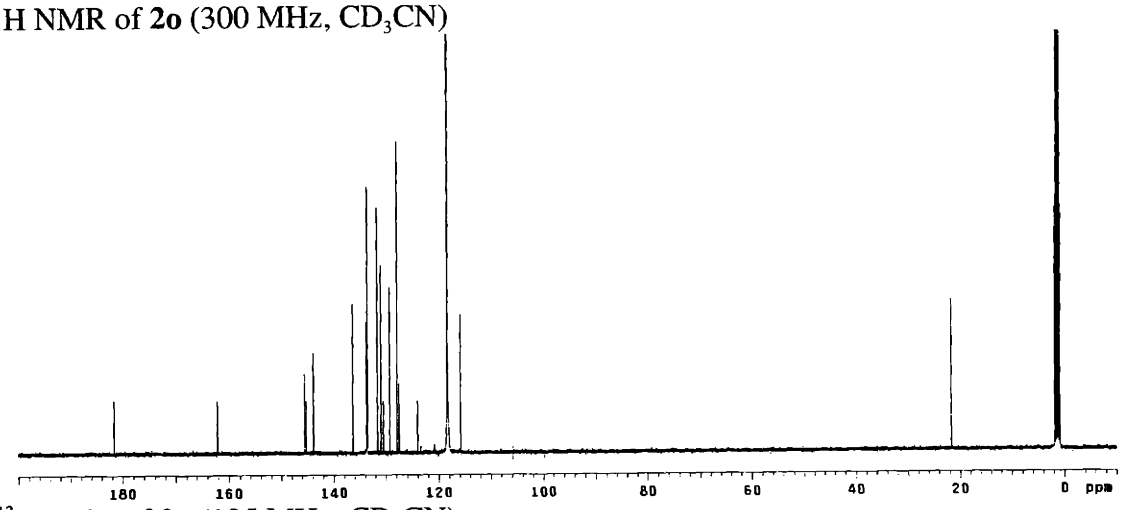

^{13}C NMR of **2o** (125 MHz, CD_3CN)

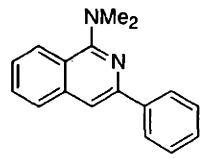

3c

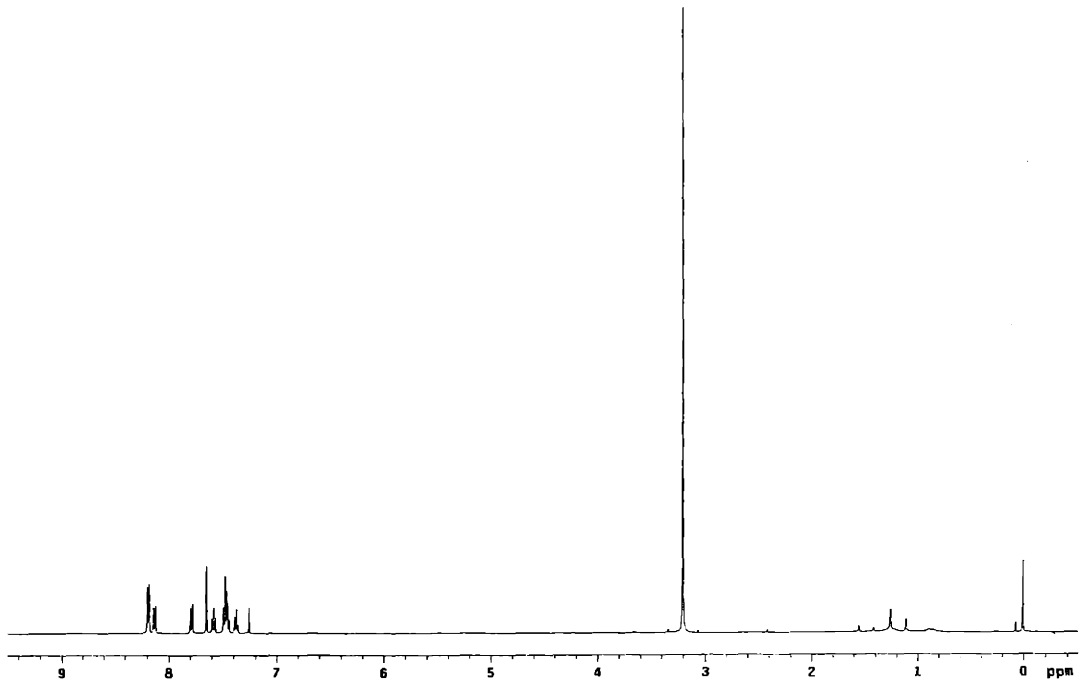

^{1}H NMR of **3c** (500 MHz, $CDCl_3$)

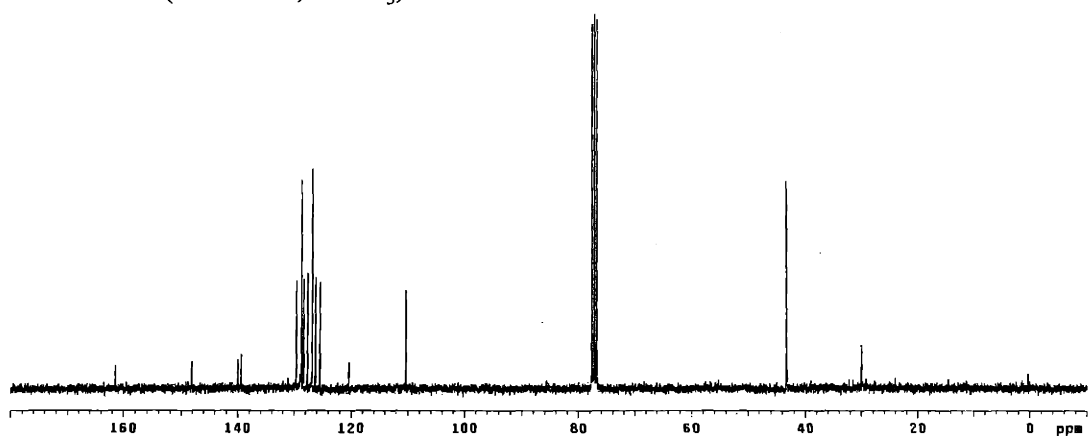

^{13}C NMR of **3c** (75 MHz, $CDCl_3$)

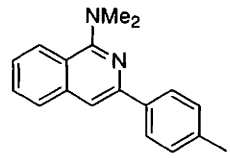

3d

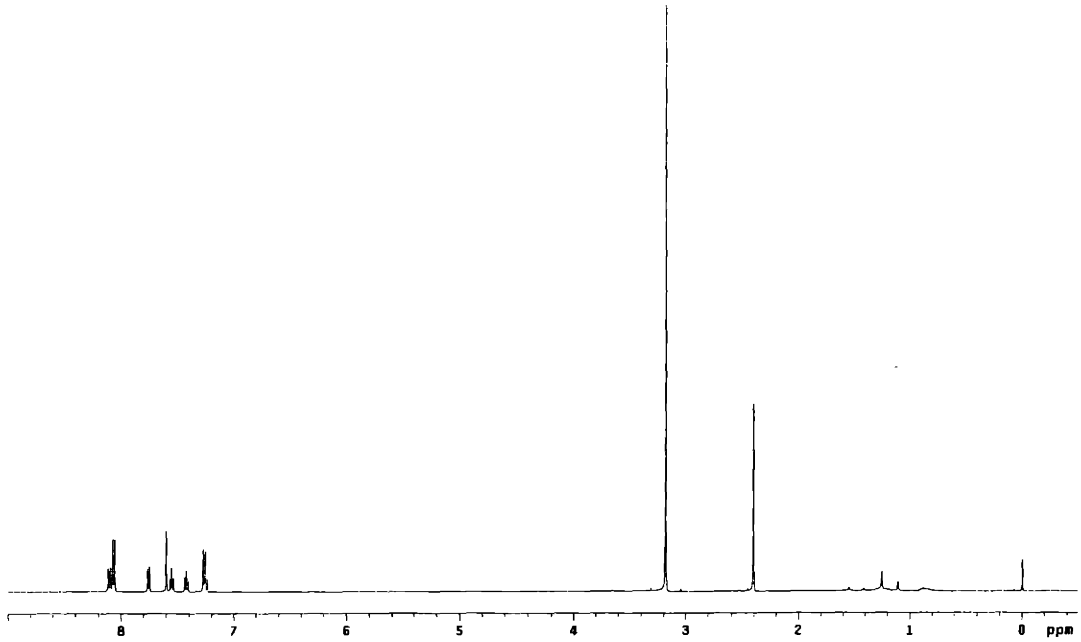

^{1}H NMR of **3d** (500 MHz, $CDCl_3$)

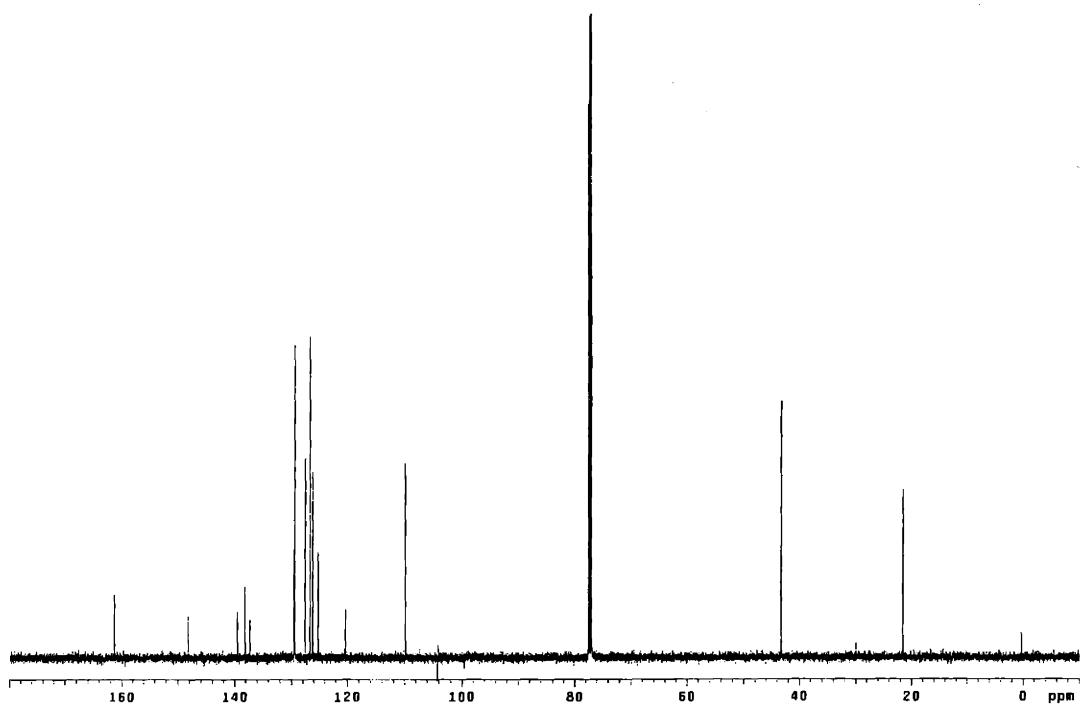

^{13}C NMR of **3d** (125 MHz, $CDCl_3$)

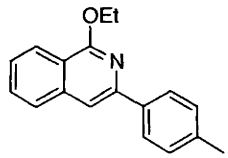

3h

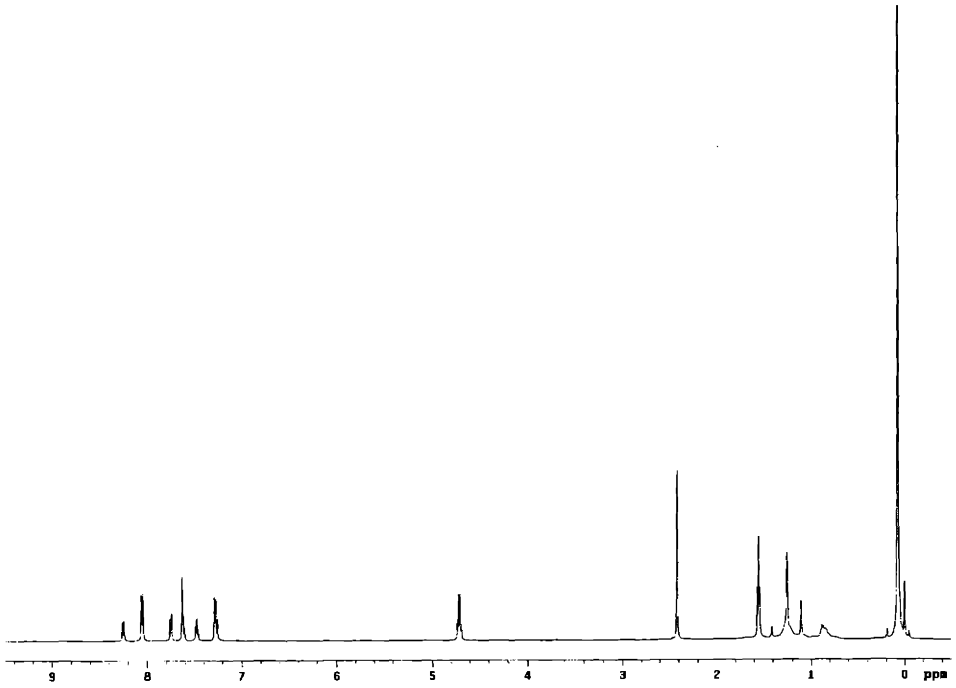

^{1}H NMR of **3h** (500 MHz, $CDCl_3$)

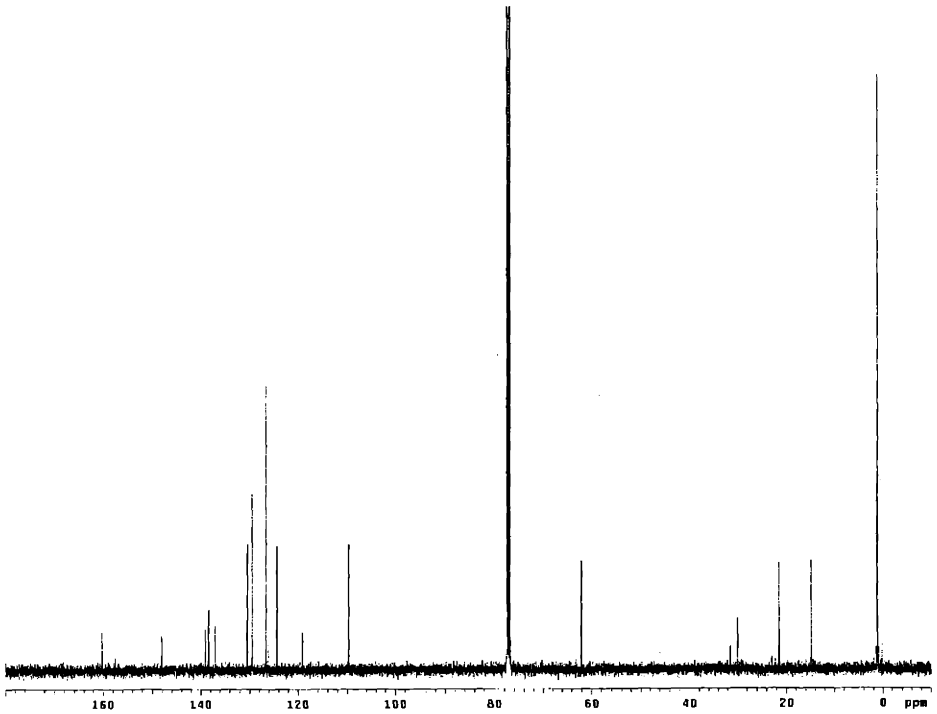

^{13}C NMR of **3h** (125 MHz, $CDCl_3$)

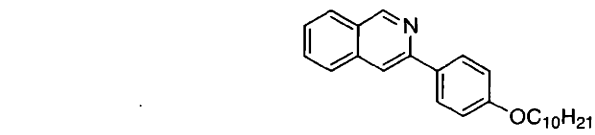

3m

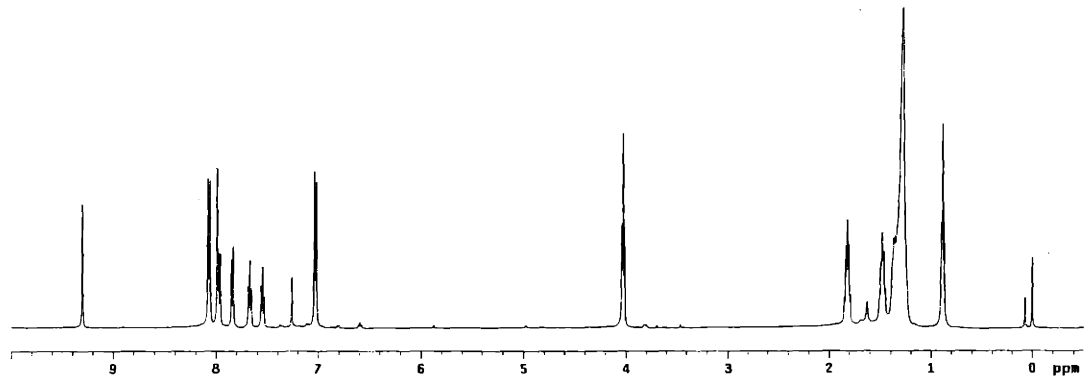

^{1}H NMR of **3m** (500 MHz, $CDCl_3$)

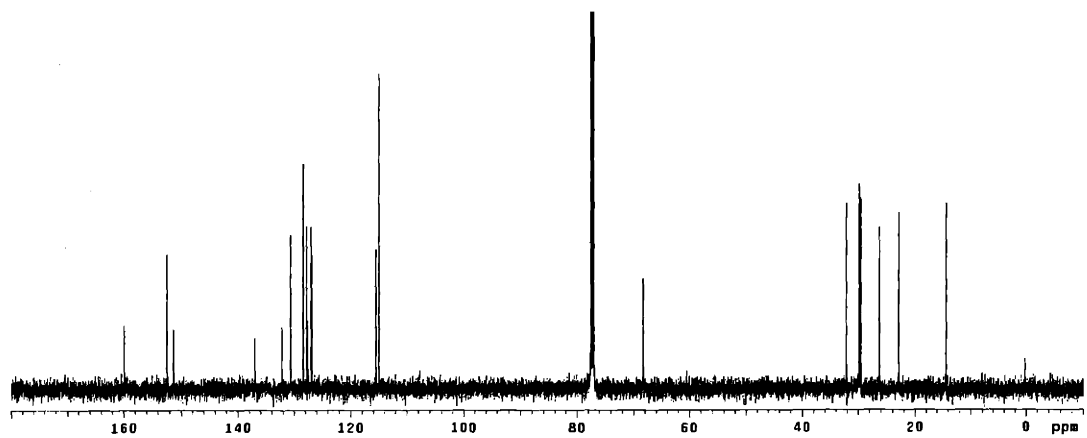

^{13}C NMR of **3m** (125 MHz, $CDCl_3$)

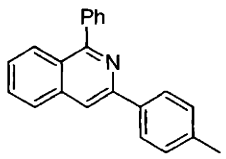

3o

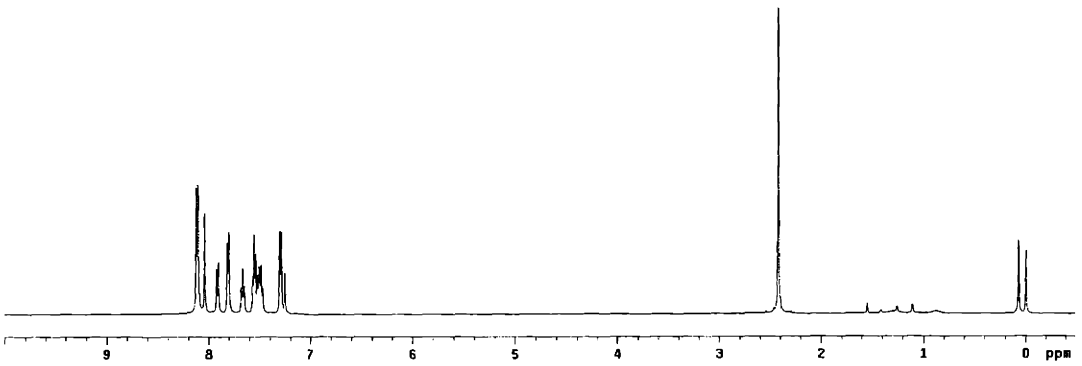

^{1}H NMR of **3o** (500 MHz, $CDCl_3$)

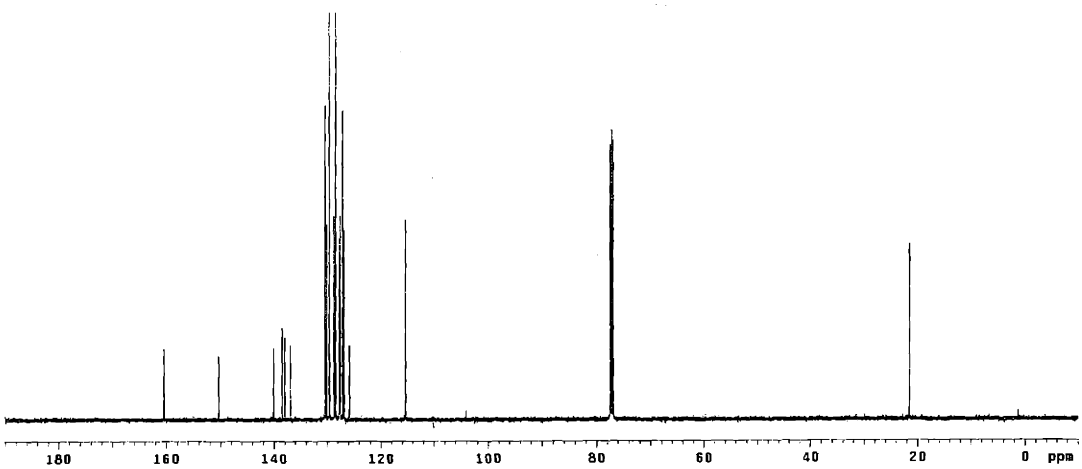

^{13}C NMR of **3o** (125 MHz, $CDCl_3$)

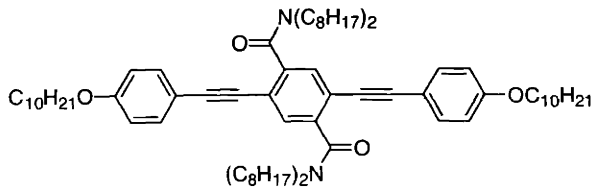

6

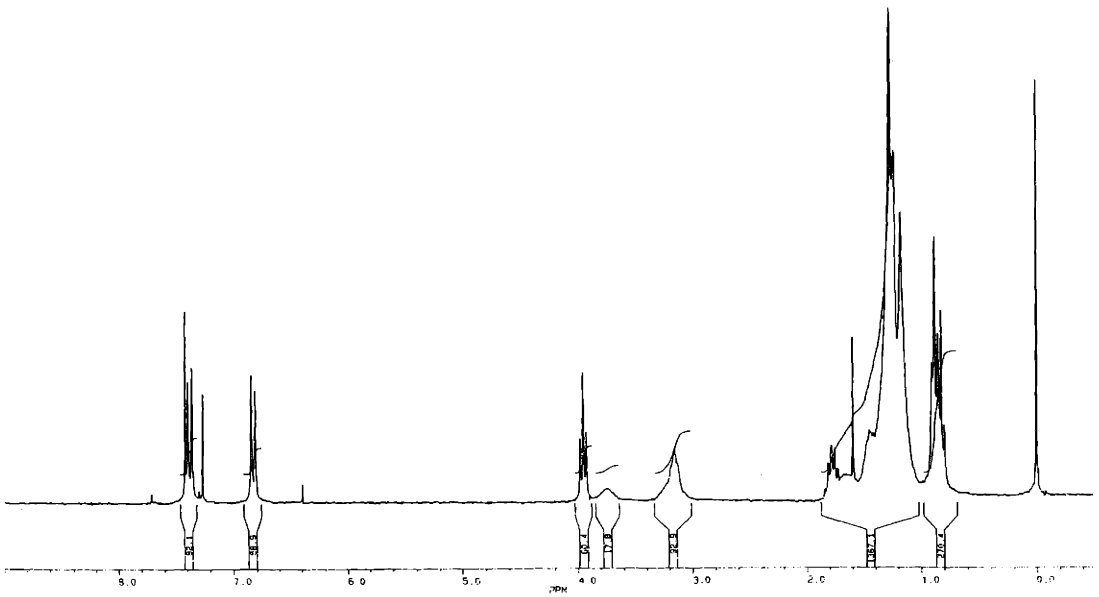

^{1}H NMR of **6** (250 MHz, $CDCl_3$)

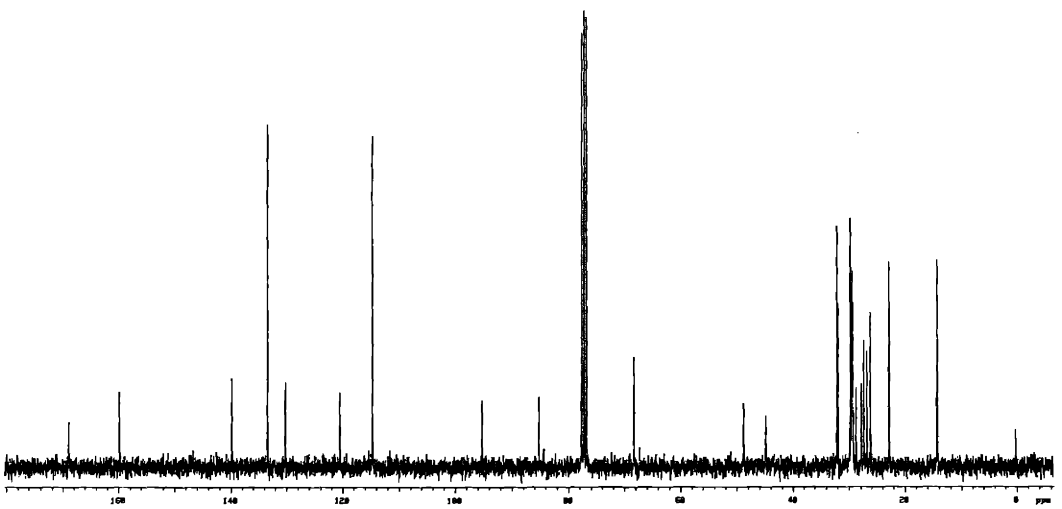

^{13}C NMR of **6** (75 MHz, $CDCl_3$)

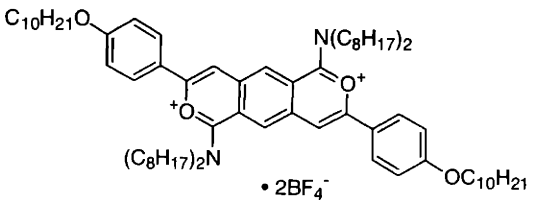

7

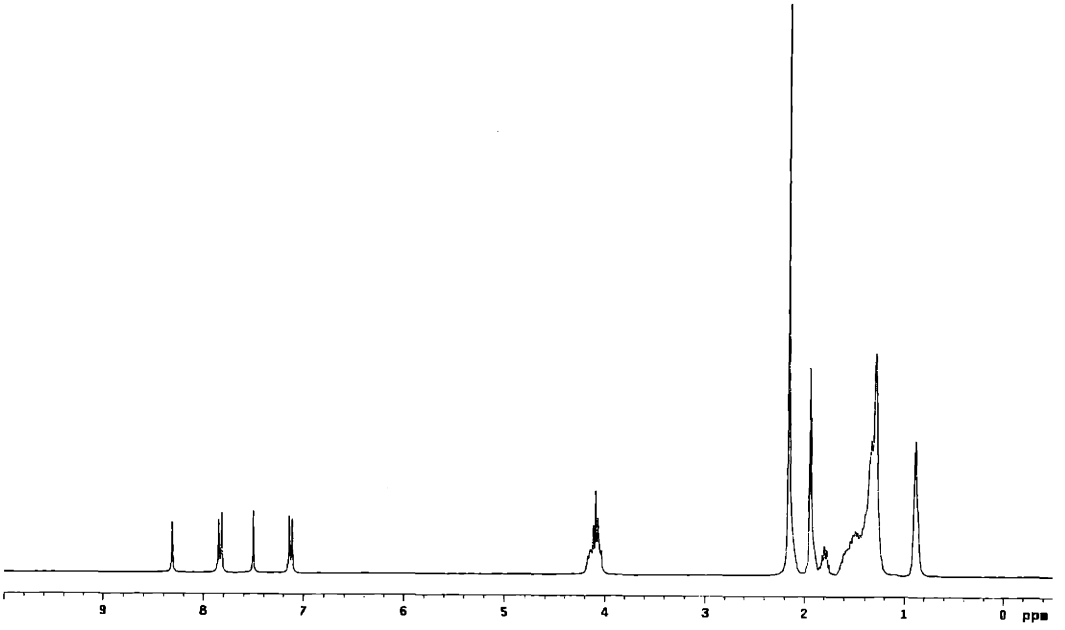

^{1}H NMR of **7** (300 MHz, CD_3CN)

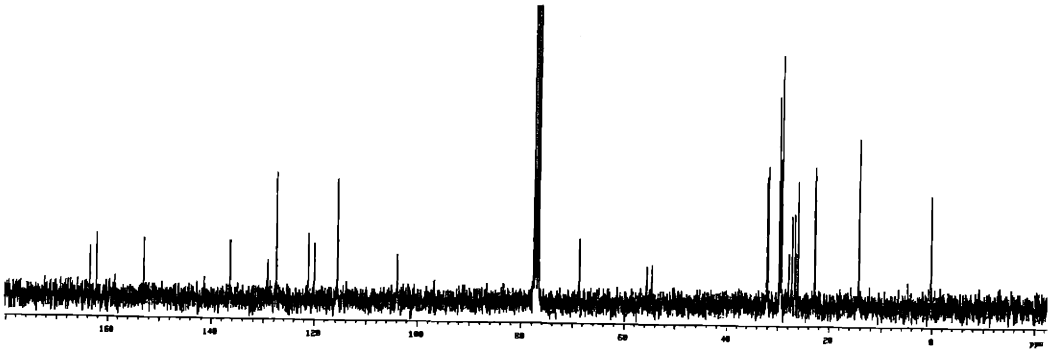

^{13}C NMR of **7** (75 MHz, $CDCl_3$)

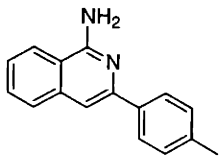

8d (and **h**)

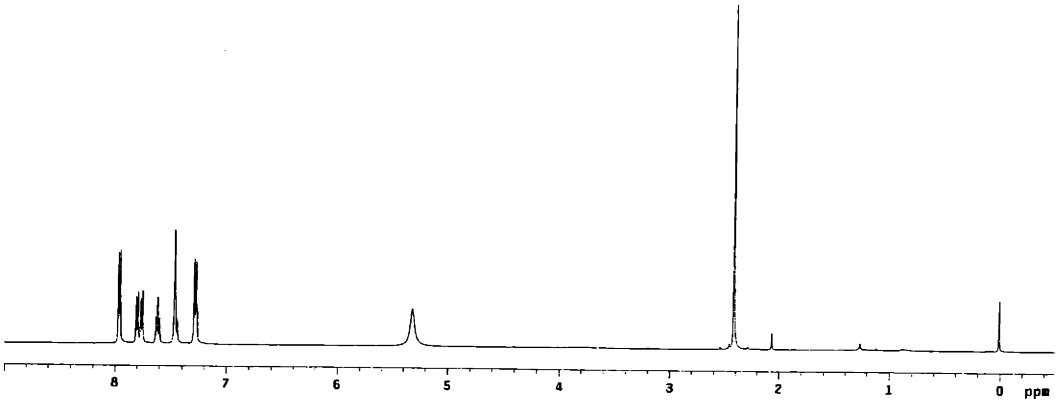

^{1}H NMR of **8d** (500 MHz, $CDCl_3$)

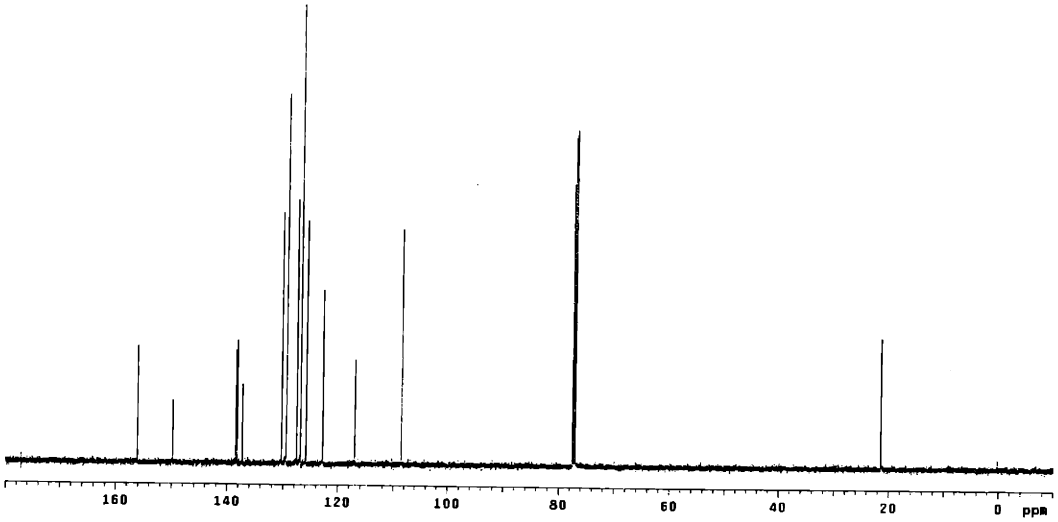

^{13}C NMR of **8h** (125 MHz, $CDCl_3$)

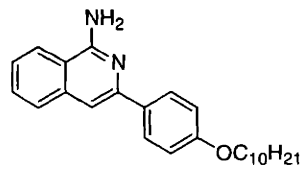

8e

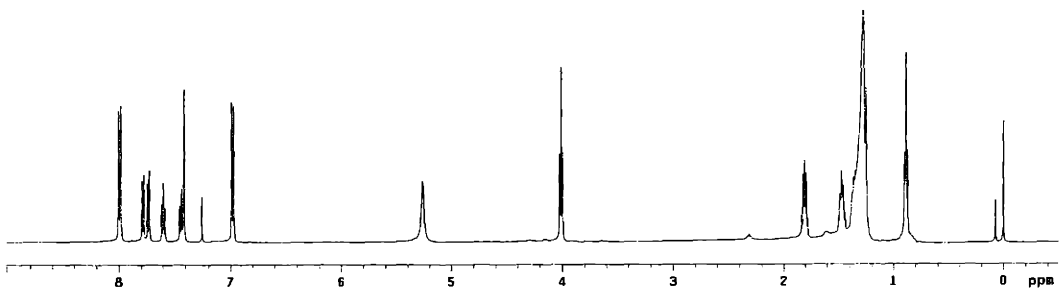

^{1}H NMR of **8e** (500 MHz, $CDCl_3$)

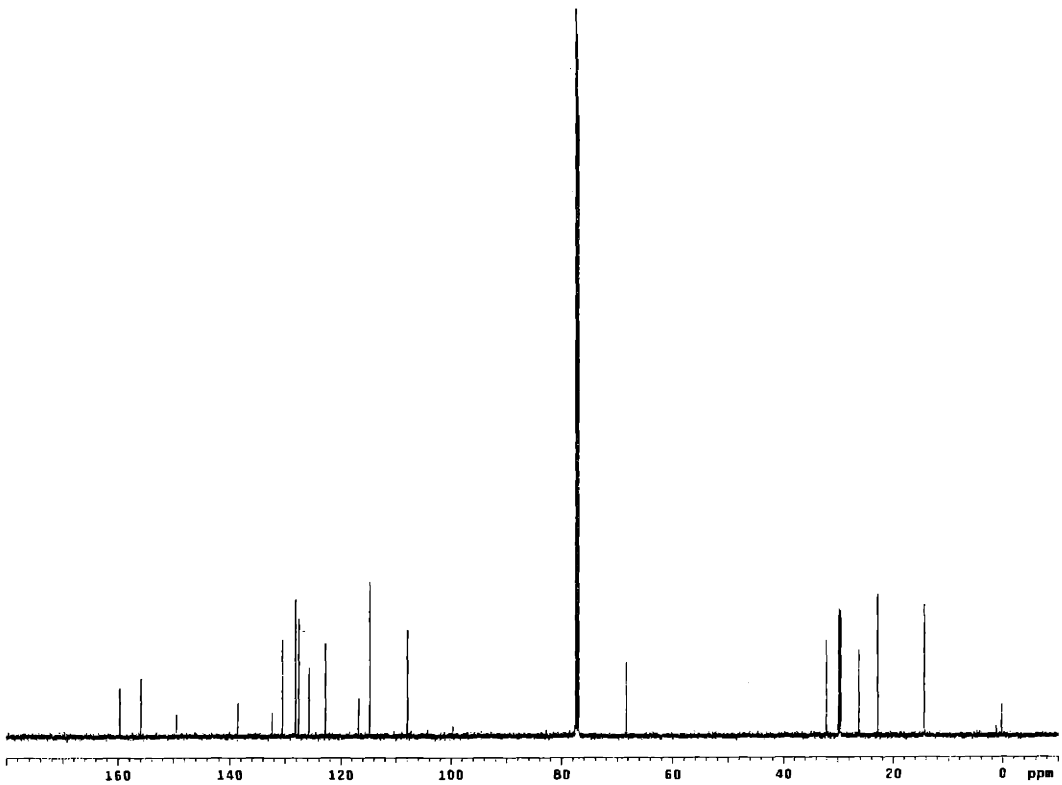

^{13}C NMR of **8e** (125 MHz, $CDCl_3$)

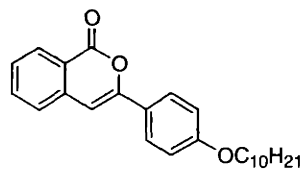

9i

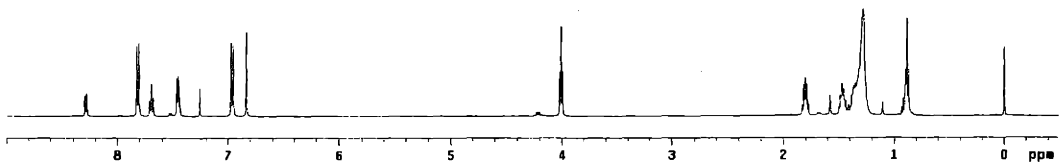

^{1}H NMR of **9i** (500 MHz, $CDCl_3$)

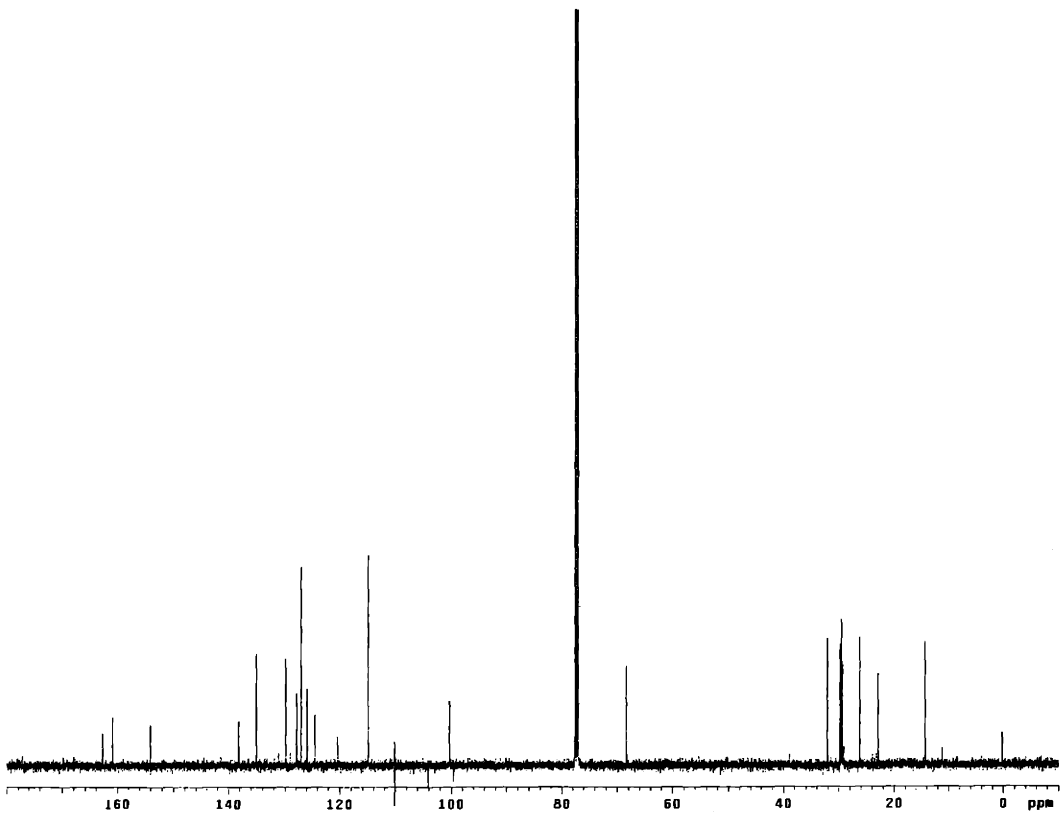

^{13}C NMR of **9i** (125 MHz, $CDCl_3$)

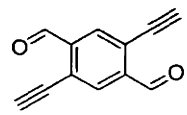

14

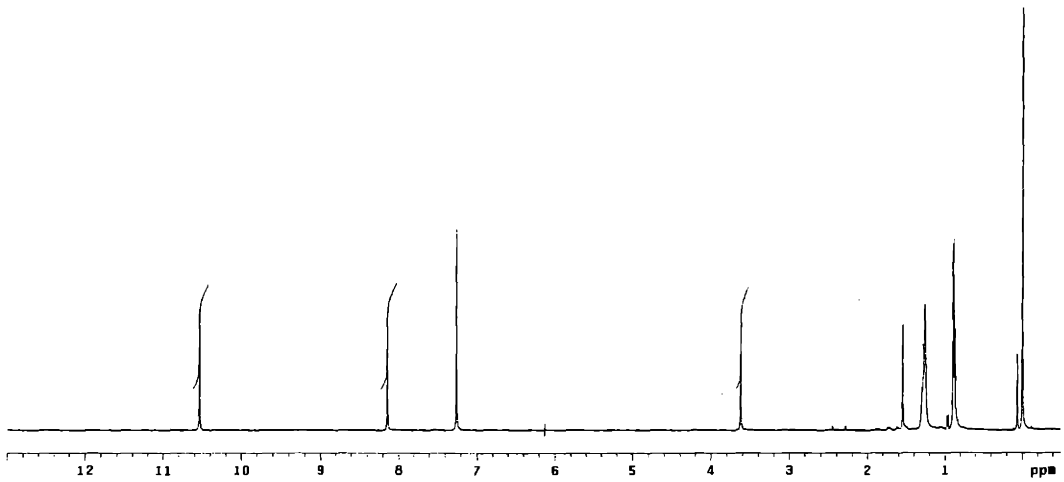

^{1}H NMR of **14** (500 MHz, $CDCl_3$)

Appendix 3:

^{1}H and ^{13}C NMR spectra for Chapter 3

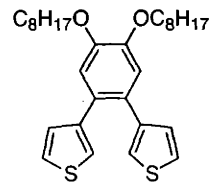

1a

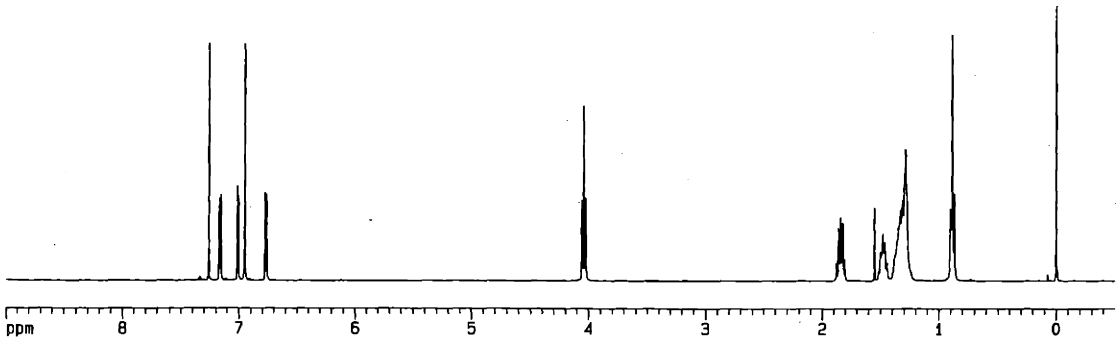

^{1}H NMR of **1a** (400 MHz, $CDCl_3$)

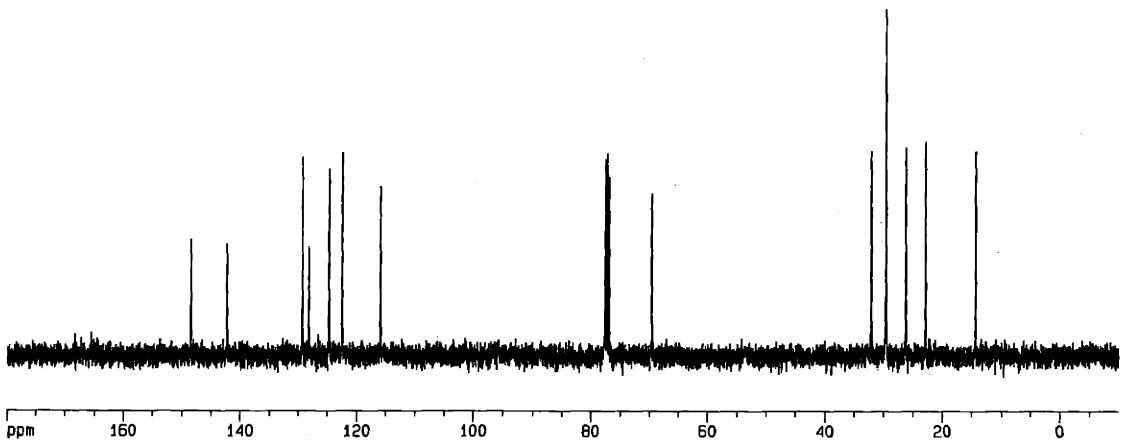

^{13}C NMR of **1a** (100 MHz, $CDCl_3$)

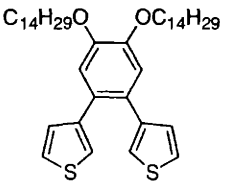

1b

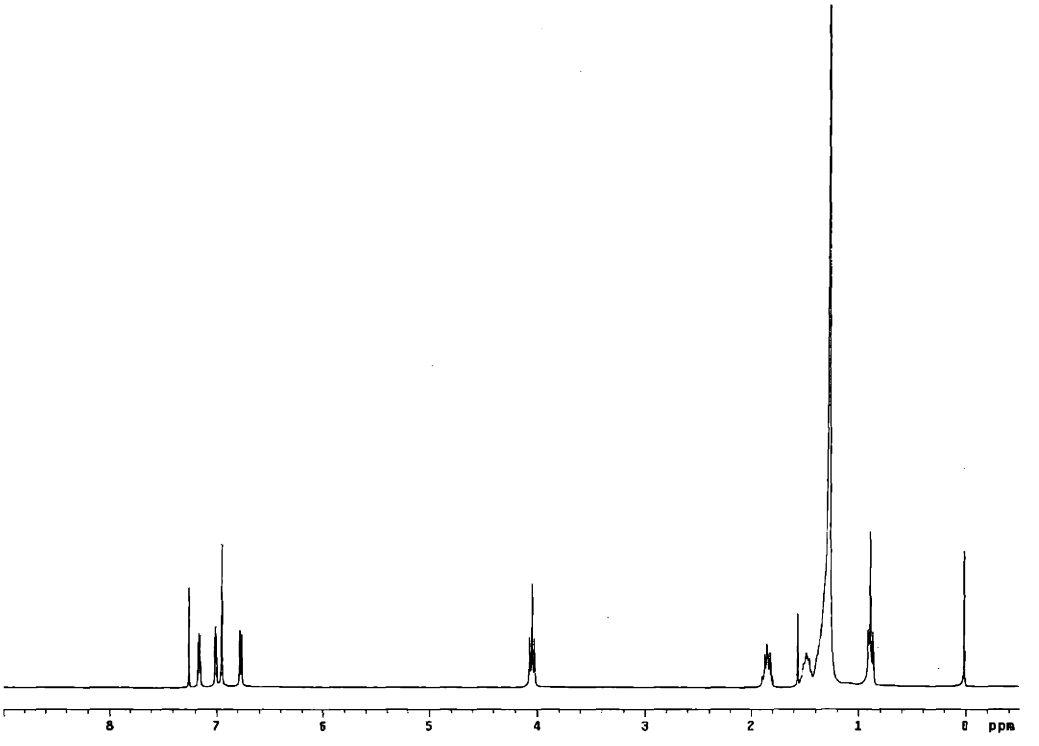

^{1}H NMR of **1b** (300 MHz, $CDCl_3$)

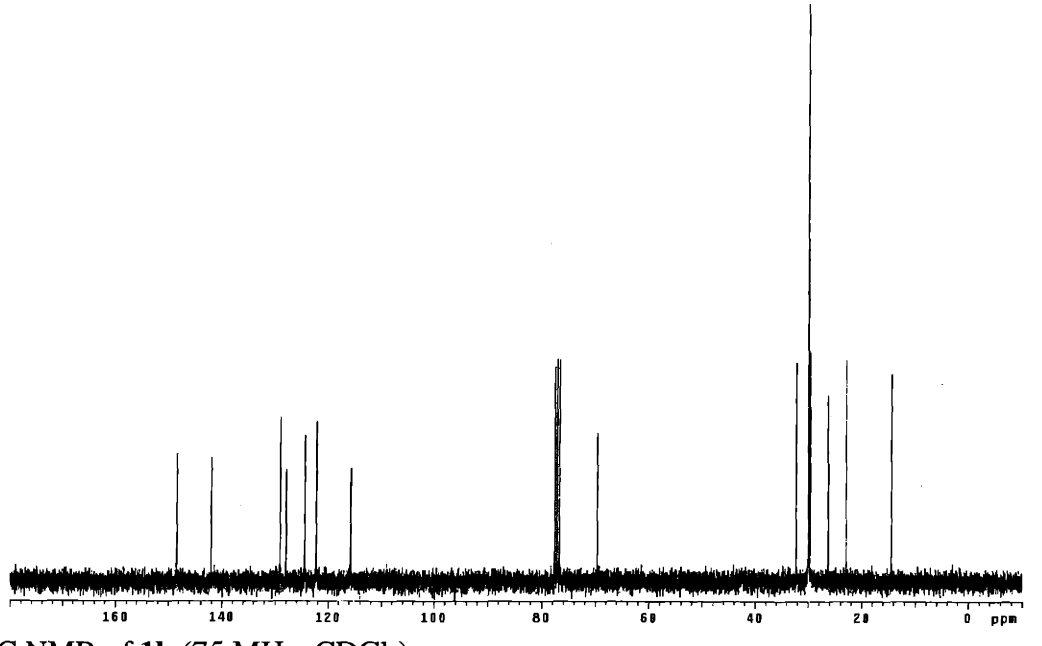

^{13}C NMR of **1b** (75 MHz, $CDCl_3$)

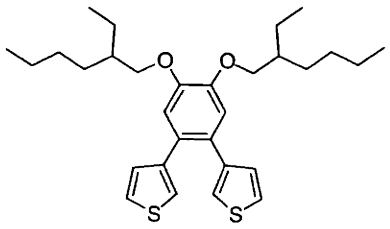

1c

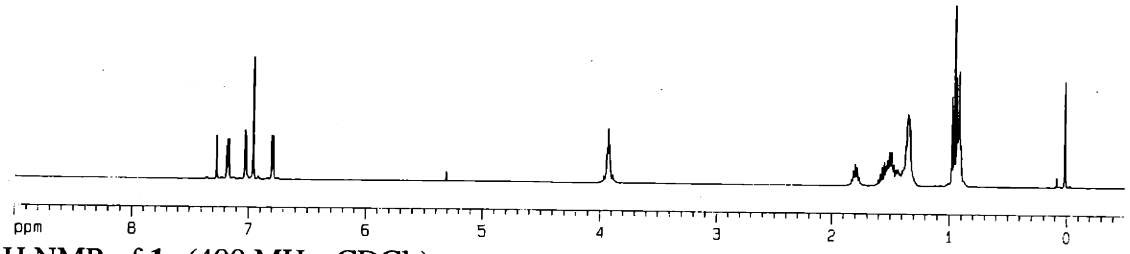

^{1}H NMR of **1c** (400 MHz, $CDCl_3$)

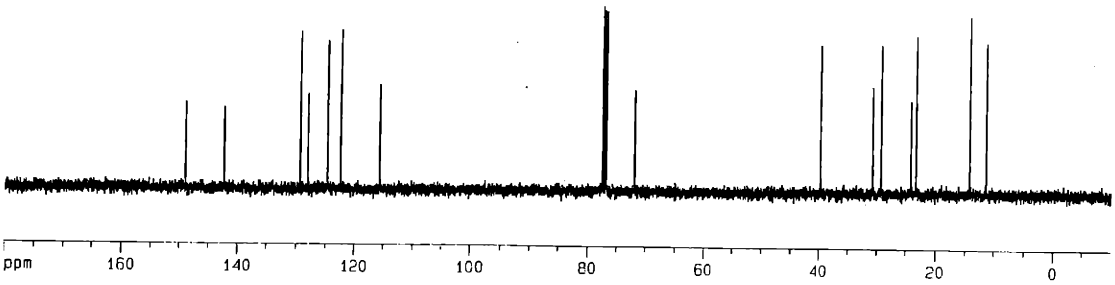

^{13}C NMR of **1c** (100 MHz, $CDCl_3$)

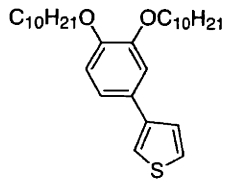

monoβ

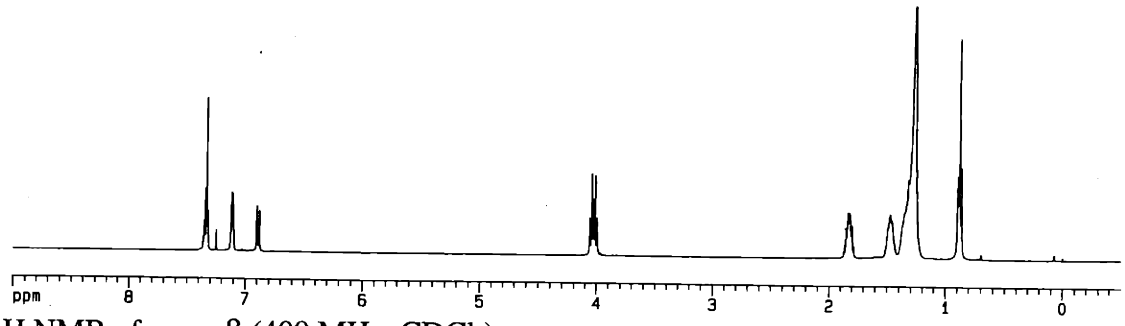

^{1}H NMR of **monoβ** (400 MHz, $CDCl_3$)

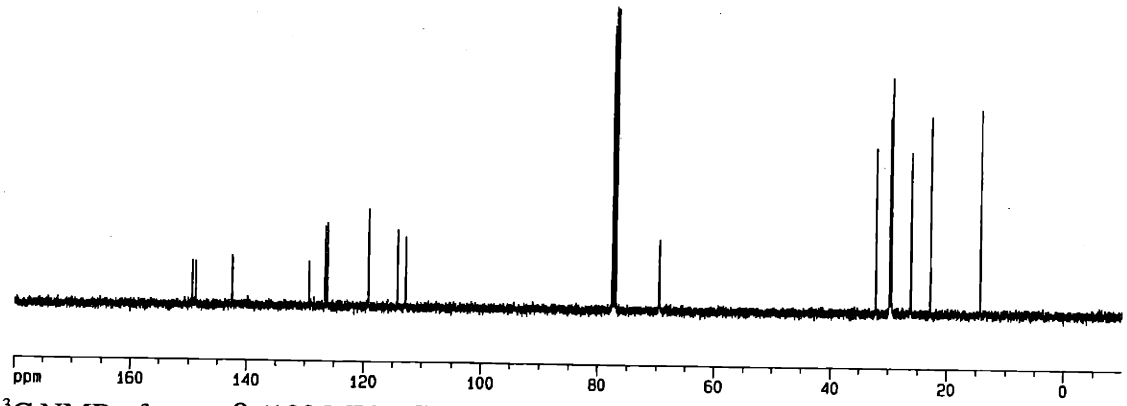

^{13}C NMR of **monoβ** (100 MHz, $CDCl_3$)

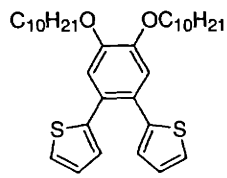

α-1

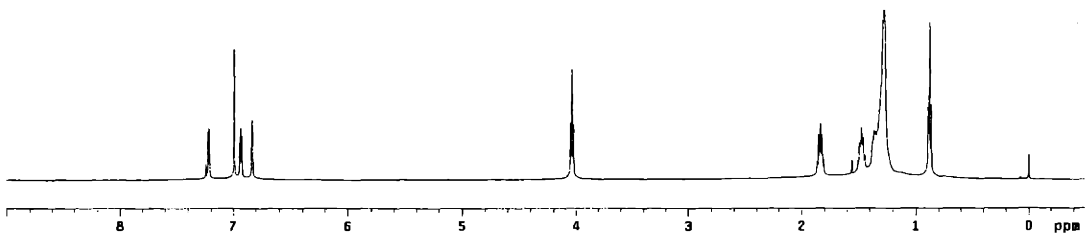

^{1}H NMR of **α-1** (500 MHz, $CDCl_3$)

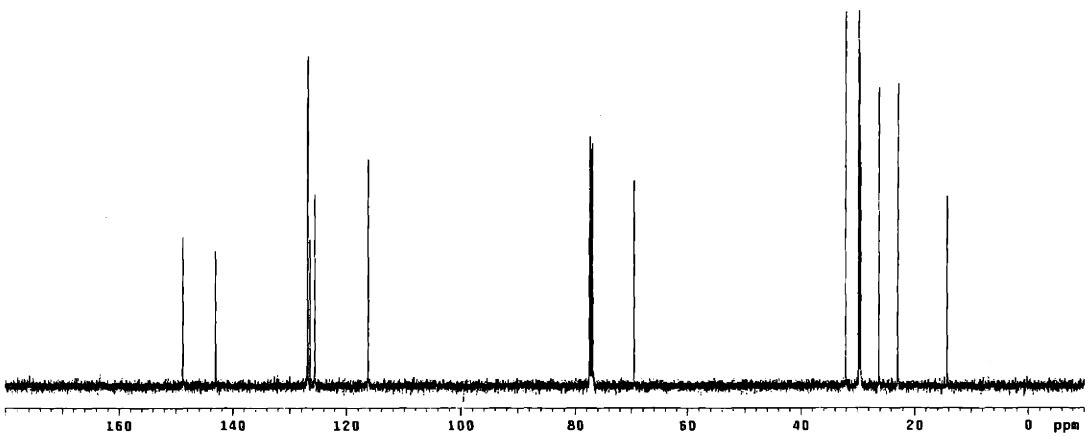

^{13}C NMR of **α-1** (125 MHz, $CDCl_3$)

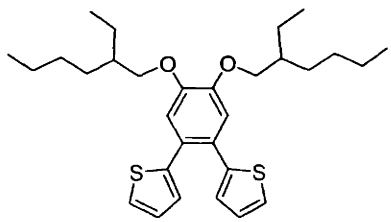

α-1 (EH)

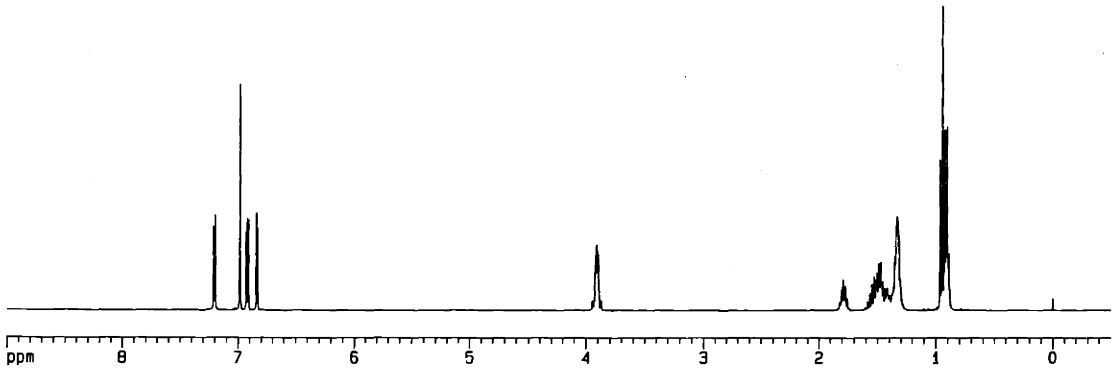

^{1}H NMR of α-**1** (400 MHz, $CDCl_3$)

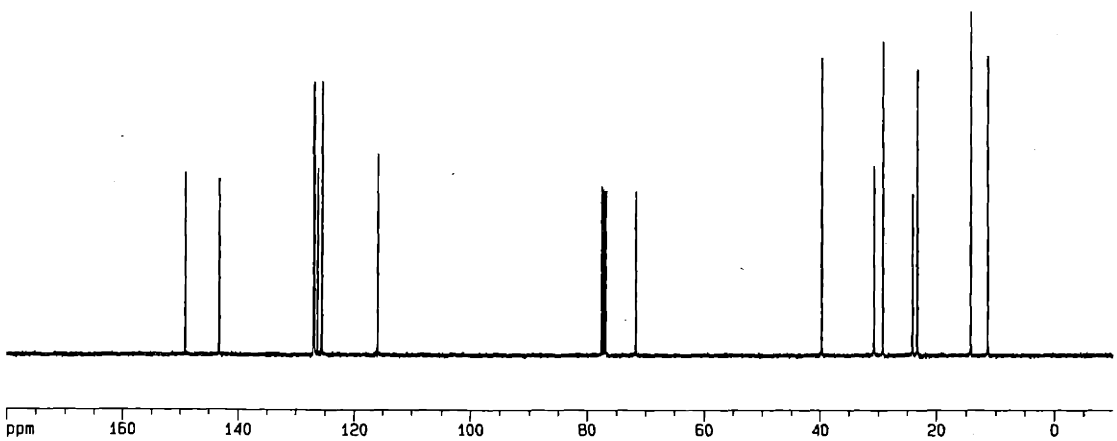

^{13}C NMR of α-**1** (100 MHz, $CDCl_3$)

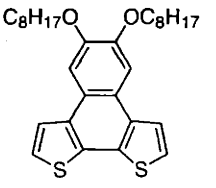

2a

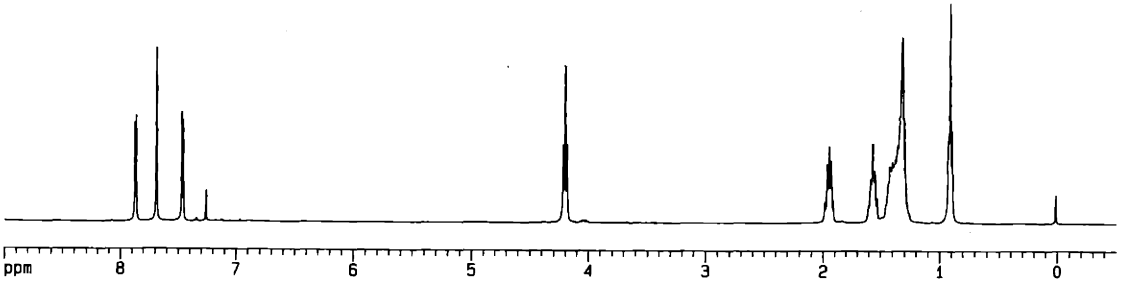

^{1}H NMR of **2a** (400 MHz, $CDCl_3$)

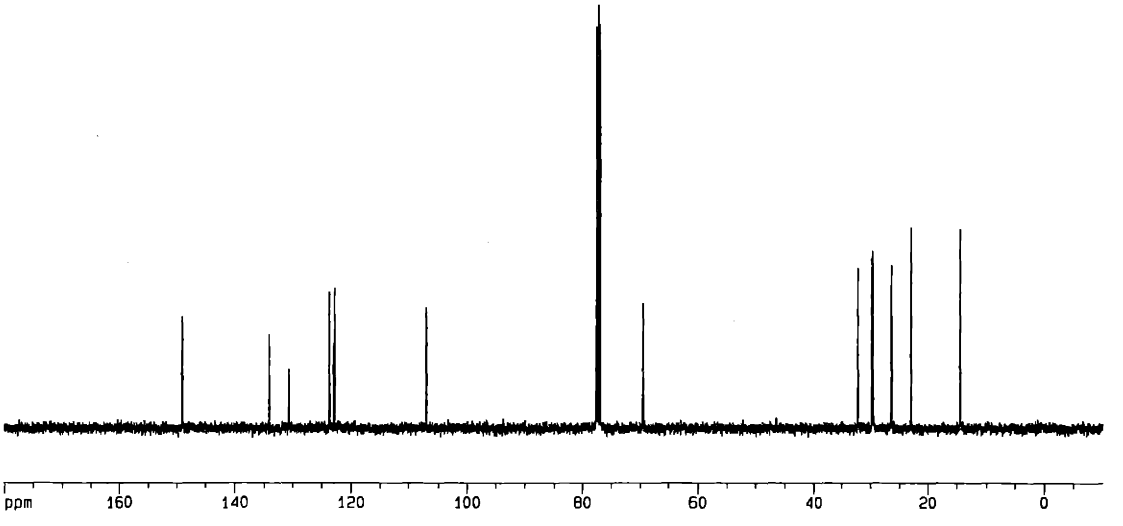

^{13}C NMR of **2a** (100 MHz, $CDCl_3$)

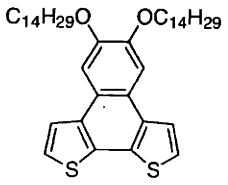

2b

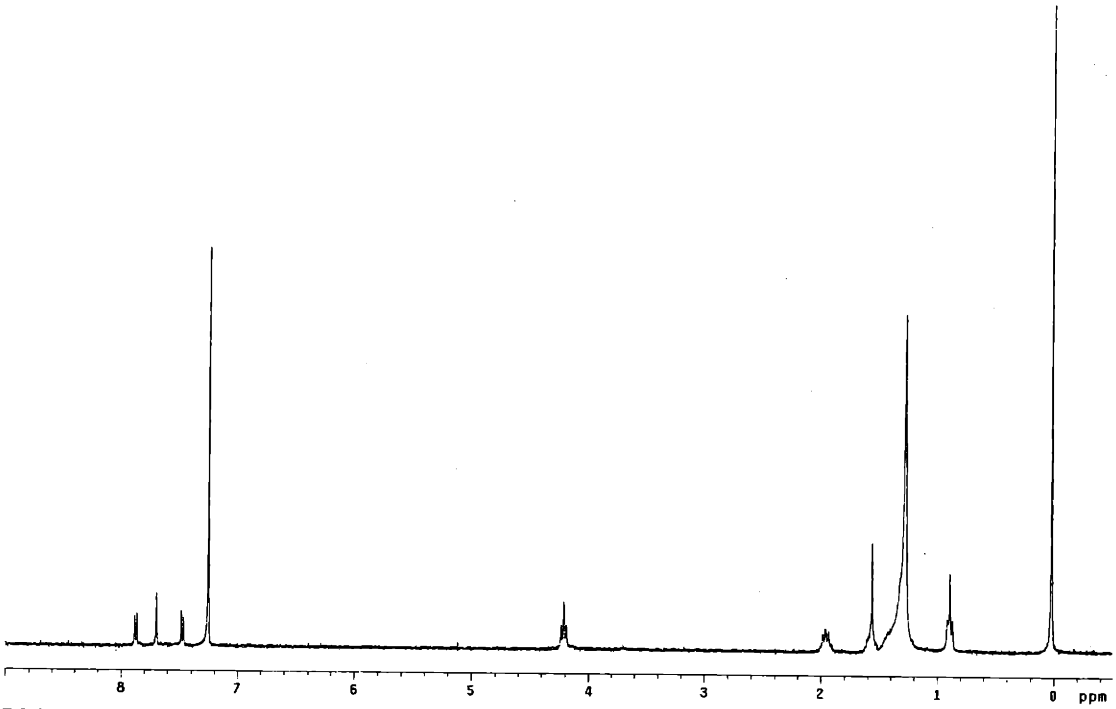

^{1}H NMR of **2b** (300 MHz, $CDCl_3$)

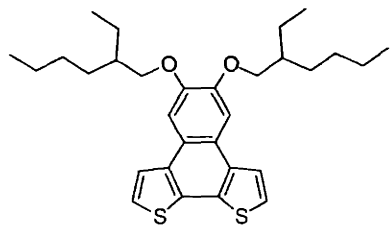

2c

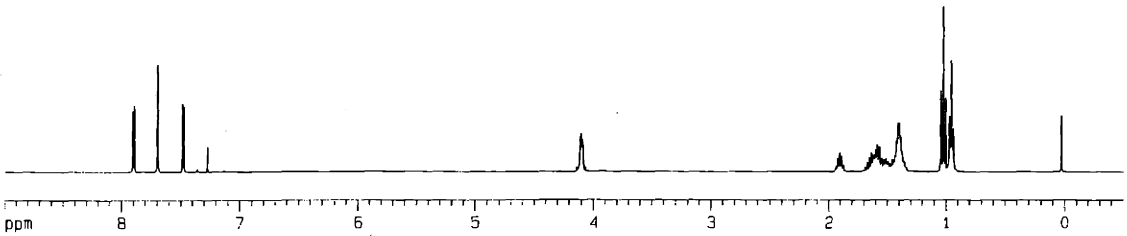

^{1}H NMR of **2c** (400 MHz, $CDCl_3$)

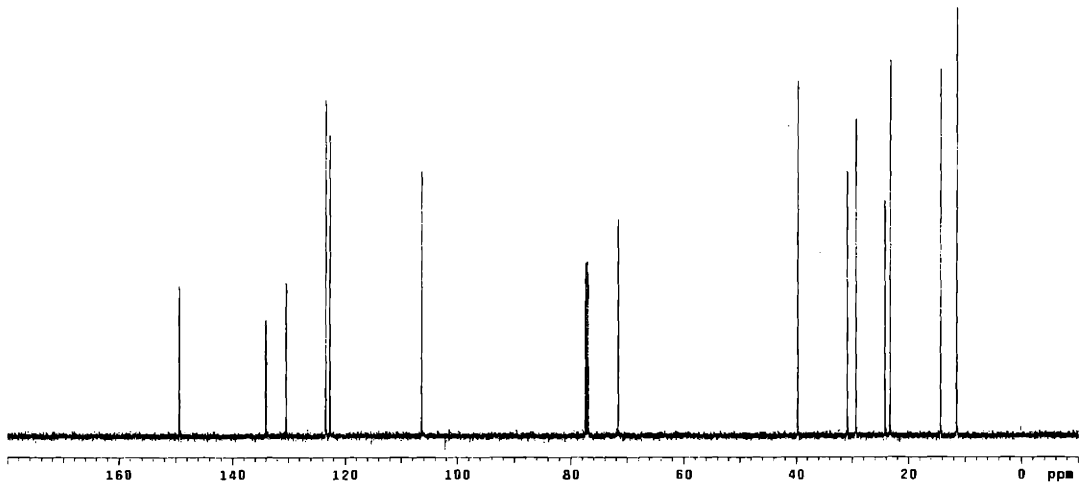

^{13}C NMR of **2c** (125 MHz, $CDCl_3$)

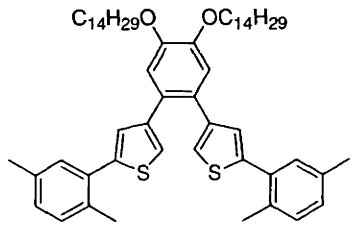

3

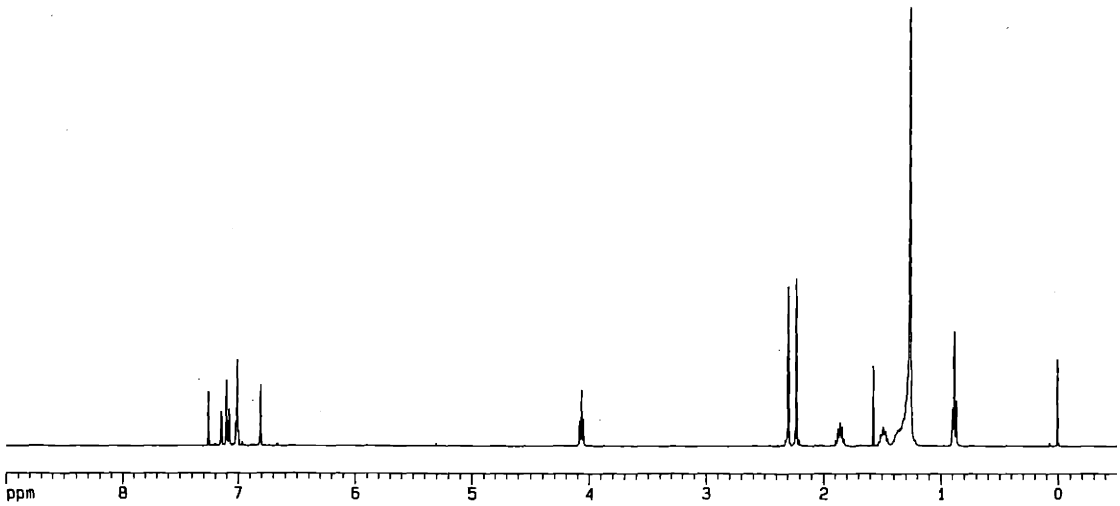

^{1}H NMR of **3** (400 MHz, $CDCl_3$)

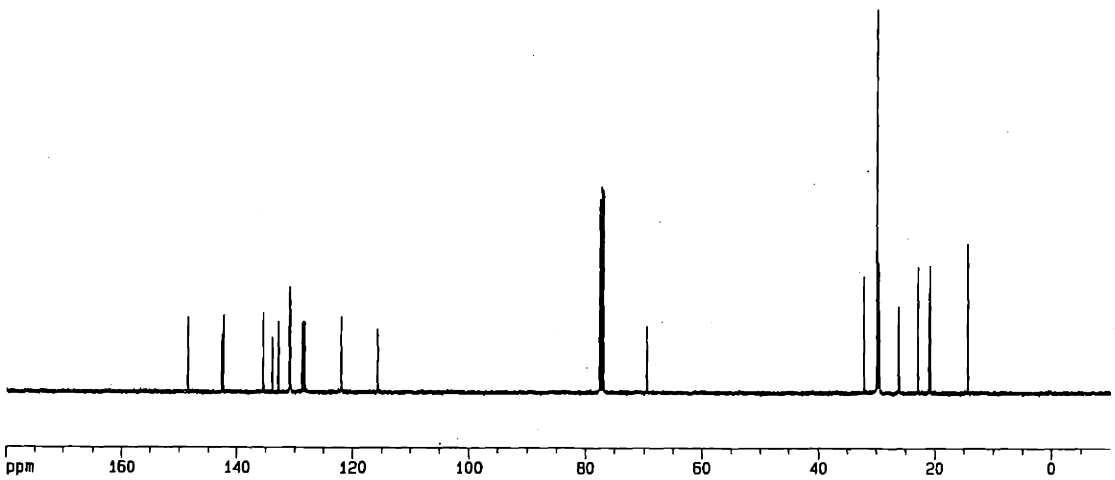

^{13}C NMR of **3** (100 MHz, $CDCl_3$)

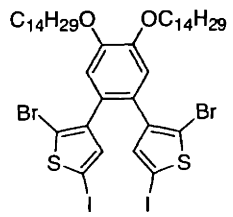

4

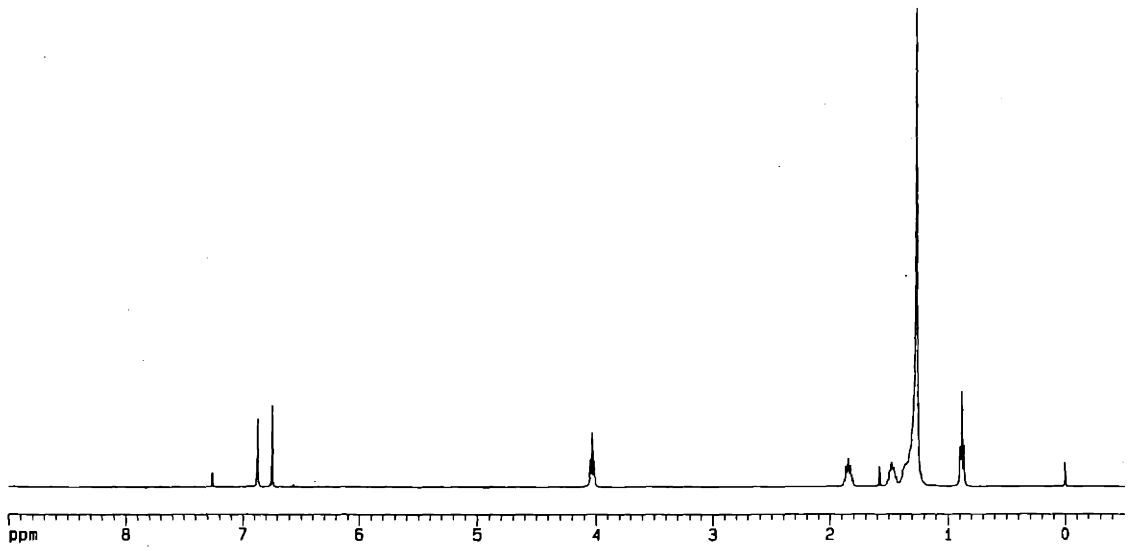

^{1}H NMR of **4** (400 MHz, $CDCl_3$)

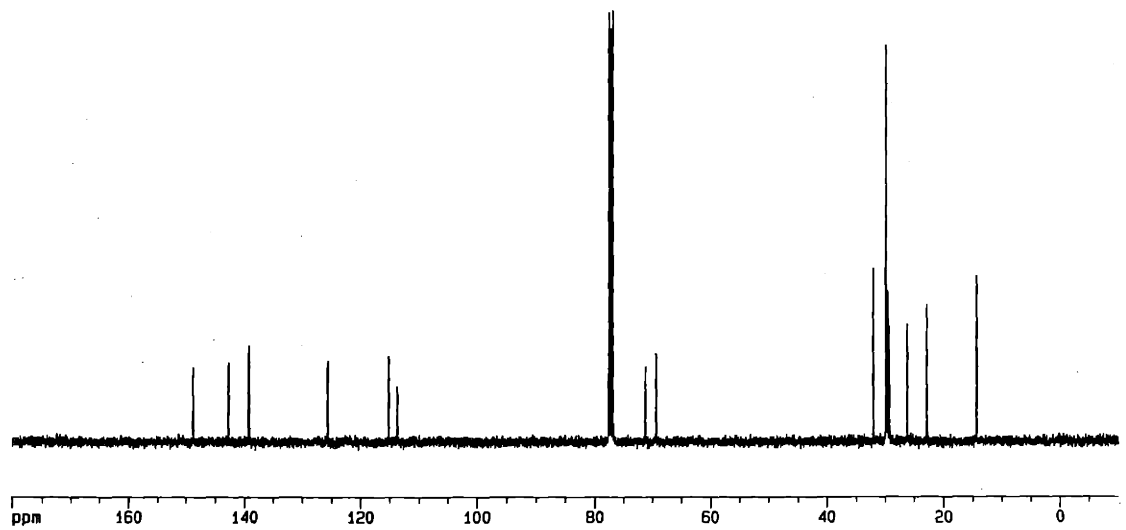

^{13}C NMR of **4** (100 MHz, $CDCl_3$)

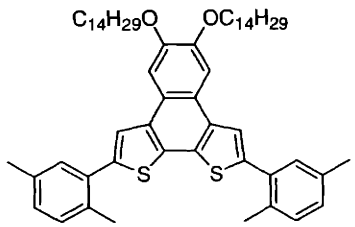

5

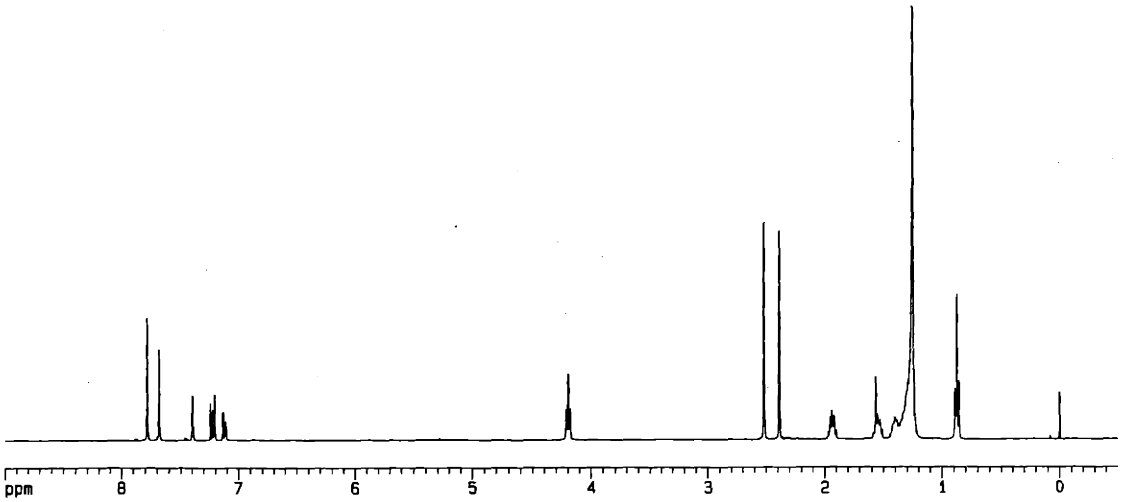

^{1}H NMR of **5** (400 MHz, $CDCl_3$)

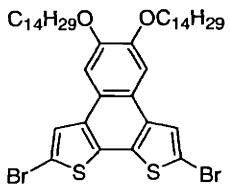

7

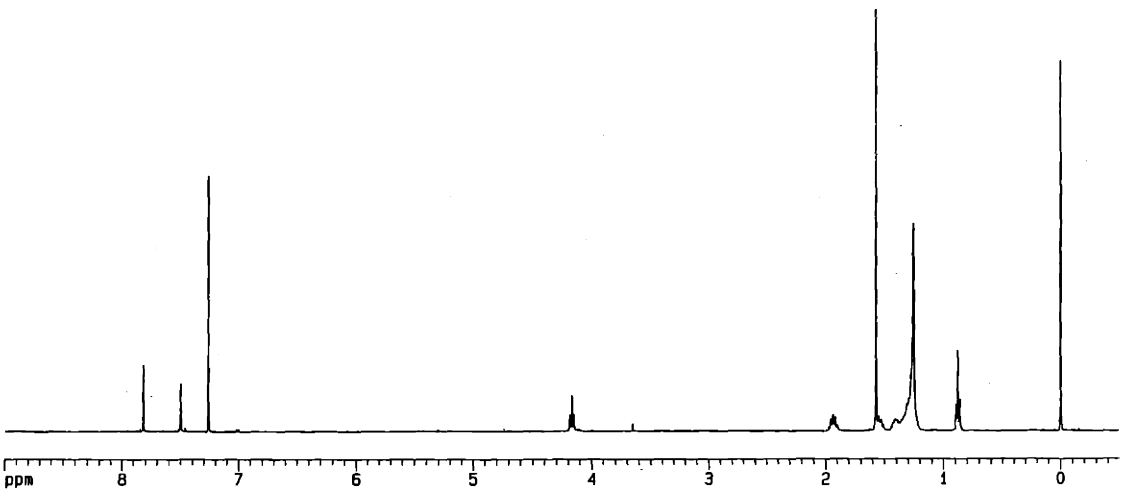

^{1}H NMR of **7** (400 MHz, $CDCl_3$)

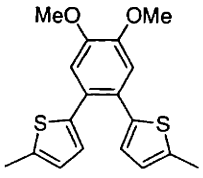

8

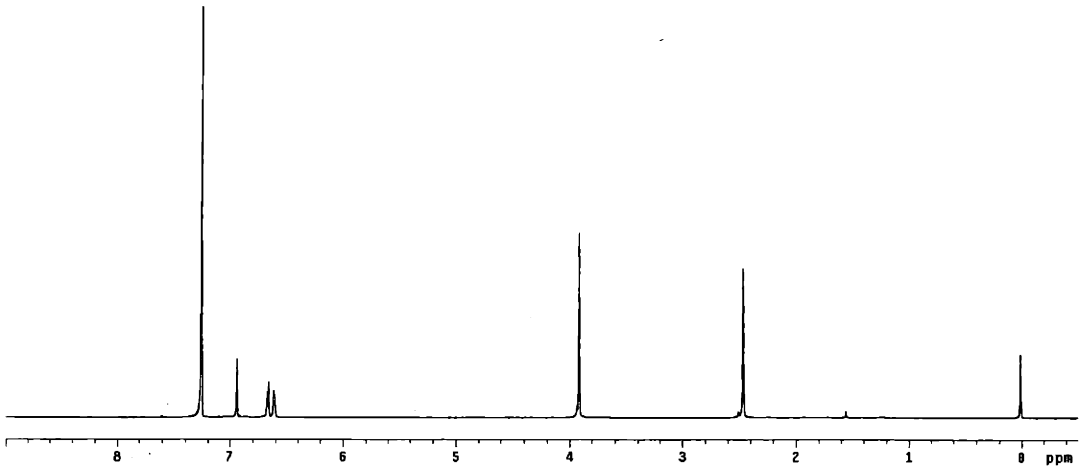

^{1}H NMR of **8** (300 MHz, $CDCl_3$)

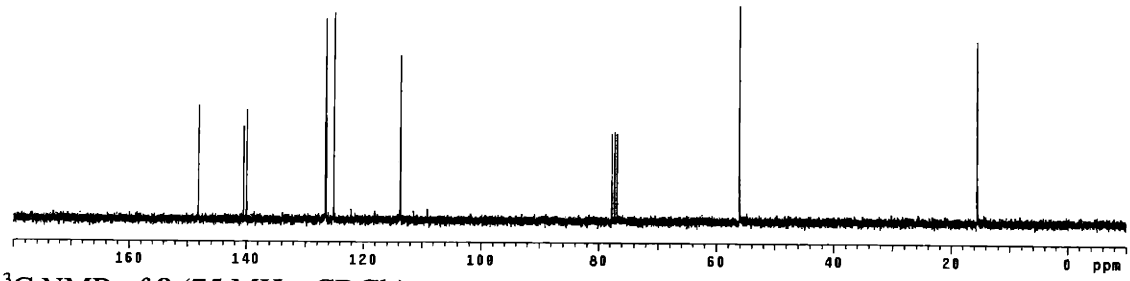

^{13}C NMR of **8** (75 MHz, $CDCl_3$)

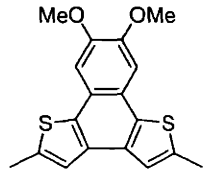

9

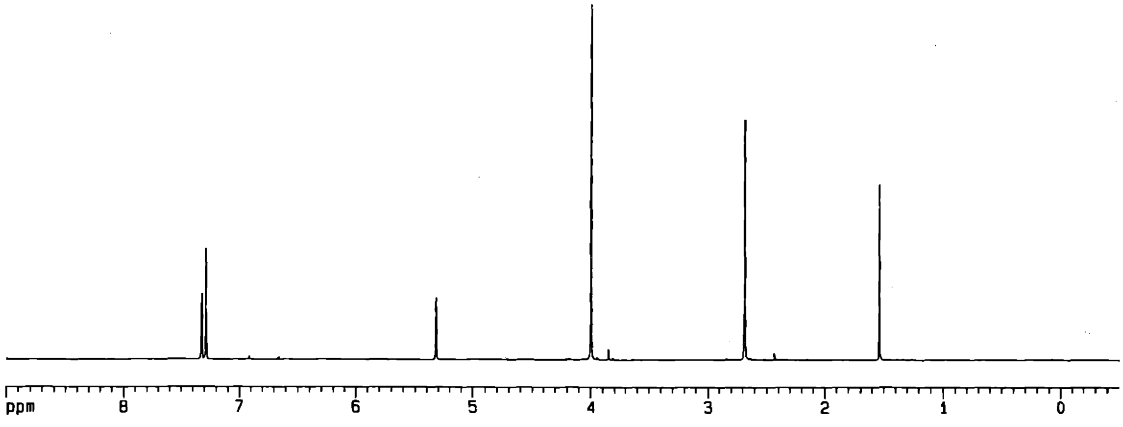

^{1}H NMR of **9** (400 MHz, CD_2Cl_2)

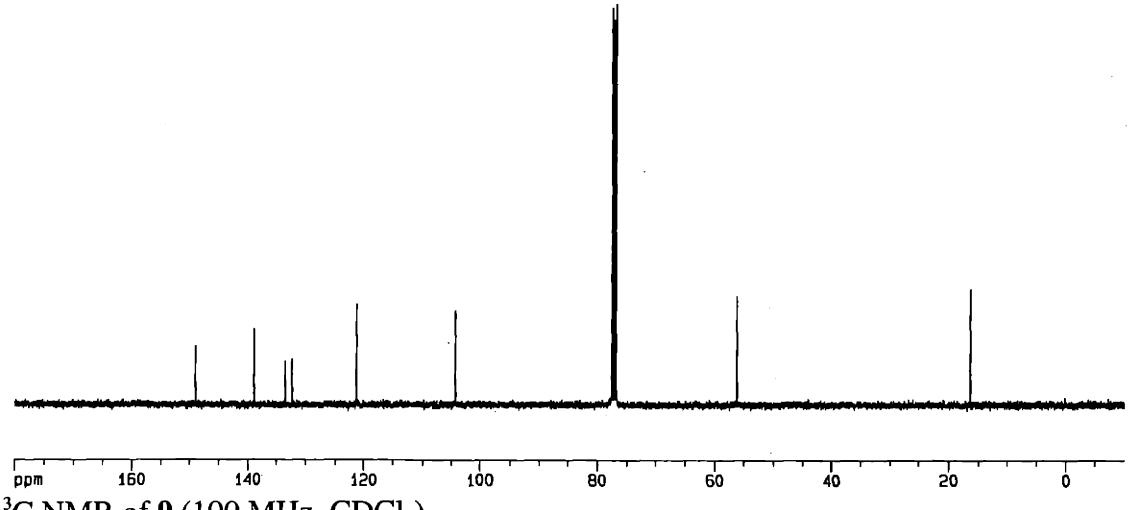

^{13}C NMR of **9** (100 MHz, $CDCl_3$)

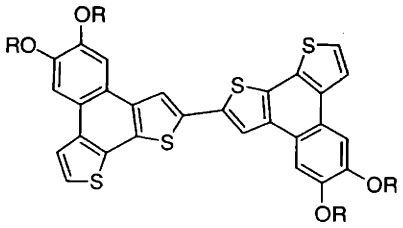

10 (R = 2-ethyl hexyl, n=0)

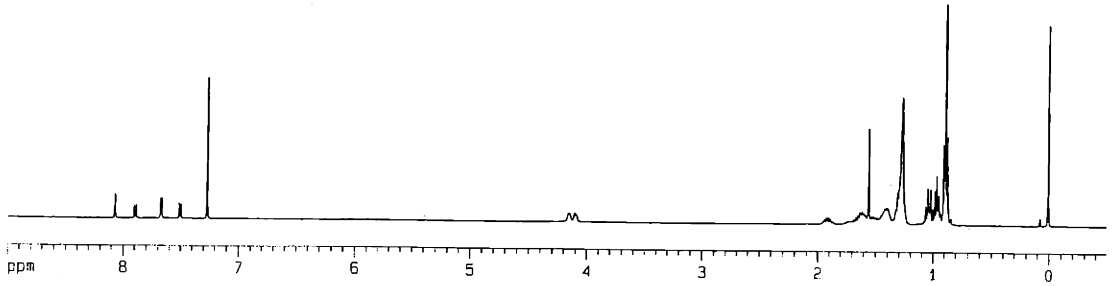

^{1}H NMR of **10** dimer (400 MHz, $CDCl_3$)

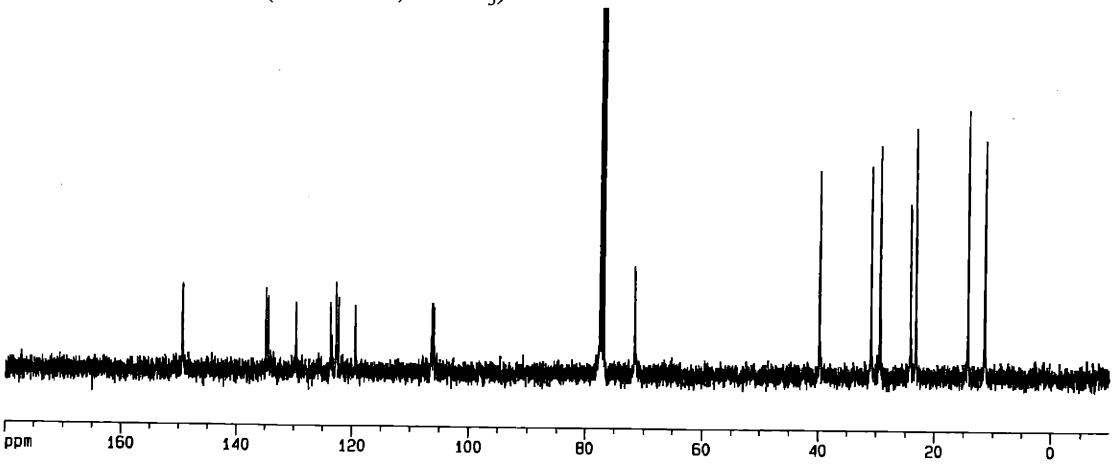

^{13}C NMR of **10** dimer (100 MHz, $CDCl_3$)

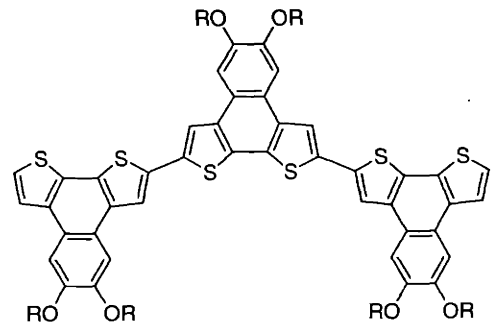

10 (R = 2-ethyl hexyl, n=1)

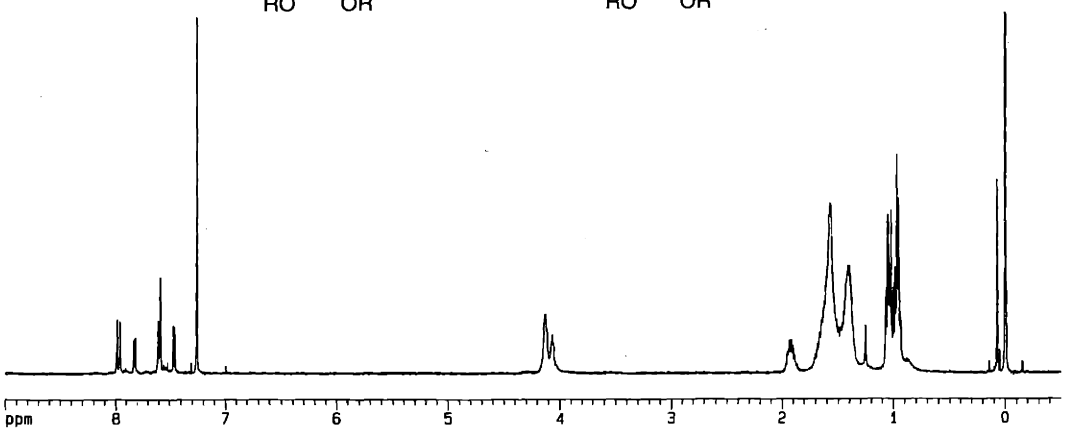

^{1}H NMR of **10** trimer (400 MHz, $CDCl_3$)

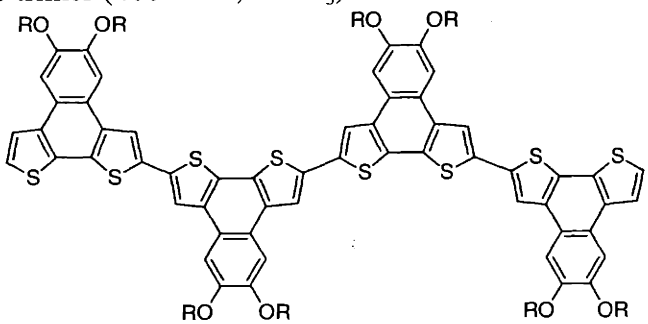

10 (R = 2-ethyl hexyl, n=2)

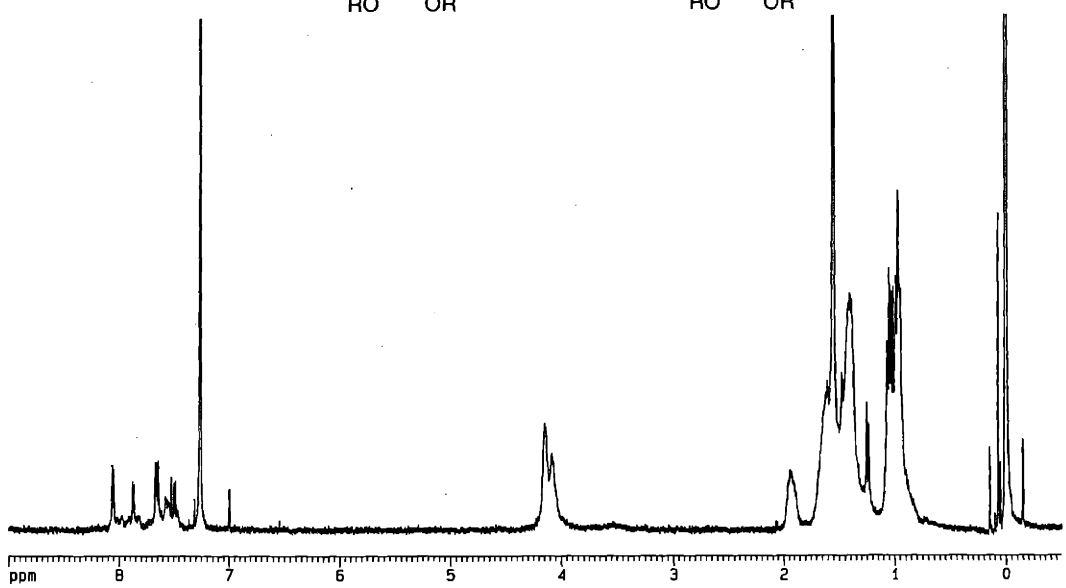

^{1}H NMR of **10** tetramer (400 MHz, $CDCl_3$)

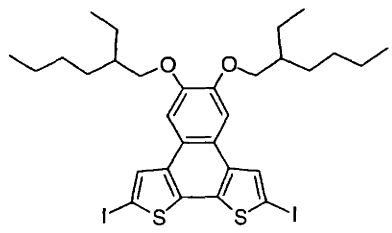

12

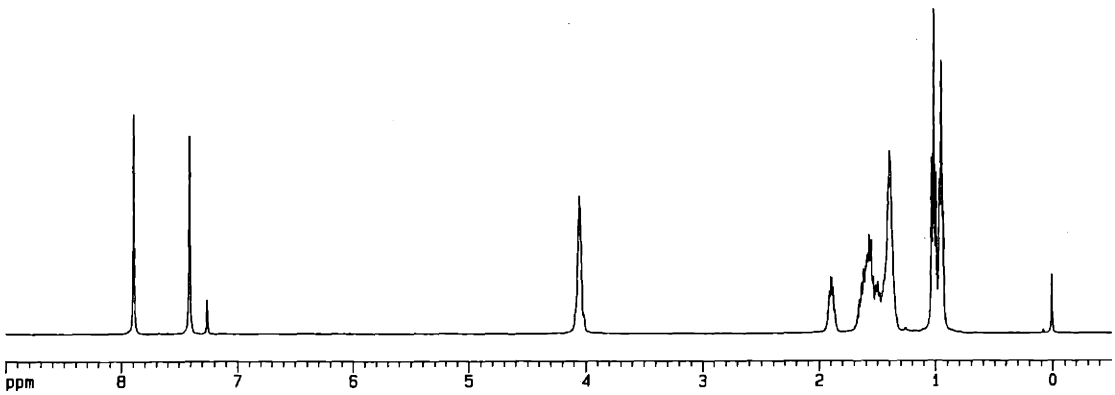

^{1}H NMR of **12** (400 MHz, $CDCl_3$)

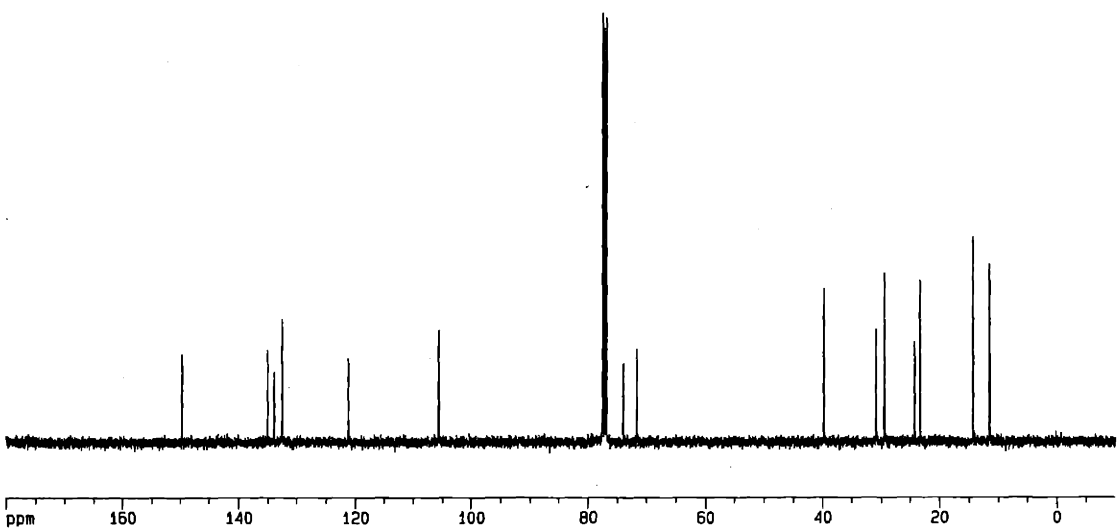

^{13}C NMR of **12** (100 MHz, $CDCl_3$)

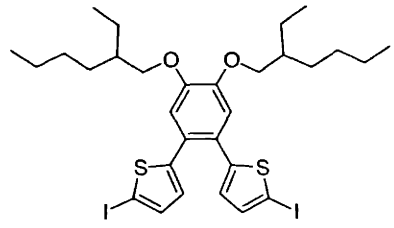

13

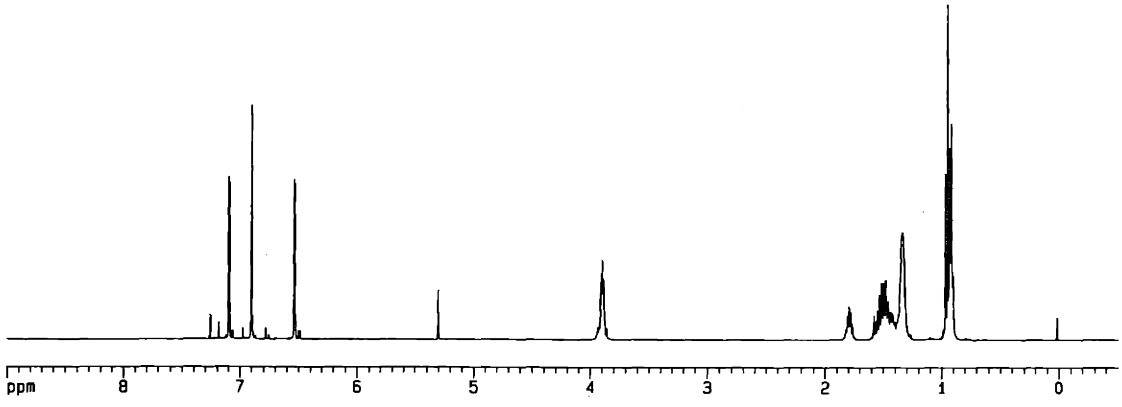

^{1}H NMR of **13** (400 MHz, $CDCl_3$)

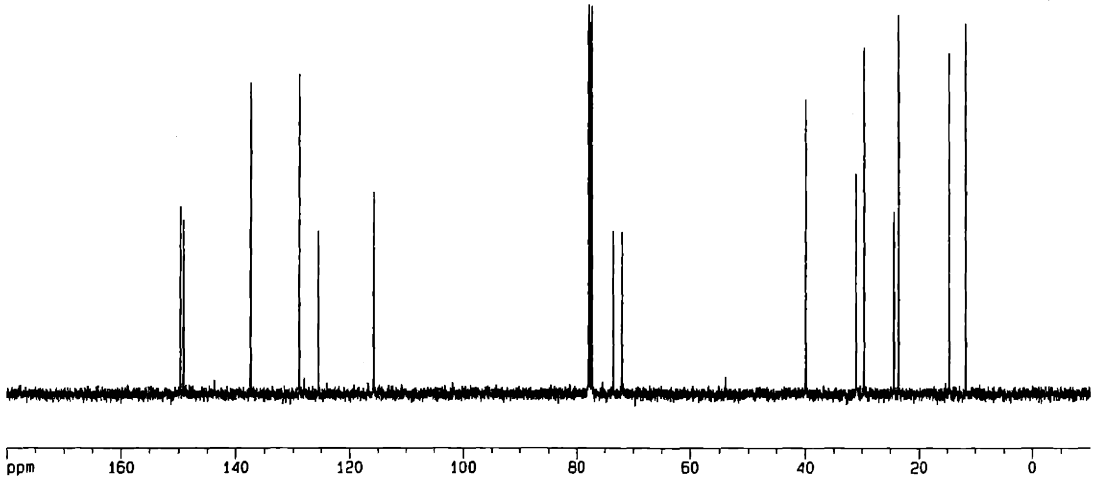

^{13}C NMR of **13** (100 MHz, $CDCl_3$)

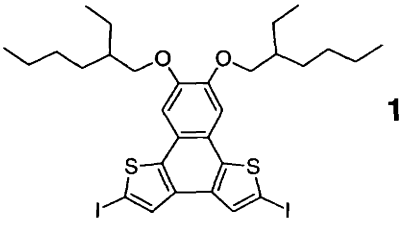

14

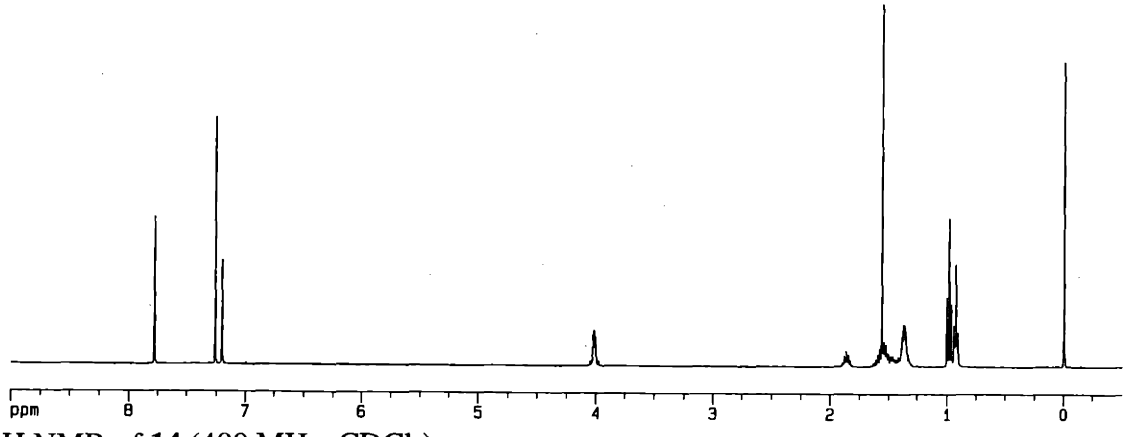

^{1}H NMR of **14** (400 MHz, $CDCl_3$)

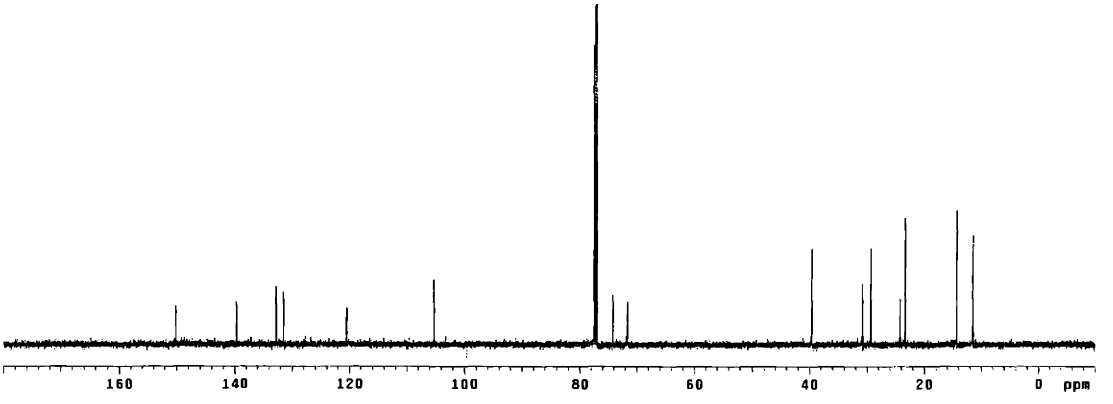

^{13}C NMR of **14** (125 MHz, $CDCl_3$)

Appendix 4:

^{1}H and ^{13}C NMR spectra for Chapter 4

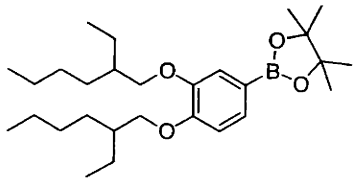

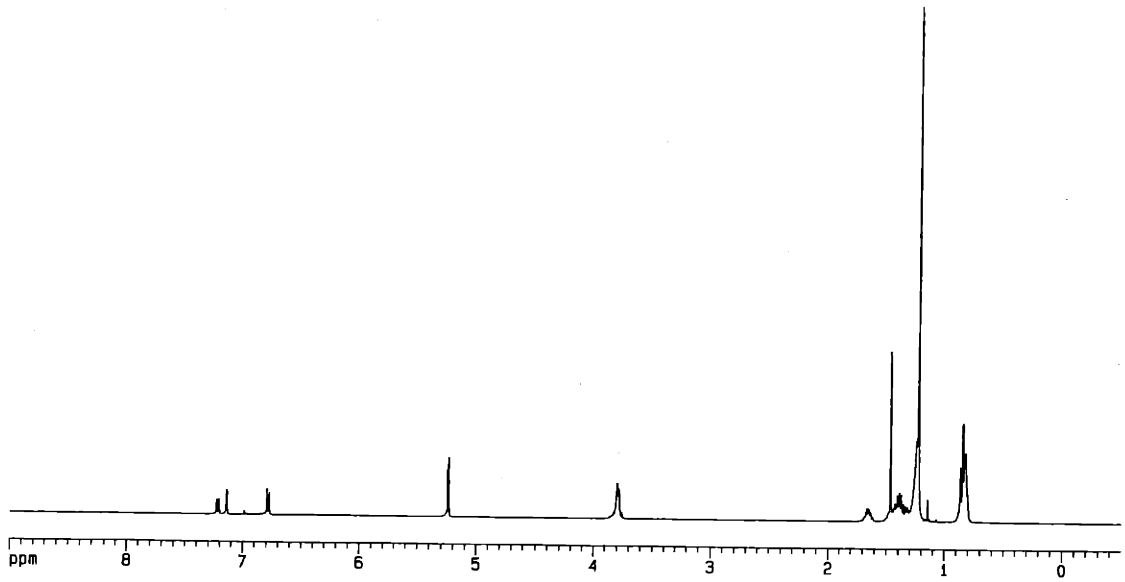

^{1}H NMR (400 MHz, $CDCl_3$)

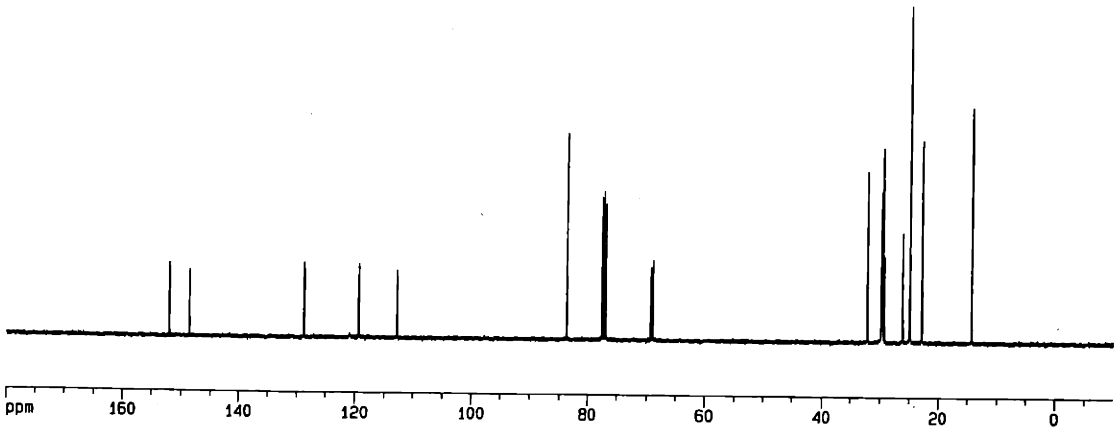

^{13}C NMR (100 MHz, $CDCl_3$)

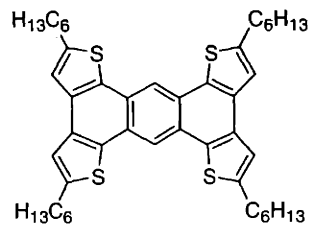

1

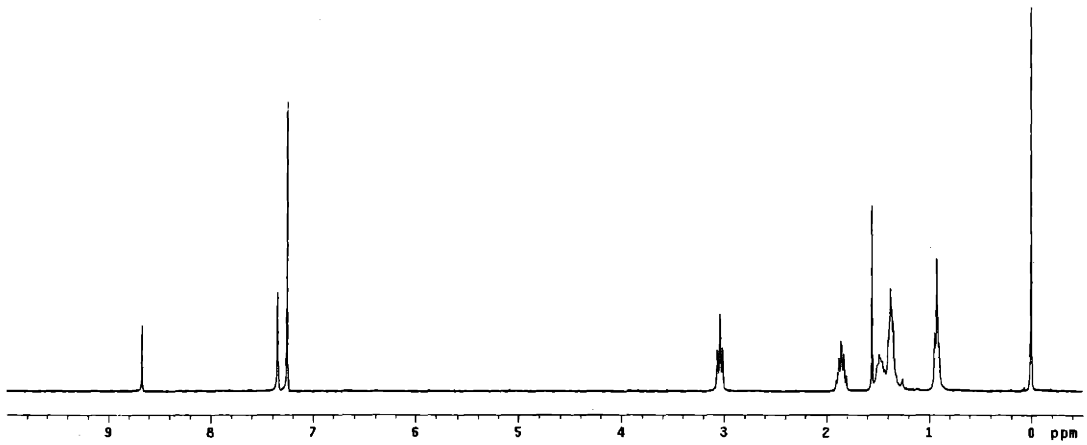

^{1}H NMR of **1** (300 MHz, $CDCl_3$)

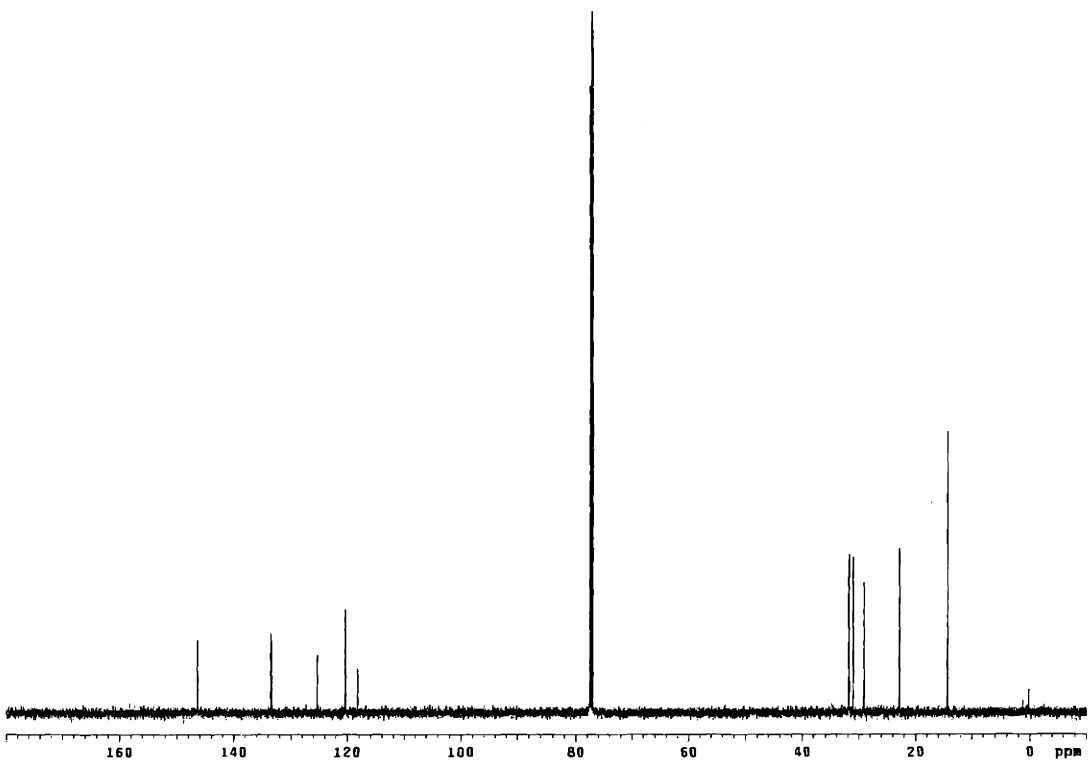

^{13}C NMR of **1** (125 MHz, $CDCl_3$)

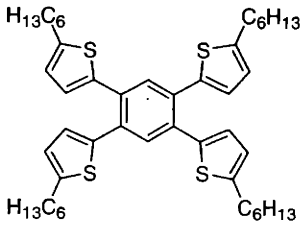

2

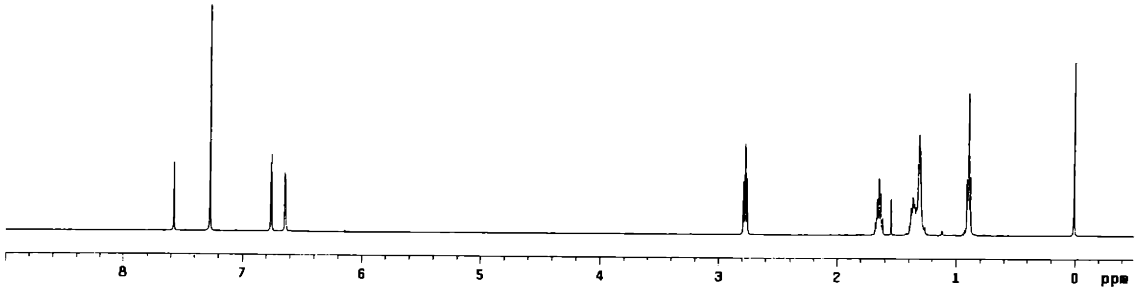

^{1}H NMR of **2** (500 MHz, $CDCl_3$)

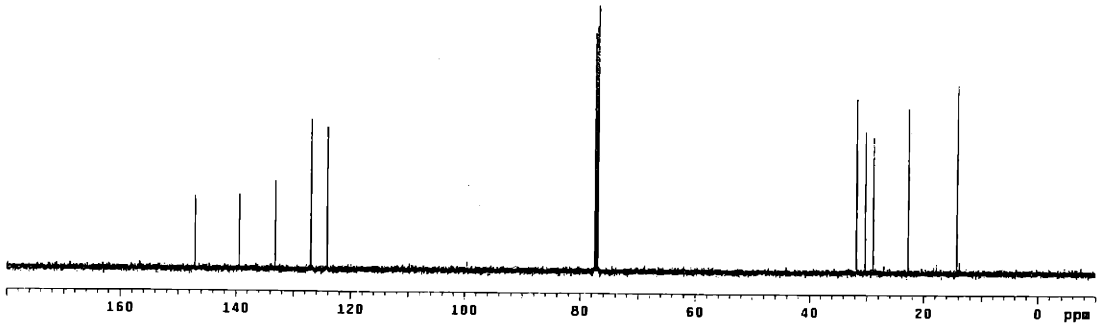

^{13}C NMR of **2** (125 MHz, $CDCl_3$)

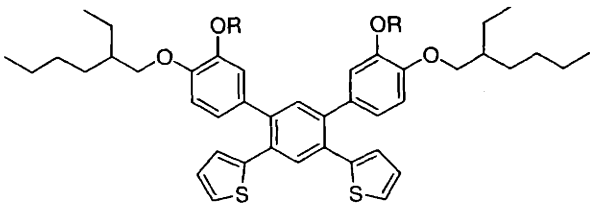

4 (R = 2-ethylhexyl)

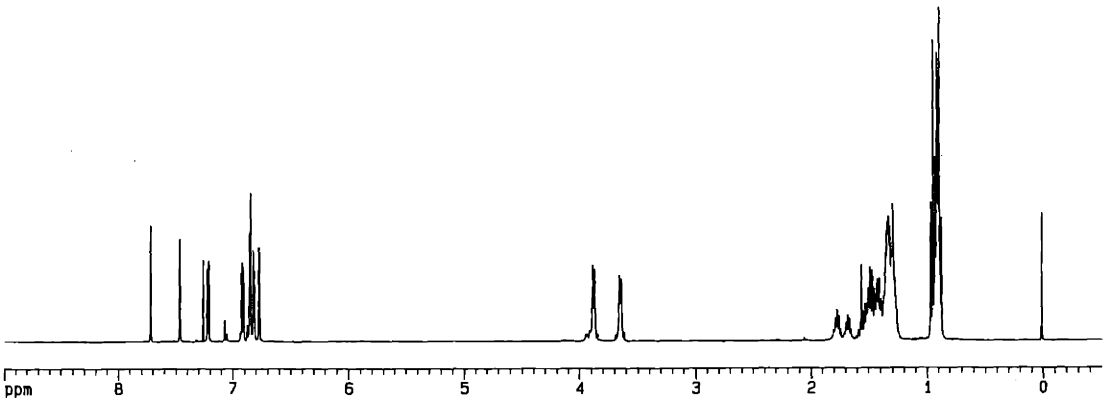

^{1}H NMR of **4** (400 MHz, $CDCl_3$)

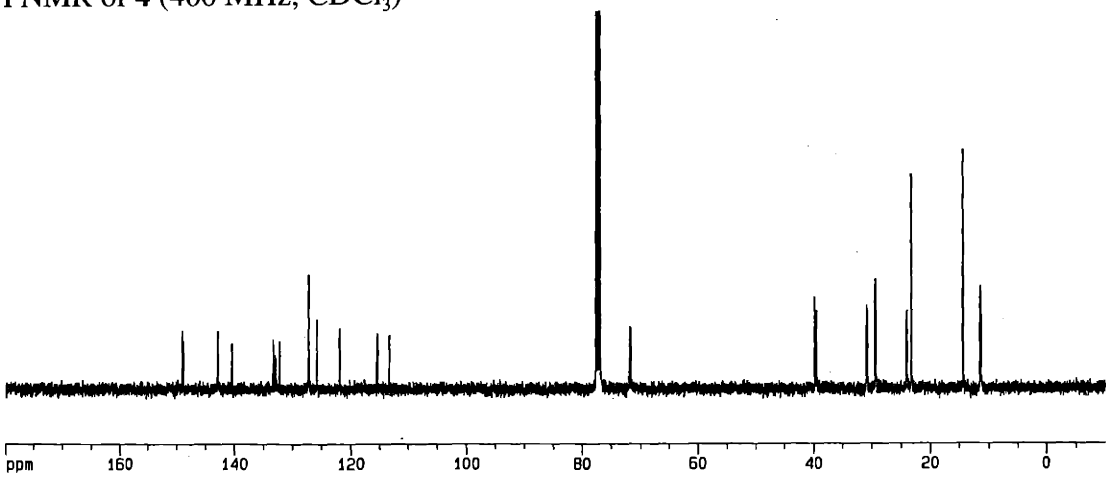

^{13}C NMR of **4** (100 MHz, $CDCl_3$)

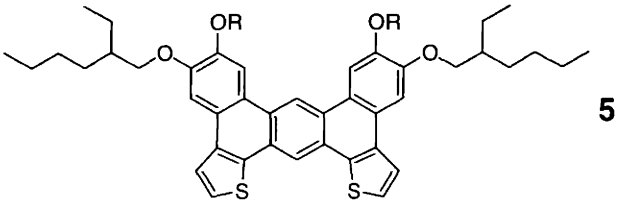

5 (R = 2-ethylhexyl)

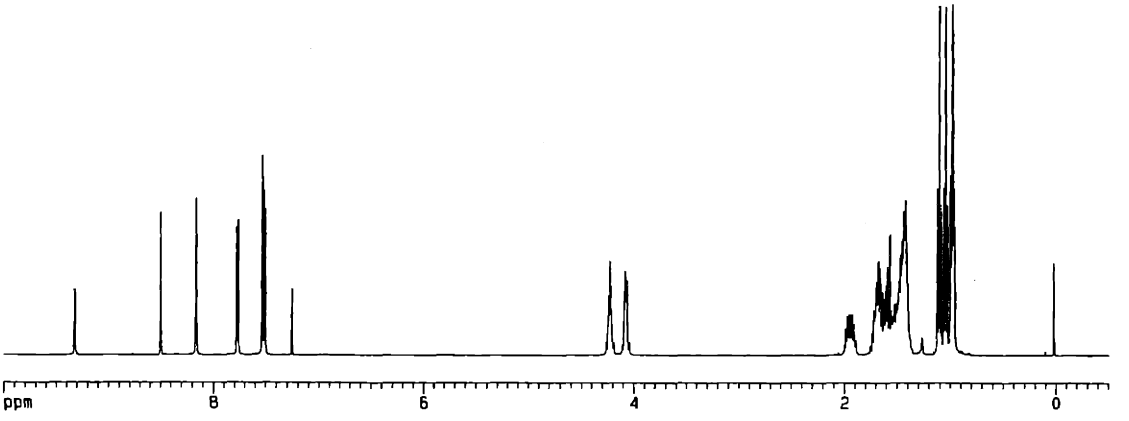

^{1}H NMR of **5** (400 MHz, $CDCl_3$)

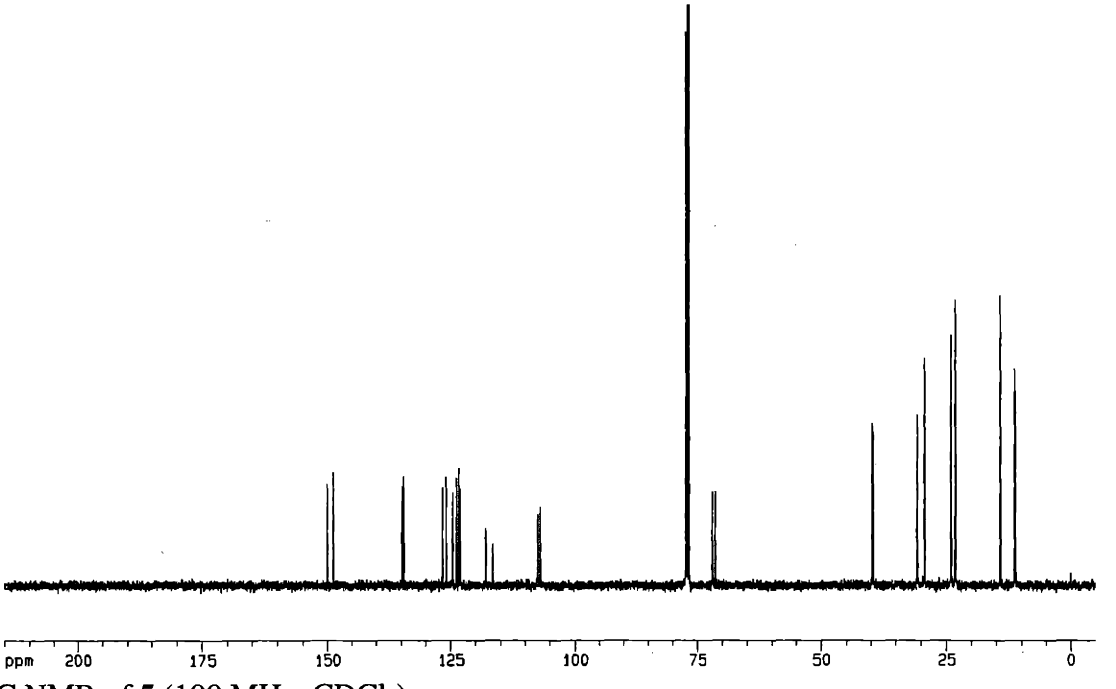

^{13}C NMR of **5** (100 MHz, $CDCl_3$)

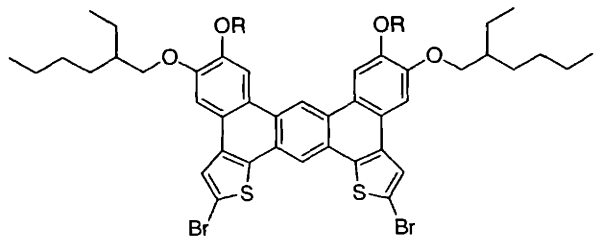

6 (R = 2-ethylhexyl)

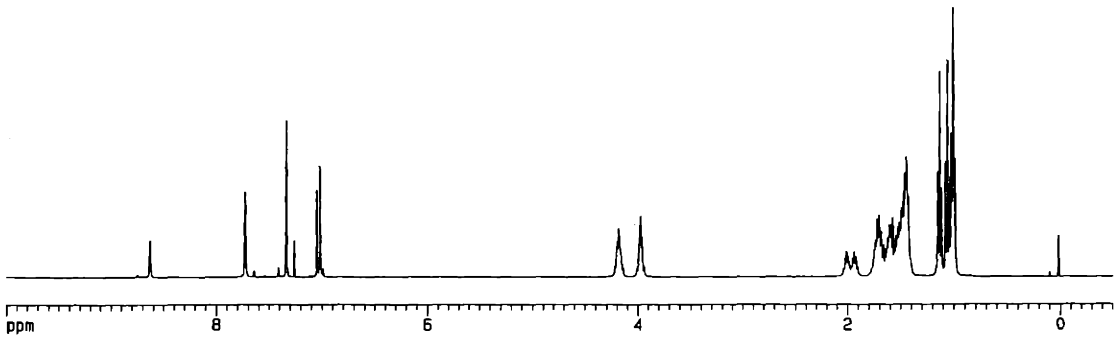

^{1}H NMR of **6** (400 MHz, $CDCl_3$)

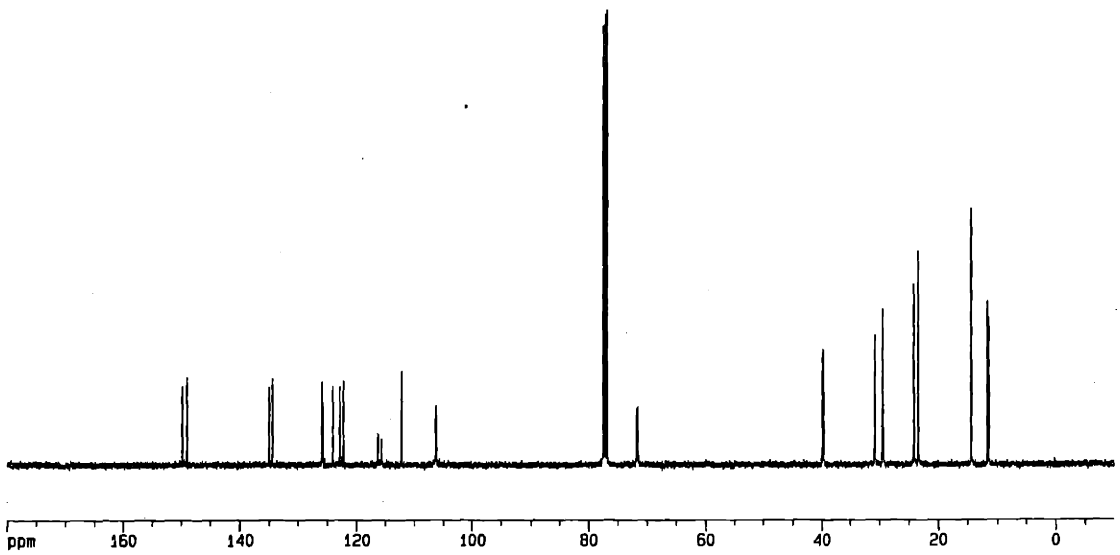

^{13}C NMR of **6** (100 MHz, $CDCl_3$)

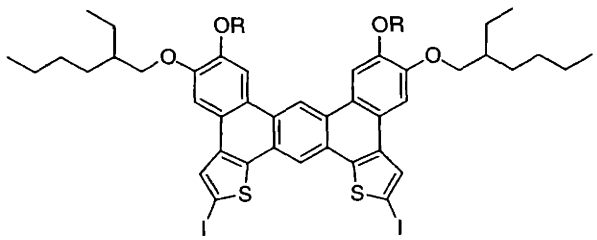

7 (R = 2-ethylhexyl)

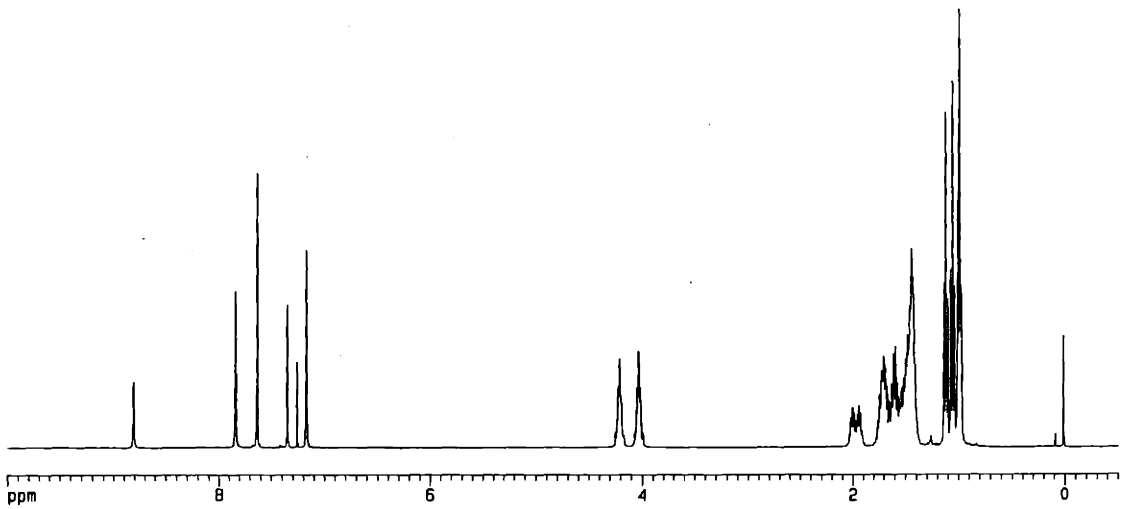

^{1}H NMR of **7** (400 MHz, $CDCl_3$)

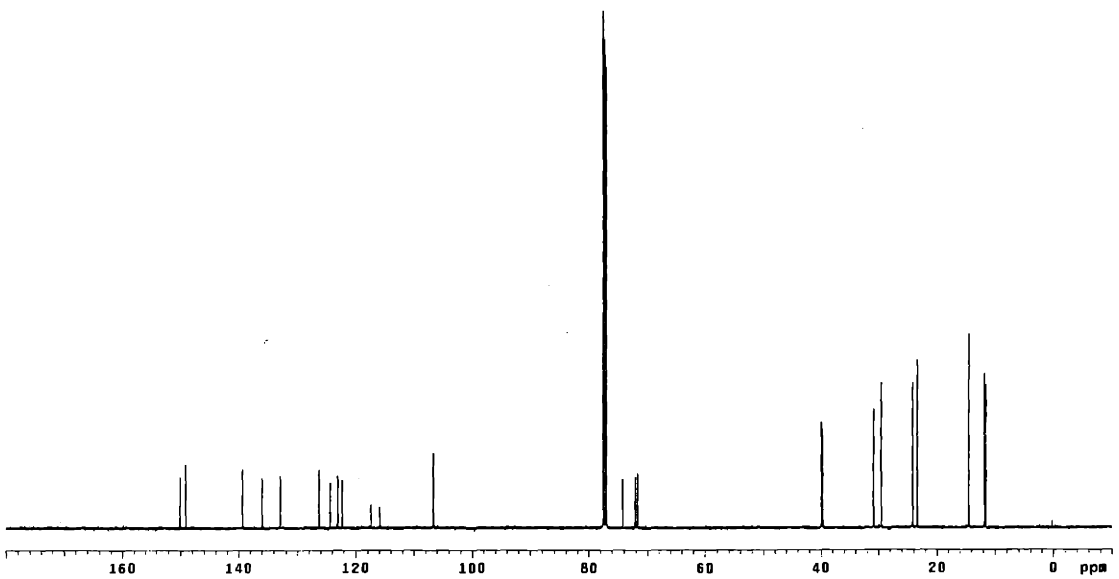

^{13}C NMR of **7** (125 MHz, $CDCl_3$)

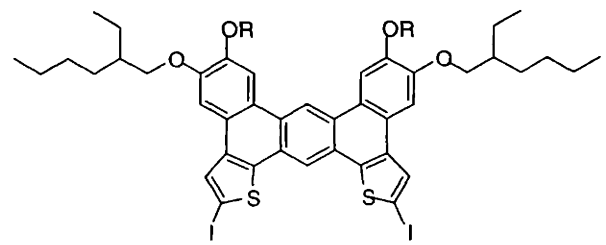

7 (R = 2-ethylhexyl)

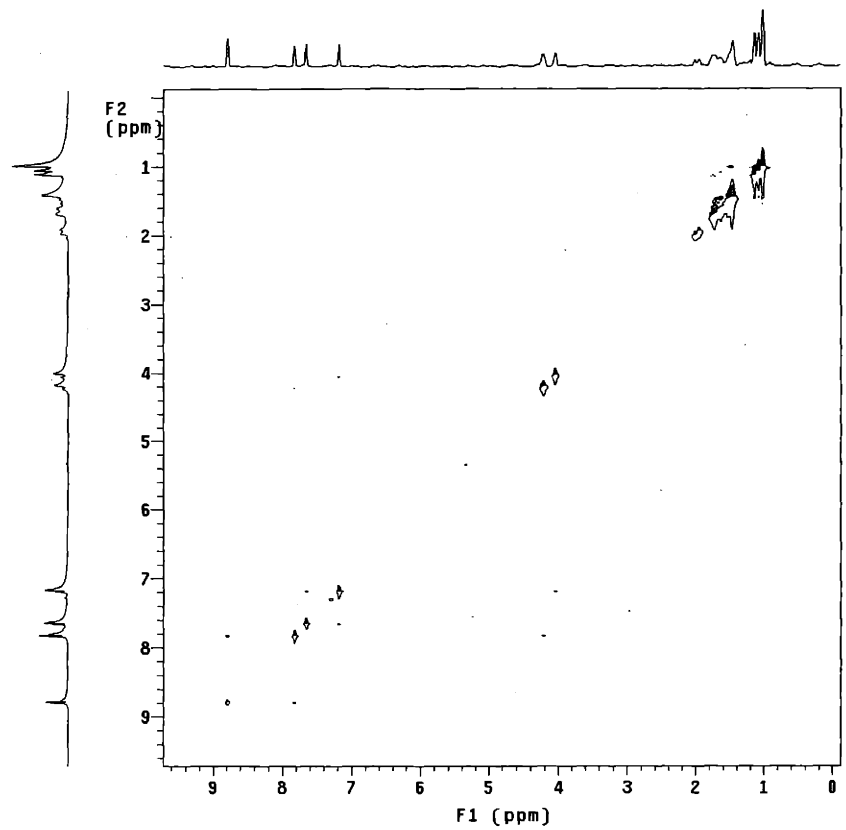

ROESY of **7** (500 MHz, CD_2Cl_2)

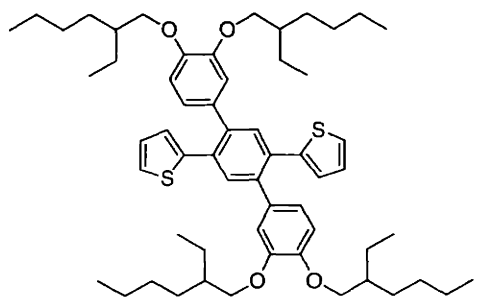

9

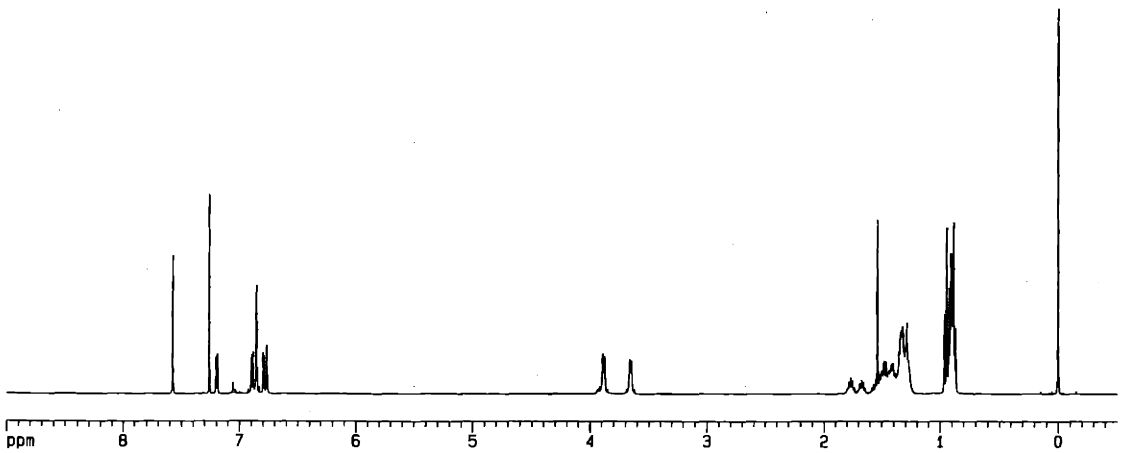

^{1}H NMR of **9** (400 MHz, $CDCl_3$)

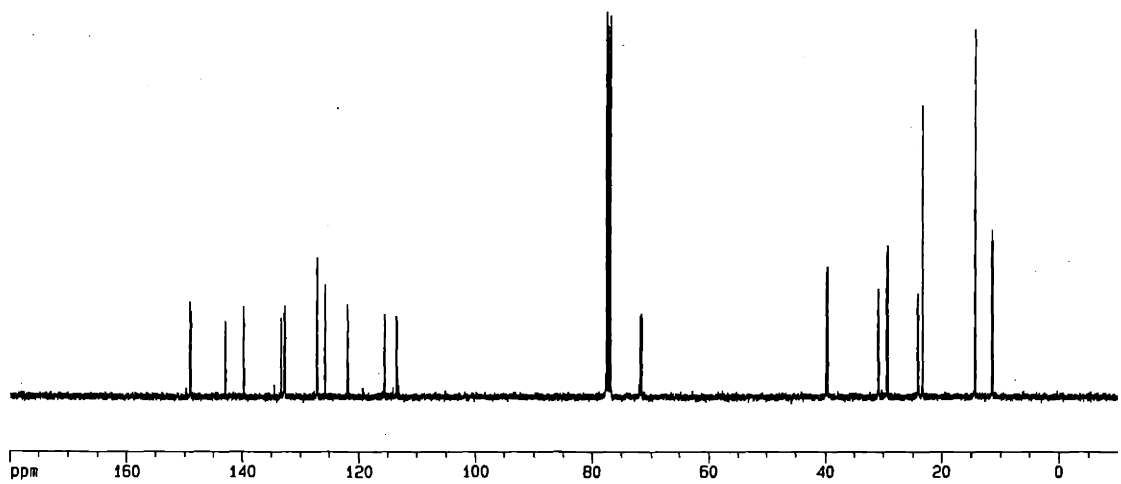

^{13}C NMR of **9** (100 MHz, $CDCl_3$)

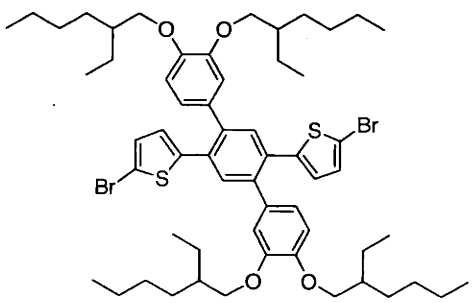

10

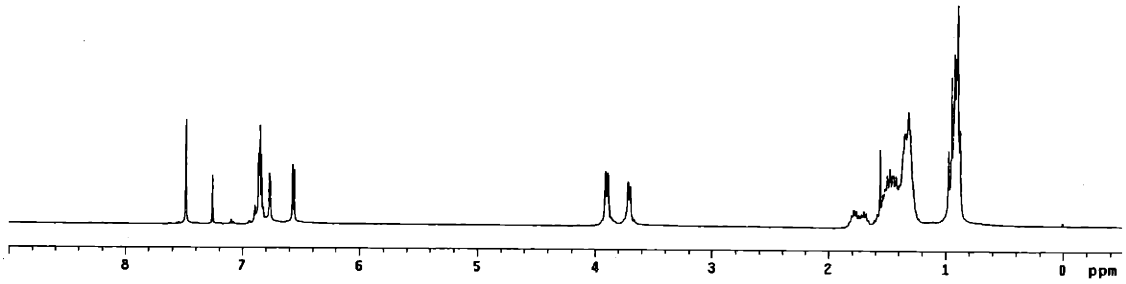

^{1}H NMR of **10** (300 MHz, $CDCl_3$)

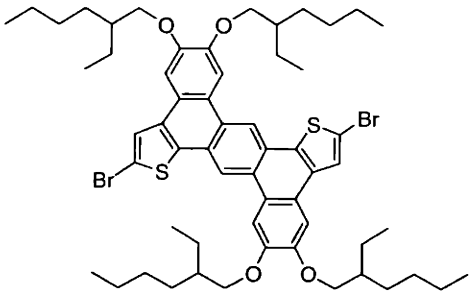

12

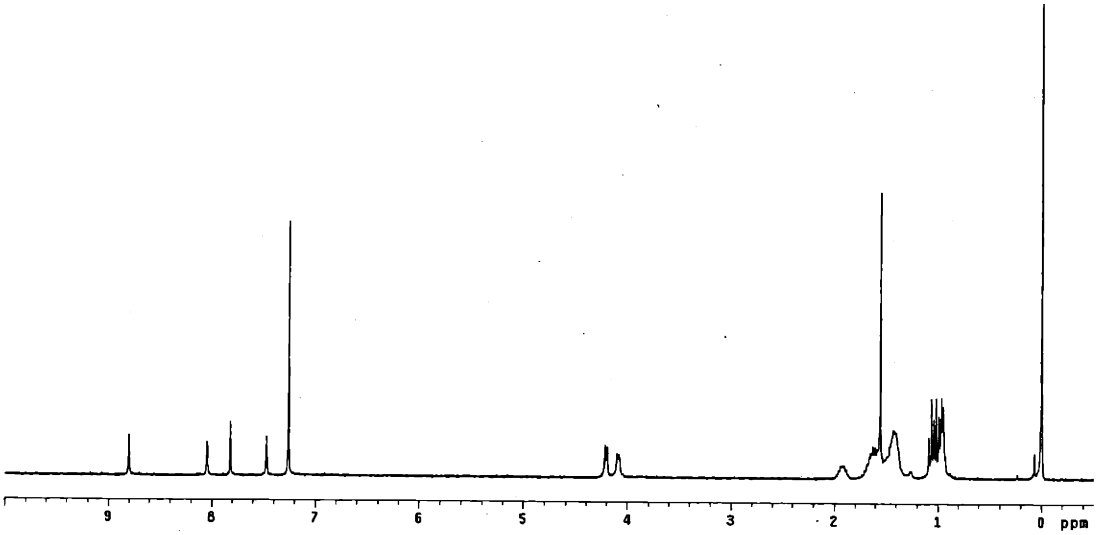

^{1}H NMR of **12** (300 MHz, $CDCl_3$)

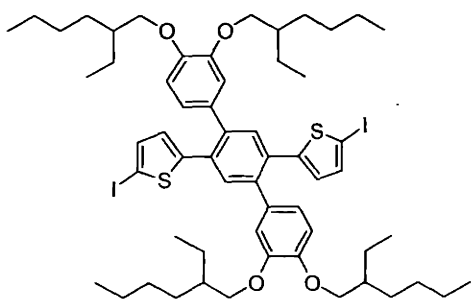

11

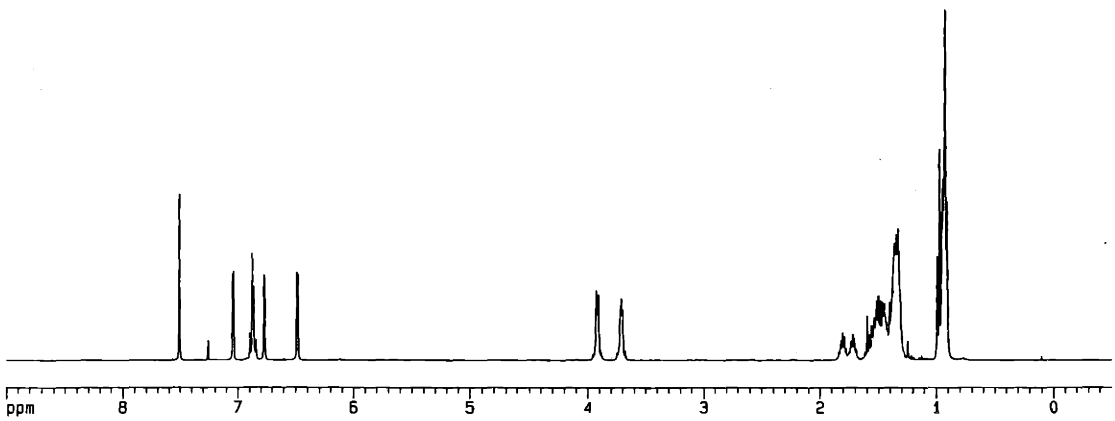

^{1}H NMR of **11** (400 MHz, $CDCl_3$)

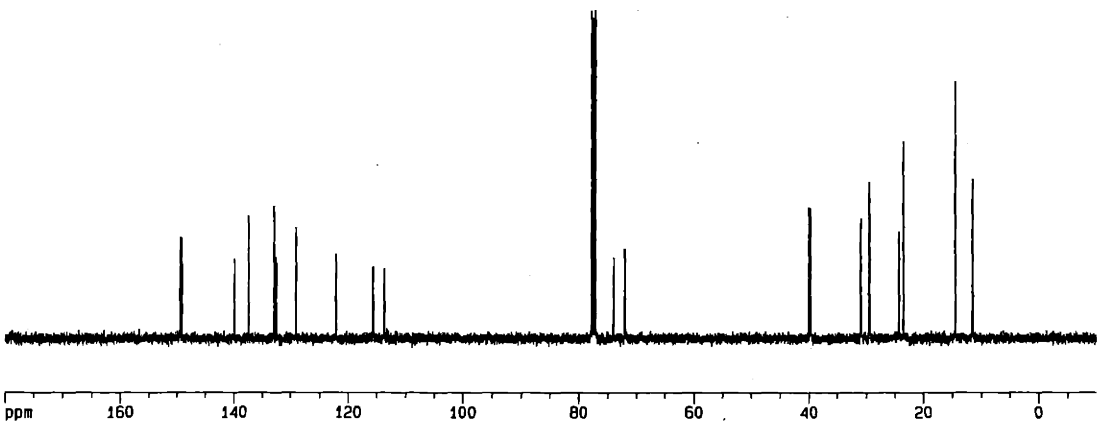

^{13}C NMR of **11** (100 MHz, $CDCl_3$)

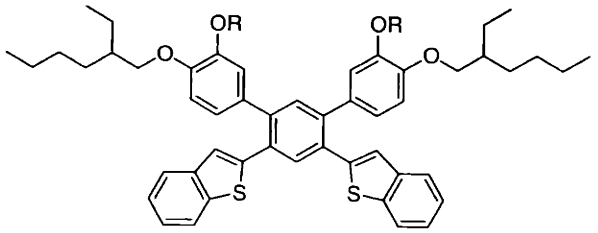

13 (R = 2-ethyl hexyl)

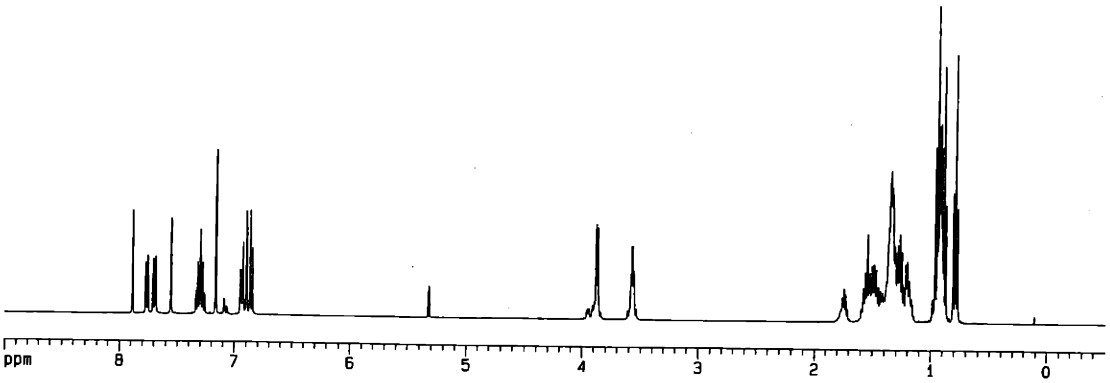

^{1}H NMR of **13** (400 MHz, CD_2Cl_2)

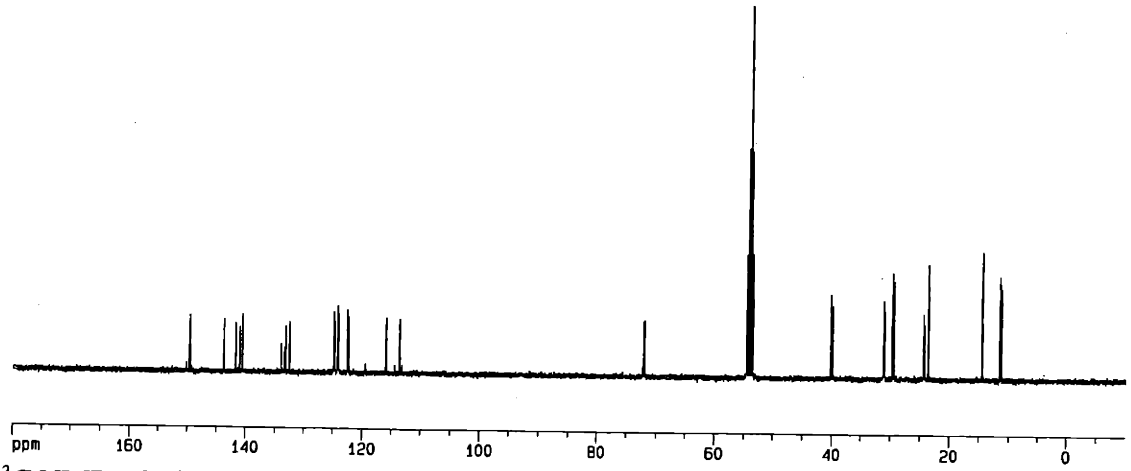

^{13}C NMR of **13** (100 MHz, CD_2Cl_2)

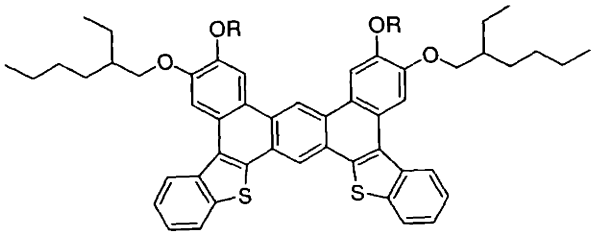

14 (R = 2-ethyl hexyl)

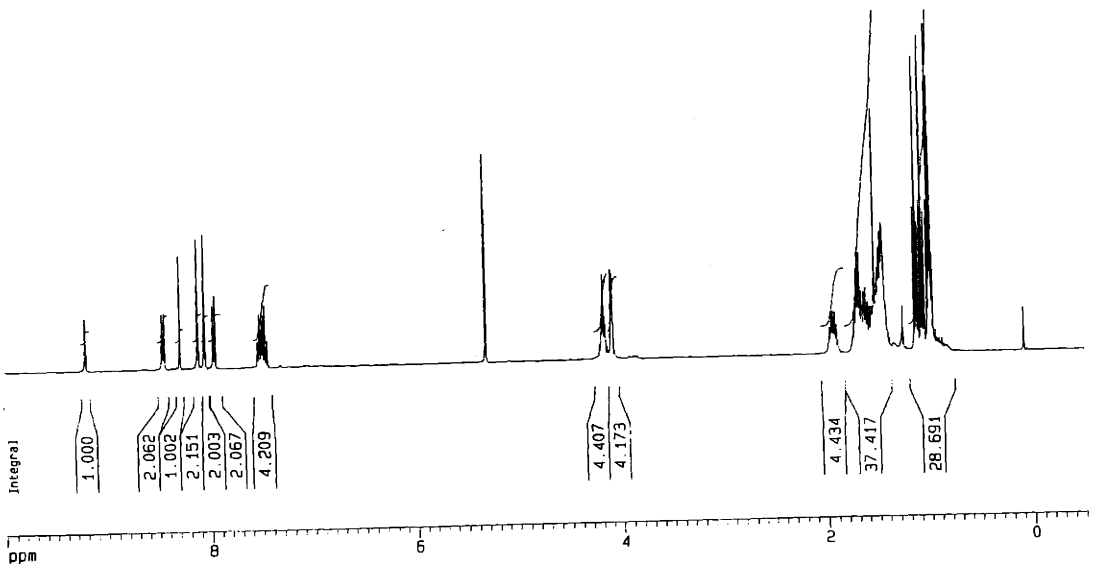

^{1}H NMR of **14** (400 MHz, CD_2Cl_2)

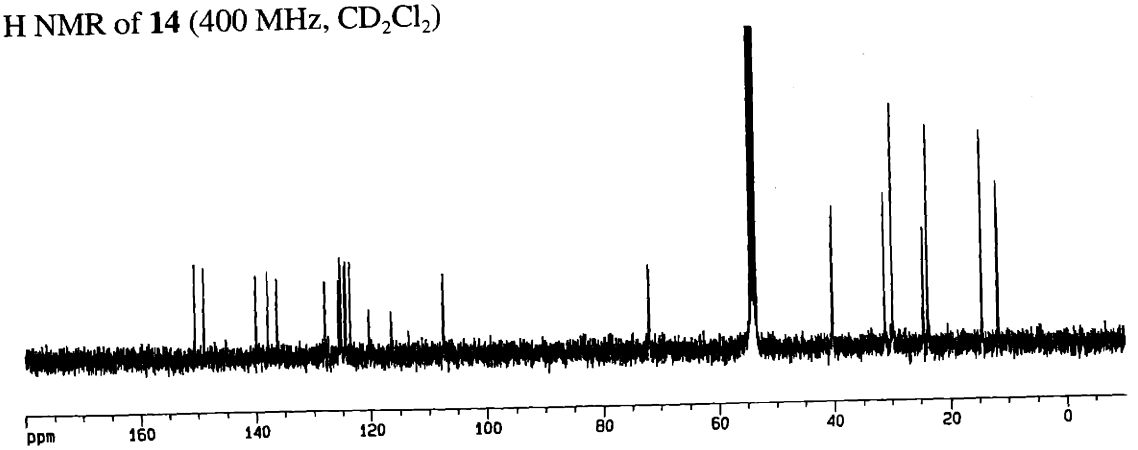

^{13}C NMR of **14** (100 MHz, CD_2Cl_2)

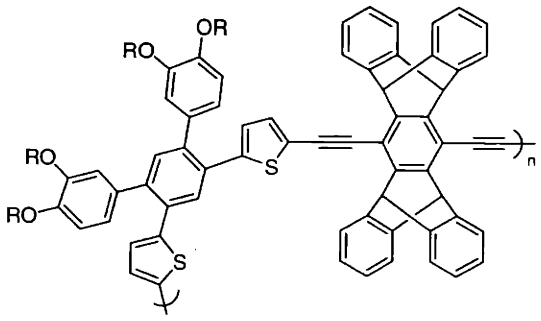

16 (R = 2-ethyl hexyl)

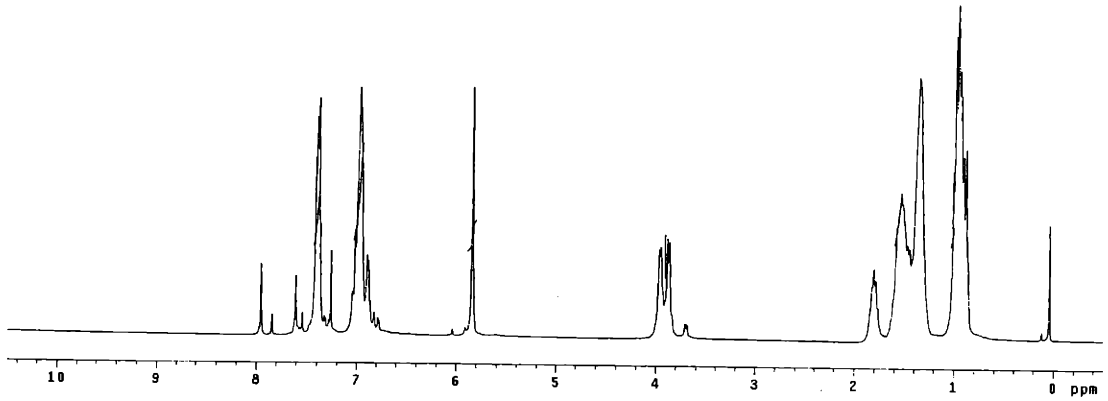

^{1}H NMR of **16** (300 MHz, $CDCl_3$)

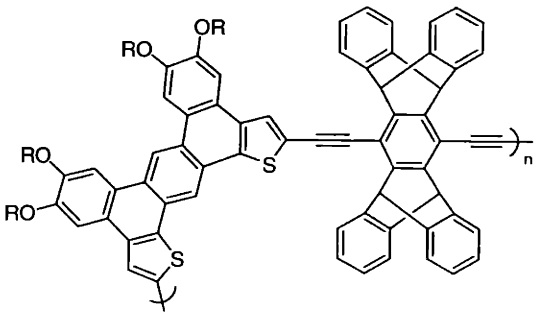

17 (R = 2-ethyl hexyl)

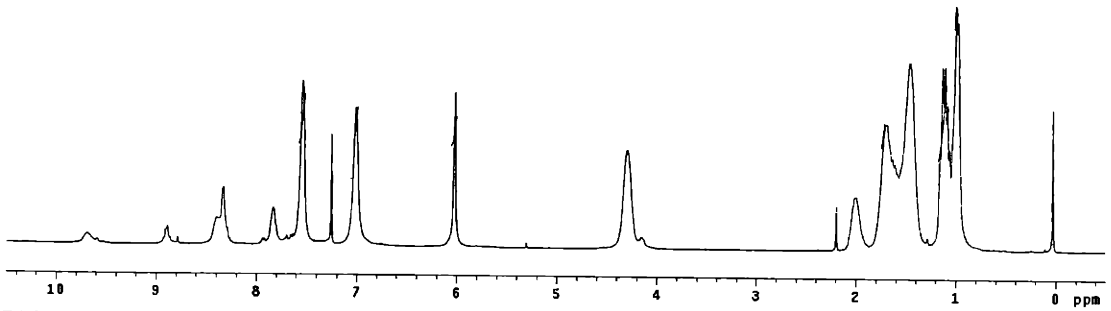

^{1}H NMR of **17** (300 MHz, $CDCl_3$)

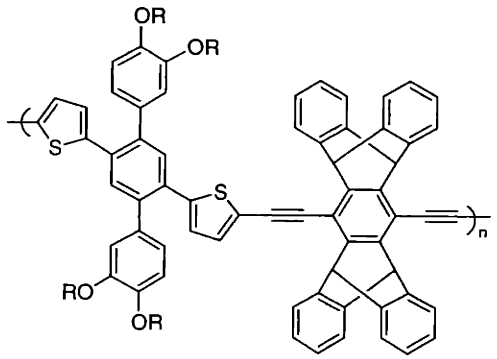

18 (R = 2-ethyl hexyl)

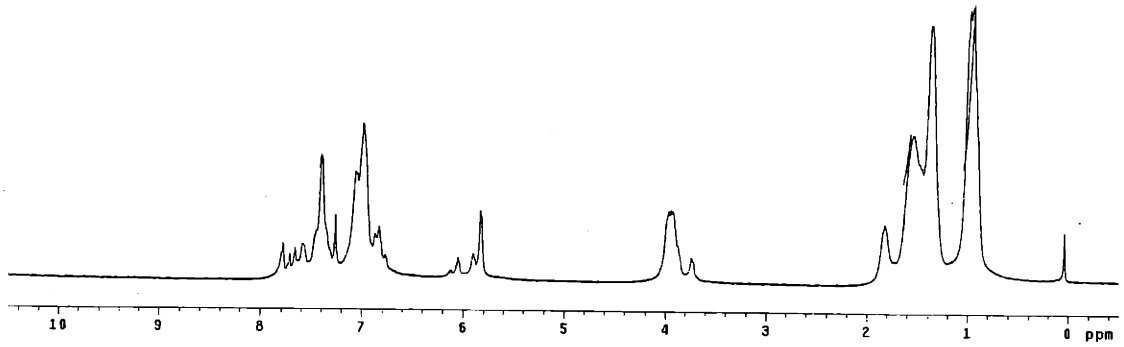

^{1}H NMR of **18** (300 MHz, $CDCl_3$)

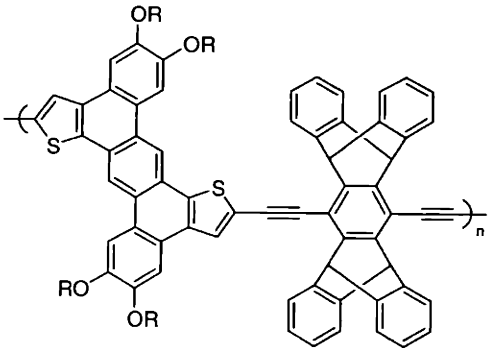

19 (R = 2-ethyl hexyl)

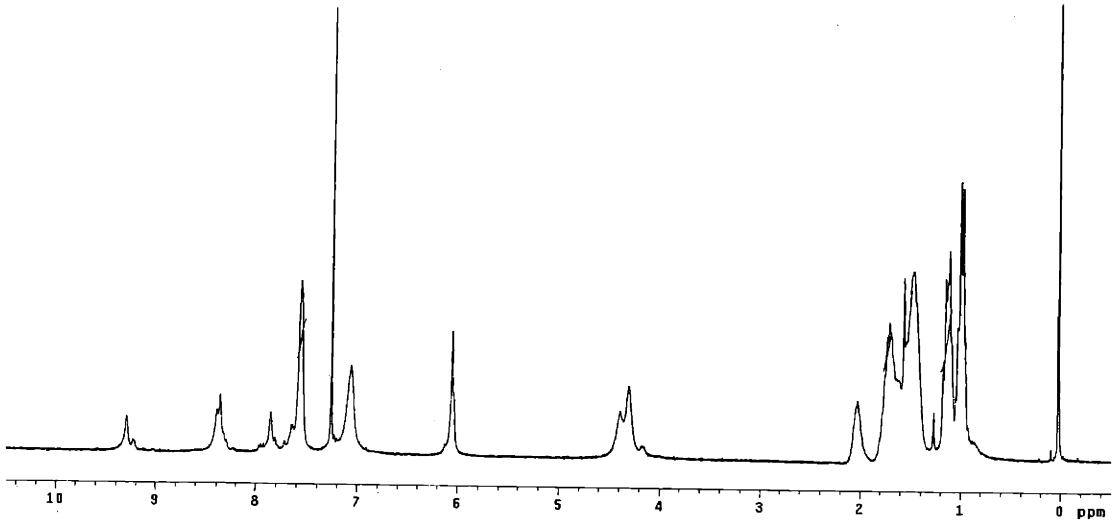

^{1}H NMR of **19** (300 MHz, $CDCl_3$)

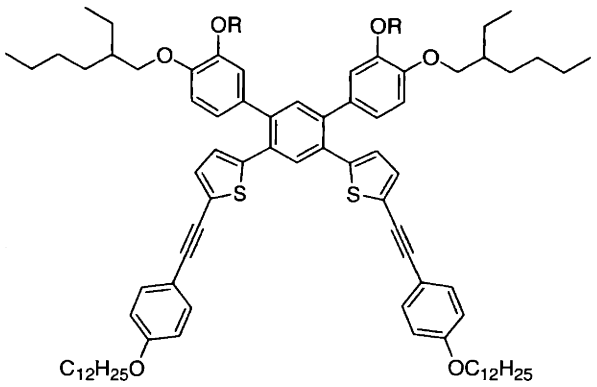

20 (R=2-ethyl hexyl)

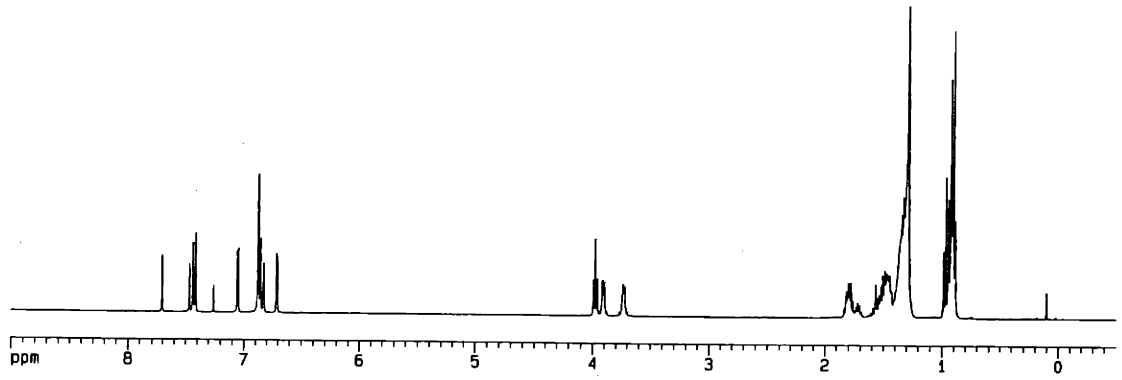

^{1}H NMR of **20** (400 MHz, $CDCl_3$)

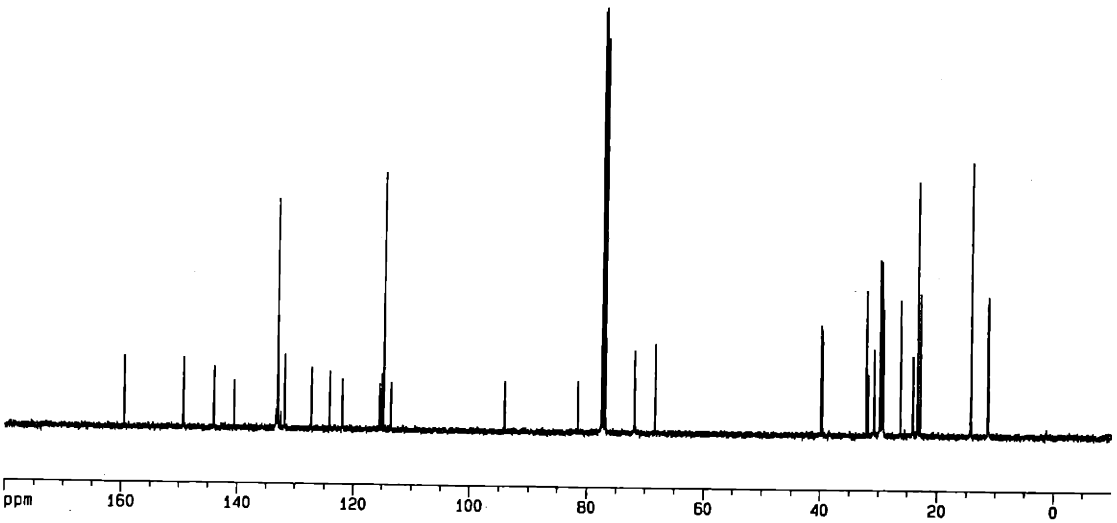

^{13}C NMR of **20** (100 MHz, $CDCl_3$)

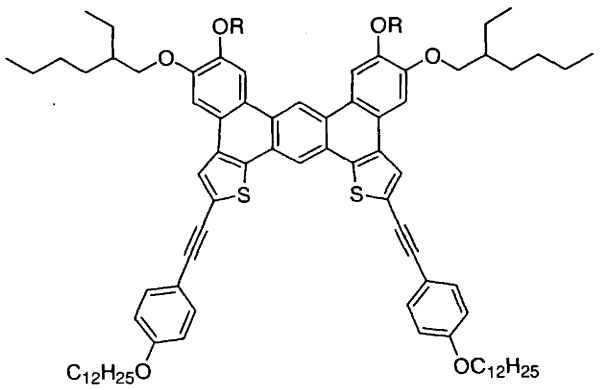

21 (R=2-ethyl hexyl)

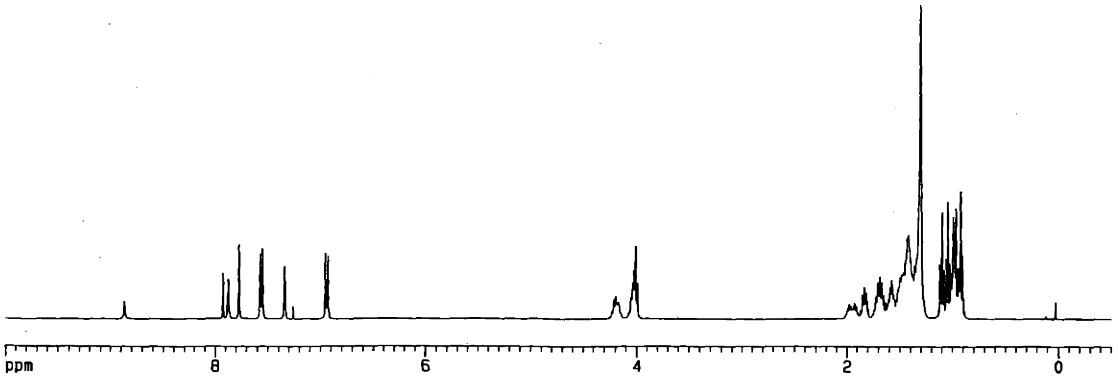

^{1}H NMR of **21** (400 MHz, $CDCl_3$)

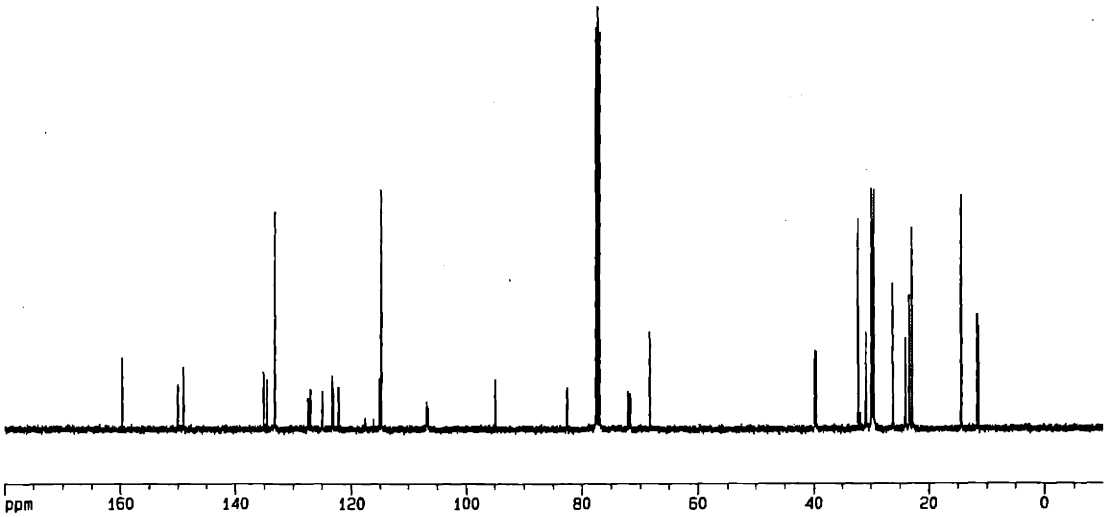

^{13}C NMR of **21** (100 MHz, $CDCl_3$)

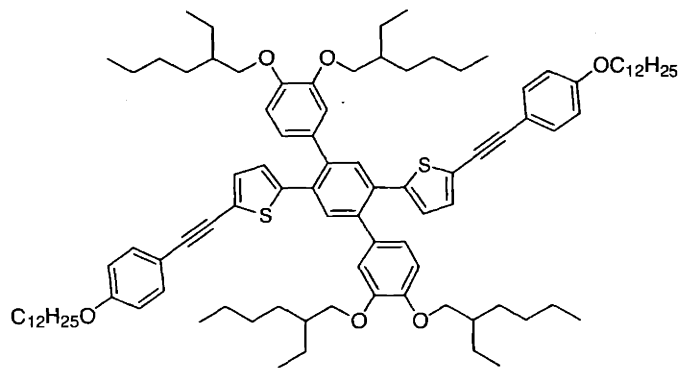

22

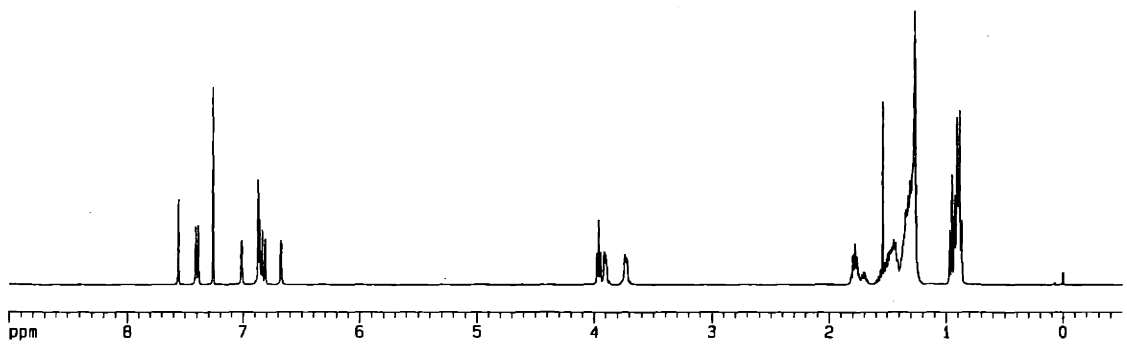

^{1}H NMR of **22** (400 MHz, $CDCl_3$)

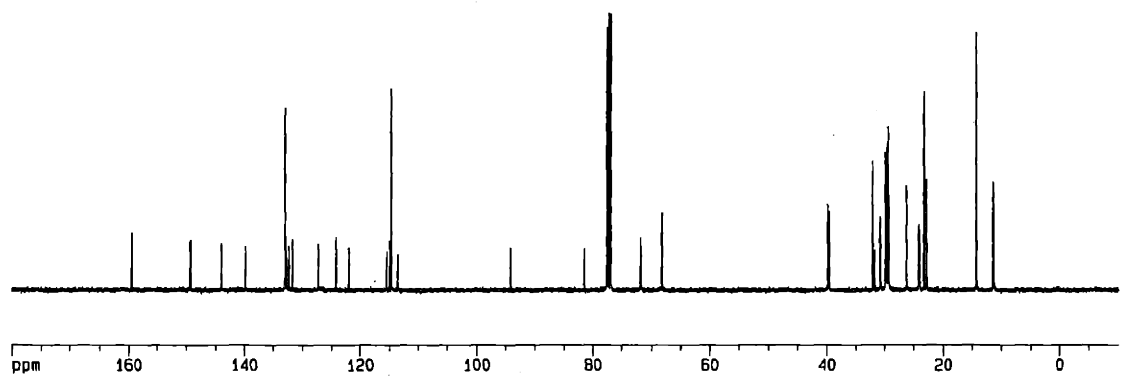

^{13}C NMR of **22** (100 MHz, $CDCl_3$)

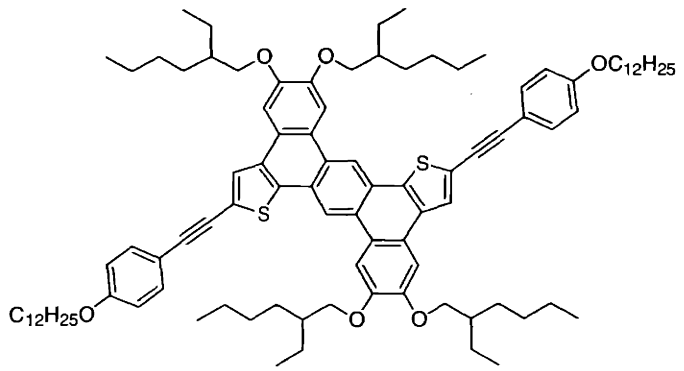

23

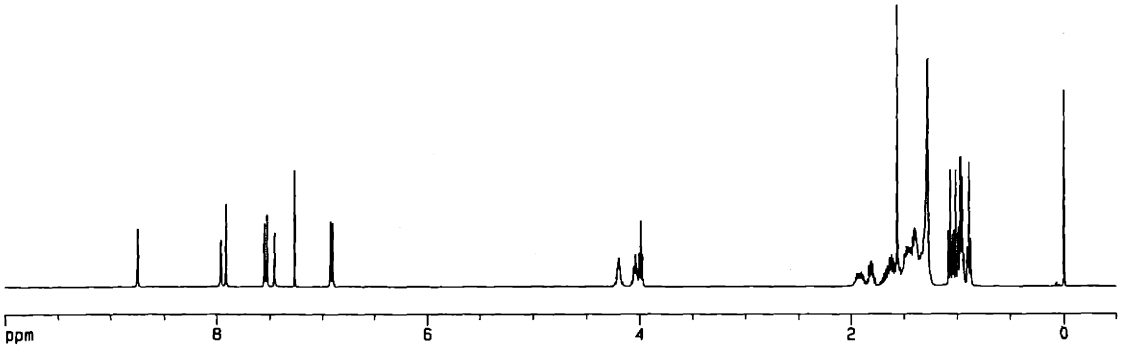

^{1}H NMR of **23** (400 MHz, $CDCl_3$)

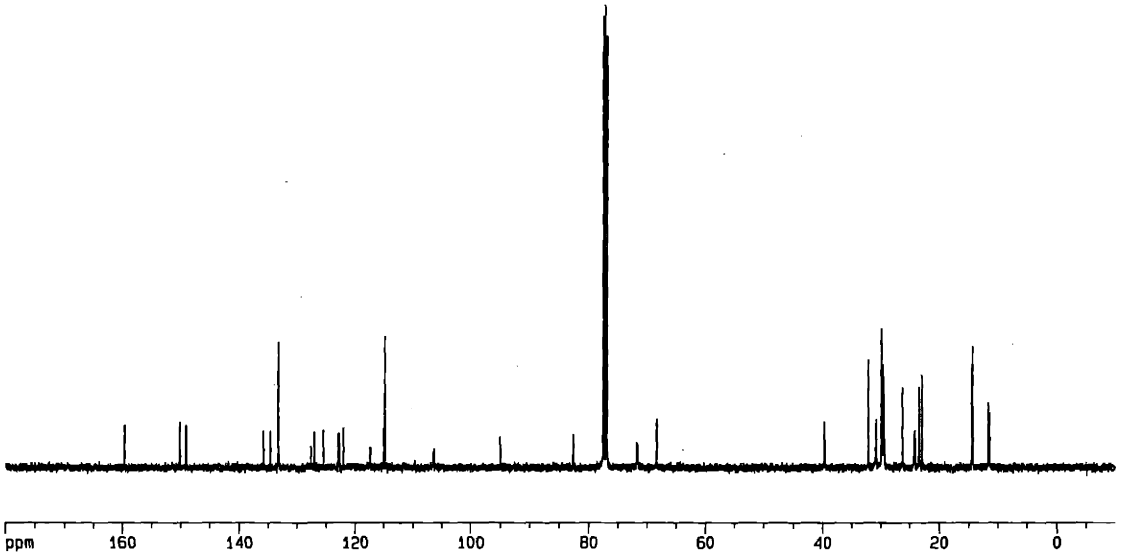

^{13}C NMR of **23** (100 MHz, $CDCl_3$)

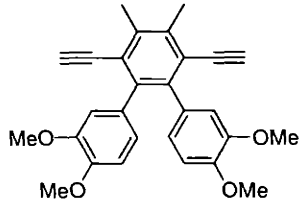

25

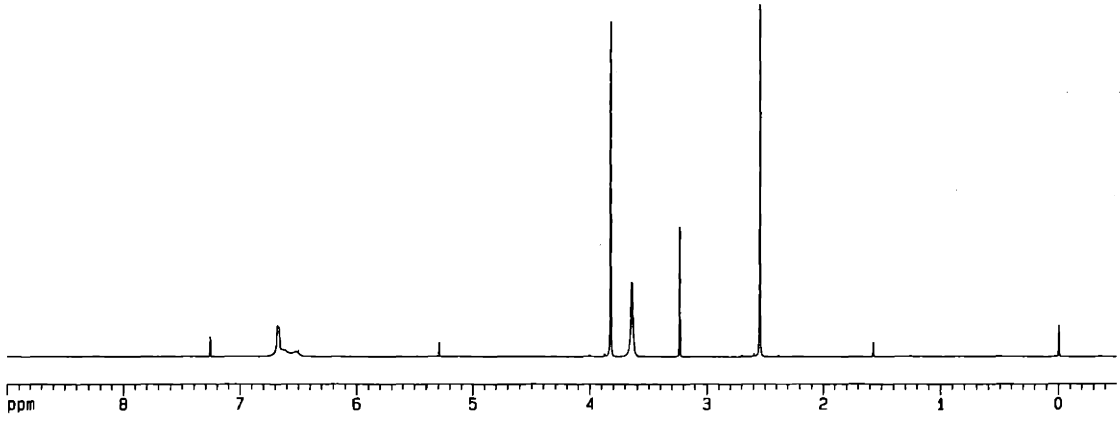

^{1}H NMR of **25** (400 MHz, $CDCl_3$)

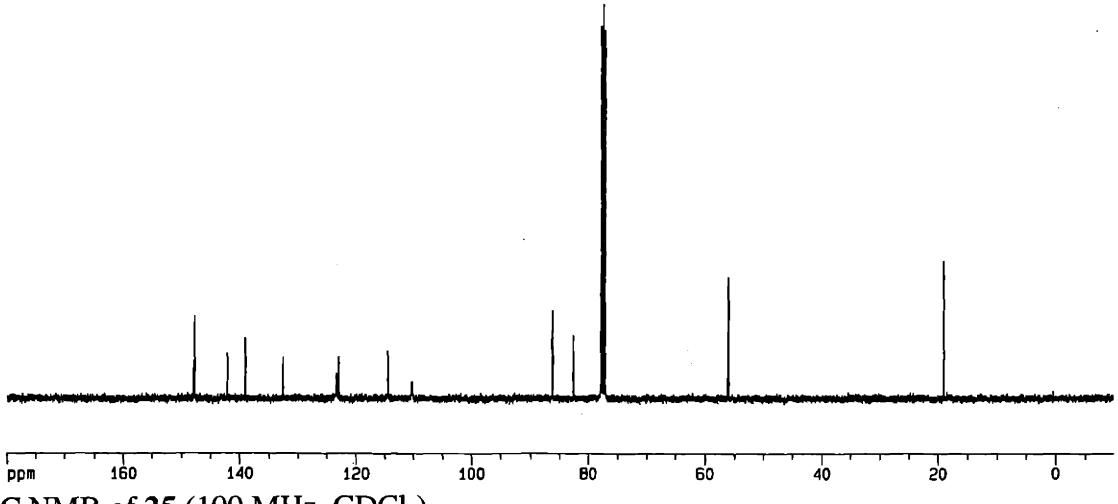

^{13}C NMR of **25** (100 MHz, $CDCl_3$)

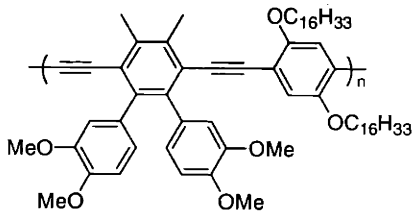

26

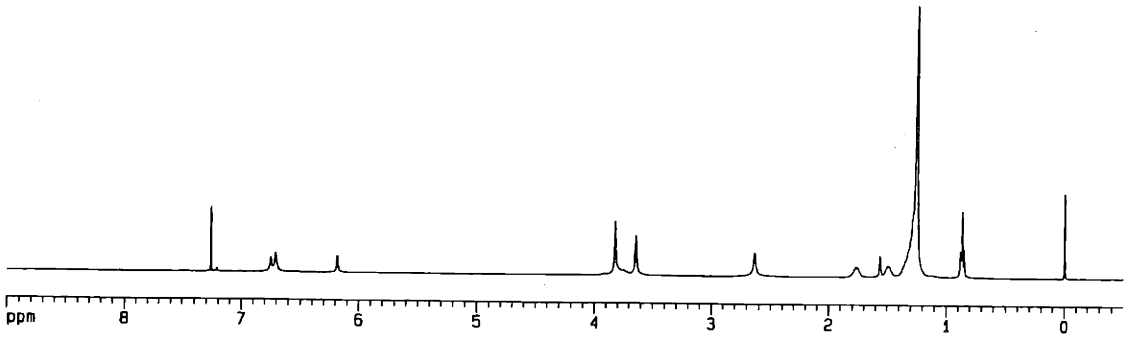

^{1}H NMR of **26** (400 MHz, $CDCl_3$)

Appendix 5:

^{1}H and ^{13}C NMR spectra for Chapter 5

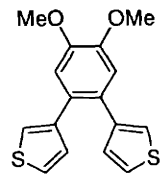

1a

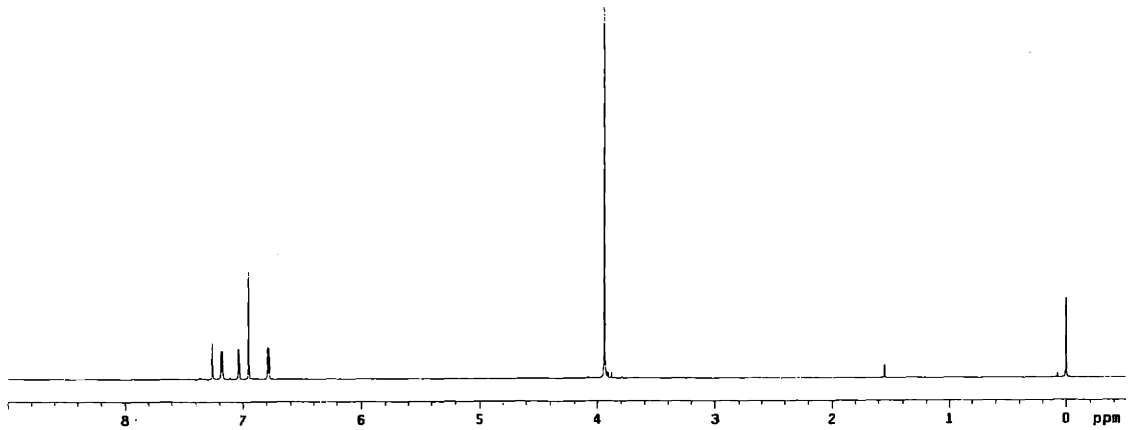

^{1}H NMR of **1a** (500 MHz, $CDCl_3$)

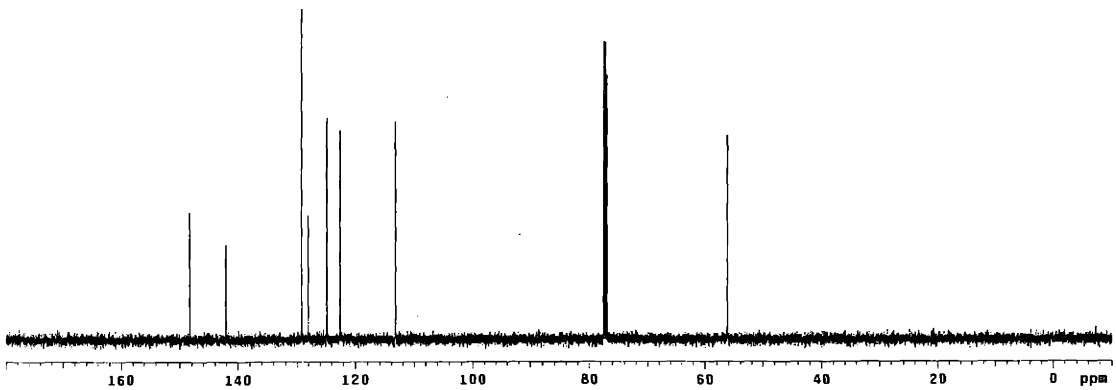

^{13}C NMR of **1a** (125 MHz, $CDCl_3$)

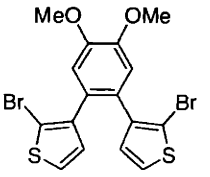

2a

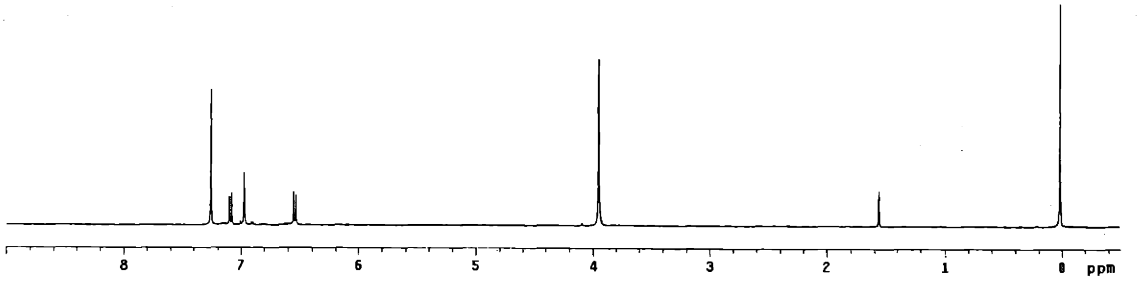

^{1}H NMR of **2a** (300 MHz, $CDCl_3$)

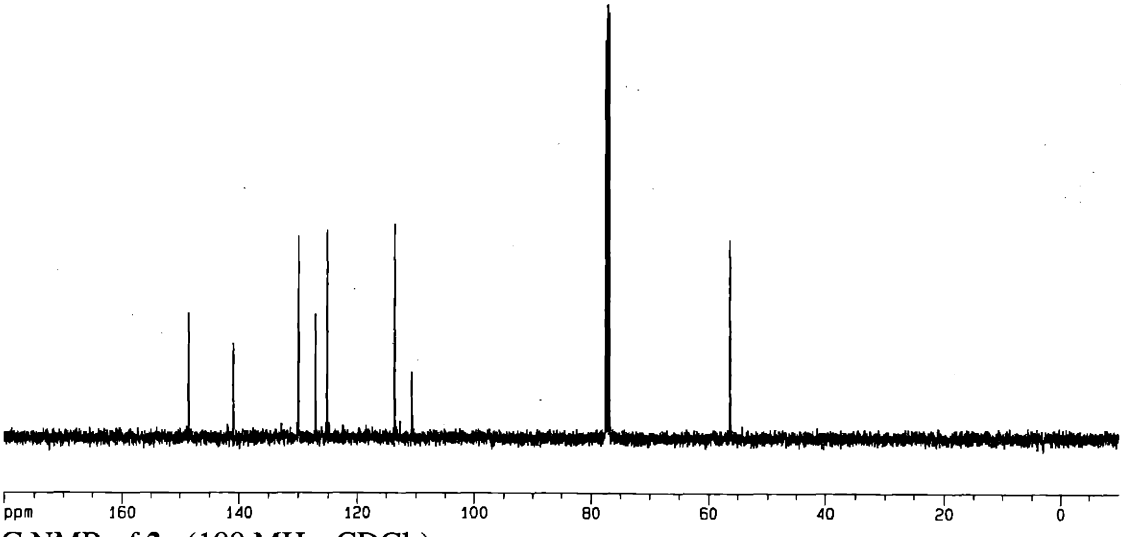

^{13}C NMR of **2a** (100 MHz, $CDCl_3$)

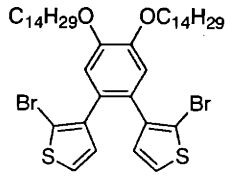

2b

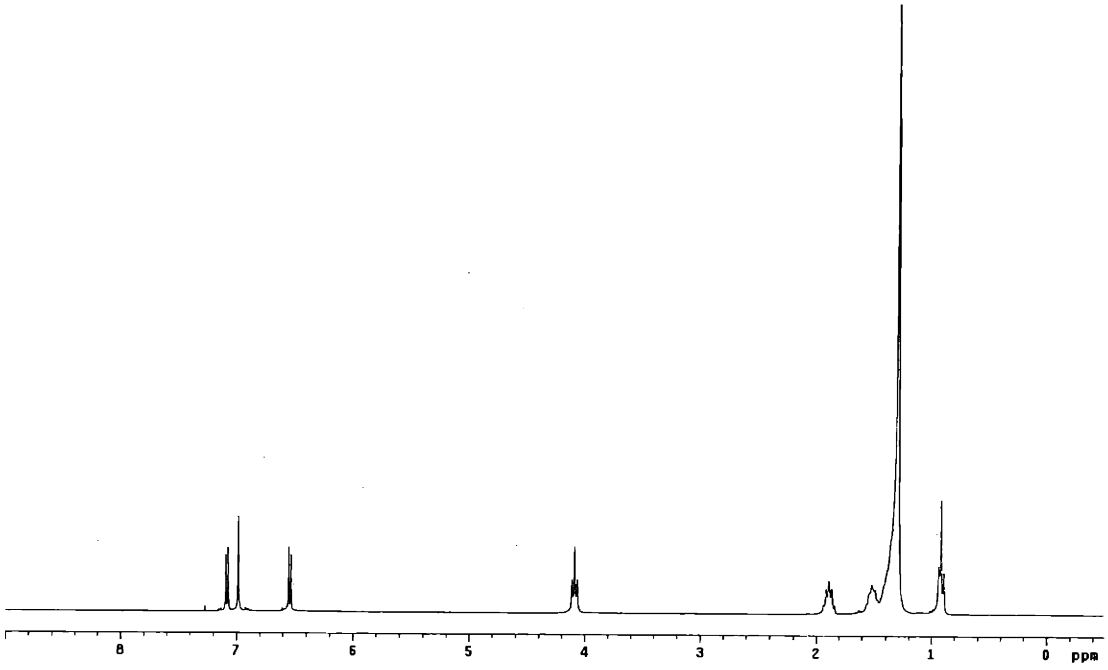

^{1}H NMR of **2b** (300 MHz, $CDCl_3$)

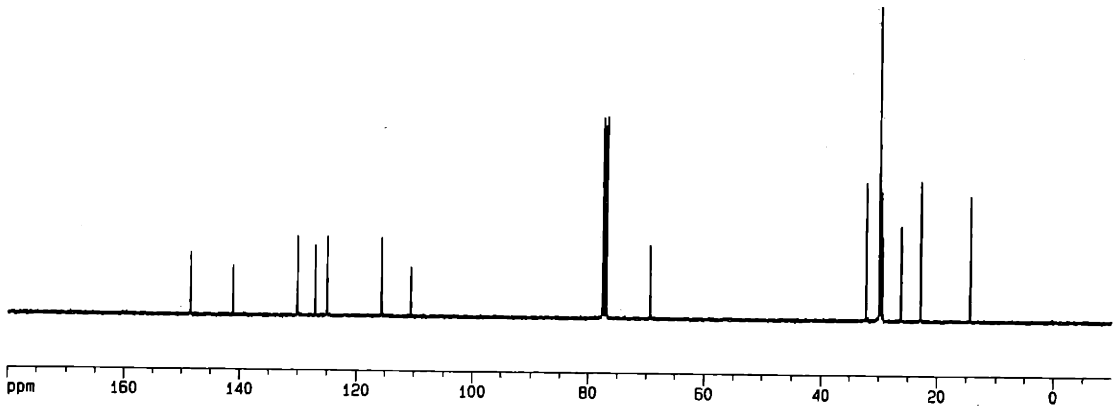

^{13}C NMR of **2b** (100 MHz, $CDCl_3$)

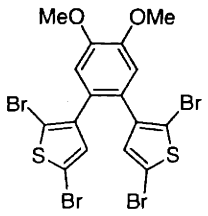

3

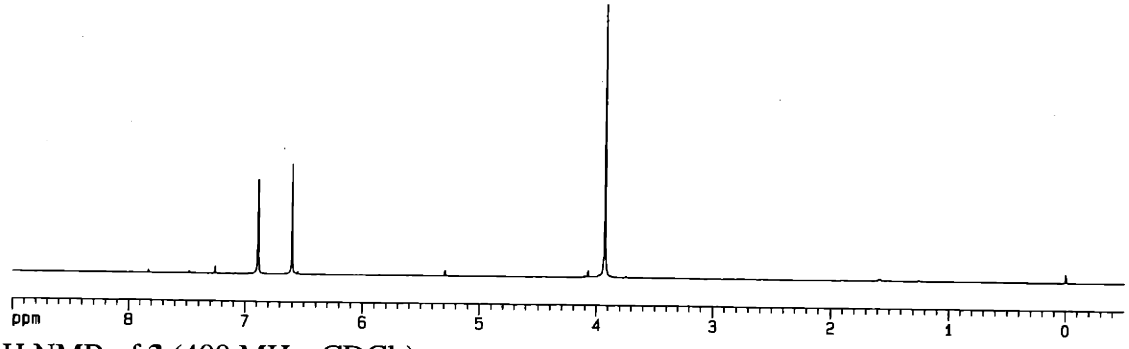

^{1}H NMR of **3** (400 MHz, $CDCl_3$)

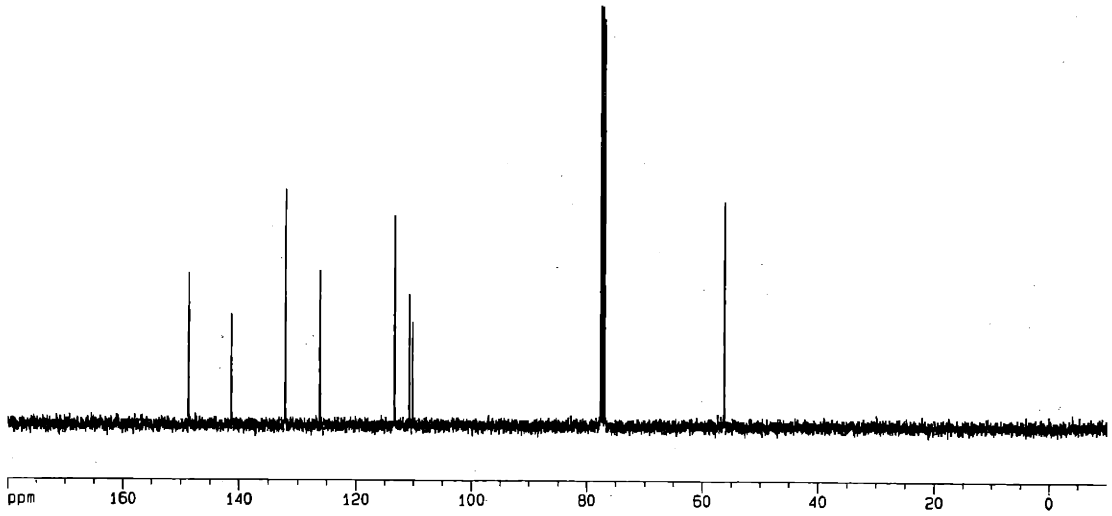

^{13}C NMR of **3** (100 MHz, $CDCl_3$)

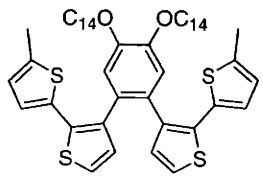

4

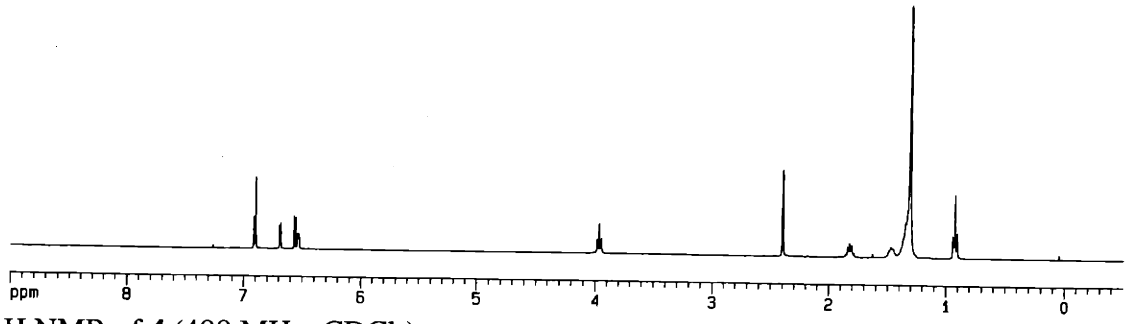

^{1}H NMR of **4** (400 MHz, $CDCl_3$)

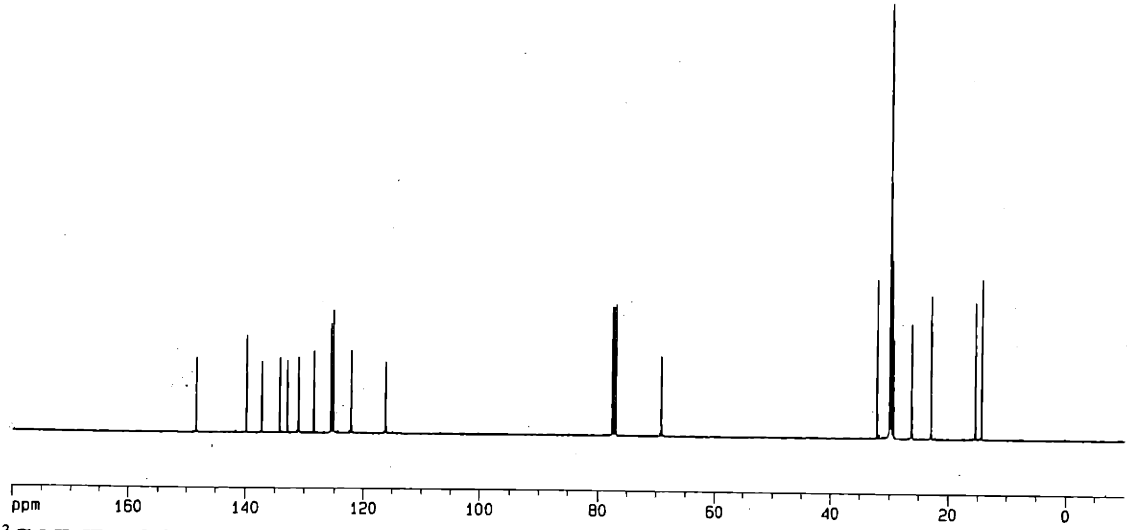

^{13}C NMR of **4** (100 MHz, $CDCl_3$)

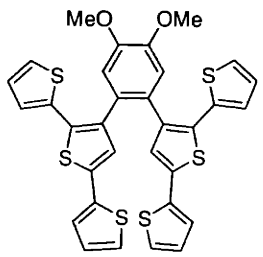

5

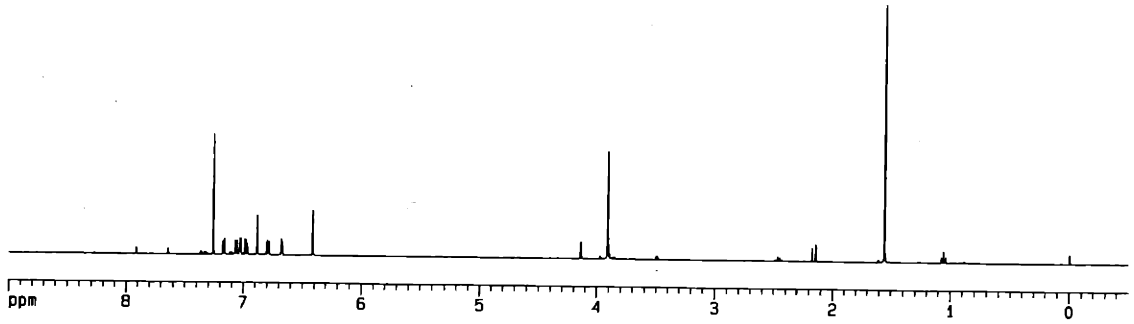

^{1}H NMR of **5** 400 MHz, $CDCl_3$)

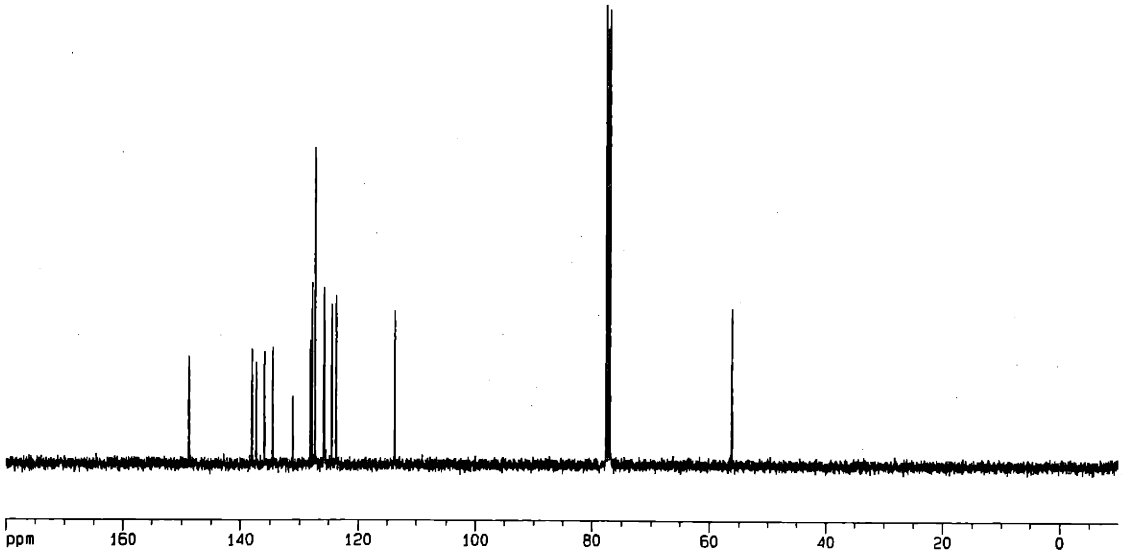

^{13}C NMR of **5** (100 MHz, $CDCl_3$)

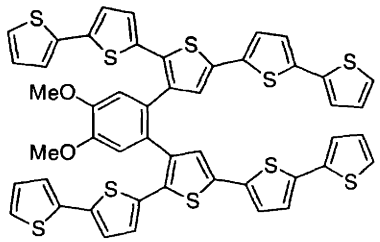

6

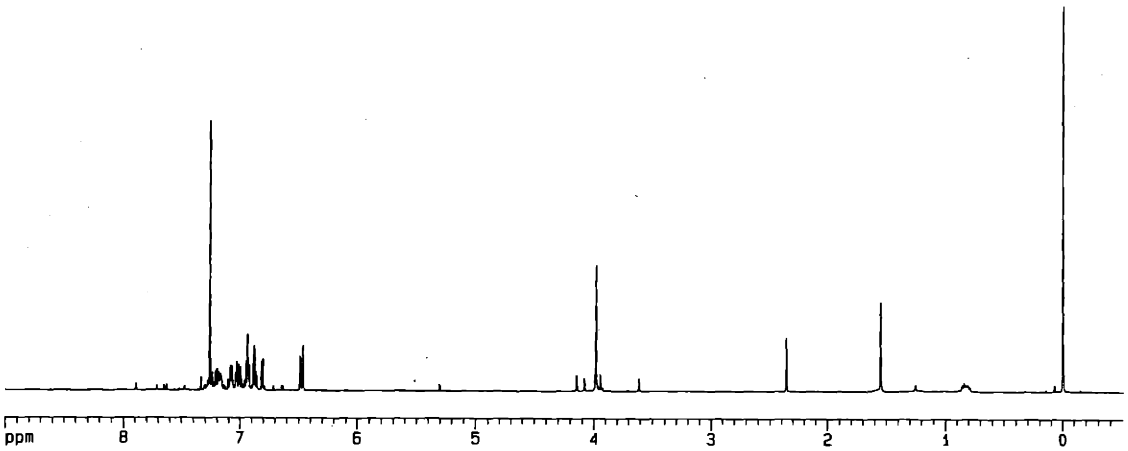

^{1}H NMR of **6** (400 MHz, $CDCl_3$)

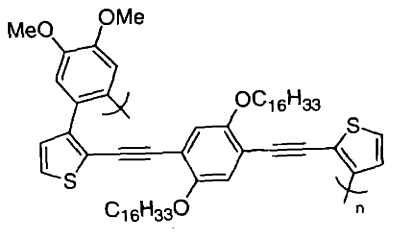

9

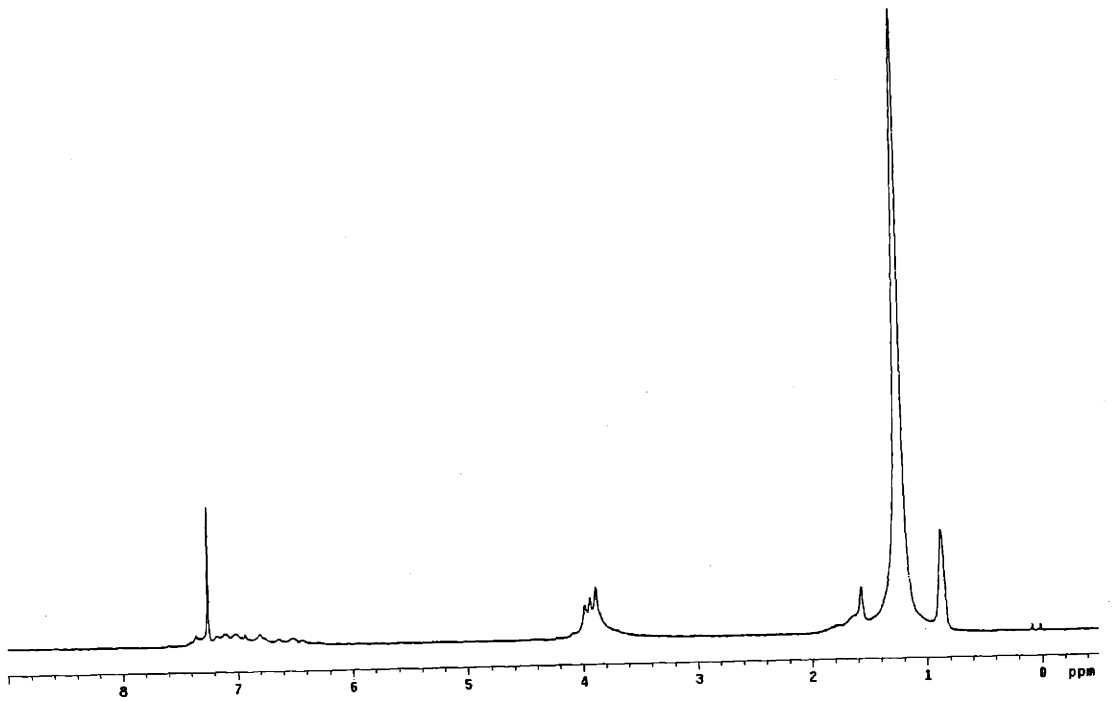

^{1}H NMR of **9** (300 MHz, $CDCl_3$)

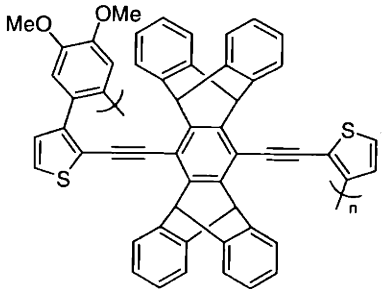

10

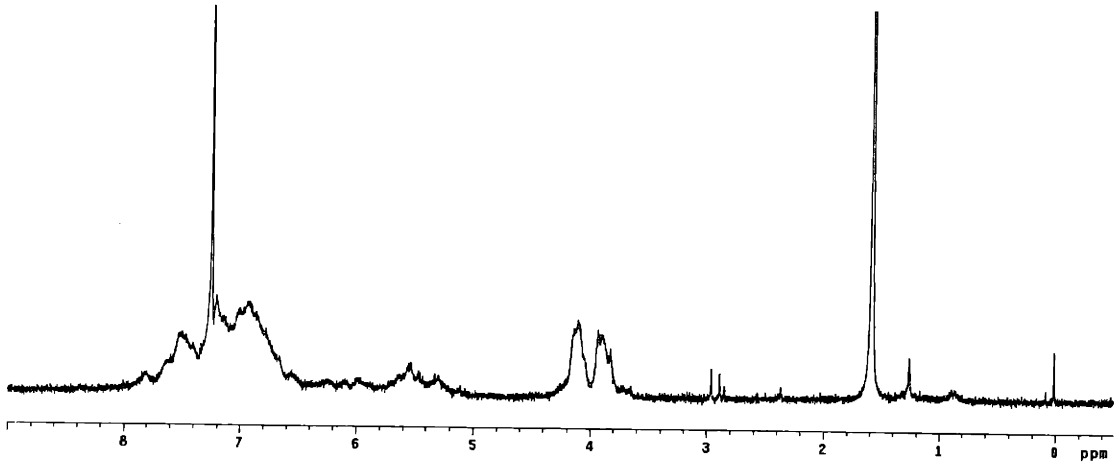

^{1}H NMR of **10** (300 MHz, $CDCl_3$)

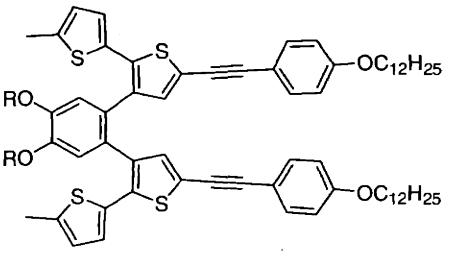

11

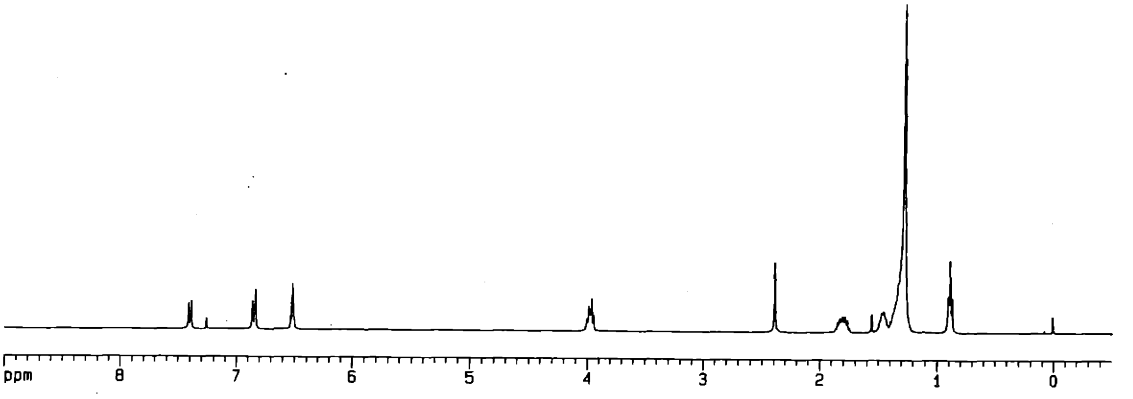

^{1}H NMR of **11** (400 MHz, $CDCl_3$)

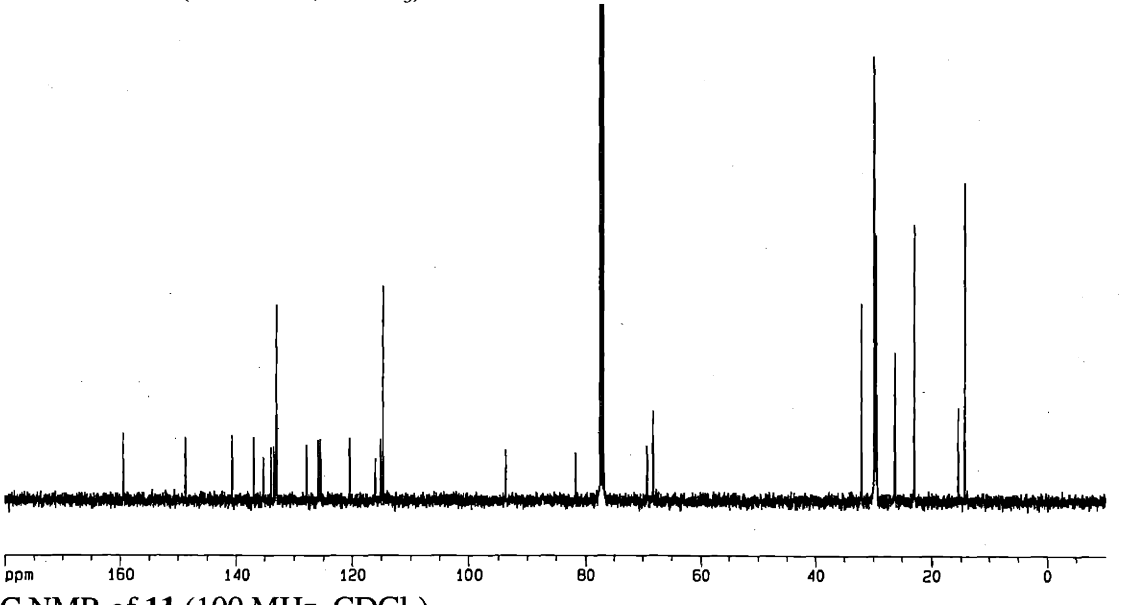

^{13}C NMR of **11** (100 MHz, $CDCl_3$)

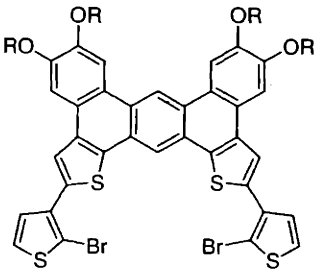

14

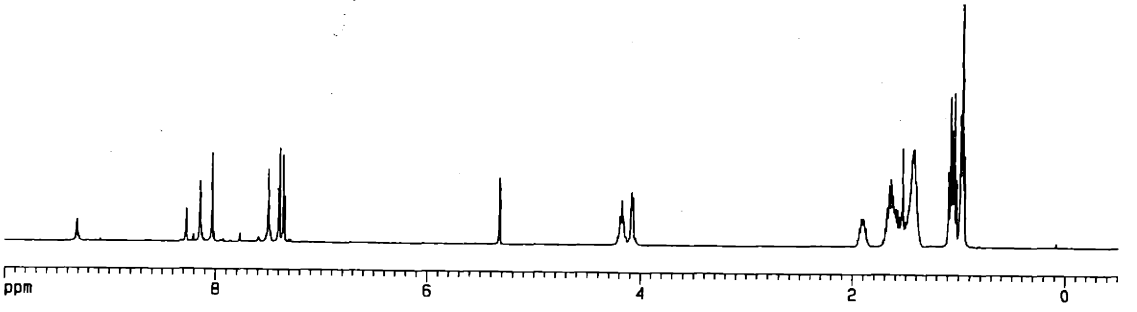

^{1}H NMR of **14** (400 MHz, CD_2Cl_2)

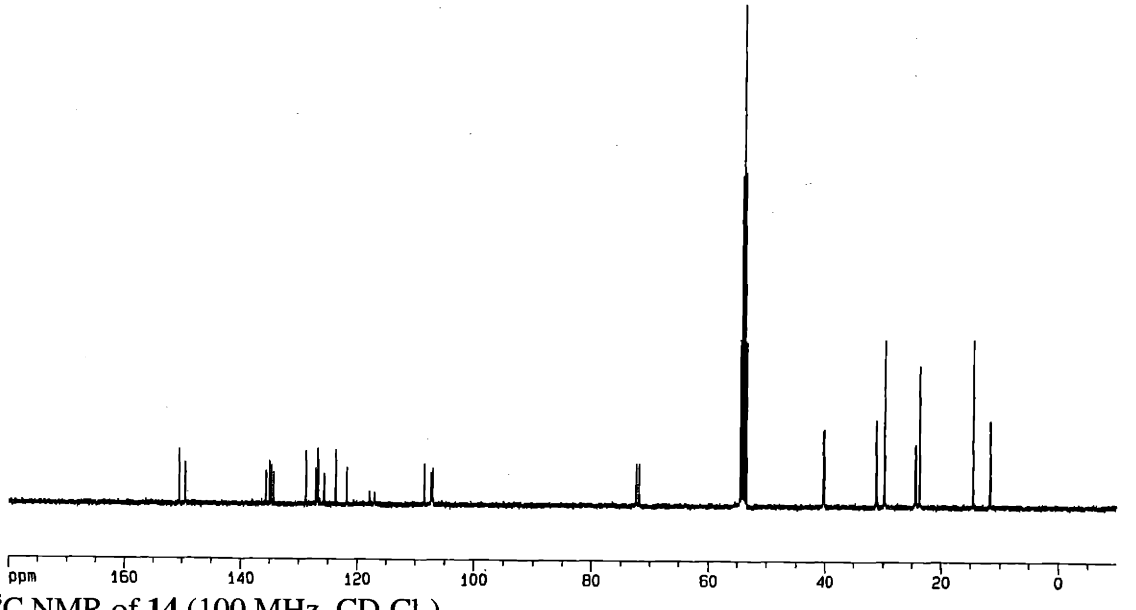

^{13}C NMR of **14** (100 MHz, CD_2Cl_2)

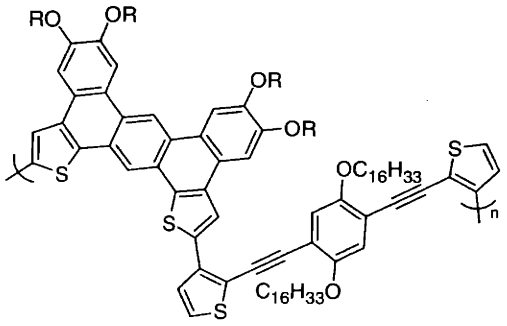

15 (R = 2-ethyl hexyl)

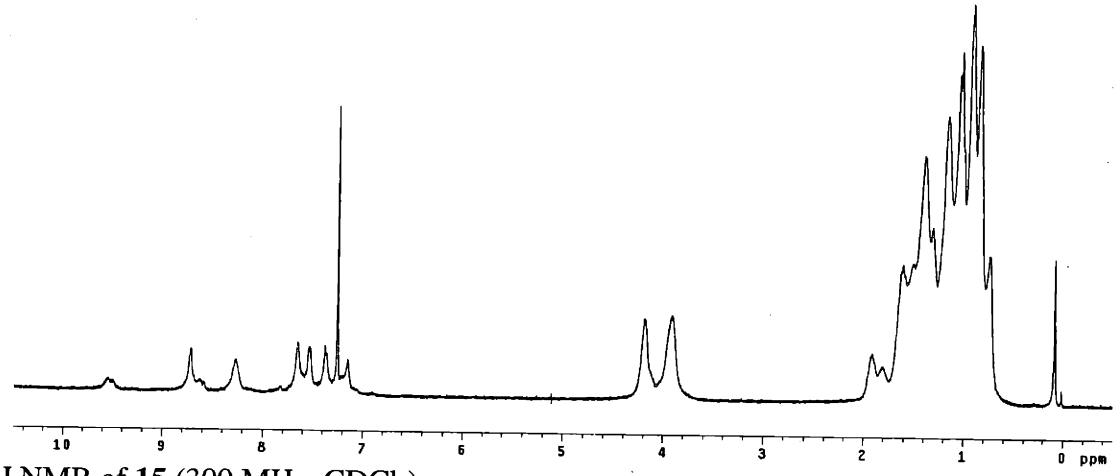

^{1}H NMR of **15** (300 MHz, $CDCl_3$)

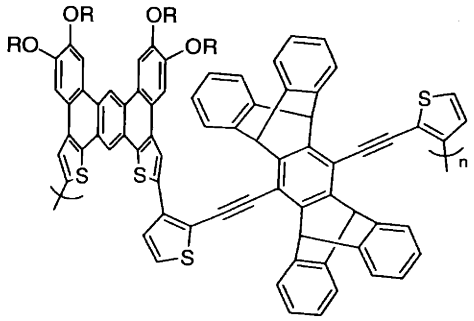

16 (R = 2-ethyl hexyl)

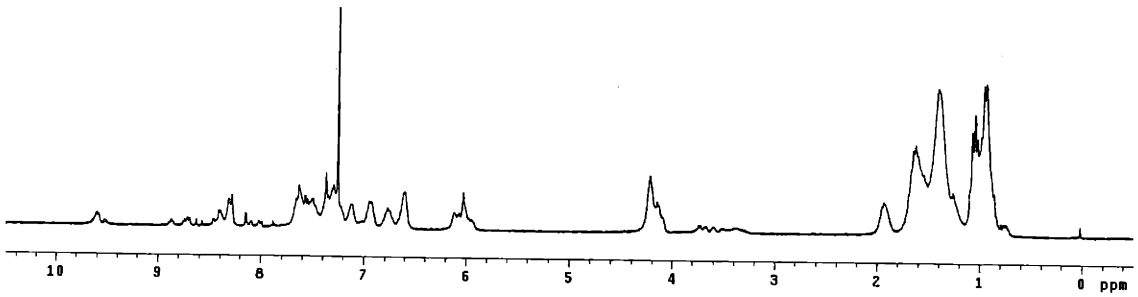

^{1}H NMR of **16** (300 MHz, $CDCl_3$)

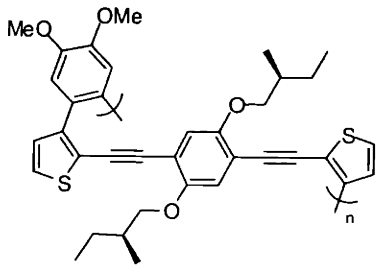

18

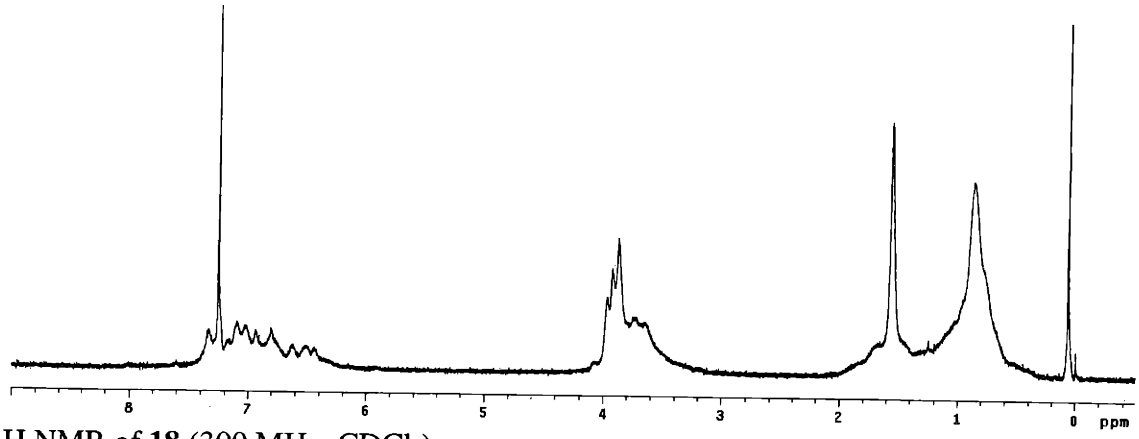

^{1}H NMR of **18** (300 MHz, $CDCl_3$)

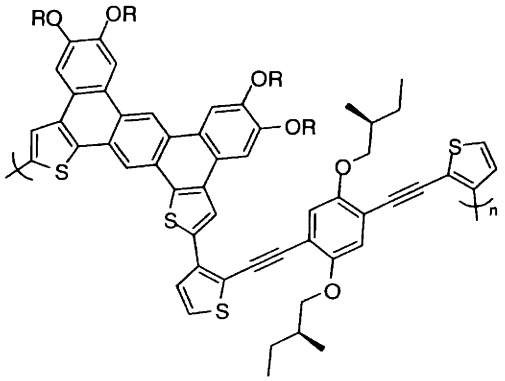

19 (R = 2-ethyl hexyl)

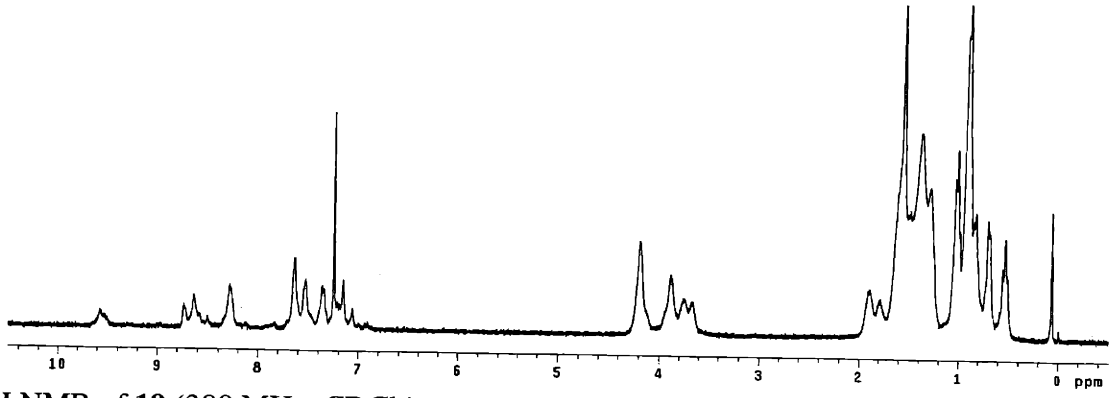

^{1}H NMR of **19** (300 MHz, $CDCl_3$)